



Abstract Volume 8th Swiss Geoscience Meeting

Fribourg, 19th – 20th November 2010

sc | nat 

Geosciences
Platform of the Swiss Academy of Sciences



Department of
Geosciences

Edited by the Swiss Academy of Sciences

Cover page images:

Large picture: Lava field and fumarole near Landmannalaugar, Iceland, Author: Pierre Dèzes, SCNAT

Small picture: Pahoeoe fountain south of Pu'u Kahaualea, Author: J.D. Griggs, USGS

8th Swiss Geoscience Meeting, Fribourg 2010

Table of contents

Organisation	2
Abstracts	
0. Plenary Session	4
1. Structural Geology, Tectonics and Geodynamics	8
2. Mineralogy-Petrology-Geochemistry	58
3. Himalayan Geology: A tribute to Augusto Gansser on his 100th anniversary	100
4. Paleontology and Paleobiodiversity	112
5. Lithostratigraphic units for the swiss geological maps: state of the art	126
6. Natural Hazards and Risks in Alpine Geology	132
7. Geomorphology	148
8. Quaternary Research	174
9. Trusting on soils in a changing world?	208
10. Open Cryosphere Session	228
11. Meteorology and Climatology	254
12. Phenology and Seasonality	266
14. Geoscience and Geoinformation - From data acquisition to modelling and visualisation	282
15. Decision oriented modelling of the geosphere	298
16. Hydrological and Limnological Perspectives in Times of Global Changes	302
17. Groundwater and Climate change	322
18. Troubling water: modes of socialization of a natural resource	338
19. The global / local in our research	344
20. Geotopes and Geoparks	348
21. Mars: water, climate & geology	354

Organisation

Host Institution

Department of Geosciences of the University of Fribourg

Patronnage

Platform Geosciences, Swiss Academy of Sciences

Program Committee

Gilles Borel

Lionel Cavin

Pierre Dèzes

Hans-Rudolf Egli

Charles Fierz

Karl Föllmi

Alain Geiger

Bernard Grob  ty

Martin Hoelzle

Hans Hurni

Adrian Jakob

Ronald Kozel

Neil Mancktelow

Franziska Nyffenegger

Nils Oesterling

Adrian Pfiffner

Rolf Philipona

Frank Preusser

Eric Reusser

Bruno Sch  dler

Manfred Th  ring

Helmut Weissert

Adrian Wiget

Fran  ois Zwahlen

Local Organizing Committee

Jean-Pierre Berger

Reynald Delaloye

Martin Hoelzle

Christian Hauck

Olivier Graefe

Bernard Grob  ty

Jon Mosar

Silvia Spezzaferri

Andr   Strasser

Participating Societies and Organisations

Etablissement cantonal d'assurance des bâtiments, Fribourg (ECAB)
 Federal Office of Meteorology and Climatology (MeteoSwiss)
 Federal Office of Topography (swisstopo)
 Institute of Geology and Hydrogeology (Chyn)
 International Union of Geodesy and Geophysics, Swiss Committee (IUGG)
 International Geographical Union (IGU)
 International Union of Geological Sciences, Swiss Committee (IUGS)
 Kommission der Schweizerischen Paläontologischen Abhandlungen (KSPA)
 Mars Society Switzerland
 Oeschger Centre for Climate Change Research (Uni Bern)
 Service des constructions et de l'aménagement du canton de Fribourg (SeCa)
 Swiss Academic Society for Environmental Research and Ecology (SAGUF)
 Swiss Association of Geologists (CHGEOL)
 Swiss Commission for Remote Sensing (SCRS)
 Swiss Committee for Stratigraphy (Platform Geosciences)
 Swiss Geodetic Commission (SGC)
 Swiss Geography Association (SGV-ASG)
 Swiss Geological Society (SGG/SGS)
 Swiss Geological Survey (swisstopo)
 Swiss Geomorphological Society (SGGm/SSGm)
 Swiss Geophysical Commission (SGPK)
 Swiss Geotechnical Commission (SGTK)
 Swiss Hydrogeological Society (SGH)
 Swiss Hydrological Commission (CHy)
 Swiss Society for Hydrology and Limnology (SGHL / SSSL)
 Swiss Meteorological Society (SGM)
 Swiss Paleontological Society (SPG/SPS)
 Swiss Society for Quaternary Research (CH-QUAT)
 Swiss Soil Science Society (SSSS)
 Swiss Snow, Ice and Permafrost Society (SIP)
 Swiss Society of Mineralogy Petrography (SMPG / SSMP)
 Swiss Tectonics Studies Group (Swiss Geological Society)
 Swiss Working Group on Geotopes (Platform Geosciences)

Plenary Session, Friday November 19th

Hot and Cold: Extreme Climates in Space and Time

Auditoire J. Deiss, Pérolles 2, Fribourg

13:30 - 13:50	Bernhard Grobéty President SGM 2010	Opening address by the President of the Geoscience Department, University of Fribourg
13:50 - 14:30	Paul F. Hoffman Harvard University	The snowball Earth hypothesis and its recent progress (<i>Joint IUGS-CH & IUGG-CH Union Lecture</i>)
14:30 - 15:10	James Zachos UC Santa Cruz	Extreme warming and ocean acidification 55 million years ago: lessons for the future?
15:10 - 15:20	<i>Musical Interlude</i>	<i>Swiss Ice Fiddlers</i>
15:20 - 16:00	Hubertus Fischer University of Bern	Climate studies on ice cores – tepid, warm and piping hot
16:00 - 16:20	<i>Coffee Break</i>	
16:20 - 17:00	John M. Reynold Reynolds Internat. Ltd	Assessing and managing glacial hazards in a changing climate
17: 00 - 17:05	<i>Musical Interlude</i>	<i>Swiss Ice Fiddlers</i>
17:05 - 17:15	Guido Vergauwen	Address by the rector of the University of Fribourg
17:15 - 17:30	Pierre Ecoffey ECAB	Impact of global change on the insurance business
17:30 - 18:15	Helmut Weissert Helmut Weissert Gilles Borel Daniele Biaggi Michael Dunga	Communications Platform Geosciences Presentation SGM 2011 in Zurich Swiss Geological Society Award CHGEOL Award Paul Niggli Medal
18:15 - ??:??	Swiss Geoscience Party	

0. Plenary Session

- 1 Hoffman P.F.: The snowball Earth hypothesis and its recent progress
- 2 Zachos J.: Global warming and ocean acidification 55 million years ago: Lessons for the future?
- 3 Fischer H.: Climate studies on ice cores – tepid, warm and piping hot
- 4 Reynolds J.M.: Assessing and managing glacial hazards in a changing climate

1

The snowball Earth hypothesis and its recent progress

Paul F. Hoffman

Dept of Earth and Planetary Sciences, Harvard University, Cambridge, MA, USA

School of Earth and Ocean Sciences, University of Victoria, Victoria, BC, Canada

The snowball Earth hypothesis invoked runaway ice-albedo feedback, also called ‘the large ice-cap instability’, to account for geological evidence that Neoproterozoic ice sheets reached sea level close to the palaeoequator and also on marine carbonate platforms, diagnostic of the warmest parts of the surface ocean. This occurred during two discrete glaciations and it was hypothesized that both terminated abruptly when ocean-atmosphere CO₂ (which accumulated over time because of diminished silicate weathering) achieved a critical greenhouse radiative forcing. In the decade since the hypothesis was first widely discussed, its empirical basis (stratigraphic, palaeomagnetic and geochronologic) has been verified for both glaciations, its theoretical foundations have been tested in a variety of climate models, and the key prediction that highly anomalous CO₂ levels were required for deglaciation has been supported by boron, carbon and, most convincingly, by large mass-independent oxygen isotope (negative δ¹⁷O) anomalies in both synglacial and syndeglacial sulfates.

Existing U-Pb dates imply that the older (‘Sturtian’) glaciation lasted for 50-57 Myrs and began at 717 Ma. The younger (‘Marinoan’) glaciation lasted no more than 24 Myr and it terminated at 635 Ma. The two were separated by an interval less than 15 Myr in duration when large ice sheets were apparently absent. Between 717 and 635 Ma, the continents were mainly situated between 30°N and 60°S latitudes. All but the southernmost land areas bore dynamic ice sheets that flowed directly into the ocean at palaeolatitudes as low as 22°N (Sturtian, Yukon Territory) and 14°N (Marinoan, South Australia). During pan-glacial times, the ocean presumably shrunk by up to 25%, with a proportional increase in salinity, because ice sheets must have grown sufficiently thick (i.e. ~2.0 km above sea level) to reach dynamic steady-state. Field evidence from Namibia for tropical tidewater ice sheets, ice streams and large changes in relative sea level will be presented.

Compatible evidence for substantial subglacial meltwater production and open water in proglacial marine settings has wrongly been hailed as refuting the snowball Earth hypothesis: the hypothesis predicts that snowball glaciations began cold and dry, but ended warm and wet. Won’t the surviving glacial sedimentary record be dominated by the period of most rapid ice sheet drainage, which would have followed after the buttress of an unlimited ice shelf (‘sea glacier’) was removed? Deposition of classic Marinoan glacial sequences at the (warm and wet) glacial termination is consistent with U-Pb dating (Nantuo Formation, South China) and triple-oxygen CO₂-proxy data (Wilsonbreen Formation, NE Svalbard).

Many leading Proterozoic palaeontologists consider that a totally ice-covered ocean of geological duration is not consistent with the observed survival of many eukaryotic algal and protistan clades. This judgement was not audibly withdrawn after sea-glacier dynamic modeling showed that crack systems would have perpetually existed on a snowball Earth along marine ice grounding-lines subjected to lateral shear. Palaeontologically-based skepticism encouraged climate modelers to renew testing the plausibility of a snowball Earth under reasonable Neoproterozoic forcings, and also to seek stable solutions in which tropical ice sheets on land coexisted with ice-free tropical or equatorial oceans. In the first half of the last decade, climate models were interpreted as indicating that a Neoproterozoic snowball Earth was implausible, that it could not be terminated in a geologically permissible timeframe, and that biologically more benign intermediate solutions were not only stable but more probable. In the more comprehensive and sophisticated models of the second half of the decade, the once promising intermediate solutions appear less and less likely to be stable solutions, and something closer to the original snowball hypothesis appears plausible, both to initiate and to terminate.

The origin of multicellularity in animals (i.e. demosponges) is closely tied to the pan-glacial intervals by microfossils (South China) and biomarkers (Oman). Genomic studies indicate that many, if not all, of the genes required for multicellularity in animals (and plants) are far more primitive than multicellularity itself. Accordingly, the argument that the duration of a snowball Earth was too short to have impacted the protracted evolution of those genes is transformed into a new question. Did a snowball Earth create a selective situation in which existing genes were coopted for multicellularity in animals?

2

Global warming and ocean acidification 55 million years ago: Lessons for the future?

James C. Zachos

*Earth and Planetary Sciences Dept., University of California, Santa Cruz, CA
(jzachos@pmc.ucsc.edu)*

Over the last century roughly 380 Pg C has been emitted to the atmosphere contributing to nearly 1°C of global warming. Of the total emissions, the ocean has absorbed more than 30%. Because the ocean is thermally stratified and the vertical mixing time of the ocean is slow (~ 500 y), most of the absorbed CO₂ has accumulated in the thin surface layer. As a consequence, both the pH and carbonate saturation state of seawater are measurably decreasing. With unabated carbon emissions over the next several centuries, the pH of the surface ocean is projected to decrease by as much as 0.7 pH units. In addition, as the atmosphere and upper ocean warm, the % of emitted carbon absorbed by the ocean is likely to decrease partly as a consequence of the pH change, but also because of increased stratification (Friedlingstein et al., 2006; Le Quere et al., 2009).

In terms of rate, the anthropogenic carbon cycle perturbation appears to be unprecedented in Earth history. The closest analog is the release of carbon that triggered the Paleocene-Eocene Thermal Maximum (PETM; ~56 Mya), a transient global warming of 5 to 6°C. The primary evidence for the carbon cycle perturbation is a large negative carbon isotope excursion (CIE), and widespread dissolution of seafloor carbonate. New estimates on the rate and magnitude of the CIE and extent of carbonate dissolution (Zachos et al., 2005) have proved critical for quantifying several features of the event including the magnitude of ocean pH change and hence the mass of carbon released during the PETM. Simulations using box and earth system models suggest that the total mass of carbon released was between 4500 to 6000 PgC (Panchuk et al., 2008; Zeebe et al., 2009). Although this is similar to the projected anthropogenic mass (~4500 PgC), the flux was spread over 5 to 10 ky, a period significantly longer than the turnover time of the ocean, thus enabling some degree of buffering by mixing with the deep sea and dissolution of carbonate sediment. As a consequence, the magnitude of peak warming, and impacts on surface ocean saturation state were nominal. The changes in deep-sea carbonate chemistry, however, were clearly severe and long lasting (>100 ky).

Given the faster rate of release (a few 10² vs. 10³y), most impacts of the current and projected anthropogenic carbon emissions should be more severe than observed for the PETM, particularly the magnitude of global warming and surface ocean acidification. However, other impacts and responses will be similar, for example the undersaturation of the deep sea, as well as the long time scale for C sequestration and climatic recovery (>100 k.y.). Finally, the large mass of carbon released during the PETM is difficult to reconcile with just a single source. Aside from possible volcanic driven emissions (e.g., Svensen et al., 2004) which would have been rate limited, the largest potential sources with sufficient capacity are the two large reservoirs of reduced carbon, soil peat and marine hydrates (CH₄), raising the specter of a predominantly feedback driven carbon release.

REFERENCES

- Friedlingstein, P., Cox, P., Betts, R., Bopp, L., et al., 2006: Climate-carbon cycle feedback analysis: Results from the (CMIP)-M-4 model intercomparison. *Journal of Climate*, 19, 3337-3353.
- Le Quere, C., Raupach, M.R., Canadell, J.G., Marland, et al., 2009: Trends in the sources and sinks of carbon dioxide. *Nature Geoscience*, 2, 831-836.
- Panchuk, K., Ridgwell, A., and Kump, L.R., 2008: Sedimentary response to Paleocene-Eocene Thermal Maximum carbon release: A model-data comparison. *Geology*, 36, 315-318.
- Svensen, H., Planke, S., Malthes-Sorensen, A., Jamtveit, B., Myklebust, R., Eidem, T.R., and Rey, S.S., 2004: Release of methane from a volcanic basin as a mechanism for initial Eocene global warming. *Nature*, 429, 524-527.
- Zachos, J.C., Rohl, U., Schellenberg, S.A., Sluijs, A., Hodell, D.A., Kelly, D.C., Thomas, E., Nicolo, M., Raffi, I., Lourens, L.J., McCarren, H., and Kroon, D., 2005: Rapid acidification of the ocean during the Paleocene-Eocene thermal maximum. *Science*, 308, 1611-1615.
- Zeebe, R.E., Zachos, J.C., and Dickens, G.R., 2009: Carbon dioxide forcing alone insufficient to explain Palaeocene-Eocene Thermal Maximum warming. *Nature Geoscience*, 2, 576-580.

3

Climate studies on ice cores – tepid, warm and piping hot

Hubertus Fischer

*Climate and Environmental Physics, Physics Institute, & Oeschger Centre for Climate Change Research, University of Bern
(hubertus.fischer@climate.unibe.ch)*

In view of the recent ongoing human induced climate change the natural variability in climate (temperature, precipitation) and greenhouse gas concentrations becomes of major concern. Direct atmospheric observations of these parameters, however, are restricted to a few centuries when it comes to temperature and only a few decades when it comes to greenhouse gases. Accordingly, reliable records from natural climate archives are the only way to extend such observations back in time.

Ice cores from both polar regions represent one of the most important of such climate archives, providing quantitative climate data over up to 800,000 years back in time in very (in many cases seasonal) resolution. Moreover, bubble enclosures in ice core represent the only archive of the air composition in the past. Here the latest highlights of climate and greenhouse gas reconstructions using ice cores from both polar ice sheets will be presented, and put into relation to the current climate.

4

Assessing and managing glacial hazards in a changing climate

Prof. John M. Reynolds

*Reynolds International Ltd, Unit 17, Mold Business Park, Wrexham Road, Mold, Flintshire, CH7 1XP, UK
(jmr@reynolds-international.co.uk)*

Glaciers around the world are undergoing considerable retreat and downwasting with a few exceptions. As a result, the number of glacial lake systems is increasing as is the volume of water stored behind moraine dams; so the hazard is growing. At the same time, communities and infrastructure are being developed in remote mountain environments, especially associated with hydropower schemes and mining, thereby increasing local vulnerability. Taken together, the overall risks in mountain environments are also rising. This has been apparent in the Swiss Alps, for example, for many years and is attracting growing publicity.

The scientific community has a responsibility to develop robust techniques by which mountain hazards, and in the present case, glacial hazards, can be assessed objectively. This is important so as to be able to advise responsible agencies as to the relative priority of hazardous lakes. Appropriate vulnerability assessments can then be made with a view to managing the overall and consequent risks.

It is important that the underlying physical processes at work and affected by changing climate are understood so that the methods of hazard assessment reflect our best knowledge of those environments. Key processes, such as the destabilisation of high mountain walls by thawing permafrost coupled with changing thermal regimes of steep glaciers, need to be much better understood, as they are likely to trigger more rock/ice avalanches into the future. The impact of these into glacial lakes can be potentially devastating. Avalanche push waves in excess of 100 m high can be formed that repeatedly overtop unstable moraines and can lead to pulsed flood events downstream.

In this presentation, examples of glacial hazard assessment will be provided from the Himalayas, and from the Peruvian Andes. Case histories of successful mitigation will also be presented including details of a major rock/ice avalanche that occurred in April 2010 in the Cordillera Blanca, Peru, which demonstrated the effectiveness of earlier mitigation works that saved many lives earlier this year. Reference will also be made to other examples of glacial hazards projects in Chile, Kyrgyzstan and Pakistan.

1. Structural Geology, Tectonics and Geodynamics

Neil Mancktelow, Guido Schreurs, Paul Tackley

Swiss Tectonics Studies Group of the Swiss Geological Society

- 1.1 Armann M., Gerya T.: Spontaneous initiation of subduction at passive margins – 3D modelling
- 1.2 Bagheri S., Nabavi M., Salari T., Buchs D.: Late Eocene-Oligocene tectonic events in the Anarak area, Central Iran
- 1.3 Baitsch Ghirardello B., Gerya T.: Physical controls of intra-oceanic arc extension and trench migration: numerical modelling
- 1.4 Beltrán-Triviño A., Winkler W., von Quadt A.: Orogenic development of the Northeastern Andes (Colombia) as revealed by detrital zircons -preliminary results
- 1.5 Beltrán-Triviño A., Winkler W., von Quadt A.: Geodynamics of the Alpine Tethys as traced by detrital zircons (in-situ U/Pb dating and high resolution provenance analysis) - a project layout
- 1.6 Bruijn R.H.C., Mainprice D., Burlini L.: High temperature compaction of hot-pressed Rochester shale powder
- 1.7 Bussien D., Gombojav N., Winkler W., von Quadt A.: Preliminary geodynamic reconstruction of the Late Paleozoic-Jurassic Mongol-Okhotsk Belt in NE Mongolia
- 1.8 Cardello G.L. & Mancktelow N.: Neogene oblique normal faults and veins in the Rawil Depression (SW Switzerland)
- 1.9 Cavargna-Sani M., Epard J.-L., Masson H.: Discovery of fossils in the Adula nappe, new stratigraphic data and tectonic consequences (Central Alps)
- 1.10 Crameri F., Tackley P., Meilick I., Gerya T., Kaus B., Keller T.: One-sided subduction in self-consistent models of global mantle convection: the importance of a free surface and a weak crustal layer
- 1.11 Duretz T., Kaus B.J.P., Schulmann K., Gapais D.: Lower crust extrusion triggered by indentation: Insight from analogue and numerical modelling
- 1.12 Dymkova D., Gerya T., Podladchikov Y.: 2D Numerical modelling of a porous flow in a deforming viscoplastic matrix with finite differences and marker-in-cell techniques
- 1.13 Egli D., Mancktelow N.: Neogene tectonics of the Mont Blanc area
- 1.14 Frehner M., Exner U., Mancktelow N., Grujic D.: The not-so-simple effects of boundary conditions on models of simple shear
- 1.15 Galster F., Epard J.-L., Masson H.: The Soja and Luzzzone nappes : discovery of a Briançonnais element below the front of the Adula (NE Ticino, Central Alps)
- 1.16 Gonzalez L., Pfiffner O.A.: Morphologic evolution of the Central Andes of Peru
- 1.17 Haertel M., Herwegh M., Pettke T.: Ti in quartz geothermometry in mylonites of the Simplon fault zone. What can we learn?
- 1.18 Ibele T., Matzenauer E., Mosar J.: Northern Alpine foreland deformation in western Switzerland: New insights from field and seismic data of the Plateau Molasse
- 1.19 Kaus B.J.P., Yamato P., Mouthereau F., Castellort S.: Dynamic constraints on crustal-scale rheology from the Zagros Mountains
- 1.20 Keller T., Boris J. P. B.: Numerical modeling of two-phase flow: Interaction of magmatism with active tectonics
- 1.21 Kounov A., Schmid S.M.: Fission-track constraints on the thermotectonic evolution of the Apuseni Mountains (Romania)
- 1.22 Madonna C., Tisato N., Boutareaud S., Burg J.-P.: State of the art of SWAM: Seismic Wave Attenuation Module

- 1.23 Manzotti P., Robyr M., Zucali M., Engi M.: Tectonic amalgamation and reworking of a sedimentary cover within a polydeformed basement in a subduction-collision zone: an example from the Western Italian Alps
- 1.24 Matzenauer E., Mosar J.: Thrusting and faulting in the Préalpes Médiannes
- 1.25 May D.A, Kaus B.J.P.: An optimal, scalable finite element based forward model for gravity computations
- 1.26 Mosar J., Meier B., Sommaruga A., Abednego M., Eichenberger U., Ibele T, Matzenauer E., Sprecher Ch., Vouillamoz N.: The Fribourg Structure and Fribourg Zone: an Active fault system or The Röstli Graben - Geologic evidence!
- 1.27 Norton K.P., Schlunegger F.: Glacially enhanced fluvial erosion and rock uplift in the Swiss Alps
- 1.28 Pleuger J., Mancktelow N.: The Canavese Fault west of Valle d'Ossola
- 1.29 Précigout J., Hirth G. and Kunze K.: B-type Olivine LPO in the Ronda Peridotite (Spain): Evidence of high-Strength sub-Continental Mantle
- 1.30 Reverman R.L., Fellin M.G., Willett S.D.: Low-temperature thermochronological constraints on the Miocene exhumation of the Adamello Complex, Southern Alps, Italy
- 1.31 Rolf T., Tackley P.: Influence of continents in mantle convection models with self-consistent plate tectonics
- 1.32 Ruh J.B., Kaus B.J.P., Burg J.-P.: Accretionary wedge dynamics: A numerical approach
- 1.33 Ruiz G., Negro F., Babault J., Frizon de Lamotte D., Stuart F., Stockli D., Foeken J., Sebti S., Saddiqi O., Di Nicola L., Thomsen T.: Tectono-thermal evolution of the Atlas system (SW Morocco), insights from low-temperature thermochronology and Raman spectroscopy on carbonaceous material
- 1.34 Scheiber T., Pfiffner O.A., Schreurs G.: Strain accumulation during basal accretion – case study Suretta nappe (eastern Switzerland)
- 1.35 Schenker F. L., Fellin M. G., Burg J.-P.: Structural and cooling history of the Eastern Pelagonian metamorphic core complex (northern Greece)
- 1.36 Schreurs G., Buiter S. and the GeoMod2008 Analogue Team: Quantitative comparisons of analogue thrust wedge experiments
- 1.37 Sommaruga A., Eichenberger U., Marillier F.: Seismic Atlas of the Swiss Molasse Basin : two example transects across the western and the eastern parts
- 1.38 Tackley P., Nakagawa T., Armann M., Keller T., van Heck H.: Modelling the thermo-chemical evolution of the interiors of Earth, Venus, Mars, Mercury and super- Earths
- 1.39 Thielmann M., Kaus B.J.P.: Shear heating and subduction initiation
- 1.40 Thust A., Heilbronner R., Stünitz H.: Dislocation glide in experimentally deformed natural quartz single crystals
- 1.41 Tisato N., Madonna C., Boutareaud S., Burg J.-P.: A new instrumentation to measure seismic waves attenuation
- 1.42 Tumarkina E., Misra S., Connolly A.D.J.: The effect of deformation on partial melting of metapelitic rock: an experimental study
- 1.43 van Heck H.J., Tackley P.J.: Mantle Convection, Stagnant Lids and Plate Tectonics on Super-Earths.
- 1.44 Vogt K., Gerya T., Castro A.: Dynamics of crustal growth at active continental margins: numerical modeling
- 1.45 von Niederhäusern B., Manzotti P., Engi M., Rubatto D., Zucali M., Darling J.: Evidence of Permian HT metamorphism in Austroalpine units of the Internal Western Alps?
- 1.46 Wrobel-Daveau J.C., Ruiz G.H.H., Stuart F.M., Ringenbach J.C., Frizon de Lamotte D.: Structural evolution of the Zagros Fold-Thrust-Belt: Insights from the U-Th/He Thermochronometry (Ap. and Zr.)

1.1

Spontaneous initiation of subduction at passive margins – 3D modelling

Armann Marina & Gerya Taras

Institut, für Geophysik, ETH Zürich, Sonneggstrasse 5, 8092 Zürich (marina.armann@erdw.ethz.ch, taras.gerya@erdw.ethz.ch)

The initiation of subduction is a poorly understood process, though subduction is the key process for plate tectonics on Earth. Oceanic lithosphere becomes denser than the underlying asthenosphere within 10 - 50 Ma after it forms at a mid-ocean ridge due to the cooling from the surface. However, despite the favorable gravitational instability and ridge-push, the bending and shear resistance of the lithosphere prevent subduction from arising spontaneously. Subduction initiation at passive margins has been recently investigated numerically in 2D (Nikolaeva et al., 2010), with (i) positive buoyancy and (ii) thinning (e.g. rifting) of the continental lithosphere been the main factors controlling this process. Nevertheless three-dimensional (3D) geometry and dynamics of this process as well as influences from curvature of a passive margin remain enigmatic.

We carried out 3D numerical experiments using the code I3ELVIS to model the spontaneous onset of retreating subduction at a passive margin. We varied model parameters as the thickness of the continental lithosphere, the curvature of the passive margin and the rheological properties of the mantle and the crust.

Similarly to 2D cases (Nikolaeva et al., 2010) three main regimes of passive margin evolution are identified: stable margin, overthrusting and proper subduction. Our models demonstrate that subduction initiation is strongly affected by fluid release from the oceanic lithosphere that begins to subduct. This process is associated with an intense development of partially molten hydrated thermal chemical plumes under the extending continental plate which should result in the strong magmatic pulse related to the beginning of subduction. Our results also suggest that 3D effects arising from margin curvature can be very important for slab geometry and dynamics of subduction initiation.

REFERENCES

Nikolaeva, K., Gerya, T.V. and Marques, F.O. (2010), Subduction initiation at passive margins: numerical modeling, *Journal of Geophysical Research*, Vol 115, B03406, doi:10.1029/2009JB006549

1.2

Late Eocene-Oligocene tectonic events in the Anarak area, Central Iran

Bagheri Sasan¹, Nabavi Mehdi¹, Salari Tayebbeh¹ & Buchs David²

¹Department of Geology, University of Sistan and Baluchestan, Zahedan, 981674-5785, Iran

²Research School of Earth Sciences, Australian National University (sasan_bagheri@yahoo.com)

The Anarak-Jandaq Terrane comprises a Variscan-Eocimmerian metamorphic basement and a Cretaceous-Cenozoic sedimentary cover exposed along the Paleo-Tethys suture in the NW margin of the Central-East Iranian micro-continent (Bagheri & Stampfli 2008) (figure 1). Although tectono-stratigraphy of the Anarak area is thought to record pre-Triassic subduction processes along the Paleo-Tethys Ocean, closure of this ocean in the Triassic, and Neo-Tethyan back-arc rifting in the Late Cretaceous (Bagheri & Stampfli 2008), our knowledge of the tectonic development of the area is still limited. We have studied structural patterns based on field observations and satellite images. Our results provide a new insight into tectonic development of the Central-East Iranian micro-continent during the Cenozoic and show the Anarak area has experienced at least two deformation events between the Late Eocene-Oligocene and Miocene-Pliocene.

Lithostratigraphic units recognized on geological maps and satellite images in the studied area allow to identify a "mushroom-shaped" structural pattern similar to Type 2 fold interference of Thiessen and Means (1980) (figure 1). This pattern has a symmetry plane oriented NW-SE on a map view. A Miocene-Pliocene deformation phase is characterized by NW-trending open folds observed at some kilometers-scale. Restoration of these folds allowed to recognize an older, Late Eocene-Oligocene deformation phase outlined by SE-vergent, NE-trending closed folds and associated far-displaced nappe thrusts. Newly-recognized deformation events could be related to Neo-Tethyan back-arc closure at the present position of the NE-striking Doruneh Fault and its Late Cretaceous mélange (figure 1). Our results suggest the most prominent struc-

tural patterns of the Anarak area essentially reflect the youngest events of a long tectonic history that remains to be characterized in detail.

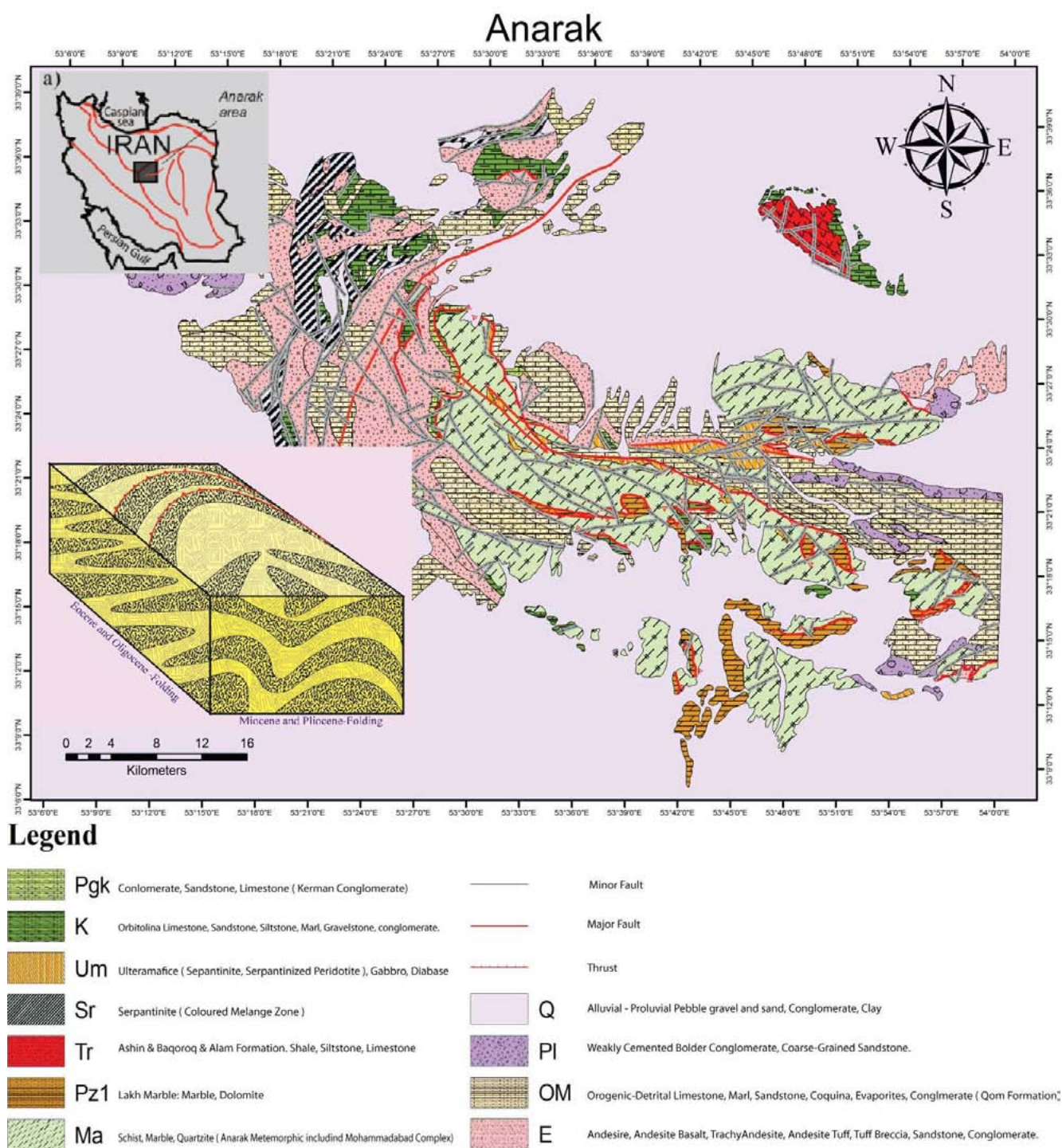


Figure 1

REFERENCES:

- Bagheri, S., & Stampfli, G. M. 2008: The Anarak, Jandaq and Posht-e-Badam metamorphic complexes in central Iran: New geological data, relationships and tectonic implications, *Tectonophysics* 451:123–155.
- Thiessen, R. L., & Means, W. D., 1980, Classification of fold interference patterns: a reexamination. *Journal of Structural Geology*, 2, 311-316.

1.3

Physical controls of intra-oceanic arc extension and trench migration: numerical modelling

Bettina Baitsch Ghirardello, Taras Gerya

Institute of Geophysics, Department of Earth Science ETH Zurich, Switzerland

Modern intra-oceanic subduction zones often develop series of magmatic chains and basins (Stern et al., 2002), (Takahashi, 2008/09), (Larter 2003) and it is not yet fully understood how and why these structures develop. We performed systematic numerical experiments with a 2D coupled petrological-thermo-mechanical numerical model of an intra-oceanic subduction process. Our model includes different slab push velocities, different weakening effects (dehydration of the subducted crust, aqueous fluid transport, partial melting of both crustal and mantle rocks and melt extraction processes), different ages of the subduction slab and the overriding plate as well as spontaneous slab bending. With a long-term model of subduction dynamics, we tested the effects of geometry, rheology, composition, dehydration and melting processes and their influences to the development of extension or compression in intra-oceanic arcs. Based on numerical results we established three different types of extension regimes: i) extension in the fore-arc, ii) extension within the magmatic arc, and iii) no extension, but compression. In general, in all our experiments, the first spreading episode mostly occurs in the fore-arc. Such fore-arc spreading can be observed in the very eastern part of the Aleutian arc system, where decompression melt pierces the thin crust and/or pushes the magmatic arc away from the trench and it becomes a paleoarc, similar to the Kyushu-Palau Ridge (Stern et al., 2003). At the same time a new magmatic arc grows between the trench and the spreading centre. Some experiments show an intra-arc-spreading, such as the active Mariana arc and the inactive West Mariana Ridge (split an initially homogeneous arc into two distinct parts), (Stern et al., 2003). We also found four different trench migration patterns depending on the degree of coupling between the plates: i) trench retreating, ii) episodic retreating and advancing with a total retreat of the trench, iii) trench advancing, iv) stable trench position over time. Our numerical results on episodic trench movements match well with natural observations (Clark et al., 2008) concerning the periodicity in the back-arc tectonic regimes.

1.4

Geodynamics of the Alpine Tethys as traced by detrital zircons (in-situ U/Pb dating and high resolution provenance analysis) - a project layout

Beltrán-Triviño Alejandro¹, Winkler Wilfried¹, and von Quadt Albrecht²

¹ETH Zürich, Geologisches Institut, Sonneggstrasse 5, CH-8092 Zürich (alejandro.beltran@erdw.ethz.ch) (wilfried.winkler@erdw.ethz.ch)

²ETH Zürich, Institut f. Geochemie und Petrologie, Clausiusstrasse 25, CH-8092 Zürich (albrecht.vonquadt@erdw.ethz.ch)

The Triassic-Tertiary Alpine orogenic cycle is recorded in a variety of sandstone-bearing formations. The detrital composition of the sandstone deposits: (i) preserves the record of the source rocks, exposed on the Earth's surface at particular geological times, and (ii) allows to corroborate large scale tectonic movements which trigger processes like uplift, exhumation and erosion.

In the Alpine range, these deposits include the initial rift and the subsequent continental drift related sediments, then, they are followed by sedimentary units related to continental convergence with lithosphere subduction and as well with the final continent-continent collision stage.

Although in the past, facies and standard provenance analyses (heavy minerals and modal composition of sandstones) have allowed to propose quite comprehensive tectono-sedimentary models, several paleogeographic and tectonics problems still are ambiguous because the complexity of the nappe-tectonics has veiled the original source - basin relationships. Furthermore, the standard provenance analyses have reached their limits of resolution and hardly can provide more details in order to refine paleogeographic models of the Alpine Tethys.

The present research project started at the beginning of year 2010. It is aimed at re-evaluating the geodynamics of the Alpine Tethys by the systematic analysis of detrital zircons in various extension and compression related sandstone units in the Central and Eastern Alps. A widespread sandstone sampling across various paleogeographic domains has been done

(Fig. 1). New concepts and analytical methods are applied in this research to complete the standard provenance analyses: (1) U/Pb laser ablation ICP-MS dating of detrital zircons (e.g. Martin-Gombojav and Winkler 2008). This method provides the magmatic and metamorphic crystallization age of the detrital zircons. Concordia diagrams are used to eliminate the odd age points, age range histograms and probability density curves define statistically valid age populations. (2) Trace element contents of the dated zircon (essentially using P, Y, Th, U, Nb, Ta, REE and Hf concentrations) are analyzed in order to determine the igneous rock type, in which grains had crystallized, following the Belousova et al. (2002) method. (3) Hafnium $^{176}\text{Hf}/^{177}\text{Hf}$ isotope analysis (e.g. Hawkesworth and Kemp 2006). These isotopes can be related to the crustal residence age (model age) or to the average time elapsed since the source of the magmas, from which the zircons crystallized, were extracted from a mantle reservoir. The $^{176}\text{Hf}/^{177}\text{Hf}$ ratio fingerprint the nature of the magmatic source rocks with respect to their derivation from depleted mantle (which indicates that the zircon were formed during the process of new crust formation) or recycled continental crust. Conveniently, as the different measurements can be performed on the same grain, the straight correlation of geological age and geochemical signatures is provided.

The first results from sandstone formations of different paleogeographic origin in the Alpine Tethys show promising results. Mesozoic and Cenozoic deposits of the Central Alps show a wide detrital zircon age range including also reworked Proterozoic grains. A prominent Late Devonian - Permian (350 - 270 Ma) age population is common in various sandstones, which correlates with the Variscan orogeny and post-Variscan extension.

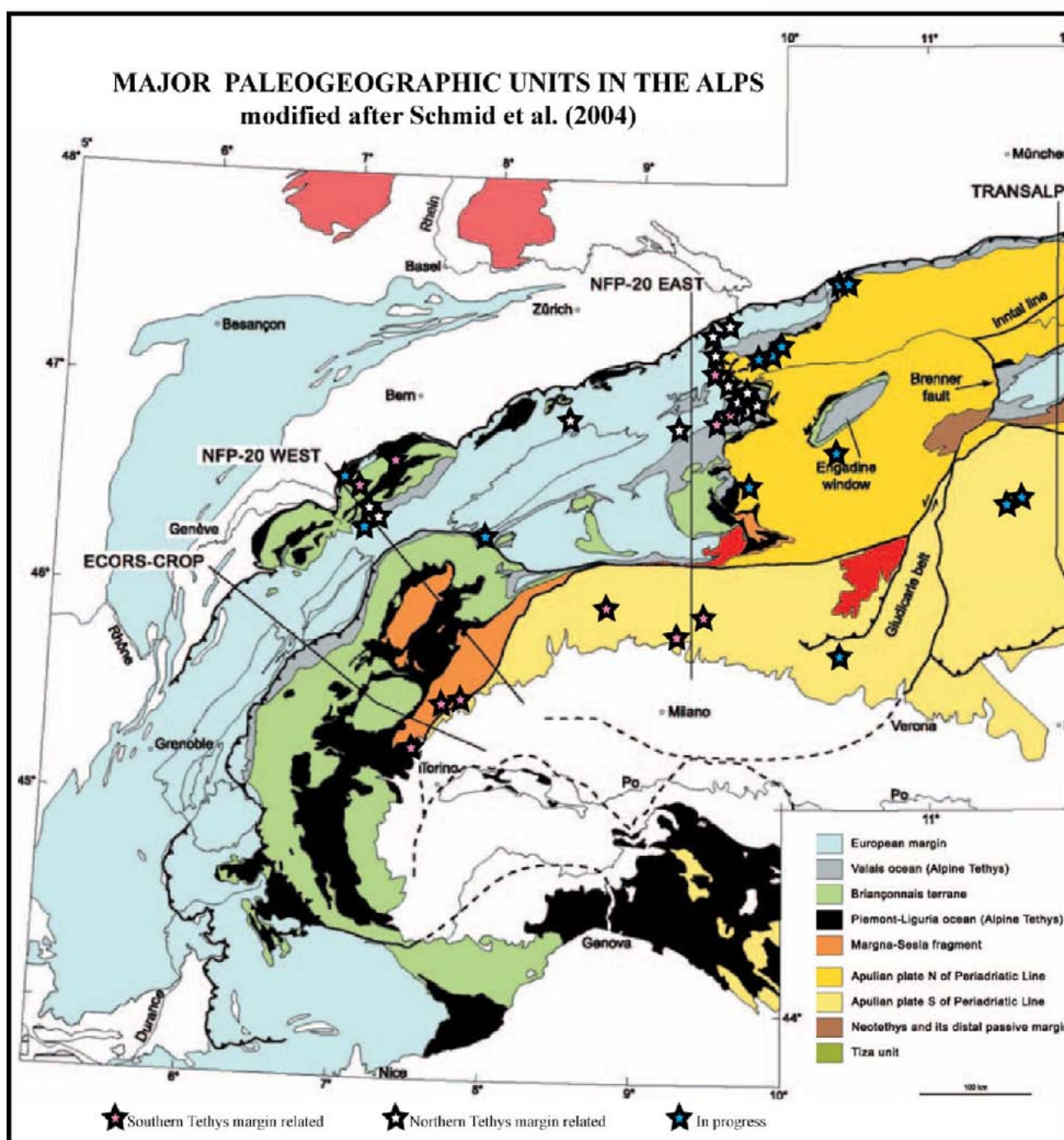


Figure 1. Major paleogeographic units in the Alps showing the location of collected samples for this research

REFERENCES

- Belousova, E.A., Griffin, W.L., O'Reilly, S. Y., Fisher, N.I. 2002. Igneous zircon: trace element composition as an indicator of source rock type. *Contrib. Mineral. Petrol.* 143, 602-622.
- Hawkesworth, C.J., Kamp, A.I.S. 2006. Using hafnium and oxygen isotopes in zircons to unravel the record of crustal evolution. *Chemical Geology* 226, 144-162.
- Martin-Gombojav, N., Winkler, W. 2008. Recycling of Proterozoic crust in the Andean Amazon foreland of Ecuador: implications for orogenic development of the Northern Andes. *Terra Nova* 20, 22-31.
- Schmid, S.M., Fügenschuh B., Kissling, E., Schuster, R. 2004. Tectonic map and overall architecture of the Alpine orogen. *Ecl. Geol. Helv.* 97, 93-117.

1.5

Orogenic development of the Northeastern Andes (Colombia) as revealed by detrital zircons - preliminary results

Beltrán-Triviño Alejandro¹, Winkler Wilfried¹, and von Quadt Albrecht²

¹ETH Zürich, Geologisches Institut, Sonneggstrasse 5, CH-8092 Zürich (alejandro.beltran@erdw.ethz.ch) (wilfried.winkler@erdw.ethz.ch)

²ETH Zürich, Institut f. Geochemie und Petrologie, Clausiusstrasse 25, CH-8092 Zürich (albrecht.vonquadt@erdw.ethz.ch)

The Meso-Cenozoic orogenic history of the Northern Andes is mirrored by a variety of sedimentary deposits, and especially sandstone-bearing formations are of special interest. In the Northeastern Andean range, these deposits include the syn-rift and the subsequent post-rift sequences and the deposits related to the retro-arc foreland basin formation. The detrital composition of the sandstone deposits reveals the source rocks, which were exposed on the Earth's surface at particular geological times. Therefore, the study allows corroborating large-scale tectonic movements, which trigger processes like uplift, exhumation and erosion.

The detailed timing for the initial uplift of the Eastern Cordillera of the Colombian Andes is poorly constrained; estimates range from ca. 60 to 5 Ma. The present research is aimed at evaluating the development of the Eastern Cordillera by the systematic analysis of the detrital composition of the different sandstone deposits (heavy minerals and modal composition), and by U-Pb laser ablation ICP-MS dating of included detrital zircons. The detrital composition analysis reveals the position of the basins within a plate tectonic framework and the U-Pb zircon dating reveals the magmatic and metamorphic crystallization age of the detrital zircons. Concordia diagrams are used to eliminate the odd age points; age range histograms and probability density curves define statistically valid age populations.

The detrital zircon U-Pb ages extracted from the intermontane basin (Sabana de Bogotá) along the axis of the Eastern Cordillera (Fig. 1) reveal a change of age-spectra at the Paleogene-Neogene transition by the new occurrence of Late Cretaceous to Tertiary magmatic/volcanic zircons (ca. 90 - 30 Ma). The observed change in the age populations in the intermontane basin corresponds to a change in the provenance regime from the Amazon Craton to Andean rock sources, which can be attributed to differential uplift and erosion of parts of the Eastern Cordillera. However, this shift is not noted in the Llanos foothill deposits (retro-arc foreland basin) to the east where the supply from Amazon Craton rocks continued to dominate (as also supposed by paleocurrent data, Parra et al. 2010). This suggests that a natural tectonic barrier isolated the Llanos basin from Andean input. However, minor input may also have been provided from uplifted Amazon basement in the Andean range as observed in the Oriente basin fill of Ecuador (Martin-Gombojav and Winkler 2008). Similarly, the important detrital change in the intermontane basin of the Sabana de Bogotá approx. correlates with major restructuring of the detrital source terranes during Late Eocene - Oligocene in the Andean transect of the Ecuadorian Andes (Martin-Gombojav and Winkler 2008).

REFERENCES

- Martin-Gombojav, N., Winkler, W. 2008. Recycling of Proterozoic crust in the Andean Amazon foreland of Ecuador: implications for orogenic development of the Northern Andes. *Terra Nova* 20, 22-31.
- Parra, M., Mora, A., Jaramillo, C., Torres, V., Zeilinger, G., Strecker, M. 2010. Tectonic controls on Cenozoic foreland basin development in the Northeastern Andes, Colombia. *Basin Research*, doi: 10.1111/j.1365-2117.2009.00459.x.

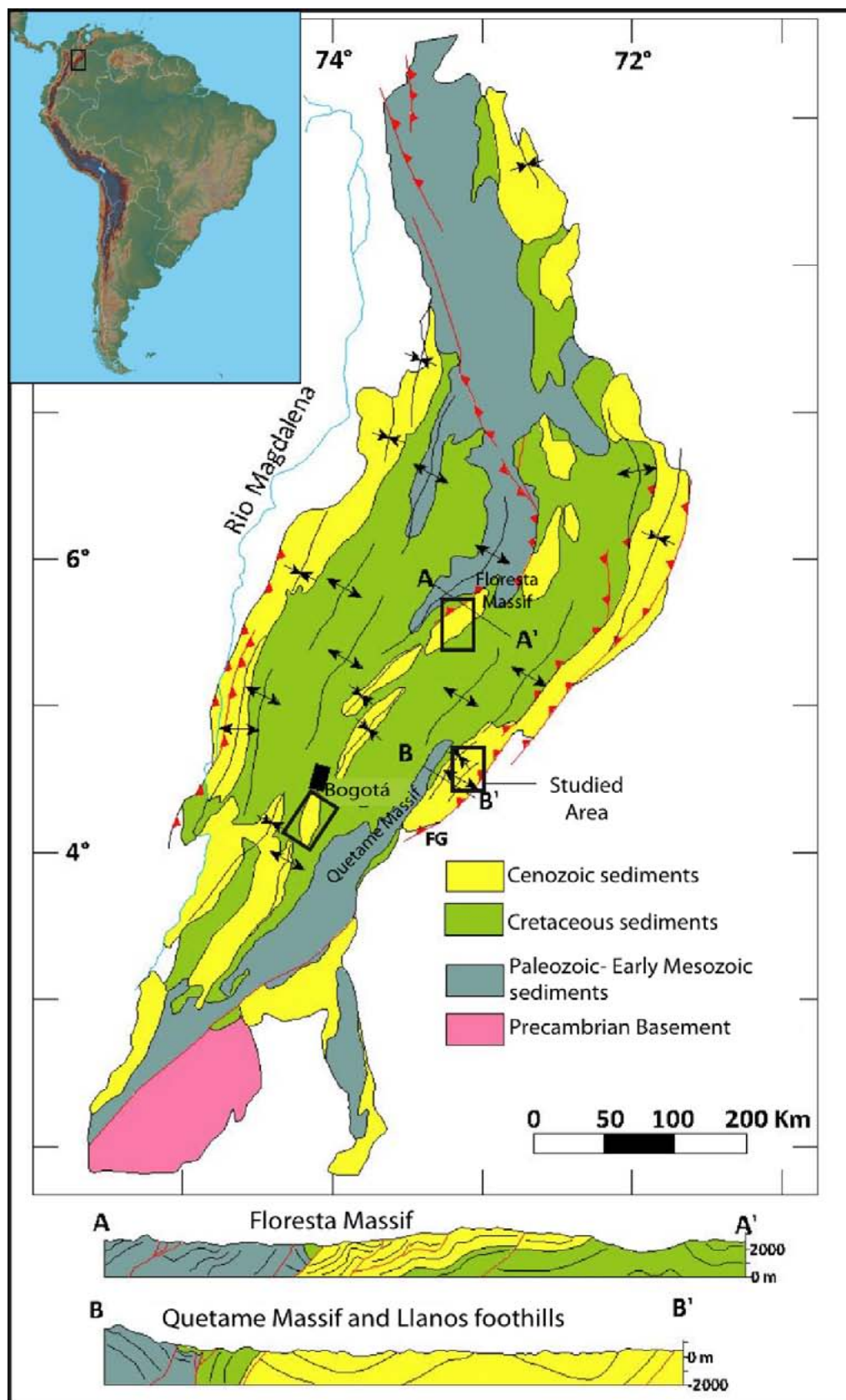


Figure 1: Simplified geological map and cross sections in the Eastern Cordillera of the Colombian Andes. Black squares represent the studied areas.

1.6

High temperature compaction of hot-pressed Rochester shale powder

Rolf Bruijn¹, David Mainprice², & Luigi Burlini

¹ Geological Institute, Sonneggstrasse 5, CH-8092 Zürich (rolf.bruijn@erdw.ethz.ch)

² Géosciences Montpellier, Place Eugène Bataillon, 34095 Montpellier, France

Samples derived from hot-pressed mineral powders are commonly used in experimental rock deformation studies. These synthetic rocks are typically more porous than their natural equivalents. Consequently, deformation is potentially accommodated by pore collapse and bulk compaction, rather than plastic flow. We performed uniaxial compression tests on porous (12.5 ± 1.2 %) hot-pressed natural shale powder to investigate the role of pore collapse and compaction in low strain deformation of phyllosilicate rich material.

Experiments were performed with a gas-medium testing machine under constant temperature (500, 650 and 700 °C), confining pressure (300 MPa) and strain rate (10^{-6} – 10^{-3} s⁻¹) conditions. Due to load cell limits and the hardness of the samples, maximum axial strain reachable in these tests was 13%. Hot-pressed (24 h at 590 °C and 160 MPa) Rochester shale powder from New York State – USA ($d < 125$ µm) was used as sample material. These samples contain 60-70 vol.% illite/mica ($d < 5$ µm) and 20-30 vol.% quartz ($20 < d < 125$ µm). Additional minor phases include biotite, K-feldspar, apatite, rutile and pyrite.

Experiments showed two distinct compaction behaviours: 1) Pure shear with pore collapse as primary porosity reducing mechanism and > 45 % compaction recovery. 2) Sample contraction with pore collapse and cementation as porosity reducing mechanisms and < 30 % compaction recovery. Pure shear compaction is characterized by strain rate insensitive work hardening to differential stress levels > 500 MPa at 8 % axial strain. All 500 and 600 °C, and vented sample 700 °C experiments followed pure shear compaction. Work hardening in contractional compaction tests was strain rate sensitive, with reducing hardening rates with decreasing strain rate. Steady state flow could not be established before 13 % axial strain and differential stress still exceeded 300 MPa. Contractional compaction occurred in 700 °C experiments without venting. Compaction behaviour defines the sample strength evolution with strain. Comparison between 700 °C vented and unvented samples under otherwise identical experimental conditions showed that at 10 % axial strain vented samples were 59 % stronger. Similarly, a comparison between unvented compacting samples at 650 and 700 °C displayed a 66 % higher flow stress for the cooler sample. The transition from pure shear to contractional compaction occurs in the temperature range coinciding with that of the dehydration reaction of illite/mica+quartz to K-feldspar+sillimanite+water, according to Perple-X modelling. Additionally, the wet-solidus was modelled at 710 °C for 300 MPa using Rochester shale compositions. Neither melt nor reaction products were observed in SEM imaging.

1.7

Preliminary geodynamic reconstruction of the Late Paleozoic-Jurassic Mongol-Okhotsk Belt in NE Mongolia

Bussien Denise (¹), Gombojav Nergui (²), Winkler Wilfried (¹), and von Quadt Albrecht (¹)

(¹) Geological Institute, ETHZ, Sonneggstrasse 5, 8092 Zurich, Switzerland (denise.bussien@erdw.ethz.ch)

(²) Pöyry Energy AG, Hardturmstrasse 161, 8037 Zurich, Switzerland

The Mongol-Okhotsk Belt extends from Central Mongolia across eastern Siberia towards the Okhotsk Sea in the northwestern Pacific. The belt was formed in a late stage of Jurassic orogeny in the composite Central Asian Orogenic Belt by the consumption of the Mongol-Okhotsk ocean (MOO) south of the Siberian Craton (Fig. 1). We investigated the Late Paleozoic-Mesozoic sediments associated with the belt in Mongolia in order to evaluate the timing and mode of ocean formation, the subduction and the collision of the framing margins. An advanced provenance analysis is applied, including (1) heavy mineral and sandstone framework grain analysis, and (2) U/Pb LA-ICPMS dating, trace element, and Hf isotope analysis of detrital zircons. The methods are useful for describing the source rock lithologies, and the age and nature of the related plutonic-volcanic input.

Three tectono-stratigraphic units are differentiated in this work: (1) the Adaatsag and Dochgol terranes, which represent the oceanic suture itself, (2) the Hangai-Hentei basin to the northwest of the suture, and (3) the Ereendavaa terrane and

the Middle Gobi volcanic belt to the southeast (Badarch et al. 2002). The latter two are considered as the northern and southern margins of the former MOO (in modern coordinates) respectively. On the northern margin ophiolitic accretionary wedge and fore-arc deposits are recognized. The southern margin is characterised by Devonian-Carboniferous sediments presumably deposited on deformed and metamorphosed Neoproterozoic-Early Paleozoic continental and ophiolitic basement, which initially was accreted against the North Asia Craton (Siberia) by the closure of northern parts of the Paleo-Asian ocean in Ordovician-Silurian (Windley et al. 2007). According to tectono-stratigraphic arguments combined with biostratigraphic and radiometric age data, the MOO is considered to open from Silurian on (Kurihara et al. 2008). Back-arc spreading within the Early Paleozoic collage due to northward subduction of the southern Paleo-Asian ocean under the accreted Mongolian margin was the possible mechanism for the MOO opening.

The Devonian and Permo-Carboniferous syn-sedimentary U/Pb detrital zircon age patterns and Hf isotopic values show similar subduction related magma production processes in the northern and southern margin. However, the two continental margins of the MOO were presumably active at different periods (i.d. later in the southern margin).

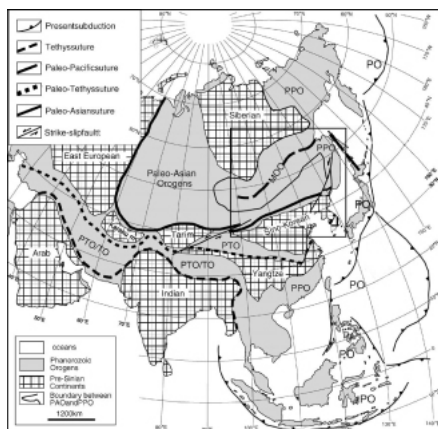


Figure 1. Approximate location and extension of the Mongol-Okhotsk Belt with its suture zone (MOO) in the Central Asian Orogenic Belt (from Li 2008).

Our results indicate that along the northern margin, from Silurian to Early Carboniferous, subduction and accretion prevailed, and was re-initiated during the Permian. Few reworked zircon grains were found in the northern margin, whereas in the contemporaneous southern margin many reworked zircon grains coming from Neoproterozoic-Early Paleozoic basement are recognized. The Silurian-Devonian southern margin depicts an extensional continental margin context that turned into an active continental margin with starting arc magmatism in the Carboniferous. Continued subduction is underlined by the occurrence of Permian and Triassic zircons. In both margins, Triassic and Jurassic continental sediments unconformably overlie tectonically deformed fore-arc series.

In the suture zone in-between, Permo-Triassic and Jurassic samples contain Permian zircon grains, and an irregular mixing with Cambrian to Carboniferous zircons is documented. The pre-Permian zircon age spectra are similar with the southern margin age patterns. Syn-sedimentary magmatic activity is recorded until Late Triassic - Early Liassic, which approximately correlates with the time of closure of the MOO in the Mongolian segment of the mountain belt.

REFERENCES

- Badarch, G., Cunningham, W. D., Windley, B. F., 2002. A new terrane subdivision for Mongolia: implications for the Phanerozoic crustal growth of Central Asia. *Journal of Asian Earth Sciences* 21, 87-110.
- Kurihara, T., Tsukada, K., Otoh, S., and 10 co-authors, 2008. Upper Silurian and Devonian pelagic deep-water radiolarian chert from the Khangai-Khentei belt of Central Mongolia: Evidence for Middle Paleozoic subduction accretion activity in the Central Asian Orogenic Belt. *Journal of Asian Earth Sciences*, 34, 209-225.
- Li, J.-Y., 2006. Permian geodynamic setting of Northeast China and adjacent regions: closure of the Paleo-Asian Ocean and subduction of the Paleo-Pacific Plate. *Journal of Asian Earth Sciences* 26, 207-224.
- Windley, B.F., Alexeiev, D., Xiao, W., Kröner, A., Badarch, G., 2007. Tectonic models for accretion of the Central Asian Orogenic Belt. *Journal of the Geological Society London* 164, 31-47.

1.8

Neogene oblique normal faults and veins in the Rawil Depression (SW Switzerland)

Giovanni Luca Cardello & Neil Mancktelow

Geologisches Institut, ETH-Zürich, CH-8092 Zürich

In the Rawil Depression between the Aar and Mont Blanc massifs, oblique normal faults are very common but, according to published maps and profiles, these faults tend to lose displacement over short distances and do not cross-cut nappe contacts or more incompetent units (e.g. shales and marls). This field study aims to establish:

- (1) the orientation and distribution of these faults
- (2) the fault geometries and kinematics
- (3) the relationship between veining and faulting.

After two field seasons of detailed mapping and fault and vein analysis in the Rawil Depression, we distinguish three post-nappe sets of veins and faults on the basis of their strike orientation: (1) NNW/NW-striking; (2) WNW/W-striking; (3) ENE-striking. Fault set (3) occurs mainly in the Rhône valley, where the fault planes are steep and with a dominant dextral strike-slip component. This set is associated with the Simplon-Rhône Fault, with activity probably throughout much of the Neogene and possibly also into the Quaternary.

Fault sets (1) and (2) generally dip at a low to moderate angle to the SW and typically develop domino-like structures. The major faults in the Rawil area are spaced around 1 km and show similar features, whereas small-scale faulting is much more diffuse. Fault sets (1) and (2) are broadly coeval, as indicated in the Rawil-Plaine Morte area by many examples of branching and bending of one set into the other and by similar displacement directions and deformation fabrics. Nevertheless, there are clear examples (e.g. along the Wildstrubelhütte segment of the Rawil Fault) of set (2) cross-cutting set (1), which establishes, at least locally, a chronological succession of faulting events.

Calcite slickenlines and fibres on fault planes (1) and (2) indicate two main slip directions. The older one is WSW-directed and generally plunges around 25° whereas the younger one plunges S, with a steeper, mainly dip-slip movement. This generally transtensional faulting must largely post-date folding, because faults of sets (1) and (2) obliquely cross-cut the fold system and the fold geometry can be matched to either side.

Folding and the initial stage of normal to oblique faulting developed under very low grade metamorphic conditions, with exhumation during the Neogene related to WSW-extension that was parallel or slightly oblique to the main Alpine fold axis-trend. Locally there is a transition from an initial more ductile mylonitic fabric to cataclasite. Since faults of sets (1) and (2) developed across the ductile-brittle transition in limestones, shales and marls, they may represent fossil seismogenic zones in rocks with high pore-fluid pressure, corresponding to the current depth of active seismic activity at around 8-12 km in the Sion-Sierre region of the Rhône valley.

Veins are very common in the Rawil area and developed throughout the deformation history, ranging from pre- to syn-folding to coeval with later transtensive faulting. A progressive increase in the number and size of veins is observed in the more competent lithologies approaching the main damage zone of oblique faults [sets (1) and (2)], implying increased fluid circulation toward the fault zones. Pressure-solution, often concentrated on stylolites, is also active until very late stages of faulting and veining. Veins in the damage zones in limestones are sheared into the initial mylonitic zones and form a major component, together with the mylonites, in the subsequently developed cataclasites. This progressive embrittlement during faulting may be due to exhumation and cooling during faulting, higher strain rates, or increased pore-fluid pressures.

Clasts of cataclasites within cataclasites establish that there have been repeated cycles of faulting resulting in cataclasis and sealing. Away from the fault damage zones, crosscutting vein relationships and the bending of vein tails indicate a progressive counter-clockwise relative rotation of the stretching direction, from WSW toward S to SSE, which is consistent with the observed change from oblique slip to subsequent dip-slip on faults of sets (1) and (2). Overall, there is an almost 180°, generally (but not exclusively) counter-clockwise change in the stretching direction, from orogen-perpendicular stretching of reclined fold limbs during NW-directed thrusting, to orogen-parallel stretching during the dominant period of veining and oblique, transtensional faulting, to a late period of limited, more orogen-perpendicular extension.

1.9

Discovery of fossils in the Adula nappe, new stratigraphic data and tectonic consequences (Central Alps)

Cavargna-Sani Mattia¹, Epard Jean-Luc¹ & Masson Henri¹

¹ Institut de Géologie et Paléontologie, Anthropole, Université, CH-1015 Lausanne (Mattia.Cavargna@unil.ch)

The Adula nappe is a large tectonic unit of the Central Alps, mainly made of highly metamorphic Paleozoic basement rocks. A Mesozoic (and younger?) cover penetrates deep into it as bands and discontinuous relics of highly metamorphic sediments. We report here the first discovery of fossils in these rocks and other stratigraphic observations at the Plattenberg (pt. 3041, 2 km S of the front of the nappe), taking advantage from the excellent quality of the outcrops.

The stratigraphic succession is the following, from basement upwards:

1. The Garenstock augengneiss forms the top of the basement in this area. It often contains brown carbonate nodules of mm size, particularly frequent in its upper part. It also contains a few amphibolite boudins in the core of which eclogite is locally preserved.
2. The gneiss is overlain with a sharp contact by a thin layer of a white quartzite, similar to the quartzite that commonly forms the base of the Triassic in many parts of the Penninic Alps.
3. This quartzite passes transitionally to a thicker alternation of white and grey-bluish dolomites. They are similar to the Triassic of several Lower Penninic nappes.
4. These dolomites are overlain with a sharp contact by a coarse detrital formation mainly made of dolomitic breccias. The dolomitic pebbles are reworked from the Triassic and they can be so closely packed that the rock looks at first sight like a genuine Triassic dolomite ("reconstituted Triassic"). The matrix is quartzitic to dolarenitic, sometimes containing also mica or calcite. At the base the quartzitic matrix can form a dm-thick layer of pure quartzite (not to be confused with the basal Triassic quartzite). Going upwards the matrix of the breccia becomes dominant and the rock gradually passes to a dolo-quartz-arenite. Near the top it may contain a few cm- to dm-thick layers of pure limestone. All these rocks form a well-characterized lithostratigraphic unit that we call the Plattenberg Formation, or Plattenberg Breccia. Discontinuous intercalations or pockets of a reddish rock rich in iron oxides and white mica occur in and at the base of the breccia. We interpret this rock as a (more or less reworked) siderolitic deposit. It gives evidence of post-Triassic emersion and continental erosion before the deposition of the breccia. Three m above the base of the breccia we found in a fine-grained calco-dolarenitic intercalation numerous plates of crinoids (with well preserved details such as the central canal). They prove that the deposition of the breccia occurred in marine (high-energy) conditions.
5. Plattenberg Breccia is overlain by a formation of metapelites passing gradually upwards to a calcschist. The metapelites contain abundant garnet and smaller amounts of kyanite, chloritoid and graphite. The amount of calcite increases upwards. At their base these metapelites also contain brownish calcareous nodules. The calcschist contains scattered pebbles of pure limestone. It forms the core of a syncline and consequently it is the youngest stratigraphic unit in this area. Cornieule (rauhwacke) is present. It is deformed and can occupy various positions in the stratigraphic column. It forms a conspicuous m-thick "layer" all along the contact of the metapelites upon the breccia in both limbs of the syncline.

Conclusions:

- A. The Adula nappe has its proper sedimentary cover (autochthonous with respect to the basement), comprised of several well-characterized stratigraphic formations.
- B. Its Triassic has no affinity with the Briançonnais Triassic. This is important for nappe tectonics, with respect to the recent discovery of a Briançonnais Triassic element below the front of the Adula (in the Luzzzone nappe, see Galster et al., this session). Consequently the Luzzzone nappe must have an ultra-Adula origin: it comes from S of the Adula and passed over it before being eventually overtaken by its front.
- C. The Plattenberg Breccia is erosive and transgressive. Its basal contact upon the Triassic must represent a large stratigraphic gap, underlined by reworked continental deposits. Comparisons with similar situations in other parts of the Alps suggest a late Early to Middle Jurassic age in a context of extensional tectonics related to the opening of the Alpine Tethys.
- D. The occurrence of relatively well preserved fossils (crinoids) in such highly metamorphic rocks is remarkable.
- E. The interpretation of the upper metapelite-calcschist unit is more uncertain, because of the intercalation of a continuous level of cornieule along its base. A large gap is possible, and even a tectonic contact can not be excluded.
- F. These results open the door to a geological study of the Adula (and similar highly metamorphic nappes) based on detailed stratigraphic analysis.

1.10

One-sided subduction in self-consistent models of global mantle convection: the importance of a free surface and a weak crustal layer

Crameri Fabio, Tackley Paul, Meilick Irena, Gerya Taras, Kaus Boris & Keller Tobias

Institut für Geophysik, ETH Zürich, Switzerland (fabio.crameri@erdw.ethz.ch)

Previous dynamical models of global mantle convection indicated that a visco-plastic rheology is successful in generating plate tectonics-like behaviour self-consistently (Moresi et al., 1998; van Heck and Tackley, 2008). Yet, these models fail to create Earth-like plate tectonics: so far in all published models subduction is two-sided and more or less symmetric, whereas terrestrial subduction is one-sided and characterized by a distinctive asymmetry.

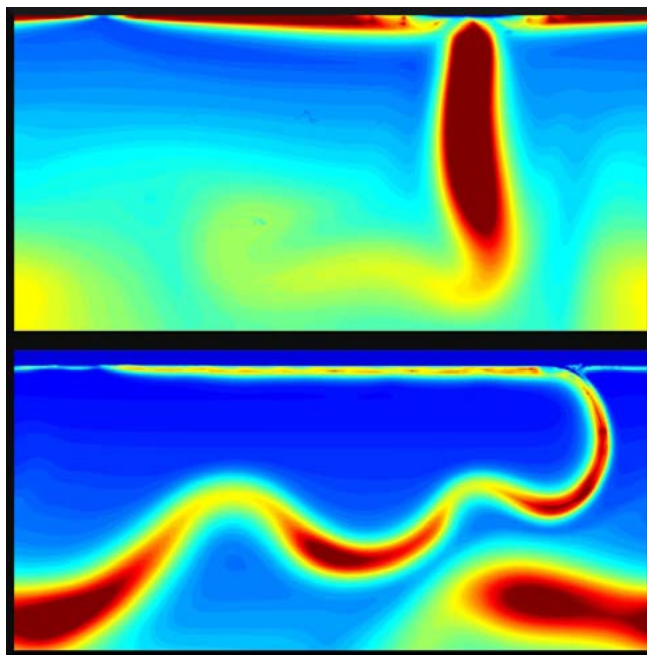


Figure 1. Viscosity fields for convection with a strongly temperature- and pressure dependent visco-plastic rheology and (top) a free-slip surface or (bottom) a free surface.

One simplification used in previous models is that of a free-slip upper boundary, in which the shear stress is zero but the vertical position of the boundary is fixed. In contrast, subduction zones display some of the largest variations in surface topography on Earth. For the case of a slab that is initially placed at the surface and allowed to freely subduct, Schmeling et al. (2008) showed that it is necessary to include a proper free surface in numerical models in order to reproduce laboratory results. According to their benchmark study, mimicking a free surface by a low viscosity, zero density layer on top of the crust is an adequate approach. For this reason, we have implemented such a “sticky air layer” in our global numerical model.

We here study the effect of a free surface on the mode of subduction in 2-D and 3-D global, fully dynamic mantle convection models with self-consistent plate tectonics. For this we use the finite volume multigrid code StagYY (Tackley, 2008) with strongly temperature- and pressure dependent viscosity, ductile and/or brittle plastic yielding, and non-diffusive tracers tracking compositional variations (the ‘air’ layer in this case).

We observe that indeed, a free surface leads to single-sided subduction, whereas identical models with a free slip upper boundary develop double-sided subduction (Figure 1). A free surface is thus an essential ingredient to obtain realistic subduction behaviour in numerical models, probably because it allows the slab to bend in a natural manner.

Although previous models appear one-sided from the temperature or viscosity fields, there is strong mechanical coupling between the slab and the mantle wedge that makes them mechanically double-sided. Regional models of subduction (Gerya et al, 2008) indicate that one requirement for stable one-sided subduction is a low strength interface between the plates achieved by the presence of metamorphic fluids in the subduction channel. Such a lubrication layer consisting of

weak hydrated sediments is implemented in the above model. It accommodates stable one-sided subduction by strain localization, while the absence of a weak shear zone leads to repeating occurrence of mechanically two-sided subduction since in this case the plastic strength of the entire plates needs to be sufficiently low to allow for subduction.

In conclusion, a free surface is the key ingredient to obtain thermally one-sided subduction, while additionally including a weak crust is essential to obtain subduction that is both mechanically and thermally one-sided.

REFERENCES

- Moresi, L., & Solomatov V. 1998: Mantle convection with a brittle lithosphere - Thoughts on the global tectonic styles of the Earth and Venus. *Geophys. J. Int.* 133, 669-682.
- van Heck, H. & Tackley P. J. 2008: Planforms of self-consistently generated plate tectonics in 3-D spherical geometry. *Geophys. Res. Lett.* 35, doi:10.1029/2008GL035190.
- Schmeling, H., Babeyko A., Enns A., Faccenna C., Funiciello F., Gerya T., Golabek G., Grigull S., Kaus B. J. P., Morra G., Schmalholz S. & van Hunen J. 2008: A benchmark comparison of spontaneous subduction models – towards a free surface: *Phys. Earth Planet. Int.* 171, 198-223.
- Tackley, P. J. 2008: Modelling compressible mantle convection with large viscosity contrasts in a three-dimensional spherical shell using the yin-yang grid. *Phys. Earth Planet. Int.*, doi:10.1016/j.pepi.2008.08.005.
- Gerya, T. V., Connolly J. A. D. & Yuen, D. A. 2008: Why is terrestrial subduction one-sided? *Geology* 36, 43-46.

1.11

Lower crust extrusion triggered by indentation: Insight from analogue and numerical modelling

Thibault Duretz¹, Boris J.P. Kaus¹, Karel Schulmann² & Denis Gapais³

¹ Department of Earth Sciences, Swiss Federal Institute of Technology (ETH Zurich) CH-8092 Zurich, Switzerland (thibault.duretz@erdw.ethz.ch)

² UDS Institut de Physique du Globe, UMR EOST 7516, 1 Rue Blessig, F-67084 Strasbourg, France

³ Université de Rennes 1, UMR 6118, CNRS, 263 Avenue du General Leclerc, F-35042 Rennes, France

Recent petrological, structural and geochronological studies of the eastern margin of the Bohemian Massif (Czech Republic) suggest a conceptual geodynamical model to explain exhumation of lower-crustal (20 kbar, 800 °C) felsic rocks. The model involves indentation of a weak orogenic lower crust by an adjacent rigid mantle lithosphere, resulting in crustal scale buckling of the weak orogenic lower/middle crust interface followed by extrusion of a ductile nappe over the rigid promontory.

The hypothesis has been checked using both analogue and numerical models. Analogue experiments using a three layer sand-silicone setup were carried out in Rennes laboratory (France). Results show that the most important features of the conceptual model can be reproduced: extrusion of lowermost silicone over the indenter and flow of horizontal viscous channel underneath a rigid lid above the actively progressing promontory. Furthermore, experimental results show that a plateau develops above the channeling lower crust.

Two sets of sandbox scale numerical simulations were performed. The first set of experiments is designed to study the influence of viscosity stratification within the crust on the extrusion process. A second set of experiments were performed in order to quantify the influence of the viscosity and the geometry of the indenter. Non-dimensional scaling laws were derived to predict the maximum extrusion rates associated with the indentation mechanism. Such laws enable to compute vertical extrusion rates that are in good agreement with natural exhumation rates

1.12

2D Numerical modelling of a porous flow in a deforming viscoplastic matrix with finite differences and marker-in-cell techniques

Dymkova Diana¹, Gerya Taras¹, Podladchikov Yury²

¹ *Institut für Geophysik, ETH Zürich, Sonneggstrasse 5, CH-8092 Zurich (diana.dymkova@erdw.ethz.ch)*

² *University of Oslo, PGP, Oslo, Norway*

Numerical modelling of a porous flow has a wide range of applications in geosciences and industrial engineering. For example, numerical modelling of subduction-related magmatic arcs includes the process of generated magma migration to the region above the subducting slab through the porous medium. This kind of fluid transport is a coupled chemical, thermal and mechanical process.

We created a two-dimensional model of a two-phase flow in a porous media solving a coupled Darcy-Stokes system of equations for two incompressible media for the case of visco-plastic rheology of solid matrix. We use a finite-difference method with fully staggered grid in a combination with marker-in-cell technique for advection of fluid and solid phase. We performed a comparison with a simple benchmark of a thermal convection in a closed bottom-heated box to verify the interdependency of Rayleigh and Nusselt numbers with theoretical ones.

In the future we plan to include elasticity of a solid phase, fluid/solid compressibility and melting in our numerical model as a function of pressure, temperature, water content and composition.

Ultimate goal is to simulate in a realistic self-consistent manner fluid and melt generation and transport in subduction zones including fluid/melt focussing phenomena.

1.13

Neogene tectonics of the Mont Blanc area

Egli Daniel¹ & Neil Mancktelow¹

¹ *Geologisches Institut, ETH-Zürich, Sonneggstrasse 5, CH-8092 Zürich (daniel.egli@erdw.ethz.ch)*

The Mont Blanc massif forms part of the chain of External Crystalline Massifs, has the highest topography in Europe (up to 4'810 m) and has had a young exhumation history, with apatite fission-track ages ranging down to 1.4 Ma (Seward & Mancktelow 1994). There is now a quite extensive low-temperature thermochronology data set that can be used to estimate exhumation rates in the Mont Blanc region during Neogene times (e.g. Seward & Mancktelow 1994; Leloup et al. 2005; Glotzbach et al. 2008). Glotzbach et al. (2008) propose an episodic exhumation with rates changing from relatively fast (~2.5 km/Ma before 6 Ma) to a slow phase (<0.5 km/Ma between 6 and 3.5 Ma), in turn followed by acceleration to ~1 km/Ma after 3 Ma. Various models have been proposed to explain this young exhumation but detailed structural studies to critically assess and constrain the proposed kinematic models are largely lacking.

The tectonic framework of the Mont Blanc area is dominated by three major structures. On the western side, the massif is bordered by the Chamonix zone, which is dominated by north-westward thrusting of the Mont Blanc massif over its sedimentary cover. Leloup et al. (2005) dated this thrusting to be active around 16 Ma. Dextral movements along the Chamonix zone were described by Gourlay & Ricou (1983) and this zone has been proposed to be the direct southward continuation of the dextral transpressive Rhône-Simplon fault zone.

On the eastern side of the massif, the most prominent structure is the Frontal Pennine Thrust, which several authors have suggested might have been reactivated with a normal movement sense in the Late Neogene, contributing to exhumation of the Mont Blanc massif (e.g. Seward & Mancktelow 1994).

The third important structure is a major back-thrust proposed by previous authors ("Mont Blanc back-thrust", e.g. Leloup et al. 2005, Rolland et al. 2007). This has been described as a relatively steeply north-west dipping thrust bringing the Mont Blanc basement back over the tectono-stratigraphically higher Helvetic and Ultrahelvetic metasediments. The current

study presents new structural data from all around the Mont Blanc massif and the adjacent sediments. It focuses on the three main tectonic structures and addresses the tectonic evolution and late stage exhumation history of the massif. We can show that normal reactivation of the Pennine Frontal Thrust is either very small or non-existent and we therefore consider that reactivation along this fault does not play an important role in the exhumation of the Mont Blanc massif. Leloup et al. (2005) describe the Mont Blanc back-thrust as being reactivated at around 2.5 Ma and to be responsible for the latest pulse of exhumation of the Mont Blanc massif. However, this back-thrust is actually slightly folded, with a younger weak axial plane cleavage cross-cutting the thrust, and therefore is unlikely to be responsible for the very young exhumation of the Mont Blanc massif.

Strike-slip movements with nearly horizontal lineations, slickenfibres, or striae can be observed throughout the whole field area. For both ductile and brittle structures, the main direction is oriented NE-SW with a right-lateral sense of shear. Paleo-stress reconstructions from the eastern side of the massif indicate a local NE-SW compression. For such a compression direction, the Mont Blanc massif would lie in the position of a restraining bend within the Rhône-Simplon fault system, possibly resulting in a positive flower structure that would exhume the massif. However, since no young structures directly related to exhumation have been found, we expect this situation to have been active earlier in the exhumation history (Miocene?) and not to be related to the final uplift. We therefore suggest that the most recent uplift of the Mont Blanc relative to its surroundings is more widely distributed and not restricted to discrete structures bounding the massif itself.

REFERENCES

- Glotzbach, C., Reinecker J., Danisik, M., Rahn, M., Frisch, W. & Spiegel, C., 2008: Neogene exhumation history of the Mont Blanc massif, western Alps, *Tectonics*, 27.
- Gourlay, P., & Ricou, L.-E., 1983: Le jeu décrochant dextre tardif de la suture de Chamonix (Alpes françaises suisses): *Comptes Rendus de l'Académie des sciences Paris*, v. 296, p. 927-932.
- Leloup, P. H., Arnaud, N., Sobel, E. R. & Lacassin, R., 2005: Alpine thermal and structural evolution of the highest external crystalline massif: The Mont Blanc, *Tectonics*, 24.
- Rolland, Y., Corsini M., Rossi, M., Cox, S. F., Pennacchioni, G., Mancktelow, N. & Boullier, A. M., 2007: Comment on «Alpine thermal and structural evolution of the highest external crystalline massif: The Mont Blanc» by P. H. Leloup, N. Arnaud, E. R. Sobel, & R. Lacassin.» *Tectonics*, 26(2).
- Seward, D. & Mancktelow N. S., 1994: Neogene kinematics of the central and western Alps: Evidence from fission-track dating, *Geology*, 22, 803-806.

1.14

The not-so-simple effects of boundary conditions on models of simple shear

Frehner Marcel¹, Exner Ulrike¹, Mancktelow Neil² & Grujic Djordje³

¹ Department for Geodynamics and Sedimentology, University of Vienna, Althanstrasse 14, A-1090 Vienna (marcel.frehner@univie.ac.at)

² Geological Institute, ETH Zurich, Sonneggstrasse 5, CH-8092 Zurich

³ Department of Earth Sciences, Dalhousie University, Edzell Castle Circle, Halifax NS, B3H 4J1, Canada

Analogue modeling of geological structures, such as the behavior of inclusions in a matrix or folding instabilities commonly employs a linear simple shear or general shear rig. In theory, a homogeneous plane strain flow is prescribed at the boundaries of such deformation rigs, but, in practice, the resulting internal deformation of the analogue material (commonly paraffin wax or silicone putties) often strongly deviates from the intended homogeneous strain field. This can easily lead to misinterpretation of such analogue experiments.

We present a numerical finite element approach to quantify the influence of imperfect simple shear boundary conditions on the internal deformation of a homogeneous viscous analogue material. The results (Figure 1) demonstrate that imperfect circumferential boundary conditions in the simple shear plane (x-y-plane) lead to the heterogeneous strain observed in some analogue experiments (Price and Torok, 1989; Sengupta and Koyi, 2001), depending on their design.

However, in other experiments, the analogue material lies on top of a weak lubricating material (e.g. Vaseline) or is sandwiched between two such materials (Ildefonse and Mancktelow, 1993; Grujic and Mancktelow, 1995). These layers lead to a viscous drag force acting on the surface of the analogue material that represents imperfect simple shear boundary conditions in the third dimension (z-direction). For this experimental configuration, the numerical results (Figure 2) show that the lubricating layers are responsible for the heterogeneous strain observed in analogue models.

The resulting errors in internal strain can be as high as 100% and these important boundary effects, which are difficult to avoid, must be considered when interpreting analogue simple shear experiments.

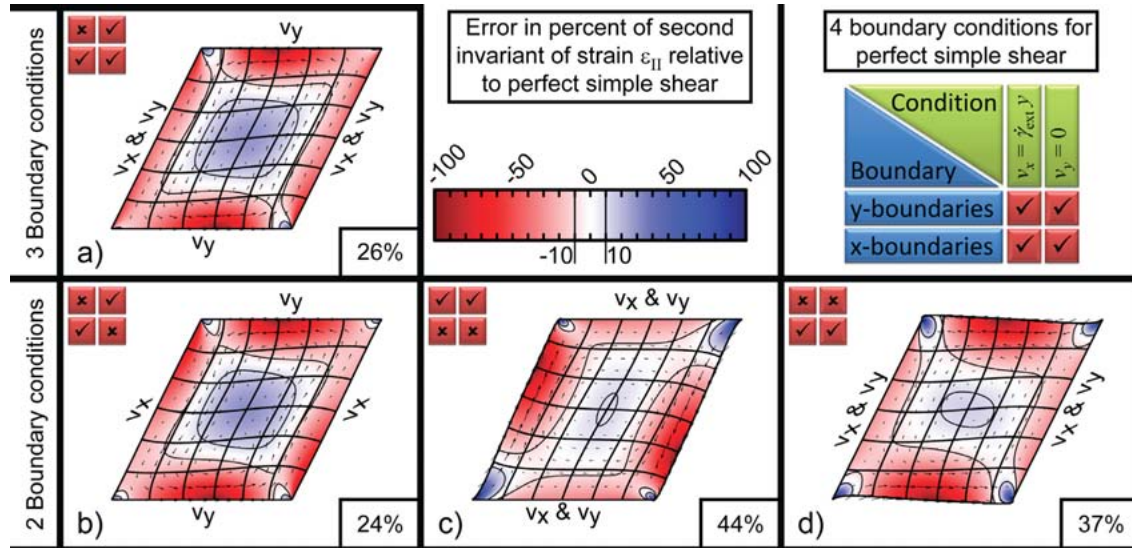


Figure 1. Numerically deformed homogeneous square with an applied simple shear strain $g_{\text{ext}} = 0.5$. The for boundary conditions for perfect simple shear are given in the table. In a), only three and in b) to d), only two of them are applied. The applied boundary conditions are noted at each boundary. Thick black lines are passive marker lines. The color represents the second invariant of finite strain, plotted as the error in percent relative to perfect simple shear. Thin black lines are the $\pm 10\%$ contour lines. The area with an absolute error smaller than 10% is given in the lower right corner of each subfigure. Arrows represent the finite perturbation strain.

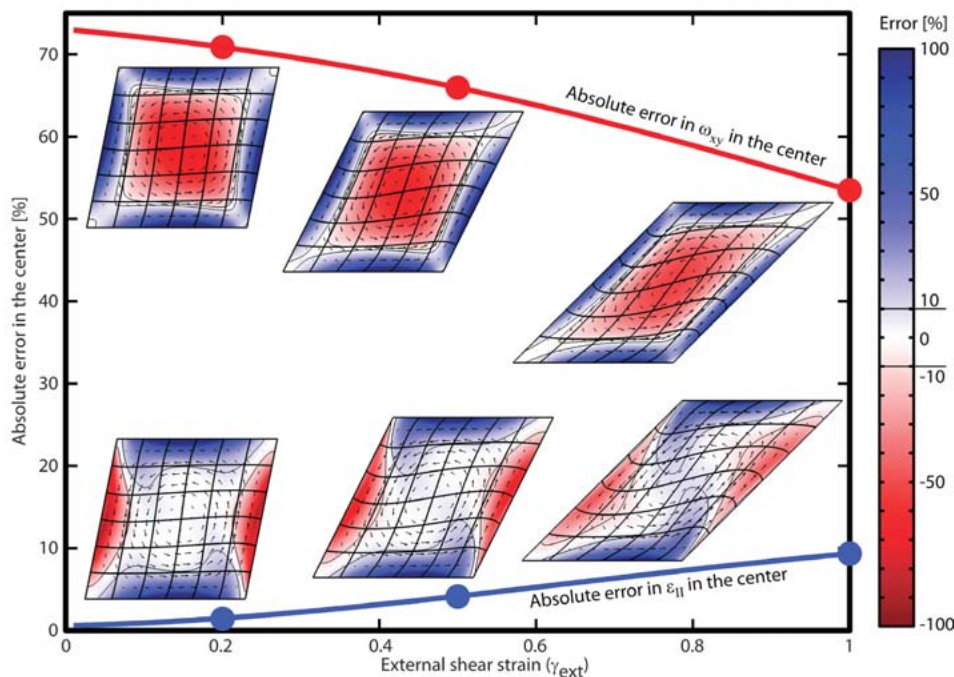


Figure 2. Numerically deformed homogeneous square with increasing applied simple shear strain g_{ext} , perfect simple shear boundary conditions in the x-y-plane and viscous drag-boundary conditions in the third (z-) direction. The color represents the finite shear strain (lower inset figures) and the finite rotation angle (upper inset figures), respectively, both plotted as the error in percent relative to perfect simple shear. Thin and thick black lines and arrows are the same as in Figure 1. The bold blue and red line represent the finite shear strain and the finite rotation angle at the very center of the model, respectively.

REFERENCES

- Grujic, D. & Mancktelow, N.S. 1995: Folds with axes parallel to the extension direction - An experimental study, *J. of Structural Geology*, 17, 279-291.
- Ildefonse, B. & Mancktelow, N.S. 1993: Deformation around rigid particles - The influence of slip at the particle-matrix interface, *Tectonophysics*, 221, 345-359.
- Price, G.P. & Torok, P.A. 1989: A new simple shear deformation apparatus for rocks and solids, *Tectonophysics*, 158, 291-309.
- Sengupta, S. & Koyi, H.A. 2001: Modifications of early lineations during later folding in simple shear, *Geological Society of America Memoir*, 193, 51-68.

1.15

The Soja and Luzzzone nappes : discovery of a Briançonnais element below the front of the Adula (NE Ticino, Central Alps)

Galster Federico¹, Epard Jean-Luc¹ & Masson Henri¹

¹ Institut de Géologie et Paléontologie, Université de Lausanne, CH-1015 Lausanne (Federico.Galster@unil.ch)

The Soja nappe is a small tectonic unit situated below the front of the Adula nappe in NE Ticino. It is classically characterized by a dm- to hm-thick sliver of paragneiss of presumed Late Paleozoic age, partly conglomeratic (sometimes called "Verrucano"), and is traditionally considered as rooted below the Adula nappe.

Stratigraphic and structural analysis based on detailed mapping of this gneissic body and its Mesozoic cover reveals the following facts:

1. The classical Soja nappe consists of two distinct parts separated by a wide landslide:
 - a. A southern part extends over 3.5 km NW of Val Soi (the type-locality) before it disappears below the landslide.
 - b. NE of the landslide, the gneiss can be followed over 7.5 km in the slopes S of the Lago di Luzzzone and in the Valle di Garzora.

Each part is homogeneous in its stratigraphic content, while there are significant differences between the southern and the northern parts, as explained below. Consequently their connection below the landslide is improbable and we better consider them as two distinct tectonic elements. The southern element is by definition the Soja nappe s.str.. We call the northern element the Luzzzone nappe.

Both nappes have the structure of an isoclinal anticline with a Paleozoic core. Mesozoic is well developed in both limbs of the Luzzzone nappe, but only in the normal limb of the Soja s.str. nappe.

2. Old gneiss: The Soja s.str. element contains an anticlinal core of gneiss with hints of pre-Alpine metamorphism. The Luzzzone nappe shows no evidence of such an old, polymetamorphic gneissic basement.
3. Late Paleozoic paragneiss: This is the characteristic lithology of the classical Soja nappe.
 - a. Luzzzone nappe: It mainly consists in well-bedded, fine-grained, micaceous and chloritic arkosic meta-sandstones. Dark brown spots of an ankeritic carbonate are omnipresent. In its upper part it may contain thin layers of dolomite and conglomeratic intercalations. This formation shows definite affinities with the Moosalp Formation in central Valais, of Permian age, which is a characteristic lithostratigraphic unit of the external part of the Paleozoic Briançonnais paleogeographic domain, or, in tectonic terms, of the lowest tectonic elements of the Grand St-Bernard nappe S of Visp (Zone Houillère and the overlying St-Niklaus syncline).
 - b. Soja nappe s.str.: The general lithology is similar but the carbonate spots or intercalations are rarer. In the inverse limb of the nappe the stratigraphically upper part is enriched in conglomerates. The Moosalp-type characteristics are less obvious.
4. Triassic: In both nappes the paragneiss is overlain by a white, pure quartzite (presumed of Early Triassic age) that passes transitionally to a thick series of limestones and dolomites. This carbonate series differs in the N and S elements:
 - a. Luzzzone nappe: The carbonate series displays typical characteristics of the Triassic Briançonnais domain. Even if tectonic deformation prevents to draw a complete stratigraphic column, very characteristic facies can be identified. Most typical is the St-Triphon Formation (of Anisian age), characterized by its calcaires vermiculés with their specific ichnofossils. The stratigraphic transition from the quartzite to the carbonate sequence, well exposed at several places with alternating layers of quartzites, greenish metapelites and dolomites underlying a first m-thick bed of yellow dolomite, can also be convincingly parallelised with the base (Dorchaux Member) of the St-Triphon Limestone in classical Briançonnais cross-sections. The Carnian dolomitic breccia has also been recognized. These

features definitely assign the Luzzzone Triassic to the Triassic Briançonnais domain.

b. Soja nappe s.str.: The dolomites predominate, but thin layers of limestone are also present at the base. Several distinct levels of dolomite have been identified and present a good lateral continuity. No typical Briançonnais feature has been observed.

5. Jurassic: Absent in Soja s.str.. It is well developed in both limbs of the Luzzzone nappe as a dm- to hm-thick series of dark blue or black pelitic schists and calcschists, classically presumed Liassic (to early Dogger?), an age that we consider as very probable. Our observations confirm that the contact of this series upon the Luzzzone Triassic is stratigraphic. This series is overthrust by another one with a very similar lithology, where the presence of a Sinemurian ammonite (*Arnioceras* sp., A. Uhr, unpubl.) supports the stratigraphic interpretation. Both together belong to the Piz Terri – Lunschania zone of the literature. This means that a large part of the Piz Terri – Lunschania zone belongs to the Luzzzone nappe, which extends considerably the surface of this tectonic unit towards NE. Characterized by two relatively coarse detrital inputs above a mainly marly base and topped by a black calcite-free pelite, these series show a clear affinity with the Helvetic (s.l.) Liassic stratigraphy.

Conclusion:

The most important point is the typical Briançonnais affinity of the Paleozoic and Triassic sections of the Luzzzone nappe. Particularly in the Triassic, the observed features belong to the core of the definition of the Briançonnais domain s.l. (i.e. including the Subbriançonnais) and of its use as a tool for paleogeographic correlations along the Alpine arc (Briançon Alps, Vanoise, Préalpes Médiannes and Grand St-Bernard nappe in central Valais). As the Adula Triassic is not Briançonnais (see Cavargna-Sari et al., this session), the Luzzzone nappe (including a large part of the Piz Terri – Lunschania zone) must have an ultra-Adula homeland. Originating S of the Adula, it must have passed over it, probably during subduction of the Adula, to be finally overtaken by its front when the Adula nappe was exhumed.

Another remarkable point is the Helvetic affinity of the Liassic section of the same Luzzzone nappe. The stratigraphic superposition of a Jurassic series of Helvetic (s.l.) type over a typically Briançonnais Triassic has major paleogeographic implications.

The classical Soja nappe is often correlated with the Lebendun nappe of NW Ticino and Italy. Our observations in both areas show that the similarity of the Lebendun gneiss with the Soja or Luzzzone gneisses is superficial. The Soja s.str and the Luzzzone nappes have nothing to do with the Lebendun.

1.16

Morphologic evolution of the Central Andes of Peru

Gonzalez Laura¹ & Pfiffner O. Adrian¹

¹Institut für Geologie, Baltzerstr. 1+3, CH-3012 Bern (Adrian.pfiffner@geo.unibe.ch)

We analysed the morphology of the Andes of Peru and its evolution based on the geometry of river channels, their bed-rock profiles, stream gradient indices and the relation between thrust faults and morphology.

The rivers of the Pacific basin incised Mesozoic sediments of the Marañon thrust belt, Cenozoic volcanics and the granitic rocks of the Coastal Batholith. They are mainly bedrock channels with convex upward shapes and show signs of active ongoing incision. The changes in lithology do not correlate with breaks in slope of the channels (or knick points) such that the high gradient indices (K) with values between 2000-3000 and higher than 3000 suggest that incision is controlled by tectonic activity. Our analysis reveals that many of the ranges of the Western Cordillera were uplifted to the actual elevations where peaks reach to 6000 m above sea level by thrusting along steeply dipping faults. We correlate this uplift with the Quechua phase of Neogene age documented for the Subandean zone (see Fig. 1).

The rivers of the Amazon Basin have steep slopes and high gradient indices of 2000-3000 and locally more than 3000 in those segments where the rivers flow over the crystalline basement of the Eastern Cordillera affected by vertical faulting. Gradient indices decrease to 1000-2000 within the east-vergent thrust belt of the Subandean zone. Here a correlation between breaks in river channel slopes and location of thrust faults can be established, suggesting that the young, Quechua phase thrust faults of the Subandean zone, which involve Neogene sediments, influenced the channel geometry. In the eastern lowlands these rivers become meandering and flow parallel to anticlinal structures that formed in the hanging wall of Quechua phase thrust faults, suggesting that the river courses were actively displaced outward into the foreland.

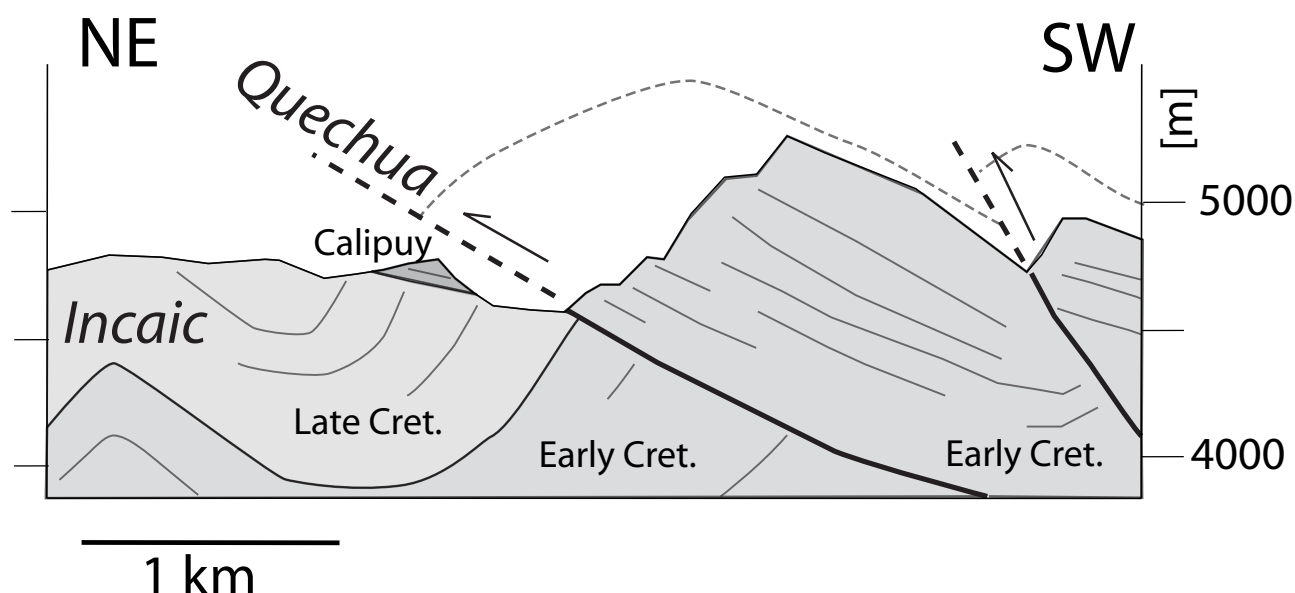


Figure 1. Morphologic expression of Neogene thrusting (Quechua phase) in the Central Highlands (near Abra la Viuda). The schematic cross section shows the geometry of thrusting responsible for the uplift of the Early Cretaceous strata. Incaic phase folding of the Cretaceous strata is pre-Calipuy (pre-Oligocene), while Quechua-phase thrusting is post-Calipuy (post-Oligocene).

1.17

Ti in quartz geothermometry in mylonites of the Simplon fault zone. What can we learn?

Härtel, Mike, Herwegh, Marco; Pettke, Thomas

University of Bern, Institut for Geological Sciences, Baltzerstrasse 1+3, 3012 Bern (mike.haertel@geo.unibe.ch)

The Simplon Fault zone (SFZ) is a major detachment fault between the Upper and Lower Penninic Units in the Central Alps and comprises mylonitic quartz microstructures deformed under the presence of water (Mancktelow & Pennacchioni 2004 and references therein) at metamorphic conditions ranging from lower greenschist facies (N) to upper amphibolite facies conditions (S). In order to study strain localization history in this large-scale structure, different sample series were collected in profiles across the Simplon fault to investigate the changes in dynamic recrystallization mechanisms and recrystallized grain size of quartz.

In the case of pure quartz mylonites (former qtz veins and qtz lenses), fine-grained recrystallized and large ribbon quartz grains occur within a 500 meter wide high strain zone. The recrystallized grain size in this fault zone generally is reduced compared to the undeformed veins, but the degree of grain size reduction varies strongly. The mechanisms of dynamic recrystallization are not only a function of the distance to the SZ, but also of strain localization, depending on the particular strain rate and temperature conditions (Hirth and Tullis, 1992 and Stipp et al. 2002, 2010). In order to track down the effect of temperature, titanium-in-quartz geothermometry (TitaniQ, Wark & Watson 2006) was applied using LA-ICPMS on thick slices of quartz, displaying both, host grains (also ribbons) as well as dynamically recrystallized grains. In this way, a sample series covering a range of distances to the shear zone from 3 m to 1866 m was investigated. Temperatures were calculated using the equation of Wark & Watson 2006 and Ti activities of 0.6, 0.8 and 1.0:

$$T(^{\circ}\text{C}) = \frac{-3765}{\log(X_{\text{qtz}}^{\text{Ti}}) - 5.69} - 273$$

In the studied quartz microstructures we obtain a temperature variation from 360 up to 470°C. Interestingly, the samples at the farthest locations to the shear zone center display the highest temperatures, whereas samples near the SZ center yield temperatures of around 360 °C. Despite this general temperature trend, local deviations enable interesting insights into the timing and the processes involved into chemical equilibration of Ti in quartz. For example, in the case of strongly elongated quartz ribbons, which were deformed under low temperature plasticity under absence of dynamic recrystallization, still the 460°C temperature event is preserved. This observation suggests that the quartz grains survived a first stage of large-scale strain localization and was only deformed during a late deformation event during which dynamic recrystallization was disabled in quartz. On the other hand, host quartz grains embedded in a fine-grained recrystallized quartz mylonite display the same low temperatures as found in the surrounding recrystallized aggregates. In this case, we assume a synkinematic formation of the quartz veins under low temperature conditions, where the host quartz was only partly recrystallized. We therefore conclude that most of the host grains show inherited temperatures reflecting either high or low temperature deformation, depending on their age of formation. Only the combination with measurement of the recrystallized matrix allows a further discrimination with this respect. In this sense, TitaniQ can indeed be a powerful geothermometer in quartz mylonites, provided that the measurements are accompanied by careful microstructural analyses and the careful selection of the samples with respect to the kinematic framework of the large-scale shear zone.

REFERENCES:

- Hirth, G. and Tullis, J. 1992: Dislocation creep regimes in quartz aggregates. *J. Struct. Geol.*, 14(2): 145-159.
- Mancktelow, N.S. and Pennacchioni, G. 2004: The influence of grain boundary fluids on the microstructure of quartz-feldspar mylonites. *Journal of Structural Geology*, 26(1): 47-69.
- Stipp, M., Stünitz, H., Heilbronner, R. and Schmid, S.M. 2002: Dynamic recrystallization of quartz: correlation between natural and experimental conditions. In: S. de Meer, M.R. Drury, J.H.P. de Bresser and G.M. Pennock (Editors), *Deformation Mechanisms, Rheology and Tectonics: Current Status and Future Perspectives*. Special Publications. Geological Society, London, pp. 171-190.
- Wark, A. W. and Watson, E. B. 2006: TitaniQ: a titanium-in-quartz geothermometer. *Contrib Mineral Petrol* 152: 743-754

1.18

Northern Alpine foreland deformation in western Switzerland: New insights from field and seismic data of the Plateau Molasse

Ibele, Tobias¹, Matzenauer, Eva¹, Mosar, Jon¹

¹Département de Géosciences Université de Fribourg, Chemin du Musée 6, CH-1700 Fribourg (tobias.iblele@unifr.ch)

In our study we investigate the Late Cenozoic tectonic evolution in the northern foreland of the western central Alps in a field based approach.

The western Swiss Molasse basin rests passively on top of a decollement that developed as the Jura Mountains formed the thin-skinned northern alpine foreland fold and thrust belt. Asymmetric Oligo-Miocene foreland basin sedimentation led to a thickening of the sedimentary pile towards southeast. In the Jura Mountains the distal Molasse deposits became eroded from top of the strongly folded frontal part of the foreland fold and thrust belt. In contrast the thicker sediments of the Plateau Molasse in the internal parts are only very gently folded.

Structural field mapping in the Plateau Molasse of the larger Fribourg area revealed regional extended strike slip tectonics, expressed in NW-SE striking dextral and N-S striking sinistral fault zones. In the sandstones, mudstones and rare conglomerates of the Lower Freshwater and Upper Marine Molasse (USM and OMM) of the Plateau- and Subalpine Molasse we observed the following brittle structures: joints and fractures, slickensides, brittle deformation bands in sandstones and pitted pebbles in conglomerates. The brittle deformation is not uniformly distributed. Areas of undisturbed rock are present, separated by strongly fractured areas with well developed meso-scale faults containing cataclasites and fault gouges. The faults are arranged in en-echelon geometries forming Riedel-shear type fault zones. The established paleo-stress field was found to be homogeneous with σ_1 orientated NNW-SSE.

The seismic activity in the region is low to moderate, fitting well the meso-scale soft linked discrete faults mapped in the surface outcrops. The focal mechanisms of instrumentally recorded earthquakes during the last decades reveal predominantly strike slip faulting located in the Mesozoic and Tertiary cover units. The stresses derived from these focal mecha-

nisms indicate a NW-SE compression and hence roughly the same as paleostresses derived from the mapped structures in the Molasse and from large scale fold- and thrust orientations in the Jura Mountains. This suggests that post mid-Miocene deformation is a continuous process until present.

The deep structure of the region is given by recent seismic interpretation and reveals a decoupling into three structural levels, representing the basement and the Mesozoic and Tertiary cover units. While basement and Mesozoic strata are pre-fractured, the Tertiary Molasse was undeformed prior to upper Miocene decollement tectonics. The basement is pre-fractured by Permo-Carboniferous normal faults of ENE-WSW strike. In the Mesozoic strata evidence is given for probably synsedimentary N-S striking normal faults. In response to the NW-SE compression of the Miocene to recent stress field the normal faults in the basement should become reactivated as reverse faults and the ones in the Mesozoic as sinistral strike slip faults. While sinistral strike slip faulting probably translates to the surface, reverse faulting in the basement is only evident from seismicity in the frontal parts of the Jura Mountains. The previously undeformed Molasse develops a conjugate dextral and sinistral fault zones system composed of Riedel-type arranged meso-scale faults. Direct kinematic linkage between the three structural levels is lacking. Instead a clear decoupling between basement and cover by the mechanically weak Triassic evaporites and a change of structural style from reactivation of structures to initial faulting between Mesozoic and Tertiary cover units is evident.

1.19

Dynamic constraints on crustal-scale rheology from the Zagros Mountains

Kaus Boris J.P.¹, Yamato Philippe², Mouthereau Frédéric³, Castelltort Sébastien¹

¹ Department of Earth Sciences, ETH Zürich, Switzerland (kaus@erdw.ethz.ch)

² Geosciences Rennes, UMR CNRS 6118, Université de Rennes 1, France

³ UPMC Univ Paris 06, UMR 7193, Institut des Sciences de la Terre de Paris, F-75005, Paris, France

The Zagros Mountains are a spectacular example of a mountain belt that consists of crustal-scale folds with a regular spacing of ~15 km. Despite excellent geological constraints, the formation of these structures remains enigmatic. Here, we therefore use visco-elasto-plastic numerical models to understand the dynamics of the Zagros on geological time scales. Models with a brittle crust and a single basal salt layer produce fault-related deformation structures that are inconsistent with the data. If, on the other hand, we take into account the observation that there might be up to 3 intermediate weak layers within the brittle crust, our models produce crustal-scale folds with the correct wavelength. Physically, this is caused by a folding instability whose wavelength mainly depends on the friction angle of the crust and the viscosity of the detachment layers. By combining a new semi-analytical technique with independent constraints on the effective viscosity of salt, we show that the friction angle of the crust in Zagros should be smaller than ~10° to reproduce observations. Our results have implications for the deformation of the crust as they highlight the importance of thin detachment layers. Moreover, our results show how geological observations put constraints on the long-term rheology and dynamics of the crust.

1.20

Numerical modeling of two-phase flow: Interaction of magmatism with active tectonics

Tobias Keller¹ and Boris J. P. Kaus¹

¹*Institute of Geophysics, ETH Zürich, 8092 Zürich, Switzerland (keller@erdw.ethz.ch)*

We investigate the behaviour of a two-phase system that involves production and percolation of partial melt through a viscoelastoplastic continental lithosphere and crust under ongoing tectonic deformation. Using two-dimensional numerical simulations we examine the coupled magmatic and tectonic processes leading to intrusive rock formation.

The numerical modeling approach is based on the assumption that the melt fraction is equal to the porosity of the rock and that porosity change reflects, apart from melting and crystallization, the compaction or dilation of the matrix framework due to both viscous and elastic processes. Both modes of compaction are connected to the local effective pressure, which is obtained as the difference between the bulk pressure over both phases and the local fluid pressure. The magmatic model is chosen to represent a typical melt evolution starting with an arc-type basaltic melt that will fractionate into mafic cumulates and more highly evolved melt, which will again crystallize as a felsic plutonite rock. Compositional contamination by melting of crustal rocks during the magma's ascent is taken into account.

The model setup involves a continental crust of 50 km thickness and 100 km of the underlying mantle. At the lithosphere-asthenosphere transition, we introduce a source region for partial melt by applying an initial temperature slightly above a wet mantle solidus. The melt production and propagation depends on the evolution of temperature and dynamic pressure in the lithosphere and crust as the region is being deformed tectonically. Here, we focus on extensional tectonics as they provide the best conditions for the extraction of mantle melt. Compressional and transpressional tectonics will be the subject of further investigations.

First results indicate that melt propagation is strongly related to the regional stress field, and that brittle fault zones form important conduits for the propagation of partial melt, especially through the more competent parts of lithosphere and lower crust. Where the partial melt reaches either mechanical barriers or neutral buoyancy with respect to the host rock, regions of magma accumulation may quickly evolve into magma chambers with melt content exceeding 80%. There, the melt may either reside until it crystallizes or fractionate until the more evolved rest of the melt has obtained new buoyancy to force its way further through the crust.

A possible application of such models is to deepen the understanding of the processes involved in, and the geometry and field relations expected from, the emplacement of hydrated slab melts into the overriding continental plate in an ocean-continent subduction setting.

1.21

Fission-track constraints on the thermotectonic evolution of the Apuseni Mountains (Romania)

Kounov Alexandre¹ & Schmid Stefan¹

¹*Geologisch-Paläontologisches Institut, Bernoullistrasse 32, CH-4056 Basel (a.kounov@unibas.ch)*

The Apuseni Mountains, located inside of the Carpathian arc and bounding the Transylvanian basin to the west, constitutes the largest outcropping part of the Tisza block. This crustal fragment consists of a stack of several nappe sequences formed in response to continental collision, which followed the closure of the Neotethys Ocean. The northwestern part of the Apuseni Mountains represents a coherent nappe sequence consisting of the Bihor and Codru nappe systems. The tectonically highest Biharia nappe system, previously considered as part of Tisza plate (Csontos and Vörös 2004), is attributed to the Dacia Mega-Unit (Schmid et al., 2008).

The first Alpine tectonic event in the area was probably related to the obduction of the Eastern Vardar Ophiolitic unit (Transylvanides) onto parts of the Dacia Mega-Unit (Biharia) in the latest Jurassic. This was followed by late early-Cretaceous final closure of the Neotethys remnants and the collision between Tisza and Dacia blocks producing top-E nappe stacking. The final emplacement of the nappes in the Apuseni Mountains involving top-W to NW superposition of the Biharia, Codru and Bihor nappe systems have taken place in the Turonian. Subsequent compressional deformations in the area are reported for the end of the Cretaceous and the Eocene.

The Jurassic volcanics of the Transylvanides, their sedimentary cover and the underlying Baia de Aries nappe (the highest structural unit of the Biharia nappe system) exhibit late early-Cretaceous zircon fission-track (FT) ages (Aptian and Albian, 120-103 Ma). The more westerly and structurally lower units (Biharia nappe of the Biharia nappe system, Codru and Bihor nappe systems), however, exhibit Late Cretaceous (Turonian to Campanian, 95-71Ma) zircon FT ages. The late early-Cretaceous zircon FT ages from the Baia de Aries nappe, together with the Jurassic ophiolites and their sedimentary cover, suggest that these rocks must have been buried to a minimum of 8km during this time. Such temperatures have probably been attained during underthrusting of these units below the Tisza megatectonic unit (thrusting being top-east).

The ages obtained from the Bihor, Codru and Biharia nappes (Turonian to Campanian, 95-71Ma) correspond to the age of the late Cretaceous top-NW event that led to the present-day nappe stack in the Apuseni Mountains. The internal parts of the Baia de Aries nappe and the overlying Transylvanides were not reheated during this second event since they occupied the highest tectonic position. Zircon FT ages, combined with thermal modelling of the apatite FT data, show that rapid post-tectonic cooling of the area during the late Cretaceous was followed by relatively slow cooling during the early Paleogene.

REFERENCES

- Csontos, L., & Vörös, A. 2004: Mesozoic plate tectonic reconstruction of the Carpathian region, *Paleogeography Paleoclimatology Paleocology* 210, 1–56.
- Schmid, S.M., Benoulli, D., Fügenschuh, B., Matenco, L., Schefer, S., Schuster, R., Tischler, M. & Ustaszewski, K. 2008: The Alpine-Carpathian-Dinaridic orogenic system: correlation and evolution of tectonic units. *Swiss Journal of Geosciences*, 101, 139-183.

1.22

State of the art of SWAM: Seismic Wave Attenuation Module

Claudio Madonna¹, Nicola Tisato¹, Sébastien Boutareaud¹, Jean-Pierre Burg¹

¹ *Geologisches Institut, Sonneggstrasse 5, CH- 8092 Zürich (claudio.madonna@erdw.ethz.ch)*

The study of wave attenuation in partially saturated porous rock over a broad frequency range provides valuable information about the fluid system in reservoirs, which is inherently a multiple phase fluid system. Until now, few laboratory data have been collected in the seismically relevant low frequency range. Therefore, actual data on partially saturated rock are very limited. The main goal of our work is to accurately measure the bulk seismic attenuation at in situ conditions in laboratory. Bench top results show consistency with the few reported experimental data of dry, partially and fully saturated rocks.

We report the new apparatus setup to measure seismic wave attenuation at room pressure and temperature on a rock sample of 60mm length and 25.4mm diameter. Our method uses bulk strain measurements, accomplished by measuring the strain across the whole sample with micro-linear variable differential transformers. We can cover the frequency range from 10-1-102 Hz.

The results on a sample of Berea Sandstone, with different degrees of saturation, and the calibration data obtained with a standard aluminium sample are described. The acquisition software and the hardware are presented, together with the final goal: the implementation of the attenuation module within a Paterson gas-medium apparatus. This adaptation will allow conducting experiments at confining pressure and depth-temperatures.

1.23

Tectonic amalgamation and reworking of a sedimentary cover within a polydeformed basement in a subduction-collision zone: an example from the Western Italian Alps

Paola Manzotti¹, Martin Robyr¹, Michele Zucali² & Martin Engi¹

¹ University of Bern, Baltzerstrasse 1+3, 3012 CH-Bern (manzotti@geo.unibe.ch)

² Dipartimento di Scienze della Terra «Ardito Desio», Università degli Studi di Milano, via Mangiagalli 34, 20133 I-Milano

The Dent Blanche nappe belongs to the Austroalpine domain of the Western Italian Alps and is classically divided into two units, the Valpelline and the Arolla Series. The Valpelline Series consists of metapelites, mafic and carbonate rocks with a dominant metamorphic imprint under amphibolite to granulite facies conditions of pre-Alpine age. The Arolla Series is mainly composed of Permian age granite, diorite and gabbro, all metamorphosed and deformed to orthogneiss, Wm-Am-bearing gneiss and schist during the Alpine tectonometamorphic evolution.

The Roisan Zone is considered to be the Mesozoic metasedimentary cover of the Dent Blanche nappe. It comprises ophiolite-free metasedimentary sequences, including Triassic dolomite, Jurassic and Cretaceous calcschist and Qtz-bearing micaschist. This cover is dismembered into metric to hectometric bands and pods and is frequently associated with the Arolla tectonites and mylonites.

The Dent Blanche nappe records a complex structural evolution in which the kinematics of the deformation vary both spatially and temporally. The present study investigates variations in structural style, intensity and geometry of deformation in the Arolla Series and in the Roisan zone. Our data indicate a complex kinematic history involving both crustal extension and shortening during the Pre-Alpine and Alpine evolution. An Alpine polyphase deformation is well developed both in the basement and cover units. The structural evolution comprises two phases of isoclinal folding associated with the development of a penetrative mylonitic foliation. Progressive tectonic modifications of geometric relationships within the whole lithostratigraphic sequence of the Roisan Zone (tectonic amalgamation with a pre-existing basement, re-foliation, transposition) severely alter the original successions of sedimentary layers and the lithologic relationships with the Arolla intrusive complex.

During Alpine deformation phases the igneous and metamorphic protoliths were mylonitized and largely converted to strongly foliated and lineated tectonites. However, heterogeneous strain distribution at the scale of the Dent Blanche nappe allowed for the preservation, at a range of scales, of pre-Alpine relics of all protoliths.

In the Arolla Series strain gradients and the partitioning of deformation are responsible for the juxtaposition of three fabric styles (coronitic, tectonitic and mylonitic domains), which lead to further differentiation. The Arolla unit displays, as a whole, a widespread Alpine reworking that is most evident in the mostly fine-grained Wm±Gln±Chl-bearing orthogneisses and mylonites. Despite this pervasive Alpine imprint, large scale relic bodies of undeformed Permian protoliths (i.e. granite and quartzdiorite) occur as kilometric and hectometric pods. These preserved cores (termed coronitic domains) are surrounded by medium- to high-strain domains, characterized by tectonitic to mylonitic Wm±Gln±Chl-bearing gneiss. Metric bands of flaser quartzdiorites to mylonites delimit these undeformed pods within the unit. Transitions from massive metagranitoids to mylonitic types are commonly outlined by coarse augengneisses to very fine-grained derivatives. Tectonitic fabrics represent a moderate deformational overprint and permit the inference of a chronological succession of deformational phases, going from coronitic to fully reequilibrated mylonitic domains. In the latter are usually devoid of relics.

1.24

Thrusting and faulting in the Préalpes Médiannes

Matzenauer Eva¹, Mosar Jon¹

¹ Département de Géosciences Université de Fribourg, Chemin du Musée 6, CH-1700 Fribourg
(eva.matzenauer@unifr.ch; jon.mosar@unifr.ch)

The study of tectonic and neotectonic structures of the Préalpes Klippen with focus on the investigation of fracture families and their possible attribution to an appropriate tectonic event is the scope of an ongoing PhD research.

The Préalpes klippen are formed by a series of nappes that were detached from their Briançonnais homeland as result of its incorporation into the orogenic wedge. Subsequently, they were transported towards the N-NW and emplaced onto the foreland, where they remain as several tectonic klippen along the northern front of the Swiss and French Alps and in the NW of the Helvetic nappes. The most important and best exposed nappe, the Préalpes Médiannes, is subdivided into two parts: the Préalpes Médiannes Plastiques (PMP), mainly governed by large-scale fault-related folds, and the Préalpes Médiannes Rigides (PMR), dominated by imbricated thrust slices dipping to the N/NW.

Field investigations mainly in limestone, but also in marls and shales of both parts of the Préalpes Médiannes exposed a whole suite of brittle tectonic features: joints and fractures, slickensides, vein arrays and stylolithes as well as strongly deformed brittle shear zones. Field measurements combined with more large-scale structural observations in the field, on maps, digital elevation models or orthophotographs allow us to distinguish several structural elements we would like to present:

- Thrusts developed during the emplacement of the Préalpes Médiannes were responsible for the folding of the nappe. For this reason, they are for the most part hidden below anticlines. Their general movement direction is top to the NW, however, as observed in the Schopfenspitze area (PMP), important backthrusts with top to the SE orientation exist. The Schopfenspitze backthrust is characterised by an important fault zone of several meters width with well developed shear bands.
- Several faults are oriented transverse or even perpendicular to the fold-axis and induce therefore a segmentation of the large folds. The succession of several normal faults lead to more pronounced plunging of the fold axis. Slickenside and vein data as well as the morphological observations expose axial parallel extension in the Dent de Broc region (PMP).
- Out-of-sequence thrusts - post-dating the emplacement of the nappes - clearly cross-cutting and off-setting pre-existing folds were found both at the Schopfenspitze and the Gros Haut Crêt area (PMP), where due to lateral ramp thrusting a strike-slip component is added.
- Elsewhere, a strike-slip component prevails over the normal fault movement. Throughout the Préalpes Médiannes, fracture analysis shows two major fault orientations: right lateral WNW-ESE and left lateral NNW-SSE striking faults. These two fault families are possibly linked to a common conjugate fault system.

Comparison of fault patterns in the Molasse Basin and Préalpes Médiannes show striking similarities in fault and stress orientation but the connection of these is still part of discussions.

1.25

An optimal, scalable finite element based forward model for gravity computations

Dave A. May¹ & Boris J.P. Kaus¹

¹Geophysical Fluid Dynamics, Institute of Geophysics, ETH Zurich, Sonneggstrasse 5, CH-8092 Zurich (dave.may@erdw.ethz.ch,kaus@erdw.ethz.ch)

The use of forward models to compute synthetic gravity signals is necessary to conduct an inversion of the density structure in the subsurface. Numerous forward models exist, the most common of which is a direct summation approach employing an analytic expression to compute the gravity over a rectangular prism. To permit the description of a detailed density structure, the domain is discretised into a set of prisms, each of which possess a unique density. The gravity at a single point s , is computed by evaluating the closed form expression for the gravity over each element, and summing the result.

The summation approach has several disadvantages. The operator F (i.e. the matrix) describing the forward model is completely dense. For inversions, the operator $F^T F$ or $F F^T$ is often required, and both these products will be dense if F is dense. Consequently the storage requirements is large for high spatial resolution 3D inversions if these products are required to be stored. Another drawback of the summation approach is the algorithmic scaling. If the domain contains $N \times N \times N$ voxels, we are required to perform $O(N^3)$ operations per point of interest s . Hence the increasing the number of gravity stations which are used as data in the inversion increases the computational cost of the method.

An alternative to the summation approaches is to solve a Poisson problem for the gravitational potential and then compute the gradient of the resulting potential to obtain the gravity. Using such a PDE based forward model has the advantage that the operator F is sparse, and there the computational cost is independent of the number of gravity stations used in the inversion. Recently, Cai & Wang (2005), proposed a more accurate boundary condition to circumvent the need to try to impose that the potential should vanish at infinity. These authors utilised a finite element discretisation as it provided high geometric fidelity to define their gravity anomaly. In contrast Farquharson & Mosher (2009), used a finite domain with zero Dirichlet boundary conditions on the potential and used a finite difference discretisation. Whilst both of these forward models do not have an algorithmic scaling dependent on the number of gravity stations, the time required to obtain the potential field using their iterative solvers is dependent on the grid resolution used to discretise the subsurface.

Here we describe a parallel finite element based forward model to solve the Poisson problem. This method incorporates several new features. Firstly it permits locally refined meshes to be used near the gravity anomaly and in the regions of free space, the grid resolution is quite coarse. We also incorporate the near-field boundary conditions of Cai & Wang (2005), thus improving the approximation that the potential should be zero at infinity. In addition, we introduce a second order accurate recovery procedure to compute the gravity field from the potential. We also introduce an optimal multilevel preconditioner to solve the Poisson problem. This feature is necessary to ensure the forward model is remains efficient for high resolution 3D inversions. We demonstrate that the preconditioner is robust with respect to the aspect ratio of the elements used in the grid and that the solution time scales linearly with respect to the number of elements in the domain. The accuracy, speed and scaling with respect to the number of elements and the number of gravity stations of the new forward will be compared with a classical closed form summation forward model.

REFERENCES

- Cai, Y., Wang, C., 2005. Fast finite-element calculation of gravity anomaly in complex geological regions. *Geophys. J. Int.* 162, 696–708.
- Farquharson, C., Mosher, C., 2009. Three-dimensional modelling of gravity data using finite differences. *J. Appl. Geophys.* 68, 417–422.

1.26

The Fribourg Structure and Fribourg Zone: an Active fault system?**or****The Röstli Graben – Geologic evidence!**

Mosar Jon¹, Meier Beat², Sommaruga Anna³, Abednego Martinus¹, Eichenberger Urs³, Ibele Tobias¹, Matzenauer Eva¹, Sprecher Christian⁴ & Vouillamoz Naomi¹

¹ Département de Géosciences – Sciences de la Terre, Université de Fribourg, Ch. Du Musée 6, CH - 1700 Fribourg (Jon.Mosar@unifr.ch).

² Interoil E&P Switzerland AG, Seefeldstrasse 287, CH - 8008 Zürich, Switzerland.

³ Institut de Géophysique, Université de Lausanne, Bâtiment Amphipôle, UNIL-Sorge CH - 1015 Lausanne.

⁴ Sprecher Consulting GmbH, Aehrenweg 27, CH-5430 Wettingen / Switzerland.

Located between the Jura mountains to the North and the Alps to the South the larger Fribourg region has been, possibly since Oligocene, and is still subjected to compressive stresses resulting from the alpine orogenic processes. The subsurface geology of the Fribourg area is basically a layer cake with 3 main levels: the Tertiary Molasse sediments overlying the Mesozoic units detached along a basal décollement in the Triassic evaporites, and below the Basement s.l. including possible Permo-Carboniferous graben structures, and Paleozoic rocks.

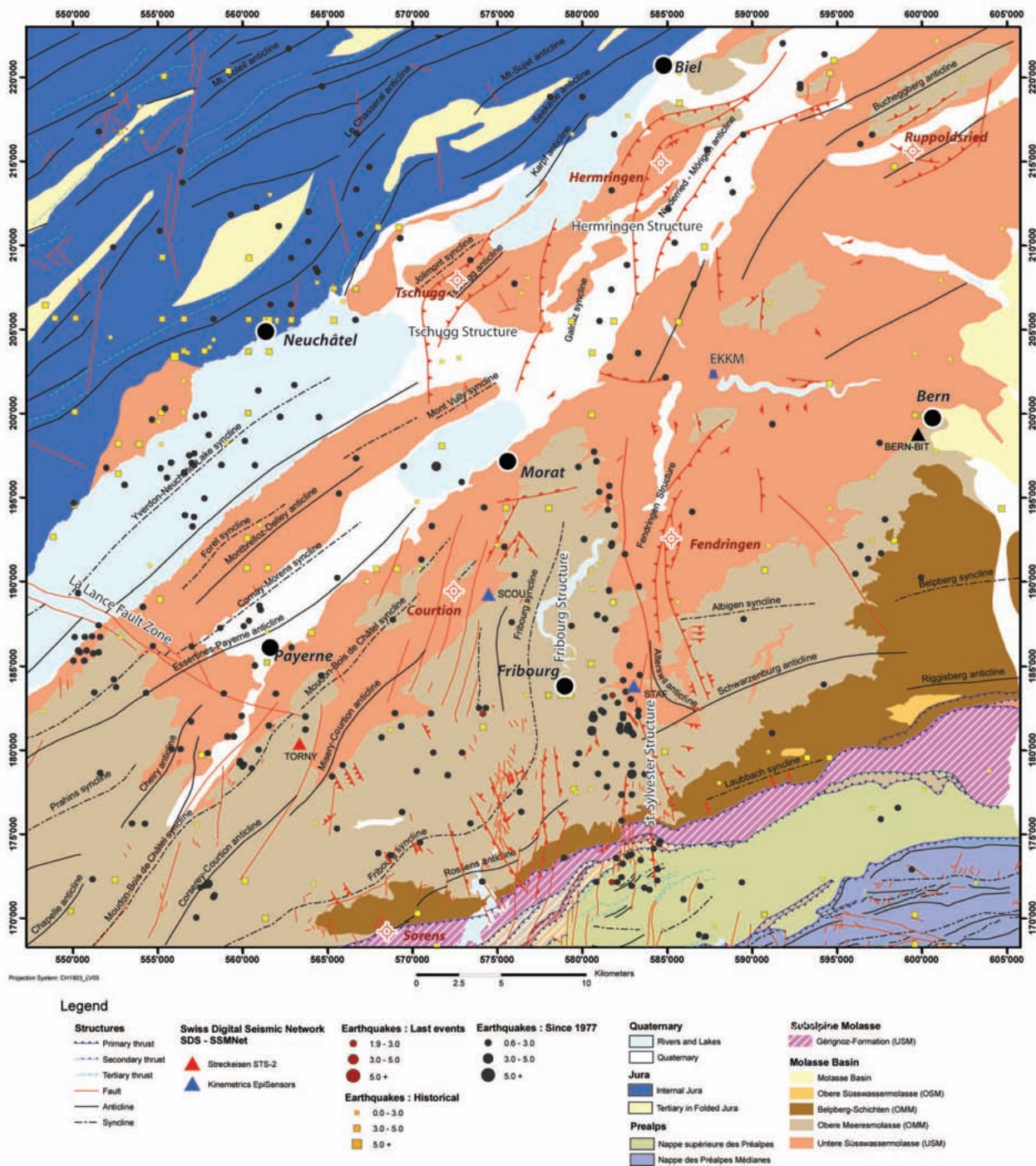
In the Fribourg area we observe a deviation from this general trend with folds, as well as major faults trending N-S to NNE-SSW. This extends some 17 km to the North and 10 km to the South of the city of Fribourg. Around Fribourg its width in an E-W direction is about 10-12 km. This whole tectonic zone is called the Fribourg Structure (FS) and its central part forms the Fribourg syncline (known from surface data). It has been suggested that recent earthquakes align along a more or less N-S oriented line, running just east of the city of Fribourg (Swiss Seismological Service). This alignment is called a lineament and was dubbed the Fribourg Zone (FZ) and corresponds to the eastern edge of the Fribourg Structure.

The regional tectonic elements result from a complex sequential and spatial evolution combining extensional and strike-slip faults as well as thrusts and folds. The deformation affects the basement and the cover series to different degrees. During the foreland evolution and contemporaneously to the fold-and-thrust development of the Jura (classically given between 15 and 4 My), the Molasse basin of W Switzerland was detached above the Triassic evaporites and transported to the N by some 25km ("Fernschub"). During this period we see the formation of a series of thrusts and related folds with a general NE-SW alpine trend that started out as gentle folds above salt pillows. Some zones, such as in the Tschugg and Hermrigen area, form complex structures with frontal ramps and N-S trending lateral ramps with a strike-slip motion component at their western edges. In the Fribourg area a graben-like structure associated with salt migration deforms the overlying sedimentary cover to develop a N-S oriented depression. This structure is associated with a series of normal faults developing at the eastern and western edges. Subsequently, as a result of alpine compression, the sedimentary cover deforms in a strike-slip regime. This causes the faults at the eastern edge of the graben to be reactivated. The faults are reactivated as an N-S en-échelon Riedel shear system. Comparing the model to the present-day distribution of earthquake activity suggests that the southern portion of the FZ is an "active fault".

Reinterpretations of reflection seismic data (440 km of lines in Fribourg area interpreted by B. Meier - InterOil, basinwide interpretation by A. Sommaruga, U. Eichenberger - Inst. Géophysique Lausanne Project with Swiss geophysical Commission) demonstrate that the faults presently active in a strike-slip mode, are clearly seen only found in the sedimentary cover and they do not extend into the basement. The new interpretation also confirms that faults are of modest dimension and arranged as a Riedel shear system.

The Fribourg Structure and the Fribourg Zone should be considered in the broader context of the deformation of the Molasse foreland basin. Unlike the situation further east where the foreland basin is in a general state of extension, the western Swiss Molasse foreland basin is in a compressional tectonic setting. This is clearly substantiated by the numerous fold and thrust structures that develop between Bern and the western termination of the Basin SW of Geneva, in the Chambéry area. In this whole zone the Molasse basin is not acting as a foreland basin but it is behaving as a wedge-top basin in the south and southeast, behind the Jura Mountains whose northernmost external thrust represents the present orogenic front.

In this framework the Molasse basin in the Fribourg – Lausanne area appears to be deforming at present mainly by large strike-slip fault zones. Several major zones form a pattern of conjugate fault systems or corridors that allow the basin to deform and shorten. Each of these corridors corresponds to a Riedel shear systems developing its own sets and subsets of fractures. Two main directions are observed: N-S sinistral and NW-SE dextral.



Structural map of the larger Fribourg area. Based on a compilation of existing surface data (mainly maps) and a new interpretation of reflection seismic data). Seismicity from SED catalogue; deep oil exploration wells are indicated (red circle and cross).

1.27

Glacially enhanced fluvial erosion and rock uplift in the Swiss Alps

Kevin P. Norton & Fritz Schlunegger

Institut für Geologie, Universität Bern, Baltzerstrasse 1+3, CH-3012 (norton@geo.unibe.ch)

The Swiss Alps are one of the most thoroughly studied mountain landscapes in the world. Nearly two centuries of intensive geologic research has lead to an unparalleled database of bedrock properties, erosion rates, and geomorphic and tectonic parameters. One result of these data is an ongoing debate as to the meaning of apparent correlations between surface denudation and modern rock uplift.

In the simplest case the Swiss Alps can be considered an isostatically compensated, non-convergent orogen. Theory suggests that rock uplift rates should be positively correlated with denudation rates (with a coefficient of 0.8) for such a system. Assuming that this is true, the next major challenge is to search for process linkage; denudation is a very broad term, encompassing such varied processes as chemical weathering, soil creep, and rockfall. Therefore, simply claiming that rock uplift is driven by denudation provides us with little additional insight.

Here, we show how individual fluvial and hillslope processes contribute to the denudational budget of the Alps, and provide a causal link between surface processes and resultant rock uplift rates. An analysis of stream channel steepness shows that oversteepened streams are associated with glacially perturbed landscapes (Figure 1; Norton et al., 2010a). These glacially impacted regions also exhibit up to 10-fold higher denudation rates than adjacent fluvial basins (Norton et al., 2010b). This results in a spatial focusing of erosion which elevates fluvial incision rates, driving associated hillslope responses such as landsliding and rockfall, which are intimately tied to the underlying lithology. Norton et al. (2010a) show that channel steepness is a function of bedrock erodibility for steady-state streams, but that this correlation breaks down in the non-steady state case, where channels are oversteepened, regardless of bedrock erodibility. Likewise, lithologies such as the schists of the Bündnerschiefer, are loci for enhanced landsliding and rock uplift.

Finally, if there is no longer active convergence in the Swiss Alps, one must question the mechanism which maintains both denudation and rock uplift at such high rates. We postulate that the effect of repeated Pleistocene glacial perturbations has been the continual renewal of transient river segments, resulting in rapid, focused fluvial incision, enhanced landsliding on adjacent slopes, and a concomitant increase in rock uplift due to isostatic compensation to the erosional mass loss.

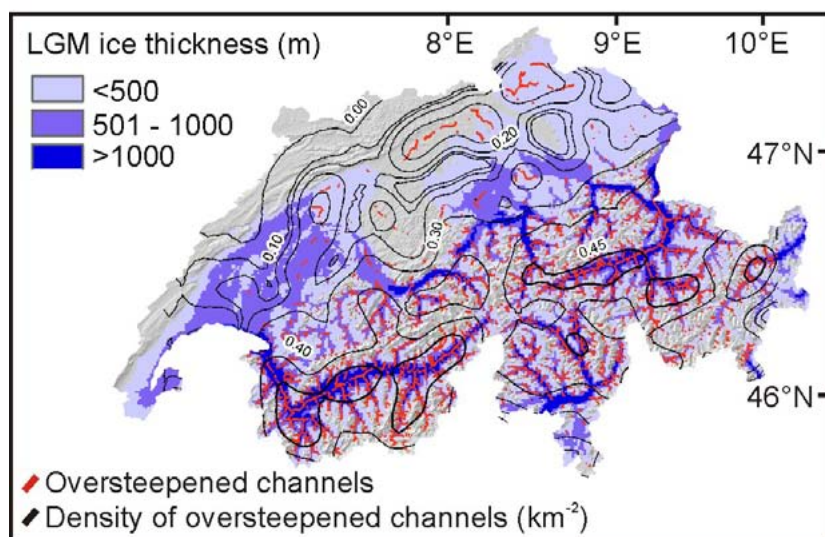


Figure 1. Patterns of LGM ice thickness and over-steepened streams (individual segments in red, and density of streams in black) in Switzerland (figure modified after Norton et al. (2010a)).

REFERENCES

- Norton, K.P., Abbühl, L.M., Schlunegger, F. 2010a. Glacial conditioning as an erosional driving force in the Central Alps. *Geology*, 38, 655-658.
- Norton, K.P., von Blanckenburg, F., Kubik, P. 2010b. Cosmogenic nuclide-derived rates of diffusive and episodic erosion in the glacially sculpted upper Rhone Valley, Swiss Alps. *Earth Surface Processes and Landforms*, 35, 651-662.

1.28

The Canavese Fault west of Valle d'Ossola

Pleuger Jan¹ & Mancktelow Neil¹¹Geologisches Institut, ETH Zürich, Sonneggstraße 5, CH-8092 Zürich (jan.pleuger@erdw.ethz.ch)

The Periadriatic Fault system has had an important influence on Neogene Alpine kinematics and is commonly taken to have partly accommodated crustal convergence between the European and Apulian plates in the Oligocene to Early Miocene. The total amount of the dextral strike-slip component on this major fault is controversial, ranging from a few tens of kilometres to many hundreds.

Fieldwork along the Canavese Fault (i.e. the Periadriatic Fault west of Lago Maggiore) has corroborated the results of earlier studies (Schmid et al. 1987, 1989) that the Canavese Fault comprises several greenschist-facies mylonite belts. These belts accommodated different relative motions between the Southern and Penninic Alps at different times.

In the Valle d'Ossola, the Canavese Fault comprises mylonites with N-side-up shear sense mostly derived from the Sesia Zone and mylonites with a dextral shear sense mostly derived from the Ivrea Zone (see also Schmid et al. 1987). In some places, the dextral mylonites have a strong S-side-up component of displacement. The N-side-up mylonite belt appears to be consistently overprinted by the dextral belt. West of Valle d'Ossola, the volumes of both the dextral and the N-side-up mylonites diminish rapidly. Toward the west, they can be traced until Valle Strona and Valle Mastallone, respectively. From Valle Strona to the west, the N-side-up mylonites are paralleled by a belt of greenschist-facies S-side-up mylonites to the north which generally have a sinistral displacement component. The age relation between the N-side-up and S-side-up mylonites could not yet be determined. Between Valle Mastallone and river Dolca in Valle Sessera, another belt of S-side-up mylonites, in this case with a dextral strike-slip component, is developed within the Ivrea Zone. This mylonite belt is identical with mylonite belt 1 of Schmid et al. (1989; also mapped by Handy et al. 2005) except that we interpret mylonites of belt 2 of Schmid et al. (1989) in the Valle Sessera to belong to the same belt. The volume of Canavese Fault mylonites decreases toward southwest. In the Valle Sessera and further southwest, the thickness of Canavese mylonites does not exceed a few tens of metres.

Since the dextral mylonite belts mentioned above are not continuous along the Canavese Fault, strike-slip displacement in the order of 100 km, as postulated by various authors, can only be explained if displacement was transferred away from the Canavese Fault into the Penninic domain. Splays branching off the Canavese Fault, as postulated by Handy et al. (2005), may provide the explanation for the eastward accumulation of dextral displacement between the Western and Central Alps with respect to the Southern Alps (Schmid et al. 1989, Handy et al. 2005, Pleuger et al. 2008). These splays need verification because the assumption of dextral displacement on the order of 100 km requires a set of continuous faults that were active at the same time.

REFERENCES

- Handy, M.R., Babist, J., Wagner, R., Rosenberg, C.L. & Konrad, M. 2005. Decoupling and its relation to strain partitioning in continental lithosphere - insight from the Periadriatic Fault system (European Alps). In: *Deformation mechanisms, rheology and tectonics: From minerals to the lithosphere* (Ed. by Gapais, D., Brun, J.P. & Cobbold, P.R.). Geol. Soc., London, Spec. Publ., 243, 249–276.
- Pleuger, J., Nagel, T.J., Walter, J.M., Jansen, E. & Froitzheim, N. 2008. On the role and importance of orogen-parallel and -perpendicular extension, transcurrent shearing, and backthrusting in the Monte Rosa nappe and the Southern Steep Belt of the Alps (Penninic zone, Switzerland and Italy). In: *Tectonic aspects of the Alpine-Dinaride-Carpathian system* (Ed. by Siegesmund, S., Fügenschuh, B. & Froitzheim, N.). Geol. Soc., London, Spec. Publ., 298, 251–280.
- Schmid, S.M., Zingg, A. & Handy, M. 1987. The kinematics of movements along the Insubric Line and the emplacement of the Ivrea Zone. *Tectonophysics*, 135, 47–66.
- Schmid, S.M., Aebli, H.R., Heller, F. & Zingg, A. 1989. The role of the Periadriatic Line in the tectonic evolution of the Alps. In: *Alpine Tectonics* (Ed. by Coward, M.P., Dietrich, D. & Park, R.G.). Geol. Soc., London, Spec. Publ., 45, 153–171.

1.29

B-type Olivine LPO in the Ronda Peridotite (Spain): Evidence of high-Strength sub-Continental Mantle

Précigout Jacques¹, Hirth Greg² & Kunze Karsten¹

¹ ETHZ, Geologisches Institut, Sonneggstrasse 5, CH-8092 Zürich, Switzerland (jacques.precigout@erdw.ethz.ch)

² Brown University, Department of Geological Sciences, Providence RI 02912, USA

Experimental rheological laws of olivine predict the presence of high-strength lithosphere mantle beneath the continental crust (Brace & Kohlstedt, 1980). Analogue and numerical models have shown that such a stiff uppermost mantle - stronger than the crust - is required to form a subduction or a narrow continental rift (Gueydan et al., 2008). In contrast, based on “indirect” geophysical observations, recent studies concluded for a sub-continental mantle weaker than the crust (Thatcher & Pollitz, 2008). In this study, we document data of olivine Lattice Preferred Orientation (LPO) in the Ronda continental peridotite (southern Spain) that provide new constraints on the mantle strength through “direct” observations. The Ronda massif exposes 300 km² of sub-continental peridotites that were exhumed in the internal Betics during the Oligocene-early Miocene. During their exhumation, they suffered intense ductile deformation that formed a kilometre-scale mylonite beneath a strongly thinned continental crust. This mylonite of extremely condensed peridotites deformed at about 850-900 °C during decompression from 18 to 10 kbar (Morishita et al., 2001). Across this domain, olivine LPOs revealed changing slip system of dislocations from A-type fabric ((010)[100]) to B-type fabric ((010)[001]) toward the overlying crust. Based on recent experimental data (Jung et al., 2006), A-type fabric implies low-stress deformation of anhydrous olivine (< 400 MPa), while B-type fabric characterizes olivine deformation at more than 400 MPa of differential stress, regardless of the water content. The occurrence of high-stress deformation in the sub-crustal Ronda peridotite confirms therefore the prediction of high-strength mantle beneath the continental crust. Nonetheless, by comparing the deformation conditions of the Ronda mylonite (850 °C and 400 MPa) with the predicted strength of the mantle lithosphere, these results suggest that olivine rheological laws largely underestimate the «real» strength of the sub-continental mantle.

REFERENCES

- Brace, W. F. & Kohlstedt, D. L. 1980: Limits on Lithospheric Stress Imposed by Laboratory Experiments. *Journal of Geophysical Research* 85, 6248-6252.
- Gueydan, F., Morency, C. & Brun, J.-P. 2008: Continental rifting as a function of lithosphere mantle strength. *Tectonophysics* 460, 83-93.
- Jung, H., Katayama, I., Jiang, Z., Hiraga, T. & Karato, S.-I. 2006: Effects of water and stress on the lattice-preferred orientation of olivine. *Tectonophysics* 421, 1-22.
- Morishita, T., Arai, S. & Gervilla F. 2001, High-pressure aluminous mafic rocks from the Ronda peridotite massif, southern Spain: significance of sapphirine- and corundum-bearing mineral assemblages. *Lithos* 57, 143-161.
- Thatcher, W. & Pollitz, F. F. 2008 : Temporal evolution of continental lithospheric strength in actively deforming régions. *GSA Today* 18, 4-11.

1.30

Low-temperature thermochronological constraints on the Miocene exhumation of the Adamello Complex, Southern Alps, Italy

Reverman Rebecca L. ¹, Fellin M. Giuditta¹ & Willett Sean D. ¹

¹ Eidgenössische Technische Hochschule Zürich, Switzerland (rebecca.reverman@erdw.ethz.ch)

The Adamello Complex is the largest of the Periadriatic intrusions and is located at the intersection of the Periadriatic Fault System (locally called the Tonale line) and the South Giudicarie line. More than seven kilometers of overburden has been removed since its emplacement in the late Eocene-early Oligocene and modern overall relief is over 2 km. Major rivers which dissect the complex flow into overdeepened valleys inferred to be areas of maximum incision from the Messinian Salinity Crisis (MSC). This makes it an ideal location to determine the role and magnitude of inferred tectonic events (Giudicarie phase shortening in the late Miocene) and superimposed erosional events driven by climatic or other external environmental conditions (MSC and Neogene glaciation) as drivers of near surface exhumation.

Low-temperature thermochronometers, such as, apatite (U-Th-Sm)/He dating (AHe) and apatite fission-track dating (AFT), constrain near-surface (<5 km) exhumation rates that can be used to characterize climate or tectonic forcing. In this study we present AHe and AFT ages for samples collected in the two largest valleys of the Adamello Complex. The ages determined in this study span the Miocene and display a normal age-elevation relationship, where age increases with elevation. All AFT ages along with the high elevation (3600-2700 m) AHe samples record early to mid-Miocene ages, while samples located below 2700 m record nearly identical AHe ages, within error, of 6.5 ± 1 Ma. This pattern reveals the possible base of an exhumed AHe partial retention zone located at a modern elevation of ~2700m, which suggests that a minimum of 3-4 km of exhumation has occurred since ~8 Ma.

The fast cooling of the low elevation samples as recorded by their AHe ages indicate that at least 2 km of rock was exhumed rapidly between 8-6 Ma. The magnitude and timing of this event suggested by our results constrain a period of transpressional activity along the South Giudicarie line and Val Trompia thrust inferred from thermal modelling of fission-track data from the area and structural evidence (Castellarin et al., 2006; Martin et al., 1998). Furthermore, the ages were modelled using Pecube (Braun, 2003), a 3-D heat conduction model including topographic relief and erosion and the recently developed GLIDE program (Fox et al., 2010), which extracts exhumation rates from thermochronological data. Both models confirm a rapid increase in exhumation rates at ~8 Ma and continuing until ~6 Ma.

REFERENCES

- Braun, J. 2003: Pecube: a new finite-element code to solve the 3D heat transport equation including the effects of time-varying, finite amplitude surface topography. *Computers & Geosciences* 29, 787–794.
- Castellarin, A., Vai, G. B. & Cantelli, L. 2006: The Alpine evolution of the Southern Alps around the Giudicarie faults: A late Cretaceous to Early Eocene transfer zone. *Tectonophysics* 414, 203–223.
- Fox, M., Herman, F. & Willet S.D. 2010: The Inversion of Low-Temperature Thermochronometry to Extract Spatially Varying Exhumation Rates. *EGU Geophysical Research Abstracts* 12 EGU2010-1167.
- Martin, S., Bigazzi, G., Zattin, M., Viola, G. & Balestrieri, M. L. 1998: Neogene kinematics of the Giudicarie fault (Central-Eastern Alps, Italy): new apatite fission-track data. *Terra Nova* 10, 217–221.

1.31

Influence of continents in mantle convection models with self-consistent plate tectonics

Rolf Tobias¹, Tackley Paul¹

¹*Institute of Geophysics, ETH Zürich, Sonneggstrasse 5, CH-8092 Zürich (tobias.rolf@erdw.ethz.ch)*

It is now well accepted that mantle convection and plate tectonics form an integrated system and cannot be treated independently. Although this is a promising improvement in understanding Earth, there is still a striking feature, which is nowadays not yet included in this integrated system, namely the existence of a lithospheric heterogeneity - in other words - the difference between oceans and continents.

The present study focusses on the effect of continents in a model of self-consistent plate tectonics in spherical geometry. As a simplification these continents are realized as strong cratons with homogeneous composition and they differ from the rest of the mantle in buoyancy and rheology. In contrast to many former studies where continents are idealized as rigid and/or immovable units, we treat continents in the same manner as normal mantle, but with different physical properties. Numerically a tracer approach is used, which allows more consistent movement and deformation of the continents.

It has been shown before that continents might have a first-order effect on the dynamics of the Earth as they might modulate convective wavelength, surface heat loss and - due to thermal insulation - the internal temperature. Increasing the latter causes a decrease in convective stresses and we studied how this effect strengthens the lithospheric lid, what finally leads to a transition from mobile lid to stagnant lid convection. Existence and timescale of this transition depend on the initial strength of the lithosphere and are most sensitive to internal temperature variations, but less sensitive to relative continental buoyancy.

The mentioned transition will be studied into more detail. A question of particular interest is, if the system behaviour changes, if the continents are no longer embedded in the thermal boundary layer. For answering this question it is necessary to modify the rheology of the continental material, namely to consider a viscosity, that depends on composition, and to make sure that continents are initially cold.

1.32

Accretionary wedge dynamics: A numerical approach

Ruh Jonas B.¹, Kaus Boris J.P.², Burg Jean-Pierre¹

¹ Geological Institute, Sonneggstrasse 5, CH-8092 Zurich (jonas.ruh@erdw.ethz.ch)

² Institute of Geophysics, Sonneggstrasse 5, CH-8092 Zurich

Subduction accretion adds material to the front of a convergent margin by thrusting and stacking sediment onto the subducting plate. Accretionary wedges have been the focus of much investigation because they provide key information on sediment deformation in a generally submarine and tectonically active environment. Because most of the modern accretionary wedges are not exposed on land (Barbados, Costa Rica, Nankai, Gulf of Cadiz, Eastern Mediterranean), their large-scale characteristics are interpreted from seismic profiles (e.g. Grando and McClay, 2007), and their bulk behaviour and growth is commonly simulated in analogue experiments (e.g. Smit et al., 2003). Based on a wealth of data, principally due to Oceanic Deep Sea Drilling, we believe that accretionary wedges form over a major décollement. Off-scraping removes material from the subducting plate and the wedge grows both vertically and horizontally by addition of oceanic sediment and shallow crustal material.

An important characteristic of accretionary wedges is the contemporaneous activity of deformation and sedimentation, which leads to the formation of growth structures (Figure 1).

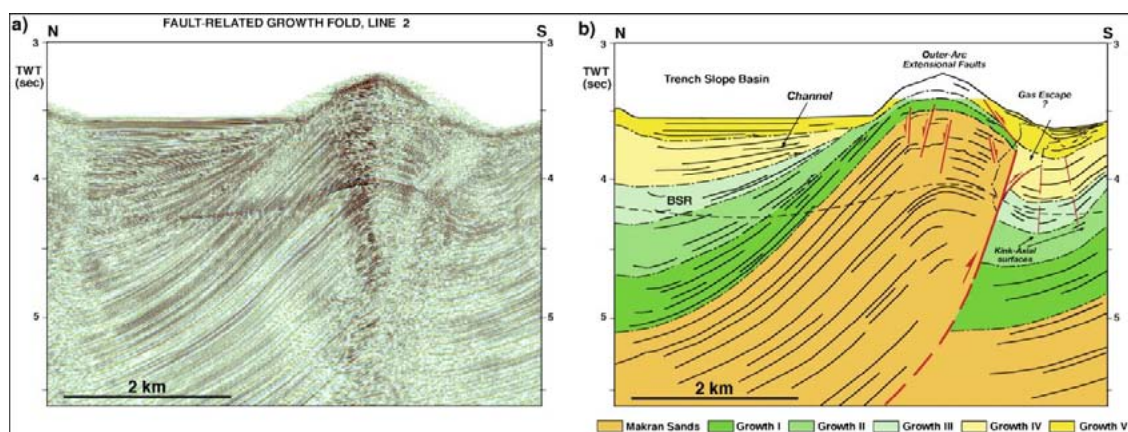


Figure 1. Interpreted seismic profile of an imbricated fan segment offshore Makran from Grando and McClay (2007) indicating progressive unconformity development on the back limb of growing fault-propagation folds. Vertical exaggeration is ~ 2 , as 1 s (TWT) is ~ 1.1 – 1.2 km depth.

One of the biggest and still active accretionary complex is Makran, in Iran and Pakistan. The essentially Eocene–Holocene wedge results from the still on-going subduction of the oceanic lithosphere flooring the Gulf of Oman. The present shore-line follows a complex fault zone that approximately separates an active, submarine and frontal southern half from a less active, exposed northern half. Water provided by dewatering of the accreting sediments apparently lubricates the basal décollement.

The influence of surface processes on thrust wedges has drawn increasing attention during recent years: Experimental studies have tested the effects of syntectonic erosion and sedimentation on the mass distribution in the wedge and thus its geometry and evolution (e.g. Barrier et al., 2002). However, these models do not satisfactorily explain the geometry of growth strata cropping out in Makran, their relation to thrusting, and their influence on wedge dynamics. One reason is that most current models of thrust wedges are derived from purely frictional experimental studies in which syntectonic erosion and sedimentation are included either as a predefined temporal or continuous mass redistribution or as a static system of evolving thrusts and growing folds.

Fieldwork on the Iranian Makran led us to identify several types of growth structures in the Miocene–Pliocene sequences, documenting complex relationships between sedimentation and regional tectonics. From our field observations we noticed that these growth structures and the related thrusts and folds are also not satisfactorily explained by existing numerical models.

We present results of new 2D numerical models in which we test the influence of sedimentation in thrust wedges and the interplay between thrusts, folds and growth strata both at wedge scales and at the scale of single structures (Figure 2). We use a visco-elastoplastic finite element code to simultaneously take the brittle overburden and the ductile substratum into account, which in the Makran is formed by shale-rich (at least initially) water-saturated soft units like marls.

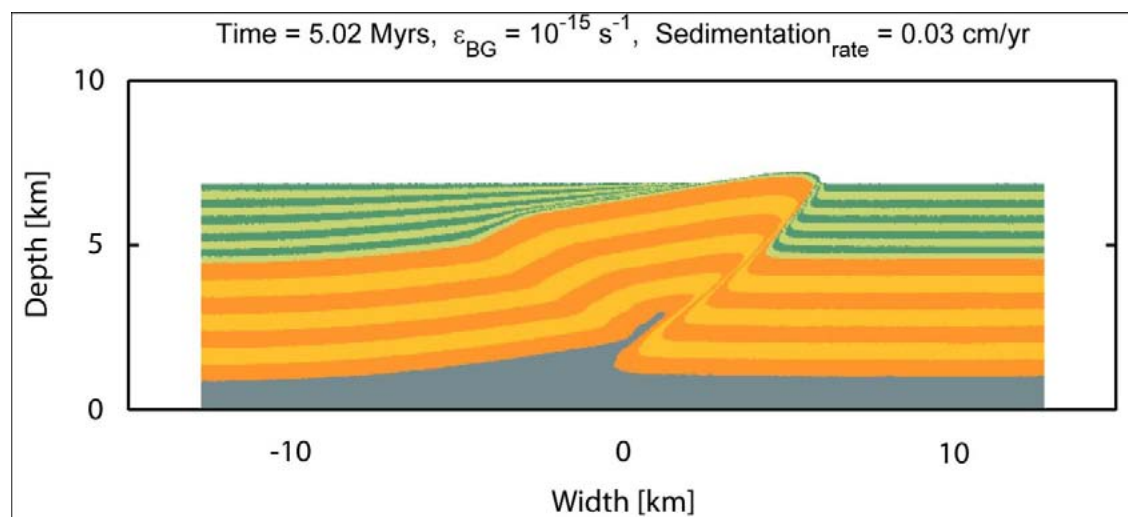


Figure 2. Numerical model with a ductile décollement (grey layer) and brittle overburden. Pre-growth sediments have reddish-yellowish stripes, growth strata is defined by greenish colours. Syn-deformational sedimentation leads to progressive unconformities on the back limb of a faulted detachment fold.

REFERENCES

- Grando, G. and K. McClay (2007). "Morphotectonics domains and structural styles in the Makran accretionary prism, offshore Iran." *Sedimentary Geology* 196(1-4): 157-179.
- Smit, J. H. W., J. P. Brun, et al. (2003). "Deformation of brittle-ductile thrust wedges in experiments and nature." *Journal of Geophysical Research-Solid Earth* 108(B10): 2480.
- Barrier, L., T. Nalpas, et al. (2002). "Influence of syntectonic sedimentation on thrust geometry. Field examples from the Iberian Chain (Spain) and analogue modelling." *Sedimentary Geology* 146(1-2): 91-104.

1.33

Tectono-thermal evolution of the Atlas system (SW Morocco), insights from low-temperature thermochronology and Raman spectroscopy on carbonaceous material

Ruiz Geoffrey¹, Negro Francois², Babault Julien³, Frizon de Lamotte Dominique⁴, Stuart Fin⁵, Stockli Dani⁶, Foeken Jurgen⁷, Sebti Samira⁸, Saddiqi Omar⁸, Di Nicola L.5 & Thomsen Tonny⁹

¹ IMG, Uni. Lausanne, CH-1015 (geoffrey.ruiz@unil.ch)

² CHYN, CH-2009 Neuchâtel

³ UAB, Spain

⁴ Uni. Cergy-Pontoise, France

⁵ SUERC-Glasgow, UK

⁶ Uni. Kansas, USA

⁷ VU Amsterdam, NL

⁸ Uni. Casablanca, Morocco

⁹ Uni. Stockholm, Sweden

In Morocco, the High and Middle Atlas of Morocco are intra-continental fold-thrust belts situated in the southern foreland of the Rif orogen (Fig. 1). It is a key natural laboratory because it 1) is the southern and westernmost expression of Alpine-Himalayan orogeny, and 2) possibly encompasses Pre-Cambrian to recent evolution of the region. Phases of shortening and exhumation of this orogen remain however ill constrained and the few available quantitative data do not allow the present-day high topography (over 4000m) to be explained. In order to put constraints on the recent orogenic growth of the Atlas system, we investigated the temperature-time history of rocks combining extensive low-temperature thermochronological analysis (Fission tracks and (U-Th)/He on zircon and apatite) and peak temperature estimation by Raman spectroscopy of carbonaceous material (RSCM) and U-Pb ages. The target area is a NE-SW oriented transect crossing the different structural segments of the western Atlas away from present-day fault systems (Fig. 1). Results are much contrasted from one domain to the other. Pre-Cambrian bedrocks from the Anti-Atlas domain yield old Fission-Track ages on zircon (340-300 Ma), apatite (180-120 Ma) but also U-Th/He (150-50 Ma) still on apatite. These datasets are interpreted, with

the help of thermal modelling, to record passive margin up and down movements during the break-up of the Pangea. U-Th/He pair dating on both apatite (80-55°C) and zircons (200-160°C) minerals are much younger in the High-Atlas once the Tizi N°Test Fault System (TNT), or SAF (Fig. 1) passed to the north, ranging between ~35-5 Ma and 85-30 Ma respectively. Similarly, maximum peak temperatures vary across the TNT, with maximum temperatures of 500-450°C in the axial zone and less than 250-200°C in the Souss plain to the south. Once all datasets combined, they indicate that uplift occurred in the Axial Zone in the Oligocene due to tectonic inversion and crustal shortening and remain constant since allowing a 6-7 km thick pile to be eroded. Low-thermochronological analyses have also been performed on Cretaceous deposits in the region. Results indicate that these deposits have been reset to temperatures greater than 80°C. This suggests that a post Cretaceous sedimentary pile of at least 3 km in thickness is missing, and as a result that a 3-4 km thick pile of substratum have been eroded in the Axial Zone. Our extensive thermochronological dataset provide for the first time constraints that evidence heterogeneous exhumation history across and along the chain. All these constraints are put together with structural, geochemical and geophysical informations to discuss the recent tectono-thermal evolution of the Atlas system in the frame of the Africa-Europe convergence and thinning of the lithosphere.

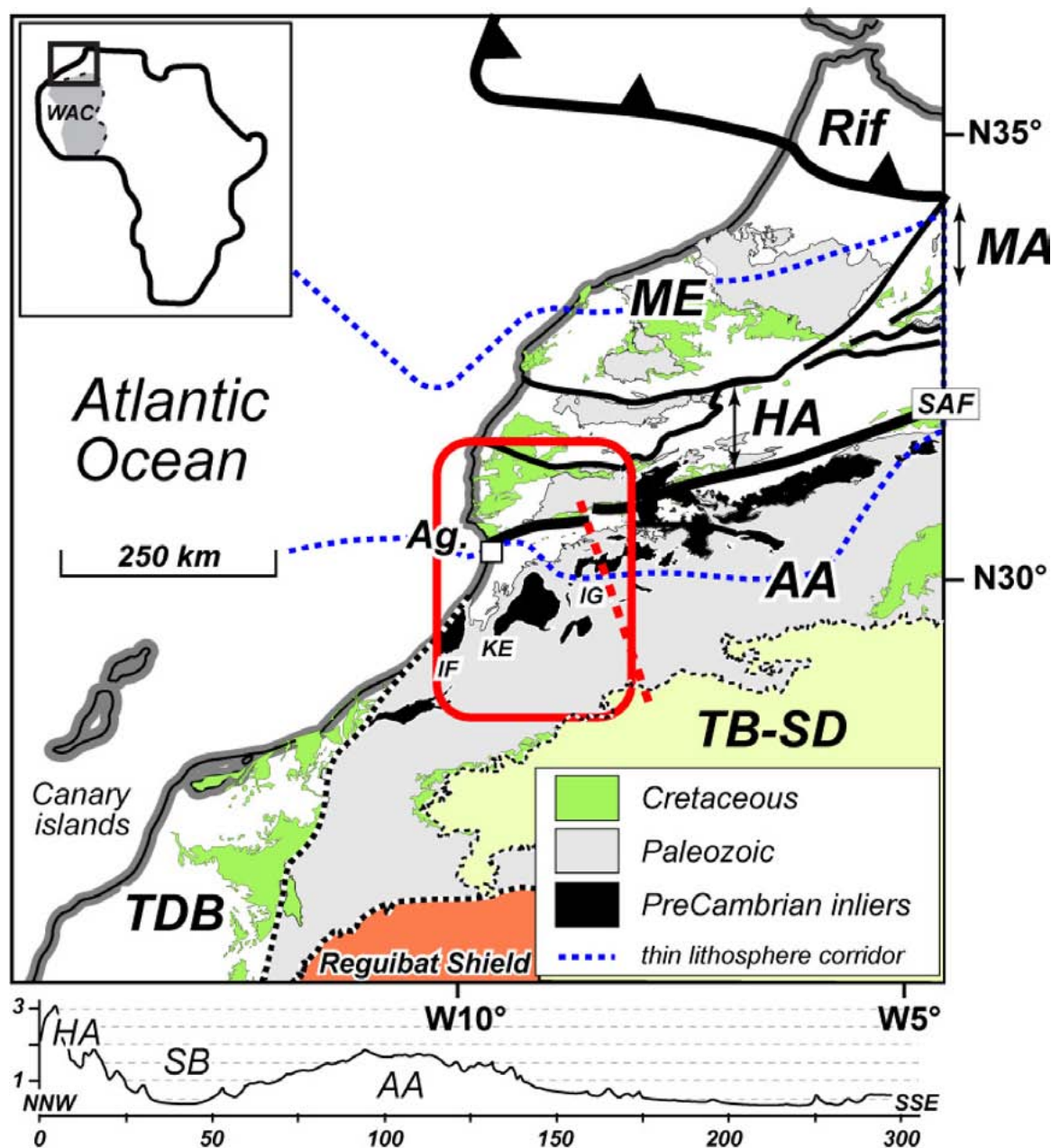


Figure 1. Top: Schematic map of northern Africa showing the main domains in Morocco, i.e. from north to south Rif-Tell, Meseta (ME), Middle-Atlas (MA), High-Atlas (HA), Anti-Atlas (AA), Tindouf Basin (TB) -Saharan Domain (SD) and Reguibat Shield towards the West Africa Craton (WAC) and finally the Tarfaya-Dakhla Basin (TDB) to the SW along the Atlantic Ocean. The studied area (red rectangular) south of Agadir corresponds to the western segment of the Atlas system than encompasses Precambrian inliers, i.e. the Ifni (IF), Kerdous (KE) and Igherm (IG) within the Paleozoic Anti-Atlas domain. SB: Souss Basin. Ag.: Agadir. Thin dashed blue line: corridor for <110 km thick lithosphere (Fullea et al., in press). Bottom: Topographic profile across the region against the strike of the orogen (x10 vertical exaggeration) - see thick dashed red line for location, horizontal and vertical axis in kilometres.

1.34

Strain accumulation during basal accretion – case study Suretta nappe (eastern Switzerland)

Scheiber Thomas, Pfiffner O. Adrian, Schreurs Guido

Institut für Geologie, Baltzerstrasse 3, CH-3012 Bern (scheiber@geo.unibe.ch)

Using a field-based approach we investigate basal accretion processes in the Alps to better understand the stacking of crystalline basement nappes as observed in the core of many orogens. In eastern Switzerland, the Suretta nappe comprises a stack of lithospheric slices derived from the Briançonnais domain and assembled in a south-dipping subduction zone during the Cenozoic orogenic cycle. The present axial plunge of about 30° towards the ENE exposes the basal thrust of the Suretta nappe over tens of kilometres and provides nearly continuous outcrop from bottom to top of the nappe.

In order to understand fold-thrust relationships in the Suretta nappe, a partial retro-deformation was performed, because the Eocene top north directed stacking (Ferrera phase after Milnes & Schmutz, 1978; Schmid et al, 1997) predates a phase of backfolding (Niemet-Beverin phase).

Emphasis was laid on the frontal part of the nappe composed essentially of late to post-Variscan intrusive rocks of the Rofna porphyry complex. Detailed structural mapping combined with strain analyses using the center-to-center (Fry) method based on the distribution of K-feldspar clasts (Genier and Epard, 2007) yield different strain patterns of the porphyry.

In the lower and interior parts of the nappe, weakly to undeformed boudins are generally surrounded by L-tectonites indicating WSW-ENE stretching; foliated equivalents reveal various strain intensities. The upper part of the nappe which was strongly affected by retro-shearing and backfolding generally shows higher strains. In this part of the nappe, the dominant WSW-ENE constrictional strain is overprinted by a more N-S directed stretching component. This leads to an oblate finite strain ellipsoid.

Mylonites were not only detected at the base of the Suretta nappe, but also at the base of internal thrust slices overlying strongly deformed autochthonous Triassic sediments ("nappe separators"). These mylonites bear NW-SSE trending stretching lineations, which are related to Ferrera phase nappe stacking. Despite the fact that shear sense indicators are generally rare, a top-to-the NNW directed transport can be assumed. Thrust-related deformation took place in a temperature regime of about 400°C where quartz deformed by dislocation creep and feldspar was the stronger mineral. Intercalations of Triassic sediments in the upper parts of the nappe that could be interpreted as isoclinal folds at first sight seem to be influenced by thrust tectonics as well.

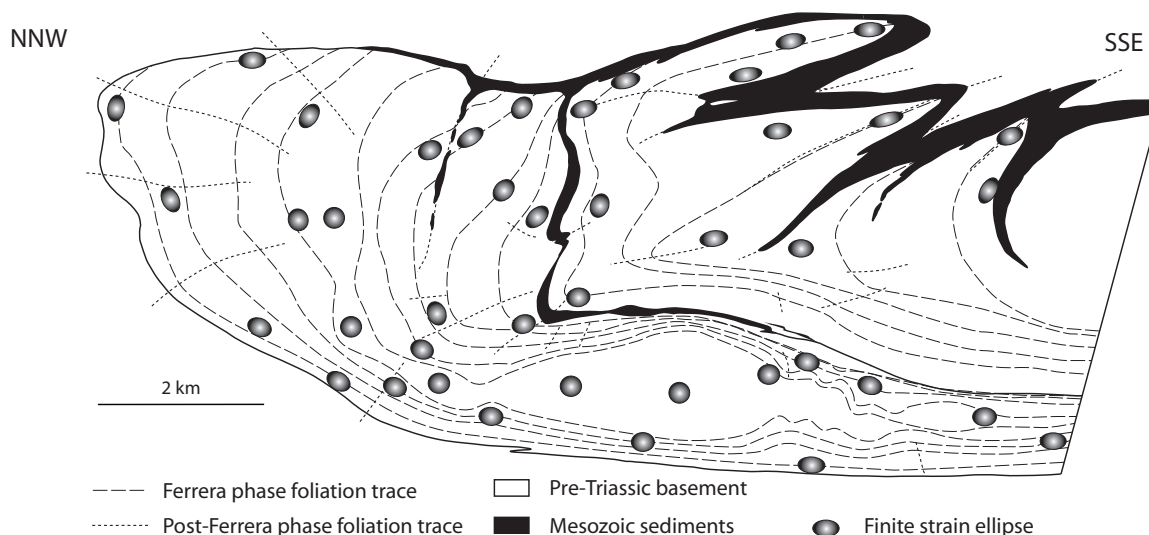


Figure 1. Finite strain ellipses in the Suretta nappe (cross-sectional view).

REFERENCES

- Schmid, S. M.; Pfiffner, O. A.; Schreurs, G. 1997: Rifting and collision in the Penninic Zone of eastern Switzerland. Deep Structure of the Swiss Alps: Results of NRP 20, Birkhäuser Verlag: 160-185.
- Milnes, A.G. & Schmutz, H.-U. 1978: Structure and history of the Suretta nappe (Pennine zone, Central Alps) – a field study. *Eclogae geologicae Helveticae*, 71/1, 19-33.
- Genier, F.; Epard, J.L. 2007: The Fry method applied to an augen orthogneiss: Problems and results. *Journal of Structural Geology*, 29, 209-224.

1.35

Structural and cooling history of the Eastern Pelagonian metamorphic core complex (northern Greece)

Schenker Filippo Luca¹, Fellin Maria Giuditta, Burg Jean-Pierre.

ETHZ, Department of Earth Sciences, Sonneggstrasse 5, CH-8092 Zürich

¹ (filippo.schenker@erdw.ethz.ch)

The Pelagonian Zone in continental Greece is the westernmost unit of the Internal Hellenides and is characterized by a structural and topographic high trending approximately NNW-SSE. We present mapping, petrographic, structural and thermochronologic data that are evidence of a metamorphic core complex in the eastern part of the Pelagonian. The area lies north and east of the Aliakmon River artificial lake (between the village of Servia in the west and the village of Kolindros in the east). The denuded metamorphic dome is about 20 x 15 km with the long axis striking NNW-SSE.

The main lithologies (gneiss, marbles and amphibolites) show a shallow-dipping foliation whose bending defines the dome. On the foliation plane aligned micas and amphiboles, and elongated quartz and feldspar form a pervasive lineation that trends SW-NE. The systematic record of asymmetric structures in the XZ-plane of finite strain ellipsoid indicates two senses of shear: (i) a regional top-to-the-SW sense of shear (Direction: $243^{\circ} \pm 25$; Plunge: $8^{\circ} \pm 15$) characterized by a strain gradient from protomylonite to ultramylonite, and related to recumbent, isoclinal and occasional sheath folds; (ii) a top-to-the-E sense of shear (Direction: $88^{\circ} \pm 20$; Plunge: $11^{\circ} \pm 16$) found in narrow (20 to 100 m) low angle shear zones located on the eastern flank of subdomes. In the footwall of the top-to-the-E detachments, migmatitic orthogneisses and amphibolites vary from metatexite, with partial melting associated with folding, to diatexite. Leucosomes cut the main foliation. Thus, the metamorphic peak and the main fabric-forming event are coeval.

Zircon fission-track ages of about 24 Ma on both sides of the top-to-the-E shear zones show that the ductile fabric is older than the late Oligocene. Fission-track data on apatites indicate cooling at $<110^{\circ}\text{C}$ during the early to middle Miocene. These cooling ages show that extensional tectonics in the Pelagonian were contemporaneous with the Aegean extension (Mykonos, Naxos, etc.).

1.36

Quantitative comparisons of analogue thrust wedge experiments

Guido Schreurs¹, Susanne Buitert² and the GeoMod2008 Analogue Team³

¹ Institute of Geological Sciences, University of Bern, Switzerland (schreurs@geo.unibe.ch)

² Geological Survey of Norway (susanne.buitert@ngu.no)

Analogue (sandbox) experiments have a long history of modelling orogenic wedge processes, examining, for example, out-of-sequence thrusting, surface slope evolution and the roles of basal friction or surface processes. However, as for all models, their results bear a signal of the initial conditions, the choice of materials, the modelling apparatus and the technique of building model. This may make it difficult to compare model results directly. In order to evaluate the variability among models and to appraise the reproducibility and limits of interpretation, we have performed a direct comparison of experimental results of 15 analogue modelling laboratories for three different thrust experiments. Our quantitative analysis of the results has direct implications for comparisons between structures in analogue models and natural field examples.

All laboratories used the same frictional analogue materials (quartz and corundum sand) and model-building techniques (sieving rate, sieving height and levelling). Although each laboratory used its own experimental apparatus, the same type of self-adhesive Alkor foil was used to cover the base and the four vertical walls of the experimental apparatus in order to guarantee identical shear stresses at the boundaries. Temperature and humidity was not controlled and was found to have varied between laboratories.

Three experimental set-ups using only brittle frictional materials were examined (Fig. 1). In each of the three set-ups, the model was shortened by a vertical wall, which moved with respect to the fixed base and the three remaining sidewalls. The minimum width of the model (dimension parallel to mobile wall) was prescribed at 25 cm. In the first experimental set-up (experiment 1A, Fig. 1), a quartz sand wedge with a surface slope of $\sim 20^{\circ}$ was pushed by a mobile wall. All models

conformed to the critical taper theory, maintained a stable surface slope and did not show internal deformation. In the next two experimental set-ups (experiments 1B and 2, Fig. 1), a horizontal sand pack consisting of alternating quartz sand and corundum sand layers was shortened from one side by the mobile wall. In experiment 2 a thin rigid sheet covered part of the model base and was attached to the mobile wall (i.e. a basal velocity discontinuity distant from the mobile wall)

In experiment 1B a basal rigid sheet was absent and the basal velocity discontinuity was located at the mobile wall. In both experiments, models accommodated initial shortening by forward- and backward-verging thrusts. In all experiments, boundary stresses created significant drag of structures along the sidewalls. We therefore compared the surface slope and the location, dip angle and spacing of thrusts in sections through the central part of the model.

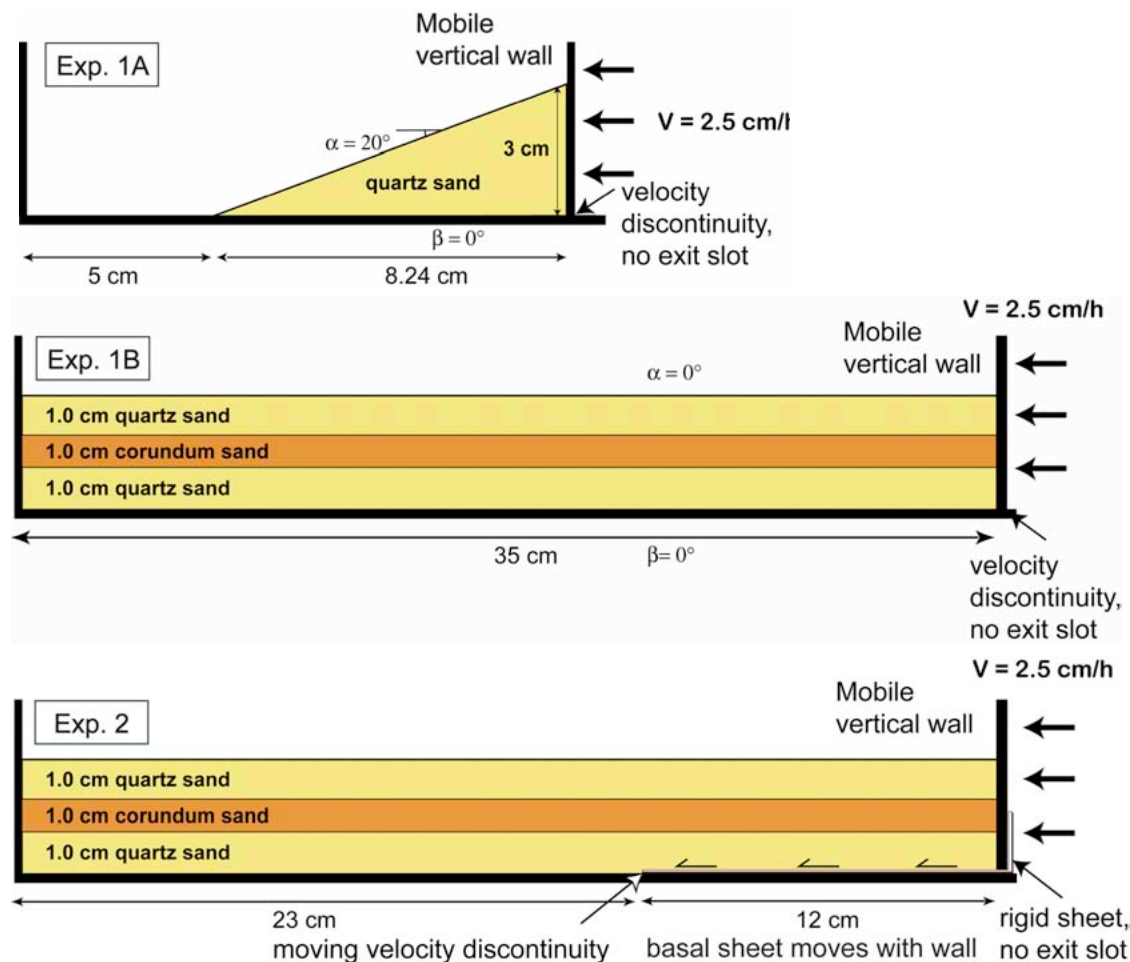


Fig. 1. Experimental set-ups used in our analogue model comparisons

All analogue models show similar cross-sectional evolutions demonstrating reproducibility of first-order experimental observations. Forward shear zones in the models develop at Mohr-Coulomb dip angles. However, the surface slopes of experiments 1B and 2 do not reach a critical taper. In addition, we find significant along-strike variations of structures in map view, highlighting the limits of interpretations of analogue model results. These variations between models may be related to model width, differences in laboratory climatic conditions and/or “the human factor”. The latter may result in small differences in model building techniques and therefore in models with slightly heterogeneous layer densities, which would affect the mechanical properties of the granular material.

³ GeoMod2008 Analogue Team: Caroline Burberry, Jean-Paul Callot, Cristian Cavozi, Mariano Cerca, Ernesto Cristallini, Alexander Cruden, Jian-Hong Chen, Leonardo Cruz, Jean-Marc Daniel, Florian Hofmann, Victor H. Garcia, Caroline Gomes, Céline Grall, Yannick Guillot, Cecilia Guzmán, Triyani Nur Hidayah, George Hilley, Chia-Yu Lu, Matthias Klinkmüller, Hemin Koyi, Jenny Macauley, Bertrand Maillot, Catherine Meriaux, Faramarz Nilfouroushan, Chang-Chih Pan, Daniel Pillot, Rodrigo Portillo, Matthias Rosenau, Wouter P. Schellart, Roy Schlische, Andy Take, Bruno Vendeville, Matteo Vettori, M. Vergnaud, Shih-Hsien Wang, Martha Withjack, Daniel Yagupsky, Yasuhiro Yamada

1.37

Seismic Atlas of the Swiss Molasse Basin : two example transects across the western and the eastern parts.

Sommaruga Anna¹, Eichenberger Urs¹ & Marillier François¹

¹ UNIL, Institut de géophysique, Amphipôle, CH-1015 Lausanne, Switzerland. (anna.sommaruga@unil.ch)

A regional seismic synthesis based on the interpretation of reflection profiles from the oil industry was conducted on the Swiss Plateau as a multiyear project of the Swiss Geophysical Commission. It will result in the publication by swisstopo of a "Seismic Atlas of the Swiss Molasse Basin" that will include more than 20 large printed plates. The interpreted seismic lines (263 lines representing a total of 4358 km) cover the entire Swiss Molasse Basin from Canton Geneva to Lake Constance. These lines represent about 1/3 of all the ones shot in Switzerland since the sixties into the nineties. The western part of the Molasse Basin is especially well covered because of a larger number of surveys carried out there (especially in the Cantons of Vaud and Fribourg). In eastern Switzerland, less surveys resulted in broader seismic line spacing. More than 20 deep wells helped calibrating the seismic interpretation.

Only few seismic lines are publicly available. They include a small number of very deep reaching seismic lines, along two Alpine traverses, from a Swiss National Science Foundation project (NFP20), oil industry lines older than 10 years collected in Canton Vaud, lines published by NAGRA, lines published in scientific papers and 52 oil industry seismic lines deposited in 1992 at the geological archive of swisstopo. The public lines all together add up to a 15% of the total number of 2D lines ever shot in Switzerland. The rest is confidential.

The seismic interpretation focussed on Mesozoic units and faults affecting them. It took into account larger features within the pre-Mesozoic and Tertiary units and was carried out entirely on paper seismic sections (at 1:25'000 or 1:20'000 scale). Eight seismic horizons were interpreted and correlated between intersecting lines: Near Base Tertiary, Near Base Cretaceous/Near Top Late Malm, Intra Early Malm, Near Top Dogger, Near Top Liassic, Near Top Late Triassic, Near Top Early Triassic, and Near Base Mesozoic. The horizons were digitized and introduced in a GIS data base. The digitized horizons were first adjusted to a common reference level of 500 m. Because of differing parameters used by the several companies that processed the data some two-way travel time (TWT) offsets (so-called "misties") remained between seismic sections of different surveys. Misties were reduced with a procedure that minimized their mean values over the entire data set. For each interpreted seismic horizon a TWT map was computed by kriging. The TWT maps were converted to depth using seismic velocity maps elaborated from well data. From the depth maps, vertical thickness maps were computed for the following units: Quaternary and Tertiary, Cretaceous, Late Malm, Early Malm, Dogger, Liassic, Late Triassic, Early Triassic.

In addition to the TWT-, velocity- and depth maps, the Seismic Atlas will contain 15 transects across the Swiss Molasse Basin. Thirteen transects are dip sections at 1:80'000 scale extending from the foot of the Jura Mountains to the Subalpine Molasse and the Alpine nappes. Two transects are strike sections that extend across the entire Swiss Molasse Basin from Canton Geneva to Lake Constance at a scale 1:250'000 with vertical exaggeration (1:80'000 in vertical scale). Each transect plate includes three sections: on top, the seismic profile (in TWT) that is a composed seismic section without interpretation in order to display the quality of the available seismic data; in the centre, the geological interpretation superimposed on the seismic section (in TWT) with the wells and only seismically supported elements (horizons and faults) within the Tertiary, the Mesozoic and the Pre-Mesozoic units; at the bottom, the depth converted seismic section is shown with additional features (conceptual faults and horizons) based on geological information (geological maps, well reports, published papers, confidential reports). The identified seismic reflections are differentiated in three quality classes: well defined, fairly well defined and poorly defined. A similar classification is introduced for faults but with only two classes: well defined and fairly well to poorly defined. All these criteria apply to the Tertiary and Mesozoic units, whereas different quality classes are defined in the pre-Mesozoic (reflective, intermediate and non-reflective zone), because of the poorer quality of the seismic data in this unit.

The poster will present two selected transects, one from the eastern and one from the western part of the Swiss Molasse Basin. These two transects highlight the stratigraphical and structural differences between the western and the central to eastern parts of the basin. Based on these transects, new insights and important conclusions can be drawn despite a somewhat unevenly distributed data set (looser grid in the central and eastern parts). The western area, comprising the Cantons of Geneva, Vaud, Fribourg and parts of Canton Bern, displays thicker Mesozoic strata, thicker Triassic evaporitic beds and more Mesozoic normal, reverse and tear faults than the central and eastern parts. Little evidence is found for faults extending over long distances. Rather, en echelon fault patterns appear to be the dominant structural style. In the western most part, structures in the Mesozoic sequence are characterized by generally NE-SW oriented synclines and anticlines of low amplitude, with cores of Middle-Early Triassic evaporite layers. The latter represent the detachment zone of the western

Swiss Molasse Basin. Tertiary sediments within the Plateau Molasse are slightly folded (very low amplitude) requesting a detachment horizon at the base of the Tertiary unit or within shaly beds of this unit. In the Subalpine Molasse, folds are related to thrust faults rooting at the Base Tertiary strata.

By contrast to the western area, Cretaceous unit layers were not preserved in the central and eastern areas. There, Triassic evaporites are reduced to a few tens of meters in some locations. Below the Plateau Molasse, a few normal or reverse faults occur. They represent the major structures within the Mesozoic beds. However, below the Subalpine Molasse and the Alpine nappes, south of Lake Lucerne and Lake Zürich, many more of such faults are observed within the Mesozoic units. At Tertiary level, the strata are displaced along thrusts and back-thrusts, representing a triangle zone. These faults root in a detachment level within the Tertiary sequence. In the easternmost part of the Swiss Molasse Basin, we observe normal faults cutting through Mesozoic and Palaeozoic units. This area is (was) clearly under extension. The transition from the eastern to the western Molasse Basin structures takes place in Canton Bern. Unfortunately, in that area the density of data is low and the quality of seismic lines is poor.

1.38

Modelling the thermo-chemical evolution of the interiors of Earth, Venus, Mars, Mercury and super-Earths

Tackley Paul, Nakagawa Takashi, Armann Marina, Keller Tobias, van Heck Hein

Institut für Geophysik, ETH Zürich, Sonneggstrasse 5, 8092 Zürich (ptackley@ethz.ch)

The latest generation of the global 3-D spherical convection model StagYY [Tackley, PEPI 2008] allows the direct computation of a planet's thermo-chemical evolution, including self-consistent lithospheric behavior (e.g., rigid lid, plate tectonics, or episodic plate tectonics [van Heck and Tackley, GRL 2008]), chemical differentiation induced by melting, large viscosity variations, a parameterized core heat balance, and a realistic treatment of phase diagrams and material properties. Global models allow the computation of planetary secular cooling including prediction of how the core heat flux varies with time hence the evolution of the geodynamo, and possible transitions in plate tectonic mode. Modern supercomputers and clusters allow increasingly higher resolution, with up to 1.2 billion unknowns possible on only 32 dual-processor nodes of an opteron cluster. In ongoing research, this tool is being applied to understand the evolution of Earth, Mars, Venus, Mercury, and super-Earths. Studying several bodies using an integrated approach facilitates a more systematic and holistic understanding of planetary behaviour both inside and outside our solar system.

With our Venus models we are studying the modes of heat loss, the origin of the inferred surface age and understanding the admittance (gravity/topography) ratio. Of particular interest is whether a smooth evolution can satisfy the various observational constraints, or whether episodic or catastrophic behaviour is needed, as has been hypothesised by some authors. Simulations in which the lithosphere remains stagnant over the entire history indicate that over time, the crust becomes at least as thick as the mechanical lithosphere, and delamination occurs from its base. The dominant heat transport mechanism is magmatic. A thick crust is a quite robust feature of these calculations. Higher mantle viscosity results in larger topographic variations, thicker crust and lithosphere and higher admittance ratios; to match those of Venus, the upper mantle reference viscosity is about 10^{20} Pa s and internal convection is quite vigorous. The most successful results in matching observations are those in which the evolution is episodic, being in stagnant lid mode for most of the evolution but with 2-3 bursts of activity caused by lithospheric overturn. If the last burst of activity occurs ~1 Ga before present, then the present day tends to display low magmatic rates and mostly conductive heat transport, consistent with observations. In ongoing work we are examining the effect of crustal rheology and a more accurate melting treatment.

Our Mars models [T. Keller and P.J. Tackley, Icarus 2009] show that with an appropriate viscosity profile, convection rapidly develops a 'one ridge' planform consisting of a single ridge-like upwelling and small-scale downwellings below a stagnant lid, and that this produces a dichotomous crustal distribution that bears a striking first-order resemblance to the crustal distribution on Mars. The actual boundary of the crustal dichotomy on Mars is not hemispherical but rather like the seam on a tennis ball, and this is reproduced by our models, with the highland region being located above the upwelling. Furthermore, the elevation difference between the highland and lowland regions is very similar to that on Mars, although the average crustal thickness is higher than thought to be appropriate for Mars. Melting is found to have a dramatic influence on thermal evolution particularly during the early stages.

Due to the absence of an atmosphere and proximity to the Sun, Mercury's surface temperature varies laterally by several 100s K, even when averaged over long time periods. The dominant variation in time-averaged surface T occurs from pole to equator (~225 K). Here we demonstrate, using models of mantle convection in a 3-D spherical shell, that this stationary lateral variation in surface temperature has a small but significant influence on mantle convection and on the lateral

variation of heat flux across the core-mantle boundary (CMB). We evaluate the possible observational signature of this laterally-varying convection in terms of boundary topography, stress distribution, gravity and moment of inertia tensor.

The discovery of extra-solar planets with terrestrial composition and sizes up to twice that of Earth, so-called “super-Earths”, has prompted interest in their possible mantle dynamics and evolution. The pressure at the core-mantle boundary (CMB) of a 2^{*} Earth-sized super-Earth is about eight times the pressure at Earth’s CMB, which has a strong effect on physical properties such as thermal expansivity, diffusivity and viscosity. The mantle of such a super-Earth would be made mostly of post-perovskite (PPv), which has different physical properties than perovskite, the major mineral of Earth’s lower mantle. Here we use the newly-computed rheological parameters for PPv, computed using density function theory [Ammann, Brodholt and Dobson, 2008] in simulations of super-Earths of up to twice Earth size. The models assume a compressible anelastic approximation that includes the depth-dependence of material parameters. Rheological parameters for minerals other than PPv are based on those for perovskite. Plastic yielding at low pressures facilitates plate-like lithospheric behaviour. Results demonstrate that super-Earths are equally likely or more likely than an equivalent Earth-sized planet to be undergoing plate tectonics, and that the low viscosity of PPv has a strong and previously unseen effects on the mantle dynamics of super-Earths.

REFERENCES

- Keller, T. & Tackley P. J. 2009: Towards self-consistent modelling of the Martian dichotomy: The influence of low-degree convection on crustal thickness distribution, *Icarus*, 202, 429-443.
- Tackley, P. J. 2008: Modelling compressible mantle convection with large viscosity contrasts in a three-dimensional spherical shell using the yin-yang grid, *Phys. Earth Planet. Inter.*, 171, 7-18.
- van Heck, H. & Tackley P. J., Planforms of self-consistently generated plate tectonics in 3-D spherical geometry, *Geophys. Res. Lett.* 35, L19312, doi:10.1029/2008GL035190.

1.39

Shear heating and subduction initiation

Thielmann Marcel¹, Kaus B.J.P¹

¹ *Geophysical Fluid Dynamics, ETH Zürich (marcel.thielmann@erdw.ethz.ch)*

Despite it’s importance in geodynamics, the processes that result in subduction initiation remain incompletely understood. Shear heating has been put forward as a mechanism to create lithospheric-scale shear zones (e.g. Ogawa 1987, Regenauer-Lieb et al. 2001). A scaling analysis highlighted the governing parameters that control shear localization (Kaus and Podladchikov 2006), and showed that the boundary between localization and no localization is quite sharp. Recently, this scaling analysis was extended to include more realistic lithospheric rheologies and structures and it could be demonstrated that shear-heating induced lithospheric scale localization might occur for Earth-like parameters (Cramer and Kaus, 2010).

It is however unclear if all lithospheric-scale shear zones evolve into self-sustaining subduction zones. Here, we therefore extend the models used by Cramer and Kaus to greater depths and take into account an underlying asthenospheric mantle.

Using visco-elasto-plastic numerical models, we show that for certain parameters, lithospheric shear zones evolve into subduction zones when convergence is forced.

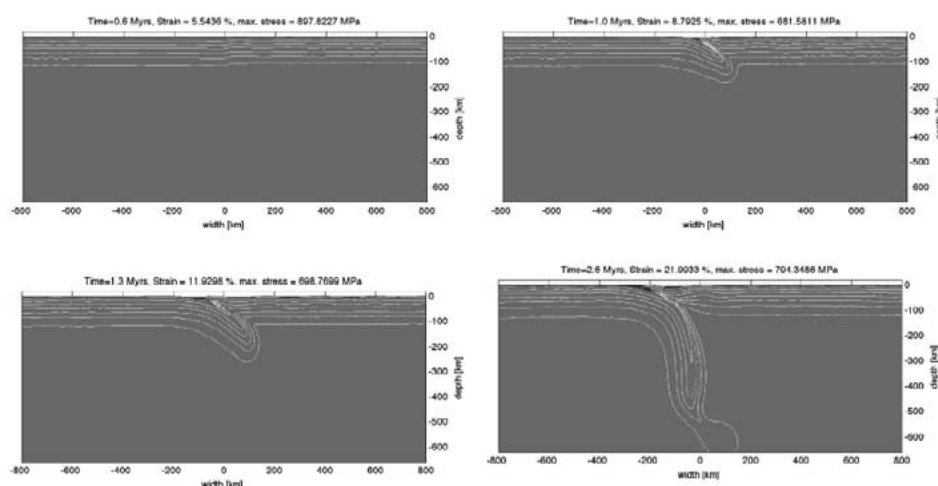


Figure 1: Subduction resulting from forced convergence of two oceanic plates of different age. Colors show composition, white contour lines denote isotherms.

1.40

Dislocation glide in experimentally deformed natural quartz single crystals

Thust Anja¹, Heilbronner Renée¹, Stünitz Holger

¹Geologisch-Paläontologisches Institut, Bernoullistrasse 32, CH-4056 Basel (anja.thust@unibas.ch)

²Institutt for geologi, Universitetet i Tromsø, Dramsveien 201, N-9037 Tromsø

Samples of natural milky quartz were deformed in a Griggs deformation apparatus at different confining pressures (700 MPa, 1000 MPa, 1500 MPa), with constant displacement rates of 10^{-6}s^{-1} , axial strains of 3 - 19%, and temperatures of 700°C to 1000°C. The single crystal starting material contains a large number of H₂O-rich fluid inclusions. Directly adjacent to the fluid inclusions the crystal is essentially dry (determined by FTIR).

The samples were cored from a narrow zone of constant “milkyness” (i.e. same density of fluid inclusions) in a large single crystal in two different orientations (1) normal to one of the prism planes ($\perp\{m\}$ orientation) and (2) 45° to $\langle a \rangle$ and to $\langle c \rangle$ (O^+ orientation). During attaining of the experimental P and T conditions, numerous fluid inclusions decrepitate by cracking. Rapid crack healing produces regions of very small fluid inclusions (“wet” quartz domains). Only these regions are subsequently deformed by dislocation glide/ dislocation climb, dry quartz domains without cracking and decrepitation of fluid inclusions remain undeformed. Sample strain is not sufficient to cause recrystallization, so that deformation is mainly restricted to dislocation glide. In experiments at lower temperatures there is abundant cracking and semi-brittle deformation, indicating that 800-900°C, represents the lower temperature end of crystal plastic deformation in these single crystals.

Peak strengths (at 900°C) range between 150 and 250 MPa for most samples of both orientations. There is a tentative of decreasing strength with increasing confining pressure, as described by Kronenberg and Tullis (1984) for quartzites, but the large variation in strength due to inhomogeneous sample strain precludes a definite analysis of the strength/pressure dependence in our single crystals.

In the deformed samples, we can distinguish a number of microstructures and inferred different slip systems. In both orientations, deformation lamellae with a high optical relief appear in the usual sub-basal orientation; often they are associated with “fluid inclusions trails”, cracks, or en echelon arrays.

In $\perp\{m\}$ orientation, conjugate misorientation bands sub-parallel to the prism planes can be observed. The misorientation is strongly localized and in some cases extremely high (up to 60° w/r to host c-axis). The deformed-shape of the samples is consistent with prism $\langle a \rangle$ slip. Unfortunately, as subgrain tilt boundaries in prism $\langle a \rangle$ slip do not rotate the c-axis orientation, it is expected that a c-axis orientation image does not show misorientation. Nevertheless, changes in the c-axis orientation are observed, indicating the activity of an additional slip system. TEM observations indicate many dislocations with other than pure $\langle a \rangle$ Burgers vector.

In O^+ orientation, we observe the formation of internally kinked shear bands. They are up to 2 mm wide and oriented at $\alpha \sim 90^\circ$ w/r to the host c-axis, slightly oblique to the sense of shear. The width of the kinked domains is $\sim 20\text{-}40\ \mu\text{m}$ and their average misorientation is 5°. Individual kink bands, crossing shear zone boundaries, show higher misorientations w/r to the host c-axis (up to 20°). The dispersion of c-axis orientation with synthetic rotation of the c-axis is evidence of basal $\langle a \rangle$ slip.

REFERENCES:

Kronenberg, A.K. & Tullis, J. 1984: Flow strength of quartz aggregates: grain size and pressure effects due to hydrolytic weakening. JGR Vol. 89, 4281-4281.

1.41

A new instrumentation to measure seismic waves attenuation

Nicola Tisato¹, Claudio Madonna¹, Sebastien Boutareaud¹, Jean-Pierre Burg¹

¹ ETH Zurich, Geological Institute, Zurich, Switzerland (nicola.tisato@erdw.ethz.ch)

Attenuation of seismic waves is the general expression describing the loss of energy of an elastic perturbation during its propagation in a medium. As a geophysical method, measuring the attenuation of seismic waves is a key to uncover essential information about fluid saturation of buried rocks.

Attenuation of seismic waves depends on several mechanisms. In the case of saturated rock, fluids play an important role. Seismic waves create zones of overpressure by mobilizing the fluids in the pores of the rock. Starting from Gassmann-Biot theory (Gassman, 1951), several models (e.g. White, 1975; Mavko and Jizba, 1991) have been formulated to describe the energy absorption by flow of fluids.

According to Mavko et al. (1998) for rock with permeability equals or less than 1 D, fluid viscosity between 1 cP and 10 cP and low frequencies seismic wave (< 100 Hz), the most important processes that subtract energy from the seismic waves are squirt flow and patchy saturation. Numerical models like Quintal et al. (2009) calculate how a patchy saturated vertical rock section (25 cm height), after stress steps of several kPa (i.e. 30 kPa) show a dissimilar increase in pore pressure between gas-saturated and liquid-saturated layers.

The Rock Deformation Laboratory at ETH-Zürich has designed and set up a new pressure vessel to measure seismic wave attenuation in rocks at frequencies between 0.1 and 100 Hz and to verify the predicted influence of seismic waves on the pore pressure in patchy saturated rocks. We present this pressure vessel which can reach confining pressures of 25 MPa and holds a 250 mm long and 76 mm diameter sample. Dynamic stress is applied at the top of the rock cylinder by a piezoelectric motor that can generate a stress of several kPa (> 100 KPa) in less than 10 ms. The vessel is equipped with 5 pressure sensors buried within the rock sample, a load cell and a strain sensor to measure axial shortening while the motor generates the seismic waves.

The sensor conditioning system has been designed and realized by us and the acquisition software has been developed in Matlab. We present the first results, at room pressure and temperature, based on the measurements of pore fluid pressure increase in a sandstone sample with a permeability of 200 to 500 mD and partially saturated with water and air.

These preliminary results show the reliability of this new instrumentation to measure seismic wave attenuation at low frequency and to verify the pore fluid flow driven by seismic waves.

REFERENCES

- Gassmann, F. "Über die elastizität in porösen medien." *Der Natur*, 96, 1951: 1–23.
- Mavko, G., and D. Jizba. "Estimating grain-scale fluid effects on velocity dispersion in rocks." *Geophysics*, 56, 1991: 1940-1949.
- Mavko, G., T. Mukerji, J. Dvorkin. "The Rock Physics Handbook: Tools for Seismic Analysis of Porous Media" Cambridge, 1998.
- Quintal, B., S. M. Schmalholz, and Y. Y. Podladchikov. "Low-frequency reflections from a thin layer with high attenuation caused by interlayer flow." *Geophysics* 74 (1), 2009: N14-N22.
- White, J. E. "Computed seismic speeds and attenuation in rocks with partial gas saturation." *Geophysics*, 40, 1975: 224-232.

1.42

The effect of deformation on partial melting of metapelitic rock: an experimental study.

Tumarkina Elizaveta¹, Misra Santanu¹, Connolly A.D. James²

* Experimental Rock Deformation Laboratory, Geological Institute, ETH., Sonneggstrasse 5, Zurich, CH-8092, Switzerland (elizaveta.tumarkina@erdw.ethz.ch; santanu.misra@erdw.ethz.ch)

** Institute for Geochemistry and Petrology, ETH, Clausiusstrasse 25, Zürich, CH-8092, Switzerland (james.connolly@erdw.ethz.ch)

Most of the existing experimental and/or theoretical investigations in the partial melting process emphasized on the role of pressure, temperature and water activity, but did not consider significantly the role of deformation during metamorphism. Natural rocks, however, generally experience phase changes simultaneously with tectonic stress. In this study, we investigated dry, synthetic quartz-muscovite (Fe-rich) system to explore the role of deformation on the reactions kinetics. Torsion experiments were conducted in an internally heated gas medium deformation apparatus at 750°C and at confining pressure of 300 MPa with a constant strain rate of 3×10^{-4} /s (1 shear strain ~ 1 hour). Static experiments were performed under same P-T conditions as for the deformation ones.

In both static and dynamic experiments the partial melting of muscovite and quartz produces melt + biotite + sillimanite + K-feldspar. The rates of melting and crystallization are independent of imposed conditions (static/dynamic) during the first 1.5 hours of experiments. After this time, deformation takes over and gradually become effective in determining the kinetics. The results indicate that the melt fraction in dynamic experiments is higher than static experiments at the same nominal P-T conditions. It is observed that kinetics of partial melt generation is 1.7 times higher in dynamic conditions compared to static ones. We propose few different explanations for this phenomenon: strain energy, local pressure drop and subsequent melt transportation, overheating because of shear, additional surface energy because of crushing of mineral grains during deformation and effect of viscosity. In this study we attempt a first order assessment of the feasibility of each mechanism.

1.43

Mantle Convection, Stagnant Lids and Plate Tectonics on Super-Earths

van Heck Hein¹, Tackley Paul¹

¹ Institut für Geophysik, Sonneggstrasse 5, Zürich (hvanheck@erdw.ethz.ch)

The discovery of extra-solar super-Earths has prompted interest in their possible mantle dynamics and evolution, and in whether their lithospheres are most likely to be undergoing active plate tectonics like on Earth, or be stagnant lids like on Mars and Venus.

The origin of plate tectonics is poorly understood for the Earth, likely involving a complex interplay of rheological, compositional, melting and thermal effects, which makes it impossible to make reliable predictions for other planets.

Nevertheless, as a starting point it is common to parameterize the complex processes involved as a simple yield stress that is either constant or has a “Byerlee’s rule” dependence on pressure (e.g., [Tackley, GCubed 2000ab] in 3D cartesian geometry; [van Heck and Tackley, GRL 2008] in 3D spherical geometry).

Because the simplifying assumptions made in developing analytical scalings may not be valid over all parameter ranges, numerical simulations are needed; the one numerical study on super-Earths to date (O’Neill and Lenardic, GRL 2007) finds that plate tectonics is less likely on a larger planet, in apparent contradiction of analytical results.

To try and understand this we here present new calculations of yielding-induced plate tectonics as a function of planet size, focusing on the idealized endmembers of internal heating or basal heating as well as different strength profiles, and compare to analytical scalings.

We conclude that for internally heated convection plate tectonics is equally likely for terrestrial planets of any size. For basally heated convection plate tectonics gets more likely with increasing planet size.

1.44

Dynamics of crustal growth at active continental margins: numerical modeling

Vogt Katharina¹, Gerya Taras^{1,2}, Castro Antonio³

¹ Department of Earth Sciences, ETH Zurich, Switzerland (katharina.vogt@erdw.ethz.ch)

² Department of Geology, Moscow State University, Russia

³ Department of Geology, University of Huelva, Spain

The dynamics of crustal growth under active continental margins were analyzed by using a coupled 2D petrological-thermomechanical numerical model of an oceanic-continental subduction process. This model includes spontaneous slab retreat and bending, dehydration of subducted crust, aqueous fluid transport, partial melting, melt extraction and melt emplacement in form of both extrusive volcanics and intrusive plutons. Depending on variable model parameters such as plate velocities and degree of rheological weakening induced by fluids and melts, the following three geodynamic regimes of crustal growth were identified:

- (i) stable subduction without plume development
- (ii) subduction associated with plume emplacement
- (iii) subduction accomplished by lithosphere extension and back arc spreading.

Crustal growth in a stable subduction setting results in the emplacement of flattened intrusions within the lower crust of mainly basaltic to andesitic composition. At first melts extracted from partially molten rocks located atop the slab (i.e. hydrated mantle, sediments and basalts) intrude into the lower crust followed by mantle-derived (wet peridotite) basaltic melts from the mantle wedge. Thus, extending plutons form associated with low crustal growth rates (15 km³/km/Myrs) and a successively increasing mantle component.

In a plume-present regime, crustal growth is accomplished by the formation and emplacement of silicic plumes. In the course of subduction localization and partial melting of basalts and sediments along the slab induces Rayleigh Taylor instabilities. Hence, buoyant silicic plumes are formed, composed of partially molten sediments, basalts (oceanic crust) and serpentinite. Subsequently, these plumes ascend, crosscutting the lithosphere before they finally crystallize within the upper crust in form of silicic batholiths. Additionally, basaltic intrusions within the lower crust are formed derived by partial melting of rocks located atop the slab and inside the plume.

Crustal growth rates increase with time before reaching a steady state (60km³/km/Myrs). The mantle component of the newly produced crust decreases with time. Subduction in an extensional arc setting results in decompression melting of dry peridotite. The backward motion of the subduction zone relative to the motion of the plate leads to thinning of the overriding plate. Thus, hot and dry asthenosphere rises into the neck as the slab retreats, triggering decompression melting of dry peridotite. As a result crustal growth rates increase to values of about 100km³/km/Myrs.

1.45

Evidence of Permian HT metamorphism in Austroalpine units of the Internal Western Alps?

Brigitte von Niederhäusern¹, Paola Manzotti¹, Martin Engi¹, Daniela Rubatto², Michele Zucali³, Bénédicte Cenki-Tok¹, James Darling¹

¹ Institut für Geologie, Universität Bern, Baltzerstrasse 1+3, CH-3012 Bern (vonniederhaeusern@geo.unibe.ch)

² Research School of Earth Sciences, Australian National University, Canberra

³ Dipartimento di Scienze della Terra «Ardito Desio», Università degli Studi di Milano, via Mangiagalli 34, 20133 I-Milano

The Internal Western Alps comprise predominantly continental terranes that were assembled during the oblique Alpine convergence of S-Europe and the thinned Apulian margin. Terranes derived from Apulia are termed Austroalpine units; these are well exposed in the Sesia Zone, the Dent Blanche nappe, and a few smaller tectonic outliers. Basement rocks are dominant in all of these units, but Permian intrusive masses are widespread, and thin trails of post-Variscan sediments have locally been recognized. Despite the HP/LT Alpine overprint (blueschist to eclogite facies) of all units, relics of an earlier HT metamorphic history are abundant. The Alpine HP-imprint is most distinctly developed in mylonites, both wi-

thin the various terranes and along contacts to adjacent ones; pre-Alpine HT assemblages are commonly preserved in less deformed rocks.

The present study focussed on samples from shear-zones with clear evidence of the Alpine HP metamorphism. To date specific metamorphic stages, detailed microstructural and petrologic analysis of select samples was followed by in-situ U-Th-Pb dating of allanite, titanite, and zircon. Much to our surprise, most ages do not reflect the Alpine HP-stage, even though robust U-Th-Pb chronometers were employed. Predominant are Permian ages. Examples presented here are chosen to document striking similarities, from SW-Sesia to the Dent Blanche, i.e. across the well established Austroalpine HP-units.

- (1) SW Sesia zone (II DK unit: 'seconda zona diorito-kinzigitica', Apulian lower crust)
 - Locality Vasario (Valle di Ribordone): Across a m-scale shear zone within the II DK unit (metabasites with thin slices of intermediate rocks), blueschist-facies assemblages are best developed in the core of the shear zone; glauc + pheng ± clz define the mylonitic foliation. Zircon grains in the mylonites of intermediate composition show igneous cores with sector-zoned metamorphic overgrowths. Such rims are typical of granulite-facies; LA-ICP-MS data reveal a Permian age (275 Ma).
 - Locality Pasturera (Val Soana): A shear zone developed along the northern contact of II DK to Gneiss Minuti in the SW Sesia zone. Strongly deformed parts near the contact show a greenschist-facies (ep + ab + chl) overprint. However, the less deformed margins of the shear zone retain blueschist-facies assemblages (glauc + pheng) with large euhedral allanite. Preliminary LA-ICP-MS data for allanite from the blueschist-facies sample yield ages of 280-330 Ma.
- (2) Dent Blanche nappe
 - Locality N of Lago Cignana (Valtournanche):
Tightly folded metacherts and carbonates contain blueschist facies assemblages (riebe-grt-qtz-ep). SHRIMP data from titanite in siliceous marbles and allanite in metacherts yield reproducible age data in three groups: 160-190 Ma, 270-290 Ma, and 300-350 Ma. The younger ages are thought to reflect heating associated with the Jurassic rifting that preceded the Alpine collision; the oldest ages represent Hercynian relics, but again there are Permian growth zones. Garnet in impure metacherts contain metamorphic allanite inclusions dated at 290 Ma as well.
- (3) Dent Blanche nappe (polymetamorphic Valpelline basement)
 - Locality Thoules (Valpelline): granulitic-facies assemblages are well developed in paragneisses (grt-sil-bt-pl-qtz). EMP geochronological data for monazite from the granulitic sample yield preliminary ages of 220-260 Ma.

While a definitive interpretation of these isolated age data is surely premature, the consistency of the data from several settings is remarkable and demands a discussion in the regional framework. Permian magmatism is of course well established in many parts of the Alps, with mafic intrusives (mostly gabbros) and more evolved types (e.g. Mucrone granodiorite, Arolla granite) occurring in the internal Western Alps. However, the widespread and diverse settings of the present observations is unlikely to represent contact-metamorphic phenomena. Regional metamorphism in the Permian is now well established in the Eastern Alps (Schuster and Stüwe, 2008). In the Western Alps, there is only sparse evidence for Permian metamorphism (e.g. Rebay and Spalla, 2001), quite possibly because Variscan rocks in the corresponding Austroalpine units are generally of upper amphibolite facies to migmatitic grade, rendering difficult the recognition of a subsequent Permian phase. Certainly the model of Permian rifting producing a high heat-flow regime that caused large-scale magmatic underplating and LPHT-metamorphism, as advocated by Schuster and Stüwe (2008), deserved further attention and scrutiny in the Western Alps.

The present communication comes out of our comprehensive effort aimed at documenting the Alpine PTdt-history in the Internal Western Alps. Why then do the shear zones we investigated, which were chosen for their clearly identifiable HP assemblages, retain the pre-Alpine chronometers so well? An obvious possibility is that these shear zones were set up during pre-Alpine tectonic activity (Jurassic rifting, Permian or Variscan or even older orogenies) and reactivated during late-Cretaceous and early Tertiary Alpine convergence.

REFERENCES

- Rebay G. & Spalla M.I., 2001. Emplacement at granulite facies conditions of the Sesia-Lanzo metagabbros: an early record of Permian rifting? *Lithos*, 58: 85-104
- Schuster R. & Stüwe K., 2008. Permian metamorphic event in the Alps. *Geology*, 36(8): 603-606.

1.46

Structural evolution of the Zagros fold-thrust-belt : insights from the U-Th/He thermochronometry (Ap. and Zr.)

J.C. Wrobel-Daveau ^{1, 2}, G.M.H. Ruiz ³, F.M. Stuart ⁴, J.C. Ringenbach ² & D. Frizon de Lamotte ¹

¹ Université de Cergy-Pontoise, Géosciences et Environnement, F95 000 Cergy-Pontoise, France. (jean-christophe.wrobel-daveau@u-cergy.fr)

² Total, Service de Géologie Structurale, CSTJF, F64 000 Pau, France.

³ IMG, University of Lausanne, Switzerland.

⁴ Isotope Geosciences Unit, Scottish Universities Environmental Research Centre, East Kilbride G750QF, UK

The Zagros Fold-Thrust Belt (ZFTB) is located south of the Arabian-Eurasian plates' suture.

Deformation and uplift in the ZFTB have been triggered by collision at about 35 Ma. However, the timing of the deformation since 35Ma is debated because it is, up to now, ill-constrained by quantitative methods.

Combining structural analysis and low temperature thermochronology (AHe and ZHe) helps to constrain vertical movements related to the building of this orogen.

The samples come from Cambrian sandstones, Paleogene Flysh and Neogene Molasse. In this study, AHe ages are used to quantify the burial history of the Paleogene flysh and Neogene molasse basins, and interpret the kinematic evolution of the ZFTB. With ZHe ages, it is possible to estimate the thickness of the total Phanerozoic sedimentary pile.

AHe and ZHe ages on detrital samples are presented on two regional cross-sections at crustal scale of the Lurestan and the Kuhzestan regions (Fig. 1).

The only available AHe and ZHe ages have been provided by Gavillot et al. (2010) in the Kuhzestan along the main thrusts, in salt plugs and in the syn-collisional conglomerate Fm.

In Lurestan, the samples of the base of the Neogene molasse show partially reset (~75°C) AHe ages, which indicates 2-3 km of burial for this formation and a thinning toward the interland.

Paleogene flysh AHe ages are also partially reset which is interpreted as a minimum burial of 2-3 km in the central Lurestan. Toward the north, completely reset ages suggest a thickening of this formation toward the interland. Finally, AHe ages lead to propose that exhumation linked to the last compressional deformation stage occurred after 12Ma along the suture and in the most internal parts of the Fold-Thrust Belt, and subsequently propagated toward the foreland, with exhumation younger than 2-3 Ma in the frontal folds.

In Kuhzestan, partial reset of ZHe ages (200-160°C) at the base of the Cambrian Fms. is evidence for a maximum burial of 7-9 km. Whereas near the top, ZHe ages at 350 Ma, not affected by the subsequent Phanerozoic sedimentary pile, allow questioning about the meaning of this signal commonly mentioned in different studies all around the Arabian plate (e.g. Kohn et al., 1992)

REFERENCES

- Gavillot, Y., Axen, G.J., Stockli, D.F., Horton, B.K. and Fakhari, M.D. (2010). Timing of thrust activity in the High Zagros fold-thrust belt, Iran, from (U-Th)/He thermochronometry. *Tectonics*, doi:10.1029/2009TC002484, in press.
- Kohn, B.P., Eyal, M. and Feinstein, S. (1992). A major late Devonian-early Carboniferous (Hercynian) Thermotectonic event at the NW margin of the Arabian-Nubian shield: Evidence from zircon fission track dating. *Tectonics*, 11, 5; 1018-1027.

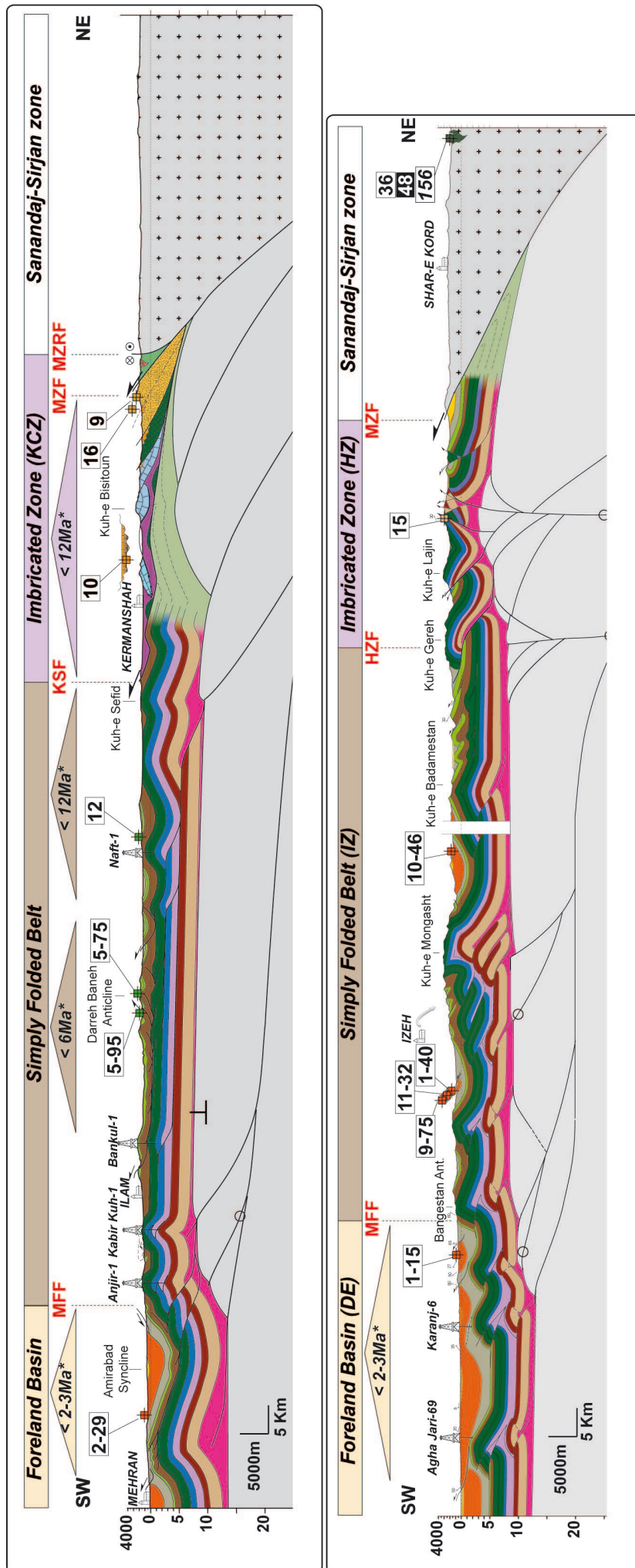


Figure 1: Cross-sections of the Lurestan (upper section) and south Kuhzestan (lower section). Thermochronological ages (AHe and ZHe) are located (white and black rectangles respectively). Triangles above the section indicate minimum age for exhumation in each structural domain. MZF: Main Zagros Fault, HZF: High Zagros Fault, IZ: Izeh Zone, DE: Dezful embayment, Kermanshah Crust Zone, HZ: High Zagros, IZ: Izeh Zone, DE: Dezful embayment

2. Mineralogy-Petrology-Geochemistry

Eric Reusser

Swiss Society of Mineralogy and Petrology (SSMP)

- 2.0 Abidi R., Slim-Shimi N., Hatira N., Marignac Ch., Gasquet D., Mejri Z.: Approche microthermométrique pour la détermination de l'origine hydrothermal de fluide minéralisateur du gisement à Pb-(Zn)-Sr-Ba d'El Aguiba (Tunisie septentrional)
- 2.1 Bader T., Franz L., de Capitani C., Ratschbacher L., Hacker B.R., Weise C., Popp M.: Tectonometamorphic evolution of the Wudang Complex (central China)
- 2.2 Bauer K., Vennemann T., Mulch A.: Reconstruction of Neogene paleoelevation and paleoclimatic conditions of the European Alps and the circum-Alpine region by stable isotope analyses
- 2.3 Cavargna-Sani M., Epard J.-L., Bussy F., Ulianov A.: Zircon U/Pb dating of the Late Carboniferous Zervreila Orthogneiss, Adula Nappe.
- 2.4 Diamond L.W., Tarantola A., Stünitz H.: Effects of deviatoric stress on natural fluid inclusions in quartz: an experimental study
- 2.5 El Korh A., Schmidt S.Th., Ballèvre M., Bruguier O.: U-Pb geochronology of an orthogneiss discovered within the HP-LT metamorphic rocks of the Ile de Groix, Armorican Massif, France
- 2.6 Hermann J., Rubatto D.: Pre-Alpine metamorphism in the classical Alpine staurolite-garnet schist of Campolungo
- 2.7 Huber C., Bachmann O., Dufek J.: Thermo-mechanical reactivation of locked crystal mushes: melting-induced internal fracturation and assimilation processes in magmas
- 2.8 Hunziker D., Caddick M., Reusser E., Burg J.-P., Müller E.: The influence of ferric/ferrous iron ratios in bulk and minerals of blueschists from the Inner Makran (SE Iran) on thermobarometric recalculations
- 2.9 Hürlimann N., Müntener O., Ulmer P.: Subvolcanic mafic to intermediate dike-systems: constraints on post-plutonic activity (S-Adamello, N-Italy)
- 2.10 Katona I., Serneels V.: The pigments of the medieval painters in Fribourg: Investigation of a top quality mural painting from the Cordeliers Church in Fribourg.
- 2.11 Kayani S.: Combustion analysis of a meteorite debris
- 2.12 Khozyem H.M., Adatte T., Tantawy A.A., Spangenberg J.E., Keller G., Föllmi K.: Nature and Tempo of the PETM (Paleocene-Eocene thermal maximum) events, new insights from the GSSP Dababyia section (Luxor, Egypt).
- 2.13 Kocsis L., Ounis A., Chaabani F., Naili S. M.: New isotope data from the Late Cretaceous and Paleogene phosphate beds of the Gafsa Basin, Tunisia
- 2.14 König D., Serneels V.: Geochemical and mineralogical examinations of roman crucibles from Autun (France)
- 2.15 Lambrecht G., Diamond L. W.: Fluid boiling and mixing during latest stage orogenic gold mineralization at Brusson, NW Italian Alps
- 2.16 Maggetti M., Morin D., Serneels V., Neururer C.: Kiln furnitures from the faience manufacture of Granges-le-Bourg (Haute Saône, France): contrasting recipes
- 2.17 Maggetti M., Rosen J., Serneels V., Neururer C.: The faience manufacture Le Bois d'Épense (North-eastern France, 18/19th century)
- 2.18 Marolf A.R., Vennemann T.W., Bonzon J.: Forensic geology: characterisation of light element stable isotopes in soil samples of the Swiss Plateau
- 2.19 Martin L.H.J., Schmidt M.W., Hametner K., Günther D.: Element partitioning between immiscible silicate and carbonatite melts by centrifuge experiments
- 2.20 Mattsson H.B., Bosshard S.A., Hetényi G., Almqvist B.S.G., Hirt A.M., Caricchi L., Caddick M.: Internal flow structures in columnar jointed basalt from Hrepphólar, Iceland
- 2.21 Mavris C., Egli M., Plötze M., Götze J., Mirabella A., Giaccai D., Haeblerli W.: Mineral weathering along a soil chronosequence in a high Alpine proglacial area: a multiple approach

- 2.22 Meier M.F., Grobéty B.: Fumarolic aerosols from El Chichón volcano, Mexico
- 2.23 Monsef R., Emami M. H., Rashidnejad Omran N., Monsef I.: Petrogenetic evolution of Neogene volcanism in northern Uromieh-Dokhtar Magmatic Belt: Insights on the origin of post-collision magmatism
- 2.24 Moulas E., Connolly J., Burg J.-P., Kostopoulos D.: Refining the granulite-facies metamorphism in the Rhodope metamorphic complex - Greece
- 2.25 Ortelli M., Moritz R., Voudouris P., Cosca M., Spangenberg J.: Tertiary Porphyry and Epithermal Association of the Sapes-Kassiteres District, Eastern Rhodopes, Greece
- 2.26 Parmigiani A., Huber C., Bachmann O., Chopard B.: Reactive multiphase flow at the pore-scale: the melting of a crystalline framework during the injection of buoyant hot volatiles.
- 2.27 Pretet C., Felis T., Samankassou E.: Constraining calcium isotope fractionation in corals
- 2.28 Regis D., Engi M., Rubatto D., Darling J.: Complex dynamics in the Sesia Zone subduction system deduced from multiple generations of white mica and allanite: the power of microtextural analysis combined with petrochronology
- 2.29 Serneels V.: Thousand Years of massive Iron Production in the Dogon Country (Mali, West Africa): Technology – Economy – Environment
- 2.30 Skopelitis A., Schaltegger U., Ulianov A., Brack P.: The Adamello batholith (Italy): a fossil magma chamber or accumulation of magma pulses?
- 2.31 Soullignac R.: Mineralogical techniques and ethnoarchaeology applied to the study of smithing slags in Mali (Africa)
- 2.32 Tămas C.G., Munteanu G., Cauuet B., Mut G.: Mining archaeological studies in Eastern Pyrenees, France: Baillestavy iron mining area
- 2.33 Thierrin-Michael G.: Fossiliferous pottery in Ajoie (NW Switzerland) and adjacent regions from La Tène and Gallo-roman sites: Information on production and distribution through microscopic and chemical analyses
- 2.34 Tritschack R., Grobéty B.: Insights into the dehydroxylation kinetics of lizardite and chrysotile
- 2.35 Verberne R., Ulmer P., Müntener O.: Calculating rheologic properties of magmas from field observations combined with experimental data.
- 2.36 Vils F., Elliott T., Smith-Duque C.E., Alt J.C., Teagle D.: How long does seawater and oceanic crust interact?
- 2.37 von Allmen K., Böttcher M.E., Samankassou E., Nägler T.F.: Barium isotope fractionation in natural barium minerals and precipitation experiments: A first glimpse at the global barium cycle
- 2.38 Westermann S., Stein M., Matera V., Fiet N., Adatte T., Föllmi K. B.: Palaeoredox change during OAE 1a: new insights from phosphorus and redox-sensitive trace elements
- 2.39 Wongfun N., Furrer G., Brandl H., Plötze M.: Influence of extrinsic weathering factors on mineral dissolution in Damma glacier forefield
- 2.40 Zurfluh F.J., Hofmann B.A., Gnos E., Eggenberger U.: Water-soluble salts and temperature variation in meteorites recovered in the hot desert of Oman

2.0

Approche microthermométrie pour la détermination de l'origine hydrothermal de fluide minéralisateur du gisement à Pb-(Zn)-Sr-Ba d'El Aguiba (Tunisie septentrional)

Riadh ABIDI ¹, Najet SLIM-SHIMI ², Nouri HATIRA ³, Christian MARGNAC ⁴, Dominique GASQUET ⁵, Zouhair MEJRI ¹

¹ Faculté des sciences de Bizerte, département de géologie, Jarzouna-Bizerte.7021. Tunisie. (Abidi1riadh@yahoo.com)

² Faculté des sciences mathématiques, physiques naturelles de Tunis. Campus Universitaire. 1060 Tunis. Tunisie.

³ Faculté des sciences de Gabes (Faculté des Sciences de Gabès, Cité Riadh, Zirig 6072 Gabès)

⁴ Ecole Nationale Supérieure des Mines de Nancy, Parc de Saurupt, 54042 Nancy, France.

⁵ Université de Savoie – CISM Laboratoire EDYTEM Bâtiment Belledonne Campus de Technolac 73370 LE BOURGET DU LAC

Le gîte d'El Aguiba représente l'un des plus importants gîtes de la zone des flyschs. Il est situé sur la bordure orientale du massif triasique du Jebel Hamra. Ce Trias fait partie des lames triasiques extrusives le long de l'accident Ghardimaou–Cap Serrat (Décrochement senestre orienté NE-SW), et forme avec des terrains argilocarbonatés d'âge crétacés-paléocène (Unité Ediss), une fenêtre tectonique dans l'unité Numidienne (argilo-gréseuse d'âge oligocène supérieur-miocène inférieur).

Le corps minéralisé, constitué d'une brèche argilo-dolomitique, est situé dans la zone de broyage entre le Trias qui représente le toit du gîte et le paléocène qui représente le mur du gîte. La minéralisation est discordante par rapport à la roche encaissante et se présente sous plusieurs formes : ciment des brèches de dissolution, remplissage des fractures et des cavités de dissolution dans les bancs de dolomie noire d'âge triasique et remplacement de la roche encaissante (dolomie d'âge triasique). Ce gisement présente une paragenèse simple composée par la galène, la sphalérite, la marcasite et la pyrite qui sont accessoirement présents avec une gangue représentée par la célestite (gangue principale), la barytine, la calcite et le quartz.

Les mesures microthermométriques, réalisées essentiellement dans des inclusions primaires et secondaires biphasées (liquide + vapeur) dans la célestite et la calcite du gîte d'El Aguiba, ont été effectuées sur une platine chauffante réfrigérante de type « Linkam MDS-600® »

1. Célestite

La salinité du fluide contenu dans les inclusions fluides primaires biphasées, est comprise entre 5.41-10.36 % poids éq. NaCl avec une moyenne de 8.13 % poids éq. NaCl. Pour les inclusions fluides secondaires biphasées la salinité varie entre 5.56 et 15.96 % poids éq. NaCl avec un maximum de fréquence vers 8 à 9 % poids éq. NaCl. La composition du fluide en CaCl_2 contenu dans les inclusions primaires et secondaires biphasées varie entre 0 et 3.4 Wt. % CaCl_2 ; tandis que la composition du fluide en NaCl contenu dans les inclusions primaires et secondaires varie entre 5 et 12 Wt. % NaCl. La température d'homogénéisation du fluide contenu dans les inclusions primaires biphasées varie entre 149 et 230°C avec une moyenne de 184°C. Pour les inclusions secondaires biphasées, la température d'homogénéisation varie entre 130 et 230°C avec une température moyenne de 174°C. Le fluide a une densité moyenne de 1.03 et une pression moyenne de 190.71 bars. La variation du changement d'état des phases d'une inclusion biphasée dans la célestite est résumée dans la figure .1.

2. Calcite

Les inclusions fluides primaires biphasées montrent une salinité qui varie entre 4.03 % et 10.36 % poids éq. NaCl avec une moyenne de 6.7 % poids éq. NaCl, une composition moyenne en CaCl_2 de 2.6 wt. % CaCl_2 et une température d'homogénéisation qui varie entre 151° et 225.7°C avec une moyenne de 178°C. Dans les inclusions secondaires, la salinité moyenne est de 7.4 % poids éq. NaCl et la température d'homogénéisation varie entre 130.7° et 240.1°C avec une moyenne de 177°C. Le fluide a une densité moyenne de 1.03 et une pression moyenne de 200.34 bars

Le fluide minéralisateur du gîte d'El Aguiba correspondrait donc à un mélange à tendance adiabatique de plusieurs fluides chauds de différentes origines hydrothermales où la température résulte seulement du mélange de fluides sans échange de chaleur avec la roche aux alentours. Le fluide contenu dans la célestite et la calcite montre une salinité moyenne à faible et une température élevée et variable. Ce fluide serait un mélange de saumures du bassin avec un fluide magmatique - météorique.

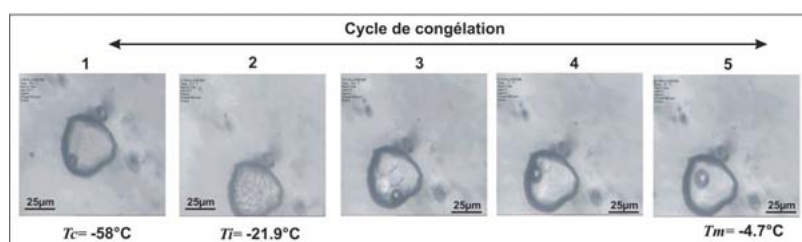


Figure 1. Evolution du changement d'état d'une l'inclusion fluide primaire biphasée (L+V) dans la célestite du gîte d'El Aguiba au cours du cycle de congélation. (Tc température de congélation, Ti température de début de fusion de la glace et Tm température de fin de fusion de la glace).

2.1

Tectonometamorphic evolution of the Wudang Complex (central China)

Bader Thomas¹, Franz Leander¹, de Capitani Christian¹, Ratschbacher Lothar², Hacker Bradley R.³, Weise Carsten², Popp Michael²

¹ Mineralogisch-Petrographisches Institut, Universität Basel, CH-4056 Basel
(thomas.bader@unibas.ch)

² Institut für Geologie, Technische Universität Bergakademie Freiberg, D-09599 Freiberg

³ Geological Sciences, University of California, Santa Barbara, CA-93106

Located in the Paleozoic-Mesozoic Qinling-Dabie-Sulu-belt in central China, the Wudang Complex is composed of Neoproterozoic siliciclastic meta-sediments and marbles with intercalated acidic and basic meta-volcanics and is overlain by Cambrian-Ordovician limestones and dolomites. During the Triassic collision of the Yangtze and the Sino-Corean plates, the Wudang Complex, which belongs to the subducted Yangtze plate, underwent a high pressure metamorphism. This study investigates this metamorphic overprint combining thermodynamic modeling using the DOMINO-THERIAK programs (de Capitani & Petrakakis 2010) with conventional geothermobarometry.

Felsic gneiss sample 76017A from the central part of the Wudang Complex, displays the peak metamorphic assemblage garnet – albite – phengite – biotite – quartz – rutile. Based on garnet core composition and the Si-content of phengite, DOMINO modeling (MnTNCKFMASH system, excess H₂O) yields 510°C at 1.2 GPa most likely representing the pressure peak of the PT path. Identical results were obtained from garnet gneiss 76032C taken ~30 km further north. The matrix of another garnet gneiss from the same outcrop shows a retrograde recrystallization to stilpnomelane, albite, quartz, and minor clinozoisite pointing to a late overprint at ~320°C and >0.3 GPa.

Several metabasic schists from Wudang's northern part display the assemblage chlorite – phengite – amphibole – epidote – albite – quartz – titanite. Amphiboles are bluish magnesioriebeckite/winchite or pale green actinolite. Phengite has high Si-contents of 3.4-3.5 p.f.u. Based on chlorite-phengite-quartz equilibria (Vidal et al. 2005; Dubacq et al. 2009) metamorphic conditions of 280-330°C at 0.5-0.8 GPa were derived. Phengite's Si p.f.u.-isopleths calculated with DOMINO point to pressures of 0.7-0.8 GPa at these temperatures. Discrete domains of stilpnomelane – calcite – phengite – chlorite – schist 753011A preserved records of an early metamorphic stage at 250-320°C at 0.5-0.9 GPa while other domains point to a subsequent overprint at 400-420°C and 0.5 GPa.

These petrological data highlight the high-pressure blueschist to greenschist facies metamorphic overprint of the Wudang Complex during the subduction of the leading edge of the Yangtze plate. The central part was buried to greater depths although the same geothermal gradient of ~12°C/km is, within errors of geobarometry, also appropriate for the low-grade metamorphic northern part. Ar/Ar dating of amphiboles and K white micas (Mattauer et al. 1985; Ratschbacher et al. 2003) demonstrate that this happened in the Late Triassic. During subduction, the Wudang formed a continuous portion of the downgoing slab and, during exhumation, was delaminated and imbricated along south-directed thrust faults (Huang, 1993).

The critical assemblage stilpnomelane – albite – clinozoisite in sample 76032D indicates, that the exhumation of the central part occurred rather fast, as the stability of stilpnomelane is indicative for elevated pressures at temperatures below ~320°C while the northern part, at least locally, underwent a medium-pressure overprint at ~400°C and 0.5 GPa.

REFERENCES

- De Capitani, C. & Petrakakis, C. 2010: The computation of equilibrium assemblage diagrams with Theriak/Domino software. *Am. Mineral.* 95, 1006-1016.
- Dubacq, B., Vidal, O. & De Andrade, V. 2009: Dehydration of dioctahedral aluminous phyllosilicates: thermodynamic modelling and implications for thermobarometric estimates. *Contrib. Mineral. Petrol.* 159, 159-174.
- Huang, W. 1993: Multiphase deformation and displacement within a basement complex on a continental margin: the Wudang Complex in the Qinling Orogen, China. *Tectonophysics* 224, 305-326.
- Mattauer, M., Matte, P., Malavieille, J., Tapponnier, P., Maluski, H., Xu, Z.Q., Lu, Y.L. & Tang, Y.Q. 1985: Tectonics of the Qinling belt: build-up and evolution of eastern Asia. *Nature* 317, 496–500.
- Ratschbacher, L., Hacker, B.R., Calvert, A., Webb, L.E., Grimmer, J.C., McWilliams, M., Ireland, T., Dong, S. & Hu, J. 2003: Tectonics of the Qinling Belt (Central China): Tectonostratigraphy, geochronology, and deformation history. *Tectonophysics* 366, 1-53.
- Vidal, O., Parra, T. & Vieillard, P. 2005: Thermodynamic properties of the Tschermak solid solution in Fe-chlorites: application to natural examples and possible role of oxidation. *Am. Mineral.* 90, 347-358.

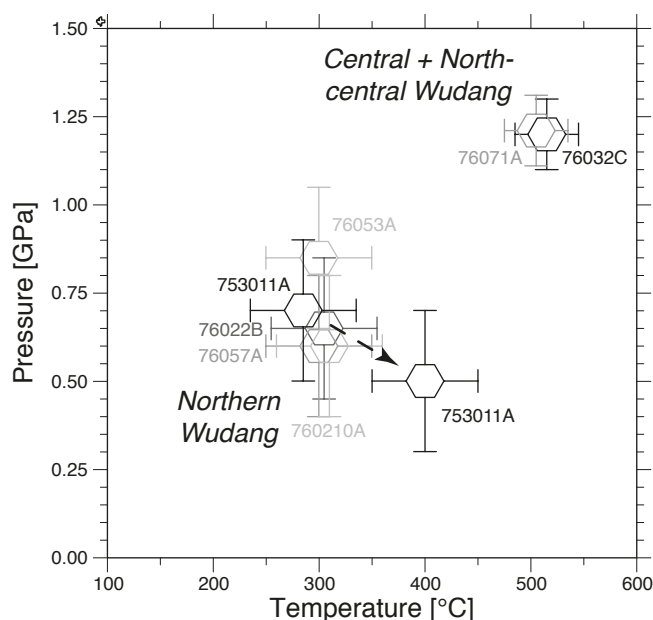


Figure 1. Summary of the metamorphic evolution of the Wudang Complex

2.2

Reconstruction of Neogene paleoelevation and paleoclimatic conditions of the European Alps and the circum-Alpine region by stable isotope analyses

Bauer Kerstin^{1,2}, Vennemann Torsten¹, Mulch Andreas²

¹ Institut de Minéralogie et Géochimie, Anthropôle, Université de Lausanne, CH-1015 Lausanne, Switzerland (Kerstin.Bauer@unil.ch)

² Institut für Geologie, Leibniz Universität Hannover, Callinstr. 30, 30167 Hannover, Germany

The stable isotope composition of oxygen and hydrogen in rain water correlates with the air temperature and with the altitude of precipitation. If meteoric water is taken up into the structure of minerals with a known water-mineral fractionation factor, it is possible to determine its original $\delta^{18}\text{O}$ and δD values and thereby the former altitude of precipitation from measurements of the isotopic composition of the host mineral and knowledge of the ambient temperature conditions (e.g. Mulch et al. 2004).

This study will apply this approach to Miocene precipitation in the circum-Alpine region via the analyses of hydrous clay minerals (e. g. Mulch & Chamberlain 2007). Previous paleontological and geochemical analyses of fossils (e.g. Janz & Vennemann 2005, Kocsis et al. 2009), from the same samples to be used for the clay mineral analysis will help to constrain the paleoclimatic conditions that existed during the formation of the clays during the Miocene. The combination of the marine paleoclimatic as well as other terrestrial fossil records with the detrital record of the clays may allow estimates on the changes in elevation of the Alpine region during orogenesis.

Measured $\delta^{18}\text{O}$ values of between 15.4 and 21.2‰, suggest that the clays were formed in the presence of meteoric water that had a comparable isotopic composition to that of modern water in the Alpine region and at temperatures of formation that correspond to typical surface temperatures.

However, the treatment of the sample material is challenging due to its extremely small grain size and hygroscopic behavior, which makes the δD values difficult to interpret. A trend to lower values for smaller grain size fractions hints to possible contamination or a mix of several components. XRD analyses show that the separates do not consist of pure smectite, but a varying mixture of smectite and illite and also mixed-layer minerals, which may also falsify the values obtained. Further tests and experiments to investigate these possibilities are in progress.

Furthermore, new sample material will be collected to fill the gaps between the existing data. Drill cores or more detailed profiles would give better constraints on the temporal and spatial distribution of the results. In addition, samples from

altered volcanic material such as bentonites may provide better absolute age constraints compared to the present approach of using biostratigraphy of individually placed sample localities. Material with a higher content of clay will be of advantage to achieve a higher yield for the sample preparation and will possibly limit some of the contaminating effects.

Another aspect of the research project will involve the investigation of recently formed Alpine soils at different altitudes. The isotope composition of the clay size fraction will be investigated in combination with precipitation and soil water isotope composition in order to study the direct interaction of meteoric water with the minerals during soil formation.

REFERENCES

- Janz, H. & Vennemann, T. W., 2005: Isotopic composition (O, C, Sr and Nd) and trace element ratios (Sr/Ca, Mg/Ca) of Miocene marine and brackish ostracods from North Alpine foreland deposits (Germany and Austria) as indicators for paleoclimate. *Palaeogeography, Palaeoclimatology, Palaeoecology* 225 (2005), 216-247.
- Kocsis, L., Vennemann, T. W., Hegner, E., Fontignie, D., & Tütken, T., 2009: Constraints on Miocene oceanography and climate in the Western and Central Paratethys: O-, Sr-, and Nd-isotope compositions of marine fish and mammal remains. *Palaeogeography, Palaeoclimatology, Palaeoecology* 271 (2009), 117-129.
- Mulch, A., Teyssier, C., Cosca, M. A., Vanderhaeghe, O., & Vennemann, T. W., 2004: Reconstructing paleoelevation in eroded orogens. *Geology* 32, 6 (2004), 525-528.
- Mulch, A. & Chamberlain C. P., 2007: Stable Isotope Paleoaltimetry in Orogenic Belts – The Silicate Record in Surface and Crustal Geological Archives. *Reviews in Mineralogy & Geochemistry* 66 (2007), 89-118.

2.3

Zircon U/Pb dating of the Late Carboniferous Zervreila Orthogneiss, Adula Nappe.

Mattia Cavargna-Sani¹, Jean-Luc Epard¹, François Bussy² & Alexey Ulianov²

¹ Institut de Géologie et Paléontologie, Université de Lausanne, Bâtiment Anthropole, 1015 Lausanne (mattia.cavargna@unil.ch)

² Institut de Minéralogie et Géochimie, Université de Lausanne, Bâtiment Anthropole, 1015 Lausanne

The Zervreila Orthogneiss is one of the dominant lithologies of the northern Adula Nappe (Jenny et al. 1923). However, the age of magmatic emplacement of this rock was never determined precisely. This age is important to better understand the lithologies (lithostatigraphy) and the geometry of the Adula Nappe.

Geochemical data show that the protolith of the Zervreila Orthogneiss is a Si-rich granite. Zircons from this orthogneiss form a very homogeneous population. Inherited cores and evidences of metamorphic growth are absent. According to Pupin classification (1980), these are mainly P-type zircons similar to zircons found in alkaline granites from extensional tectonic environments. We have dated the zircons from the Zervreila Orthogneiss by LA-ICPMS using an Element XR sector-field instrument interfaced to an UP-193 excimer ablation system. A 5 Hz repetition rate and an on-sample energy density of 2-2.4 J/cm² were applied to minimise the laser induced fractionation. A GJ-1 zircon was used as a primary standard. Analyses were performed on oscillatory magmatic growth zones recognisable in cathodoluminescence images.

Samples dated come from four localities in the northern Adula Nappe: Val Scaradra, Zervreila, and two closely situated outcrops from Zapport. The U/Pb ages of these samples are largely concordant; the 206/238 age values are 296.10 (+2.90 -1.80) Ma, 291.20 (+8.10 -3.00) Ma, 288.65 (+3.25 -4.75) and 293.60 (+3.90 -2.00) Ma, respectively. Within the analytical error, these four ages are interpreted to result from the same magmatic event and to correspond to the intrusion time of a granitic body, probably emplaced within the Adula paragneisses in the late Variscan post-orogenic context.

REFERENCES

- Jenny, H., Frischknecht, G. & Kopp, J. 1923: Geologie der Adula. Beitr. Geol. Karte Schweiz (N.F.) 51, 1-123.
- Pupin, J. P. 1980: Zircon and granite petrology. *Contributions to Mineralogy and Petrology* 73, 207-220.

2.4

Effects of deviatoric stress on natural fluid inclusions in quartz: an experimental study

Diamond Larryn W.,¹ Tarantola Alexandre¹, Stünitz Holger

¹ Rock–Water Interaction Group, Institute of Geological Sciences, University of Bern, Baltzerstrasse 3, CH-3012 Bern, Switzerland (diamond@geo.unibe.ch)

² Department of Geology, University of Tromsø, Dramsveien 201, 9037 Tromsø, Norway

Fluid inclusions in quartz are known to modify their shapes, textures and densities during shear deformation. Modifications of chemical composition are also suspected. However, such changes have not been experimentally demonstrated, their mechanisms remain unexplained, and no criteria are available to assess whether deformed inclusions preserve information on paleofluid properties and paleostress conditions.

To address these issues, quartz crystals containing natural CO₂-H₂O-NaCl fluid inclusions have been experimentally subjected to deviatoric stresses of 90–250 MPa at 700 °C and ~600 MPa confining pressure. Strains of up to 1% cause the inclusions to develop irregular shapes (Fig. 1, 2a) and to generate microcracks in crystallographic planes oriented subperpendicular to the major compression axis, σ_1 . The uniform alignment of the microcracks imparts a planar fabric to the samples (Fig. 1b). Inclusion expansion due to microcracking reaches 20%, producing low fluid densities that bear no relation to physical conditions outside the sample. Nevertheless, the composition of the precursor inclusions is preserved (Fig. 2b). The microcracks heal and form swarms of tiny satellite inclusions with a wide range of densities, the highest reflecting the stress value of σ_1 . These new inclusions lose H₂O via diffusion, thereby passively increasing their salt and gas contents, and triggering plastic deformation of the surrounding quartz via H₂O-weakening. Consequently, the quartz samples deform plastically only in domains originally rich in inclusions.

This study shows that fluid inclusions deformed by deviatoric stresses may record information on paleostresses and on pre-deformation fluid composition, and that they play a key role in facilitating crystal-plastic deformation of quartz.

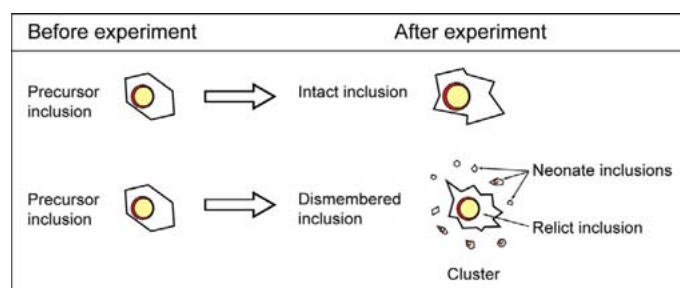


Figure 1. Summary and nomenclature of shape changes accompanying ~1% plastic strain. View looking down σ_1 .

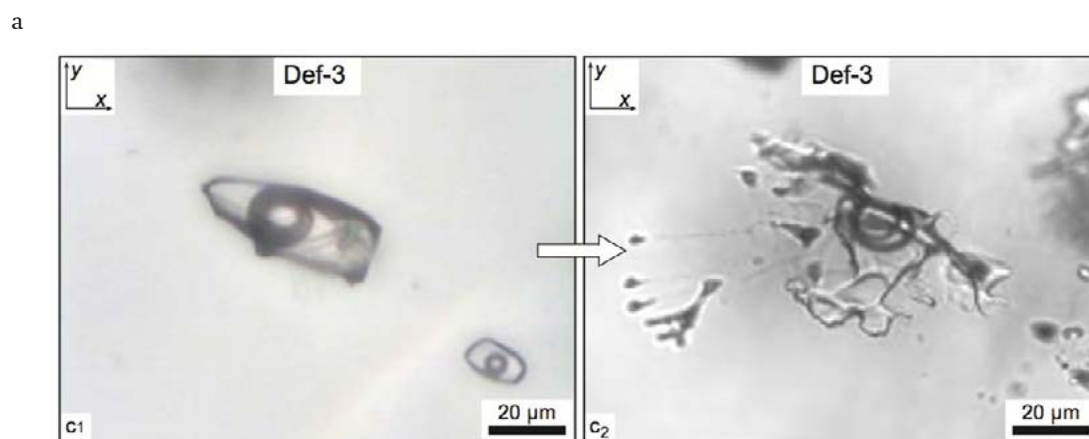


Figure 2a. Shape changes accompanying ~1% plastic strain: Example view looking down σ_1

b

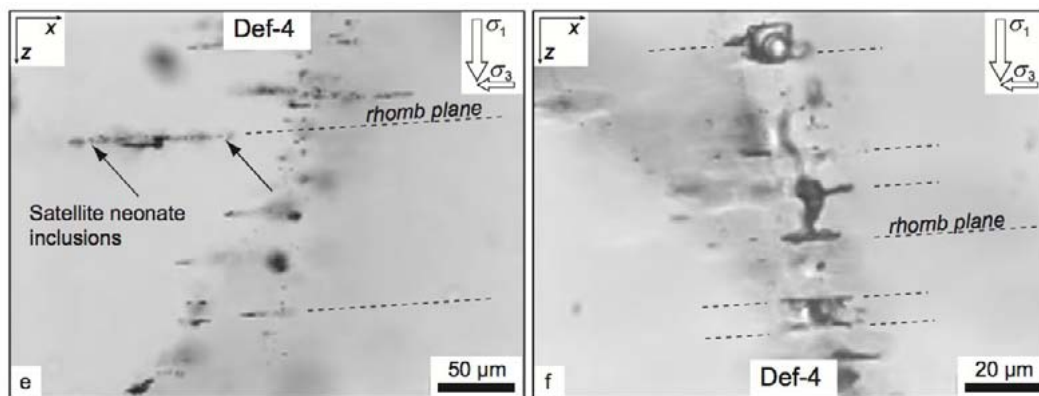


Figure 2b. Shape changes accompanying ~1% plastic strain: Example view looking perpendicular to σ_1 .

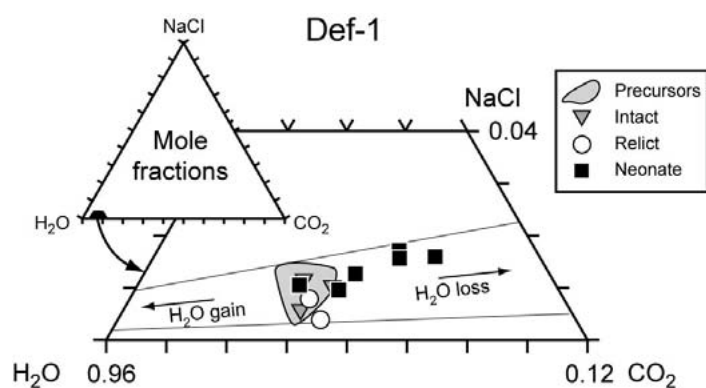


Figure 3. Compositional changes accompanying ~1% plastic strain.

REFERENCES

- Diamond, L. W., Tarantola, A. & Stünitz, H., 2010: Modification of fluid inclusions in quartz by deviatoric stress II: Experimentally induced changes in inclusion volume and composition. *Contributions to Mineralogy and Petrology* DOI 10.1007/s00410-010-0510-6.
- Tarantola, A., Diamond, L. W. & Stünitz, H., 2010: Modification of fluid inclusions in quartz by deviatoric stress. I: Experimentally induced changes in inclusion shapes and microstructures. *Contributions to Mineralogy and Petrology* DOI 10.1007/s00410-010-0509-z.

2.5

U–Pb geochronology of an orthogneiss discovered within the HP–LT metamorphic rocks of the Ile de Groix, Armorican Massif, France

El Korh Afifé¹, Schmidt Susanne Th.¹, Ballèvre Michel² & Bruguier Olivier³

Département de Minéralogie, Université de Genève, Rue des Maraîchers 13, CH-1205 Genève, Suisse
(Afife.ElKorh@unige.ch, Susanne.Schmidt@unige.ch)

² Géosciences Rennes (UMR CNRS 6118), Université de Rennes 1, Campus de Beaulieu, F-35042 Rennes Cedex, France
(michel.balleve@univ-rennes1.fr)

³ Géosciences Montpellier (UMR CNRS 6250), Université de Montpellier 2, Place Eugène Bataillon, F-34095 Montpellier Cedex 05, France
(olivier.bruguier@gm.univ-montp2.fr)

For the first time, an albitic orthogneiss has been recognised and dated within the HP–LT blueschist facies metabasites and metapelites of the Ile de Groix. It is part of the remnants of an accretionary complex formed after subduction and exhumation of an oceanic crust and its sedimentary cover (Bernard-Griffiths et al., 1986). The HP–LT event (blueschist

facies) is dated at 358–365 Ma with the $^{40}\text{Ar}/^{39}\text{Ar}$ (phengite) and Rb–Sr (whole rock, phengite and epidote) methods (Bosse et al., 2005).

The albitic orthogneiss occurs as 40 cm thick layers within HP-LT metapelites and is composed of an assemblage of albitic plagioclase, perthitic porphyroclasts of K-feldspars, quartz, phengite, epidote rimming metamict allanite, and garnet. Accessory minerals consist of titanite, apatite and zircon. The major element composition corresponds to that of peraluminous leucogranites, characterised by very high contents of SiO_2 (75.5 wt %), low CaO contents (1.7 wt %) and high Al/CNK ratios (1.5). The $[\text{FeOt}/(\text{FeOt}+\text{MgO})]$ ratio is high (0.8). The trace element composition of the orthogneiss displays high LILE, Th and U contents, MORB-like HREE abundances and moderate Nb and Y values. Despite the peraluminous orogenic signature, the chemical composition of the studied orthogneiss, as well as the presence of accessory allanite, apatite, titanite and zircon indicate a within-plate anorogenic or a volcanic arc origin.

Titanite and zircon were dated by LA-ICPMS, at the Universities of Montpellier and Lausanne, respectively, both using an Element XR spectrometer. Titanite (40 to 200 μm) was analysed in-situ in thin sections. Zircons (25 to 100 μm long) were extracted and separated following the conventional mineral separation procedures using gravimetric and magnetic methods. Titanite and zircon U–Pb data are represented together in a Tera-Wasserburg diagram (Fig. 1). No common lead correction was applied. The data define a Concordia intercept at 480.9 ± 3.1 Ma, with a MSWD of 12, interpreted as the age of the magmatic emplacement during the early Ordovician. Additional zircon grains yield late Neoproterozoic (i.e. Cadomian) ^{206}Pb – ^{238}U ages [546.6–606.0 Ma].

Titanite and zircon U–Pb ages indicate that the felsic magmatism from the Ile de Groix is contemporaneous with the granitic to rhyolitic, pre-orogenic plutonism widely recognized in the internal zones of the Variscan belt, related to the Ordovician continental rifting. This event led to the opening of the Rheic and Galicia-Southern Brittany oceans, and to the detachment of the microcontinent Armorica from Gondwana.

The magmatic protolith probably inherited its specific chemical composition from a combination of orogenic and anorogenic signatures due to partial melting of the Cadomian basement during granite emplacement in a continental rifting environment.

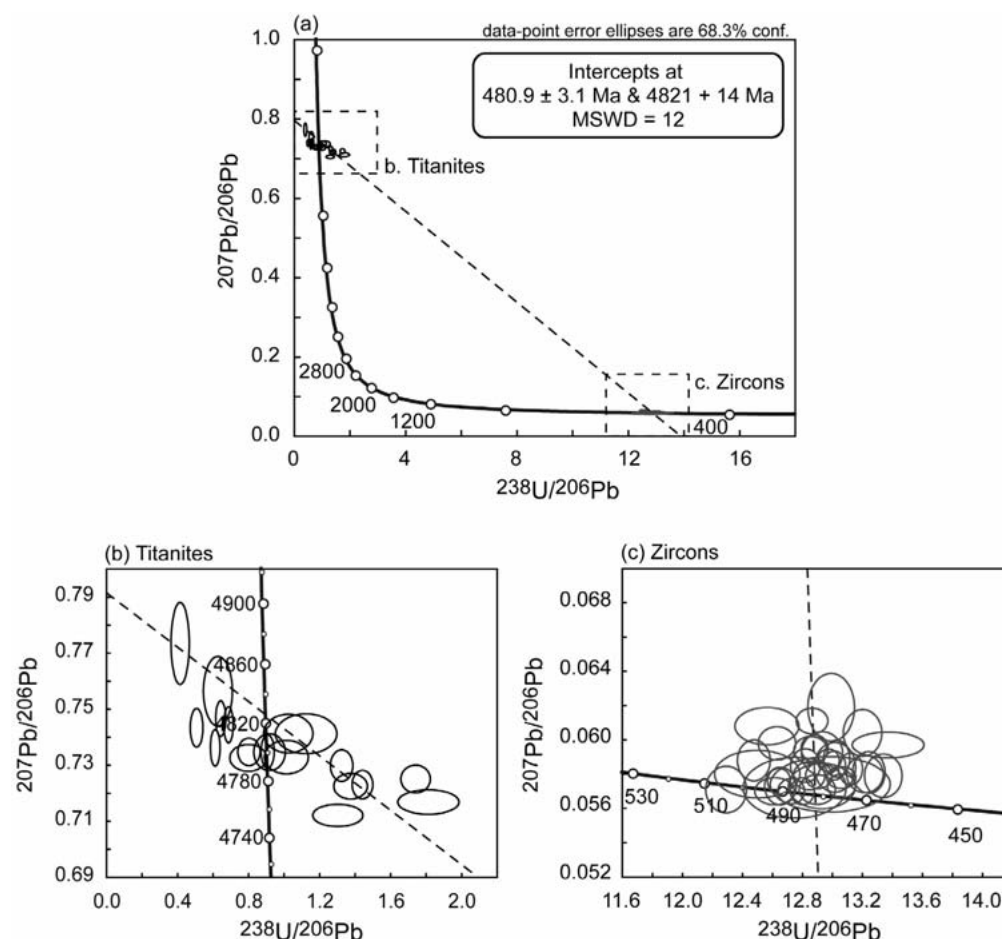


Figure 1. Tera-Wasserburg plots for titanite and zircon grains from orthogneiss GROA 115a. (a) All data, (b) titanites, (c) zircons.

REFERENCES

- Bernard-Griffiths, J., Carpenter, M.S.N., Peucat, J.-J. & Jahn, B.M. (1986). Geochemical and isotopic characteristics of blueschist facies rocks from the Ile de Groix, Armorican Massif (northwest France). *Lithos* 19, 235–253.
- Bosse, V., Feraud, G., Ballèvre, M., Peucat, J.-J. & Corsini, M. (2005). Rb–Sr and $^{40}\text{Ar}/^{39}\text{Ar}$ ages in blueschists from the Ile de Groix (Armorican Massif, France): Implications for closure mechanisms in isotopic systems. *Chemical Geology* 220, 21–45.

2.6

Pre-Alpine metamorphism in the classical Alpine staurolite-garnet schist of Campolungo

Jörg Hermann^{1,2} & Daniela Rubatto^{1,2}

¹ Research School of Earth Sciences, The Australian National University, AU-0200 Canberra (joerg.hermann@anu.edu.au)

² Present Address: Institute of Mineralogy and Geochemistry, Université de Lausanne, Anthropole, CH-1015 Lausanne

The Campolungo area, Ticino, represents one of the classical areas where Alpine metamorphism, structure and tectonics have been investigated. The area exposes a well-preserved Mesozoic stratigraphy (Bianconi, 1971) ranging from basal quartzites to dolomites (presumed Triassic deposition age) to Bündnerschiefer (presumed Jurassic deposition age). This sequence shows a series of overprinting Alpine structures (Grujic & Mancktelow, 1996) and associated metamorphism reaches amphibolite facies peak conditions (~6.5 kbar at the thermal peak of ~600°C; Todd & Engi, 1997). Staurolite-garnet schists outcrop stratigraphically below the quartzites. The schists display a comparable structural and metamorphic evolution to the Mesozoic rocks and thus have been interpreted as late Paleozoic clastic sediments that were metamorphosed during the Alpine orogeny.

We investigated in detail staurolite-garnet schists in the vicinity of the Capanna Leit. The samples consist of phengite, quartz and fine-grained graphite, marking a penetrative foliation that is also refolded. A second generation of phengite is present in the axial plane cleavage of the crenulation. Garnet occurs as porphyroblasts, partly overgrowing the foliation. Staurolite also forms postkinematic porphyroblasts. Late biotite flakes overprint the main foliation. Rutile cores are overgrown by ilmenite, and accessory tourmaline, monazite and zircon are dispersed throughout the samples. Especially in graphite rich rocks, monazite contains oriented graphite inclusions providing evidence that monazite formed syn to post-kinematic to the main foliation (Fig. 1).

Monazite grains were separated for SHRIMP dating from two staurolite-garnet schists. Despite its textural position, monazite consistently yielded pre-Alpine ages of ~330 Ma, corresponding to the known Variscan metamorphism. No trace of Alpine (~30 Ma) metamorphism was found in monazite in these samples. This indicates that at least part of the foliation in the rocks is not of Alpine age and that the staurolite-garnet schists represent a crystalline basement to the Mesozoic sediments.

A multistage evolution is also preserved in the garnet. Whereas Mn, Fe and Mg elemental maps do not show any zoning, the Ca-map displays a strong discontinuity separating a large, zoned garnet core from a small, homogenous rim. The transition is characterized by a highly irregular surface that crosscut previous zoning and is enriched in Ca. It is important to note that garnet in the nearby Bündnerschiefer (that experienced only Alpine metamorphism) do not show any of these features.

Trace element profiles across the garnet display a Y and HREE rich core with marked trace element depletion towards the intermediate garnet zone, typical of prograde growth zoning. Phosphorous increases steadily from core to the intermediate zone. At the discontinuity, visible in the Ca maps, Y and HREE increase by a factor of 5, indicating resorption of pre-existing garnet. In the rim, Y and HREE decrease drastically again, while P, after showing a significant drop at the interface, increases to values observed in the intermediate garnet zone. We interpret these observations as the Alpine prograde growth of a garnet rim on a previously, partly resorbed, Variscan garnet. The garnet core contains inclusions of chloritoid and staurolite, whereas only staurolite was found in the garnet rim. Therefore, the petrographic observations, major element mapping and trace element profiles in garnet combined with the dating of monazite indicate that the investigated mica-schists at Campolungo experienced staurolite-garnet grade metamorphism during Variscan as well as during Alpine metamorphism.

REFERENCES

- Bianconi, F., 1971. Geologia e petrografia della regione del Campolungo. Beiträge zur Geologischen Karte der Schweiz, vol. 142. Kümmerly & Frey, Bern.
- Grujic, D., & Mancktelow, N.S., 1996. Structure of the northern Maggia and Lebendun Nappes, Central Alps, Switzerland. *Eclogae Geologicae Helveticae* 89, 461–504.
- Todd, C.S., & Engi, M. 1997. Metamorphic field gradients in the Central Alps. *Journal of Metamorphic Geology*, 15, 513–530.

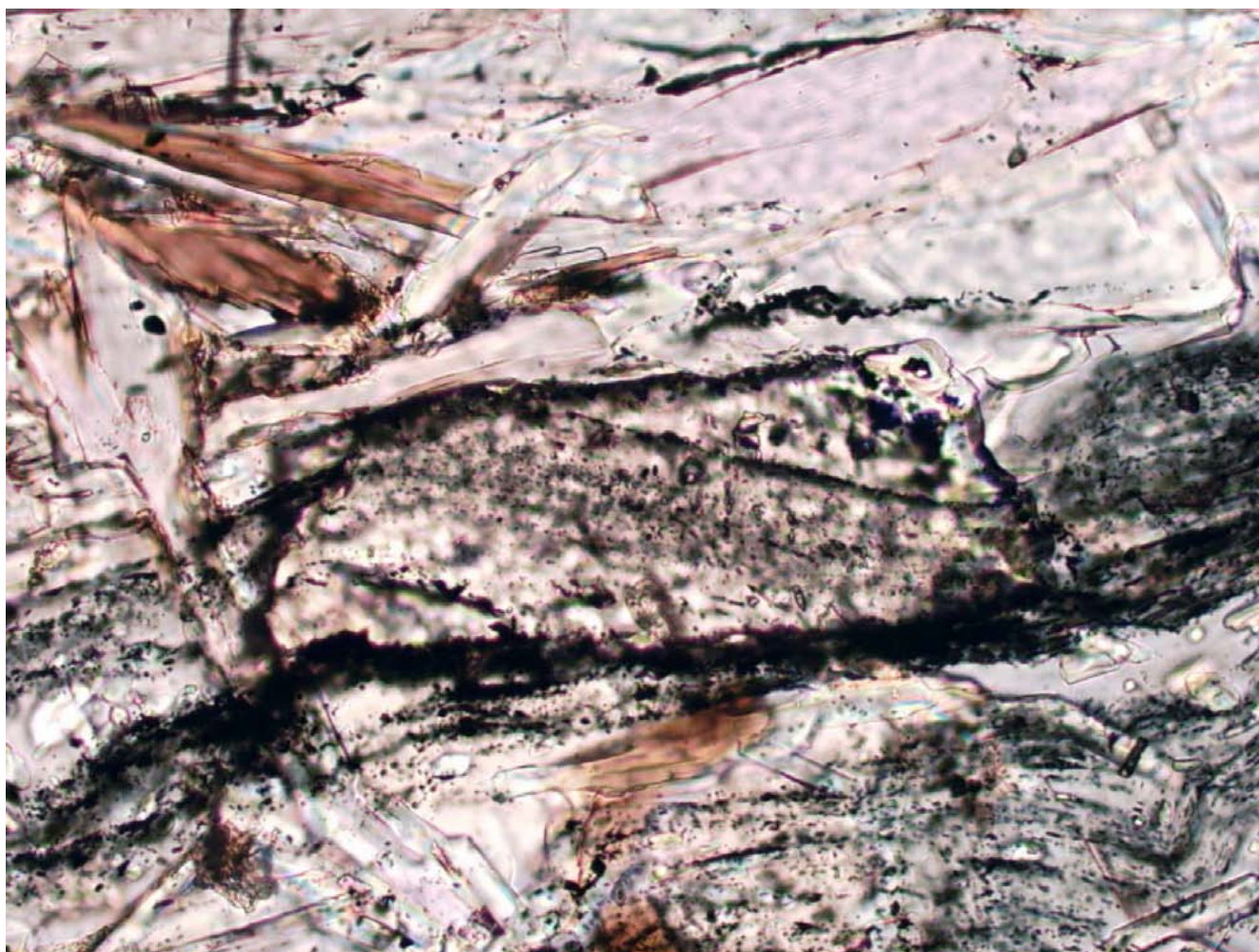


Figure 1. Monazite crystal (200 μm long) with internal graphite foliation from a staurolite-garnet schist. The age of monazites in this sample is ~ 330 Ma, indicating that pre-Alpine metamorphism and deformation is present in the Campolungo area.

2.7

Thermo-mechanical reactivation of locked crystal mushes: melting-induced internal fracturation and assimilation processes in magmas

Huber Christian¹, Bachmann Olivier² & Dufek Josef¹

¹ School of Earth and Atmospheric Sciences, Georgia Institute of Technology, Ferst drive 311, Atlanta, GA, USA (christian.huber@eas.gatech.edu)

² Department of Earth and Space Science, University of Washington, Seattle,

Thermal reactivation of locked crystal mushes in the upper crust is a fundamental step towards triggering volcanic eruptions of crystal-rich magmas. Models of such reactivation events indicate that partial melting of the crystalline framework is energetically costly and lead to average crystallinities that are lower than those observed in many erupted crystal mushes. Here, we show that internal overpressurization of the mush induced by small amounts of melting (10-20 %) breaks the crystalline framework by microfracturation and allows for efficient unlocking. Hence, this melting-induced overpressurization, enhanced by addition of gas in wet magmatic systems, plays an important role in generating volcanic deposits with crystal contents close to the rheological lock-up (~ 50 vol % crystals) by accelerating the incorporation of highly crystalline parts of the magma chamber (self-assimilation). It can also participate in disintegrating pieces of country rock that are commonly scavenged in magmas, leading to bulk assimilation of crustal lithologies in shallow reservoirs.

2.8

The influence of ferric/ferrous iron ratios in bulk and minerals of blueschists from the Inner Makran (SE Iran) on thermobarometric recalculations

Hunziker Daniela¹, Caddick Mark², Reusser Eric², Burg Jean-Pierre & Müller Elisabeth³

¹ Geological Institute, Structural Geology and Tectonics, ETH Zurich, Sonneggstrasse 5, NO E69, CH-8092 Zurich (daniela.hunziker@erdw.ethz.ch)

² Institute for Mineralogy and Petrology, ETH Zurich, Clausiusstrasse 25, CH-8092 Zurich

³ Electron Microscopy ETH Zurich (EMEZ), HP D11, CH-8093 Zurich

To reconstruct subduction parameters like depth of burial and subsequent exhumation the thermobarometric conditions of recrystallization of blueschist facies rocks has to be well constrained.

Calculations and models involve charge balance-based assumptions concerning the Fe³⁺/Fe²⁺ ratio of mineral phases. However, these ratios are poorly known for most minerals, especially for sodic amphiboles.

We approach the problem by studying the petrography, geochemistry and thermobarometry of scarcely studied blueschists in the Inner Makran of Southeast Iran. Comparing metamorphic pressure and temperature conditions calculated with different ferric/ferrous iron ratios of bulk and minerals illustrates the strong influence of this ratio. Recalculations using the true bulk Fe³⁺/Fe²⁺ ratio of the Makran blueschists measured by colorimetric titration and an estimated value from mineral parageneses differ largely. This is probably due to inaccurate amphibole models, which tend to consider a too low ferric/ferrous iron ratio. Using electron energy-loss spectroscopy (EELS) quantitative analyses of all paragenetic mineral phases will be analyzed and cross-checked with micro-X-ray absorption near-edge structure (XANES) analysis and Mössbauer spectroscopy.

The results entered into amphibole models will improve pressure/temperature recalculations of blueschist-facies and other amphibole-bearing metamorphic rocks.

2.9

Subvolcanic mafic to intermediate dike-systems: constraints on post-plutonic activity (S-Adamello, N-Italy)

Hürlimann Niklaus¹, Müntener Othmar¹ & Ulmer Peter²

¹ Institute of Mineralogy and Geochemistry, Anthropole, CH-1015 Lausanne, Switzerland (niklaus.hurlimann@unil.ch)

² Institute of Geochemistry and Petrology, Clausiusstrasse 25, CH-8092 Zurich, Switzerland

Various scales of dike geometries provide a record of strain during their emplacement. Distinct dike generations might record strain-evolution through time. In addition, dike rocks are generally close to liquid compositions, in particular mafic compositions, relative to plutonic rocks. Here we present field evidence of structural relationships and first petrological and geochemical data that characterize the evolution of post-batholith subvolcanic magmatic activity during cooling of a plutonic-suite in the Southern Adamello massif (Italy).

At least three different generations of mafic to intermediate dikes of picrobasaltic to andesitic composition postdate a succession of large volume pluton emplacement (Schaltegger et al. 2009, Hansmann and Oberli 1991, Del Moro et al. 1985). Early, partially deformed dike generations appear to reflect more local strain whereas later ones reflect a much more regional strain pattern that appears to be independent of interplutonic and wallrock contacts. Subvertical dikes are characterized by composite, multiple stage textures and are often phenocryst/xenocryst-rich whereas subhorizontal types are related to simpler one stage or pulse emplacement.

Subhorizontal types show a wide range of phenocryst phases such as olivine, clinopyroxene, amphibole and plagioclase. Evolved phases such as allanite-epidote, titanite, apatite and zircon are mainly associated with more felsic zones or bands within the dikes. Plagioclase in these felsic zones shows a large range of compositional variation. Such felsic zones appear to represent evolved liquid segregations from rather closed system fractionation (equilibrium crystallization).

Bulk rock geochemistry and petrography indicate an evolution to more evolved magmas towards younger generations and pulses. Particularly the later dike generations carry variable proportions of xenocrystic material. Major and trace element concentrations of bulk rocks indicate that aphyric dike margins in single pulse systems display a more evolved 'hydraulic head' followed by a trailing that is more primitive indicated by increasing contents of MgO, Fe₂O₃, Cr and Ni from the dike margin towards the center.

We will present major and trace elements of the aphyric-matrix obtained by Laser-Ablation-ICP-MS, to determine actual liquid compositions and to test equilibrium with respect to zoned phenocrysts. We will provide constraints on contamination and its sources with quantitative estimates on xenocryst content in individual samples with regard to dikes or magma pulses that show less or no contamination. Particular well established compositional zoning patterns in clinopyroxene-phenocrysts will further allow application of respective geospeedometers to constrain reservoir residence times with regard to cation interdiffusion (Chakraborty et al. 2008).

REFERENCES

- Chakraborty, S., Dohmen, R., Mueller, T., Beaker, H.W. & Ter Heege, J. 2008: Fe-Mg interdiffusion coefficients in clinopyroxene: experimental determinations using nanoscale films. AGU, Fall Meeting 2008, abstract #MR21C-04.
- Del Moro, A., Pardini, G., Quercioli, C., Villa, I.M. & Callegari, E. 1985: Rb/Sr and K/Ar chronology of Adamello granitoids, Southern Alps. *Memorie della Società Geologica Italiana*, 26, 261-284.
- Hansmann, W. & Oberli F. 1991: Zircon inheritance in an igneous rock suite from the southern Adamello batholith (Italian Alps). *Contributions to Mineralogy and Petrology*, 107, 501-518.
- Schaltegger, U., Brack, P., Ovtcharova, M., Peytcheva, I., Schoene, B., Stracke, A. & Bargossi G. 2009: Zircon and titanite recording 1.5 million years of magma accretion, crystallization and initial cooling in a composite pluton (southern Adamello batholith, northern Italy). *Earth Planetary Science Letters*, 286, 108-218.

2.10

The pigments of the medieval painters in Fribourg: Investigation of a top quality mural painting from the Cordeliers Church in Fribourg.

Ildiko Katona & Vincent Serneels

Department of Geosciences, University of Fribourg, Chemin du Musée 6, CH-1700 Fribourg (ildiko.katonaserneels@unifr.ch)

During the 80's, thousands of fragments of mural painting dating back to the late medieval period (15th century AD) were found during restoration works in the church of the Cordeliers in Fribourg. For 25 years, they remain unexploited at the Archaeological Service of Fribourg until their extraordinary esthetic quality was recognized.

Since 2009, an interdisciplinary team of researchers has been set up and the project has been supported by the SNF. It includes the reconstruction of the entire scene -20'000 fragments- (S. Garnerie), the art historical (B. Pradervand, J. Bujard) and the technical studies (J. James, V. Serneels, I. Katona). The aim of this study is the identification of the materials (pigments, binders, supports) and the description of the painting technique.

Chemical (XRF) and mineralogical (XRD) analyses are used together with microscopical observations of the surface and dispersed powder microscopy for the identification of components. As this major work of art is already fragmented, it offers an exceptional opportunity for the systematical sampling of the whole painted layer and the production of numerous small polished sections. This makes possible the use of SEM as a major method of investigation. On the other hand, the burial of the fragments under the ground inside the church allows a very good preservation of the fragile painted layer.

The medieval artist, still unidentified, was using a large variety of mineral pigments, including high quality ones, like red cinnabar, blue azurite, artificial Sn-Pb yellow and even gold. His technique was highly sophisticated with pigments mixtures for the production of specific shades and superposition of layers to obtain complex visual effects. First mineralogical results on this material will be presented.

2.11

Combustion analysis of a meteorite debris

Kayani Saheeb-Ahmed

National University of Sciences and Technology, H-12, Islamabad-44000, Pakistan (saheebk@ceme.nust.edu.pk)

A meteorite ablation debris has been identified near village Lehri (33°09'09"N; 73°33'35"E) in district Jhelum, Pakistan by Kayani (2009). In this research study, total carbon content of the meteorite debris has been determined and this abundance has been compared with values reported in literature to identify the origins of the parent body of this meteorite debris.

Carbon is one of the most important elements in nature. It can exist in many stable forms and the chemical structure of carbonaceous matter depends upon available environmental conditions. The abundance, composition and structure of carbon can be analyzed to gather information about the initial formation process and following environmental changes to the carbonaceous matter (Murae et al. 1993). In carbon rich chondrites (stony meteorites), carbonaceous matter has been identified as graphite, amorphous, kerogen-like, in some cases diamond, and mostly as a structurally unclear insoluble high molecular organic compound. In iron and stony-iron meteorites, carbon is found as graphite or less ordered graphitic matter (Murae et al. 1993; Swart et al. 1983; Amari et al. 1990).

In light of the above, it seems that carbon abundance can serve as a useful clue to identify the nature and origin of a particular meteorite. Further more it can also be used to detect alterations in the structure of the original matter (of the meteorite) due to impacts or collisions etc. For the meteorite debris under study, through XRD analysis magnetite and wustite have been detected as predominant iron phases (Kayani 2009). Presence of wustite shows a reducing environment which may have existed either due to collision of the parent body with an other celestial object or due to high pressure and temperature caused by resistance from the atmosphere of earth. As the meteorite debris has been found lying over the site in form of small stones, it seems on entry into earth's atmosphere, the parent meteoroid succumbed to increasingly high pressure and temperature and at a certain height exploded into innumerable small pieces that came to rest on this particular site. This kind of behavior is typically observed with chondrites as they are more vulnerable to high pressure and temperature effects due to their composition and structure.

In order to determine the abundance of carbon and sulphur in the meteorite debris, a specimen was tested through combustion analysis using the facilities at Petroleum Geochemistry Laboratory of Hydrocarbon Development Institute of Pakistan in Islamabad. In combustion analysis of meteorites, carbon is released over three different heating ranges. Recent contaminants are detected below 500°C while weathering products (i.e. carbonates) decompose around 1000°C. The spallogenic components (from metals and silicates) are identified during melting. Heating up to 1000°C is used to determine the weathering age where as the melt is analyzed to establish a terrestrial or residence age for the meteorite. The testing results are: Carbon 0.43 wt% and Sulphur 0.04 wt%.

The carbon abundance for this meteorite debris is in conformity with median carbon abundance value for enstatite chondrites (i.e. 0.4 wt%) as reported by Moore and Lewis (1965). This carbon value and the elemental composition determined through XRF analysis by Kayani (2009) supports the idea that the parent meteoroid body of this debris may have been an enstatite chondrite. Enstatite chondrites have a high iron content (up to 30 wt%) and contain a magnesium-silicon mineral enstatite ($\text{Mg}_2\text{Si}_2\text{O}_6$). The silicon and magnesium abundance values detected through XRF analysis are 3.93 wt% and 0.342 wt% respectively (Kayani 2009). The increased relative abundance of iron (56.28 wt%) in the meteorite debris is attributed to ablation effects experienced by the parent meteoroid body on its entry into earth's atmosphere and its subsequent explosive disintegration into small meteorites. This meteoroid may be related to a primitive undifferentiated parent body or an asteroid. Such asteroids represent the earliest rocky bodies that originated with in the solar system. Most of these asteroids float around the sun with in the orbits of Mars and Jupiter (the so called asteroid belt).

On the basis of the analysis included above, the meteorite debris is identified as that of an enstatite chondrite. The parent body of this meteorite debris may have originated from the asteroid belt. It may have been hurled (as a result of a collision with a neighboring celestial object) into a trajectory that ultimately brought it into close proximity of earth and was finally pulled down by earth's gravity causing it to crash on this particular site.

REFERENCES

- Amari, S., Anders, E., Virag, A. & Zinner, E. 1990: Interstellar graphite in meteorites. *Nature*, 345, 238-240.
- Kayani, SA. 2009: Using combined XRD-XRF analysis to identify meteorite ablation debris. In: Proceedings of IEEE International Conference on Emerging Technologies, Islamabad, October 19-20, 219-220.
- Moore, C. & Lewis, C. 1965: Carbon abundances in chondritic meteorites. *Science*, 149, 317-317.
- Murae, T., Kagi, H. & Masuda, A. 1993: Structure and chemistry of carbon in meteorites. In: *Primitive Solar Nebula and Origin of Planets* (Ed. by Oya, H.). Tokyo: Terra Scientific Publishing Company.
- Swart, P., Grady, M., Pillinger, C., Lewis, R. & Anders, E. 1983: Interstellar carbon in meteorites. *Science*, 220, 406-410.

2.12

Nature and Tempo of the PETM (Paleocene-Eocene thermal maximum) events, new insights from the GSSP Dababyia section (Luxor, Egypt).

Hassan M. Khozyem¹, Thierry Adatte¹, Abdel Aziz Tantawy², Jorge E. Spangenberg³, Gerta Keller⁴ & Karl Föllmi¹

¹ Institut de Géologie et de Paléontologie (IGP), Université de Lausanne. Hassanmohamed.Saleh@unil.ch

² Department of Geology, South Valley University, Aswan 81528, Egypt.

³ Institut de Minéralogie et Géochimie (IMG), Université de Lausanne.

⁴ Department of Geosciences, Princeton University, Guyot Hall, Princeton, NJ 08544, USA

The Paleocene-Eocene Thermal Maximum GSSP have been carefully selected by The International Union of Geological Sciences (IUGS) located at the base of a characteristic lithologic succession (the Dababyia Quarry Beds) that occurs in the lower part of the Esna Shale, a well known formation that outcrops extensively throughout Egypt. This selection was based on: (1) the organic carbon isotope excursion (CIE), located at the base of Bed 1 of the Dababyia Quarry Beds of the El Mahmiya Member in the Esna Formation. (2) the mass extinction of abyssal and bathyal benthic foraminifera (*Stensioina beccariiiformis* microfauna), which is reflected at shallower depths by a minor event; (3) the transient occurrence of taxa among the planktonic foraminifera (*Acarinina africana*, *A. sibaiyaensis*, *Morozovella allisonensis*) during the $\delta^{13}\text{C}$ excursion; (4) the transient occurrence of the *Rhomboaster* spp. – *Discoaster araneus* (RD) assemblage; and (5) an acme of the dinoflagellate *Apectodinium* complex. The GSSP-defined Paleocene/Eocene boundary is approximately 0.8 my older than the base of the standard Eocene Series as defined by the Ypresian Stage in epicontinental northwestern Europe (Aubry, M.-P et al., 2007).

High-resolution sampling has been achieved from two sections located at the left and right side of the original Dababyia GSSP. 62 samples from the left side section and 42 samples from the right side section have been subjected to micropaleontological (nannofossils), sedimentological, mineralogical and geochemical analysis in order to reconstruct the paleoenvironmental conditions and climatic changes occurring during the PETM. Preliminary fieldwork, sedimentological and stable isotopes data suggest that the Dababyia GSSP section has been deposited in a small channel structure which can be traced over 200m, with the basal units a and b (Aubry et al., 2005) thinning towards the edges of the outcrop and finally disappearing. The Paleocene-Eocene GSSP is consequently only complete over a 2-3 meters width, in the center of the outcrop. Geochemically, (1) both organic and bulk rock carbon isotopes show a long-term gradual decreasing and reach maximum negative values at the mid of bed. 2, (2) a severe and persistent decrease in $\delta^{15}\text{N}_{\text{org}}$ to $\sim 0\text{‰}$, (3) Sharp decrease in productivity at the CIE interval followed by a significant increase up to the end of the PETM, (4) A change in redox condition from oxic below the PETM to anoxic conditions in the lowermost PETM, followed by normal oxic conditions, (5) A maximum humidity (kaolinite peak) coinciding with the base of the PETM. Despite, the lack of lateral continuity, the Dababyia GSSP is one of the most complete PETM section and reveals interesting and unique features that may be crucial for a better understanding of the PETM events.

2.13

New isotope data from the Late Cretaceous and Paleogene phosphate beds of the Gafsa Basin, Tunisia

Kocsis László¹, Ounis Anouar², Chaabani Fredj² & Naili Salah Mohamed³

¹ Institut de Minéralogie et Géochimie, Faculté des Géosciences et Environnement, Université de Lausanne, Switzerland

² Laboratoire des Ressources Minérales et Environnement, Faculté des Sciences de Tunis, Université de Tunis El Manar, Tunisia

³ Compagnie de Phosphate de Gafsa, Direction de Géologie, Métlaoui, Tunisia

During the Late Cretaceous and Paleogene Tunisia was located in the southern margin of Tethys and it was a part of the main Tethyan giant phosphorite belt. At this period Tethyan waters covered most of the Tunisian landmass and only some areas like the Djefara and Kasserine islands emerged. Between these islands located the intracratonic Gafsa Basin that was connected to the open sea westward and sometimes water exchange occurred in the east through the Chamsi Pass (Fig. 1). Sedimentation in the Gafsa Basin was conducted in a semi-closed sea, where inner neritic and coastal environment alternated (e.g. Chaabani, 1995, Zaïer et al., 1998). Phosphate beds occurred first on the Hard Ground of the Abiod Formation in the Early Maastrichtian, where the layers can reach locally one meter in thickness, while later, during the Paleocene-Early Eocene more massive and economically important phosphorites were deposited in the area (Chouabine Formation).

The first detailed stable isotope study of the phosphate remains (shark teeth and coprolites) from the Gafsa Basin was conducted by Ounis et al. (2008). The carbon isotope analyses resulted in a pronounced negative carbon isotope excursion (CIE) of 3–4 ‰ at the limit of Unit-C and Unit-D of the Chouabine Formation, which was identified in two different sections and in two different archives (Fig. 1). Initially, therefore this CIE was proposed to mark the Paleocene-Eocene (P/E) boundary in the phosphate series.

The oxygen isotopic compositions of the fossils indicate a stable warm, tropical climate during the deposition of the phosphate layers. At the P/E boundary, however a global hyperthermal event (PETM – Paleocene Eocene Thermal Event) occurred reflected by a negative oxygen isotope shift in benthic foraminifera record (e.g. Zachos et al. 2001). The absence of any thermal anomaly at the PETM in the Gafsa sections was explained by the tropical position and the shallow, semi-closed condition of the Gafsa Basin (Ounis et al., 2008). However whether this preceding result is only due to this special local condition or rather a global phenomenon at low latitudes is not utterly clear.

Further investigation, therefore is necessary focusing on the connection of the Gafsa Basin with the global ocean, the possible effects of diagenetical processes and the verification of wider occurrence of CIE in the region. Hence other isotope systems such as Sr and Nd have been involved and applied for the same sample suits previously investigated in the Alima and Bliji Mountains (Ounis et al., 2008). In addition, shark teeth from the different phosphate layers of the Chouabine and Métlaoui Formations in the Kef Eddour region (Métlaoui) were collected and analyzed for Sr isotopic ratios.

The $^{87}\text{Sr}/^{86}\text{Sr}$ ratios are widely in the expected range of the Late Cretaceous and Paleocene-Eocene open seawater however the younger samples show more pronounced deviations from the global Sr-evolution curve. The ϵ_{Nd} values of the few sample analyzed are quite variable and they vary from -8.8 to -10.7. These preliminary data indicate either enhanced continental reworking or increased influence of early diagenetic fluid on the samples which is most possibly relating to the gradual closing of the basin during the Paleogene.

For further investigating the subject, in the Kef Eddour region a detailed section of the Chouabine Formation were sampled focusing not only the phosphate but the intercalated marls and carbonate layers especially across the supposed P/E boundary. Bulk sediment, total organic matter, phosphate remains and foraminifers are the initial targets for stable isotope analyses critical to the P/E boundary.

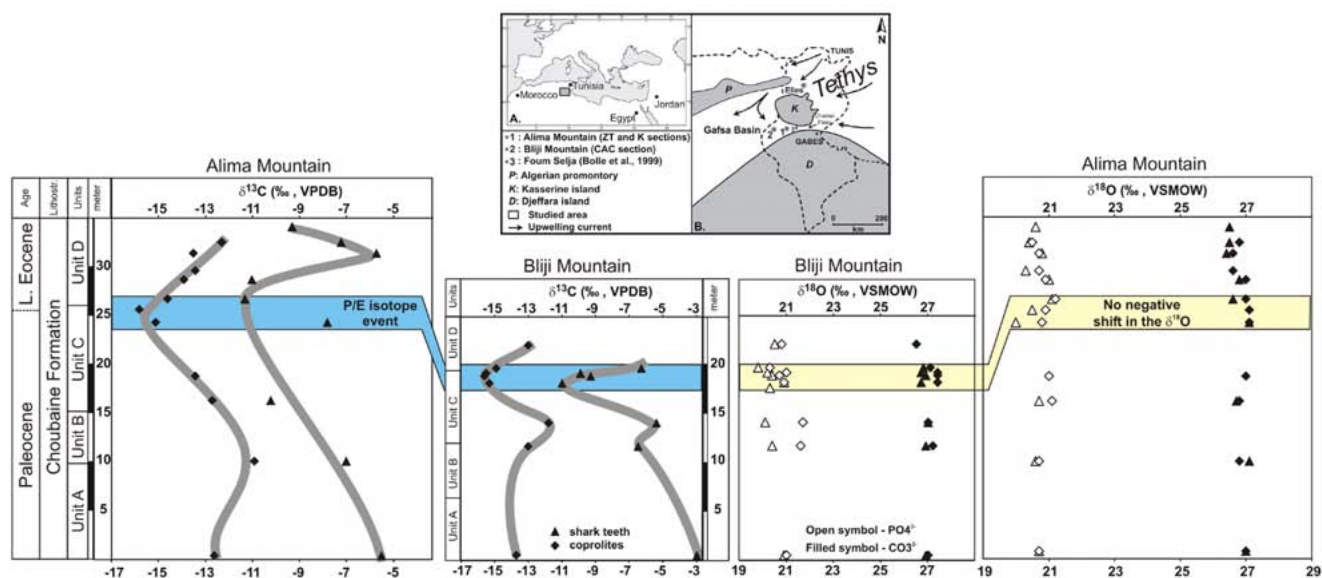


Figure 1. Palaeogeographical map of the studied Gafsa Basin in Tunisia and the obtained oxygen and carbon isotope distributions along two Paleocene–Eocene sequences in the Chouabine Formation (Ounis et al., 2008). Note the negative CIE at the limit of Unit-C and Unit-D, but no variation in the oxygen isotope record.

REFERENCES

- Chaabani, F., 1995. Dynamique de la partie orientale du bassin de Gafsa au Crétacé et au Paléogène: Etude minéralogique et géochimique de la série phosphatée Eocène, Tunisie méridionale. Thèse Doc. Etat. Univ. Tunis II. Tunisie.
- Ounis, A., Kocsis, L., Chaabani, F. & Pfeifer H.-R. 2008: Rare earth element and stable isotope geochemistry (d^{13}C and d^{18}O) of phosphorite deposits in the Gafsa Basin, Tunisia. *Palaeogeogr. Palaeoclimatol. Palaeoecol.*, 268, 1–18.
- Zachos, J., Pagani, M., Sloan, L., Thomas, E. & Billups, K. 2001: Trends, rhythms, and aberrations in global climate 65 Ma to present. *Science* 292, 686–693.
- Zaïer, A., Beji-Sassi, A., Sassi, S. & Moody, R.T.J. 1998: Basin evolution and deposition during the Early Paleocene in Tunisia. In: Macgregor, D.S., Moody, R.T.J. and Clark-Lowes, D.D. (Eds.), 1998. *Petroleum Geology of North Africa*. Geol. Soc. London Spec. Publ. 132, pp. 375–393.

2.14

Geochemical and mineralogical examinations of roman crucibles from Autun (France)

Daniela König & Vincent Serneels

Department of Geosciences, University of Fribourg, Chemin du Musée 6, CH-1700 Fribourg (daniela.koenig@unifr.ch)

The investigated crucible fragments arise from an archaeological excavation of the site of the Lycée militaire in Autun (France). During the excavation of a large craftsman quarter at the Roman town of Autun, several hundred kilos of crucible fragments have been collected. There are obvious evidences for foundry work but the production of copper-based alloys (Zn, Sn, Pb) is also supposable. The archaeological site is dated to the Gallo-Roman period (Chardon-Picault & Pernot, 1999).

This study aims to specify the structure of the ceramics to identify the raw material and describe the technology of production. For this, used analytical methods comprise optical microscopy, SEM and SEM-EDX analyses on wall cross-sections, X-ray diffraction analyses (XRD) from differentiable parts of the inner wall layer as well as X-ray fluorescence spectroscopy (XRF) on the different layers of the crucibles.

In general, the crucibles show a multilayered wall structure, which are made up of two to three layers of different ceramic materials. Each layer possesses distinct thicknesses and fabric characteristics. The first (outer) and the second (inner) layer, which are present in all crucibles are optically distinguishable by the differing colour and the glass-matrix composition. These features suppose major mineralogical heterogeneities between single layers and individual fragments. An innermost (third) layer, which is missing in some of the investigated fragments, is probable a kind of inner protecting layer. The fabric is influenced by two more important factors. Firstly, the strong gradient of temperature between the inner and the outer part are based on the high external fieriness. Secondly, the fabric is influenced by interaction between the inner metallic charge, the ceramic and the contribution gases from outside.

The first results show remarkable differences between the two main layers. The inner layer is characterised by a high content of mullite, low-cristobalite, quartz and in some cases orthoclase, whereas the low-cristobalite is often ill crystallised. Therefore, firing temperatures are proposed to have reached approximately 1100°C to 1300°C. In contrast the outer layer is dominated by a higher content of mullite bearing glass. Additionally, some samples contain secondary analcime in the first layer, which was formed during the burial stage. XRF analysis documents a ten times higher CaO concentration in the first (outer) layer as in the second (inner) one. The sporadically occurring third layer has also a differing CaO concentration, which is higher than the concentration in the second (inner) one. This feature could be a first hint of different source materials for the single layers.

REFERENCES

Chardon-Picault, P. & Pernot, M. (1999): Un quartier antique d'artisanat métallurgique à Autun - Le site du Lycée militaire. Paris: MSH, 320 p.

2.15

Fluid boiling and mixing during latest stage orogenic gold mineralization at Brusson, NW Italian Alps

Lambrecht Glenn¹, Diamond Larryn¹

¹ Rock-Water Interaction Group, Institute of Geological Sciences, University of Bern, Switzerland (lambrecht@geo.unibe.ch)

We are investigating fluid inclusions in hydrothermal quartz-carbonate-sulphide veins from the abandoned Fenilia Mine at Brusson, northwestern Italian Alps. Studied quartz samples contain early primary and pseudosecondary inclusions that can be approximated by the CO₂-H₂O-NaCl system. Two types are observed (Fig. 1): first, abundant low-XCO₂ L_{aq}L_{car}V inclusions that homogenize to liquid at ~230 °C and have an aqueous salinity of 3.7 mass% NaCl_{equiv}; second, high-XCO₂ L_{aq}L_{car} inclusions with similar homogenization behaviour and an aqueous salinity of 2.2 mass% NaCl_{equiv}. The two contras-

ting inclusion types were described by Diamond (1990) and interpreted to have formed during boiling (phase separation into “vapour” and “liquid”) of the low- XCO_2 -type ore-bearing solution.

New charge-contrast imaging has revealed fine overgrowths of quartz on the main-stage crystals (quartz zone 3 in Fig. 2c). These host late-primary inclusion assemblages, which consist of rare low- XCO_2 $\text{L}_{\text{aq}}\text{L}_{\text{car}}\text{V}$ inclusions (identical to those described above) coexisting with abundant $\text{L}_{\text{aq}}\text{V}$ inclusions. The latter were previously unknown at this deposit. Their carbonic phases have variable volume fractions $[\varphi(\text{car})]$ ranging from 0.075 to 0.47 ($\pm 4\%$) (Fig. 1a), which, along with element partitioning data, is diagnostic of boiling. These inclusions homogenize at 3180°C via the transition $\text{L}_{\text{aq}}\text{V} \rightarrow \text{L}_{\text{aq}}$.

Raman analysis revealed CO_2 , CH_4 and N_2 within the carbonic phases of all $\text{L}_{\text{aq}}\text{V}$ inclusions, but the molar ratios of the gases vary systematically. In Fig. 1b these analyses reveal a linear array stretching from compositions close to those of low- XCO_2 $\text{L}_{\text{aq}}\text{L}_{\text{car}}\text{V}$ and high- XCO_2 $\text{L}_{\text{aq}}\text{L}_{\text{car}}$ inclusions (end-member no. 1 in Fig. 1) to compositions of about 4.4 mol.% CO_2 , 91.4 mol.% N_2 and 4.2 mol.% CH_4 (end-member no. 2 in Fig. 1).

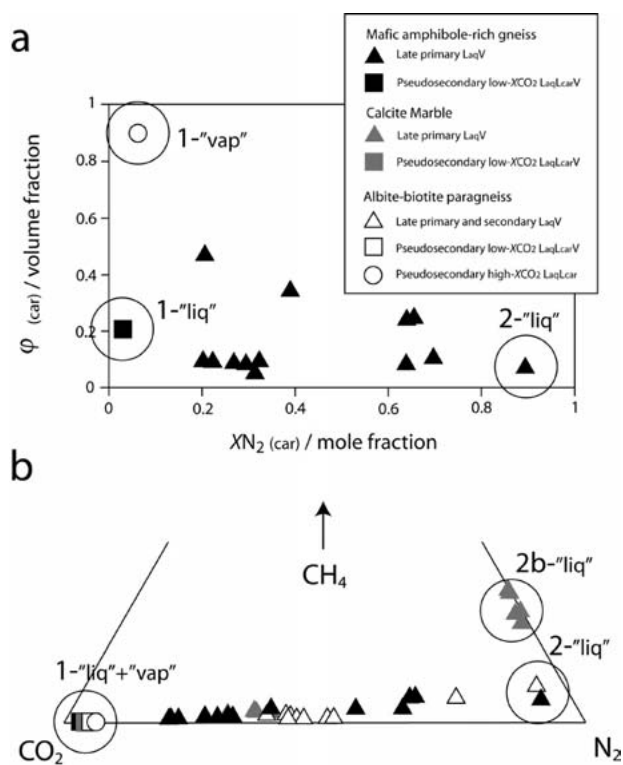


Figure 1. (a) Relationship between volume fraction of the carbonic phase $[\varphi(\text{car})]$ and mole fraction of N_2 in the carbonic phase $[\text{XN}_2(\text{car})]$ and (b) molar composition of the carbonic phase in $\text{L}_{\text{aq}}\text{V}$, low- XCO_2 $\text{L}_{\text{aq}}\text{L}_{\text{car}}\text{V}$, and high- XCO_2 $\text{L}_{\text{aq}}\text{L}_{\text{car}}$ inclusions from quartz-vein samples hosted by different types of wall rock.

The liquid end-members 1, 2 and 2b are mutually miscible at the entrapment temperature of the low- XCO_2 liquid, 230°C . Therefore, the linear compositional trend of the late primary $\text{L}_{\text{aq}}\text{V}$ inclusions in Fig. 1b can be interpreted as a mixing line. Thus, it appears that boiling and mixing occurred simultaneously in the vein system during precipitation of quartz zone 3 (Fig. 2c).

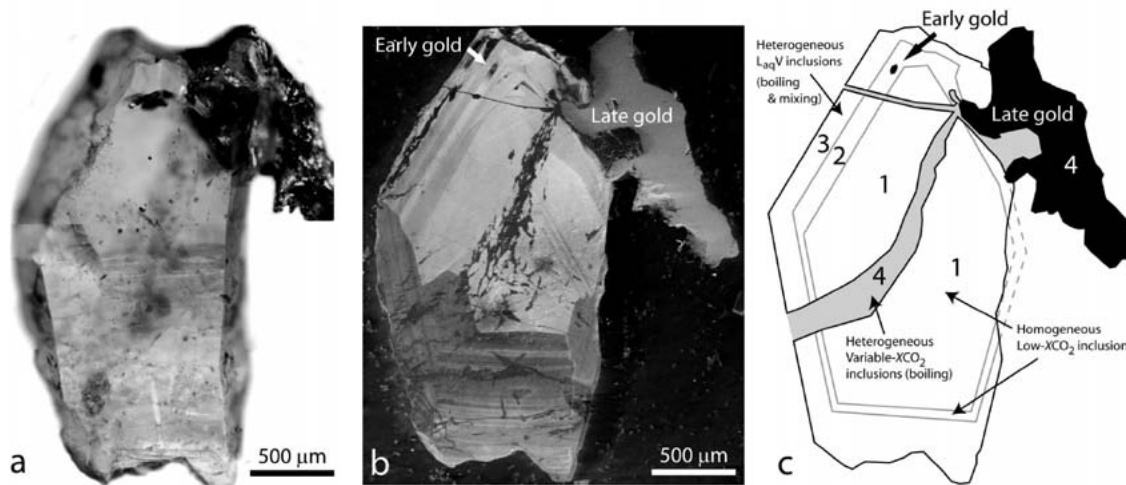


Figure 2. (a) Photograph of quartz crystal with free gold deposited on the surface. (b) SEM charge-contrast image of a polished section through this crystal. (c) Schematic interpretation of the charge-contrast image in b. See text for further details.

The quartz sample in Fig. 2 exhibits two generations of gold: small inclusions within a late growth zone (Early gold in zone 2, Fig. 2c); and free gold mostly overlying the outer crystal surface (Late gold, Fig. 2c). Charge-contrast imaging reveals that this late gold is younger than the fine crystal growth zone 3 (Fig. 2c) that hosts the late primary $\text{L}_{\text{aq}}\text{V}$ inclusion assemblages. The late gold is also in direct contact, and therefore coeval, with healed fractures (zone no. 4 in Fig. 2c) that host a secondary assemblage of variable- XCO_2 inclusions (including both low- XCO_2 $\text{L}_{\text{aq}}\text{L}_{\text{car}}\text{V}$ and high- XCO_2 $\text{L}_{\text{aq}}\text{L}_{\text{car}}$ types). These

new temporal and compositional deductions are used to reconstruct the history of quartz growth in the Fenilia vein: First, a low- XCO_2 -type carbonic liquid forms main-stage quartz (zone 1 in Fig. 2c) and alters the adjacent wall rock. Subsequent simultaneous precipitation of gold and quartz is presumably triggered by cooling or by wall-rock reactions. Progressive cooling and reduction in fluid pressure owing to on-going uplift of the Western Alps induces boiling of the main-stage fluid (Diamond, 1990). Pore fluid from the wall rocks simultaneously seeps into the open vein, where it mixes with boiling carbonic fluid. At this moment the late primary $\text{L}_{\text{aq}}\text{V}$ inclusions are trapped (zone 3 in Fig. 2c). Finally, a new pulse of boiling, ore-bearing carbonic fluid enters the mine level, fracturing the existing quartz crystals and depositing the late gold on top of them (zone 4 in Fig. 2c). Without any evidence for wall-rock pore waters at this stage, it seems most likely that partitioning of gold-complexing ligands (aqueous HS^- and H_2S) from the liquid into the carbonic vapour triggered deposition of the late gold.

REFERENCES

Diamond, L.W. 1990: Fluid inclusion evidence for P-V-T-X evolution of hydrothermal solutions in late-alpine gold-quartz veins at Brusson, Val-d'Ayas, Northwest Italian Alps. *American Journal of Science*, 290, 912-958.

2.16

Kiln furnitures from the faience manufacture of Granges-le-Bourg (Haute Saône, France): contrasting recipes

Maggetti Marino¹, Morin Denis², Serneels Vincent¹, Neururer Christoph¹

¹ Department of Geosciences, Mineralogy and Petrography, University of Fribourg, CH-1700 Fribourg (marino.maggetti@unifr.ch)

² CNRS, TRACES - UMR 5608, Université de Toulouse, F-31058 Toulouse

During archaeological excavations of the brickworks (16th - 19th c.) from Granges-le-Bourg (Morin & Morin-Hamon 2004), faience waste was found from an unknown late 18th/early 19th c. production. In Granges-le-Bourg, coarse, as well as fine ceramic was therefore produced simultaneously. Archaeometric analysis included 35 samples of kiln furniture or technical ceramic (firing plates, saggars, spacers, props, wads), 5 bricks and tiles and 7 clays in order to study the chemical - mineralogical composition of these objects. Analytical techniques were optical microscopy, X-ray fluorescence, X-ray diffraction and scanning electron microscopy, coupled to an energy-dispersive X-ray spectrometer.

A first group of kiln furniture (firing plates, saggars and props) is, as to be expected, calcium- and magnesium-poor, well suited to support high firing temperatures as well as several firing cycles. The coarse ceramic (bricks & tiles) has an identical chemical composition. Saggars and bricks are grog-tempered. The second group of spacers and wads is calcium- and magnesium-rich (between 5-10 wt. % CaO resp. MgO), matching the chemical composition of the faience production. The ancient potters obviously used two recipes for the kiln furniture: the brick & tile recipe and the faience paste recipe. The use of a non refractory paste for the spacers and wads is puzzling. Ceramic objects with such high flux (CaO , MgO) will melt around 1100°C - they are not very well suited to resist high firing temperatures of a faience kiln, nor to support many firing cycles. Were these objects used only once? Local Triassic (Anisian) marls contain much dolomite and are chemically similar to the High-Mg group. As shown by vertical profiles of two raw materials outcrops, there is a decarbonatisation towards the surface. The top layers correspond chemically well to the MgO -poor objects. The potters used such local raw material and not imported, specific refractory clays. A coating of either tin glaze (with significantly less tin oxide than the faience pieces) or lead glaze has been applied to the interior of the saggars. For these objects, a small glaze-ceramic body interface has been observed only for the lead glaze. The absence of any significant reaction zone indicates that the glaze suspension was applied on already (biscuit) fired saggars.

REFERENCE

Morin, D., & Morin-Hamon H. J. 2004: La tuilerie-faïencerie de Granges-le-Bourg, *Bulletin de la société d'Histoire et d'Archéologie de l'Arrondissement de Lure*, 23, 94-104.

2.17

The faience manufacture Le Bois d'Épense (North-eastern France, 18/19th century)

Maggetti Marino¹, Rosen Jean², Serneels Vincent¹, Neururer Christoph¹

¹ Department of Geosciences, Mineralogy and Petrography, University of Fribourg, CH-1700 Fribourg (marino.maggetti@unifr.ch)

² DR CNRS, UMR 5594, Faculté des Sciences, Université de Dijon, F-21000 Dijon

The French factory Le Bois d'Épense was an important tin-glaze pottery production site in the years 1735-1742 and 1764-1848, with almost 200 workers at the top of its activity. We present the analytical results for 56 faïences (= tin-opacified lead glazed earthenware), 28 samples of technical ceramic (saggars and spacers) and 6 local clays. Analytical techniques were optical microscopy, X-ray fluorescence (XRF), X-ray diffraction (XRD) and scanning electron microscopy, coupled to an energy-dispersive X-ray spectrometer (EDS).

As shown by XRF analysis, the faïence is very homogeneous and has a typical calcareous faïence body (16-24 wt.% CaO). No chemical difference can be evidenced between the biscuits and the faïences with a "grand feu" or an enamel decoration. The products from this site can easily be distinguished from the actually known French faïence reference groups. The spacers were made from the same paste as the faïence, but the saggars with a imported refractory clay, rich in Al_2O_3 . For the faïence body, a mixing of two local clays has been reported in a paper from 1877. However, the prospected local Cretaceous (Middle Albian) clays never exceed 12 wt.% CaO. An addition of a CaO-rich material is undoubtedly necessary to reach the 16-24 wt.% CaO of the faïence. This is not a local marl, but most probably a very pure chalk from the Champagne. Firing temperatures were inferred by XRD and lie < 950°C for the biscuits and between 950-1050°C for the glazed pieces, indicating a two chambered kiln. The quality of the tin glaze is in general good, showing rare rounded quartz crystals, very few newly crystallized phases (K-feldspars, cristobalite ?) and bubbles. Contrasting, the cassiterite crystals are heterogeneously dispersed, forming clusters. The absence of any glaze-body interface is consistent with the application of the liquid glaze to an already fired body. Area measurements show that all tin opacified glazes can be classified as SiO_2 -PbO glazes (~ 80 wt.%) containing about 9 wt. % SnO_2 , with other oxides in concentrations < 5 wt.%. Spot analyses of the glass matrix indicate a much lower tin oxide amount of about 2 wt.% as compared to the area measurements.

2.18

Forensic geology: characterisation of light element stable isotopes in soil samples of the Swiss Plateau

Marolf André¹, Vennemann Torsten¹ & Bonzon Jeanne²

¹ Institut de minéralogie et géochimie, Université de Lausanne, Bâtiment Anthropole, CH-1015 Lausanne (andre.marolf@gmail.com)

² Musée cantonal de géologie, Université de Lausanne, Bâtiment Anthropole, CH-1015 Lausanne

The purpose of this work is to characterise soil samples from the Swiss Plateau for their stable carbon and oxygen isotope compositions as a basis for forensic and geological research. Five sampling locations were chosen in the cantons of Geneva, Vaud, Fribourg and Valais, and six in the canton of Zurich. The coordinates of the latter locations have been taken from real crime scenes (anonymised). Fourteen samples per location were collected for all localities except for the canton of Zurich where six samples per location were chosen, following a regular pattern for all localities. All the soil samples were characterised for their carbon and oxygen isotopic composition via Isotope Ratio Mass Spectrometry (IRMS). Organic compounds have been removed and carbonates and silicates analysed separately with a GasBench II, respectively a CO_2 -laser based extraction line, both linked to an IRMS.

The results indicate that carbon and oxygen isotopes are a promising tool to investigate variations in soils from the Swiss Plateau, but distinguishing between locations in the same region is still challenging. Despite these difficulties, three major domains can be clearly distinguished and the data shows that isotopes can be an additional, new fingerprint of soils. The domains of Valais (Martigny), the Romandie (Lausanne, Genève, Yverdon) and the Zürich region (Gockhausen, Hausen-am-Albis, Kindhausen, Oetwil-an-der-Limmat, Wallisellen and Wiesendangen) can be distinguished. A fourth domain (Fribourg), however, slightly overlaps the Zürich region and the Romandie domain and hence remains ambiguous.

The fact that other samples of carbonate, quartz and clay minerals that have been analysed from the Molasse show similar values to the soils analysed here, could indicate that the Molasse and the corresponding reworked Quaternary deposits are the main sources of inorganic soil material. Even if the formation and evolution of soils are still not well understood in detail, biological activity is unlikely to influence the mineralogy of soils analysed here in a major way, although local differences related to organic acids may be present. The data provide new insight into chemical and physical processes of soil formation and may thus be of help for interpretations of the geology, pedology, and for forensics. More analyses of soils will certainly help to provide further and additional constraints on soil provenance in time and space.

2.19

Element partitioning between immiscible silicate and carbonatite melts by centrifuge experiments

Martin Lukas H.J.¹, Schmidt Max W.¹, Hametner Kathrin² & Günther Detlef²

¹ Institute of Geochemistry and Petrology, ETH, Clausiusstrasse 25, CH-8092 Zürich (Lukas.martin@erdw.ethz.ch)

² Laboratory of Inorganic Chemistry, ETH, Wolfgang-Paulistr. 10, CH-8093 Zürich

Carbonatite are known for their economic importance as they are enriched in rare incompatible elements, which are exploited for technical industry. The mechanisms which can form carbonatites are: (a) very small degree of partial melting of a CO₂-rich mantle, (b) extreme differentiation of a CO₂-rich undersilicified magma, (c) by silicate-carbonatite liquid immiscibility.

This study is focused on liquid immiscibility and it aims to determine trace element partition coefficients (K_D) between carbonatite and silicate melts in experiments. The K_D values will then be applied to natural conjugate melt pairs occurring in volcanoes erupting both silicate and carbonatite magmas.

The strategy of this study is to obtain liquid immiscibility by experiments, segregate the coexisting liquids by centrifuging and determine element partition coefficients for highly sodic and highly potassic carbonatite-silicate melt systems. These partition coefficients are then applied to test whether liquid immiscibility was the process forming kamafugite-carbonatite pairs. In comparison with the only existing previous centrifuge study from Veksler et al. (1998), we study close-to-natural systems and determine ≥ 40 element partition coefficients. The investigated sodic system is from Lee & Wyllie (1997), the potassic system simulates the Italian intra-appeninic kamafugite-carbonatite suite. Kamafugites are highly silica undersaturated, have extreme K₂O contents and K₂O/Na₂O > 5, crystallizing phlogopite, olivine, leucite, melilite, and also kalsilite. They are associated with carbonatites, which at some localities carry mantle xenoliths indicating that they originate from depths > 45 km.

Immiscible carbonatite-silicate melts devoid of crystals are produced at 1 GPa, 1230 °C and 1.7 GPa, 1220-1250 °C for the sodic and ultrapotassic systems, respectively. The trace element spiked starting materials were first equilibrated in static experiments, reloaded in a single stage piston cylinder mounted on a centrifuge as described by Schmidt et al. (2006), and rerun at identical P-T conditions at 700 g for 3-5 hours to physically separate the liquids. LA-ICPMS analyses were performed on seven centrifuged experiments representing the two systems.

The results indicate that the partition coefficients are close to unity. The alkali and alkali earth elements have a affinity to partition into the carbonatite melt as well as P and Mo whereas the HFSE have a strong affinity for the silicate melt. The LREE elements partition weakly into the carbonatite melt whereas the HREE prefer the silicate melt. The weak partitioning of the LREE into the carbonatite melt indicates that liquid immiscibility is not the process enriching the carbonatites in REE.

REFERENCES

- Lee, W. J. & Wyllie, P. J. 1997: Liquid immiscibility between nephelinite and carbonatite from 1.0 to 2.5 GPa compared with mantle melt composition. *Contributions to Mineralogy and Petrology*, 127, 1-16.
- Schmidt, M. W., Connolly, J. A. D., Gunther, D. & Bogaerts, M. 2006: Element partitioning: The role of melt structure and composition. *Science*, 312, 1646-1650.
- Veksler, I. V., Petibon, C., Jenner, G. A., Dorfman, A. M. & Dingwell, D. B. 1998: Trace element partitioning in immiscible silicate-carbonatite liquid systems: an initial experimental study using a centrifuge autoclave. *Journal of Petrology*, 39, 2095-2104.

2.20

Internal flow structures in columnar jointed basalt from Hrepphólar, Iceland

Mattsson Hannes B.¹, Bosshard Sonja A.¹, Hetényi G.¹, Almqvist Bjarne S.G.², Hirt Ann M.², Caricchi Luca³ & Caddick Mark¹

¹ *Institute of Geochemistry and Petrology, ETH Zürich, Clausiusstrasse 25, 8003 Zurich (hannes.mattsson@erdw.ethz.ch)*

² *Institute of Geophysics, ETH Zürich*

³ *Department of Earth Sciences, University of Bristol, U.K.*

Columnar jointed basalt from Hrepphólar in southern Iceland display spectacular internal structures when cut. These structures follow the overall orientation of the columns and display semi-circular to circular features when cross-cut. It was previously believed that these internal structures formed as a result of alteration due to circulation of meteoric water within the column-bounding fractures after emplacement. However, new field observations of viscous fingering within the columns and the fact that approximately 80% of the semi-circular features are found within the column whereas the remaining 20% are cut by the column-bounding fractures clearly shows that these internal structures must have formed prior to crack-propagation (and are thus primary features).

Here we present the results of textural and petrological analyses through a cross-section of a column, in combination with magnetic susceptibility and anisotropy measurements of the same samples. The variation in textures and geochemistry can be attributed to the presence of diffuse banding caused by variations in the modal proportions of the main phenocryst phases (i.e., plagioclase, clinopyroxene, olivine and titanomagnetite/ilmenite). Orientation of plagioclase laths and titanomagnetite crystals (based on measurements in thin sections and AMS-measurements) are consistent with vertical flow alignment. Nowhere in the column can evidence for downwards flow be found (excluding the possibility of small-scale convection cells generating these features).

It is proposed here, that the volume decrease associated with solidification (typically 10-15 vol.% for basaltic systems) and the increasing weight of the overlying crust results in upwelling of partially crystallized material into the centre of the columns. Preliminary numerical modeling indicates that the isotherms within individual columns become steeper with increasing depth in a lava flow (allowing for larger displacement distances). We propose that this upwelling can be a rather common phenomenon in nature, but without the presence of chemically distinct compositions (or textural banding) it can be difficult to recognize such features in the field.

2.21

MINERAL WEATHERING ALONG A SOIL CHRONOSEQUENCE IN A HIGH ALPINE PROGLACIAL AREA: A MULTIPLE APPROACH

Christian Mavris¹, Markus Egli¹, Michael Plötze², Jens Götze³, Aldo Mirabella⁴, Daniele Giaccai⁴, Wilfred Haeberli¹

¹ Department of Geography, University of Zurich, Zurich, 8057, Switzerland (christian.mavris@geo.uzh.ch)

² ETH Zurich, Institute for Geotechnical Engineering, Zurich, 8093, Switzerland

³ Institute of Mineralogy, TU Bergakademie Freiberg, Freiberg, D-09596, Germany

⁴ Istituto Sperimentale per lo Studio e la Difesa del Suolo, Centro di ricerca per l'Agrobiologia e la Pedologia, Firenze, Italy

Climate change and glacier melting feed the need for understanding the processes related to weathering of recently exposed areas. Past studies in high Alpine environments show that clay mineral formation rates are higher in younger soils (<1000 yr) than in older soils (>10000 yr). However, investigations of processes that occur in the first decades of soil formation are rare.

In the present study we investigated the mineral weathering in a recently exposed high Alpine chronosequence. The study was undertaken in the Morteratsch glacier forefield, located in SE Switzerland. The progressively exposed proglacial area offers a full time sequence from 0 to 150 yr old surfaces. The rock basement is the Bernina crystalline unit, mostly constituted of Variscan granitoid rocks (Büchi, 1994). Previous mineralogical studies carried out in the soils of the proglacial forefield (Mavris et al., 2010) show a decrease of biotite and epidote as a function of time in the fine earth fraction (<2 mm). Mineralogical measurements of the clay fraction (<2 µm) were now carried out using XRD and DRIFT. Furthermore, analysis in the d(060) range were carried out. The decreasing content of trioctahedral phases with time in the clay fraction confirms active chemical weathering and formation and transformation of parent rock mineralogy. Measurement of layer charges allowed the detection of smectite and vermiculite and the attribution of the parent phases. Along the selected chronosequence, the smectite content increased steadily. Furthermore, the combination of cathodoluminescence (CL) and Nomarski DIC microscopy for the observation of the fine earth fraction (<2 mm) allowed the observation of compositional and weathering features in both the parent material and the soils. The mineral formation and transformation processes detected within the considered time span confirm the high reactivity of freshly exposed sediments.

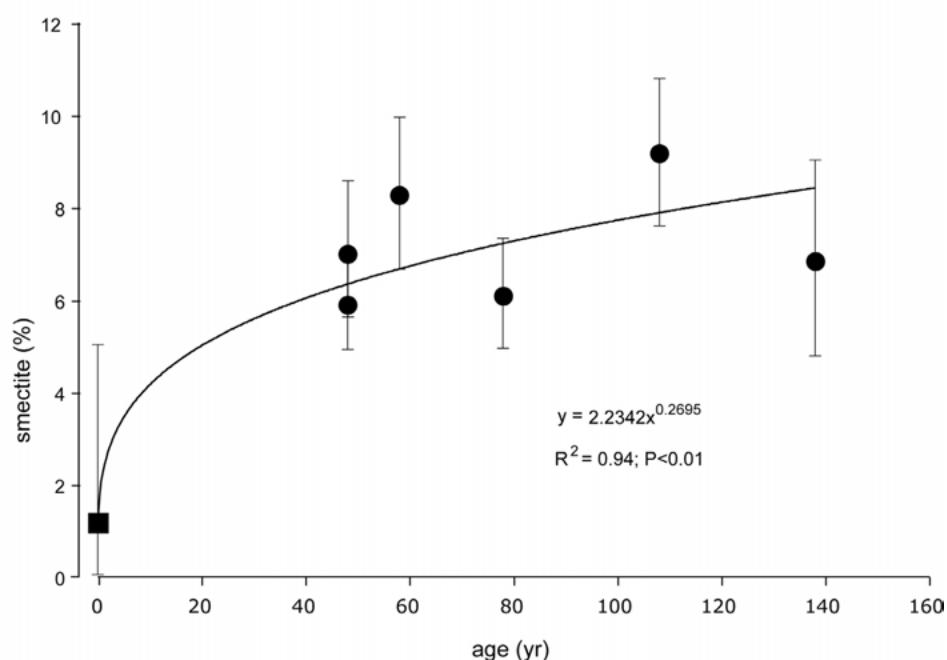


Fig. 1. Smectite content as a function of pedogenesis. Square dot = glacial till, dot = topsoils along the proglacial area.

REFERENCES

- Büchi H. 1994: Der variskische Magmatismus in der östlichen Bernina (Graubünden, Schweiz). Schweizerische Mineralogische und Petrographische Mitteilungen, 74, 359-371
- Mavris, C., Egli, M., Plötze, M., Blum, J.D., Mirabella, A., Giaccai, D., Haeberli, W. (2010) – Initial stages of weathering and soil formation in the Morteratsch proglacial area (Upper Engadine, Switzerland). Geoderma, 155, 3-4, 359-371.

2.22

Fumarolic aerosols from El Chichón volcano, Mexico

Meier Mario Federico¹, Grobéty Bernard^{1, 2}

¹ Department of Geosciences, University of Fribourg, Chemin du Musée 6, CH-1700 Fribourg (mario.meier@unifr.ch, bernard.grobety@unifr.ch)

² Fribourg Center for Nanomaterials (FriMat), University of Fribourg, CH-1700 Fribourg

Quiescent volcanoes are emitting continuously aerosol particles by fumarolic and diffuse degassing into the troposphere. The impact of these particles on the environment, e.g. on the radiation budget, may be considerably. However, only scarce information about the nature and the evolution of such particles is available (e.g. Mather et al. 2003; Pfeffer et al. 2006). The aim of this study is to characterize chemically and morphologically fumarolic particulate matter from El Chichón volcano (Chiapas, South Mexico, 1150 m.a.s.l.).

For that purpose aerosol particles were sampled actively onto polycarbonate Nuclepore filters and Transmission Electron Microscopy (TEM) grids in 2009. The sampling devices, an active PM10 and a corrosion resistant electrostatic sampler, were used at the crater rim (CR) and close to the fumaroles inside the crater. The samples were analyzed by TEM and Computer Controlled Scanning Electron Microscopy (CCSEM), both combined with simultaneous Energy Dispersive Spectroscopy analysis (EDX).

Several thousands of particles in the size fraction 0.4 – 10 µm have been analyzed and classified by CCSEM. The solid particle concentration inside the crater was around 3000 particles/liter, whereas on the rim the concentration was half as high. At both sites most of the particles were containing sulfur. The dominant fumarolic particle species were sulfur/sulfuric acid particles and Na-, K-, Na-K- respectively Ca-sulfates. Total sulfur containing particle flux is estimated to be 0.1 kgs⁻¹. Alkali chlorides could also be detected. Clays are considered to have a non-fumarolic origin. Their abundance is the same at both sampling sites. Aluminum containing particles (Al-oxides) are clearly more abundant at the CR. That points to a higher influence of soil particles on the total particle concentration outside the crater. Many particles sampled inside the crater are composite particles. Some of them contain Na-sulfate needles and pseudo-hexagonal Na-K-sulfate crystals. Other composite particles are containing P, S, K, Na, K, (Mg), (Al), (Zn) and (Pb). The phosphorus points to a non magmatic source (Obenholzer et al. 2003). Most of the composite particles, including the P rich particles, are no longer present at the CR.

The fumaroles at El Chichón emit hydrothermal steam rich in CO₂ and lower amounts of H₂S, acidic species such as SO₂ and HCl are nearly absent (Rouwet et al. 2009). During the sampling period, the gas emissions were accompanied by geyser activity with increased discharge of Na-Cl-SO₂ waters. Sulfate particles can be derived from both types of activity. The presence of the different sulfates can be partially interpreted as precipitation products resulting from the evaporation of geyser derived liquid droplets. The precipitation sequence for sodium dominated neutral (Ca)-Na-K-SO₄ water is (arcanite)-aphtitalite followed by a Na-sulfate phase, as observed. More data about fumarolic aerosols are crucial for a better understanding of formation processes and their impact on the environment.

REFERENCES

- Mather, T.A., Pyle, D.M. & Oppenheimer, C., 2003: Tropospheric volcanic aerosol. In Robock, A. & Oppenheimer, C., eds.: *Volcanism and the Earth's atmosphere*. Geophysical Monograph 139, Washington D.C., AGU, 189-212.
- Obenholzer, J.H., Schroettner, H., Golob, P. & Delgado, H., 2003: Particles from the plume of Popocatepetl volcano, Mexico – the FESEM/EDS approach. In Oppenheimer, C., Pyle, D.M. & Barclay, J., eds.: *Volcanic degassing*. Geological Society, London, Special Publications, 213, 123-148.
- Pfeffer, M.A., Rietmeijer, F.J.M., Brearley, A.J. & Fischer, T.P., 2006: Electron microbeam analyses of aerosol particles from the plume of Poás Volcano, Costa Rica and comparison with equilibrium plume chemistry modelling. *Journal of Volcanology and Geothermal Research*, 152, 1-2, 174-188.
- Rouwet, D., Bellomo, S., Brusca, L., Inguaggiato, S., Jutzeler, M., Mora, R., Mazot, A., Bernard, M., Cassidy, M. & Taran, Y., 2009: Major and trace element geochemistry of El Chichón volcano-hydrothermal system (Chiapas, Mexico). *Geofísica internacional*, 48 (1), 55-72.

2.23

Petrogenetic evolution of Neogene volcanism in northern Uromieh-Dokhtar Magmatic Belt: Insights on the origin of post-collision magmatism

Monsef Reza¹, Emami Mohamad Hashem², Rashidnejad Omran Nematallah³ & Monsef Iman⁴

¹ Islamic Azad University, Estahban Branch, Iran (zaos13000@yahoo.com)

² Islamic Azad University, Islamshahr Branch, Iran

³ Geology Department Basic Science Faculty, Tarbiyat Modares University, Tehran, Iran

⁴ Shahid Beheshti University, Faculty of Earth Sciences, Tehran, Iran

The Neogene volcanic rocks were exposed northern part of the Uromieh-Dokhtar Magmatic Belt, along which the Neo-Tethyan oceanic lithosphere was closed during a period between Eocene and Oligocene.

The collision-related volcanic rocks, which were most evident during the Early Miocene to Early Pliocene, span the whole compositional range from andesitic basalt to pargasitic andesite and display calc-alkaline character. These activities formed in relation to localized extensional basins and were dominated by pargasitic andesite to andesitic basalt lava flows and andesitic basalt dykes.

Major and trace elements geochemistry data exhibit enrichment in LILE and LREE relative to HFSE ($(La(N)/Yb(N)) = 3-9.7$ and $(La(N)/Nb(N)) = 2.5-4.5$), depletion in Nb, Ta and Ti, and also high Th/Yb and Ce/Nb ratios relative to Mantle array. The HFSE data demonstrate that volcanic lavas have high abundances of Nb/Yb and Nb/Ta ratios.

Our geochemical data indicate that calc-alkaline volcanic rocks were derived from the mantle metasomatized enriched source with effective of liquid and sediment flux components inherited from a pre-collision subduction slab.

After collision between Arabian plate and Central Iran Block in Early Cenozoic, this region has experienced of lithospheric thinning and volcanism activity formed in relation to localized extensional regime during the Early Miocene to Early Pliocene. The volcanism postdates continental collision, occurring in transtensional tectonic environment.

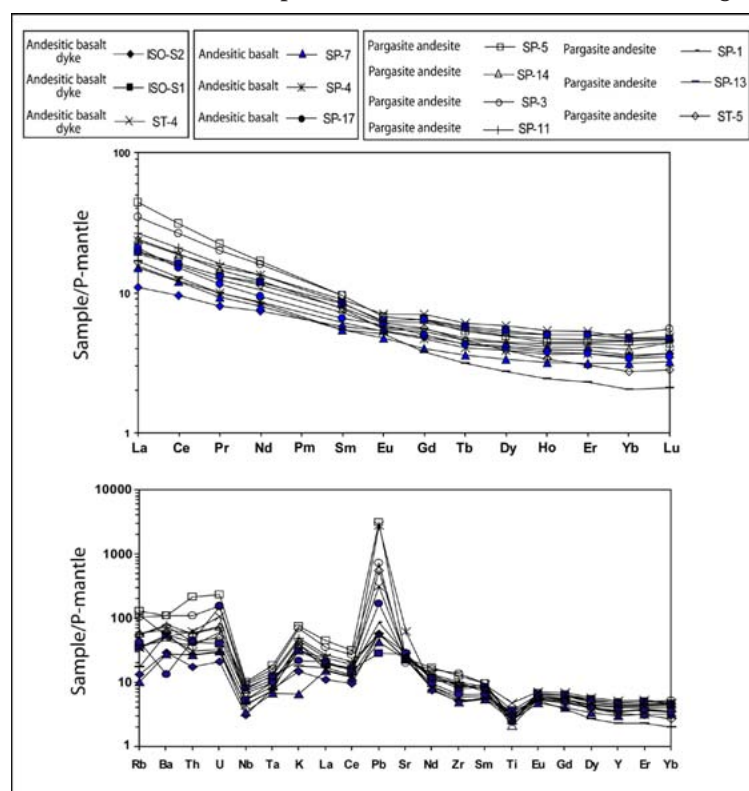


Fig 1: P-mantle normalized REE and trace element patterns for selected Neogene post-collision volcanic rocks in Uromieh-Dokhtar Magmatic Belt. The P-mantle normalizing values are from Sun & McDonough 1989.

REFERENCES

- McCulloch, M.T. & Gamble, J.A., 1991: Geochemical and geodynamical constraints on subduction zone magmatism. *Earth and Planetary Science Letters*, 102, 358-375.
- Sun, S.S. and McDonough, W.F., 1989: Chemical and isotopic systematics of oceanic basalts: implications for mantle composition and processes. In: Saunders, A.D. and Norry, M.J. (Eds.): *Magmatism in Ocean Basins*. Geological Society Special Publication London, 313-345.

2.24

Refining the granulite-facies metamorphism in the Rhodope metamorphic complex – Greece

Moulas Evangelos¹, Connolly James¹, Burg Jean-Pierre¹ & Kostopoulos Dimitrios²

¹ Department of Earth Sciences – ETH-Zurich, Sonneggstrasse 5, CH-8092 Zurich (evangelos.moulas@erdw.ethz.ch)

² Department of Mineralogy and Petrology, Panepistimioupoli Zographou, 15784 Athens, Greece

The Rhodope metamorphic complex (RMC) in northern Greece - southern Bulgaria is a stack of synmetamorphic nappes thrust mostly during Mesozoic times and having experienced extension coeval with magmatic activity during the Cenozoic, in particular during the Oligocene. The high-pressure (HP) metamorphic rocks of the central Rhodope are overprinted by granulite and amphibolite-facies metamorphism. The granulite-facies metamorphism has previously been interpreted to record high-pressure, we show here that the pressure of granulite metamorphism was unexceptional.

A retrogressed kyanite-eclogite from the intermediate thrust sheets of the RMC (outcrop near Thermes village - northern Greece) was investigated to establish the metamorphic conditions during decompression from eclogite-facies.

Textures indicating kyanite replacement by symplectites of corundum + plagioclase (An_{40-60}) and spinel ($Sp_{50}-Hc_{50}$) + plagioclase (An_{40-60}) reveal micro-scale metasomatic processes. We used free energy minimization and compositional phase diagrams (X-X sections) for the $Na_2O-CaO-FeO-MgO-Al_2O_3-SiO_2$ (NCFMAS) system to define the pressure and temperature (PT) space in which these symplectites have formed. The thermodynamic modelling reveals that the granulite-facies overprint occurred at a pressure < ca 1.0 GPa. The PT conditions of the kyanite breakdown are bounded by the univariant phase fields:

garnet = plagioclase + sillimanite + spinel

and

sapphirine + sillimanite = spinel + cordierite

Our results show that modelling of the symplectitic mineralogy in the simplified MASH system is inappropriate for NCFMAS symplectites.

2.25

Tertiary Porphyry and Epithermal Association of the Sapes-Kassiteres District, Eastern Rhodopes, Greece

Melissa Ortelli¹, Robert Moritz¹, Panagiotis Voudouris², Michael Cosca³ and Jorge Spangenberg⁴

¹ Département de Minéralogie, Rue de Maraîchère 13, CH-1205 Genève (melissa.ortelli@unige.ch)

² University of Athens, 15784 Athens, Greece

³ US Geological Survey, Denver Federal Center, Denver 80225, USA

⁴ Institut de Minéralogie et de Géochimie, Anthropole, CH-1015 Lausanne

The Sapes-Kassiteres district belongs to the Eastern Rhodopes and is located 20 km northwest of Alexandroupoli, Thrace, Greece. Tertiary magmatism associated with various types of mineralization in northeastern Greece and Bulgaria is related to post-orogenic extension (Voudouris et al. 2003, Marchev et al. 2005). This extensional context resulted in the formation of N-oriented fault systems controlling the ascent of magma and the emplacement of ore deposits. The Sapes-Kassiteres district contains the St-Demetrios, Viper and the St-Barbara prospects and is described as an association of porphyry and epithermal gold deposits hosted by volcano-sedimentary rocks (Voudouris et al. 2003, Michael 2004). Our study area, together with the well-known Perama Hill project, is part of a zone in the Eastern Rhodopes straddling Greece and Bulgaria, which is the focus of continuous exploration interest for gold by mining companies over the last decade.

The earliest mineralizing event is the Konos Mo (-Cu) porphyry hosted by a granodiorite-tonalite and containing mainly disseminated pyrite and some Cu-mineralization in sericitic altered host rocks, which is crosscut by molybdenite-pyrite

veins, dark-grey banded quartz veins (B-veins) and sulfide-rich gypsum veins. Epithermal events form the predominant mineralization of the district, starting with high-sulfidation mineralization at St-Demetrios with hydrothermal vuggy silica breccia and native gold associated with tellurides, sulfides and sulfosalts, followed by two different low/intermediate-sulfidation events characterized by amethyst-chalcedony veins related to quartz adularia alteration and milky quartz base metal veins related to sericitic alteration.

Fluid inclusion microthermometric data were collected from quartz, calcite, sphalerite of the mineralized veins from the Sapes-Kassiteres district, and show an evolution of homogenization temperatures (without pressure correction) ranging from 560°C, corresponding to the high-temperature porphyry system, to 160°C, related to a superficial or epithermal environment. An early boiling assemblage around 500 °C is crosscut by brine inclusion trails yielding homogenization temperatures around 240 °C with salinities between 30 and 50 wt. % NaCl equiv. Fluid inclusions related to the epithermal veins (Viper amethyst-chalcedony veins, and milky quartz-calcite veins) yield homogenization temperatures between 170 to 315°C and salinities below 6 wt. % NaCl equiv.

Oxygen isotope values combined with fluid inclusion data reveal the presence of a magmatic source for mineralizing fluids related to the porphyry system and the epithermal veins, with meteoric water contributing to the oxygen isotopic composition of the epithermal veins.

According to the $^{40}\text{Ar}/^{39}\text{Ar}$ data, the Sapes - Kassiteres district includes magmatic and mineralizing events, which took place between 31.3 and 33.1 Ma. This study reveals that the Sapes - Kassiteres magmatism and mineralization were contemporaneous at about 32 Ma with other Eastern Rhodopes ore districts in Bulgaria, like Madjarovo and Zvezdel. At the district scale, the $^{40}\text{Ar}/^{39}\text{Ar}$ ages tend to confirm the chronology of the magmatism and mineralization events observed in the field (Figure 1). The porphyry mineralization (biotite cooling age: 32.6 ± 0.5 Ma) precedes the biotite age of the potassic alteration at 32.0 ± 0.5 Ma. Adularia from the low/intermediate sulfidation system yielded an age of 31.5 ± 0.2 Ma. One set of the magmatic steam alunites has a plateau ages of 31.9 ± 0.2 Ma overlapping with the biotite and adularia ages. Another magmatic steam alunite yields a slightly younger age of 31.2 ± 0.4 Ma.

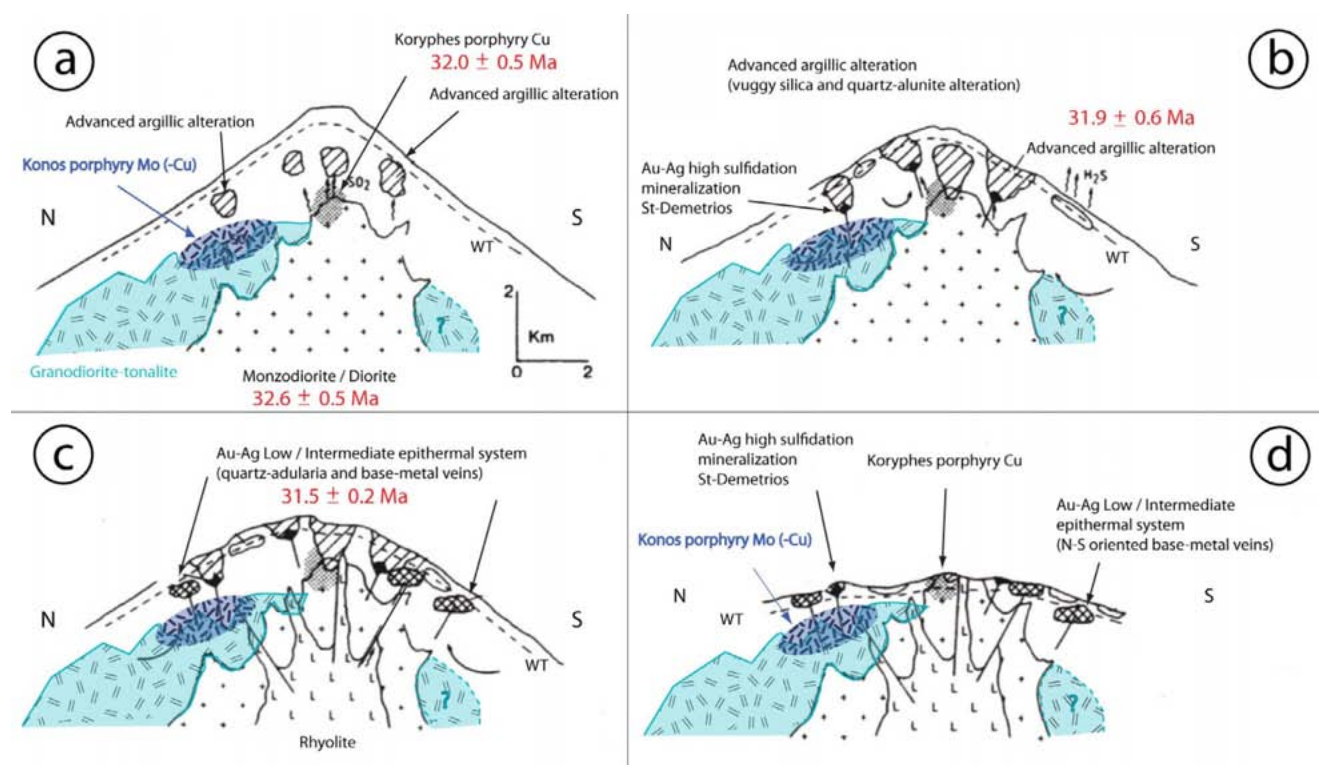


Figure 1. Modified genetic model by Voudouris (1993). The colored items highlight the new contributions of this study.

REFERENCES

- Marchev, P., Kaiser-Rohrmeier, M., Heinrich, C., Ovtcharova, M., von Quadt, A., Raicheva, R., 2005, Hydrothermal ore deposits related to post-orogenic extensional magmatism and core complex formation: The Rhodope Massif of Bulgaria and Greece : Ore Geology Reviews 27, p. 53-89.
- Michael, C., 2004, Epithermal systems and gold mineralization in western Thrace (North Greece) : Bulletin of the Geological Society of Greece vol. XXXVI, p. 416-423
- Voudouris, P., 1993, Mineralogische, mikrothermometrische und geochemische Untersuchungen an epithermalen Au-Ag Gangmineralisationen bei Kassiteres/Sape (Nordostgriechenland). PhD Thesis at Hambourg University.
- Voudouris, P., Melfos, V., Vavelidis, M., Arikas, K., 2003, Genetic relation between the Tertiary porphyry Cu (-Mo) and the epithermal Au (-Ag) deposits in the Rhodopes metallogenic province, Thrace region, Northern Greece : Eliopoulos et al. (eds) Mineral Exploration and Sustainable Development, SGA meeting Athens August 2003, p. 542-544.

2.26

Reactive multiphase flow at the pore-scale: the melting of a crystalline framework during the injection of buoyant hot volatiles.

Parmigiani Andrea¹, Huber Christian², Bachmann Olivier³ & Chopard Bastien¹

¹ Computer Science Department, University of Geneva, CH-1211 Geneva 4, Switzerland
(andrea.parmigiani@unige.ch)

² School of Earth and Atmospheric Sciences, Georgia Institute of Technology, GA 30332, USA.

³ Department of Earth and Space Sciences, University of Washington, WA, USA.

Multiphase reactive flows occur naturally in various environments in the shallow subsurface, e.g. CO₂ injections in saturated reservoirs, exsolved methane flux in shallow sediments and H₂O-CO₂ volatiles in magmatic systems. Because of their multiphase nature together with the nonlinear feedbacks between reactions (dissolution/melting or precipitation) and the flow field at the pore-scale, the study of these dynamical processes remains a great challenge.

In this study we focus on the injection of buoyant hot volatiles exsolved from a magmatic intrusion underplating a crystal-rich magma (porous medium). We use some simple theoretical models and a pore-scale multiphase reactive lattice Boltzmann model to investigate how the heat carried by the volatile phase affects the evolution of the porous medium spatially and temporally. We find that when the reaction rate is relatively slow and when the injection rate of volatiles is large (high injection Capillary number), the dissolution of the porous medium can be described by a local Peclet number (ratio of advective to diffusive flux of heat/reactant in the main gas channel). When the injection rate of volatile is reduced, or when the reaction rate is large, the dynamics transition to more complex regimes, where subvertical gas channels are no longer stable and can break into disconnected gas slugs.

For the case of the injection of hot volatiles in crystal-rich magmatic systems, we find that the excess enthalpy advected by buoyant volatiles penetrates the porous medium over distances $\sim r$ Pe, where r is the average radius of the volatile channel (\sim pore size). The transport of heat by buoyant gases through a crystal mush is therefore in most cases limited to distances $<$ meters. Our results also suggest that buoyant volatiles can carry chemical species (Li, F, Cl) far into a mush as their corresponding local Peclet number is several orders of magnitude greater than that for heat, owing to their low diffusion coefficients.

2.27

Constraining calcium isotope fractionation in corals

Pretet Chloé¹, Felis Thomas² & Samankassou Elias¹

¹Département de géologie et paléontologie, rue des maraîchers 13, CH-1205 Genève, Switzerland (chloe.pretet@unige.ch)

²MARUM-Center for Marine Environmental Sciences, University of Bremen, 28359 Bremen, Germany

Based on a multi-proxy dataset consisting of $\delta^{44}\text{Ca}$, $\delta^{18}\text{O}$ and Sr/Ca, this preliminary report discusses the parameters that control the calcium isotope fractionation in tropical corals.

Potential factors that control the calcium isotope ratio in coral skeleton include biological factors (vital effects), temperature and salinity. Currently the calcium pathway and isotopic fractionation in corals is not fully constrained. Therefore, detailed measurements and a multi-proxy approach appear fundamental for the understanding of parameters that influence the fractionation.

Our dataset is based on fossil last deglacial coral samples from Tahiti, cored during the IODP Expedition 310 (Camoin et al., 2007). For an accurate record, the coral skeleton was micro-drilled at subseasonal resolution. Ca and O isotopic composition as well as the Sr/Ca ratio were measured, using the same sample. For Ca, we used a TIMS Finnigan Triton T1, following the method described in Heuser et al. (2002).

Our preliminary results show that the fractionation is almost constant within error bars. No relationship between precipitation rate and coral $\delta^{44}\text{Ca}$ is recognized.

Subseasonal temperatures variations reconstructed from coral $\delta^{18}\text{O}$ signal and Sr/Ca ratio are not mirrored in coral $\delta^{44}\text{Ca}$. The weak temperature dependence reported by Böhm et al. (2006) is possibly not the only parameter that is responsible for the fractionation.

Removing sea-surface temperature component from the coral $\delta^{18}\text{O}$ signal ($\delta^{18}\text{O}_{\text{seawater}}$) results in a coral $\delta^{44}\text{Ca}$ record that reveals some similarity to the reconstructed $\delta^{18}\text{O}_{\text{seawater}}$ record, pointing to salinity as a potential factor that affects coral $\delta^{44}\text{Ca}$. However, we note that in modern corals the seasonal cycle of salinity at Tahiti cannot be resolved (Cahyarini et al., 2008). These preliminary results require further investigation, including measurements of skeleton originating from corals cultured under well-monitored environmental conditions.

Furthermore, we plan to measure the isotopic composition of different microstructural parts of corals (e.g., calcification center versus fibers) in order to better constrain the calcium isotope fractionation processes.

REFERENCES

- Böhm, F., Gussone, N., Eisenhauer, A., Dullo, W., Reynaud, S., & Paytan, A. 2006: Calcium isotope fractionation in modern scleractinian corals. *Geochimica et Cosmochimica Acta*, 70 (17), 4452-4462.
- Cahyarini S. Y., Pfeiffer M., Timm O., Dullo W., & Schönberg D. G. 2008: Reconstructing seawater $\delta^{18}\text{O}$ from paired coral $\delta^{18}\text{O}$ and Sr/Ca ratios: Methods, error analysis and problems, with examples from Tahiti (French Polynesia) and Timor (Indonesia). *Geochimica et Cosmochimica Acta*, 72, 2841-2853.
- Camoin, G.F., Iryu, Y., McInroy, D. & the IODP Expedition 310 Scientists 2007: Proceedings of the IODP 310. Integrated Ocean Drilling Program Management International, Inc, Washington, DC.
- Heuser, A., Eisenhauer, A., Gussone, N., Bock, B., Hansen, B.T., Nägler, T.F. 2002: Measurement of calcium isotopes ($\delta^{44}\text{Ca}$) using a multicollector TIMS technique. *International Journal of Mass Spectrometry*, 220, 385-397.

2.28

Complex dynamics in the Sesia Zone subduction system deduced from multiple generations of white mica and allanite: the power of microtextural analysis combined with petrochronology

Daniele Regis¹, Martin Engi¹, Daniela Rubatto², James Darling¹

¹ Institut für Geologie, Universität Bern, Baltzerstrasse 3, CH-3012 Bern (daniele.regis@geo.unibe.ch)

² Research School of Earth Sciences, Australian National University, Canberra

Research worldwide on the evolution of terrains with high-pressure (HP) rocks aims to elucidate the geodynamically fundamental processes at convergent margins. The Western Alps, notably their internal parts (Sesia-Lanzo Zone, Dent Blanche nappe, and smaller klippen units), have long been recognized as a classic HP terrane: a substantial area of predominantly continental, polycyclic basement transformed to blueschist or eclogite facies in the Alpine orogeny. However, recent regional work (Babist et al., 2006) has indicated substantial gaps and inconsistencies in the classic view of the Western Alps, and new models emphasizing the sequence of regional poly-deformation and poly-metamorphism have been proposed. To retrace the steps of this complex evolution, it is essential to link the detailed petrography and microchemical analysis of the major and accessory phases with their microtextural relations and subgrain-scale geochronology, using a retentive isotopic system.

We present a case study on a single poly-deformed eclogite facies sample from the Sesia Zone (Italian Western Alps), which contains phengite and allanite crystals with multiple metamorphic domains.

The sample, collected in the Scalero valley, consists of quartz (60%), phengite (20%), allanite/epidote (10%), detrital feldspar (2%) and albite (5%) with accessory monazite, apatite, titanite and zircon. Two foliations are marked by white mica of different composition: Phengite (Wm²-Phe²) marking the main foliation (S3) contains large relic flakes (Wm¹-Phe¹, pre-S3). Texturally old phengite cores (Phe¹) are rimmed by muscovite (Wm¹), the composition of which is identical to that of white mica cores in S3 (Wm²). The latter are in turn surrounded by phengite rims (Phe²). Occasionally, Phe¹ forms relic cores in the mica aligned along S3.

In the same quartzite REE-rich allanite cores have a first rim of REE-poor allanite and an external rim of epidote. Corroded relics of monazite are occasionally present in the allanite core. The allanite contents decrease from core (Aln core: REE+Y 0.5-0.44 a.p.f.u.) to rim (Aln rim: REE+Y 0.3-0.24 a.p.f.u.) to the epidote rim (Ep: REE+Y < 0.05 a.p.f.u.). Both types of allanite are Ce-dominated, incorporating only small amounts of La and Nd. The zoning seen in BSE images is due to differences in REE, Th and U contents, which generally decrease from core to rim. The epidote rim is Fe- and Sr-rich.

Allanite cores and rims contain minute phengite inclusions. These were analyzed by EMP to compare their composition with that of mica marking the S3 foliation. Abundant mica inclusions in the allanite cores are identical in composition to the texturally oldest phengite preserved in the sample (Phe¹). Allanite rims contain inclusions of micas, the composition of which are indistinguishable from those of the low pressure micas (Wm¹/Wm²).

The two generations of allanite were dated by ion microprobe using the Th-Pb system. The epidote rim was too rich in common Pb to obtain reliable age data. The REE-rich allanite cores yield consistent ²⁰⁸Pb/²³²Th ages with weighted mean of 75.6±0.8 Ma (10 analyses, MSWD 1.02). The REE-poor allanite mantle is systematically younger at 69.8±0.8 Ma (11 analyses, MSWD 1.8). The two allanite populations are thus indicative of two metamorphic stages that pre-date the ~65 Ma HP assemblage that has generally been accepted as the age of the eclogite facies metamorphism in the Sesia Zone (Inger et al. 1996, Duchêne et al. 1997, Rubatto et al. 1999). The latter is likely represented by the texturally late HP foliation (Phe²) preserved in the sample. This may explain the remarkable diversity of Ar-Ar age data reported by Venturini (1995) for samples from many localities in the Sesia Zone, including the Cima Bonze area, where the present sample was taken.

This study reveals that the subduction-collision history has produced a complex record in single rock samples, in this case an impure quartzite. Combining microtextural analysis and petrochronology, specified stages of the metamorphic evolution and polyphase deformation were discerned; SHRIMP dating of select growth domains of allanite yielded a (minimum) duration of ~ 6 Ma for the age difference between two stages of the HP-evolution. It is not clear why the eclogite stage at 65 Ma simply left no imprint in this type of sample, whereas earlier stages did. According to the regional tectonic framework (Babist et al. 2006), the two main basement blocks of the Sesia Zone (i.e. the Bard and Mombarone units) were amalgamated with the trail of Bonze metasediments between them at HP-conditions, prior to the complex exhumation history.

REFERENCES

- Babist J., Handy M.R., Hammerschmidt K. & Konrad-Schmolke, M., 2006. Multi-stage exhumation of high pressure rocks from a sliver of continental crust: an example from the Sesia zone, Italian Western Alps. *Tectonics*, 26: 25.
- Duchêne S., Blichert-Toft J., Luais B., Télouk P., Lardeaux J.-M., Albarède F. 1997. The Lu-Hf dating of garnets and the ages of the Alpine high-pressure metamorphism. *Nature* 387, 586.
- Inger S., Ramsbotham W., Cliff R. A., & Rex D. C., 1996. Metamorphic evolution of the Sesia-Lanzo Zone, Western Alps: time constraints from multi-system geochronology. *Contrib. Mineral. Petrol.* 126, 152.
- Rubatto D., Gebauer D. & Compagnoni R., 1999. Dating of eclogite-facies zircons: the age of Alpine metamorphism in the Sesia-Lanzo Zone (Western Alps). *Earth Planet. Sci. Lett.* 167, 141.
- Venturini, G., 1995. Geology, geochemistry and geochronology of the inner central Sesia Zone (Western Alps, Italy). *Mémoires de Géologie (Lausanne)*, 25: 148 p.

2.29

Thousand Years of massive Iron Production in the Dogon Country (Mali, Western Africa) : Technology – Economy - Environment

Serneels Vincent¹

¹Department of Geosciences, University of Fribourg, Chemin du Musée 6, CH-1700 Fribourg (vincent.serneels@unifr.ch)

In pre-industrial societies, iron tools are essential for agriculture and iron weapons for warfare and political power. Iron production took place everywhere in Africa, long time ago (at least 2'500 years) and well before the colonisation. The production technique is always based on the "blooming process": solid state reduction of iron oxides into metal by reaction with the carbon monoxide from the combustion of charcoal. All over Africa, societies developed an incredibly high number of different production lines to obtain iron from a huge range of ores using very different furnaces (very small to very large, wind or bellows driven, free standing or sunked, etc). The reason for this technological variability remains unexplained.

For ten years, the ancient iron production in the dogon Country (central Mali, West Africa) is investigated on the field and in the laboratory. The aim of the study is the understanding of the technologies and the measure of the impact of this production on the societies and the environment.

In the studied area (15'000 km²), about 150 production sites have been located. Seven different technological traditions have been characterised in different areas. A very remarkable concentration of remains has been identified in a restricted area (500 km²), around the village of Fiko.

The systematic survey of the production sites revealed about 15 large complexes, characterised by huge heaps of slag and furnace remains. The slag heaps are mapped in detail during fieldwork and the volumes of waste are calculated. Furnace remains are excavated and stratigraphic trenches are cut into the heaps. Slags, ores, linings and charcoal are systematically sampled for laboratory studies (XRF, XRD, SEM-EDS). Dates are obtained by ¹⁴C on charcoal.

The technology is always the same, based on very large furnace (3-4 m³) using charcoal and natural draft and no bellows (low temperatures 1100°C / long times > 24h). Lateritic ores, mined in several points all over the area, are used. Grades are low in the natural ore (Fe₂O₃ 55 – 65 %) but enrichment by hand sorting allows to increase it significantly. Tapped slags containing fayalite and few free wüstite are the typical wastes (FeO 45 – 50 %).

The sizes of the heaps range from 5'000 to 40'000 tons. The total amount of slag from the technological tradition of Fiko can be evaluated to 300'000 tons. The quantity of iron can be estimated on the basis of a chemical balance calculated between the ore and slag. The total quantity of iron must have been over 100'000 tons.

The production started probably around 500 AD but developed mainly between 1000 and 1750 AD at the time of the rise of the Mali Empire. The production rose up to a quasi industrial level (100 tons / year), involving a large part of the local population and with a significant impact on the wood resources (2000 tons wood / year).

This study is part of the global interdisciplinary project "Human Population and Paleoclimatic Evolution in West Africa" led by prof. E. Huysecom (Geneva) and funded by the SNF, the SLSA and several additional sources. The various aspects of the archaeometallurgical studies involved several European and African researchers: V. Serneels, S. Perret, M. Mauvilly, I. Katona, R. Soulignac (Fribourg), C. Brunner (Geneva – Toulouse), B. Eichhorn (Frankfurt), B. Traoré (Bamako – Paris), A. Dembélé (Bandiagara).

2.30

The Adamello batholith (Italy): a fossil magma chamber or accumulation of magma pulses?

Skopelitis Alexandra¹, Schaltegger Urs¹, Ulianov Alexey² & Brack Peter³

¹ Département de Minéralogie, Rue de Maraîchers 13, CH-1211 Genève 4 (alexandra.nowak@unige.ch, Urs.Schaltegger@unige.ch)

² Institut de minéralogie et géochimie, Anthropole, CH-1015 Lausanne (Alexey.Ulianov@unil.ch)

³ Departement Erdwissenschaften, ETH Zürich, CH-8092 Zürich (peter.brack@erdw.ethz.ch)

We want to study plutons and batholiths in detail to elucidate their modes of formation, and in particular, to reconstruct the time required for their emplacement. This latter information is linked to the overall thermal budget of the intruded area and the cooling rate of the intruded magmatic bodies. It is important to know how the timescales of solidification relate to the time elapsing between the emplacement of two consecutive magma batches. In other words, we want to know to what extent which parts of a pluton were present in a, at least partially, molten state.

This study focuses on the time needed to build the Adamello batholith in the Italian Alps, mainly in the northern part, which comprises the Ré di Castello (RdC), the Adamello, the Avio and the Presanella superunits (Fig.1). Previous age determinations from the Adamello rocks show a younging towards the north, based on U-Pb zircon data and K-Ar and Rb-Sr results (summaries in Callegari & Brack, 2002; Schaltegger et al., 2009). The south of the batholith is characterized by more mafic compositions ranging from gabbroic to tonalitic, whereas the north is composed principally of tonalite, leucotonalite and trondhjemite rocks (Brack, 1983). Moreover, previous isotope studies across the Adamello showed an increase of the $^{87}\text{Sr}/^{86}\text{Sr}$ and $^{18}\text{O}/^{16}\text{O}$ ratios from south to north, indicating an increasing crustal contamination towards the north (Del Moro et al., 1983; Dupuy et al., 1982), confirmed by petrographical changes in the tonalites, such as increasing abundance of biotite compared to amphibole in the same direction. In this project, geochronology and whole rock as well as mineral chemistry will be used to understand the formation of the tonalites. We attempt understanding and distinction of inherited geochemical characteristics from the source and those acquired during fractionation and crystallisation.

Rocks from the center and the north of the Adamello show a restricted range in composition (diorite-granodiorite, 63-70% wt SiO_2) although the rocks have different mineralogy, grain size and texture. Indeed, the textures observed in rocks from the north-eastern border areas are specific because of their foliation, probably due to deformation in connection with the adjacent Tonale Line. The preliminary geochemical data highlight that the RdC has a metaluminous composition, whereas the others units - younger and situated northwards - are more peraluminous. Laser ablation-ICP-MS U-Pb age determinations on zircon from tonalites originating from the central and northern parts of the batholith have been carried out to determine the age of crystallization and reconstruct the intrusion sequence. First results confirm that the center and northern part of the Adamello emplaced between 43 and 34 Ma (Fig.1). With our present analytical precision of 0.4-1% (N=8-32) of the $^{206}\text{Pb}/^{238}\text{U}$ age we can demonstrate our ability to resolve such age differences and have arguments that the Adamello batholith formed incrementally by several pulses younging towards the north and showing different composition. The CL imaging performed before LA-ICP-MS analysis revealed well crystallized magmatic zonations and xenocrystic cores in particular for northern units. Finally, these results clearly favour an amalgamation of distinct magmatic pulses over millions of years that previously differentiated in a deeper magmatic system as the process forming the Adamello batholith.

We acknowledge funding of FNS in the frame of ProDoc project Adamello 4-D.

REFERENCES

- Brack, P. 1983: Multiple intrusions examples from the Adamello batholith (Italy) and their significance on the mechanisms of intrusions. *Mem. Soc. Geol. It.* 26, 145-157
- Callegari, E. & Brack, P. 2002: Geological map of the Tertiary Adamello batholith (Northern Italy) explanatory notes and legend. *Mem. Sci. Geol.* 54, 19-49
- Del Moro, A., Ferrara, G., Tonarini, S. & Callegari, E. 1983: Rb-Sr systematics on rocks from the Adamello Batholith (Southern Alps). *Mem. Soc. Geol. It.* 26, 261-284
- Dupuy, C., Dostal, J. & Fratta, M. 1982: Geochemistry of the Adamello Massif (Northern Italy). *Contrib. Min. Pet.* 80, 41-48
- Schaltegger, U., Brack, P., Ovtcharova, M., Peytcheva, I., Schoene, B., Stracke, A. & Bargossi, G. 2009: Zircon and titanite recording 1.5 million years of magma accretion, crystallization and initial cooling in a composite pluton (southern Adamello batholith, northern Italy). *Earth Planet. Sci. Lett.* 186, 108-218

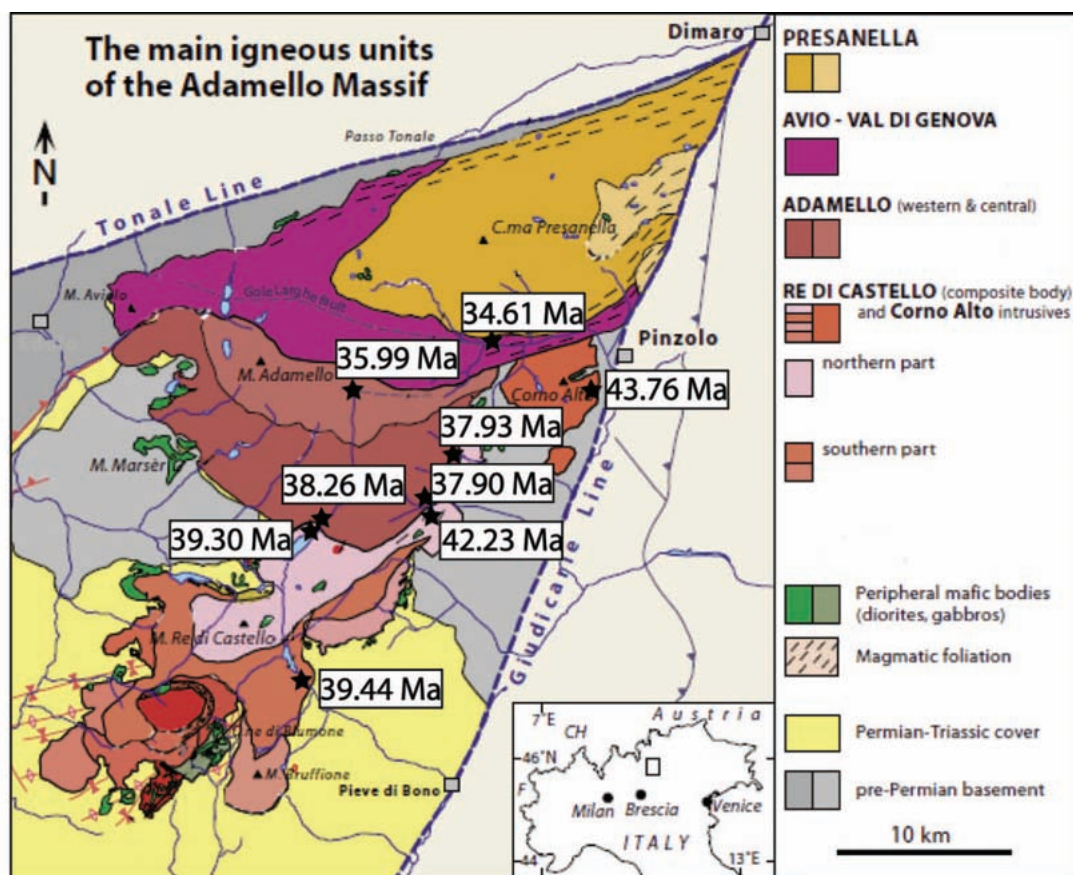


Figure 1. Geological map of the Adamello batholith, indicating our new LA-ICP-MS U-Pb ages on zircon (Modified after Brack et al., unpublished)

2.31

Mineralogical techniques and ethnoarchaeology applied to the study of smithing slags in Mali (Africa)

Soullignac Raphaëlle¹

¹Department of Geosciences, Chemin du Musée 6, CH – 1700 Fribourg (raphaëlle.soullignac@unifr.ch)

Archaeological excavations often reveal hemispherical pieces of slag that are the waste resulting of the smithing of iron in a hearth. They are formed by the accumulation of several fused materials at the base of the hearth, between the lighting and the extinction of the fire. Smithing slags show a high variability (size, weight, shape, internal structure, materials they are made of) reflecting the complexity of the smithing work: variability of starting materials, thermomechanic treatments, skills of the smith, economic pressure.

With this intention to understand in more details those slags, we undertook an ethnoarchaeological approach with traditional smiths of the Dogon group in Mali. This ethnoarchaeological approach is based on the observation and the record of the production of 126 traditional hoes of iron or “daba” in 4 villages of 2 ethnical groups with several smiths. They were given each time various starting materials with different composition (%C : 0.17, 0.35, 0.45) or shape (bars of 4x4 cm, 2x2 cm, 1x1 cm etc). The wastes (slags and hammerscales) have been collected after one single forging or after one working day. They are under study in the lab, using mineralogical techniques : XRF, XRD, SEM-EDXS. The first results will be discussed.

It appears that for one single piece of iron, the quantity of iron lost during the operation varies from 7 to 25 %. If the smith has to weld together 2 pieces of iron, then the length of the operation increases and also the amount of iron lost, up to 60 %.

2.32

Mining archaeological studies in Eastern Pyrenees, France: Baillestavy iron mining area

Călin G. Tămaş^{1,2}, Gabriel Munteanu³, Béatrice Cauuet³ & Gérard Mut³

¹ Department of Geosciences, University of Fribourg, 6, chemin du Musée, CH-1700 Fribourg (calin-gabriel.tamas@unifr.ch)

² Faculty of Biology and Geology, University Babeş-Bolyai, 1, M. Kogălniceanu str., 400084, Cluj-Napoca, Romania

³ Laboratoire des Travaux et Recherches Archéologiques sur les Cultures, les Espaces et les Sociétés (TRACES), Université Toulouse 2 Le Mirail, CNRS UMR 5608, Maison de la Recherche, 5 allées Antonio-Machado, 31 058 Toulouse Cedex 09, France

Several iron deposits hosted in Lower Cambrian limestones and dolomites (Canaveilles Formation) are known in the northern part of Canigou Massif, Eastern Pyrenees, France (Guitard et al., 1998). According to the above mentioned authors several deposits like Batère, Escaro-Escoums, Aytua-Torrent, Casteil-Falguerosa, Sahorre, Fillols-Taurinya, le Llech, la Coume have been mined until mid 20th century when the mining activity finally stopped.

Baillestavy is a small village situated close to la Coume deposit. This locality represents a mining site but in the same time it is known due to the large amount of iron slags. Archaeological diggings carried out within the slag deposit of the church St. Andrew from Baillestavy (Mut, 2001) pointed out a metallurgic activity back to Gaul and Roman times (2nd century BC – 1st century AD). Instead of the presence of Ancient slag waste dumps in Baillestavy, according to Finot (1902) the iron exploitation started only in 1830.

Mining archaeological studies started recently in Baillestavy area having several aims:

- to make an up to date review of the accessible mining vestiges and their conservation state;
- to identify different periods of mining based on peculiarities of digging techniques;
- dating of the oldest mining activity.

The study developed during three field work campaigns being focused on surface and underground exploration, identification of all accessible mining works, topography of the works, archaeological observations, geological mapping, and archaeological diggings. Four mining sites have been investigated in the vicinity of Baillestavy: Mas Morer, Peña Blanca, la Coume and Mas Bourasse.

Taking into account the digging technique, at least three periods of activity have been observed:

- 1 – hand tools with narrow traces;
- 2 – Catalan type chisel;
- 3 – blast holes (two types).

The ore bodies and their host rocks have been mapped for all the identified mining sites. The geological study of the underground works gave more informations concerning the genesis of the ore bodies and helped to better understand the development of the mines.

The archaeological diggings conducted in the underground works from Mas Bourasse mining sector, situated north-west of la Coume deposit, allowed Munteanu (2010) to certify that the iron ores were mined during 1st century AD.

REFERENCES

- Guitard, G., Laumonier, B., Autran, A., Bandet, Y. & Berger, G.M. 1998: Carte géologiques de la France à 1/50.000. Notice explicative de la feuille Prades, 198 p.
- Finot, M. 1902: Procès-verbal de visite des recherches de mines de fer de la Société de Pauillac à Baillestavy et Estoher. Ministère des Travaux Publics, Service des Mines, Dépt. des Pyrénées Orientales, Prades, no. 1246, 8p.
- Munteanu, G. 2010: Le district minier de Baillestavy (Pyrénées Orientales). La production du fer de l'Antiquité à l'époque moderne – exploration, topographie, chronologie et géologie des mines souterraines. Master II, Université Toulouse le Mirail (unpubl.).
- Mut, G. 2001: Les forges de Baillestavy, in Sablayrolles, R. (ed.), Les ressources naturelles des Pyrénées. Leur exploitation durant l'Antiquité, Entretiens d'archéologie et d'histoire, St-Bertrand-de-Comminges, 2001, p. 141-153.

2.33

Fossiliferous pottery in Ajoie (NW Switzerland) and adjacent regions from La Tène and Gallo-roman sites: Information on production and distribution through microscopic and chemical analyses

Thierrin-Michael Gisela

Department of Geosciences, University of Fribourg, ch. du musée 6, 1700 Fribourg et Section archéologie et paléontologie, Office de la culture du Canton du Jura, 2900 Porrentruy

Fossiliferous, also called “shell-tempered”, pottery is presented as a phenomenon in late La Tène and Gallo-roman periods in several regions – like Normandy, Belgium and South England. In most cases these ceramic productions are linked to clay outcrops in the same region. In some instances, however, these wares are thought to have been widely distributed from one production area.

Fossiliferous pottery is the most important fabric group at mid to late La Tène sites in Ajoie and remains significant among Gallo-roman material (7 sites considered). Hand-formed bowls of different dimension are the most frequent form. These findings allowed a diachronic study of this pottery, spanning over 300 years answering following questions: which raw materials were used?, the same clay(s) throughout?, same or differing preparation in time?

The presence of fossiliferous pottery is also well documented on contemporary sites in the nearby Basel region, among them the kiln-site of Sissach-Brühl (Basel-Landschaft, Switzerland). While very coarse pieces from Ajoie are distinctive and seem to occur only there, a finer fabric is present on all sites. Macroscopically, the material from different sites is undistinguishable. Were there only few production sites and exchange, or many productions? In order to determine this, pieces from Sissach-Brühl and three La Tène settlements (mostly hand-formed bowls), as well as sherds of hand-formed cooking pots from the Roman town Augusta Rauricorum (Basel-Landschaft, Switzerland) and surrounding villae, were compared to the finds from Ajoie.

Macroscopic, microscopic and chemical (XRF-WDS) comparison to virgula marl from the upper Jurassic (Kimmeridgian) proved this particular clay to be used in Ajoie – either pure or crushed and mixed with non-calcareous quarternary clays. Outcrops of the marly layer are easily accessible from all the sites. Some gallo-roman pieces revealed another preparation: crushed spathic limestone, locally available, mixed with non-calcarous clay.

The sherds from the Basel region all show fossil assemblages different from the Ajoie pottery. Fossiliferous marly layers from the Dogger certainly provided the raw materials for some of them, while others appear to be mixtures (natural or intentional) of different not yet identified clays (the identification is difficult also, because thin sections from ceramic sherds do not always show diagnostic fossil fragments and assemblages). This diversity in raw material supports the assumption that this ware rarely travelled far from the production site in the discussed region of NW Switzerland. During the La Tène period at least, there is no evidence of distribution from more important production sites, in spite of a certain popularity suggested by the high percentages of fossiliferous pottery among the ceramic material in the settlements.

2.34

Insights into the dehydroxylation kinetics of lizardite and chrysotile

Trittschack Roy & Grobéty Bernard

University of Fribourg, Department of Geosciences, Chemin du Musée 6, CH-1700 Fribourg (roy.trittschack@unifr.ch)

Lizardite and chrysotile represent two prominent trioctahedral 1:1 phyllosilicates of the serpentine mineral group. Lizardite ($\text{Mg}_3\text{Si}_2\text{O}_5(\text{OH})_4$) has a conventional sheet silicate structure, whereas in chrysotile the same TO-layers are rolled to cylinders. The chrysotile structure has thus not a classical 3D-symmetry, but only rotational and no radial symmetry. Physical properties are, therefore, expected to reflect also this non-conventional symmetry.

The aim of this study is to understand the influence of special symmetry of chrysotile on the mechanism and the rate determining steps of the dehydroxylation reaction. The dehydroxylation kinetics of lizardite serves, thereby, as reference.

Theoretical deprotonation and water forming schemes were compared with results of in-situ High-Temperature X-ray diffraction, in-situ IR-spectroscopy, FTIR and Differential Thermogravimetry experiments on well characterized chrysotile and lizardite samples. In-situ IR and HT-XRD experiments under ambient pressure gave starting temperatures for the dehydroxylation of lizardite between 500°C and 550°C which lies in the range of former investigations (Frank et al. 2005).

Chrysotile dehydroxylation depend on structural features like the inner and outer tube diameter which itself dictate the physical properties. The dehydroxylation starts at the outermost layers at around 450°C and 500°C, whereas innermost layers breakdown about 600°C (Metraux et al. 2002). The initial dehydroxylation product of both polymorphs is X-ray amorphous, but crystallizes after a certain time to forsterite. These phase transformations were also followed by FTIR analyses, which offer a detailed insight into the structural recombination during the dehydroxylation.

Kinetic data were calculated from two independent methods, in-situ High-Temperature X-ray diffraction and Differential Thermogravimetry techniques for different atmospheres (N₂, O₂, air, etc.). Assuming proportionality between the integral intensity of diffraction peaks and the amount of serpentine present, the reaction rate can be extracted from the rate of intensity decrease. Data from isothermal runs have been treated with the conventional Avrami method as well as the “time to a given fraction” (TGF) method. Latter one offers the possibility to discover changes in the activation energy E_a during the course of dehydroxylation (Putnis 1992). The same reaction progress dependency of E_a can also be obtained by the isoconversional Friedman analysis from a series of dynamic DTG data.

Isothermal HT-XRD experiments on lizardite yielded E_a of around 340 kJ mol⁻¹ (Avrami method). Data treated with the TGF method showed a progressive increase of the E_a with the fraction transformed from around 200 kJ mol⁻¹ ($\alpha=0.1$) to 340 kJ mol⁻¹ ($\alpha=0.9$). Non-isothermal DTG analyses on lizardite with different heating rates and under a controlled nitrogen atmosphere confirmed the TGF results and enabled a much more detailed resolution of the E_a during the dehydration progress. A preliminary mechanistic interpretation of these results will be given.

REFERENCES

- Frank, M.R., Earnest, D.J., Candela, P.A., Wylie, A.G., Wilmot, M.S. & Maglio, S.J. 2005 (abstract): Experimental study of the thermal decomposition of lizardite up to 973K, Salt Lake City Annual Meeting 2005
- Metraux, C., Grob  ty, B. & Ulmer, P. 2002: Filling of chrysotile nanotubes with metals, *Journal of Material Research*, 17, 1129-1135.
- Putnis, A. 1992: *Introduction to Mineral Sciences*, Cambridge University Press, 457 p.

2.35

Calculating rheologic properties of magmas from field observations combined with experimental data.

Verberne Roel¹, Ulmer Peter², M  ntener Othmar¹

¹ *Institut de Min  ralogie et G  ochimie, batiment Anthropole, CH-1015 Lausanne (roel.verberne@unil.ch)*

² *Institut f  r Geochemie und Petrologie, Clausiusstrasse 25, CH-8092 Z  rich*

In order to investigate the emplacement processes that occur in shallow level plutonic magma reservoirs, we try to relate phase assemblages and mineral composition to the emplacement history of a particular rock suite by combining field and experimental approaches to understand the physical, rheological and temporal evolution of crystallizing batholiths.

Here we present a case study of the Listino Ring Structure of the Adamello Batholith, N-Italy, where processes of interaction between felsic and mafic magmas, such as mafic dike injection in partly crystallized silicic magmas, dike disaggregation, enclave formation, and near-solidus shearing were studied in glacier-polished outcrops. Most of these phenomena are generally assigned to fluid dynamic processes operating in a magma reservoir (Turner & Campbell, 1986), where rheological barriers (e.g. viscosity contrast) inhibit chemical mixing of mafic magmas with crystal-rich silicic magmas (Sparks & Marshall, 1986; Blundy & Sparks, 1992).

Our approach centers around the determination of mineral assemblages and crystal fractions present at the time of the process under investigation. The mineral assemblage at the time of injection of mafic magmas, can be determined from the observation that minerals from the host magma are being mechanically incorporated as phenocrysts into the

mafic enclaves before quenching occurs. In the case of synmagmatic deformation, the crystals present during deformation can possibly be identified by determining the crystal fraction displaying plastic deformation.

Having determined the modal mineralogy and composition of phases, combining with whole rock chemistry of both magmas and a pressure estimate obtained from Al-in-Hornblende barometry by Blundy & Caddick (unpublished), allows us to constrain the temperature and H₂O-content of the host magma. The melt fraction and composition of the host magma can then be calculated from available experimental data, and the melt composition can be further constrained by the chemical analysis of assemblages found in (back)veins, which are thought to represent the melt component of the system.

Observed crosscutting relationships between the different magmatic phases combined with their respective offset along synmagmatic shear zones can be used to determine strain and possibly strain rates through dating of the various phases. Having determined the composition, pressure, temperature and crystallinity of the host magma, its relative viscosity can be calculated using the experimentally calibrated relationship between relative viscosity and the particle volume fraction (Costa et al., 2009 and references therein).

REFERENCES

- Blundy, J.D. and Sparks, R.J.S., 1992. Petrogenesis of mafic inclusions in granitoids of the Adamello Massif, Italy. *Journal of Petrology*, 33: 1039-1104.
- Costa, A et al., 2009. A model for the rheology of particle-bearing suspensions and partially molten rocks. *Geochim. Geophys. Geosyst.*, 10, Q03010, doi:10.1029/2008GC002138.
- Sparks, R.S.J. and Marshall, L.A., 1986. Thermal and mechanical constraints on mixing between mafic and silicic magmas. *J. volc. geotherm. res.*, 29: 99-124.
- Turner, J.S. and Campbell, I.H., 1986. Convection and mixing in magma chambers. *Earth. Sci. Rev.*, 23: 255-352.

2.36

How long does seawater and oceanic crust interact?

Flurin Vils¹, Tim Elliott¹, Christopher E. Smith-Duque², Jeffrey C. Alt³ & Damon Teagle²

¹ University of Bristol, BS8 1RJ Bristol, United Kingdom († correspondence: flurin.vils@bristol.ac.uk)

² National Oceanography Centre, SO14 3ZH Southampton, United Kingdom

³ University of Michigan, MI 48109-1005, USA

After having been formed at mid-ocean ridges, oceanic plates cool as they move away from the ridges and become older. Much of this cooling is related to hydrothermal alteration by seawater infiltrating the plates. During seawater-rock interaction, primary minerals are transformed into secondary minerals. This transformation can mobilize elements, which are leached of or enriched in the oceanic crust and is therefore influencing the bulk rock composition.

Two processes mainly control element abundances in the oceans: continental weathering and hydrothermal activity in the oceanic plate. The hydrothermal activity is further divided into high-T (near ridge) and low-T (off the ridge) alteration. High-T alteration processes can be easily studied in hydrothermal vent regions. As low-T alteration processes in the oceanic crust are rather diffuse and slow, their limits and conditions (time, temperature, etc.) are largely unknown and thus investigation of off-ridge alteration is important. This study investigates the alteration processes of mid-ocean ridge basalts (MORB) in the low-T environments and constructs a time frame for seawater-rock interaction in these regions.

Weathering of the continental plates keeps the U-series decay chain in the ocean (a ²³⁴U/²³⁸U-ratio of ~1.14) in disequilibrium. On the other hand, MORB formed at the ridge are in secular equilibrium. Thus any seawater alteration of MORB leads to an enriched ²³⁴U/²³⁸U-ratio and after ~5 half-life times of uranium the MORB are again in secular equilibrium. Preliminary ²³⁴U/²³⁸U-data on old oceanic crust from ODP Site 1179 (~129Ma) and ODP Site 843 (~94Ma) shows that altered MORB are mostly in secular equilibrium. Nevertheless, higher U concentrations in the altered MORB compared to fresh MORB on both Sites suggests that seawater alteration occurred earlier, but outside the radiogenic detection window of ~1.25Ma for the ²³⁴U/²³⁸U decay chain. Altered MORB from younger ODP Sites (e.g. ODP Site 1301, ~3.5Ma) show disequilibrium, representing recent seawater-rock interactions. Additional U-series measurements on ODP Sites are currently proceeding to further constrain the alteration time-window.

2.37

Barium isotope fractionation in natural barium minerals and precipitation experiments: A first glimpse at the global barium cycle

Katja von Allmen ^(1,3), Michael E. Böttcher ⁽²⁾, Elias Samankassou ^(1,3), and Thomas F. Nägler ⁽⁴⁾

⁽¹⁾ Department of Geosciences, Chemin du Musée 6, University of Fribourg, CH-1700 Fribourg, Switzerland (katja.vonallmen@unifr.ch),

⁽²⁾ Leibniz Institute for Baltic Sea Research (IOW), Geochemistry & Isotope Geochemistry Group, D-18119 Warnemünde, FGR (michael.boettcher@io-warnemuende.de),

⁽³⁾ present address: Section of Earth and Environmental Sciences, University of Geneva, Rue des Maraîchers 13, CH-1205 Geneva, Switzerland (Elias.Samankassou@unige.ch),

⁽⁴⁾ Institute of Geological Science, Baltzerstr. 3, University of Bern, CH-3012 Bern, Switzerland (naegler@geo.unibe.ch)

We present results from an ongoing investigation on the stable barium (Ba) isotope fractionation in the natural Ba cycle. Stable Ba isotope signatures of international IAEA reference materials (synthetic barium sulfate and barium carbonate), natural Ba minerals and Ba precipitates have been analyzed to evaluate potential discriminating processes in the global geochemical barium cycle.

In the modern ocean, dissolved Barium (Ba) shows a variable concentration and a nutrient-type behavior (Chan et al., 1976). As a non-conservative element, Ba has a relatively short residence time of 11kyrs (Edmond et al., 1979). Ba concentrations are reduced in the upper waters of the open ocean and enriched in deep waters and areas of nutrient upwelling (e.g., Church, 1979). Variations in the accumulation rate of Ba bound to carbonate and sulfate in marine sediments are thought to be indicative of variations in marine biological productivity through time (e.g., Church, 1979; Paytan & Griffith, 2007). Detrital sources of Ba from continental runoff, hydrothermal alteration, and diagenetic Ba mobility are hard to constrain with Ba concentrations alone. Thus, we propose the fractionation of stable Ba isotopes as a new tool to constrain Ba behavior in the global element cycle.

Measurements were carried out on a multi-collector ICP-MS applying a ¹³⁰Ba/¹³⁵Ba double spike. Data are given as per mil deviations from a laboratory Ba nitrate standard solution in the $\delta^{137/134}\text{Ba}$ notation (external 2s stdev < 0.1 per mil). Various synthetic solid standards and the p.a. quality synthetic barium chloride used for the precipitation experiments show very similar isotope results close to the nitrate standard solution. The terrestrial barium gangue minerals (four barites, one norsethite [BaMg(CO₃)₂]) were depleted in the heavy isotope ($\delta^{137/134}\text{Ba}$ values between 0 and -0.2 per mil).

A natural barite from an undisclosed Chinese locality gave an isotope value of -0.4 per mil. High ³⁴S/³²S and ¹⁸O/¹⁶O ratios in this sample indicate that this barite has been formed under influence of microbial sulfate reduction, probably in a marine diagenetic environment. The largest Ba isotope fractionation with -0.5 per mil was found in a diagenetic barite. This value is also accompanied by high ³⁴S/³²S and ¹⁸O/¹⁶O ratios indicating formation under influence of microbial sulfate reduction. The observed natural discriminations are by far larger than the analytical uncertainty of the isotope measurements, indicating isotope discrimination in the natural barium cycle (von Allmen et al., 2010).

Precipitation experiments from aqueous barium chloride solutions at temperatures of 20° and 80°C indicate that the light Ba isotope is enriched in pure barium carbonate or barium sulfate compared to the aqueous solution. A maximum isotope fractionation of -0.3 per mil is observed, for both barium carbonate and sulfate. This fractionation seems to be influenced by precipitation rate (BaCO₃) and/or the aqueous speciation, but less by temperature.

REFERENCES:

- Chan, L.H., Edmond, J.M., Stallard, R.F., Broecker, W.S., Chung, Y.C., Weiss, R.F. & Ku, T.L., 1976: Radium and barium at GEOSECS stations in the Atlantic and Pacific. *Earth Planet. Sci. Lett.*, 32, 258-267.
- Church, T.M., 1979: Marine barite, in Burns, R.G. (Editor), *Marine minerals*. Mineralogical Society of America, *Reviews in Mineralogy*, 6, 175-209.
- Edmond, J.M., Measures, C., McDuff, R.E., Chan, L.H., Collier, R., Grant, B., Gordon, L.I. & Corliss, J.B., 1979: Ridge crest hydrothermal activity and the balances of the major and minor elements in the ocean - Galapagos data. *Earth Planet. Sci. Lett.*, 46, 1-18.
- Paytan, A. & Griffith, E.M., 2007: Marine barite: Recorder of variations in ocean export productivity: Deep-Sea Research: Part II, *Topical Studies in Oceanography*, doi: 10.1016/j.dsr2.2007.01.007.
- von Allmen, K., Böttcher, M.E., Samankassou, E., & Nägler, T.F., (2010): Barium isotope fractionation in the global barium cycle: First evidence from barium minerals and precipitation experiments. *Chem. Geol.*, (in press) doi:10.1016/j.chemgeo.2010.07.011

2.38

Palaeoredox change during OAE 1a: new insights from phosphorus and redox-sensitive trace elements

Stéphane Westermann¹, Melody Stein², Virginie Matera³, Nicolas Fiet⁴, Thierry Adatte² & Karl B. Föllmi²

¹Department of Earth Sciences, University of Bristol, Wills Memorial, BS81RJ, Bristol, UK (stephane.westermann@bristol.ac.uk)

²Institut de géologie et de paléontologie, Université de Lausanne, CH-1015, Lausanne, Switzerland

³I.N.R.S., Avenue de Bourgogne, 54500 Vandoeuvre-les-Nancy, France

⁴AREVA, 33 rue La Fayette, 75442 Paris, France

The Early Aptian records an episode of severe environmental change including an oceanic anoxic event (OAE), a platform drowning episode and a biocalcification crisis. This episode, the so-called OAE 1a, corresponds to one of the most studied anoxic events and is characterized by an increase in the $\delta^{13}\text{C}$ values preceded by a negative spike. Here, we propose to trace changes in ocean chemistry during OAE 1a to improve our understanding of such phenomena and test the proposed models. Thus, we investigate phosphorus (P) and redox-sensitive trace-element (RSTE) distributions in sections along a basin-shelf transect in the western Tethys through lower Aptian sediments. We complement our geochemical analysis by the analysis of organic-matter contents.

We selected three representative sections: Gorgo a Cerbara (central Italy) in the Umbria Marche basin, Glaise (SE France) located in the Vocontian Trough and Cassis/La Bédoule (SE France) located along the Provencal platform.

In the sections of Glaise and Cassis/La Bédoule, P contents show first an increase at the onset of the Early Aptian event, just above the $\delta^{13}\text{C}$ negative spike, and then, during the OAE 1a, followed by lower values. A second increase is observed at the end of the carbon-isotopic excursion. This suggests an increase in nutrient input, whereas the return to lower values through the first part of the anoxic event may be related to a weakened capacity to retain P in the sedimentary reservoir due to bottom-water oxygen depletion. This general pattern is contrasted by the data of Gorgo a Cerbara. Surprisingly enough, the sediments deposited during the OAE 1a (the Selli level) shows P-enrichments (mainly authigenic P) associated with maximum in TOC values and high $C_{\text{org}}:P_{\text{tot}}$ ratios. A part of the remobilized P appears to have been trapped in the sediments and was as such prevented from returning to the water column.

In the section of Gorgo a Cerbara, U, V, Mo, Co and As distributions present similar behaviour with a low background level along the main part of the section, contrasted by different maxima in concentrations within the Selli level. In the Glaise section, a weak increase is observed just after the negative spike in $\delta^{13}\text{C}$ whereas in the Cassis/La Bédoule section, no significant enrichments have been observed in sediments equivalent to the Selli level. The different behaviour of the RSTE in the studied sections may be related to the palaeogeographic setting of the studied sections. Our data seem to indicate the development of anoxic conditions in basin settings during OAE 1a. In shallower-water environments, conditions may have been less reducing. Moreover, in Gorgo a Cerbara, two distinct enrichments have been observed. This is in favour of fluctuations in the intensity of water-column anoxia during the shift in $\delta^{13}\text{C}$.

Our results show that the expression of the OAE 1a is different following the palaeogeographic settings. The stratigraphic evolution of P contents suggests an increase in nutrient input at the onset of the anoxic event, just after the negative spike in $\delta^{13}\text{C}$. RSTE and high $C_{\text{org}}:P_{\text{tot}}$ values may indicate anoxia conditions in the deep environment characterized by several anoxic phases with intermittent return to less oxygen-depleted conditions. These rapid changes in redox conditions may be related to a fluctuating oxygen-minimum zone and suggest that oceanic productivity has played a key role in bottom-water oxygen depletion during OAE 1a.

2.39

Influence of extrinsic weathering factors on mineral dissolution in Damma glacier forefield

Wongfun Nuttakan¹, Furrer Gerhard¹, Brandl Helmut² & Plötze Michael³

¹ *Inst. of Biogeochemistry and Pollutant Dynamics, ETH Zürich, Universitätsstrasse 16, CH-8092 Zürich (nuttakan.wongfun@env.ethz.ch)*

² *Inst. of Evolutionary Biology and Environmental Studies, Universität Zürich, Winterthurerstrasse 190, CH-8057 Zürich*

³ *Inst. for Geotechnical Engineering, ETH Zürich, Schafmattstrasse 6, CH-8093 Zürich*

Initial weathering processes and soil formation are of particular interest in alpine postglacial areas due to their crucial role on life under harsh conditions (Bernasconi & BigLink project members 2008). At near-neutral pH under aerobic conditions, the availability of nutrients in fine-grained rock material and soil is usually very low. To overcome this limitation, microorganisms and plants modify their local environment by various exudates including organic ligands, siderophores and also cyanide. Cyanide can be a very important agent during the initial period of colonization and soil formation.

We study mechanisms of weathering of primary rock-forming minerals in terms of intrinsic (e.g. mineralogy, grain-size, surface area) and extrinsic (e.g. pH, Eh, concentrations of ligands) weathering factors. Rock samples and samples from weathered stream sediments were obtained from the Damma glacier forefield area (Central Alps, Switzerland) at approximately 2000 m a.s.l. The stream sediment samples were collected distinguishing four water regimes regarding the distance from the main water stream and the accessibility of water.

Mineralogical compositions determined by X-ray diffraction and Rietveld analysis show similarity in mineralogical heterogeneity of the metagranitic material throughout the glacier forefield. Grain-size distribution and accordingly the mineralogical composition are influenced by hydrological factors such as temporal availability and flow velocity of water.

In addition to field observations, weathering of crushed granite is investigated in controlled lab experiments. At 25 °C, the influences of oxalate, citrate and cyanide are studied in batch reactors. The concentration of cyanide is maintained by a constant partial pressure of hydrogen cyanide through gas bubbling. Thus, the concentration of cyanide anion strictly depends on pH. Preliminary results show that citrate exhibits the most distinct effect and the presence of cyanide suppressed the mobilization of iron.

REFERENCES

Bernasconi, S.M. and BigLink project members. 2008: Weathering, soil formation and initial ecosystem evolution on a glacier forefield: a case study from the Damma Glacier, Switzerland. *Mineral Mag.* 72, 19-22.

2.40

Water-soluble salts and temperature variation in meteorites recovered in the hot desert of Oman

Zurfluh Florian¹, Hofmann Beda², Gnos Edwin³ & Eggenberger Urs¹

¹ *Institut für Geologie, Baltzerstrasse 1+3, CH-3012 Bern (florian.zurfluh@geo.unibe.ch)*

² *Naturhistorisches Museum Bern, Bernastrasse 15, CH-3005 Bern*

³ *Muséum d'Histoire naturelle, route de Malagnou 1, CP 6434, CH-1211 Genève*

One of the major goals of our longstanding meteorite search and research collaboration between the Ministry of Commerce and Industry, Sultanate of Oman and institutions from Switzerland is to collect a statistical significant number of well documented meteorite samples to perform studies on find density (Gnos et al. 2010), weathering and contamination (Al-Kathiri et al. 2005). Here we present an ongoing study on the interaction of ordinary chondrites with the desert soil with the focus on water-soluble salts.

During terrestrial residence the components first attacked in an ordinary meteorite are the iron minerals kamacite and taenite and the iron sulfide troilite (Wlotzka 1993, Lee & Bland 2004, Al-Kathiri et al. 2005). Beside oxygen, water and microbes, salts derived from the soil accelerate weathering of these minerals in the meteorite. Chlorine is an important constituent involved in the formation of the iron hydroxide akaganéite (Buchwald & Clarke 1989).

A first survey of water-soluble salts in meteorites gave interesting results: Aqueous leaching was performed on 16 small (3 – 6 g) cubes from the interior of 200 – 400 g individual stones. We detected Mg^{2+} , Ca^{2+} , SO_4^{2-} and Cl^- as the major ions. The signal is dominated by either chlorine or sulphate. Chlorine, calcium and a part of the sulphate are derived from the soil, whereas magnesium and some of the sulphate is of meteoritic origin. The total concentration of water-soluble ions varies from 1860 ppm to 10500 ppm in the solid (Zurfluh 2008).

Currently we perform additional tests to optimize the experimental setup of aqueous leaching. Multiple cubes from one meteorite piece were leached during various time periods to get an idea of salt solubility as a function of time. Additionally, the experiment was performed under N_2 atmosphere to prevent oxidation of iron during leaching.

Until now all extraction data are collected from samples of the large JaH 091 strewn field, a common L5 S2 W2-4 ordinary chondrite (Russel et al. 2004, Gnos et al. 2006, Zurfluh 2008, Gnos et al. 2010).

The process of contamination with these salts is not understood in detail. One important parameter may be the daily temperature fluctuation that causes a pumping effect. We suppose that due to the dark colour, meteorites undergo a much larger temperature range compared to the surrounding soil.

To obtain data on temperature variations inside a meteorite, a sample from JaH 091 strewn field was equipped with a thermocouple connected with a temperature data logger and placed in the desert. A second temperature sensor was placed in an aluminium disc and buried at a depth of 30 cm in the soil. The experiment was run from June 2009 until January 2010. Currently a new logger is collecting data at the same location to cover the whole year. The highest temperature in the meteorite was measured in mid July reaching 66.3°C and the daily min-max temperature differences in the meteorite averages 34.3°C. In contrast, the maximum temperature recorded in the soil is 54.8°C and the daily variation averages 21.6°C. This temperature variation in the meteorite is maybe enough to produce a pumping effect that transports ions solved in water into the pore space of the meteorite (average porosity of ordinary chondrites: $8.9 \pm 4.9\%$; Consolmagno et al. 2008). Water is available from morning dew and the low annual precipitation, typically <40 mm that occurs normally between January and March (Fisher 1994). During hot periods the water evaporates and the salts remains in the meteorite. Because of the long residence time of the meteorite and the large number of these cycles high concentrations of salts results.

REFERENCES

- Al-Kathiri, A., Hofmann B. A., Jull A. J. T., and Gnos E. 2005: Weathering of meteorites from Oman: Correlation of chemical/mineralogical weathering proxies with ^{14}C terrestrial ages and the influence of soil chemistry, *Meteoritics & Planetary Science*, 40, 1215-1239.
- Buchwald V. F. and Clarke R. S. 1989: Corrosion of Fe-Ni alloys by Cl-containing akaganéite (beta-FeOOH) - The Antarctic meteorite case. *American Mineralogist* 74, 656-667.
- Consolmagno G. J., Britt D. T. and Macke R. J. 2008: The significance of meteorite density and porosity. *Chimie der Erde-Geochemistry* 68, 1-29.
- Fisher M. 1994: Another look at the variability of desert climates, using examples from Oman. *Global Ecology and Biogeography Letters* 4, 79-87.
- Gnos, E., Eggimann M. R., Al-Kathiri A. and Hofmann B. A. 2006: The JaH 091 strewn field, *Meteoritics & Planetary Science* 41 Suppl., A64
- Gnos, E., Hofmann, B., Walbrecker, J., Zurfluh, F., Eggenberger, U., Greber, N., Opitz, C., Bretscher, A. and Trappitsch, R. 2010: „ The 2010 Oman meteorite search campaign with a magnetic survey of the main impact site of the JaH 091 strewn field, Abstract Swiss Geoscience Meeting 2010, Fribourg.
- Lee M. R. and Bland P. A. 2004: Mechanisms of weathering of meteorites recovered from hot and cold deserts and the formation of phyllosilicates. *Geochimica et Cosmochimica Acta* 68, 893-916.
- Russell S. S., Folco L., Grady M. M., Zolensky M. E., Jones R., Righther K., Zipfel J. and Grossmann J. N. 2004: The Meteoritical Bulletin, No. 88, 2004 July. *Meteoritics & Planetary Science* 39, A215-A272.
- Wlotzka F. 1993: A Weathering scale for the ordinary chondrites (abstract). *Meteoritics* 28, 460.
- Zurfluh F. J. 2008: Meteorites in the Sultanate of Oman - Effects of terrestrial weathering in the Jiddat al Harasis (JaH) 091 Strewn field. MSc-thesis, University of Berne, 138pp.

3. Himalayan Geology: A tribute to Augusto Gansser on his 100th anniversary

Guido Schreurs, Neil Mancktelow, Ruedi Hänni, Jean-Pierre Burg

*Swiss Tectonics Studies Group of the Swiss Geological Society
Swiss Society of Mineralogy and Petrology*

- 3.1 Baud A.: A geological account of South Tibet: 1936 Gansser's diary to the holy Kailas
- 3.2 Dolati A., Bernoulli D., Burg J.-P., Smit J., Müller C., Spezzaferri S., Sergey S.: Sedimentology and stratigraphy of the Makran accretionary wedge in Iran
- 3.3 Dolati A., Burg J.-P., Smit J., Bernoulli D.: Structural analysis of central Makran accretionary wedge (SE Iran)
- 3.4 Dolati A., Seward D., Smit J., Burg J.-P.: Tectonic evolution of Makran accretionary wedge (SE Iran) using low temperature thermochronology and tectono-stratigraphic evidences
- 3.5 Grasemann B.: Fold growth in the Zagros fold-and-thrust belt in Kurdistan (NE-Iraq)
- 3.6 Grujic D., Warren C. J., Kellett D. A., Wooden J. L.: Syn-collisional exhumation of the continental lower crust
- 3.7 Jalali A., Dolati A., Bernoulli D., Burg J.-P.: Preliminary results of Cretaceous-Eocene sediment analysis of Makran accretionary wedge in SE Iran
- 3.8 Molnar P.: The upward and outward growth of northeastern Tibet and geodynamic implications
- 3.9 Monsef I., Rahgoshay M.: Compositional variations and geodynamic implications of the Mesozoic island arc magmatism in the Sanandaj-Sirjan arc-basin system
- 3.10 Rahn M., Wang H.: Metamorphic and denudation patterns of the Songpan-Garzê flysch in Sichuan Province, China
- 3.11 Rubatto D., Chakraborty S., Dasgupta S.: Protracted melting in the Higher Himalayan Crystalline (Sikkim, India)
- 3.12 Steck A., Epard J.L.: Structural development of the Tso Moriri ultra high pressure nappe of the Ladakh Himalaya

3.1

A geological account of South Tibet: 1936 Gansser's diary to the holy Kailas.

Baud Aymon

BGC, Parc de la Rouvraie 28, CH-1018 Lausanne (aymon.baud@unil.ch)

As brilliantly told in his famous book “Thron der Götter” and reported in the “Central Himalaya, Geological observations of the Swiss expedition 1936”, August Gansser, staying then close to the Tibet border, grabbed his chance of two pilgrims going to the Kailas and he decided within few hours to follow them and to enter in the forbidden Land. Disguised in Tibetan monk, his itinerary brought him through the Mangshang pass to the Raksas valley and “daemon” lake. This way lead him to discover a whole chain of exotic mountains: the Amlang-la flysch with two zones of blocks, some similar to the famous Kiogar Exotics with reefal, Dachstein type Triassic limestone, the other called the Chirchun Exotics of deep water facies (red Triassic ammonoid limestone and radiolarites), both topped by a thick sheet of peridotite (called Jungbwa from the nomad camp West the Raksas lake). Arriving at the foot of the holy Kailas peak, he was again surprised to find the same flysch with exotic blocks and peridotite, with southward dipping tectonic contact (Great Counter thrust) with what he called the Transhimalaya Kailas conglomerate. As he had to hide his camera, hammer and notebook and take care when collecting and storing samples, the quality and the subtlety of his observation in such adverse environment are astounding. His report with drawings, panorama and pictures on South Tibet geology in 1939 and in his famous “Geology of the Himalayas” book (1964), with already the concept of the Indus suture zone, of large southward movements of oceanic Exotic thrust mass and the “underthrusting of the Indian shield against Tibetan mass” were ready to be incorporated and to give convincing arguments into the plate tectonic theory that has been expounded respectively thirty-one and six years later.

Now, on the Gansser's panorama section of the Amlang-la, there are apparently no new detailed reports and we will have just to label it as Amlang-la accretion prism overlain by obducted (or supra-subduction) Jungbwa ophiolites. The Gansser's Indus suture became “Indus-Yalu Suture zone” that separates the Indian block from the Lhasa block.

About the Exotic blocks of the area, the Kiogar facies can be now interpreted as shallow Triassic oceanic island (seamount) and the Chirchun facies is corresponding to Permian seamounts. It is only this year that a Tibetan Permian-Triassic section of the Chirchun Facies has been described in detail.



It is also interesting to note that during his first very short two days trip to Purang (Taklakot) in the forbidden land, August Gansser not only recognized the arch shape of the 7700 m. high Gurla Mandhata but observing tilting of terraces along the mountainside and the fresh erosive morphology, he reported this very recent, incredible high up-doming. We actually know that the Gurla Mandhata is part of large recent extensional domes of gneiss that occur north the High Himalaya Range. Only recently, more than sixty years after Gansser's report, detailed descriptions have been published and the interpretation of tectonic exhumation or erosion-driven exhumation is now subject of large discussions.

The written geological accounts of August Gansser, our great geological field-explorer, are models of the genre and remain of a great topicality.

August Gansser as a Tibetan Pilgrim (Heim, A & Gansser, A., 1938, Thron der Götter, Morgaten Verlag, Zürich, f. 72)

3.2

Sedimentology and stratigraphy of the Makran accretionary wedge in Iran

Dolati Asghar¹, Bernoulli Daniel¹, Burg Jean-Pierre¹, Smit Jeroen¹, Müller Carla², Spezzaferri Silvia³ & Sergey Sergeev⁴

¹Earth Sciences, ETH-Zurich, Sonneggstr. 5, CH-8092 Zurich (dolati@erdw.ethz.ch)

²6 bis r Haute 92500 RUEIL MALMAISON, France

³Department of Geosciences, University of Fribourg, ch du Musée 6, 1700 Fribourg

⁴Karpinskii All-Russia Research Institute of Geology (VSEGEI), Srednii pr. 74, St. Petersburg, 199026 Russia

The Makran Accretionary Prism (MAP) results from the convergence, initiated during the Late Cretaceous, between the Arabian and Eurasian plates. The active MAP has grown seawards by frontal accretion and underplating of trench-fill sediments since the Miocene. Today, the system is characterized by a shallow dipping slab ($<2^\circ$), great sediment thickness (>7 km) in the foreland of the Oman Sea and a wedge width of >500 km, >300 km of which are exposed onshore.

New mapping and structural sections document the stratigraphic and structural developments of the central Makran Accretionary Wedge (MAW) in southern Iran. Four main tectono-stratigraphic provinces were distinguished, which are from north to south: North-, Inner, Outer and Coastal Makran. North Makran is dominated by mafic to intermediate igneous rocks (Fannuj Unit) and tectonic mélanges in which igneous rocks and Cretaceous deep-water marine sediments are involved (Maskutan). Locally, Upper Cretaceous shallow-water limestone unconformably covers deformed Lower Cretaceous sediments and igneous rocks. The first turbiditic sequences containing mafic fragments were deposited during the Late Cretaceous. To the south, above the Ghasr Ghand Thrust (Inner Makran), Lower Eocene deep-marine sediments and volcanic rocks of the Pip Unit grade into the deeper marine turbiditic sequences of the Eocene Tang Sarheh Unit, which shows a general thickening- and coarsening-upward trend. Well preserved nummulitids in turbiditic sandstones and hundred meters across exotic blocks of Eocene shallow-water limestone in the Tortonian olistostrome indicate shallow-water carbonate deposition north of the turbidite basin. The turbidites become more terrigenous and proximal (channelized) during Early–Late Oligocene, which suggests progradation of submarine fans (Markan and Pirdan Units), followed by more distal deposition during the Late Oligocene (Rask Unit). The pro-delta turbidites grade up-section into Lower Miocene sandstones which are deposited on a shelf dominated by waves and tidal currents. The Lower Miocene sediments, crops out in both Inner and Outer Makran, are mainly marls with gypsum (Ghasr Ghand Unit) were deposited in basins with restricted circulation. These deposits grade laterally into bioclastic sandstones and marls (Pishamak and Roksha Units) and coral limestones (Vaziri Unit) bordering the basin. Plant remains suggest an emerging area to the north. Middle Miocene sediments (Peersohrab Unit) crop out mainly in Outer Makran, between the Ghasr Ghand and Chah Khan Thrusts. However the passage from the Lower to Middle Miocene is not observed but the Middle Miocene sediment starts with deep-marine turbidite to the south of Gativan Thrust which grade up-section into shallower facies. Coastal Makran, to the south of Chah Khan Thrust, exposes sediments mostly younger than the Late Miocene. These sediments represent a wedge-top basin with a shallowing-upwards sequence from slope marls to coastal and continental deposits. All the provinces, Coastal Makran excepted, are covered unconformably by a large olistostrome including giant blocks of igneous and sedimentary rocks from North Makran and of sediments from Inner Makran. This olistostrome was emplaced during the Tortonian (11.6–9.6 Ma).

3.3

Structural analysis of central Makran accretionary wedge (SE Iran)

Dolati Asghar¹, Burg Jean-Pierre¹, Smit Jeroen¹ and Bernoulli Daniel¹

¹ Earth Sciences, ETH-Zurich, Sonneggstr. 5, CH-8092 Zurich (dolati@erdw.ethz.ch)

The Makran Accretionary Prism (MAP) is formed by active convergence between the Eurasian and the Arabian plates. The oceanic crust of the Arabian plate is subducting to the north under the Eurasian continent, thereby building the MAP. This wedge is characterized by a shallow subduction angle ($<2^\circ$), great sediment thickness on the Oman Sea and a wedge width of >500 km, which more than half is exposed onshore.

New mapping and structural sections document the structural developments of the central Makran Accretionary Wedge (MAW) in southern Iran. Four main tectonic units are defined, which from north to south are: North-, Inner, Outer and Coastal Makran. All these units are delimited by regional thrusts. The uppermost tectonic unit, North-Makran, contains Cretaceous rocks which in general contain open folds with wavelength (>200 m) trend ENE–WSW. The unit is thrust over the Eocene turbidites, exposed in Inner Makran by north-dipping Bashakerd Thrust and an Imbricate Zone. Toward south, Eocene-Oligocene turbidites contain S-vergent, tight to isoclinal folds with a general WNW–ESE trend. In contrast, the Miocene sediments contain gentle and symmetrical folds with large wavelength (>500 m) which implies strain differences, stronger in pre-Oligocene and weaker in Miocene sediments. Growth strata in Middle Miocene turbidites indicate folding and thrusting during this time. All major faults are N-dipping thrusts associated with flat and ramp systems. According to the new geological map and cross sections, the main décollement has developed in Oligocene shale layers. The Ghasr Ghand Thrust brings the Inner Makran on Lower–Middle Miocene sediments exposed in Outer Makran. These sediments are folded symmetrically and gently with large wavelength (>500 m) and trend E–W. Usually large box folds (wavelength >100 m) dominate this tectonic unit. Potential décollement horizons are Oligocene or Middle Miocene shales. The N-dipping Chah Khan thrust separate Outer Makran in the north from Coastal Makran., which contains sediments younger than Upper Miocene. Folds are symmetric, open-gentle, rounded-blunt with very long wavelength (>10 km) and low amplitudes. They trend E–W. Planar and bookshelf normal faults cutting sediments younger than Upper Miocene characterize this unit.

Calculation of paleostress tensors indicate regional NNE–SSW compression which is consistent with mapped fold trends and major thrusts as well as with the present day convergence direction between the Arabian and Iranian plates. These results clearly show a stable stress field for the structural development of MAW from Cretaceous to recent. Extension characterizes a more complex and timely less stable system. Coastal Makran recorded regional, radial and active extension. Local extensional events in North-Makran area are local features like in releasing bends of strike-slip faults.

3.4

Tectonic evolution of Makran accretionary wedge (SE Iran) using low temperature thermochronology and tectono-stratigraphic evidences

Asghar Dolati, Diane. Seward, Jeroen. Smit and Jean-Pierre Burg

Earth Sciences, ETH-Zurich, Sonneggstr. 5, CH-8092 Zurich (dolati@erdw.ethz.ch)

Low temperature thermochronology (apatite and zircon fission-track analysis) throughout the Makran Accretionary Wedge provides temporal constraints, that can be interpreted in terms of burial related to both sedimentary and tectonic overburden and later exhumation. Fission tracks in apatite hosted in horizons ranging in age from Late Cretaceous to Miocene (75-10 Ma) have all undergone at least partial annealing since sedimentation. A general increase in annealing with stratigraphic age reflects increased temperatures (burial depth). Samples from horizons as young as 10 Ma are slightly reset implying that temperatures $> 60^{\circ}\text{C}$ were reached prior to eventual cooling and exhumation; horizons older than about 40 Ma have reached temperatures of almost 110°C , the closure temperature of apatite. From this data and associated tectono-stratigraphic observations, it is possible to make some estimates on the timing of thrust activity. There is a regional tendency for southward thrust propagation over time. Between about 27-20 Ma the older horizons (75-63 Ma) from the northern nappe were being exhumed while other units were still being deposited. The youngest cooling/exhumation event of 10-7.9 Ma is recorded in sediments of the footwall nappes. In addition, timing of thrust activity has been influenced by the Tortonian olistostrome. The apatite fission-track results suggest that the recent outcrops took place above a décollement/décollements at a depth of about 5-6 km considering a geothermal gradient of ca. $20^{\circ}\text{C}/\text{km}$.

The fact that the apatites have not reached full annealing in most places puts an upper limit on the paleo-temperature reached such that the zircon single grain ages can be considered to represent true detrital ages. Further confirmation that they have not been reset is that no single grain zircon ages are less than the stratigraphic age from the enclosing horizons. Lag times for individual grains range from almost zero to 500 Ma. The zircon data suggests volcanic activity from Late Cretaceous to Oligocene times. It also confirms the recycling of sediment from within the accretionary wedge during the Miocene, whereby sediment from the northern upthrust units was supplied to the proximal basins.

3.5

Fold growth in the Zagros fold-and-thrust belt in Kurdistan (NE-Iraq)

Grasemann, Bernhard

*Department for Geodynamics and Sedimentology, University of Vienna, Althanstrasse 14, A-1090 Vienna, Austria
(Bernhard.Grasemann@univie.ac.at)*

Fold-growth models in fold-and-thrust belts are of major scientific and economic interest because they are estimated to contain 14% of the known and 15% of the undiscovered global recoverable hydrocarbons. Especially the Zagros fold-and-thrust belt, containing 49% of global fold-and-thrust belt related hydrocarbons has attracted numerous recent studies (e.g. Lacombe et al., 2007 and references cited therein). Whereas thorough tectonic and geomorphological investigations focused on the SE Zagros fold-and-thrust belt in the Islamic Republic of Iran, considerably less modern studies investigated the NW parts in the Parliamentary Republic Iraq.

The Zagros Fold Belt is the northeastern continuation of the Arabian Platform, where the north trending Oman line terminates its southeastern extension (Gansser 1955). The Zagros Mountains started to form as a result of the collision between the Eurasian and Arabian Plates, whose convergence began in the Late Cretaceous as part of the Alpine–Himalayan orogenic system. Geodetic and seismological data document that both plates are still converging and that the fold-and-thrust belt of the Zagros is actively growing (Gansser, 1969). Relationships between active tectonics and erosional landforms reveal differences in the type and rates of deformation and fold growth (Ramsey et al. 2008). The evolution and changes in drainage patterns as well as the influence of fold growth to their appearance are evidence for the kinematics of folds and faults. Tributary networks act very sensitive to deformation and therefore generate characteristic geomorphologic shapes that can be used for the interpretation of tectonic processes (Burbank & Anderson, 2001).

By means of structural field work and quantitative geomorphological techniques the progressive fold growth of anticlines located in the NE of the city of Erbil in the Kurdistan region of Northern Iraq were investigated. This part of the Zagros fold-and-thrust belt is dominated by open folding with wavelengths of about 10 km. The mechanical anisotropy of the formations consisting of a succession of relatively competent (massive dolomite and limestone) and incompetent (claystone and siltstone) sediments essentially controls the deformation pattern with open to gentle parallel folding of the competent layers and flexural flow folding of the incompetent layers.

The anticlines have not developed from subcylindrical embryonic folds but they have merged from different fold segments that joined laterally during fold amplification. This fold segments with length between 5 and 25 km have been detected by mapping ancient and modern river courses that initially cut the nose of growing folds and eventually got defeated leaving behind a wind gap. Fold segments, propagating in different directions force rivers to join resulting in steep gorges, which dissect the merging fold noses. Geomorphological indices of the drainage basins (spacing and elongation ratio, circularity index and shape factor) of different parts in the fore and back-limb of the anticlines demonstrate that the basins have a low maturity and that fold growth is still highly activity.

REFERENCES

- Burbank, D. & Anderson, R. S. 2001. *Tectonic Geomorphology*. Blackwell Science Inc Malden.
- Gansser, A. 1955. New aspect of the geology of the Central Iran. 3e Congr. mond. Pétrole, Actes et doc., 1, 279-300. Roma.
- Gansser, A. 1969: The large earthquakes of Iran and their geological frame. *Eclogae Geologicae Helvetiae*, 62, 2, 443-466.
- Lacombe, O., Lavé, J., Roure, F. & Verges, J. 2007: *Thrust Belts and Foreland Basins: From Fold Kinematics to Hydrocarbon Systems Series*. Springer, Berlin Heidelberg New York.
- Ramsey, L. A., Walker, R. T. & Jackson, J. 2008. Fold evolution and drainage development in the Zagros mountains of Fars province, SE Iran. *Basin Research*, 20, 23-48.

3.6

Syn-collisional exhumation of the continental lower crust

Grujic Djordje¹, Warren Clare J.², Kellett Dawn A.¹ & Wooden Joseph L.³

¹ Dalhousie University, Department of Earth Sciences, Halifax, NS B3H 4J1, Canada (dgrujic@dal.ca)

² The Open University, Earth and Environmental Sciences, Milton Keynes, MK7 6AA, United Kingdom

³ Department of Geological and Environmental Science, Stanford University, Stanford, USA

Here we present a tectonic model for the evolution of the eastern Himalaya and suggest a general model for late orogenic exhumation of the lower continental crust.

Mafic and pelitic granulites exposed in the eastern Himalayan kingdom of Bhutan preserve textural evidence for a precursor high-pressure metamorphic event, the precise conditions of which are generally unrecoverable due to the later high temperature overprint. As high pressure metamorphism is rare in the Himalayas, especially in the eastern parts of the orogen, their thermobarometrical and geochronological evolution place important constraints on the geodynamic evolution of the Himalaya in particular and continental collisions in general. We report SHRIMP trace element (REE) and U–Pb zircon, and LA-ICPMS U–Th–Pb monazite geochronological data. Combined, these data suggest that zircons crystallized at 14–15 Ma over a temperature range of ca. 705–815 °C. This age is interpreted to indicate the timing of HP metamorphism due to the lack of negative Eu anomaly, the depleted heavy REE signature and the low temperatures of crystallization. Monazites associated with sillimanite-grade metamorphism in granulite-hosting garnet-sillimanite-biotite migmatitic gneisses yield rim ages between 15.4 ± 0.8 Ma and 13.5 ± 0.5 Ma. These rocks structurally overlie older 21–16 Ma garnet-sillimanite-biotite migmatitic gneisses in which granulite-facies material is absent. The geochronological, petrological and structural data suggest that an out-of sequence thrust likely separates the two packages. These data are consistent with exhumation of GHS material from a variety of crustal depths at different times along the Himalayan orogen during the Miocene. Exhumation of eclogites and granulites in Bhutan was possibly driven by tectonic forcing over an incoming Indian crustal ramp.

3.7

Preliminary results of Cretaceous-Eocene sediment analysis of Makran accretionary wedge in SE Iran

Ali Jalali^{1,2}, Asghar Dolati¹, Daniel Bernoulli¹, Jean-Pierre Burg¹

¹ Earth Sciences, ETH-Zurich, Sonneggstr. 5, CH-8092 Zurich (ali.jalali@erdw.ethz.ch)

² Geological Survey of Iran, Meraj Avn., Azadi Sq., Tehran, Iran. Po. Box 13185-1494

Upper Cretaceous to Miocene sediments of the Makran accretionary wedge are dominated by bouma-type turbidite sandstones and shales.

Having specified the stratigraphic ages of the successive lithostratigraphic facies, this study concentrates on the source of the sediments. The heavy mineral analyses of the Cretaceous turbidites indicates contribution of ophiolite fragments exposed not far from the studied basin, as suggested by the angular shape of clastic fragments. The likely source is the Makran ophiolites that crop out along the northern boundary of the Makran accretionary wedge.

Fission track ages of zircon in Cretaceous sandstones show two main populations, one at 77 ± 6 Ma and one at 144 ± 10 Ma. These two age clusters defining two different sources.

Petrographic studies of Eocene turbidites identified Na- and K-idiomorphic feldspars as well as sanidine minerals, which all together suggest silicic volcanic sources. The Eocene turbidites also contain ophiolitic fragments, similar to those found in the Cretaceous sediments. Eocene polymictic conglomerates contain ultramafic, mafic and granite pebbles. The 86.2 ± 10.6 and 88.4 ± 12.0 Ma zircon fission track ages of granite pebbles point to plutonic source rocks older than Late Cretaceous. Since the sizes of the pebbles are large (10–50 cm), the source is not as far as the Himalayas. A closer solution would be the Sanandaj-Sirjan plutonic belt, located just N–NW of the wedge.

3.8

The upward and outward growth of northeastern Tibet and geodynamic implications

Molnar P.

Department of Geological Sciences and Cooperative Institute for Research in Environmental Science (CIRES), University of Colorado, Boulder, Colorado USA, 80309-0399 (CO, USA) (molnar@colorado.edu)

Several recent studies from northern Tibet demonstrate that faulting, folding, rapid exhumation, and rotation around vertical axes occurred shortly after India collided with southern Eurasia at 45-50 Ma; many other recent studies show enhanced deformation on the margins of Tibet and in surrounding regions beginning since ~15-10 Ma. The first implies that the essentially all of the rock now comprising Tibet was, immediately after collision, part of what grew to be the Tibetan Plateau and that as the plateau grew higher, its north-south dimension decreased. Thus, any northward propagation of deformation as India penetrated Eurasia was superimposed on this plateau-wide contraction. The presence of a strong Tarim Basin and North China craton, and perhaps of a strong Qaidam Basin, helped to concentrate deformation on its margins and therefore to confine the dimensions of Tibet. The deformation beginning near 15-10 Ma includes not only an acceleration of crustal shortening on the margins of the plateau, but also a change in the orientation of compressional strain in northeast Tibet from NNE-SSW to more nearly ENE-WSW with an important component of left-lateral shear on E-W planes. This change might be related to removal of mantle lithosphere from beneath northern Tibet. Present-day deformation of northeastern Tibet includes thrust faulting on numerous ESE-WNW-trending faults and both right- and left-lateral slip on conjugate strike-slip faults. If this deformation field is to be described in terms of relative movements of crustal blocks, many tens of blocks will be needed to such a description, which makes such a description virtually useless for understanding the dynamic processes.

3.9

Compositional variations and geodynamic implications of the Mesozoic island arc magmatism in the Sanandaj-Sirjan arc-basin system

Monsef Iman¹ & Rahgoshay Mohamad¹

¹ Shahid Beheshti University, Earth Sciences Faculty, Tehran, Iran (iman_monsef@yahoo.com)

The subduction of the Neo-Tethys ocean appears to have initiated in the south of the Sanandaj-Sirjan arc-basin system at Early Jurassic to Late Cretaceous time in Iranian convergent margin environment. These magmatic activities in the Sanandaj-Sirjan magmatic arc show significant geochemical variations during their evolutionary period. These magmatic sequences have exposed with Mesozoic age in magmatic-sedimentary-turbiditic structural zone along a 1300 km arc-basin system.

The geochemical data suggest magmatic evolution from the tholeiitic to the calc-alkaline characteristics in space and time. REE and trace element patterns show moderate to high LREE/HREE ratios, low to moderate depletion in Nb relative to Yb, and high Th/Yb ratios relative to MORB and WPB. The parent magma of Early to Late Jurassic sequences, with island arc tholeiite (IAT) compositions, has been originated from the spinel lherzolite mantle with primitive mantle (PM) composition, with effective of liquids and sediment resulted from the subducting slab. The parent magma of Cretaceous sequences with island arc tholeiite to E-MORB compositions have been resulted from the garnet - spinel lherzolite mantle with E-MORB to OIB composition.

These compositional changes may be related to high sediment and hydrothermal fluxes, resulted from the deep subducted slab into the mantle wedge. These magmatic sequences are originated during the northeastward subduction of the Neo-Tethyan ocean plate under the Sanandaj-Sirjan arc basin system, during the Early Jurassic to Late Cretaceous time, in the island arc tectonic environment. The arc-trench system collided with the Arabian passive margin in the late Cretaceous along the Main Zagros Thrust Belt. The Zagros orogen is a young Tertiary collision belt generally considered a recent analogue of the Alpine - Himalayan orogenic system.

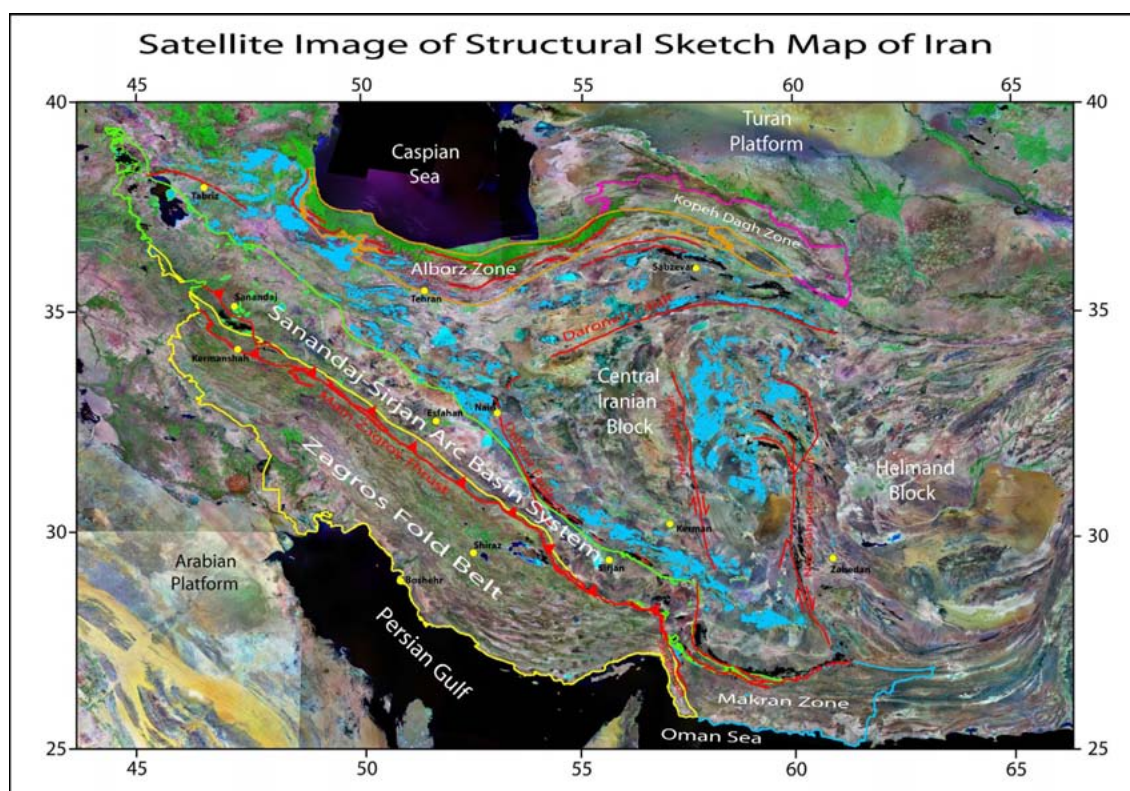


Figure 1. Satellite image of structural sketch map of Iran. The locations of major structural zones consisting of Sanandaj-Sirjan Arc-Basin System, Central Iranian Block, Alborz Zone, Kopedagh Zone, Makran Zone, Arabian Platform, Zagros Folded Belt and Helmand Block are indicated.

REFERENCES

- Pearce, J.A. & Parkinson, I.J. 1993: Trace element models for mantle melting: application to volcanic arc petrogenesis. Geological Society, London, Special Publications, 373-403.
- Pearce, J.A., Stern, R.J., Bloomer, S.H. & Fryer P. 2005: Geochemical mapping of the Mariana arc-basin system: Implications for the nature and distribution of subduction components. *Geochemistry, Geophysics, Geosystems*, 6, 7, 1-27.

3.10

Metamorphic and denudation patterns of the Songpan-Garzê flysch in Sichuan Province, China

Rahn Meinert¹ & Wang Hejing²

¹ Swiss Federal Nuclear Safety Inspectorate (meinert.rahn@ensi.ch)

² School of Earth and Space Sciences, Peking University, Beijing 100871, P. R. China

Exhumation of the Qinglin and Dabie Shan orogens from deep crustal levels in the Triassic led to the formation of large sedimentary deposits north and south of these orogens. The basins were filled with up to 10 km thick flysch sequences (Songpan-Garzê flysch, Ingersoll et al., 2003) that later underwent shortening and folding (Roger et al. 2010) in an accretionary wedge setting. The flyschs were overprinted between diagenetic to low-grade metamorphic grade (Wang et al. 2008). Exhumation of the flysch units was decoupled from the surrounding areas (e.g. the Red Basin, Richardson et al. 2008) by two extended and active fault lines, the Xianxuihe fault to the southwest and the Longmenshan fault to the southeast. Today, the Songpan-Garzê orogen forms the eastern margin of the Tibetan plateau.

The metamorphic pattern (mostly based on illite and chlorite crystallinities) is in part influenced by localized exhumation along the Longmenshan fault. Metamorphic boundaries cut across large-scale Triassic fold structures. From the metamor-

phic parameters it is evident that the Longmenshan fault system has accommodated more than 5 km of post-metamorphic vertical displacement, while for the Xianxiuhe fault 60 km of sinistral strike-slip is to be postulated.

Fission track data from 48 samples collected within the flysches and along a profile across the Longmenshan fault system vary between 3 and 136 Ma and indicate young and fast exhumation of units NW of the Longmenshan fault. Ages become older with increasing distance from the fault and reach a plateau of Lower/Upper Cretaceous values far away. It is shown by thermochronological modelling that most ages can be shown to be the result of two thermal event, i.e. a Lower Cretaceous cooling episode (140-90 Ma) and a late reheating and cooling event at around 20-15 Ma. Strong effects of a late cooling event are also found far away from the Longmenshan fault in areas of highest metamorphic overprint. It is thus concluded that the metamorphic pattern as mapped at the surface today is markedly influenced by exhumation processes along the Longmenshan fault but also along flysch-internal structures. The findings of a strong Cretaceous cooling event contrasts with the synthesis of Roger et al. (2010) who describe the Jurassic and Cretaceous as a period of tectonic quiescence.

REFERENCES

- Ingersoll, R.V., Dickinson, W.R. & Graham, S.A. 2003: Remnant-ocean submarine fans: Largest sedimentary systems on Earth. *GSA Special Paper* 370, 191–208.
- Richardson, N.Y., Densmore, A. L., Seward, D., Wipf, M., Li, Y., Ellis, M. A. & Zhang, Y. 2008: Extraordinary denudation in the Sichuan Basin: Insights from low-temperature thermochronology adjacent to the eastern margin of the Tibetan Plateau. *JGR* 113, doi:10.1029/2006JB004739.
- Roger, F., Jolivet, M. & Malavieille, J. 2010: The tectonic evolution of the Songpan-Garzê (North Tibet) and adjacent areas from Proterozoic to Present: A synthesis. *Journal of Asian Earth Sciences* 39, 254-269.
- Wang H., Rahn, M., TAO, X., Zheng, N. & Xu, T. 2008: Diagenesis and metamorphism of Triassic Flysch along profile Zoige-Lushan, Northwest Sichuan, China. *Acta Geologica Sinica* 82, 917–926.

3.11

Protracted melting in the Higher Himalayan Crystalline (Sikkim, India)

Daniela Rubatto^{1,2}, Sumit Chakraborty³, Somnath Dasgupta⁴

¹ Research School of Earth Sciences, The Australian National University, Mills Road, Canberra 0200, Australia
(daniela.rubatto@anu.edu.au)

² Present address: Institute of Mineralogy and Geochemistry, University of Lausanne, Antrophole, CH-1015 Lausanne, Switzerland

³ Institut fuer Geologie, Mineralogie und Geophysik, Ruhr-Universität Bochum, D-44780 Bochum, Germany

⁴ National Centre of Experimental Mineralogy & Petrology, University of Allahabad, 14 Chatham Lines, Bank Road, Allahabad-211002, Uttar Pradesh, India

Partial melting of the continental crust commonly occurs in orogenic settings at the root of mountain belts. The timing of melting has significant implications for the secular evolution of the planet in terms of modeling of orogenic processes, heat transfer and rheology of the crust. One of the most spectacular and complete migmatite sequence is exposed in the Sikkim Valley of the eastern Himalayas where the Lesser Himalayan Crystalline in the south and the Higher Himalayan Crystalline in the north, both reached melting conditions. The LHC consists of an inverted sequence of greenschist- to amphibolite grade metapelites, which reached muscovite-melting conditions (~675°C and 7.5 kbar, Dasgupta et al. 2009). In the HHC a similar metapelitic sequence underwent pervasive partial melting at higher grade (~800°C and 7-12 kbar). This fertile bulk composition crosses a series of melting reaction during the prograde path including paragonite melting, fluid induced melting, muscovite melting and biotite melting.

Zircon and monazite crystals in numerous leucosomes and mesosomes from the HHC show multiple growth domains (Figure 1). These domains were analysed by microbeam for age (SHRIMP) and trace element composition (LA-ICPMS) in an attempt to relate ages to conditions of formation.

Monazite preserves the best record of metamorphism. In most samples monazite yield two ages, which generally correspond to domains with different zoning pattern and composition. In two monazite samples an third, older age component is present. Zoning and trace element composition indicate that initial monazite growth occurred at amphibolite facies conditions, likely before the onset of melting. Monazite growth in the presence of melt was widespread and diachronous across samples (29-17 Ma).

Zircon was generally less reactive than monazite to metamorphism. A limited number of samples preserve up to two distinct growth zones, that for shape, zoning pattern and composition can be attributed to melting. As for monazite, the trace element composition of the distinct zircon growth zones indicates that they were produced by different melting reactions. Also for zircon, ages are diachronous across samples and vary from ~32 to 17 Ma.

The spread of ages indicates that melting continued across the HHC for more than 10-15 Ma via a series of melting reactions. The episodic record of each sample also suggests that, within this time window, zircon and monazite crystallization from the melt was diachronous within and across samples. A trend to younger ages is observed within the HHC from north (South Tibetan Detachment side) to south (Main Central Thrust side).

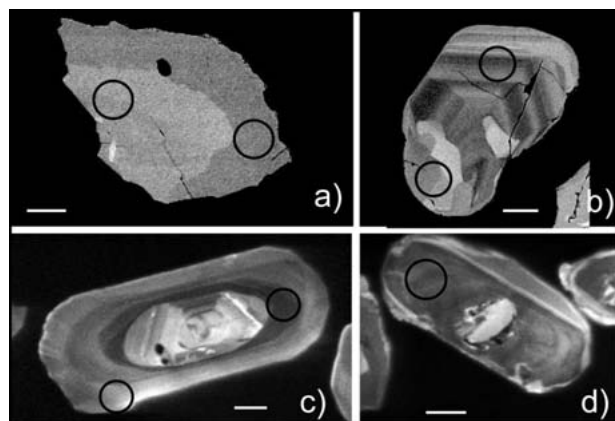


Figure 1. Back scattered electron (a and b) and cathodoluminescence (c and d) images of monazite and zircon crystals, respectively. The crystals show multiple growth zones that yield distinct ages testifying to protracted metamorphism and melting. The circles indicate the location of SHRIMP analyses. The scale bar is 2µm.

REFERENCES

Dasgupta, S., Chakraborty, S. & Neogi, S. 2009: Petrology of an inverted Barrovian sequence of metapelites in Sikkim Himalaya, India: constraints on the tectonic inversion. *American Journal of Science*, 309, 43-84.

3.12

Structural development of the Tso Morari ultra high pressure nappe of the Ladakh Himalaya

Albrecht Steck¹ and Jean-Luc Epard²

¹Institut de Minéralogie et Géochimie, Université de Lausanne, Anthropole, CH-1015 Lausanne, Switzerland.

E-mail: Albrecht.Steck@unil.ch

²Institut de Géologie et Paléontologie, Université de Lausanne, Anthropole, CH-1015 Lausanne, Switzerland.

E-mail: Jean-Luc.Epard@unil.ch

A subduction and multistage exhumation process for the Tso Morari ultra high pressure nappe is discussed. The model is constrained by a review of published thermo-barometric and age data combined with a new geological and tectonic map as well as observations on the structural and metamorphic evolution of the Tso Morari area and the North Himalayan nappes. After continental collision some 55 Ma ago, the N Indian continental crust was subducted to a depth of over 90 km below Asia. The under thrusting was accompanied by the detachment and accretion of the upper crust Late Proterozoic to Early Eocene sediments, creating the N Himalayan accretionary wedge, in front of the active Asian margin and the 103-50 Ma Ladakh arc batholith. At a depth of over 90 km, pressures of over 27 kbars and temperatures of 500 to 600°C, the basic dikes in the Ordovician Tso Morari granite were transformed to eclogites with crystallisation of coesite, some 53 Ma ago. The detachment and extrusion of the low density Tso Morari nappe, composed of 70% of the Tso Morari granite and 30% of graywackes with some eclogitic dikes, occurred by ductile pure and simple shear deformation, pushed by buoyancy forces and by squeezing between the underthrust Indian lithosphere and the Asian mantle wedge. The extruding Tso

Morari nappe reached a depth of 35 km at the base of the N Himalayan accretionary wedge some 48 Ma ago, where the whole nappe stack recrystallized under amphibolite facies conditions of a Barrovian regional metamorphism, with a metamorphic field gradient of 20°C/km. An intense schistosity with a W-E oriented stretching lineation L1 and top-to-the E shear criteria and crystallisation of oriented sillimanite needles after kyanite, testify to the phase of the Tso Morari nappe extrusion and pressure drop. Reaching the base of the N Himalayan accretionary wedge, the whole nappe stack composed from base to top of the Tso Morari, Tetraogal, Karzok and Mata – Nyimaling-Tsarap nappes, was overprinted by new schistoses with a first N-directed and a second NE-directed stretching lineation L2 and L3, characterised by top-to-the S and SW shear criteria. This structural overprint was related to an early N- and a younger NE-directed under thrusting of the Indian plate below Asia, that was accompanied by an anticlockwise rotation of India. The warping of the Tso Morari dome started already some 48 Ma ago with the formation of an extruding nappe at depth. The Tso Morari dome reached a depth of 15 km some 40 Ma ago in the eastern Kiagar La region and 30 Ma ago in the western Nuruchan region. The extrusion rate was of about 3 cm/yr between 53-48 Ma, followed by an uplift rate of 1.2 mm/yr between 48 and 30 Ma and only 0.5 mm/yr since 30 Ma. Observations on the geomorphology show that the Tso Morari dome is still affected by faults, open regional dome and basin and pull-apart structures, in a zone of active dextral transpression parallel to the Indus Suture zone.

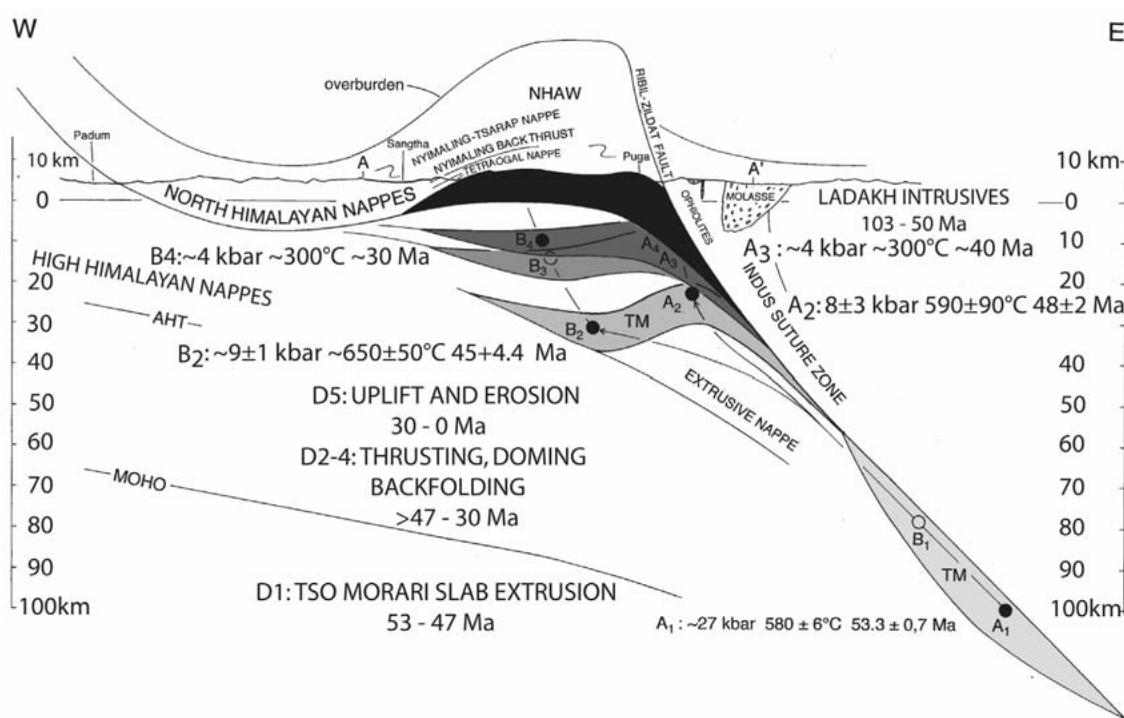


Figure 1. Structural model for the emplacement of the Tso Morari nappe.

REFERENCES

- De Sigoyer, J., Chavagnac, V., Blichert-Toft, J., Villa, I.M., Luais, P., Guillot, S., Cosca, M., Mascle G., 2000: Dating the Indian continental subduction and collisional thickening in the northwest Himalaya: Multichronology of the Tso Morari eclogites. *Geology* 28, 487-490.
- Epard, J.-L., Steck A., 2008: Structural development of the Tso Morari ultra-high pressure nappe of the Ladakh Himalaya. *Tectonophysics* 451, 242-264.
- Girard, M. Bussy, F., 1999: Late Pan-African magmatism in the Himalaya: new geochronological and geochemical data from the Ordovician Tso Morari metagranites (Ladakh, NW India). *Schweizerische Mineralogische und Petrographische Mitteilungen* 79, 399-417.
- Leech, M.L., Sing, S., Jain, A.K., Klemperer, R.M., Manickavasagam, R.M., 2005: The onset of India-Asia continental collision: Early, steep subduction required by the timing of UHP metamorphism in the western Himalaya, *Earth and Planetary Sciences Letters* 234, 83-87.
- Schlup, M., Carter, A., Cosca, M., Steck, A., 2003: Exhumation history of the eastern Ladakh revealed by $^{40}\text{Ar}/^{39}\text{Ar}$ and fission track ages: The Indus river-Tso Morari transect, NW Himalaya. *Journal of the Geological Society of London* 160, 385-399.
- Schlup, M., Steck, A., Carter, A., Cosca, M., Epard, J.-L., Hunziker, J., 2010: Exhumation history of the NW Indian Himalaya revealed by fission track and $^{40}\text{Ar}/^{39}\text{Ar}$ ages. *Journal of Asian Earth Sciences*, in press.

4. Paleontology and Paleobiodiversity

Lionel Cavin & Jean-Pierre Berger

*Schweizerische Paläontologische Gesellschaft (SPG/SPS),
Kommission des Schweizerischen Paläontologischen Abhandlungen (KSPA)*

- 4.1 Bomou B., Arnaud-Vanneau A., Adatte T.: Stratigraphy and ecology of large benthic foraminifera during the Cenomanian-Turonian transition: new insights from the Morelos-Guerrero carbonate platform, southwestern Mexico.
- 4.2 Chablais J., Feldmann R.M., Schweitzer C.E., Martini R., Rigaud S.: Triassic decapods: new data from the Arabian shelf of the northern United Arab Emirates
- 4.3 Chablais J., Martini R., Onoue T.: Upper Triassic reef biota from southwestern Japan: new data from a Panthalassan seamount
- 4.4 De Baets K., Klug C., Korn Dieter.: Early Emsian Ammonoidea: stratigraphy, intraspecific variability, and evolutionary trends
- 4.5 Klug C., De Baets K., Korn D.: Devonian pearls and ammonoid-endoparasite co-evolution
- 4.6 Klug C., De Baets K., Monnet C.: Parallel evolution controlled by adaptation and covariation in ammonoid cephalopods
- 4.7 Lavoyer T., Berger J.-P.: Stratigraphy and Paleogeography of the North- Middle Upper Rhine Graben (N-Middle URG) during the Paleogene.
- 4.8 Marty D., Paratte G., Lovis C., Jacquemet M., Meyer C.A.: Extraordinary sauropod trackways from the Late Jurassic Béchat Bovais tracksite (Canton Jura, NW Switzerland): implications for sauropod locomotor styles
- 4.9 Mennecart B., Becker D., & Berger J.-P.: Swiss *Amphitragulus* and *Dremotherium* (Mammalia Ruminantia): State of the art
- 4.10 Ospina-Ostios L.M., Ragusa J., Kindler P.: New biostratigraphic data from the Voirons Sandstones (Voirons massif, Haute-Savoie, France): implications for the paleogeographic origin of the Gurnigel Nappe
- 4.11 Pirkenseer C., Steurbaut E., Speijer R.: The evolution of Early Ypresian microfossil assemblages and stable isotopes during a distinct plankton peak in the Corbières (Aude, France) continental margin record
- 4.12 Scherler L., Becker D., Berger J.-P.: A Tooth Tale: the *Anthracotherium bumbachense* (Artiodactyla, Mammalia) from Beuchille (Delémont, Switzerland)
- 4.13 Ware D., Bucher H., Brühwiler T., Goudemand N.: Dienerian (Early Triassic) ammonoid successions of the Tethys: preliminary results from Pakistan and India

4.1

Stratigraphy and ecology of large benthic foraminifera during the Cenomanian-Turonian transition: new insights from the Morelos-Guerrero carbonate platform, southwestern Mexico.

Brahimsamba Bomou¹, Annie Arnaud-Vanneau², Thierry Adatte¹

¹ Institut de Géologie et de Paléontologie, Université de Lausanne, Unil-Dorigny, Anthropole, 1015 Lausanne, Suisse (brahimsamba.bomou@unil.ch)

² Université de Grenoble, Institut Dolomieu, 15 rue M. Gignoux, 38031 Grenoble

Contrary to the Central Atlantic and Western Tethys areas, the carbonate platform of Guerrero-Morelos, located in Southwestern Mexico, persisted up to the basal Turonian. The Axaxacualco and Baranca el Cañon sections are located at the Guerrero-Morelos carbonate platform in southern Mexico and exhibit a typical and correlateable $\delta^{13}\text{C}$ curve. In the distal part of the carbonate platform (Axaxacualco), the $\delta^{13}\text{C}$ positive excursion coincides with oligotrophic carbonate platform environments, characterized by abundant and diversified benthic microfauna and rudists, confirmed by low concentrations in phosphorus. The impact of OAE appears more significant in the proximal part of the carbonate platform at Barranca, characterized by the deposition of thick laminated microbialites indicative of mesotrophic conditions. This carbonate platform characterized by oligotrophic to mesotrophic conditions, was therefore persistent throughout the entire OAE2 in Central Mexico despite the closeness to the Caribbean plateau. The definitive drowning, marked by the deposition of black shale and turbidites, occurs only in the lower Turonian (*P. flexuosum*), well above the end of the $\delta^{13}\text{C}$ shift. This carbon isotope positive excursion, coinciding with the Oceanic Anoxic Event (OAE2), is therefore recorded in the upper part of platform carbonate deposits. That allows a better understanding of large benthic foraminifera distribution during the OAE2 event.

During the Late Cenomanian, microfauna is not extremely diversified, but some large benthic foraminifera as *Pseudorhapydionina chapianensis* and *dubia*, *Cuneolina parva*, *Dicyclina* sp., and *Chrysalidina gradata* are present. In the first part of the $\delta^{13}\text{C}$ shift (peak 1) these foraminifera still keep going, but are less abundant. Some *Cuneolina* excepted, they completely disappear in the second part of the positive excursion. These large benthic foraminifera probably linked to green symbiotic algae, are absent in uppermost part of the carbonate platform sediments. However, some endo-benthic foraminifera with thin shell and without symbiotic association persisted. They consist of trochospiralia species which belong to *Nezzazata*, *Nezzazatinella* and *Dobrogeolina* genera, suggesting significant biotic stress conditions. The demise of the Guerrero-Morelos carbonate platform is related to a regression and occurs only at the end of the $\delta^{13}\text{C}$ shift, thus significantly after the OAE2. However, the last carbonate deposits are recorded at Axaxacualco, located in a more distal part of the platform, and correspond to a falling stage system tracks. No relevant microfauna is observed. The drowning of Guerrero-Morelos carbonate platform takes place in the early Turonian, characterized by deeper and anoxic environments, which preclude large benthic fauna reestablishment.

4.2

Upper Triassic reef biota from southwestern Japan: new data from a Panthalassan seamount

Chablais Jérôme¹, Martini Rossana¹ & Onoue Tetsuji²

¹ Département de Géologie et Paléontologie, Rue des Maraîchers, 13, CH-1905 Genève (Jerome.Chablais@unige.ch)

² Department of Earth & Environmental Sciences, Kagoshima University, Kagoshima, 890-0065, Japan

Upper Triassic reefs are particularly important because they represent the renewal of metazoan reefs after the Permian crisis. A renewed diversification of metazoan reef builders and dwellers began in the Anisian and reached its maximal biodiversity only during the Late Triassic. As a result of a change from humid to arid climatic conditions that began during the Carnian and extended through the Norian, the Norian-Rhaetian interval was characterised by an extraordinary global latitudinal expansion of reefs across the northern and southern hemispheres between 33° N and 35° S (Kiessling et al., 1999; Flügel, 2002). During this time, large reef complexes developed worldwide both north and south of the Tethys Ocean and throughout the Panthalassic Ocean in displaced terranes and/or on seamounts.

Important works on Triassic reefs by several authors (Kiessling et al., 1999; Flügel, 2002; with bibliography) have thoroughly catalogued these numerous Upper Triassic reef localities throughout the world. However, most studies involve those in the Tethys realm, and few data are from Panthalassic reefs, generally corresponding to atoll-type shallow-marine carbonates accumulated over seamounts and/or oceanic plateaus in an open-ocean realm.

Because these reefs are pivotal in resolving sedimentological, paleontological and paleobiogeographic issues related to the Panthalassic Ocean and Late Triassic reefs during the Mesozoic, we intensely studied the reef limestones discovered near Inaba Cave on Shikoku Island, Japan, with respect to their microfacies, paleontology and paleoecology.

This Norian-Rhaetian reef limestone belongs to the Sambosan Accretionary Complex, a Late Jurassic to Early Cretaceous subduction-generated accretionary complex in southwestern Japan. This patch reef complex is inferred to have formed within an atoll-type carbonate system accumulated over a mid-oceanic seamount surrounded by deep-water radiolarian cherts in the Panthalassic Ocean during the Late Triassic (Chablais et al., 2010a).

Based on preserved depositional textures and biota, we described several microfacies and interpret its sedimentary environment. Due to the preservation state of the outcrop and the geological context of the Sambosan limestones (accretionary system), the sedimentological and paleontological analysis should be regarded as a characterisation of reef communities rather than of the total reef. Based on these constraints, three groups of facies can be identified: (1) boundstone reef facies, (2) interstitial reef facies, and (3) surrounding reef facies (Chablais et al., 2010b).

The reef boundstone facies is characterised by abundant coralline sponges that, in association with microbial crusts, constitute the main framebuilders. Some phaceloid and/or dendroid corals occur, but these groups are poorly represented, as are algae. Microproblematica and foraminifers exhibit rich associations, acting as secondary reef builders and/or reef dwellers. The surrounding setting comprises biotrital sponge-coral rudstone and well-preserved megalodont rudstone-floatstone. The sedimentary contact between reef and lagoon is observed for the first time within Inaba Cave, where an excellent exposure of megalodont floatstone occurs in association with a coral-sponge boundstone facies.

Finally, this Japanese Upper Triassic reef gives interesting assets for paleobiogeographic comparisons with the coeval Upper Triassic reefs of the southern Peri-Tethys area including the Northern Calcareous Alps, Sicily, and Oman. It appears that the Japanese and Peri-Gondwanian (Oman) seamount reefs resemble one another because of their similar depositional setting. Both types of reefs are characterised by a similar biodiversity of corals, sponges and foraminifers, but they exhibit significant differences in the rarity of calcareous algae and abundant endemic coral species in Japan. Nevertheless, the major similarities confirm a more southern-Hemisphere origin for Upper Triassic Japanese reefs than predicted by previous reef studies.

This project was supported by the Swiss National Science Foundation (grant RM 200021-113816).

REFERENCES

- Chablais, J., Martini, R., Samankassou, E., Onoue, T. & Sano, H. 2010a: Microfacies and depositional setting of the Upper Triassic mid-oceanic atoll-type carbonates of the Sambosan Accretionary Complex (Southern Kyushu, Japan). *Facies*, 56, 249-278.
- Chablais, J., Onoue, T. & Martini, R. 2010b: Upper Triassic reef limestone blocks of southwestern Japan: new data from a Panthalassan seamount. *Palaeogeography, Palaeoclimatology, Palaeoecology*, 293, 206-222.
- Flügel, E. 2002: Triassic reef patterns. In: Kiessling, W., Flügel, E. & Golonka, J. (Eds.), *Phanerozoic Reef Patterns*. Society of Economic Paleontologists and Mineralogists special publication, 72, 391-464.
- Kiessling, W., Flügel, E. & Golonka, J. 1999: Paleoreef maps: evaluation of a comprehensive database on phanerozoic reefs. *American Association of Petroleum Geologists Bulletin*, 83, 1552-1587.

4.3

Triassic decapods: new data from the Arabian shelf of the northern United Arab Emirates

Chablais Jérôme¹, Feldmann Rodney M. ², Schweitzer Carrie E. ³, Martini Rossana¹ & Rigaud Sylvain ¹

¹ Département de Géologie et Paléontologie, Rue des Maraîchers, 13, CH-1905 Genève (Jerome.Chablais@unige.ch)

² Department of Geology, Kent State University, Kent, OH 44242 United States of America

³ Department of Geology, Kent State University at Stark, 6000 Frank Ave. NW, North Canton, OH 44720 United States of America

Knowledge about Triassic decapod crustaceans is very limited due to the paucity of Triassic fossils throughout the world. Around 65 species of Triassic shrimps and lobsters have been reported, mainly from Tethyan and Eurasian localities, as well as a few from North America and Madagascar (Amati et al., 2004; Feldmann and Schweitzer, 2006).

One reason for the relatively small number of fossil decapod crustaceans is the susceptibility of the carapace to be consumed by many predators and scavengers and to the post mortem fragmentation of organisms by wave action. As a result, the discovery of new fossil decapod crustaceans commonly marks a notable addition to the taxonomic and systematic knowledge of the group.

Thus, the discovery of a new specimen, *Platykotta akaina* n. gen. n. sp., identified as a Triassic anomuran, from the Arabian shelf of the northern United Arab Emirates, represents important contribution to the paleontological knowledge of the crustacean fossils (Chablais et al., 2010). The generic name is derived from the Greek *platys* = flat, and *kotta* = head, in reference to the flattened surface of the metagastric region. The trivial name is derived from the Greek *akaina* = thorn or spine, in reference to the spinose nature of the cephalic region.

This crustacean fossil has been collected from the Upper Triassic carbonates of the Ghalilah Formation in the Musandam Peninsula, United Arab Emirates. The Musandam Mountains offer spectacular exposures of Permian to Cretaceous shallow-marine carbonates which were deposited on the passive margin of the Arabian Plate bordering the southern Tethys during that time (Maurer et al., 2008). The fossil decapod was found in an extensively burrowed limestone level within the Ghalilah Formation (Norian-Rhaetian) of the Wadi Naqab.

The great abundance and high biodiversity of decapod crustaceans in the shallow-water environment of the Arabian shelf during the Triassic is suggested by the large number and variety of burrows on the exposures, including large *Spongiomorpha* burrows.

Initially, only the ventral exposure of the new taxon was preserved. Using a rigorous chemical preparation by dilute organic acid (acetic) to dissolve limestone but leaving the carapace (chitin) intact, the dorsal view revealed a well-preserved, chitinous, granular carapace exhibiting characteristic carapace morphology and groove pattern of the Eocarcinoidea, the superfamily to which the new family is assigned.

The dorsal view together with the ventral surface, rarely seen in the fossil record, provides new insight into the morphology of representatives of the Eocarcinoidea. It brings new insight into the crustacean origins, dispersal, and radiation along the carbonate shelf of the Tethys during the Triassic. Until now, Triassic crustaceans known from the Southern Hemisphere only have been reported from Madagascar (Feldmann and Schweitzer 2006). This is the first known occurrence of anomurans from this part of the world. Furthermore, the new species represents the oldest occurrence of the Anomura MacLeay known to date.

This project is supported by the Swiss National Science Foundation (grant RM 200021-113816).

REFERENCES

- Amati, L., Feldmann R.M. & Zonneveld, J.-P. 2004: A new family of Triassic lobsters (Decapoda: Astacidea) from British Columbia and its phylogenetic context. *Journal of Paleontology*, 78, 150-168.
- Chablais, J., Feldmann, R.M. & Schweitzer, C.E. 2010: A new Triassic decapod, *Platykotta akaina*, from the Arabian shelf of the northern United Arab Emirates: earliest occurrence of the Anomura. *Paläontologische Zeitschrift*, DOI: 10.1007/s12542-010-0080-y.
- Feldmann, R.M. & Schweitzer, C.E. 2006: Paleobiogeography of Southern Hemisphere decapod Crustacea. *Journal of Paleontology*, 80, 83-103.
- Maurer, F., Rettori, R. & Martini, R. 2008: Triassic stratigraphy, facies and evolution of the Arabian shelf in the northern United Arab Emirates. *International Journal of Earth Sciences*, 97, 765-784.



Figure 1. Ventral view of the new specimen, *Platykotta akaina* n. gen. n. sp. (modified from Chablais et al., 2010). For the dorsal view: come to see the poster!

4.4

Early Emsian Ammonoidea: stratigraphy, intraspecific variability, and evolutionary trends

De Baets, Kenneth¹, Klug, Christian¹ & Korn, Dieter²

¹Paläontologisches Institut und Museum, Universität Zürich, Karl Schmid-Strasse 4, 8006 Zürich, (chkklug@pim.uzh.ch)

²Museum für Naturkunde, Leibniz Institute at the Humboldt University Berlin, Invalidenstraße 43, D-10 115 Berlin, Germany, (dieter.korn@mfn-berlin.de)

Ammonoids represent one of the most important groups of macro-invertebrates for dating Devonian to Cretaceous marine sediments. Ammonoids originated from bactritoids in the Early Devonian during a time of macroecological turnover in marine ecosystems (the so-called 'Devonian Nekton revolution'). Several authors noticed an evolutionary increase in coiling in embryonic and post-embryonic whorls in the lineage from Orthocerida via Bactritoidea to plesiomorphic and derived Ammonoidea. This evolutionary trend was, however, never quantified. Progressive coiling has been interpreted as adaptation towards improved swimming capabilities, an r-strategy reproduction, and increasing predation pressure by jawed fish. The taxonomy is still poorly resolved due to often fragmentary or poorly preserved material, the low amount of characters (suture line rather simple), oversplitting because of little consideration for ontogenic changes and intraspecific variability, and correlation problems. We focused on the earliest ammonoids (early Emsian), the here called *Anetoceras* faunas, many of which are loosely coiled. Most authors agree that their evolution must have proceeded rapidly, but the quantification has never been attempted, mostly due to the low stratigraphical resolution. Additional problems lie in the correlation between the more pelagic (Bohemian) facies and the more neritic (Rhenish) facies in the Pragian and Emsian stages. In the Rhenish facies, the classical Emsian was defined. Ammonoids mostly occur in Bohemian facies, but occasionally also in Rhenish facies, thus representing a valuable source to correlate neritic facies with more pelagic facies (Klug et al. 2008; De Baets et al. 2009, 2010), improving stratigraphical schemes.

Based on new material from the Moroccan Anti-Atlas, the Uzbek Zeravshan-Gissar Range, and the Rhenish Slate Mountains (Klug et al. 2008; De Baets et al. 2009, 2010; Becker et al. 2010) as well as museum materials (Berlin, Bonn, Kitab, New York, Prague, Moscow), we can now draw several conclusions. Several new taxa could be introduced and other taxa could be synonymized, integrating ontogeny and intraspecific variability. These taxonomic revisions partially extended the paleogeographic distribution of some species and decreased the overall ammonoid diversity. Some of the earliest more loosely coiled ammonoids such as *Anetoceras* and *Erbenoceras*, show a large intraspecific variability, which is in part related with their loose coiling. We report some of the earliest well-dated ammonoids from the Hunsrück Slate, which is considered to be the cradle of early ammonoids by some. The Hunsrück material provided an important window enabling the examina-

tion of the ontogeny of earliest ammonoids. Some of these specimens display the most plesiomorphic character states among ammonoids. In contemporary Moroccan layers, comparable species are only preserved as fragments.

In addition to the knowledge of early ammonoid ontogeny from the Hunsrück, the embryonic and adult conchs of several additional taxa has been described from Morocco and Uzbekistan. Interestingly, several lineages such as the Mimosphinctidae, the Mimoceratidae, the Anarcestidae, and the Agoniatitidae convergently developed a trend towards increased coiling (e.g., decrease in umbilical window size).

We could produce diversity charts with a higher resolution as before. In the early Emsian of Morocco like in many other localities, however, often too little and different ammonoid taxa can be found per section to allow for robust correlation between sections. This related with the fact, that many taxa are quite rare (e.g., *Weyeroceras* = 3 specimens have become known in 11 years time: see De Baets et al. 2010), while other taxa are quite abundant, but have long ranges (*Erbenoceras*). This supports the need to integrate several groups to augment stratigraphical resolution (ammonoids, conodonts, dacryoconarids) as has been partially attempted in the Hunsrück Slate by studying co-occurring dacryoconarids. New materials, new methods, and revisions of older materials have enabled us to study several aspects of the early evolution of ammonoids. This includes cases of parallel evolution, convergence, parasite-host-coevolution (Klug et al. in press) and several details of the links between evolution and development of early ammonoids. Of great interest is also the astonishingly rapid increase of morphologic disparity of ammonoids directly after their origin.

REFERENCES

- Becker, R.T., De Baets, K., & Nikolaeva, S. 2010. New ammonoids records from the lower Emsian of the Kitab Reserve (Uzbekistan) – preliminary results. SDS Newsletter 25, 20-28.
- De Baets, K., Klug, C., & Korn, D. 2009: Anetoceratinae (Ammonoidea, Early Devonian) from the Eifel and Harz Mountains (Germany), with a revision of their genera. Neues Jahrbuch für Geologie und Paläontologie, Abhandlungen, 252, 361-376.
- De Baets, K., Klug, C., & Plusquellec, Y. 2010. Zlíchovian faunas with early ammonoids from Morocco and their use for correlation of the eastern Anti-Atlas and the western Dra Valley. Bulletin of Geosciences, 85 (2), 317-352.
- Klug, C., Kröger, B., Korn, D., Rücklin, M., Schemm-Gregory, M., De Baets, K., & Mapes, R. H. 2008. Ecological Change during the early Emsian (Devonian) in the Tafilalt (Morocco), the Origin of the Ammonoidea, and the First African Pyrgocystid Edrioasteroids, Machaerids and Phyllocarids. Palaeontographica, Abteilung A, 283 (4-6), 83-176.
- Klug, C., De Baets, K., & Korn, D. in press. Devonian pearls and ammonoid-endoparasite coevolution. Acta Palaeontologica Polonica, 20 pp.

4.5

Devonian pearls and ammonoid-endoparasite co-evolution

Klug, Christian¹, De Baets, Kenneth¹ and Korn, Dieter²

¹ Paläontologisches Institut und Museum, Universität Zürich, Karl Schmid-Strasse 4, 8006 Zürich, chklug@pim.uzh.ch

² Museum für Naturkunde, Leibniz Institute at the Humboldt University Berlin, Invalidenstraße 43, D-10 115 Berlin, Germany, dieter.korn@mf-n-berlin.de

Raised shell projections on the inner shell walls that form pits on the internal moulds of Devonian ammonoids have been known for several decades. New specimens from Morocco reveal novel details of these structures; most, if not all, of which consist of a capsule of ammonoid shell that covers tiny tubes attached to the outer (=lateral or ventral) shell wall from the inside. In accordance with comparable Recent occurrences of similar structures in molluscs, we use the term “pearls” for these raised structures and the pits they form on the internal moulds. The nature of these encapsulated tubes is described and discussed. Because of the presence of these tubes inside the pearls, the arrangement and organization of the pearls, and their similarity to modern mollusc occurrences, the tubes are interpreted as traces of parasitoses. The pearls and pits were grouped into five types based on differences in morphology, size, and arrangement. Then, having used these traits to perform a simple cladistic analysis, the resulting cladogram was compared to the phylogeny of ammonoids. Based on this comparison, it appears likely that the parasites underwent a co-evolution with the ammonoids, which lasted 10 to 15 Ma. Patterns of evolutionary events that were detected include co-speciation, “drowning on arrival” (end of parasite lineage near base of a new host clade), and “missing the boat” (parasite lineage does not adapt to a new host clade, thus not evolving a new parasite clade). The condition of “swapping the boat” (parasites of another host clade evolving a new clade long after the emergence of a new host clade) probably did not occur. Because of the lack of fossilised soft tissue, only speculations can be made about the systematic affiliation of the parasites, their life-cycle, infection strategy and ecological framework. Some co-occurring bivalves also have pits reminiscent to structures caused by trematodes in recent forms. However, based on the available information, the tubes are interpreted as artefacts of trematode infestations, which if correct, would extend the fossil record of parasitic trematodes into the early Devonian.

4.6

Parallel evolution controlled by adaptation and covariation in ammonoid cephalopods

Klug, Christian¹, De Baets, Kenneth² & Monnet, Claude³

¹Paläontologisches Institut und Museum, Universität Zürich, Karl Schmid-Strasse 4, 8006 Zürich, chklug@pim.uzh.ch

²Paläontologisches Institut und Museum, Universität Zürich, Karl Schmid-Strasse 4, 8006 Zürich, kenneth.debaets@pim.uzh.ch

³Paläontologisches Institut und Museum, Universität Zürich, Karl Schmid-Strasse 4, 8006 Zürich, claudemonnet@pim.uzh.ch

A major goal in evolutionary biology is to understand what are the processes (and when, how, why, in which proportions, they occur) that shape the path of evolution and thus to explain evolutionary patterns documented in fossil and living organisms. Among evolutionary patterns, parallel evolution in extinct and extant lineages is a very common phenomenon, rarely studied in detail and over a time interval exceeding 1 myr. The repeated and similar large-scale morphological evolutionary trends of distinct lineages suggest that adaptation by means of natural selection (functional constraints) is the major cause of parallel evolution. However, some aspects of parallel evolution can result from other processes which are usually ignored or difficult to identify, such as developmental constraints. Hence, understanding the underlying processes of parallel evolution and ecological evolutionary feedbacks still require further research.

Herein, we present such a case study of two lineages of earliest ammonoids (extinct cephalopods with an external, chambered shell), which evolved in parallel several more or less independent shell characters. This case of parallel evolution concerns two ammonoid lineages (Auguritidae and Pinacitidae), which are of Emsian and Eifelian age (Early and Middle Devonian; ~ 405–395 Ma). Based on recent exceptional discoveries and a revised palaeobiological framework of both lineages (taxonomy, stratigraphy, phylogeny), the ammonoid shell is quantified by eight classical and biologically meaningful phenotypic characters.

This study highlights that both ammonoid lineages under consideration follow in time and through phylogenetic sequence the classical and common evolute to involute evolutionary trend throughout ontogeny (i.e. toward more tightly coiled whorls); they also show an increase of shell diameter (i.e. adult body size); they record an increasing complexity of their suture line (reflecting the complexity of the folded walls separating the gas-filled buoyancy-chambers); and they are characterized by the evolution of an umbilical lid in the most derived taxa (a shell feature unknown in any other ammonoid group). The trend of increasing involution toward shells with closed umbilicus has been widely demonstrated to reflect improving hydrodynamic properties of the shell (velocity, manoeuvrability, energy efficiency and perhaps buoyancy) and thus likely result from similar natural selection pressures. The appearance of the peculiar umbilical lid might have speculatively also added to the improvement of the hydrodynamic properties of the shell as reflected by experiments on shell models. Finally, the trend toward increasingly complex sutures likely results from covariation induced by the trends of increasing adult size and whorl overlap given the morphogenetic properties of the suture.

The morphological evolution of the two Devonian ammonoid lineages presented here follows a common parallel evolutionary path of some important shell characters during several million years through their phylogenetic sequence. Evolutionary transformations of ammonoid shell traits (e.g., increasing involution, umbilical lid) appear mainly driven by adaptation to improve the hydrodynamic properties of the shell as corroborated by earlier experiments on shell models. Most of the other characters evolving in parallel (e.g., sutural complexity) appear to be triggered by covariation of shell characters, which plays a central role in the morphogenesis of mollusc shells. This example provides evidence that parallel evolution can be driven simultaneously by different factors such as covariation (fabricational constraints) and adaptation (natural selection).

4.7

Stratigraphy and Paleogeography of the North- Middle Upper Rhine Graben (N-Middle URG) during the Paleogene.

Lavoyer Thibault & Berger Jean-Pierre

Département de Géosciences, Géologie et Paléontologie, Université de Fribourg, chemin du musée 6, CH-1700 Fribourg

Located between Strasbourg (France) in the south and Landau (Germany) in the north, the North- Middle Upper Rhine Graben (N-Middle URG) can be subdivided from west to east into three parts.

In the western part, the “champ de fracture de Saverne” is largely composed by Mesozoic sediments. The Paleogene is almost absent. It is represented mainly by the Lutetian outcrop of Bouxwiller.

The Pechelbronn oil field presents the traditional stratigraphic succession of the URG is present. In stratigraphic order: the transition zone, in contact with the underlying Jurassic limestone, the dolomitic zone, the red bed, the Lower-, Middle- and Upper Pechelbronn Beds and the “Série Grise”. There are very few outcrops in this area, but many boreholes exist because of the oil industry. Two of them will be presented more in detail: GPK4 Soultz-sous-forêt, covering the whole series, and 01983X2854 Preuschof, which is a complete cored drilling corresponding to the Upper Pechelbronn Beds with a small part of the Middle Pechelbronn Beds at the base. A particular focus will be the discovery of marine elements (especially foraminifers) along the Upper Pechelbronn Beds, in the Preuschof profile. This confirms the different facies defined by Schnaebelé (1948) for this formation.

In the Eastern part, the Central Graben and the foothill of the Black Forest don't show any Paleogene outcrops. The data comes from drillings. The stratigraphic succession is the same than in the previous part, except that the Red Beds are not present, and the whole series is overlied by the Niederroedern Formation. On the German side, some boreholes indicate the presence of “Süsswasserkalke” and “Lymnaemergel”.

A geological map of the studied area will be presented, just as a stratigraphic profile from Bouxwiller to Karlsruhe (Fig 1). According to the recent compilation of Berger (2010), a stratigraphic correlation will be exposed and the previous paleogeographical reconstitutions (Berger et al. 2005 a, Pirkenseer 2007) will be discussed.

This study is financed by the SNF Project 200020-118025 “Paleontology and Stratigraphy of the Rhine graben during the Paleogene”, including the PhD-thesis of T. Lavoyer “Paleontology and Stratigraphy of the Middle Upper Rhine Graben during the Paleogene: a key-study for the relationships between Rift system, Alpine Orogeny and Paleoclimate” (in progress). We thank Marion Kimmel (Geoderis) for giving access to the core Preuschof, Philippe Elsass (BRGM) for access to the Soultz samples and for fruitful discussions.

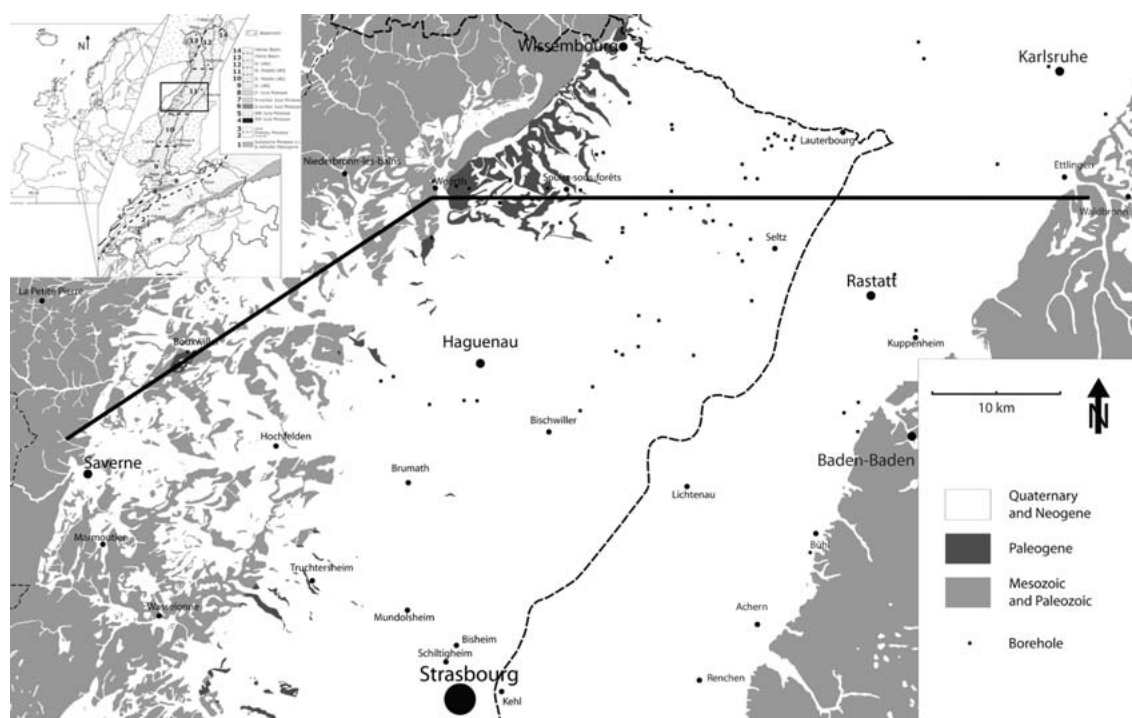


Figure 1. Location of the section and boreholes.

REFERENCES

- Berger, J.-P. 2010, Lithostratigraphic subdivision of the Swiss Molasse: first report. Molasse group meeting 2010.
- Berger, J.-P. et al., 2005a. Paleogeography of the Upper Rhine Graben (URG) and the Swiss Molasse Basin (SMB) from Eocene to Pliocene. *International Journal of Earth Sciences*, 94(4): 697-710.
- Pirkenseer, C. 2007. Foraminifera, Ostracoda and other microfossils of the Southern Upper Rhine Graben. *Palaeoecology, Biostratigraphy, Palaeogeography and Geodynamic implications*. Unpublished thesis, 1-340.
- Schnaebelen R., 1948. Monographie géologique du champ pétrolifère de Pechelbronn. – Mémoires du Service de la Carte géologique d'Alsace et de Lorraine, 7:254 S Strasbourg

4.8

Extraordinary sauropod trackways from the Late Jurassic Béchat Bovais tracksite (Canton Jura, NW Switzerland): implications for sauropod locomotor styles

Daniel Marty¹, Géraldine Paratte¹, Christel Lovis¹, Mathilde Jacquemet¹ & Christian A. Meyer²

¹ Office de la Culture, Section d'archéologie et paléontologie, Paléontologie A16, Hôtel des Halles, P.O. Box 64, 2900 Porrentruy 2, Switzerland (daniel.marty@palaeojura.ch)

² Naturhistorisches Museum, Augustinergasse 2, 4001 Basel, Switzerland

In 2008 and 2009, the Béchat Bovais tracksite, located on the future course of the A16 highway (Canton Jura, NW Switzerland), was excavated over a surface of more than 4000 m². On level 515, 2100 dinosaur tracks were uncovered and 28 sauropod trackways identified and documented by means of classical ichnological techniques, laser scanning, and photogrammetry. Layer 515 is a 5-15 cm thick, calcareous marl and its bedding plane (level 515) is a palaeosurface characterized by the presence of a dense network of reddish *Thalassinoides* burrows and true tracks with a wide range of morphologies indicating that substrate properties were not uniform across the site. Generally, on the underlying, desiccation-cracked level 510, no or only very shallow and faint undertracks are visible, indicating that level 510 was already well indurated at the time of track formation on level 515. Level 510 only broke occasionally under the pressure of the sauropod feet, leading in some places to the formation of deep tracks with steeply inclined track walls.

Pes tracks are oval in shape, longer than wide, only rarely exhibit digit and never claw impressions, and their mean length and width vary from 35.8 to 59.3, and 27.4 to 45.4 cm, respectively. Manus track morphology varies from horseshoe-shaped over semi-circular to sub-circular without any evidence for pollex claw impressions. Manus imprints are always wider than long, and their mean length and width varies from 8.5 to 28, and 20.9 to 34.3 cm, respectively.

Many of the trackways show different patterns and configurations, and marked distinctions also occur along single trackways (e.g. changes: from pes/manus to pes-only, in relative position of pes and manus tracks, in trackway gauge, in track rotation). Two extraordinary long and parallel trackways (S18 with 115 m, S19 with 105 m) show several small turns. The mean ratio between the width of the angulation pattern and the pes length ([WAP/PL]-ratio) characterizes 10 trackways as narrow, 9 as intermediate, and 9 as wide gauge. However, along several trackways (e.g., S18, 19, 21) these values change between narrow and wide over a couple of steps and demonstrate that these two locomotor styles could have been used by one and the same sauropod trackmaker and over short distances (Figure 1). This evidence – together with the fact that the studied trackways equally divide between the three different gauge categories – suggests that trackway gauge is not an unambiguous characteristic to distinguish sauropod ichnotaxa and to identify sauropod trackmakers.

The long, continuous sauropod trackways of Béchat Bovais can be used for detailed studies on the environmental and taphonomical controls of track geometry and morphology, and they may provide important new data on the habitual locomotor characteristics of sauropods such as unsteady locomotion and changes in locomotor behaviour. Locomotor variation within ichnospecies can be addressed statistically, and ontogenetic effects of size on locomotor function can be analyzed.

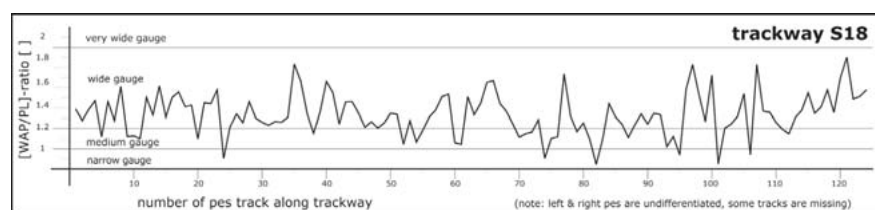


Figure 1. Variation of trackway gauge (as expressed by the [WAP/PL]-ratio) along the 115 m long sauropod trackway S18, Béchat Bovais tracksite, level 515. Even though the mean [WAP/PL]-ratio classifies the trackway as wide gauge, the ratio varies remarkably along the trackway course. Pronounced changes between narrow up to very wide gauge occur over a couple of steps and may also be associated with changes in the relative position of pes and manus tracks.

4.9

Swiss *Amphitragulus* and *Dremotherium* (Mammalia; Ruminantia): State of the art

Mennecart Bastien¹, Becker Damien² & Berger Jean-Pierre¹

¹ Département de Géosciences, Géologie et Paléontologie, Université de Fribourg, Chemin du Musée 6, 1700 Fribourg, Switzerland (bastien.mennecart@unifr.ch)

² Section d'archéologie et paléontologie, République et Canton du Jura, Office de la culture, Hôtel des Halles, Case postale 64, 2900 Porrentruy 2, Switzerland

The ruminants are typical European post- «Grande-Coupure» migrants and are quite common within the Oligo-Miocene deposits of the Swiss Molasse Basin. Nowadays, the appendages and cheek teeth allow easily differentiating the numerous extant ruminant families. However, only hornless animals with sabre teeth occurred until the Early Miocene and the tooth patterns of primitive ruminants exhibit also strong similarities. As result, the Swiss Oligocene and Early Miocene ruminants, as well the European ones, were for a long time mainly identified either as *Dremotherium* or *Amphitragulus*. At least 17 species of *Amphitragulus* had been described until the beginning of the 20th century (*A. aurelianensis*, *A. boulangeri*, *A. communis*, *A. elegans*, *A. gracilis*, *A. fenningrei*, *A. flourentianum*, *A. lemanensis*, *A. major*, *A. medius*, *A. neminoides*, *A. nouletti*, *A. podelskiscusis*, *A. pomeli*, *A. primaevus*, *A. quercyi*, *A. querey*). But, recent discoveries and studies allowed underlining within most of material wrongly assigned to *Dremotherium* or *Amphitragulus* new genus attributions (*Gelocus*, *Hydropotopsis*, *Micromeryx*, *Pomelomeryx*), intraspecific variability and synonymies (today only *A. elegans* and *A. quercyi* are valid).

The higher Pecora only appeared during the latest Oligocene (MP28; ca. 24.5 Ma) with the first representatives of *Dremotherium* and *Amphitragulus*, whereas Tragulina or Gelocidae represented the mid-Oligocene primitive ruminants. This faunal change is probably linked to the Late Oligocene Warming, migrations, and global environmental changes. *Dremotherium* and *Amphitragulus* are recorded from MP28 to MN2 (latest Oligocene to Aquitanian). The reassessment of the Swiss specimens of these two genera permits to better understand their taxonomy and ecology, and to update faunal composition of the Swiss ruminants during the Oligo-Miocene transition.

The University of Fribourg, the Swiss National Fund (project n°126420), and the “Section d’archéologie et paléontologie” (Jura Canton) fund this research.

4.10

New biostratigraphic data from the Voirons Sandstones (Voirons massif, Haute-Savoie, France): implications for the paleogeographic origin of the Gurnigel Nappe

Ospina-Ostios Lina María¹, Ragusa Jérémy¹ & Kindler Pascal¹

¹ Section of Earth and Environmental Sciences, rue des Maraîchers 13, CH-1205 Genève (lina.ospina@unige.ch)

New biostratigraphic data from the Voirons Sandstones (Voirons Massif, Gurnigel Nappe) demonstrate the importance of reworking in this turbiditic succession and suggest that it is younger than previously thought, thus raising questions about its inferred south-penninic origin.

The Voirons massif is situated in the Chablais Prealps (Haute-Savoie, France), at about 20 km to the East of Geneva. It belongs to the Gurnigel Nappe, which essentially consists of deep-water turbidites (i.e. flysch) supposedly derived from an ultrabriançonnais or south-penninic realm. This attribution, however, is controversial. In this area, the Gurnigel Nappe comprises three stratigraphic units of Paleogene age: the Voirons Sandstones, the Vouan Conglomerates and the Saxel Marls. The Voirons Sandstones consist of a monotonous alternation of shales and sandstones, locally including thin intercalations of conglomerates. Based on calcareous nannoplankton and dinoflagellate assemblages, the age of this formation has previously been constrained between the early Paleocene and the early middle Eocene.

We have logged new sections in the most important outcrops of the region and described new exposures. Sampling was performed mainly from the shaly intervals within the sandstone/shale turbidite succession. About 30 shale samples were washed with gasoline. Residues were picked and examined for foraminiferal content with a binocular microscope and a SEM. Small pieces of six out of these 30 samples were sent off for calcareous nannofossil analysis.

The obtained biostratigraphical results are controversial. Nannofossil data confirm previous research and constrain the age of the Voiron Sandstones between the early Paleocene and the early middle Eocene. In contrast, foraminiferal data suggest that, in many exposures, the Voiron Sandstones may be as young as the late Eocene.

These new results emphasize the importance of reworking phenomena in the fine fraction of turbiditic sediments and question the use of nannofossil analyses for dating these deposits. Furthermore, the youngest ages obtained by foraminiferal dating suggest that the sedimentation of the Voiron Sandstones took place in a more external basin than the Piemont Ocean, which became inverted during the middle Eocene.

Acknowledgments: we thank S. Spezzaferri (UNIFR), R. Wernli (UNIGE) and E. de Kaenel (BP Petroleum) for their micropaleontological determinations.

4.11

The evolution of Early Ypresian microfossil assemblages and stable isotopes during a distinct plankton peak in the Corbières (Aude, France) continental margin record

Pirkenseer Claudius¹, Steurbaut Etienne¹ & Speijer Robert¹

¹ University of Leuven, Celestijnenlaan 200E, B-3001 Heverlee (claudiusmarius.pirkenseer@unifr.ch)

The Corbières Foreland Basin represents the southeastern-most extension of the Aquitaine Basin. During the Ypresian a succession of marine carbonates, marine marls, brackish marls to sandstones and subsequent fluvio-lacustrine sediments were deposited in the Corbières (Aude, France) area in several sequences. The present study focuses on the middle and upper part of the neritic „Blue Marls“ close to Pradelles-en-Val. Samples from the overview section contains nannofossils indicating the nannoplankton zone upper NP11 and a fully marine, nearshore depositional environment. The lower half of the section is characterized by a strongly variable (1-85% plankton), plankton/benthos-ratio. A last pronounced peak in plankton occurrence in association with the near disappearance of all larger faunal elements (except pteropods) and a change in the ostracod assemblage was chosen for a more detailed sample campaign.

The detailed section (46 samples in 15cm intervals) pinpoints the correlation between rising P/B-ratio and abundance and composition of the ostracod assemblage. Variations in the assemblages of the planktic and small benthic Foraminifera taxa suggest rapidly changing conditions, probably triggering the speciation event in the ostracod lineage *Echinocythereis isabellana-aragonensis* (Reyment 1985). During the depleted interval ostracoda and foraminifera numbers decrease, *Pseudovigerina wilcoxensis* is nearly absent and buliminids, *Pulsiphonina wilcoxensis* as well as echinoderm spines peak. The depleted interval is slightly preceded by the first occurrence of the planktic taxa *Subbotina hornibrooki* and *Globoturborotalites bassriverensis*, the latter being considered a PETM-excursion taxon (Olsson et al. 2006). The subsequent interval is characterized by rapidly increasing P/B-ratio, a dominance of *Globoturborotalites bassriverensis* and *Pseudohastigerina wilcoxensis* as well as an altered ostracod assemblage composition. Sedimentation of clastic material larger than 63µm increases approximately 100%. Bulk $\delta^{13}\text{C}$ values generally drop from around -1.0‰ to around 1.5‰ and then increase to -0.8‰ after the plankton peak. The influence of either local factors and/or diagenesis obscuring possible global events (H-K hyperthermals, Cramer et al. 2003) remains difficult to quantify due to the lack of data from comparable marginal marine Paleogene sections and the high resolution due to the short represented timespan (upper NP11).

This project is funded by the Swiss National Science Foundation (project-nr. PBFR22-116947) and supported by the K.U.Leuven Research Fund.

REFERENCES

- Cramer, B. S., Wright, J. D., Kent, D. V. & Aubry, M.-P. 2003: Orbital climate forcing of $\delta^{13}\text{C}$ excursions in the late paleocene-early eocene (chrons c24n-c25n). *Paleoceanography*, 18(4), 1097, doi 10.1029/2003pa000909.
- Olsson, R.K., Hemleben, C., Huber, B.T. & Berggren, W.A. 2006: Taxonomy, biostratigraphy, and phylogeny of Eocene *Globigerina*, *Globoturborotalita*, *Subbotina*, and *Turborotalita*. *Cushman Foundation Special Publication*, 41, 11-168.
- Reyment, R. (1985): Phenotypic evolution in a lineage of the Eocene ostracod *Echinocythereis*. *Paleobiology*, 11(2), 174-194.

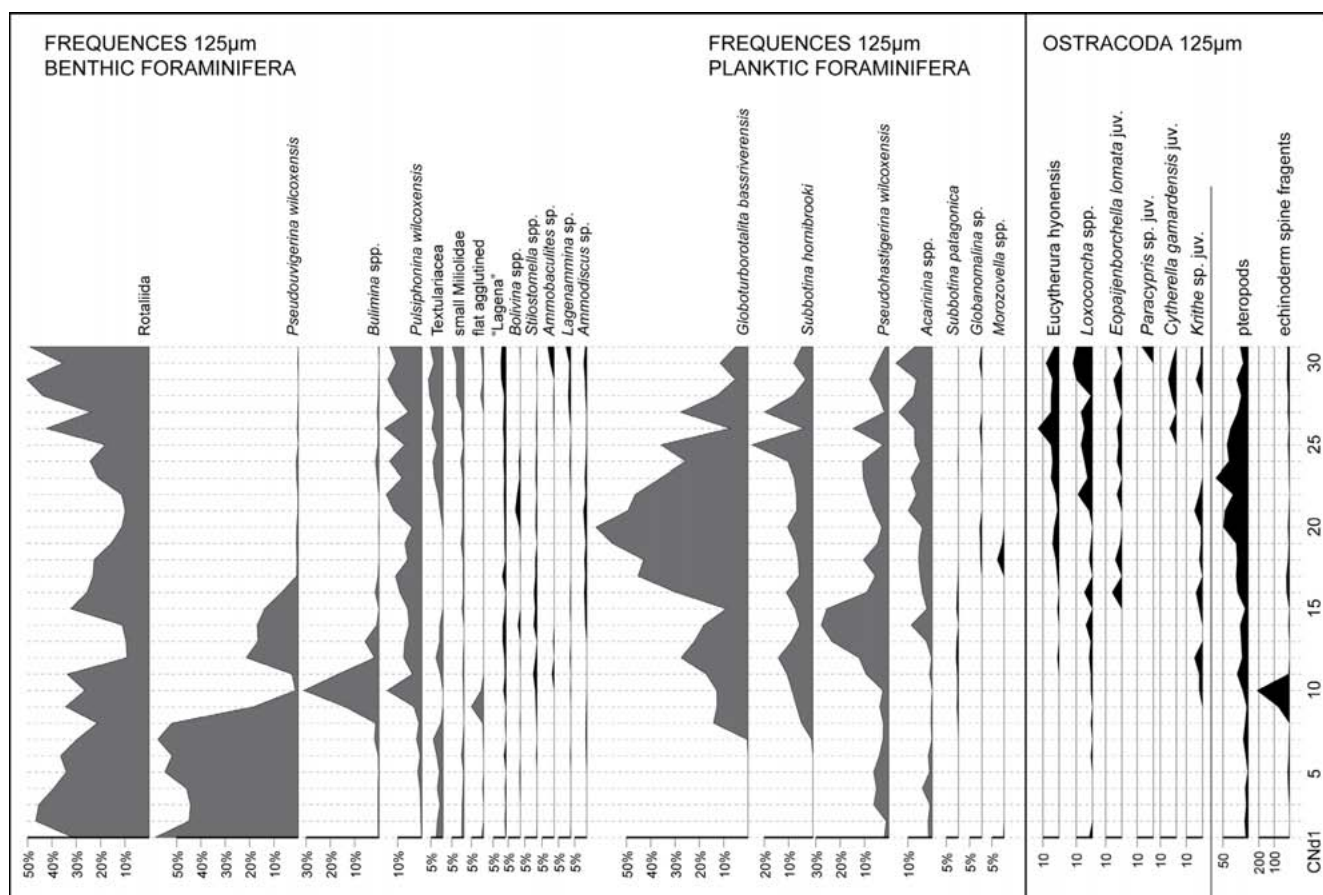


Figure 1. Microfossil frequencies in the high resolution section (sample interval is 15cm)

4.12

A Tooth Tale: the *Anthracotheirus bumbachense* (Artiodactyla, Mammalia) from Beuchille (Delémont, Switzerland).

Scherler Laureline^{1,2}, Becker Damien², Berger Jean-Pierre¹

¹ Institut de Géologie, Département des Géosciences, ch. du Musée 6, CH-1700 Fribourg (laureline.scherler@unifr.ch)

² Section d'archéologie et paléontologie, Hôtel des Halles, CP64, CH-2900 Porrentruy

The genus *Anthracotheirus* (Artiodactyla, Mammalia) originated in Asia in the middle Eocene and migrated to Europe in the Early Oligocene. Its worldwide extinction is reported to the end of the Oligocene (Lihoreau and Ducrocq, 2007). Early descriptions (e.g., Kowalevsky, 1873; Stehlin, 1910) determined fossils of this genus in Europe, widely occurring in France, Germany, and Switzerland. No less than ten species were described throughout the Oligocene, and these species were generally only differentiated by biometrical comparisons.

The species *A. bumbachense* was established by Stehlin (1910) from the locality of Bumbach in Switzerland, which is the reference locality of the Mammal Biozone MP25 (early Late Oligocene, ca. 28 Ma). Stehlin (1910) based his observations on scarce postcranial remains such as a cuboid, a phalange, and two metapods. In his monography on the genus *Anthracotheirus*, Kowalevsky (1873) had observed a morphological difference between the large specimens of the Late Oligocene (e.g., *A. magnum*, *A. valdense*) that had four digits of similar size, and the specimens of the Early Oligocene that showed a reduction of the lateral digits. *A. bumbachense* belonged to this latter group, called "Anisodactyls".

For ten years the section of paleontology of Porrentruy (Jura, NW Switzerland) excavates fossils along the Transjurane highway. In 2001, the locality of Beuchille, located in the Delémont Basin, displayed numerous remains of vertebrates such as reptiles and terrestrial mammals. Dental and postcranial remains of anthracotheriids were found and preliminarily determined as *Anthracotheirus* sp. The upper molar of *Anthracotheirus* discovered here was particularly difficult to deter-

mine at the specific level due to the fact that anthracotheres displayed highly monotonous morphological characters. This isolated tooth was not the only anthracotheriid remain found in this locality. It was also completed by a single metapod that allowed Becker et al. (2004) to assign this specimen to *Anthracotherium* cf. *bumbachense* thanks to its shape.

In 2007, an SNF-project (126420) began at the University of Fribourg on the large terrestrial mammals of the Swiss Molasse Basin from the Early Oligocene to the Early Miocene, employing two PhD students and two Master students. A review of the locality of Bumbach (old collection and new field work) was made by N'Guyen in 2008, but no molars of *A. bumbachense* were discovered. Later, a review of the material deposited in the University Claude Bernard in Lyon (France) showed two complete skulls and their mandibles from the locality of Bénisson-Dieu (France) assigned to *A. bumbachense* by Roman and Boucher (1936). It enabled a detailed description of the teeth, and especially of the upper molars. Thanks to a new method established by Boisserie et al. (2010) to describe the dental remains of bunodont artiodactyls (e.g., hippopotamuses), the European species of *Anthracotherium* could finally be systematically differentiated by the morphology of their cuspids. The molar from Beuchille could be compared to the material from Bénissons-Dieu and it could be assigned without any doubt to the species *A. bumbachense* (Fig. 1). Furthermore, a new biostratigraphic and paleogeographic frame could be proposed.

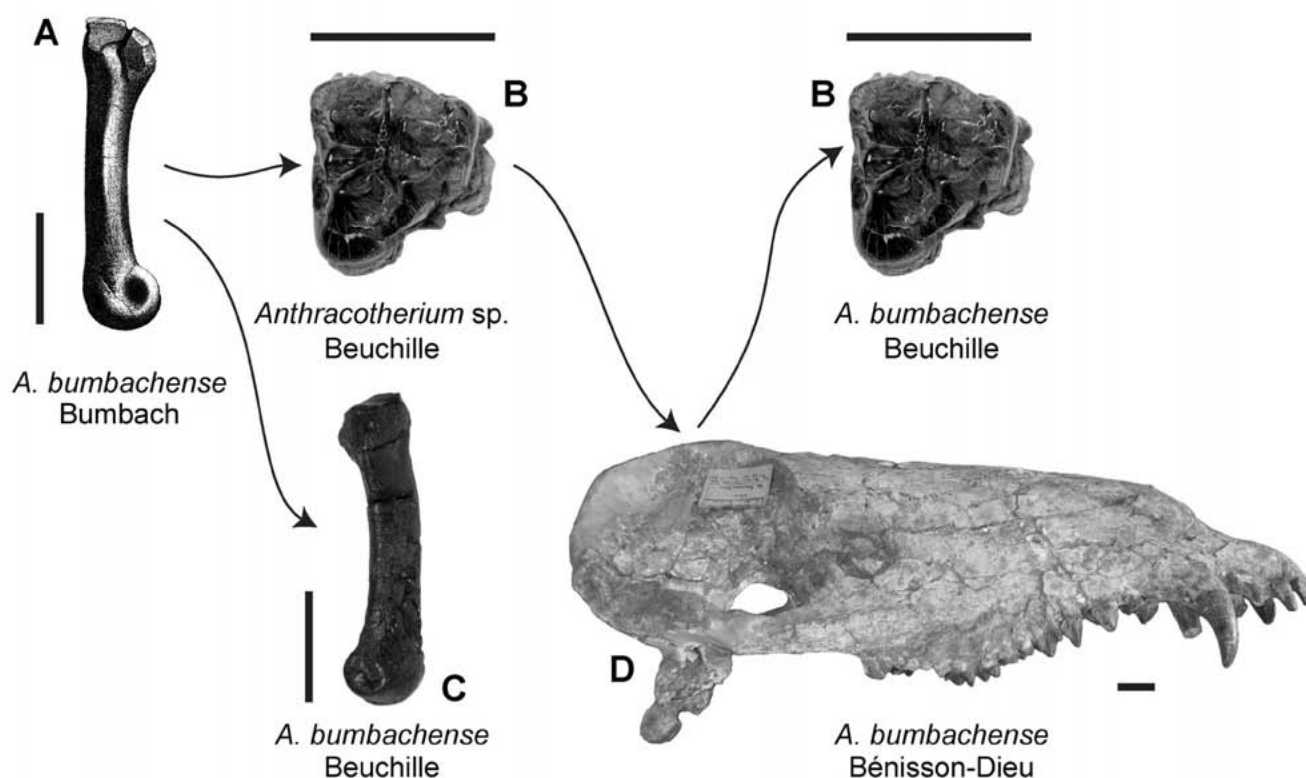


Figure 1. Synthesis of the determination of *A. bumbachense* from Beuchille. A: McII from Bumbach (drawing from Kowalevsky, 1873); B: M3 from Beuchille; C: McII from Beuchille; D: skull from Bénissons-Dieu. Scale bars equal 5 cm.

REFERENCES

- Becker, D., Lapaire, F., Picot, L., Engesser, B., & Berger, J.-P. 2004: Biostratigraphie et paléocologie du gisement à vertébrés de La Beuchille (Oligocène, Jura, Suisse). *Revue de Paléobiologie*, 9, 179-191.
- Boisserie, J.-R., Lihoreau, F., Orliac, M., Fisher, R. E., Weston, E. M., & Ducrocq, S. 2010: Morphology and phylogenetic relationships of the earliest known hippopotamids (Cetartiodactyla, Hippopotamidae, Kenyapotaminae). *Zoological Journal of the Linnean Society*, 158, 325-366.
- Kowalevsky, W. 1873: Monographie der Gattung *Anthracotherium* Cuv. und Versuch einer natürlichen Classification der fossilen Hufthiere. *Palaeontographica*, 3, 347 pp.
- Lihoreau, F. & Ducrocq, S. 2007: Family Anthracotheriidae. In: Prothero, D. R. & Foss, S. E. (Eds.): *The Evolution of Artiodactyls*. The John Hopkins University Press, Baltimore, 89-105.
- N'Guyen, T.B. 2008: Die *Anthracotherium* des Oligozäns der Schweizer Molasse: Stratigraphie, Paläoökologie und Paläoklima. Unpublished Diploma Thesis, University of Fribourg, 138 pp.
- Roman, F., & Boucher, J. 1936: Les mammifères stampiens du Bassin de Roanne (Loire): I. *Anthracotherium bumbachense*. *Travaux des Laboratoires de Géologie de la Faculté des Sciences de Lyon*, 29, 48 pp.
- Stehlin, H.G. 1910: Zur Revision der europäischen Anthracotherien. *Verhandlungen der naturforschenden Gesellschaft*, Basel, 21, 165-185.

4.13

Dienerian (Early Triassic) ammonoid successions of the Tethys: preliminary results from Pakistan and IndiaWare David¹, Bucher Hugo¹, Brühwiler Thomas¹ & Goudemand Nicolas¹¹ Paläontologisches Institut und Museum der Universität Zürich, Karl Schmid-Strasse 4, CH-8006 Zürich, Switzerland
(e-mail: david.ware@pim.uzh.ch)

In the aftermath of the Permian/Triassic mass extinction, ammonoids are one of the two fastest animal marine clades to recover (Brayard et al. 2009). It is generally assumed that diversity remained low during the Griesbachian, increased slowly during the Dienerian, and then reached a first peak in middle Smithian times. However, Dienerian faunas are only poorly known, and most recent works deal with boreal faunas whose record is strongly affected by the paucity of carbonate rocks. Recent fieldwork conducted in the Lower Triassic of the Northern Indian Margin (Salt Range, Pakistan and Spiti Valley, NW Himalaya) allow us to reassess the hypothesis of a slowly increasing diversity during the Dienerian: late Griesbachian and Dienerian ammonoid taxonomy is being completely revised and a preliminary, high resolution biochronological scheme has been constructed.

This paper focuses on the Nammal section (Salt Range), which possesses the best stratigraphic record so far (17 ammonoid-bearing beds within this 12 m interval of the section; the duration of the Griesbachian, Dienerian and lowermost Smithian together being of ca. 1.4 My, Galfetti et al. 2007). This time interval can be divided here into 5 major ammonoid zones: the first one is late Griesbachian, characterised by ophiceratids, and the other five zones are Dienerian, characterised by a succession of five phylogenetically related gyronitid genera: *Gyronites*, *Ambites*, gen. nov. C, and *Prionolobus* (in stratigraphical order). Preliminary results from other sections in the Salt Range and Spiti show that these five Dienerian zones can be recognised easily in every of these.

Diversity in the latest Griesbachian and Dienerian stays rather low and constant, with 5 to 7 species per zone, but this time interval is characterised by very high turnover rates. The supposed low increase of diversity during the Dienerian is therefore not obvious, and may just be a consequence of the previous lower time resolution combined with high turnover rates. In the earliest Smithian zones, diversity remains low (6 to 8 species), and starts increasing only at the end of the lower Smithian (Brühwiler et al., accepted).

We also note a drop of the morphological disparity among Dienerian ammonoids. The most striking fact is the loss of ornamentation: ribbed forms are still known in the *Gyronites* zone, but they completely disappear in the *Ambites* zone, and reappear only in the earliest Smithian faunas. Cadiconic forms are also absent during this time interval.

REFERENCES

- Brayard, A., Escarguel G., Bucher H., Monnet C., Brühwiler T., Goudemand N., Galfetti T., & Guex J. 2009: Good Genes and Good Luck: Ammonoid Diversity and the End-Permian Mass Extinction. *Science* 325:1118-1121.
- Brühwiler, T., Bucher, H., Brayard, A., & Goudemand, N. (accepted): High-resolution biochronology and diversity dynamics of the Early Triassic ammonoid recovery: the Smithian faunas of the Northern Indian Margin. *Palaeogeography, Palaeoclimatology, Palaeoecology*.
- Galfetti, T., Bucher H., Ovtcharova M., Schaltegger U., Brayard A., Brühwiler T., Goudemand N., Weissert H., Hochuli P. A., Cordey F., & Guodun K. 2007: Timing of the Early Triassic carbon cycle perturbations inferred from new U–Pb ages and ammonoid biochronozones. *Earth and Planetary Science Letters* 258:593-604.

5. Lithostratigraphic units for the swiss geological maps: state of the art

Jean-Pierre Berger

Swiss Committee for Stratigraphy

- 5.1 Berger J.-P., Kaelin D. & Kempf O.: Swiss Molasse Lithostratigraphy
- 5.2 Burkhalter R., Möri A.: Harmonising geological map legends – a challenge for the Swiss stratigraphic community
- 5.3 Ragusa J., Ospina-Ostios L. M. & Kindler P.: Petrography and granulometry of the Gurnigel Flysch from the Voirons and Vouan massifs (Chablais Prealps, Haute-Savoie, France): preliminary results
- 5.4 Strasser A., Weissert H.: New developments in stratigraphic nomenclature

5.1

Swiss Molasse Lithostratigraphy

Berger Jean-Pierre¹, Kälin Daniel² & Kempf Oliver²

¹ Dept. Geosciences-Earth Sciences, chemin du Musée 6, 1700 Fribourg (jean-pierre.beerger@unifr.ch)

² Swiss Geological Survey, Federal Office of Topography swisstopo, Seftigenstrasse 264, CH-3084 Wabern

In the frame of the Swiss Committee of Stratigraphy, a subgroup coordinated by J.-P. Berger is currently working on a general synthesis of the lithostratigraphy of Swiss Molasse deposits. We here present a first concept to regroup more than 900 lithostratigraphic units known in the literature. The general model will subdivide each of the four classical Molasse groups (UMM = Lower marine Molasse, USM = Lower freshwater Molasse, OMM = Upper marine Molasse, OSM = Upper freshwater Molasse) into subgroups characterized by a particular regional situation and/or a succession of facies:

- UMM I: Deep marine (turbiditic) facies actually trapped in the subalpine Molasse and the helvetic nappes. All formations (e.g. "Formation du Val d'Illeiez") are stratigraphically older than the formations of UMM II and III.
- UMM II-III: Shallow marine facies of Oligocene age actually trapped in the subalpine Molasse (UMM II, e.g. Vaulruz-Formation, Grisigen-Mergel, Horw-Sandstein) or in the Jura (UMM III, e.g. "Septarientone", "Fischschiefer").
- USM I: Oligocene units of the subalpine (alluvial fan conglomerates, "Molasse Rouge", "coal Molasse") and Plateau Molasse ("Untere Bunte Mergel", Gypsum marls) or the Jura Molasse ("Delsberger Kalke").
- USM II: Aquitanian deposits within the subalpine (e.g. conglomerates) and Plateau Molasse (e.g. "Molasse grise de Lausanne") or rarely in the Jura Molasse ("Calcaires de La Chaux", "Gres de Tavannes").
- USM III: early Burdigalian deposits within the subalpine Molasse (Sommersberg conglomerates) and limnic equivalents of the OMM (restricted to alluvial fans)
- OMM I: includes the classical "Sense-Formation" and "Luzern-Formation".
- OMM II: represented by marly, sandy and conglomeratic units of the "Belpberg-Formation" and the "St. Gallen-Formation".
- OMM III: covers the youngest part of the OMM deposited only in the Jura Molasse and is represented by the "Marnes rouges & Gompholithes".
- OSM: The subdivision of the OSM is still under debate, but a possible way will be to regionally subdivide an early OSM I (with OSM I-H in the Hörnli region below the "Hüllistein marker bed", OSM I-N in the Napf region until the top of the "Mergelzone", and OSM I-J in the Jura Molasse below the lacustrine Limestones) and a late OSM II (OSM II-H, -N, and -J above the mentioned horizons). Note that "Juranagelfluh" belongs to OSM I-II-J, and that OSM I-J is time-equivalent to OMM III.

This concept permits a clear and simple lithostratigraphic scheme on the Swiss scale. These subgroups comprise the well-known Molasse formations, which form the basal lithostratigraphic units that can be mapped at a 1:25'000 scale.

We thank the Swiss National Foundation, projects 118025 and 126420, for financial support.

5.2

Harmonising geological map legends – a challenge for the Swiss stratigraphic community

Burkhalter Reto^{1, 2} & Möri Andreas¹

¹Swiss Geological Survey (SGS), swisstopo, Seftigenstrasse 264, CH-3084 Wabern

²President, Swiss Committee of Stratigraphy, c/o SGS (reto.burkhalter@swisstopo.ch)

The demand for digital geological maps in vector format has been steeply rising during the past years. In order to fulfil this need, the Federal Office of Topography swisstopo has initiated the project *GeoCover*, with the aim of providing geological vector data sets for the entire surface of Switzerland by 2012 (one data set per map sheet 1:25'000).

The *Datenmodell Geologie* (data model geology), which is expected to be ready by the end of 2010, provides a model that allows geological vector data sets to be uniformly attributed.

The maps of the Geological Atlas of Switzerland 1:25'000 (GA25), as well as additional Geological Special Maps used for *GeoCover*, reflect the growth of geological knowledge and the development of mapping practices over the past one hundred years. As a consequence, the naming and stratigraphic allocation of the formations in Swiss geological map legends became rather heterogeneous.

The attribution of all elements in the data set requires a standardised general geological map legend, which is based on a harmonised lithostratigraphic nomenclature and a consistent chronostratigraphic allocation of the lithostratigraphic units.

In the summer of 2010 swisstopo has launched a pilot project with the objective of testing the compilation of a harmonised legend of the Mesozoic of the Swiss Jura Mountains. This pilot project is a cooperation between the Swiss Geological Survey and the study group Jura of the Swiss Committee of Stratigraphy. Besides, the Committee has initiated the development of the internet-based Stratigraphic Lexicon of Switzerland (www.stratigraphie.ch) a few years ago (Burkhalter & Heckendorn 2009).

With respect to stratigraphy, the principal goals of the harmonisation of geological map legends are (a) to define an uniform nomenclature (Remane et al. 2005) for all lithostratigraphic units (mapping units) used in the legends of the GA25, (b) to correlate the legends of the GA25 from west to east and (c) to provide the harmonised lithostratigraphic units of Switzerland (definition, description, chronostratigraphic allocation) in the Stratigraphic Lexicon of Switzerland.

REFERENCES

- Burkhalter, R. & Heckendorn, W. 2009: Das Stratigraphische Komitee der Schweiz (SKS). *Swiss Bulletin for applied Geology* 14/1+2, 159–162.
- Remane, J., Adatte, T., Berger, J.-P., Burkhalter, R., Dall'Agnolo, S., Decrouez, D., Fischer, H., Funk, H., Furrer, H., Graf, H.R., Gouffon, Y., Heckendorn, W. & Winkler, W. 2005: Guidelines for stratigraphic nomenclature (Swiss Committee of Stratigraphy). *Eclogae geologicae Helvetiae* 98/3, 385–405.

5.3

Petrography and granulometry of the Gurnigel Flysch from the Voirons and Vouan massifs (Chablais Prealps, Haute-Savoie, France): preliminary results.

Ragusa Jérémy¹, Ospina-Ostios Lina María¹ & Kindler Pascal¹

¹ Université de Genève, Section des sciences de la Terre et de l'environnement, 13 rue des Maraîchers, 1211 Genève 4
(jeremy.ragusa@unige.ch)

Preliminary compositional and granulometric analyses of turbiditic sandstones from the Gurnigel Flysch (Voirons and Vouan massifs, Haute-Savoie, France) show that these deposits mostly consist of poorly sorted subarkoses, but reveal distinctive granulometric trends within this succession. Moreover, the recognition of various facies, including globigerinid-rich limestones, suggests that future detailed petrographic and sedimentological work will contribute to refine the lithostratigraphy of this flysch.

The Voirons and Vouan massifs are located in the external part of the Chablais Prealps and belong to the Gurnigel nappe, the origin of which is controversial. They comprise three lithostratigraphic units including from bottom to top: (1) the Voirons Sandstones (VS), consisting of a thick alternation of shales and sandstones, locally interspersed with conglomerate beds; (2) the Vouan Conglomerates (VCg), forming metric beds of matrix-supported conglomerates; and (3) the Saxel Marls (SM), which is a very fine-grained, mostly shaly succession, locally comprising thin sandstone beds. These three units are interpreted as deep-water turbidite deposits. Their age has been constrained between the early and the late Eocene by planktonic foraminifer assemblages. However, these siliciclastic units have never been the object of quantitative petrographic and sedimentological analyses. Up to now, no precise criteria can be used to unambiguously identify each of these formations in complex exposures.

In this study, we have so far collected and examined more than 180 sand-sized samples, mainly from the VS and SM, from both known exposures (Charollais et al., 1998) and new outcrops. For each thin section, granulometric and compositional (point counting) analyses were performed with a petrological microscope leading to the recognition of several facies types.

Preliminary point-counting analyses indicate that most sandstones from all three units can be classified as subarkoses. Preliminary granulometric analyses show that sandstones collected from the SM are well sorted and fine- to medium-grained, whereas those from VS are poorly sorted and range from silt- to very coarse sand-size (Fig. 1). Furthermore, granulometric trends in the VS correspond with the stratonomy of this unit, but are not visible in the stratonomy of the SM. Finally, ten distinctive facies have been identified including a wide range of composition from mature glauconitic sandstones to globigerinid-rich arenaceous limestones.

REFERENCES

Charollais, J.; Plancherel, R.; Monjuvent, G. & Debelmas, J. 1998. Carte géologique de la France (1/50000e) -- Feuille d'Annemasse. BRGM - Masson

Voirons sandstone

Saxel marls

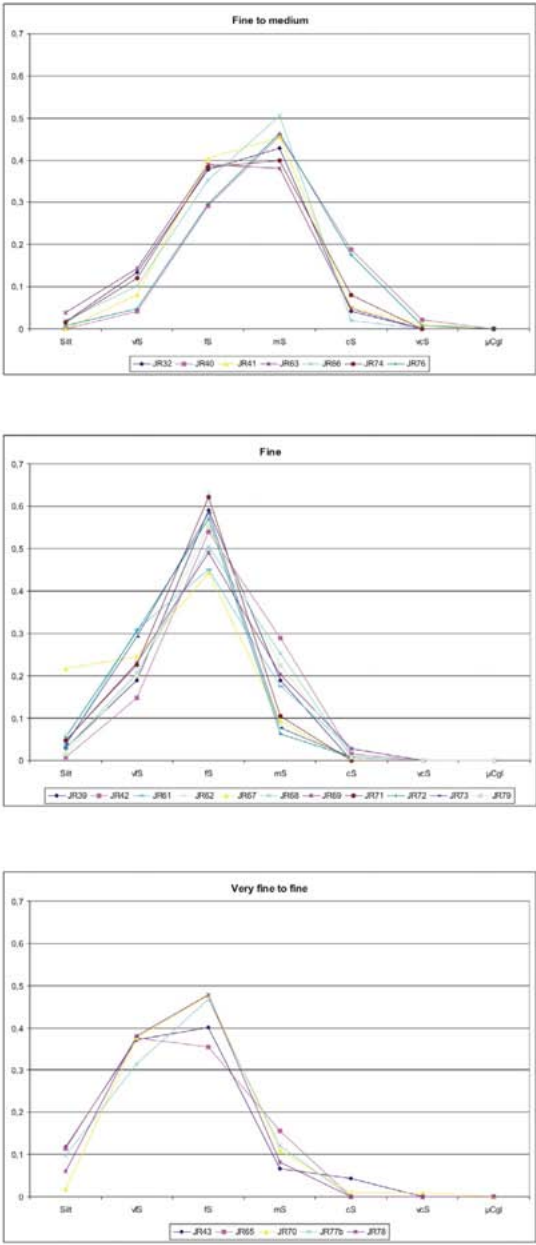
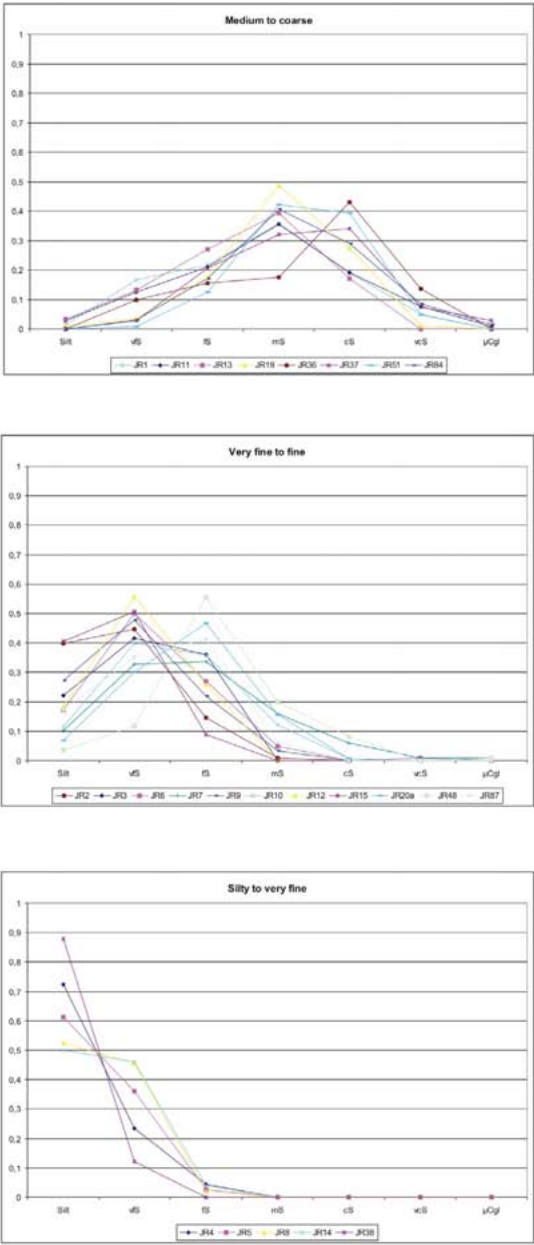


Figure 1. Granulometric distribution of sandstone from Voirons Sandstones and Saxel Marls.

5.4

New developments in stratigraphic nomenclature

Strasser André¹ & Weissert Helmut²

¹ Département de Géosciences, Ch. du Musée 6, CH-1700 Fribourg (andreas.strasser@unifr.ch)

² Geologisches Institut, ETH Zentrum, CH-8092 Zürich (helmut.weissert@erdw.ethz.ch)

Stratigraphy not only describes strata (as its name implies) but also analyses the relationship between rock units and geologic time. Thus, it furnishes the indispensable base for the interpretation of the tectonic, climatic, oceanographic, geochemical, biotic, and sedimentary processes that shaped the face of the Earth throughout its history.

In an effort to present the state of the art in stratigraphic classification, the International Subcommittee on Stratigraphic Classification (ISSC) of the International Commission on Stratigraphy (ICS), a member of the International Union of Geological Sciences (IUGS), publishes a series of articles on the various stratigraphic disciplines. So far, cyclostratigraphy (Strasser et al. 2006), chemostratigraphy (Weissert et al. 2008), and magnetostratigraphy (Langreis et al. 2010) have been treated. Papers on biostratigraphy, lithostratigraphy, sequence stratigraphy, and chronostratigraphy are in preparation. This series is not meant to be a revision but rather a complement to the International Stratigraphic Guide (Hedberg 1976, Salvador 1994) by presenting the newest concepts and by giving real-world examples from the Palaeozoic, the Mesozoic, and the Cenozoic.

An issue being currently hotly debated in the international stratigraphic community is the question if the nomenclature of stratigraphic units should be simplified as proposed by Zalasiewicz et al. (2004), i.e. no more distinction should be made between chronostratigraphy (time-rock units) and geochronology (units of geologic time). Related to this issue is the distinction between durations of stratigraphic units (expressed in yr, kyr, or Myr) and dates on the time axis (expressed in a, ka, and Ma)(e.g., Aubry 2009).

Although nomenclature should never overrule the scientific reasoning and become a research goal in itself, it is important that clear and commonly accepted definitions be available to improve the communication between scientists. A good example is the international effort to integrate the various stratigraphic methods for the establishment of the GSSPs that define stage boundaries.

REFERENCES

- Aubry, M.-P. 2009: Thinking of deep time. *Stratigraphy* 6, 93-99.
- Hedberg, H.D. (ed.) 1976: *International Stratigraphic Guide – a guide to stratigraphic classification, terminology, and procedure*. Wiley, New York, 200 pp.
- Langreis, C.G., Krijgsman, W., Muttoni, G. & Menning, M. 2010: Magnetostratigraphy – concepts, definitions, and applications. *Newsl. Stratigraphy* 43, 207-234.
- Salvador, A. (ed.) 1994: *International Stratigraphic Guide – a guide to stratigraphic classification, terminology, and procedure* (2nd ed.). Int. Union Geol. Sci. and Geol. Soc. Amer., 214 pp.
- Strasser, A., Hilgen, F.J. & Heckel, P.H. 2006: Cyclostratigraphy – concepts, definitions, and applications. *Newsl. Stratigraphy* 42, 75-114.
- Weissert, H., Joachimski, M. & Sarnthein, M. 2008: Chemostratigraphy. *Newsl. Stratigraphy* 42, 145-179.
- Zalasiewicz, J., Smith, A., Brenchley, P., Evans, J., Knox, R., Riley, N., Gale, A., Gregory, F.J., Rushton, A., Gibbard, P., Hesselbo, S., Marshall, J., Oates, M., Rawson, P. & Trewin, N. 2004: Simplifying the stratigraphy of time. *Geology* 32, 1-4.

6. Natural Hazards and Risks in Alpine Geology

Marco Schwab, Jon Mosar, Michel Jaboyedoff, Manfred Thüring

SeCA (canton Fribourg), ECAB (Canton Fribourg)

- 6.1 Bejaoui J., Samaali M., Baccouche S., Reguigui N., Ben Hamouda M.F., Azzouz Z., Trabelsi A., Bouhlel S. & Boulamia S.: Hazard of naturally occurring radioactive material from Tunisian and Algerian Phosphorite
- 6.2 Broennimann C., Michoud C., Nicolet P., Jongmans D., Baron L., Jaboyedoff M. & Tacher L.: The active Pont Bourquin landslide (Les Diablerets, VD): a combined geophysical, hydrogeological and ground-based remote sensing survey
- 6.3 Dammeier F., Moore J., Haslinger F., Loew S.: Seismic signal analysis of rockslide events in the Swiss Alps
- 6.4 Deubelbeiss Y., Graf C., McArdeall B., Bartelt P.: Numerical modeling of debris flows – Case study at Dorfbach, Randa (VS)
- 6.5 Faillettaz J., Sornette D., Funk M.: Climate warming and stability of hanging glaciers: lessons from the 1895 Altels break-off
- 6.6 Gischig V., Moore J. R., Evans K. F., Loew S.: Thermal effects on seasonal variability of deformation rate at the Randa rock slope instability, Valais
- 6.7 Glur L., Anselmetti F.L., Gilli A., Kägi R.: Detailed characterisation of thinnest lake sediment deposits using scanning electron microscopy.
- 6.8 Humair F., Pedrazzini A., Jaboyedoff M., Epard J.L., Froese C.: Movements characterization along open back crack affecting Turtle Mountain, Alberta, Canada
- 6.9 Kos A., Schaer P., Signer A., Strozzi T., Valenti G., Loew S.: A remote sensing application for hazard analysis at Alp di Roscioro, Canton Tessin.
- 6.10 Moore J.R., Burjanek J., Gischig V., Löw S., Fäh D.: Investigating the seismic response of a large rock slope instability (Randa, VS)
- 6.11 Nicolet P., Jaboyedoff M., Gerber C., Giorgis D.: Representation problems of danger and “risks” maps
- 6.12 Rudaz B., Jaboyedoff M.: Historical activity of the Saint-Barthélémy stream (VS) – old data, new look
- 6.13 Wirth S.B., Glur L., Gilli A., Anselmetti F.S.: Reconstruction of the Holocene flood history for assessing the future flood hazard in the Central Alps (FloodAlp project)

6.1

Hazard of naturally occurring radioactive material from Tunisian and Algerian Phosphorite

J. Bejaoui^{1,3}, M. Samaali⁴, S. Baccouche⁴, N. Reguigui⁴, M. F. Ben Hamouda¹, Z. Azzouz⁴, A. Trabelsi⁴, S. Bouhlef³ & S. Boulamia²

¹ Unité d'hydrologie isotopique, Centre National des Sciences et Technologies Nucléaire, Pôle Technologique - 2020 Sidi Thabet, Tunisie. (bjaoui_geo@yahoo.fr)

² Département de géologie et d'Aménagement, Faculté des sciences et sciences de la nature et de la vie, Université de Tébessa, Algérie.

³ U.R. de Minéralogie et Géochimie Appliquées, Département de Géologie, Faculté des Sciences de Tunis, Université de Tunis El Manar, 2092 Tunis, Tunisie

⁴ Unité de Recherches Maitrise et Développement des Techniques Nucléaires à caractères pacifique, Pôle Technologique - 2020 Sidi Thabet, Tunisie

In this study we investigate the radiological hazard of naturally occurring radioactive material in Tunisian and Algerian phosphorite province (Fig.1). In this province the phosphorites deposits are stratiform deposits and of sedimentary origin. The phosphorite beds occur in the Late Paleocene and Lower Eocene (Ypresian-Lutetian) in age (Sassi, 1984 et Zaïer, 1999). Twenty samples of phosphorite rocks were collected from the phosphorite mines. Activity concentrations in all the samples were measured by alpha spectrometry and gamma spectrometry.

Alpha spectrometry analyses (Fig.2) show that the specific activity values of ^{238}U , ^{234}U and ^{235}U in the samples of Tunisian phosphorite were 327 ± 7 (321–327), 326.81 ± 6 (325.7–331.39) and 14.5 ± 0.72 (13.9–15) Bq. kg⁻¹, respectively.

Specific activity concentrations measured by gamma spectrometry in the samples of the Tunisian and Algerian phosphorite show a little difference. Specific activity concentration levels of ^{40}K , ^{226}Ra , ^{232}Th , ^{235}U and ^{238}U in the phosphorite samples from Tunisia were respectively 71.10 ± 3.8 , 391.54 ± 9.39 , 60.38 ± 3.74 , 12.72 ± 0.54 and 527.42 ± 49.57 Bq kg⁻¹ and Algeria were 15.72 ± 1.73 , 989.65 ± 12.52 , 12.08 ± 1.2 , 47.5 ± 1.52 and $1148.787.3$ Bq kg⁻¹, respectively.

The measured value of specific activity of ^{232}Th and ^{40}K in the Tunisian phosphorite samples is relatively higher than that in the samples of Algerian phosphorite. The measured concentration of uranium in the Tunisian phosphorite (527 ± 49) Bq kg⁻¹ is lesser than in Algerian phosphorite. The measured concentration of uranium 238 in the Tunisian phosphorite samples was ($527-1315 \pm 65$) Bq. kg⁻¹ which is higher than its maximum background value of 110 Bq kg⁻¹ in soils of the various countries of the world (M. Tufail et al., 2006). Different geological origins of phosphorites deposits are the main reason for the large spread in worldwide specific activities. Present study reveals that phosphorite deposits contain natural radioactivity considerably higher than background level.

REFERENCES

- Beji Sassi, 1984. Pétrographie, Minéralogie et Géochimie des sédiments phosphatés de la bordure de l'île de Kasserine (Tunisie). In: Thèse 3ème cycle, Université d'Orléans (1984), p. 230.
- M. Tufail, Nasim-Akhtar, M. Waqas 2006. Measurement of terrestrial radiation for assessment of gamma dose from cultivated and barren saline soils of Faisalabad in Pakistan, Radiat. Meas. (41) 443-451.
- Zaïer A 1999. Evolution tectono-sédimentaire du bassin phosphate du centre-Ouest de la Tunisie minéralogie, pétrographie, géochimie et genèse des phosphorites. Thèse Doct. Es-Sci. Univ. Tunis II.



Fig.1. Location of phosphorite sampling sites in the area under study in Tunisia and Algeria.

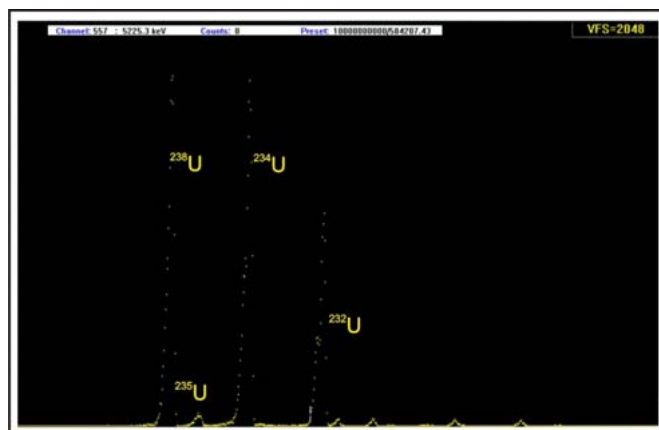


Fig.2 Spectrum of Uranium peaks.

6.2

The active Pont Bourquin landslide (Les Diablerets, VD): a combined geophysical, hydrogeological and ground-based remote sensing survey

Broennimann Cornelia¹, Michoud Clément², Nicolet Pierrick², Jongmans Denis³, Baron Ludovic⁴, Jaboyedoff Michel² & Tacher Laurent¹

¹Laboratory of Engineering and Environmental Geology, EPFL, Station 18, CH-1015 Lausanne (cornelia.broennimann@epfl.ch)

²Institute of Geomatics and Risk Analyses, UNIL, Amphipole, CH-1015 Lausanne

³Laboratoire de géophysique interne et Tectonophysique, UJF, Maison des Géosciences Campus Universitaire 1381, F-38400 Saint Martin d'Hères

⁴Institute of Geophysics, UNIL, Amphipole, CH-1015 Lausanne

First important movements of the Pont Bourquin landslide were observed in 2004. Three years later, heavy rainfall triggered an earth and debris flow with a volume of about 11'000 m³ which was cutting the cantonal road between the villages Les Diablerets and Gstaad. Recently, successive events of debris slides-earth flows and mud flows with small volumes were triggered and reached again the edge of the road.

The 250 m long Pont Bourquin landslide is located in the Western Prealps of Switzerland in a tectonically complex zone and affects mainly black shale, cornieule rocks, flysch and moraine material. Since 2008, a combined ground-based remote sensing, geophysical and hydrogeological survey of the landslide is carried out with the aim to (1) quantify its movements, (2) define the origin of the groundwater in the sliding mass and (3) create an overall conceptual model of the landslide.

Regularly, TLS (Terrestrial Laser Scanning), Differential GNSS (Digital Global Navigation Satellite System) as well as Total Station measurements are performed. Several Seismic Refraction and ERT (Electric Resistivity Tomography) profiles were made along and across the landslide. Periodically, groundwater from boreholes and springs is sampled and chemically analyzed and groundwater tables are monitored in several piezometers between 2 and 5 m depth.

The main slip surface of the landslide is localized at about 10 m depth. Important movements occur also along shallower secondary slip surfaces. In a time period of three months, a 20 m-displacement could be measured in the middle part of the landslide. Water is playing an important role for the triggering of the landslide: on one hand, meteoric water is ponding on the low permeable landslide mass and in large extensional cracks and on the other hand, water is flowing along numerous fractures in the black shale and extruding at perennial springs on the landslide.

Due to its fast and continuous movements, the Pont Bourquin landslide represents a significant example for natural hazards processes in the Alps.

REFERENCE

Jaboyedoff, M., Pedrazzini, A., Loye, A., Oppikofer, T., Güell i Pons, M. & Locat J. 2008: Earth flow in a complex geological environment: the example of Pont Bourquin, Les Diablerets (Western Switzerland). Conf. Proceeding Landslide Processes: from geomorphological mapping to dynamic modelling, Strasbourg 2009.

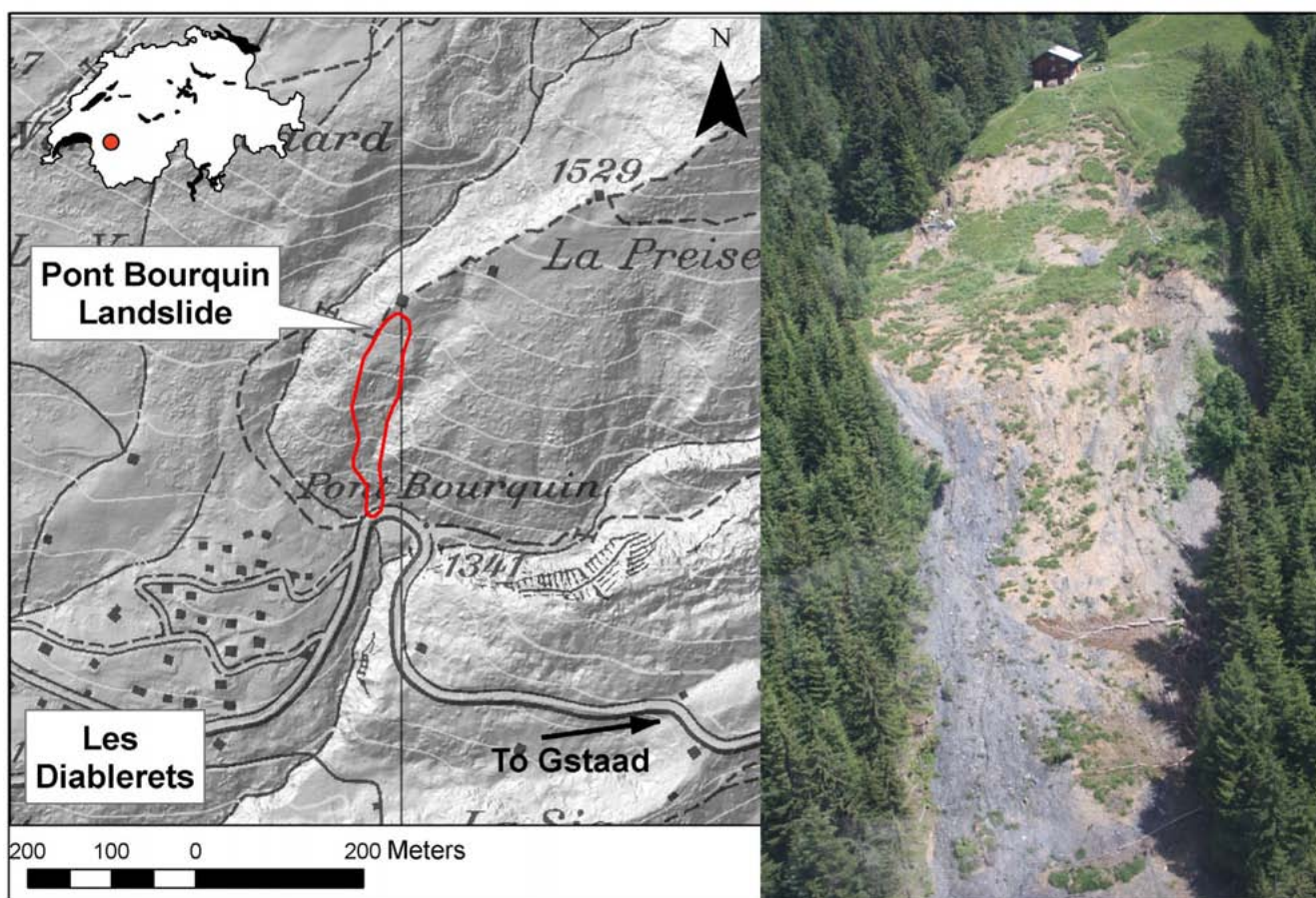


Figure 1: Left: Location of the Pont Bourquin landslide between the Les Parchets landslide to the Northwest and ancient slope instabilities to the East (data from Swisstopo: DV335.2; MNT-MO 2008 SIT). Right: Aerial photograph of the upper and middle part of Pont Bourquin landslide, (M. Jaboyedoff, July 2009).

6.3

Seismic signal analysis of rockslide events in the Swiss Alps

Dammeier Franziska¹, Moore Jeffrey R¹, Haslinger Florian², Löw Simon¹

¹ Department of Earth Sciences, Swiss Federal Institute of Technology, Zürich, Switzerland (dammeief@student.ethz.ch)

² Swiss Seismological Service, Swiss Federal Institute of Technology, Zürich, Switzerland

Seismic recordings from regional networks may be used to identify and locate rockslide events, and can provide unique information on event characteristics that could otherwise only be established by eye witnesses. Here we analyze the seismic signals from 20 large rockslide events that occurred in the Swiss and French Alps during the last twenty years. Rockslide seismic signals have a typical ‘cigar’ shape characterized by an emergent onset and slowly decaying tail. The majority of seismic energy is contained in frequencies below ~4 Hz, and near the source, the signal generally cannot be separated into different wave types. Five seismic metrics were used to quantify differences between rockslide seismograms: seismic duration, peak amplitude of the seismic velocity envelope (ePGV), average ground velocity (AGV), rise time (RT) from event onset to ePGV, and the area of the seismic velocity envelope (EA). Three seismic metrics (EA, AGV, ePGV) exhibited loglog attenuation behavior, RT exhibited semilog attenuation behavior and duration did not show any clear attenuation with distance. For comparison between events, each seismic metric was extrapolated to a common distance of 30 km; for duration the value at the nearest station was used. Event potential energy correlated well with seismic duration and ePGV, and rock/ice avalanches could be identified by unusually low ePGV. Event volume correlated with seismic duration and EA, and rock collapses could be identified by unusually low EA. Analyzing six events that occurred from the same slope with similar runout, the correlation of ePGV and event volume was better than that for all events, indicating that runout path has an important effect on ePGV. For these six events, a plot of EA versus duration showed that rockslides with more than one sub-event lie far from the fitted curve. We also attempted to match seismic waveform features to event dynamics as observed in video footage. A high amplitude signal on one horizontal component may indicate the time at which the moving mass was deflected in its runout path. An event with an initial free-fall phase exhibited an early-time high frequency signal on the vertical component, possibly resulting from impact of the rock mass on the ground.

6.4

Numerical modeling of debris flows – Case study at Dorfbach, Randa (VS)

Deubelbeiss Yolanda¹, Graf Christoph², McArdell Brian², Bartelt Perry¹

¹WSL-Institut für Schnee und Lawinenforschung SLF, Flüelastrasse 11, CH-7260 Davos Dorf (yolanda.deubelbeiss@slf.ch)

²WSL Eidg. Forschungsanstalt für Wald, Schnee und Landschaft, Zürcherstrasse 111, CH-8903 Zürich

Debris flow occurrence in mountain torrents seems to have increased over the last few years - most likely due to glacier retreat and permafrost melting in high Alpine regions [Lemke et al. (2007), IPCC report]. Additional debris material is available, which serves as starting material for catastrophic debris flow events after heavy rainfalls or snow melting. As a result, it is increasingly important to better understand the physical mechanisms governing initiation, motion and settlement of debris flows. Numerical models (such as RAMMS (Rapid Mass MovementS [Christen et al., 2010])) are used to study the dynamics and are valuable tools for hazard assessment and mitigation in inhabited Alpine regions.

Experimental and naturally-triggered debris flows indicate that entrainment and deposition processes as well as the interaction between solid material and interstitial fluid are central to understanding the dynamics of debris flows (Brian). Yet, there are only a few models in use and most of them incorporate one-phase friction relations to describe the flow behavior. It is well-known that debris flows are mixed solid-fluid (two-phase) flows. Disadvantageous is that such models often use empirically derived friction coefficients. Two-phase flow models would allow the description of the interaction between solid and fluid material by treating the phases separately but in a coupled manner. Using an adequate energy description in such models would be a major step forward in properly describing flow height, flow velocity, runout distance as well as entrainment (bulking) and deposition processes.

For the project “Hazard mapping in Mattertal (VS): Data acquisition and numerical modeling of debris flows” we placed instruments in one of the mountain torrents (Dorfbach, Randa, VS) including devices to measure front velocity and flow depths and a video camera provides visual information of an event. The newly gained data combined with existing data from Dorfbach and other locations in the Swiss Alps can be used to investigate entrainment and deposition processes along the channel. The new knowledge on the dynamics helps to optimize the existing numerical debris flow model.

We present 2D numerical simulations in a 3D terrain (Dorfbach, Randa, VS) using RAMMS. The model is based on the 2D shallow water equations and incorporates the Voellmy friction relation. We performed simulations for different scenarios in order to assess different flow paths and deposition areas, which may have disastrous consequences for the population in the Mattertal, VS. The ability to incorporate mitigation structures helps to evaluate the dimensions and the position of such structures in order to protect the populated areas. On the basis of these results we show weaknesses of the used Voellmy model.

Comparison with natural events show that the reproduction of flow heights, runout distances as well as local deposition of material causing channel blockage are problematic. The development of a more realistic two-phase flow model may improve the results concerning runout and deposition processes.

REFERENCES

- Christen, M., Kowalski, J. and Bartelt, P. RAMMS: Numerical simulation of dense snow avalanches in three-dimensional terrain. *Cold Regions Science and Technology* 63 (2010) 1–14.
- Lemke, P., J. Ren, R.B. Alley, I. Allison, J. Carrasco, G. Flato, Y. Fujii, G. Kaser, P. Mote, R.H. Thomas and T. Zhang (2007), Observations: Changes in Snow, Ice and Frozen Ground. In: *Climate Change 2007: The Physical Science Basis. Contribution of Working Group I to the Fourth Assessment Report of the Intergovernmental Panel on Climate Change* [Solomon, S., D. Qin, M. Manning, Z. Chen, M. Marquis, K.B. Averyt, M. Tignor and H.L. Miller (eds.)]. Cambridge University Press, Cambridge, United Kingdom and New York, NY, USA.

6.5

Climate warming and stability of hanging glaciers: lessons from the 1895 Altels break-off

Faillietaz Jérôme¹, Sornette Didier² & Funk Martin¹

¹ Laboratory of Hydraulics, Hydrology and Glaciology (VAW), ETH Zurich, CH-8092 Zurich (faillietaz@vaw.baug.ethz.ch)

² Department of Management, Technology and Economics, ETH Zurich, CH-8092 Zurich.

The Altels hanging glacier broke off on September 11, 1895. The ice volume of this catastrophic rupture was estimated to 4.10 cubic meters, which made this collapse the largest ever observed in the Alps. However the causes of such a collapse are not entirely clear. Based on former works, we reanalyzed this break-off with help of a new numerical model. This model, initially developed by Faillietaz et al. (2010) for gravity-driven instabilities, was applied to this glacier. It takes into account the progressive maturation of a heterogeneous mass towards a gravity-driven instability, characterized by the competition between frictional sliding and tension cracking. We use an array of slider blocks on an inclined (and curved) basal surface, which interact via elastic-brittle springs. A realistic state- and rate-dependent friction law established in the laboratory is used for the block-bed interaction. We model evolution of the inner material properties of the mass and its progressive damage eventually leading to failure, by means of a laboratory-based stress corrosion law governing the rupture of the springs.

It appears that such a break-off could only happen when the basal friction at the bedrock is reduced in a restricted area, possibly induced by a storage of infiltrated water within the glacier. This result seems to be confirmed by the exceptional hot summer preceding the collapse.

Moreover, a two-step behavior could be evidenced: (i) A first calm regime, without visible changes, its duration depending on the rate of basal change. (ii) An unstable regime with a rapid increase of basal motion within few days. As a consequence, a crow crevasse opens few days later (which was observed) and the final instability occurs. This means that the destabilization process of a hanging glacier due to a progressive warming of the ice/bed interface towards a temperate regime will occur without easily visible signs until few days prior to the collapse.

REFERENCES

Faillietaz, J., D. Sornette, and M. Funk (2010). Gravity-driven instabilities: Interplay between state-and-velocity dependent frictional sliding and stress corrosion damage cracking. *J. Geophys. Res.*, 115, B03409, doi:10.1029/2009JB006512.

6.6

Thermal effects on seasonal variability of deformation rate at the Randa rock slope instability, Valais

Gischig Valentin¹, Moore Jeffrey R. ¹, Evans Keith F. ¹, Loew Simon¹

¹ Institute of Geology, Swiss Federal Institute of Technology (ETH), Zürich

Following two catastrophic rockslides in 1991 at Randa, Switzerland, a new retrogressive instability has been observed in the area of the crown and northern margin incorporating 4 - 7.5 million m³ of fractured crystalline rock.

Geodetic measurements reveal a constant long-term displacement rate of more than 20 mm/yr. In 2000, a multi-component monitoring system was installed, including borehole inclinometers, extensometers in boreholes and at the ground surface, piezometric pressure sensors, and temperature sensors. Five years of continuous inclinometer data measured across an active discontinuity at 68 m depth reveal that the deformation rate abruptly increases as soon as the ground surface temperature drops below 0 °C in fall, and then decreases slowly after snowmelt in spring. Piezometer data in 50 and 120 m deep boreholes show that the regional groundwater table is low throughout the year, which is not unusual for the highly fractured rock mass and ridge topography of the test site.

Nevertheless, temporary perched water bodies are observed and local pore pressures are expected to reach a maximum after snowmelt. Therefore, observed annual changes in the deformation time series are contradictory to seasonal velocity variations reported for most large mass movements, where acceleration usually occurs after the onset of snowmelt.

The records from fiber optic strain sensors installed in August 2008 and monthly geodetic surveys conducted in 2008/09 confirm the temporal behavior observed in in-place inclinometer data. We hypothesize that stress changes induced by near surface thermal contraction and expansion of rock play a key role in forcing movements along active discontinuities at depth and in propagation of fractures, while pore pressure effects are of lesser importance.

The mechanisms by which thermo-elastic stresses may drive rock slope deformation are explored with numerical models applying both continuum and discontinuum approaches. The discontinuum models indicate that thermally-induced stress changes at depth can lead to permanent displacement along critically stressed fractures.

6.7

Detailed characterisation of thinnest lake sediment deposits using scanning electron microscopy.

Glur Lukas¹, Anselmetti Flavio S. ¹, Gilli Adrian² & Kägi Ralf¹

¹Eawag, Swiss Federal Institut of Aquatic Science and Technology, CH-8600 Dübendorf (lukas.glur@eawag.ch)

¹Geological Institute, ETH Zürich, Sonneggstr. 5, CH-8092 Zürich

Detailed characterisation of the sediments is in many limnogeological research questions of particular importance. One example is the distinction between background and event sediments. Within the FloodAlp! project, flood-related event deposits in numerous lakes in the alpine realm are studied. Hundreds of such layers can occur in the Holocene sediment record of alpine lakes ranging from less than a millimetre to several tens of centimetres in thickness. The specific characterisation of these deposits and the distinction between flood deposits, mass movement-related event-deposits and typical varve deposits (e.g. authigenic carbonate layers) is of crucial importance.

The characterisation of layers thicker than a few millimetre can be achieved by standard chemical, physical and mineralogical analyses, such as smear slides, thin sections, oxygen and carbon-isotope analyses, C/N ratio, total organic carbon (TOC) and inorganic carbon content (IC). In addition, the mineralogical composition as well as the grain size pattern, shape and texture of detrital grains within these event deposits are essential properties of the sediment layers that can mostly be obtained by optical microscopy of thin sections or smear-slide analyses. However, grain size and structures of fine-grained sediment layers thinner than a few millimetres, cannot be analysed due to the limited resolution of the optical microscope.

To analyse such thin and fine-grained event layers, we are using a low vacuum scanning electron microscope (ESEM) in combination with an energy dispersive x-ray analyses system (EDX). Although these techniques are well known since decades, only the recent development of EDX detectors with increased active surfaces allow recording elemental maps within a few minutes and thus enable an elemental mapping of larger areas. The combined information of the backscattered electrons (BSE) and the x-ray maps allow a mineralogical and textural characterization of millimetre to submillimetre-scaled event layers. With our current experimental setup, we are able to map sediment intervals over several millimetres in thickness continuously, which allows us for example to establish grain size distributions within individual layers.

First results from millimetres to submillimetre-scaled event-layer analyses demonstrate the potential of our approach. Sediment cores of four lakes in the northern Alps (Hinterer Schwendisee, Fälensee, Klöntalersee and Canovasee) were analysed. Thinnest flood-related event deposit could be characterized in detail and distinguished from background sedimentation as well as from mass-movement deposits, all results that could to date, at this scale, not be achieved by optical methods only. Detrital minerals are clearly detectable and upward fining gradation within the flood layers can be observed. In a few cases, an erosional base of the turbidite can be documented.

Our approach allowed us to characterise flood records of millimetres to centimetres thickness in more detail than it would have been possible with an optical microscope. The results demonstrate the high potential of this method as it increases the spatial and thus the temporal resolution of event deposits.

6.8

Movements characterization along open back crack affecting Turtle Mountain, Alberta, Canada

Humair Florian¹, Pedrazzini Andrea¹, Jaboyedoff Michel¹, Epard Jean-Luc² & Froese Corey³

¹ Institute of geomatics and risk analysis, University of Lausanne, Amphipole building-340, CH-1015 Lausanne (florian.humair@unil.ch)

² Institute of geology and paleontology, University of Lausanne, Anthropole building-4163, CH-1015 Lausanne

³ Alberta Geological Survey/Energy Resources Conservation Board, 4999-98 Avenue, Edmonton, Alberta, Canada T6B 2X3

Turtle Mountain is located in the Foothills in southwest Alberta, Canada and is formed by highly fractured Paleozoic carbonates rocks and Mesozoic clastic rocks. This area is mainly affected by two major geological structures that are the Turtle Mountain anticline and the Turtle Mountain thrust. This site became famous after a 30 M m³ rock avalanche of massive limestone and dolostone affecting the eastern mountainside of Turtle Mountain on April 1903. This resulted in the burrying of the Frank village and more than 70 casualties. However, portions of the Mountain are still unstable and some of them are currently monitored (Froese et al. 2009).

The structural features of Turtle Mountain were investigated in order to understand the potential origin of the fractures, the present day scar morphology and to identify the most important failure mechanisms (Langenberg et al. 2007; Jaboyedoff et al. 2008; Pedrazzini et al. in press; Humair et al. 2010).

This study focused on the investigation of the open back cracks that are affecting the crown area of Turtle Mountain, between North and Third Peak (Fig. 1 and 2). The analyses are based on high resolution DEM, orthophoto, aerial photogrammetric, and manual field estimation analysis. The results are compared with extensometers values of displacement. Each method attempts to provide information on the displacement vectors and on the opening of the moving rock compartments measured on the open back cracks.

Therefore, the aim is to confront the different methods in order to evaluate the relevance of any of them in such an investigation. The linkage between the global previous analysed structural pattern of discontinuities and the cracks geometry is performed. Indeed, most of the cracks show a “saw-teeth” geometry and are controlled by two or more pre-existing discontinuity sets (Fig. 3). An estimation of the cumulative displacement on the open cracks allows estimating the effect of stress release on the behaviour of the Turtle Mountain rock compartments. Depending on the orientation of the movements, different deformation zones are created. Moreover, based on the orientation, opening and persistence of the open cracks, an investigation of the volume of potentially unstable rock compartments is attempted.

REFERENCES

- Froese C R, Moreno F, Jaboyedoff M, Cruden D M. 2009. 25 years of movement monitoring on South Peak, Turtle Mountain: understanding the hazard. In: Canadian geotechnical journal. 46, 256-269.
- Humair F, Charrière M, Pedrazzini A, Guell I Pons M, Volpi M, Foresti L, Jaboyedoff M, Epard JL, Froese C. 2010. The Frank Slide (Alberta, Canada): from the contributing factors to the processes of propagation. In: Proceedings of the 63th International Canadian Geotechnical Conference of the Canadian Geotechnical Society, Calgary, AB.
- Jaboyedoff M, Couture R, Locat P. 2009. Structural analysis of Turtle Mountain (Alberta) using digital elevation model: Towards a progressive failure. In: Geomorphology, 103(1), 5-16.
- Langenberg C W, Pana D, Richards B C, Spratt D A, and Lamb M A. 2006. Structural geology of the Turtle Mountain area near Frank, Alberta. EUB/AGS Science Report 2007-01, 30 p.
- Pedrazzini, A., Jaboyedoff, M., Froese, C.R, Langenberg, C.W., and Moreno, F. In press. Structural analysis of Turtle Mountain; origin and influence of fractures in the development of rock failure. In: Geological Society of London, Special publication “Slope tectonics”.

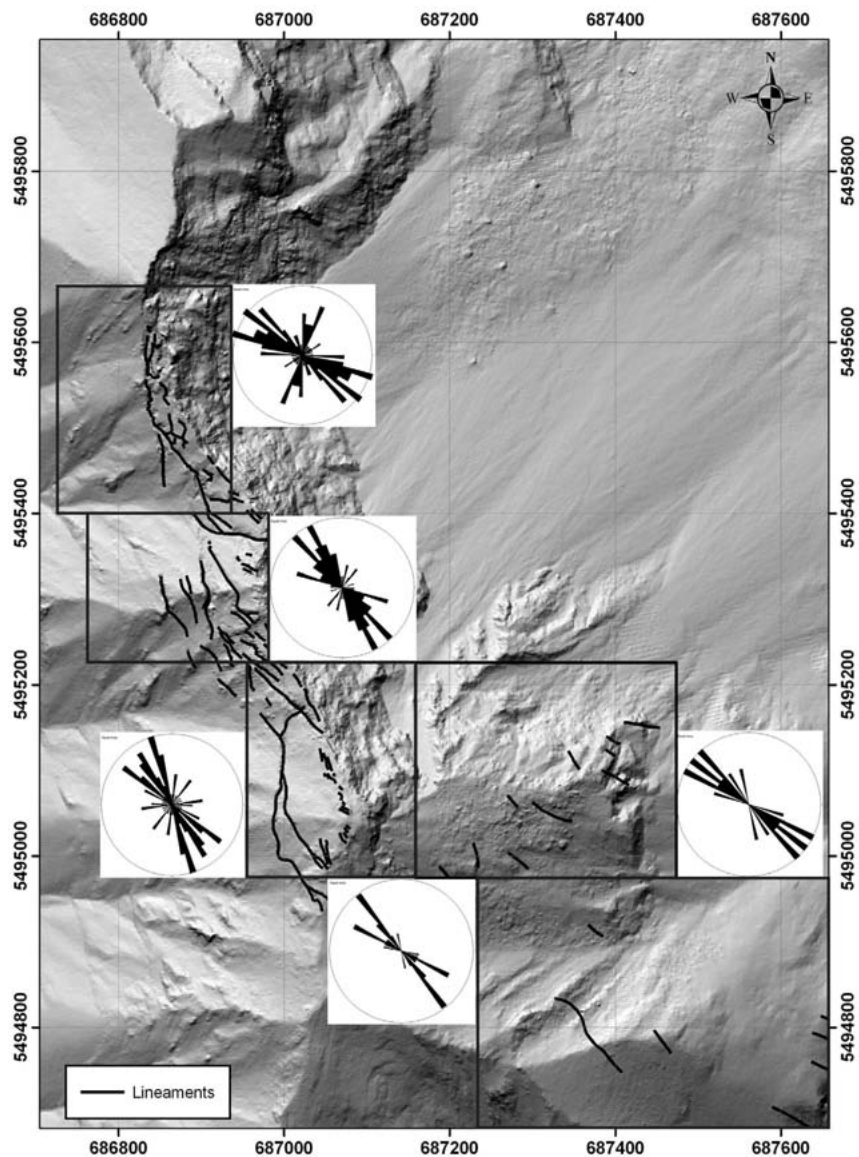


Figure 1: Main lineaments detected in different structural zones between North and Third Peak. From Pedrazzini et al. (in press).

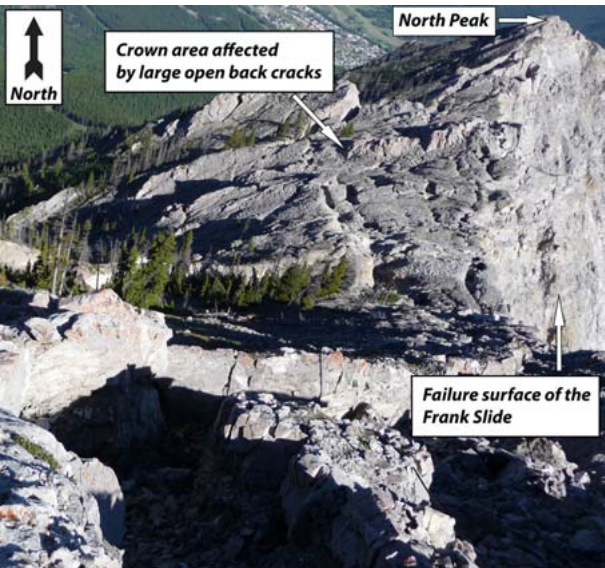


Figure 2: View of the crown area affected by multiple open cracks.

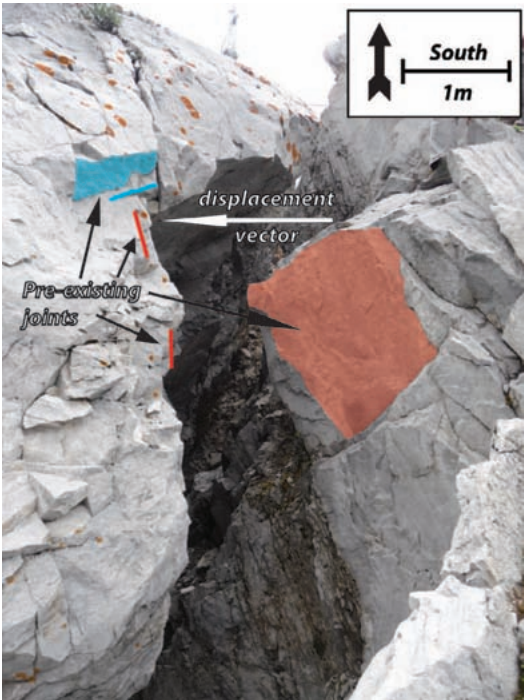


Figure 3: Field example of the control of pre-existing fractures on the crack orientation and its displacement vector.

6.9

A remote sensing application for hazard analysis at Alp di Rosciro, Canton Tessin.

Kos, Andrew^{1,2}, Schaer, Philipp³, Signer, Alexandra¹, Strozzi, Tazio⁴, Valenti, Giorgio⁵, & Loew, Simon¹.

¹ Geological Institute, ETH Zurich, Switzerland (kos@erdw.ethz.ch)

² Terrarsense Switzerland AG, Werdenberg, Switzerland

³ BSF Swissphoto AG, 8105 Regensdorf-Watt, Switzerland

⁴ Gamma Remote Sensing AG, Gümplingen, Switzerland

⁵ Sezione Forestale Cantonale, Canton Ticino, Switzerland

An unstable rock slope located on the western flank of the lower Riviera valley, above the village of Preonzo (TI), was the focus of a study using a combination of helicopter acquired lidar/imagery and ground based radar interferometry. The rock slope instability, known as Alp di Rosciro, consists of a steep 200-300 metre high, largely inaccessible scarp that endangers an industrial complex at the foot of the slope. Since 1989 the instability has been monitored by Cantonal authorities, following the discovery of large tension cracks behind the main scarp (see Figure 1). In 2002, approximately 150K m³ failed in the highly fractured southern section, with renewed activity taking place in northern section in 2010, resulting in a smaller failure of approximately 30K m³. In an effort to better understand the hazard posed by the instability terrestrial and airborne remote sensing techniques were employed for improving our understanding of the geological disposition and the distribution and volume of unstable rockmass compartments.



Figure 1. High resolution aerial image of Alp di Rosciro: The large tension cracks behind the main scarp can be clearly identified.

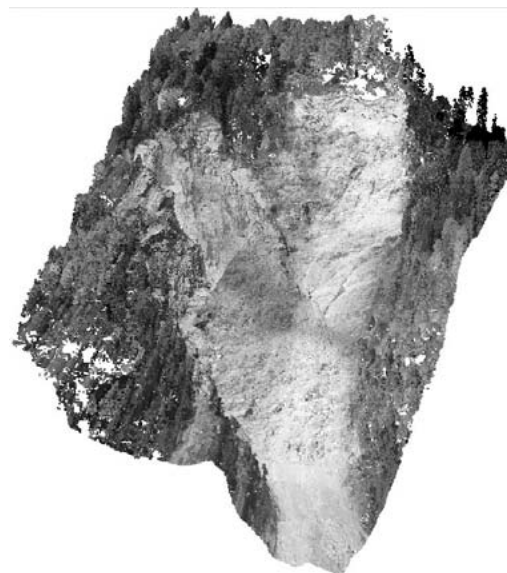


Figure 2. 3D model of the scarp combining lidar and image data

A high resolution, lidar-based digital terrain model and images were acquired by helicopter using the scan2map-system developed at EPF Lausanne and operated by BSF Swissphoto. The special “handheld” setup of the mapping system enables a high operational flexibility and allowed to perform an oblique scan of the area of interest, thus guaranteeing high mapping accuracy also in the very steep scarp beneath the Alp. The resulting 3D model, that combines the Lidar data and the oblique imagery in one (see Figure 2), was used to construct a detailed geological model and identify important structures controlling the instability. Additionally, structural data was extracted from the HRDTM for analysis of kinematic mechanisms, the results of which indicated the importance of joint intersections forming wedges.

High precision, ground-based radar interferometry (GPRI) was used to delineate the boundaries of the moving rock mass and establish an activity profile for comparison with in situ crack meters installed along the main tension crack. Similar magnitudes of displacement between interferometry and crack meter results indicated that the unstable area moves as a coherent block. As a result, dominant, steeply dipping slope sub-parallel joints (K1) become activated in tension resulting in small scale failure (as evidenced from recent activity). Ongoing research is focused on further elucidating the failure mechanism, establishing accurate volumes for unstable compartments, and defining possible failure scenarios (i.e. run out analysis).

6.10

Investigating the seismic response of a large rock slope instability (Randa, VS)

Moore Jeffrey¹, Burjanek Jan², Gischig Valentin¹, Löw Simon¹ & Fäh Donat²

¹ Department of Earth Sciences, Swiss Federal Institute of Technology, Zürich, Switzerland (jeffrey.moore@erdw.ethz.ch)

² Swiss Seismological Service, Swiss Federal Institute of Technology, Zürich, Switzerland

Several observations in the Matter valley of southern Switzerland attest to an important role of earthquake induced rock slope displacements, however owing to the long return period of large earthquakes in the area, co-seismic landslide hazards are not often fully appreciated. In this study, we investigate the seismic response of a large unstable rock mass above the village of Randa in Canton Valais. The site is the subject of numerous interdisciplinary investigations aimed to understand the internal structure and dynamic response of the roughly 5 million m³ of unstable material.

In this study, we employ ambient vibration measurements and fiber optic (FO) strain monitoring to measure the rock mass response to small nearby earthquakes. Notable amplification was observed within the unstable rock mass, with strong polarization in the direction of instability deformation. Results further highlight resonant frequencies of internal rockslide blocks, or effective compartments with similar behavior, which help us understand the rockslide internal and deformation structure.

In May 2010, a M_L 3.4 earthquake struck the area. Five km from the epicenter at Randa, we measured clear transient deformations up to 30 micrometers across surface tension cracks. Spectral peaks from the FO strain record match closely with ambient vibration measurements and new analysis of seismic data recorded during previous experiments. Comparing strain records from either side of one instrumented block, two spectral peaks at 3 and 5 Hz were apparent. 5 Hz energy was found to be exactly out of phase, indicating Eigen-mode block vibration, while 3 Hz energy was in phase, suggesting a resonant frequency of the larger unstable rock mass. 3 Hz resonance could be observed from other ambient vibration measurements distributed around the unstable rock mass, while 5 Hz peaks were visible only in the area of the instrumented crack.

The combined methodology offers a unique view into the rockslide structure, highlighting effective block assemblages and offering clues as to their size, which matches well with local geodetic displacement monitoring and structural characterization.

6.11

Representation problems of danger and “risks” maps

Nicolet Pierrick¹, Jaboyedoff Michel¹, Gerber Christian² & Giorgis David³

¹ Institute of Geomatics and Risk analysis, University of Lausanne, Amphipôle, 1015 Lausanne (Pierrick.Nicolet@unil.ch)

² Canton de Vaud, Département de la Sécurité et de l'Environnement, Secrétariat Général, Place du Château 1, 1014 Lausanne

³ Canton de Vaud, Office de l'Information sur le Territoire, Avenue de l'Université 5, 1014 Lausanne

Danger maps in Switzerland are represented with five levels of danger: white (no danger, or negligible danger), white-yellow (residual danger), yellow (low), blue (medium), and red (high). The zoning is performed on actual state, taking into account assessment measures (as long as they are considered as durable in terms of functionality and if there maintenance is guaranteed; projects cannot be integrated). These maps are then used for the land use planning and to establish protection measures. They are supposed to be checked “periodically” and updated “in case of important modification of the danger” (Lateltin, 1997). The yellow-white color is displayed for both very low occurrence/very high intensity hazards or very low danger remaining after protection measures. Thus, we identify two problems in this methodology :

- The difficulty to identify the initial state danger level and the risk of forgetting the danger (more or less willingly)
- The ambiguity of the yellow-white color

Our French neighbors have a different system. They draw their “hazard” maps (which correspond more or less with our danger maps) ignoring the existing protection measures (Besson et al. 1999; Garry & Graszk 1999). After the identification of areas with stake, they draw a regulatory zoning plan. This plan aims to classify the area into different constraints levels for the land use, regarding the level and type of danger, the existing protection measures or the possibility to build new ones and the stake. This technic offers two advantages:

- The preservation of the primary danger level
- The ability to perform openly an interests weighing

Thus, we propose to adapt the Swiss system with a new color code. The level of danger reduced by a safety measure could have the color of the original danger, with an overprinting representing the method of danger reduction and the color of the danger level considering the protection measures (fig. 1). This representation can be made whether by a point symbol or by a pattern including the symbol. As the representation of protection measures with pictograms is not easy to understand, the symbology should be tested with the assistance of psychologists. We assume that with this new symbology, the authorities and the public will be aware of the potential danger and of the reduction method and that the danger cannot then be forgotten anymore. Furthermore, the yellow-white color would only represent the very low occurrence/very high intensity hazards. This symbology would offer more tools to perform the interests weighing at the risk study level.

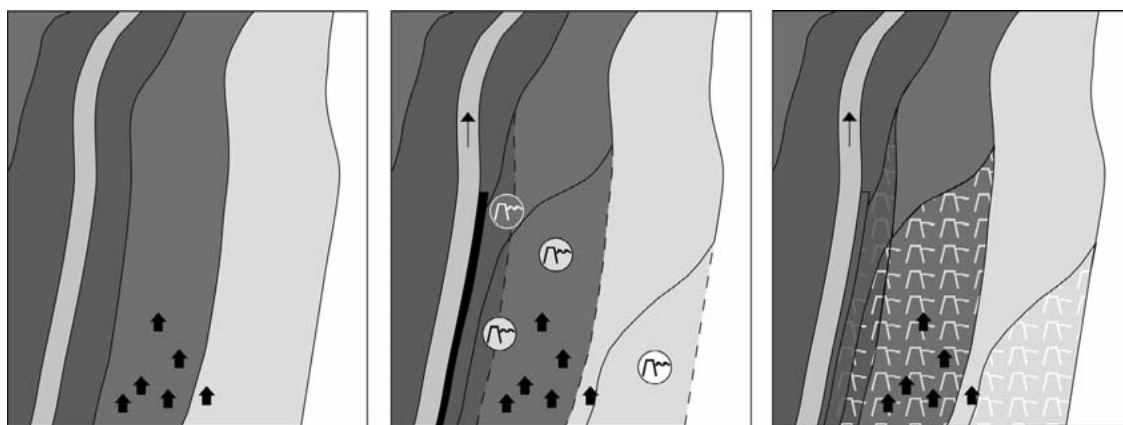


Figure 1. Examples of symbologies. The first image displays the danger map without protection measures. The second image displays the new map after the building of a dike with the “symbol” method. The third one is the same as the second one, but with the “pattern” method. In both case, the symbols takes the colour of the danger level considering the dike.

REFERENCES

- Besson, L. et al. (dir) 1999: Plans de prevention des risques naturels (PPR): Risques de mouvements de terrain. Guide méthodologique. La documentation française, Paris
- Garry, G. & Graszk, E. (dir) 1999: Plans de prevention des risques naturels (PPR). Risques d'inondation. Guide méthodologique. La documentation française. Paris
- Lateltin, O. 1997: Prise en compte des dangers dus aux mouvements de terrain dans le cadre des activités de l'aménagement du territoire, OFAT, OFEE, OFEFP.

6.12

Historical activity of the Saint-Barthélémy stream (VS) – old data, new look

Rudaz Benjamin¹, Jaboyedoff Michel¹

^{*} Institut de Géomatique et d'Analyse du Risque, UNIL, Bâtiment Amphipôle, 1015 Lausanne

The Saint-Barthélémy stream drains a 12.5 km² catchment in the canton Valais, through three geological domains. Its steep course (avg. slope 20°) connects the Dents du Midi massif down to the Rhone valley, creating a massive debris fan of 130 * 10⁶ m³.

The first records of its activity are a great subject of debate, since the Bois Noir fan is one of the supposed location of the Tauredunum event, which caused a tsunami wave on the Lake Lemman in 563 AD. The torrent is not mentioned in the archives before 1470. It has since produced series of debris flows once every century. With the arrival of natural sciences, and the increasing human activity in the Rhone valley, the mentions of the Saint-Barthélémy activity strongly increases in the XIXth century, with two majors crisis around 1835 and 1870.

The last crisis occurred between 1926 and 1930, with debris flows transporting an estimated volume of 106 m³. The instantaneous denudation rate during the crisis reached 12 mm/year. Contemporary denudation rates are ranging between 0.13 and 0.88 mm/year (Rudaz 2010). This last crisis is well documented in its chronology, by local testimonies, field visits during and after the crisis, and most importantly photographs. The behavior of this stream was already supposed to be in a pulse regime, a low background activity interrupted by strong crisis (Bardou & Jaboyedoff 2008).

Looking back on past crisis, it appears that in almost every case (1870 excepted), a rock avalanche occurred in the upper part of the catchment. Using the 1926 event as an exemple, the chronology of past crisis can be reconstructed.

The rock avalanche occurs in the steep upper gorge, and mixes with perenneal snow avalanche deposits, which lubricates the mass and allows a portion of it to reach the alluvial fan (august 1926) on an otherwise sunny day. The main volume of the rock avalanche is mobilized during intense storm precipitation (september and october 1926), forming massive debris flows, and erodes a quaternary deposit in the central part of the catchment. This activity slowly decreases as the original rock avalanche volume is exhausted. Following this crisis, the torrent was corrected by check dams in the central zone, but the main cause was not addressed. The upper cliffs and their failure are historically the source of sediment pulses and their corresponding risks.

REFERENCES

- Bardou E., Jaboyedoff M., Debris flows as a factor of hillslope evolution controlled by a continuous or a pulse process, Geological Society London, v. 296, pp 63-78, 2008
- Bolomey J., Note sur les coulées du Saint-Barthélémy et la possibilité de les combattre, Bulletin technique de la Suisse Romande, Lausanne, 1931
- Montandon F., Les éboulements de la Dent du Midi et du Grammont (examen critique de la question du Tauredunum), Le Globe, 1925
- Montandon F., Chronologie des Grands Eboulements Alpains du début de l'ère chrétienne à nos jours, Extrait des matériaux pour l'étude des calamités, Genève, 1933
- Virieux A., Nouvelle contribution à l'étude du torrent du Saint-Barthélémy, Bulletin de la Société Vaudoise des Sciences Naturelles No 57, 1931, Lausanne
- Archives photographique - Médiathèque du Valais, Martigny



Fig. 1 debris flow damage in 1930, © André Kern, Usine de Lavey, Médiathèque Valais – Martigny



Fig. 2 upper gorge with rock avalanche (a) and resulting debris flow trace (b), B. Rudaz

6.13

Reconstruction of the Holocene flood history for assessing the future flood hazard in the Central Alps (FloodAlp project)

Wirth Stefanie B.¹, Glur Lukas², Gilli Adrian¹ & Anselmetti Flavio S.²

¹Geological Institute, ETH Zürich, Sonneggstr. 5, CH-8092 Zürich (stefanie.wirth@erdw.ethz.ch)

²Eawag, Swiss Federal Institute of Aquatic Science and Technology, Department of Surface Waters, Ueberlandstr. 133, CH-8600 Dübendorf

Floods caused by extreme precipitation events represent a major natural hazard in the Alpine realm, involving enormous financial and social damage (e.g. Hilker et al. 2009). Current climate models predict even an increase in heavy precipitation in the future related to an intensification of the hydrological cycle in the context of global warming (Frei et al. 2006). In order to assess this flood hazard, knowledge about the natural variability of extreme flood events is required. Lacustrine sediment records allow the reconstruction of flood recurrence rates in the past, with the great advantage that their records reach beyond the time span covered by instrumental and historic data series.

The FloodAlp project aims to reconstruct the Holocene flood history of the Central Alps. We investigate 18 small lakes (0.01 to 3 km²) along a North-South Alpine transect from northeastern Switzerland to northern Italy covering a large range in altitude. This multi-archive approach eliminates only locally occurring events, like spatially limited thunderstorms, from the overall signal and gives evidence on the geographical distribution of the flood events. In addition, the wide altitude distribution provides information on the seasonality of the events because high-elevation lakes are, due to their ice cover in winter, only susceptible for summer/autumn rainfalls. Sedimentologically, our approach is based on the mobilisation of sediment material in the catchment during intense precipitation events and the subsequent transport of this material in the river waters to the next downstream lake. The high density of the water-sediment mixture reaching the lake leads to the formation of underflows and finally to the deposition of flood-turbidite layers on the flat basin floor. In the sediment cores, these flood layers are identified and mapped with a suite of visual, mineralogical, chemical and physical methods (Gilli et al. in press).

The flood records of the first six analysed lakes show a general trend from lower flood activity in the early and mid-Holocene to higher flood frequencies in the late Holocene (0-4 kyr). In addition, correlations to variations in the large-scale atmospheric circulation pattern as reconstructed from the GISP2 ice-core record have emerged (Mayewski et al. 2004). Furthermore, some lakes in the Northern Alps present a particularly enhanced flood activity during the last 2000 years. In these cases, land-use changes leading to more easily mobilised sediment material could play an important role, indicated by the conspicuous thickness of the deposits especially during the last millennium. The extension of our flood archive with further lacustrine records will refine these observations and interpretations and will give more evidence on the seasonal occurrence of the events.

REFERENCES

- Frei, C., Schöll, R., Fukutome, S., Schmidli, J. & Vidale, P.L. 2006: Future change of precipitation extremes in Europe: Intercomparison of scenarios from regional climate models. *Journal of Geophysical Research*, 111, D06105, doi:10.1029/2005JD005965.
- Gilli, A., Anselmetti, F.S., Glur, L. & Wirth, S.B. in press: Lake sediments as archives of recurrence rates and intensities of past flood events. In: Bollschweiler, M., Stoffel M. and Rudolf-Miklau, F. (Eds) 'Tracking Torrential Processes on Fans and Cones, Springer Series 'Advances in Global Change Research'.
- Hilker, N., Badoux, A. & Hegg, C. 2009: The Swiss flood and landslide damage database 1972-2007. *Nat. Hazards Earth Syst. Sci.*, 9, 913-925.
- Mayewski, P.A., Rohling, E.E., Stager, J.C., Karlén, W., Maasch, K.A., Meeker, D.L., Meyerson, E.A., Gasse, F., van Kreveland, S., Holmgren, K., Lee-Thorp, J., Rosqvist, G., Rack, F., Staubwasser, M., Schneider, R.R. & Steig, E.J. 2004: Holocene climate variability. *Quaternary Research*, 62, 243-255.

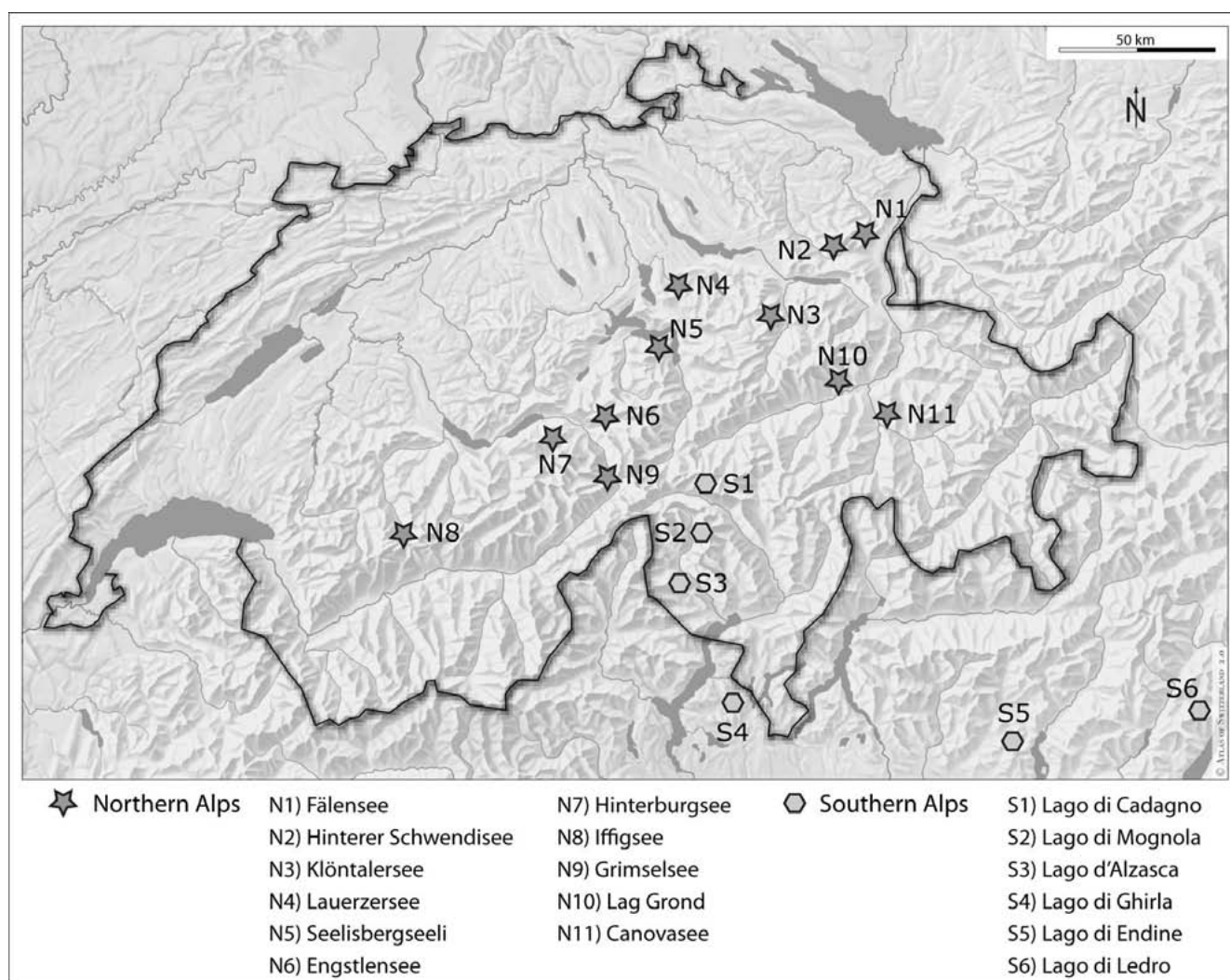


Figure 1: Map of Switzerland and surrounding regions displaying the studied lakes in the Northern and Southern Alps.

7. Geomorphology

R. Delaloye, G.R. Bezzola, M. Bollschweiler, I. Gärtner-Roer, C. Graf, H. Kienholz, N. Kuhn, E. Reynard

Swiss Geomorphological Society

- 7.1 Barboux C., Delaloye R.: Analysing the pluri-decennial development of a rock glacier crisis using repeated SAR interferometry, terrestrial and airborne optical data
- 7.2 Bast A., Gärtner H., Gärtner-Roer I.: If trees have cold feet: Tree-ring analyses of *Larix decidua* Mil. at a sporadic permafrost site in the Swiss Alps
- 7.3 Bast A., Kneisel C.: Small-scale permafrost distribution and its influencing parameters in an alpine glacier forefield
- 7.4 Beaud F., Herman F., Champagnac J.-D.: Influence of hydrology on spatial patterns of glacial erosion
- 7.5 Bennett G., Molnar P., Korup O., McArdeall B.: Modelling sediment transfer through mountain basins
- 7.6 Bergamaschi S., Delaloye R.: Year-round changes in snow cover on the east and north faces of Matterhorn
- 7.7 Bernasconi L., Reynard E.: Hydropeaking on watercourses: an analysis of the effects on erosion, transport and sedimentation of material in the Moesa and the Morobbia rivers (GR/TI)
- 7.8 Castelltort S., Champagnac J.-D.: Landscape resistance: using drainage networks as deformation markers
- 7.9 Champagnac J.-D., Molnar P., Sue C.: Relations among tectonic shortening, climate, and relief creation in mountain ranges.
- 7.10 Champagnac J.-D., Sternai P., Herman F., Guralnik B., Beaud F.: Fracture density as a controlling factor of postglacial fluvial incision rate, Granite Range, Alaska.
- 7.11 Fister W., Iserloh T., Roche M.A., Ries J.B.: Influence of land use and climate change on wind erosion susceptibility in central Aragon (Spain)
- 7.12 Guralnik B., Herman F., Lowick S.E., Preusser F., Rhodes E.J.: Preliminary constraints on the kinetics of OSL thermochronology
- 7.13 Kuhlemann J., Rahn M.: Late Miocene to Present landscape evolution in Northern Switzerland
- 7.14 Molnar P., Densmore A.L., McArdeall B.W., Turowski J.M., Burlando P.: Flood-induced changes in the step-pool morphology of a steep mountain stream
- 7.15 Salcher B.C., Kober F., Willett S.D.: Present erosion and landscape evolution in the glacially overprinted Alps
- 7.16 Scapozza C., Lambiel C., Abbet D., Delaloye R., Hilbich C.: Internal structure and permafrost characteristics of the Lapires talus slopes (Nendaz, Valais)
- 7.17 Schwanghart W., Jarmer T.: Variability of topsoil organic carbon in semi-arid areas at different spatial scales
- 7.18 Sternai P., Herman F., Fox M., Castelltort S.: Hypsometric analysis of glacial landscapes and its application to the European Alps
- 7.29 Strähl S.C., Kuhn N.J.: Vegetation border lines and border line ecotones influenced by geo morph dynamic processes. An example of the timber line development since 1920 in the area of Grindelwald (Bernese Oberland).
- 7.20 Werren G., Lasri M., Reynard E., Obda K.: Flood hazard mapping in two Moroccan watersheds
- 7.21 Zeilinger G., Kober F., Hippe K.: Morphometric parameters and denudation rates in the Eastern Cordillera, Bolivia, affected by crustal bending?

7.1

Analysing the pluri-decennial development of a rock glacier crisis using repeated SAR interferometry, terrestrial and airborne optical data

Barboux C.¹, Delaloye R.¹

¹ Department of Geosciences, Geography Unit, University of Fribourg, Ch. Du Musée 4, CH-1700 Fribourg, Switzerland
(firstname.name@unifr.ch)

Recent works based on the analysis of satellite Synthetic Aperture Radar Interferometry (InSAR) data have evidenced that 15 to 20 rock glaciers were affected by very rapid movements in the Swiss Alps between 1995 and 1999 [Delaloye et al. 2010]. Most of these rock glaciers, moving 2-5 m/year or more, exhibit transversal scarps and/or crevasses revealing some degree of destabilization and the landslide-like behavior of these landforms [Lambiel et al. 2008, Roer et al. 2008]. Nevertheless the chronological and morphological development of the destabilization phase, indicated by changes in the kinematics, geometry and modified topography and which may certainly differ for case to case, is actually not known for most rock glaciers. The aim of this study is to go back at the beginning of the destabilization phase to looking for different factors involved in this process.

In this context, the development of the Grabengufer rock glacier (Zermatt valley, Valais, Swiss Alps) has been investigated among others. This landform is suffering an extraordinary crisis since the winter 2008/2009 at least with annual surface velocities reaching up to 80 m/year [Delaloye et al. 2010]. In order to appreciate the way in which the activity of this landform has changed over the past, a backward analysis was started of both its morphology and kinematics based on repeated InSAR data from 1991 to 2009 and airborne optical data from 1930 to 2005.

The first results show that the current crisis has developed over the last 30 years or so. It began as an accelerated mass wasting (permafrost creep or landslide ?) in the upper rooting zone of the rock glacier already during the 1980's, which propagated progressively by compression to the median part of the rock glacier during the 1990's and the early 2000's, before to reach finally the front. Surface velocities during the initial phases increased maximally to 5 m/year. Once the front – located on a steep slope – was destabilized, it accelerated dramatically dragging almost the whole of the 450 m long rock glacier down. Maximal velocities up to more than 45 cm/day were observed during the second half of 2009 using both GPS as well as tachymetry survey.

The development of the Grabengufer rock glacier crisis, and its chain reaction initially caused by the pulse in rooting zone, differs dramatically from the other destabilized rock glaciers that have been analyzed so far [Roer et al. 2008]. This shows that the factors conducting to destabilization could be various. Nevertheless, looking the strong increase in air temperature that has occurred since the 1980's, these results do not challenge the potential origin of the destabilization in rheological properties of warming ice which could happen in that specific case in the rooting zone of the rock glacier.

The authors are grateful to Gamma Remote Sensing, the Swiss Federal Office for the Environnement (FOEN) and the European Space Agency (ESA) for starting cooperation on the monitoring of landslides and other mass movements using InSAR, and for including the University of Fribourg within this project by studying the detection of rock glaciers and landslides in southern Valais. We would like to thank them for providing us available SAR interferometry, terrestrial data, and airborne optical data related to the sample area.

REFERENCES

- Delaloye, R., Strozzi, T., Lambiel, C., Perruchoud, E., Raetzo, H. 2008: Landslide-like development of rockglaciers detected with ERS-1/2 SAR interferometry. Proceedings of the FRINGE 2007 Workshop, Frascati, Italy, 26-30 November 2007 (ESA SP-649, February 2008).
- Delaloye R., Strozzi T., Lambiel C., Barboux C., Mari S., Stocker A., Techel F., Raetzo H. 2010 : The contribution of InSAR Data to the early detection of potentially hazardous active rock glaciers in mountain areas. Proceedings ESA Living Planet Symposium 2010, Bergen, Norway (ESA SP-686, in press)
- Roer I., Haeberli W., Avian M., Kaufmann V., Delaloye R., Lambiel C., Käb A. 2008: Observation and considerations on destabilizing active rock glaciers in the European Alps. In Kane, D.L, Hinkel, K.M (Eds.), Ninth International Conference on Permafrost. University of Alaska, Fairbanks, USA, pp. 1505-1510
- Lambiel C., Delaloye R., Strozzi T., Lugon R., Raetzo H. 2008 : ERS InSAR for assessing rock glacier activity. In Kane, D.L, Hinkel, K.M (Eds.), Ninth International Conference on Permafrost. University of Alaska, Fairbanks, USA, pp. 1019-1025.

7.2

If trees have cold feet: Tree-ring analyses of *Larix decidua* Mil. at a sporadic permafrost site in the Swiss Alps

Bast Alexander¹, Gärtner Holger¹, Gärtner-Roer Isabelle²

¹ Swiss Federal Research Institute WSL, Dendro Sciences Unit, Zürcherstrasse 111, CH-8903 Birmensdorf, (alexander.bast@wsl.ch)

² Department of Geography, University of Zürich, Winterthurerstr. 190, CH-8057 Zürich

The study focuses on tree-growth analyses at a north facing slope, ranging in elevation from 1800 to 1900 m a.s.l., which is located in the Bever Valley, Upper Engadine/Swiss Alps. Even though the lower boundary of discontinuous permafrost in the Swiss Alps can be averaged at about 2300 m a.s.l., geophysical soundings point out, that permafrost occurs in the Bever Valley below the timberline, depending on multifaceted factors (e.g. very shaded north-face exposition with a small amount of incoming solar radiation, vegetation/moss layer, chimney effect, oftentimes cold air pockets in winter). The investigated slope is covered with a dense forest stand consisting of European larch (*Larix decidua* Mill.) and Swiss stone pine (*Pinus cembra* ssp. *sibirica*). The trees do not show any morphological differences (e.g., dwarfing) to trees adjacent to the slope, nor to trees growing on the opposite south facing slope where no permafrost is present.

Three main questions form the base of our study: (i) Is it possible to detect the presence of permafrost, or rather cold subsurface conditions round about 0°C, by analyzing ring-width variations in larch related to a local chronology established on the south facing slope vis-à-vis the study site? (ii) If so, can we combine our founded results of cold subsurface conditions with geoelectrical soundings, which can prove the presence of permafrost? (iii) Can we estimate a rough time span, where a possible permafrost evolution took place?

On the permafrost site, 88 dominant larch trees with an average age of 210 years were cored in autumn 2006 and the position of each sampled tree was documented in a detailed map of the slope. In addition, 18 trees from the south facing slope were used to establish the reference chronology.

The results show distinct growth suppression in the reference chronology from 1879 to 1890, where the average ring width is reduced by 30% compared to the average of 40 years before and after this time period. This period of reduced growth also occurs in the chronologies of 44 trees (P 1) taken from the permafrost sites, which show growth development comparable to the reference. The remaining 44 trees (P 2) from this site show a strong growth suppression (up to 80%) starting in the period 1879 to 1985 but they do not recover after 1890. Annual growth of 24 trees of P 2 remains reduced until the 1960s, then annual ring width increases again up to the level which is common for the site. The remaining 20 trees of P 2 show reduced growth until the 1990s, when a weak growth release started, not reaching the level of common growth.

Comparisons between single trees show that enduring growth reductions correspond with locations of permafrost lenses detected by ERT-soundings along two transects across the slope. Although the growth reductions cannot be related to defined permafrost conditions (ground temperature that remains at or below 0 °C for at least two consecutive years), they can certainly be related to low soil temperatures restricting root and consequently tree growth. Nevertheless, it can be assumed that the permafrost lenses at this site developed around 1879, because all trees show a comparably higher growth level for more than one hundred years before this suppression occurred. Future work will place emphasis on potential differences in wood anatomical features.

7.3

Small-scale permafrost distribution and its influencing parameters in an alpine glacier forefield

Bast Alexander¹, Kneisel Christof²

¹ Swiss Federal Research Institute WSL, Dendro Sciences Unit, Zürcherstrasse 111, CH-8903 Birmensdorf, (alexander.bast@wsl.ch)

² Department of Physical Geography, University of Wuerzburg, Am Hubland, D-97074 Wuerzburg

The study presented focuses on the small-scale variability of surface substratum and the potential incoming solar radiation (PISR). Both effect snow cover evolution and duration, ground surface temperature regimes and, hence, permafrost distribution in the subsurface.

These surface characteristics act as a buffer-system in the energy balance between atmosphere and lithosphere and, along with climate conditions and elevation determine the patchy occurrence of mountain permafrost.

The permafrost distribution will be mapped by using quasi-3D images as a new approach in periglacial environments.

The study site, a glacier forefield, ranging from 2650 to 2900 m a.s.l., is located in the Muragl Valley, in the Upper Engadine/Swiss Alps. The forefield is characterized by a complex glacier-permafrost interaction (e.g. thrust-moraine, glacial flutes) due to the polythermal regime of the former Muragl glacier.

ERT (electrical resistivity tomography) soundings were performed in summer 2008 at two sites in the glacier forefield, to establish two quasi-3D resistivity images of the subsurface to map the permafrost distribution. The two sites differ mainly in their surface material: The lower site is characterized by coarse blocky, but although fine grained material, whereas the upper site consists of a much finer grained substrate. In addition, the upper site is located in the shadow of an adjacent mountain ridge, while the lower site is more exposed to incoming solar radiation. The first image in the lower part consists of 22 merged ERT soundings (5m electrode spacing, Wenner array, 792 electrode positions, 4356 data points), covering an area of 175 x 175 m. The second image, covering an area of 72 x 72 m, consists of 17 combined ERT surveys (2m electrode spacing, Wenner Schlumberger array, 612 electrode positions, 4896 data points). The large amount of data points results in two high resolution images of the subsurface structure.

To record surface substratum geomorphological mapping of the glacier forefield was carried out in summer 2008. Furthermore, to get a higher resolution in these parts of the forefield, surface material was mapped inside the two ERT-grids at each electrode position. Ground surface temperature was measured using 15 miniature temperature loggers (MTDs), which were placed throughout the glacier forefield. In order to log ground temperatures, two boreholes (8m depth, 8 sensors) were drilled at the two ERT-grid sites in 2006. Additionally, BTS measurements (bottom temperatures of snow cover) were realized in March 2007 and 2008. PISR was calculated by using the solar analyst, integrated in the ESRI ArcGIS software package.

Surface substratum was categorized in five substrate classes ranging from coarse blocks (>630mm, often 1000-2000 mm) at the thrust-moraine, to fine-grained, detritus-sandy to loamy substrate, particularly within the streambeds of the glacier run-off. A high variability in grain-size was noticeable within short distances.

The MTDs as well as the borehole measurements illustrated the different temperature regimes of the substrate classes. In 2006-2007 mean annual ground surface temperature ranged from -1.3 °C in the coarse grained, to 1.06°C in the finer-grained substrate; resulting in an offset larger than 2.3 °C within approx. 100m. Mean annual ground temperature at a depth of 5 m was -0.59 °C (2008/09) at the lower site, which was slightly colder than at the upper site (-0.10 °C (2008/09)). Nevertheless, borehole temperature logging proved the occurrence of permafrost at both sites.

Modeled PISR clearly shows the mountain shade effect. The ERT-grid in the lower part of the forefield was more exposed to solar radiation with values ranging from 19 to 20 MJ/m²d compared to the area that is covered by the ERT-grid in the upper part, which showed energy values between 14 and 17.5 MJ/m²d.

Results of the quasi-3D images enable linking the subsurface structure with the surface maps. Resistivities of > 100 kOhm.m in the lower part of the glacier forefield below the coarse blocky material indicated higher ice contents in the voids between the blocks of the subsurface. In the marginal areas of that high resistivity anomaly, where surface substratum also changed to more fine-grained particles, resistivities decrease to values of approx. 12 kOhm.m. This suggests a lower ice content of the permafrost body. Active layer thickness increased simultaneously from 2 m to 5 - 7 m. In the case of the finest substrate class, as well as in areas with streambeds, resistivities < 10 kOhm.m in the subsurface indicated permafrost-free conditions.

Resistivities in the upper quasi-3D image, however, did not exceed the mark of 23 kOhm.m. This suggests lower ice content and/or warmer permafrost temperatures in the subsurface. The latter is proved by the borehole temperatures. Active layer thickness ranged between 5 and 8 m. Lower values of PISR have a positive impact for the permafrost body at that site.

7.4

Influence of hydrology on spatial patterns of glacial erosion

Beaud Flavien¹, Herman Frédéric¹, Champagnac Jean-Daniel¹

¹Earth Surface Dynamics, Geological Institute, ETH-Zürich, Sonneggstrasse 5, 8092 Zürich, Switzerland. flavien.beaud@gmail.com

During the Last Glacial Maximum (LGM) most of worldwide mountain ranges have undergone glacial conditions. Better understandings of glacial erosion patterns are necessary to explain relief evolution of alpine ranges.

Models have already reproduced some glacial features such as U-shape valleys and steps, nevertheless large overdeepenings, such as Lake Geneva, Switzerland and France remain without explanation. Since the early times of glaciology (De Saussure in 1779), it is expected that water play an important role for glacier sliding. Furthermore, most erosion laws scale with the sliding velocity, itself scaling with basal water pressure. However, so far, no study explicitly addresses and quantifies the role of hydrology.

To quantify the importance of hydrology on spatial erosion patterns, we develop a model that reproduces ice flow, using the First Order Approximation (FOA), and integrates hydrology.

Irrespective of the initial shape of the topography, the model without hydrology creates a smooth concave profile with no steps or overdeepenings. Integration of the glacial hydrology leads to changes in sliding pattern and thus in erosion rate pattern, creating steps, flats and overdeepenings in all the simulations. The Figure 1 shows the evolution of a synthetic fluvial profile under glacial condition: a step followed by a 15km long flattened areas are formed. Furthermore the model shows that most of erosion takes place below the Equilibrium Line Altitude, as shown in Figure 2. Thus we claim that neglecting glacial hydrology the model fail to reproduce glacial valley features, whereas with hydrology integration the model succeeds to do so. Comparison with natural longitudinal profile (Valais and Vanoise area) confirms the occurrence of steps and flats, several hundred of meters below Little Ice Age and LGM, respectively.

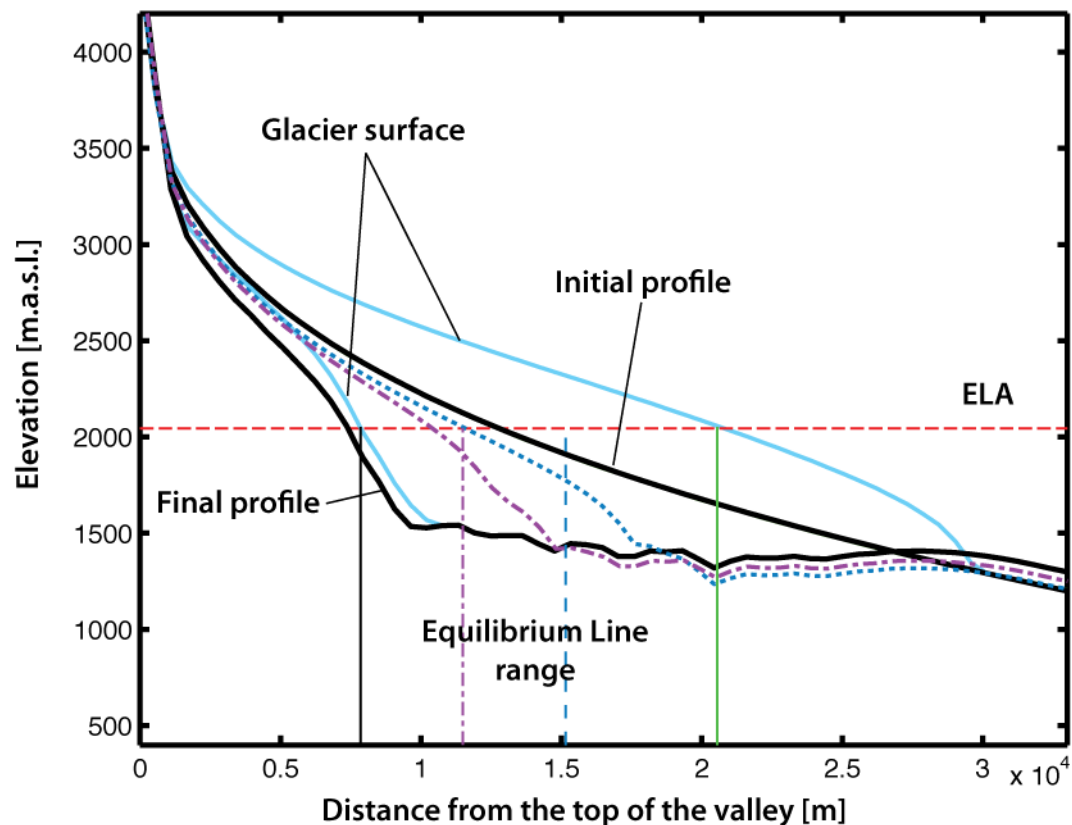


Figure 1: Evolution of a longitudinal profile that has undergone glacial erosion, with the integration of glacial hydrology.

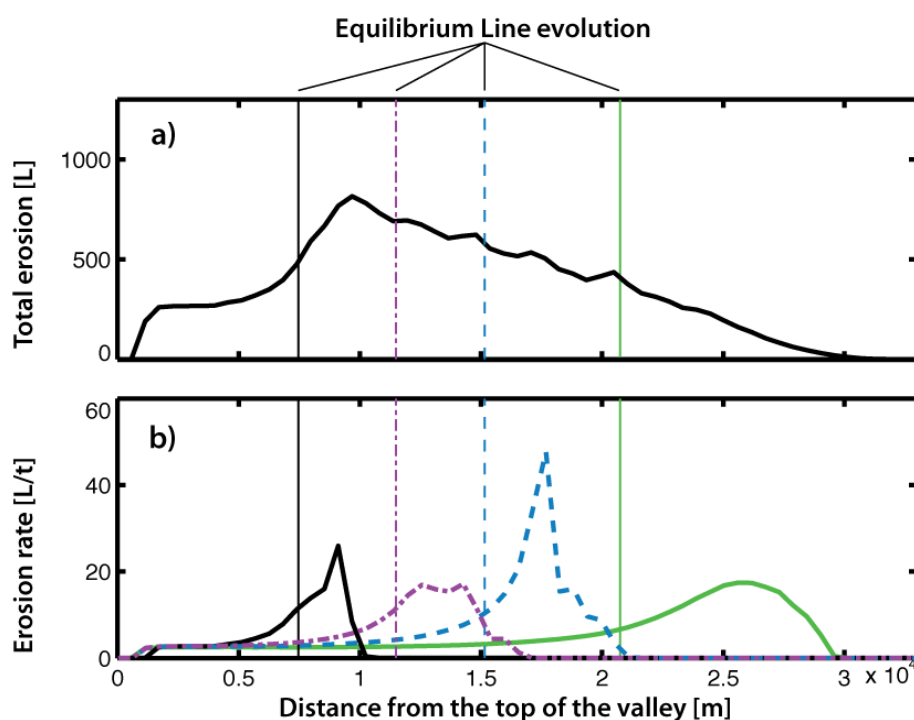


Figure 2: a) Total glacial erosion and b) erosion rate evolution during the simulation. Vertical lines are the corresponding ground position of the ELA.

7.5

Modelling sediment transfer through mountain basins

ESF TOPOEUROPE: SedyMONT

Bennett Georgina¹, Molnar Peter¹, Korup Oliver², McArdeell Brian³

¹ Institute of Environmental Engineering, ETH Zürich, Schafmattstrasse 6, ETH Hönggerberg, 8093-Zürich (bennett@ifu.baug.ethz.ch)

² Institute of Earth and Environmental Sciences, University of Potsdam, Germany

³ Swiss Federal Institute WSL, Zürcherstrasse 111, 8903 Birmensdorf

Quantifying sediment yield from mountain basins is of considerable societal interest because it is the main source of sediment transported to lowland and coastal regions and because mountain basins are particularly susceptible to environmental change, in particular to climate change. We identify the following characteristics of sediment transfer through mountain basins that need to be better understood with respect to their long term sediment yields: temporary storage of sediment, longer-term sediment storage and system thresholds.

Transfer of sediment through a system is usually treated as a one-dimensional mass conservation problem in which the difference between inputs and outputs at intermediate stages through the system are accounted for by temporary storage. The residence time of sediment in storage can be calculated as the mass of the storage component divided by the flux through it over a defined period of time. Based on this calculation, the distribution of travel times of sediment through the component is exponential with a mean equal to the residence time. It follows that all sediment in the component has an equal probability of evacuation (Lisle and Church, 2002). A certain proportion of sediment passing through the basin may be deposited into stable storage components, such as alluvial fans, with a much lower probability of remobilization over short time scales. Both temporary and longer-term storage components are vulnerable to instantaneous remobilization related to the existence of internal system instabilities, or thresholds, within the system. These thresholds thus present a major source of non-linearity and complexity in sediment transfer that may explain some of the temporal variability observed in sediment yields (e.g. Phillips, 2006). The quantification of sediment residence times in short-term storage and redeposition of sediment into longer-term storage, along with a better understanding of the role of thresholds in stochastic sediment supply will help to resolve the discrepancies between short and long-term basin sediment yields that have been observed in many studies (e.g. Kirchner et al., 2001).

We are currently investigating temporary and long-term sediment storage and system thresholds in the Illgraben catchment, SW Switzerland, using a combination of available data and data obtained from several aerial photographs spanning 1963-1998 using digital photogrammetry. Differencing of digital elevation models (DEMs) has revealed a zone of persistent sediment storage at the head of the debris flow torrent in the order of 100,000s m³ of sediment between 1963 and present. Landsliding between 1986 and 1992 delivered ~1,000,000m³ to this zone. The annual flux was calculated as the annual difference between erosion by landsliding and deposition, giving a value of ~100,000m³. Sediment residence time was calculated as ~10 years based on using the total eroded mass of sediment by landsliding over the 6 year period as the potential mass of sediment in storage and dividing this by the flux. Residence times were also calculated for several channel reaches based on estimations of the mass of stored sediment in the channel bed and sediment flux data obtained from DEM differencing and from recent channel bed monitoring by Peter Schuerch, Durham University and Catherine Berger, WSL. Initial results suggest that channel residence time decreases exponentially with distance from the channel crest. This correlates with reports downstream decreasing amplitudes of erosion and deposition by Berger et al. (2010) and sediment flux and storage by Benda and Dunne (1997a). This supports previous suggestions that the Illgraben is a transport limited system. The proportion of sediment that was redeposited annually into longer-term storage within the alluvial fan between 2007 and 2009 was calculated at 0.5%. Calculations of these residence times and redeposition along with further calculations are presented.

Based on the knowledge of sediment residence times and redeposition rates for different morphological elements of the basin system, a mountain basin can be conceptualized as a sequence of reservoirs with different storage capacities through which sediment is routed. A model is presented that will be used to investigate and compare the interactions between sediment production, short and long term storage, supply and transport limiting thresholds and net sediment yield at a number of mountain basins covering a range of climatic and geomorphic settings that are being monitored as part of the ESF TOPOEUROPE SedyMONT project. These include the Illgraben, Switzerland, where sediment transfer is dominated by debris flow activity; the Pasterze, an Alpine glaciated basin in Austria; and Erdalen and Bødalen, both glaciated fjord basins in Norway.

REFERENCES

- Benda, L. and T. Dunne (1997a). Stochastic Forcing of Sediment Supply to Channel Networks from Landsliding and Debris Flow. *Water Resources Research*. 33(12) 2849-2863.
- Berger, C., McArdell, B.W., Schlunegger, F. (2010) Sediment transfer processes at the Illgraben catchment, Switzerland: Implications for debris flow entrainment. *Earth Surface Processes and Landforms*. Accepted
- Lisle, T. E. and M. Church (2002). Sediment transport-storage relations for degrading, gravel bed channels. *Water Resources Research* 38(11).
- Kirchner, J.W., Finkel, R.C., Riebe, C.S., Granger, D.E., Clayton, J.L., King, J.G., & Megahan, W.F. (2001) Mountain erosion over 10 yr, 10 k.y., and 10 m.y. time scales. *Geology*, 29(7), 591-594.
- Phillips, J.D. (2006) Evolutionary geomorphology: thresholds and nonlinearity in landform response to environmental change. *Hydrology and Earth System Sciences*, 10(5), 731-742.

7.6

Year-round changes in snow cover on the east and north faces of Matterhorn

Bergamaschi Stefano¹ & Delaloye Reynald¹

¹Department of Geosciences, Geography, University of Fribourg, Ch. du Musée 4, CH-1700 Fribourg (name.surname@unifr.ch)

During the last century many ice carapaces adhering on steep slopes at high altitude in the Alps have partly or even completely disappeared. Between two phases of significant ice losses during the 1940s and since the end of the 1980s the ice coverage on steep slopes has nevertheless tended to slightly increase (Delaloye 2008). The processes of snow-ice transition and the consequent surface ice aggradation on steep slopes differ obviously from firnification processes on glaciers and remain not completely understood. Indeed it is assumed that:

- the ice forms mostly by refreezing of meltwater in the snowcover,
- the favorable conditions for ice formation are mostly encountered in spring and fall when alternating melting / refreezing phases are the most likely to occur,
- considering that cold snow can not accumulate significantly during winter on steep slopes, the climatic factors controlling the evolution of ice cover on steep slopes are not all the same as on glaciers,.

The Matterhorn (Matterhorn, Wallis) is a “spot” where the process of snow accumulation and ice transition may be clearly visible during all the year long. Besides to document the year-round changes in the snow coverage, the main objective of this study is to try to detect where and when melting/refreezing processes are occurring on both the northern and eastern faces of the mountain.

To achieve this goal, systematic remote measurements of the surface temperature of Matterhorn are taken for 24 hours by clear sky once every month for an all year long with a thermal camera (FLUKE TiR). This periodic measurement is permitting to better understand the spatial patterns as well as the day-night and seasonal differences of the surface temperature, that on the Matterhorn is extremely variable and able to change quickly between snowy (icy) surface and bare rock. The obtained surface temperature data also gives the opportunity to describe in details where and when melting is possibly to take place and its influence on the changes in snow coverage (Fig. 1).

Taking into consideration several parameters as the air temperature (derived from a weather station located at the Solvay hut at 4003 m asl on the Hörnli Ridge), the solar radiation (calculated with the Solar Analyst software), the slope inclination and the morphological features of the mountain (surface relief), the year-round general behaviour of the snow coverage on the two faces can be drawn. Concentrating the attention on the period where snow accumulation and melting process take place permits to explain the different and sometimes contradictory aspects that the Matterhorn reveal during the four different seasons (Fig. 2)

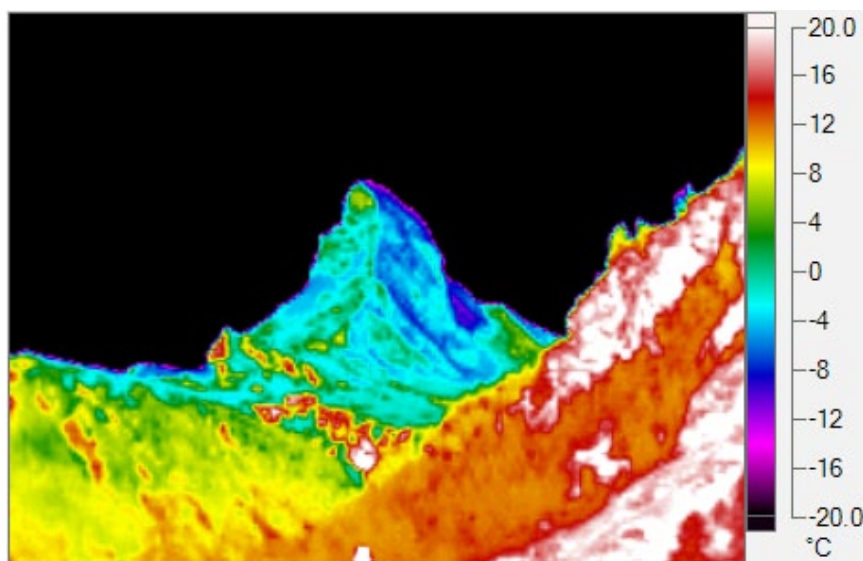


Figure 1. Thermal image of Matterhorn on 22-05-2010, 12.00h. Melting is likely to occur on most of the east face, whereas the surface temperature on the north face is almost cold.

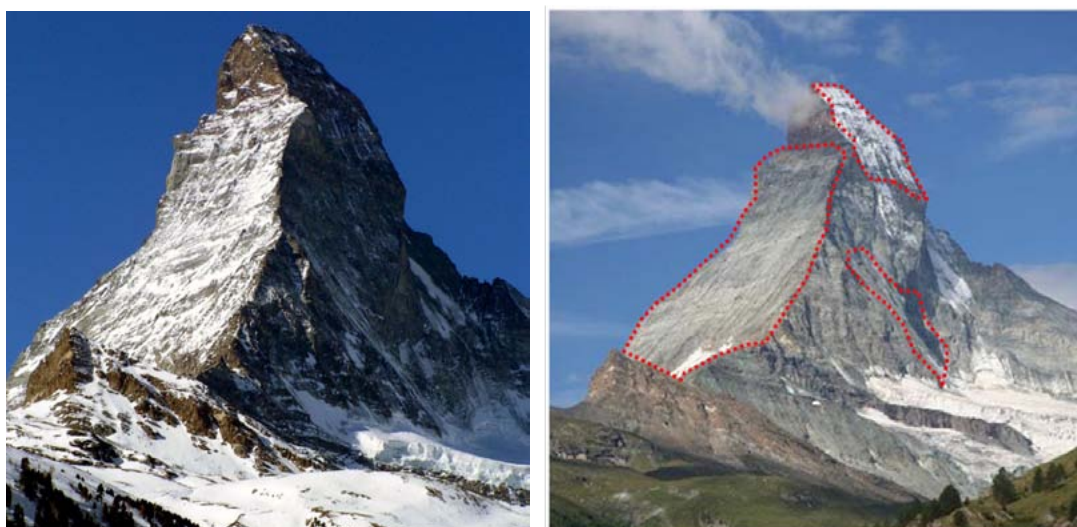


Figure 2. Examples of varying snowcover on Matterhorn between winter season (left) and summer season (right). Whereas the east face and the base of the north face are less covered by snow on the summer picture, the upper north face appears conversely to be much snowy.

REFERENCES

- Delaloye, R. 2008. Parois glaciaires... parois rocheuses : l'évolution séculaire des grandes faces alpines. Klimaveränderungen auf der Spur. Jahrestagung der Schweizerischen Geomorphologischen Gesellschaft SGmG, Samedan, 2007, pp. 93-104.

7.7

Hydropeaking on watercourses: an analysis of the effects on erosion, transport and sedimentation of material in the Moesa and the Morobbia rivers (GR/TI)

Bernasconi Laura¹, Reynard Emmanuel¹

¹ Université de Lausanne, Institut de géographie, Anthropole, Quartier Dorigny, CH 1015 Lausanne (laura.bernasconi@unil.ch) (emmanuel.reynard@unil.ch)

In recent decades, the hydrology of alpine streams has been altered by hydroelectric projects. To produce energy, plants must open storage basins located at high altitude in order to run their turbines. The water is discharged into the river downstream of the central points of restitution. These mechanisms cause an oscillation of the daily regime of rivers, passing through minimum flows during the night (low energy demand) to the maximum data rates when energy demand is high. Streams affected by this type of operation undergo substantial changes in river morphology and aquatic ecosystems (Fette, 2006). The hydropeaking (the daily oscillation) is a phenomenon that has acquired a dominant role in recent years, both for the innovative character and in the extent of its impact on the aquatic ecosystem (Baumann & Klaus, 2003).

The main purpose of this study is to bring a new contribution to research by studying the impact of hydropeaking on sediment transfer. The study is conducted on two rivers, the Moesa (GR/TI) and the Morobbia (TI), which are characterized by different daily changes. The analysis of the ecomorphology is conducted using the modular stepwise procedure for assessing the ecological status of rivers in Switzerland. In fact, it is important to understand the relationship between river morphology and the effects of hydropeaking. We also measure the runoff of the rivers, through the installation of two hydrological gauging stations. Investigations are carried out to appreciate the degree of colmatation, one of the major impacts of hydropeaking. We also carry out an analysis to understand the variation of the erosion and transport of river materials: we stain sediments before the arrival of the artificial flood. The movement of these sediments gives us information on the erosion created by the increase of water level and speed. Following this study it is possible to obtain more information about the magnitude of the effects of hydropeaking.

The poster presents the preliminary results of this study.

REFERENCES

- Baumann, P. & Klaus I. 2003: Conséquences écologiques des éclusées, étude bibliographique. Inf. conc. Pêche no. 75. Office fédéral de l'environnement, des forêts et du paysage, Berne.
- Fette, M. 2009: Schwall und Sunk: Effekte auf das Grundwasser. Eawag News, 61, 30-31.

7.8

Landscape resistance: using drainage networks as deformation markers

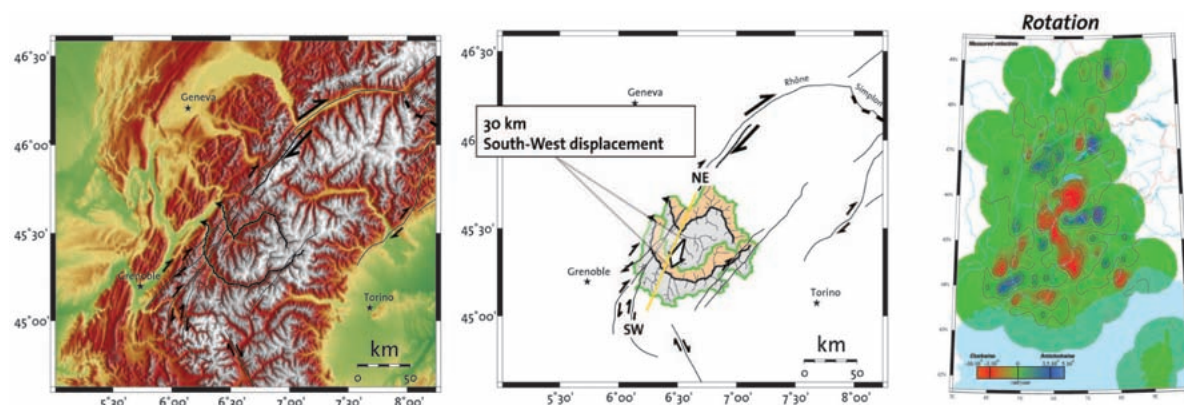
Castelltort Sébastien¹ & Champagnac Jean-Daniel¹

¹ Earth Surface Dynamics, Geological Institute, ETH-Zürich, Sonneggstrasse 5, 8092 Zürich, Switzerland

Fluvial networks determine to a large extent the structure and geometry of erosive landscapes in mountain ranges. As a consequence it is fundamental to understand how they develop and evolve in order to reconstruct and predict landscape evolution. A particularly important issue is the degree to which fluvial networks evolve and change through their existence.

Two end members can be invoked:

On one hand, river networks are very dynamic, changing and reorganizing frequently during orogen evolution. In this view, landscapes mostly reflect the present state of the tectonic forcing, with a minor component of “memory”. This has found support in a variety of observations like wind gaps, hanging valleys, sinuous shape of water divides, inferred changes of detrital sources that all evoke river captures and drainage network changes, and are reproduced in some analogue and numerical models.



Deformation of a drainage basin by horizontal movement: example of the W-Alps, and comparison with geodetic strain rates (right, Delacou et al., 2008)

On the other hand, river network can be viewed as largely resistant to deformation and change, thus potentially acting as as useful passive markers of the crustal strain. Some notorious examples are antecedent rivers and drainage systems cutting through lithological and geological structures (folds and faults), drainage systems extending behind the main drainage divide in large mountain ranges, and preservation of superficial cover rocks adjacent to valleys deeply incised into the basement. Spectacular plane deformation of large river basins also points to the large resistance of river networks to deformation and their difficulty to reorganize, especially when relief is high and / or increases [Hallet and Molnar, 2001]

Based on natural examples of tectonically deformed drainage network in the European Alps and Southern Alps of New Zealand we address two fundamental questions:

- What are the required conditions for a drainage network to be used as a marker of the deformation?
- How much deformation can record a given drainage network? Does this depends and strain rate and potential erosion rates?

It appears that drainage network can be used as strain marker if i) the initial shape of a drainage network can be constrained, and ii) the ratio between erosion and deformation allows the strain to be recorded without dramatic change (e.g. piracy). Large rivers can record more deformation than small ones, for similar strain rates. Finally, this shows that incision of the rivers (i.e. increase of the relief) makes the network more stable (and therefore more suitable to record deformation).

REFERENCES

Hallet, B., and P. Molnar (2001), Distorted drainage basins as markers of crustal strain east of the Himalaya *Journal of Geophysical Research B: Solid Earth*, 106(B7), 13697-13709.

7.9

Relations among tectonic shortening, climate, and relief creation in mountain ranges.

Champagnac Jean-Daniel¹, Molnar Peter², Sue Christian³ & Herman Frédéric¹

¹ Earth Surface Dynamics, Geological Institute, ETH-Zürich, Sonneggstrasse 5, 8092 Zürich, Switzerland. champagnac@gmail.com

² Department of Geological Sciences, and CIRES, University of Colorado, Boulder, Colorado, 80309, USA.

³ UFR Sciences et techniques, 16, route de Gray, 25030 Besançon, France.

In order to determine the relative contribution of climate and tectonics to landscape morphology, we explore the correlations among topographic, geomorphic, tectonic, and climatic variables of more than 50 mountain belts worldwide.

Topographic data, from the GTOPO30 DEM, include several parameters: maximum elevation, mean elevation, and maximum averaged elevation, calculated above sea level and above individual base levels.

Geophysical Relief (the mean elevation difference between a smooth surface connecting the highest points in the landscape and the current topography (Small and Anderson, 1998)) calculated over 3 different radius, 1km, 5km and 15km provides a measure of relief over several typical lengths and yields a thickness if normalized by area.

Tectonic parameters comprise geodetic shortening rates and average strain rates obtained by dividing shortening rate by the orogen's width.

Climatic data are mean precipitation rates and a qualitative measure of glaciation factor ranging from 1 (no glaciation) to 5 (full glaciation), for both LGM and present day. (Cosine of) latitude has also been used as a proxy for insolation, hence for (potential) glaciations.

The database has been split in two parts: one for all mountain belt, including non-convergent settings, and another one, with only actively compressional orogens. Sizes of areas considered span two orders of magnitude (the largest being the Gobi Altai, Mongolia, the smallest the Wind River Range, Wyoming, USA). Bigger orogens (Himalayas, Andes...) have been separated into several sub-orogens.

For the global database, measures of geomorphic, erosional, and tectonic parameters are self-consistent; correlation coefficients are ~0.9. Those for climate are less so, with a correlation coefficient of 0.4, as links between glaciation and precipitation are weak.

Multivariate regressions show that topography depends on 50% on convergence rate and 50% (negatively) with latitude. Topographic parameters appear to be almost insensitive to precipitations. Similarly, relief depends equally on convergence rate and latitude. However, if relief is normalised to mean belt's elevation, it is nicely negatively correlated with latitude.

A strong positive correlation also exists between the "scale length" of the relief (GR15/GR1 and exp) and the latitude. This correlation is better with only the no-convergent settings (shortening rate = zero) taken into account. This is interpreted as a signature of glacial erosion that increases the relief over small (i.e. ~1km typical length). We also note that there is no correlation between tectonic and this relief scale length.

We conclude that:

- All the morphometric parameters investigated are insensitive to large scale precipitation.
- Topography positively correlated with shortening rate, and negatively correlated with latitude by a similar amount.
- Small scale Geophysical Relief (GR1) increases when latitude increases.
- « Scaling Length » of relief (GR15/GR1, and exp. factor), and normalized relief (GR/(M-B)) strongly depends on latitude, but NOT on shortening rate.

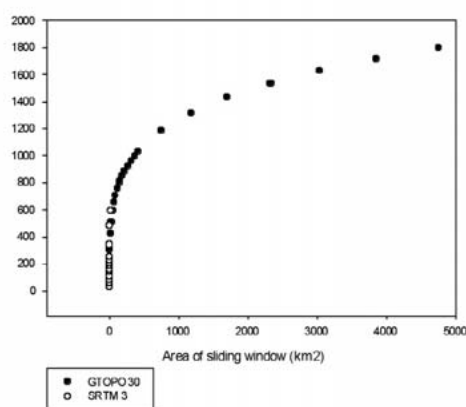


Figure 1: Power-law evolution of the geophysical relief (GR) with the area of sliding window in the Western Alps.

$$\text{MeanGR} = A * x^{\text{exp}}$$

REFERENCES

Small, E.E., and Anderson, R.S., 1998, Pleistocene relief production in Laramide mountain ranges, western United States: *Geology*, v. 26, p. 123-126.

7.10

Fracture density as a controlling factor of postglacial fluvial incision rate, Granite Range, Alaska.

Champagnac Jean-Daniel¹, Sternai Pietro¹, Herman Frederic¹, Guralnik Benny¹, and Beaud Flavien¹

¹ *Earth Surface Dynamics, Geological Institute, ETH-Zürich, Sonneggstrasse 5, 8092 Zürich, Switzerland. champagnac@gmail.com*

The nature of the relations between lithosphere and atmosphere to shape their interface (the observed landscape) is highly disputed since the last two decades or so. The classical “chicken or egg” problem (Molnar and England, 1990) raised the idea that erosion itself can promote creation of topography thanks to isostatic compensation of eroded material and subsequent positive feedback. The quaternary glaciations and the associated high glacial erosion rates are supposed to be the main agent of such process. More recently, “tectonic activity” has been considered not only as a rock uplift agent, but also as a rock crusher, that in turn promote erosion, thanks to the reduction of size of individual rock elements, more easily transported by ice and water (Clarke and Burbank, 2010; Dühnforth et al., 2010; Molnar et al., 2007).

The Granite Range in Alaska presents a contrasted morphology, all other (lithology, climate) being equal: to the west (Kiagna River watershed), glacial landscape is well preserved (vegetated “U” shaped), and subsequent fluvial incision occurs only to the downstream part of the drainage network. Oppositely, the eastern part (Goat Creek watershed) presents a strong fluvial / hillslope imprint (“V” shaped, with no vegetation) of both trunk stream and tributaries, and only a few relict surfaces supposedly related to a former glacial landscape.

Postglacial erosion related to fluvial, debris flow and hillslope processes appears to be one order of magnitude higher in highly fractured area than in less fractured area. Despite similar drainage areas between the two rivers (~600km²), Goat Creek shows a massive fan delta at its junction with its base level (Chitina River), whereas Kiagna River shows no fan delta a few tens of km downstream Chitina River.

These large discrepancies in the landscape have been determined from 1) qualitative (visual) appreciation of the landscape, 2) the volume of eroded material determined by reconstruction of the glacial landscape surface and subtraction of the actual landscape, and 3) the hypsometric quantification of the landscape.

On the field, the eastern part of the belt appears to be highly fractured, with numerous, large, penetrative faults, associated with km-thick fault gouges and cataclasites. The westernmost part shows massive bedrock (paragneiss and granite), with minor, localised faults. Fault density, determined from satellite imagery and DEM confirms the field observation: density is much higher to the east, where postglacial incision is the most important.

One cannot exclude external forcing (e.g. E-W gradient of rock uplift), or remote sensing bias (sun orientation, faults that may be more visible in bare rock area, snow and ice shielding etc.) that may quantitatively change our results. However, our qualitative observations are robust, and provide an impressive case study for tectonic-erosion interactions. This may be extrapolated in other mountain ranges (e.g. the European Alps), where the largest active debris flow system (the Illgraben, Valais, Switzerland), is located on a bend of one of the largest fault zones in the Alps (the Rhone Fault Zone), that promote production of small rock elements.

REFERENCES

- Clarke, B.A., and Burbank, D.W., 2010, Bedrock fracturing, threshold hillslopes, and limits to the magnitude of bedrock landslides: *Earth and Planetary Science Letters*.
- Dühnforth, M., Anderson, R.S., Ward, D., and Stock, G.M., 2010, Bedrock fracture control of glacial erosion processes and rates: *Geology*, v. 38, p. 423-426.
- Molnar, P., Anderson, R.S., and Anderson, S.P., 2007, Tectonics, fracturing of rock, and erosion: *Journal of Geophysical Research F: Earth Surface*, v. 112.
- Molnar, P., and England, P., 1990, Late Cenozoic uplift of mountain ranges and global climate change: Chicken or egg?: *Nature*, v. 346, p. 29-34.

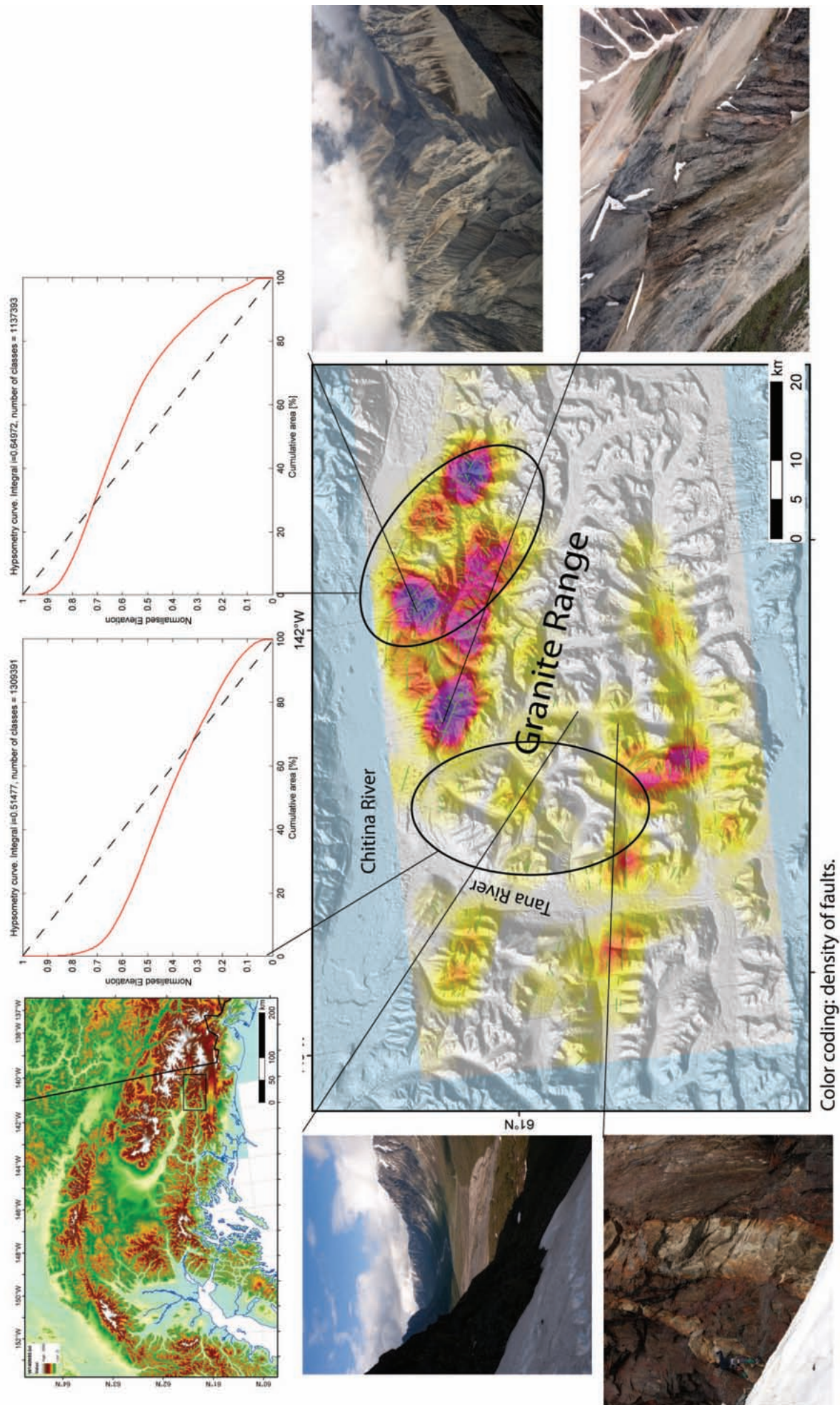


Figure 1: Localisation of working area (top left), picture of Ushaped valley (lower left), picture of massive rock (top right), picture of V shaped valley (upper right), picture of penetrative faulting and fault gouge (lower right, scale ~100m), map of fault density (center), and hypsometric integrals curves of non fractured area ($H_i=0.4$) and fractured area ($H_i=0.6$)

7.11

Influence of land use and climate change on wind erosion susceptibility in central Aragón (Spain)

Fister Wolfgang¹, Iserloh Thomas², Roche Marie A.² & Ries Johannes B.²

¹ *Physical Geography and Environmental Change, University of Basel, Klingelbergstrasse 27, CH-4056 Basel (wolfgang.fister@unibas.ch)*

² *Physical Geography, Trier University, Behringstrasse Campus II, D-54296 Trier*

For the last centuries the agricultural landscape in semi arid central Aragon (NE Spain) has been subject to climate change as well as land use change. The accompanying effects on wind erodibility of different soil surfaces in this region are largely unknown, but knowledge is required to evaluate mitigation strategies against increasing soil loss. In this study present wind erosion susceptibility is assessed based on meteorological data and land use data for the Province of Aragon in order to highlight the relative importance of climate and land use on future wind erosion susceptibility in this region.

Information about present wind erosion susceptibility in respect of the three dominating land uses in Aragon – fallow land, sheep pasturing, and dry farming – was obtained from 86 in-situ wind tunnel simulations on modified and genuine soil surfaces. Mean and maximum wind velocities at 10 m above ground and number of days with wind velocity above 10 ms⁻¹ since 1986 were analyzed, as well as mean daily precipitation and mean daily air temperature for the last five decades. The analysis of land use change focused on the development of total agricultural area, arable land, and fallow land during the last four centuries.

The considered climatic and human (land use change) impacts show a contrary signal for future development of wind erosion susceptibility in Aragon. The increase of air temperature of about 1.75°C from 1952 to 2006 and the accentuation of precipitation within the year indicate an intensification of future wind erosion susceptibility, whereas land use with increasing areas of fallow land appears to diminish it. Combined with the results of the wind tunnel test runs, which show negligible wind erosion on undisturbed, crusted surfaces (< 1 gm⁻²) and severe wind erosion on grazed (1-13 gm⁻²) and rolled surfaces (1-52 gm⁻²), reduced wind erosion susceptibility due to increasing areas of fallow land becomes evident.

Although we cannot clearly specify the relative importance of climate and land use change on wind erosion susceptibility, our results strongly suggest the importance of the combination of both in understanding future soil loss. Since human impact by land use change appears to have very immediate effects on soil loss, we conclude that mitigation strategies should focus on adapting agricultural use to minimize soil loss in the future.

7.12

Preliminary constraints on the kinetics of OSL thermochronology

Guralnik Benny¹, Herman Frederic, Lowick Sally², Preusser Frank² & Rhodes Ed³

¹ *Department of Earth Sciences, ETH, 8092 Zurich, Switzerland (benny.guralnik@gmail.com)*

² *Institute of Geological Sciences, University of Bern, Baltzerstrasse 1+3, 3012 Bern, Switzerland*

³ *Department of Earth and Space Sciences, UCLA, Los Angeles, CA 90095-1567, USA*

Utilizing the fact that temperature exerts a strong control on the retention of radiogenic products at their production sites (and hence their rate of accumulation), thermochronology is an extension of geochronology used to elucidate the cooling histories (t-T trajectories) of rocks over time (Dodson, 1973). Here we present a potential thermochronometer based on the optically stimulated luminescence (OSL) signal of bedrock quartz, with an estimated “closure” temperature of ~25-40°C (-dT/dt=10°C/Ma). In this method, the radiogenic “products” measured are electrons trapped at the naturally occurring lattice defects (electrically unbalanced sites). These electrons can be subsequently released back into the conduction band by exposure to heat and/or light. The mean lifetime τ of an electron in a particular trapping site is well described by an Arrhenius relationship of the form $\tau = s^{-1} \exp(E/kT)$, where E and s are activation energy and frequency factors, respectively, and k is Boltzmann’s constant. Reported lifetimes of the major trap types at 20°C are well beyond Ma-timescale, but for typical natural radioactivity dose rates, these traps saturate well before ~0.5 Ma.

In the current work, we analyzed the OSL signals of bedrock quartz from the KTB-VB drillhole (Southern Germany), where long-term stable temperature conditions provide a natural isothermal holding experiment at a Ma-timescale. Eleven core samples from a depth range of 560 m – 2335 m (22°C – 71°C, respectively), were processed to obtain an unbleached quartz fraction of 180-250 µm. Natural and regenerated luminescence signals were measured by stimulation with infrared and then blue light using a single-aliquot regeneration (SAR) protocol. As a function of sample depth, the measured OSL signal varies from a saturated signal at shallow depths to reset signals below a depth of 1 km (i.e., ambient rock temperature higher than 40°C). Several unstable trapping sites with potentially different closure temperatures are suggested by comparison of the natural to regenerated signals.

7.13

Late Miocene to Present landscape evolution in Northern Switzerland

Kuhlemann, J., Rahn, M.

Swiss Nuclear Safety Inspectorate ENSI, Industriest. 19, CH-5200 Brugg (KUJ@ensi.ch)

A lively discussion started in 2004, when Cederbom et al. (2004) presented new thermochronologic data from drillholes in the Swiss part of the North Alpine Foreland Basin (NAFB), which indicated an exhumation pulse by about 5 to 3.6 Ma (Early Pliocene). This time span includes the rapid increase of erosion in the Swiss Alps at the Miocene-Pliocene boundary at about 5.3 Ma and in the Eastern Alps by about 3.5 Ma (Kuhlemann et al. 2002). The drawback of all these age estimates is that they are within the range of error of the respective methods. The discussion on the implications of these ages is dedicated to the role of climate and tectonics, which is further complicated by positive feedbacks.

A potential climate trigger would be increased storminess and precipitation following an intensification of the Gulf Stream during shoaling and closure of the Panama gateway between the Atlantic and Pacific Oceans.

A potential tectonic trigger would be a slab breakoff below westernmost Swiss Alps in the latest Miocene which migrates eastward, affecting the Swiss Alps well before the Eastern Alps by rapid uplift. The NAFB would follow isostatic rebound responding to accelerated erosion in the Alps.

The problem is that both triggers potentially had much more limited effect in case of the NAFB as compared to the Alps. Strengthening of the Gulf Stream appears to have been gradual, and independent evidence of dramatically increased precipitation between 4.5 and 4.0 Ma is missing. Rapid uplift of the Alps would affect the NAFB after some response time and only by a minor part of the amount of uplift which had affected the Alps, too weak to cause a thermochronologic signal. We will present a new interpretation based on a landscape evolution model which is compatible with all existing data sets. Additional data to be considered are cemented earliest Pleistocene proglacial gravel about 300-400 m above present local base level. These prove foreland incision rates of less than 0.2 mm/a since about 2.5 Ma which limits the main pulse of erosion in the NAFB to a time between 2.5 Ma and 4.5 Ma. Moreover, within this short period of time not only a minimum of 500 m of denudation (typically 1-1.5 km must have occurred, but also a planation surface has been created which is locally covered by gravel of the paleo-Aare river.

Our solution proposes long-term uplift of the Swiss Jura foldbelt after about 11 Ma and residual subsidence of the NAFB in a piggy-back setting, controlled by aggradation in the rear of the Jura main thrust. Uplift of the Swiss Alps after 5.3 Ma enhanced erosion in the Alps and deposition of gravel in the NAFB. Maximum aggradation in the NAFB should have occurred at the eastern end of the actively deforming Swiss Jura fold belt. By a certain time, aggradation by the river paleo-Aare enabled a stepover towards the later upper Rhine valley at the boundary between the Black Forest and the Swiss Jura.

At this time, the Rhine catchment ended in the vicinity of Freiburg in the Upper Rhine graben, and the paleo-Aare was captured by a tributary of the Doubs-Rhone by about 4.2 Ma. Catchment cannibalism, however, can only held responsible for fast erosion and exhumation of the Swiss NAFB, if enough potential relief energy between the Swiss NAFB and the Doubs-Rhone has been accumulated until the capturing event. This relief energy seems to have been built up between about 11 and 4.2 Ma during northward thrusting of the Jura foldbelt on a 6°-south-dipping thrust plain. Today, gravel of the Aare-Danube are preserved at 850 altitude in the westernmost Swabian Alb which means that at the same (unknown) time before 4.2 Ma, the locus of river capture was virtually situated even higher. Certainly, the true land surface in the river bed of the Aare-Danube the locus of river capture was less high than at present, since northern Switzerland and southern Germany is subjected to long-term uplift, and rapid erosion in the Swiss NAFB must have caused additional isostatic rebound.

Much more difficult to explain is the planation phase a, after 4.2 Ma and before 2.5 Ma, given the fact that 0.5 to 1.5 km of Molasse sediments in the Swiss NAFB have been eroded during this time span, which appears to be in conflict with a phase of planation. We speculate that the erosion pulse was interrupted by a temporal blocking of the Aare-Rhone, caused by south-directed gravitational gliding of the so-called Mettau thrust sheet from the southern flank of the Black Forest into the rapidly incised valley which today hosts the upper Rhine. A single gravel deposit on this planation surface, preserved at Geissberg above the Aare valley which crosses the easternmost part of the Swiss Jura, testifies a phase of aggradation at the end of the planation phase, prior to earliest Pleistocene proglacial gravel deposition. Such a phase of Late Pliocene aggradation is not expected in the course of the inferred development of a dammed lake. Although such a lake, temporally forming behind a large landslide, should have finally been filled by river sediments, the natural landslide dam is expected to have been incised by river overflow. Hence, aggradation of gravel on the planation surface without a climate trigger is not to be expected. Possibly, the gravel aggradation was caused by the short glaciation event. Alternatively, local karst formation on the Geissberg has facilitated preservation of gravel.

REFERENCES

- Cederbom, C.E., Sinclair, H.D., Schlunegger, F., Rahn, M. 2004: Climate-induced rebound and exhumation of the European Alps. *Geology* 32, 709-712.
- Kuhlemann, J., Frisch, W., Székely, B., Dunkl, I., Kázmér, M. 2002: Post-collisional sediment budget history of the Alps: Tectonic versus climatic control. *Int. J. of Earth Sciences*, 91/5: 818-837.

7.14

Flood-induced changes in the step-pool morphology of a steep mountain stream

Molnar Peter¹, Densmore Alexander L.², McArdeell Brian W.³, Turowski Jens M.³ & Burlando Paolo¹

¹ Institute of Environmental Engineering, ETH Zurich, CH-8093 Zurich (molnar@ifu.baug.ethz.ch)

² Department of Geography, Durham University, United Kingdom

³ Swiss Federal Research Institute WSL, CH-8903 Birmensdorf

Steep mountain streams often develop a distinct step-pool morphology, in which coarse particles form a riser which spans the entire channel width and below which a plunging pool develops. Step formation is influenced by flow magnitude, local channel width, bed particle size and distribution, sediment transport, and the presence of woody debris (Chin and Wohl, 2005; Church and Zimmermann, 2007). In general, the step-pool morphology is considered to be stable for small to moderate discharges; however, high magnitude floods can destabilize many steps and generate a wave of sediment propagating through the system. There are very few field-based datasets that document these impacts and field studies are needed to quantify and interpret the nature of these changes.

It is our goal in this paper to provide a detailed field-based analysis of changes in the step-pool morphology of a well-studied mountain stream, the Erlenbach in Switzerland (WSL experimental basin in Alpthal), after the largest recorded flood in 2007 (return period of about 50 yrs). We use one pre-flood (2004) and two post-flood (2007 and 2010) longitudinal surveys of a 650 m long study reach to address two main research questions: (a) do extreme floods such as the 2007 event change the step-pool morphology into a state that is less organized (more variable); and (b) can the effect of the 2007 flood be quantified by looking at the longitudinal profiles before and after the flood with statistical scaling methods?

The longitudinal surveys were analyzed with the critical slope method of Milzow et al. (2006) to extract steps and determine their height H and spacing L (step length). The analysis of the statistical distributions of H and L before and after the flood show significant differences (Figure 1). Most notable is an increase in the variance of both distributions: the standard deviation increased by 30% for H and 50% for L after the flood. At the river reach scale, the correlations between step properties both pre- and post-flood were generally weak, and there is no evidence for self-organization into geometrically regular sequences.

By comparing the longitudinal we found that the flood led to widespread erosion of the river bed, followed by aggradation in the most recent period. Locally up to 2-3 m of vertical channel change was observed and about 1800 m³ of sediment was eroded from the study reach, which is substantially more than accumulated on the river bed in periods without large floods. The eroded volume from the study reach and the unknown input of sediment from upstream could easily supply the sediment volume collected in the retention basin after the flood which was estimated to be about 1650 m³ (Turowski et al., 2009).

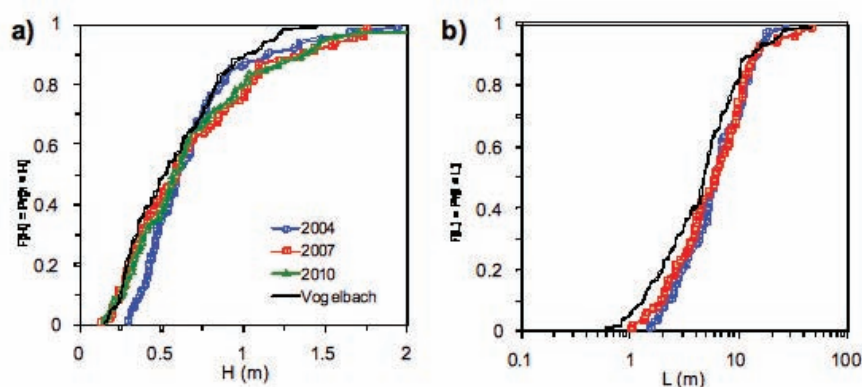


Figure 1. The empirical cumulative distribution for a) step height H and b) step spacing L in the Erlenbach pre-flood (2004) and two post flood profiles (2007, 2010). The pre-flood neighbouring stream Vogelbach is also shown.

Although steps were distributed along the whole channel length, the largest steps were constrained to the central reaches of the study reach where hillslope landslides are most active (Schuerch et al., 2006). We found that at least 60% of the steps moved during the flood, regardless of their size, which would have contributed to the destabilization of the river bed, increased sediment transport during the flood, and increased sediment supply on the river bed after it.

Finally we investigated the pre- and post-flood step-pool profiles with a statistical scaling approach which identifies the complexity of the spatial organization in the longitudinal profile. We applied the scaling technique to the increments of the resampled longitudinal profile to detect differences between the pre- and post-flood sequences. We found a multiscaling signature in the step sequences both before and after the flood, which is an indication of complex structure in the step morphology. Pool sequences also showed a strong multiscaling signature in the pre-flood profile, where pools have had time to form, and a tendency to simple scaling after the flood.

REFERENCES

- Chin, A., & Wohl, E., 2005: Towards a theory for step pools in stream channels, *Prog. Phys. Geogr.* 29, 275-296.
- Church, M., & Zimmermann, A., 2007: Form and stability of step-pool channels: research progress, *Water Resour. Res.* 43, doi:10.1029/2006WR005037.
- Milzow, C., Molnar, P., McArdeell, B.W., & Burlando, P., 2006: Spatial organization in the step-pool structure of a steep mountain stream (Vogelbach, Switzerland), *Water Resour. Res.* 42, doi:10.1029/2004WR003870.
- Schuerch, P., Densmore, A.L., McArdeell, B.W., & Molnar, P., 2006: The influence of landsliding on sediment supply and channel change in a steep mountain catchment, *Geomorphology* 78, 222-235.
- Turowski, J.M., Yager, E.M., Badoux, A., Rickenmann, D., & Molnar, P., 2009: The impact of exceptional events on erosion, bedload transport and channel stability in a step-pool channel, *Earth Surf. Process. Landforms* 34, 1661-1673.

7.15

Present erosion and landscape evolution in the glacially overprinted Alps

Salcher, B.C., Kober, F., Willett, S.D.

Geological Institute, ETH Zürich, CH-8092 Zürich, (bernhard.salcher@erdw.ethz.ch)

Glaciers overprinted mountain landscapes and generally increase the relief of landscapes. Alpine basins affected by glacial sculpting have common mean slopes between 25° and 37° except in some extremely high erodible rock settings where mean slopes can be as low as 20°. In these high mean slope basins denudation rates vary substantially. The increase of erosion rates is non-linear and insensitive to basins mean slope. Detachment-limited hillslope processes are supposed to be the dominant control in such settings (e.g. Binnie et. al, 2007)

In order to investigate factors controlling the erosion rates of glacially sculpted basins in the European Alps we derived geomorphometric data from 30 m DEMs and compiled data on erosion rates obtained from ¹⁰Be (Wittmann et al., 2007), furthermore on geology, vegetation and precipitation. We show that the total length of streams per basin exhibits a negative, linear correlation with denudation rates in basins with mean slope larger than 25°. Similar, the number channel heads per catchment decrease with increasing erosion rates. It is striking that in such basins high erodible rocks show a generally reduced drainage density in contrast to areas with low erodible rocks. Hillslope processes may counteract fluvial incision by horizontal rock mass advection (Korup and Schlunegger, 2007) and control channel initiation. In accordance, a lower drainage density reflects lower hillslope stability and higher erosion rates and vice versa. Hence, drainages per catchment might be a mirror for the hillslope activity (Howard, 1997). Different slopes of the drainage density/erosion rate regression in different parts of the Alps show that other factors may play an additional important role. Using the regressions we extrapolate recent erosion rates on a orogen scale to make statements on catchment wide denudation of Alpine basins with high mean slopes (basically most glacially sculpted basins). Drainage density also gives insights on the relation of the impact of glacial erosion and present erosion rates, indicating clear difference of basins which are affected only by peak glaciations and basins with multiple glacial erosion history.

REFERENCES:

- Binnie, S. A., Phillips, W. M., Summerfield, M. A., Fifieldm K.L., 2007: Tectonic uplift, threshold hillslopes, and denudation rates in a developing mountain range. *Geology* 35, 743-746.
- Howard, P.A. (1997): Badland morphology and evolution: Interpretation using a simulation model. *Earth Surface Processes and Landforms* 22, 211-217.
- Korup, O., Schlunegger, F., 2007: Bedrock landsliding, river incision, and transience of geomorphic hillslope-channel coupling: Evidence from inner gorges in the Swiss Alps. *Journal of Geophysical Research* 112, F03027, doi:10.1029/2006JF000710.
- Wittmann, H., von Blanckenburg, F., Kruesmann, T., Norton, P., Kubik, P.W. (2007): Relation between rock uplift and denudation from cosmogenic nuclides in river sediment in the central Alps of Switzerland. *Journal of Geophysical Research-Earth Surface* 112, doi:10.1029/2006JF000729.

7.16

Internal structure and permafrost characteristics of the Lapires talus slopes (Nendaz, Valais)

Scapozza Cristian¹, Lambiel Christophe¹, Abbet Damien², Delaloye Reynald² & Hilbich Christin³

¹Institut de Géographie, Université de Lausanne, Anthropole-Dorigny, CH-1015 Lausanne
(cristian.scapozza@unil.ch ; christophe.lambiel@unil.ch)

²Département des Géosciences, Géographie, Université de Fribourg, Chemin du Musée 4, CH-1700 Fribourg
(damien.abbet@unifr.ch ; reynald.delaloye@unifr.ch)

³Glaciology, Geomorphodynamics & Geochronology, Department of Geography, University of Zurich, Winterthurerstr. 190, CH-8057 Zurich
(christin.hilbich@geo.uzh.ch)

In order to determine the spatial extension and the characteristics of permafrost within alpine talus slopes, the Lapires site (northern orientation, 2380 – 2700 m a.s.l.), located in the western part of the Swiss Alps (Valais Alps), was studied using borehole drilling and electrical resistivity tomography (ERT) profiles. The Lapires site can be considered as a ventilated periglacial talus slope, where the special patterns of permafrost distribution can be partially related to the thermal regime influenced by internal air advection (see Delaloye & Lambiel 2005).

Three boreholes were drilled in summer 2008 along an upslope-downslope transect in the western part of the talus slope (fig. 1). Frozen sediments are present only in the two lowest boreholes, whereas the upper borehole does not present ice. The presence of permafrost is confirmed by ground temperatures registered in the boreholes. The stratigraphy of the boreholes is known thanks to direct observations and movies recorded with a hand-made borehole camera.

In borehole B11/08 (lower part of the slope, 40.0 m depth) and B12/08 (middle part of the talus, 35.0 m in depth), 4.0 m of unfrozen sediments are present above respectively 20.0 m and 16.0 m of ice and blocks. Finally, borehole B13/08 is 15.5 m depth and does not present ice. In the three boreholes, the bedrock was not reached.

Several ERT profiles were realised in summer 2008, 2009 and 2010. Two fix ERT profiles were installed in the slope in summer 2006/2007, whereas other sub-parallel ERT profiles were carried out on an upslope-downslope transect in summer 2008 and 2010. The other parallel ERT profiles are perpendicular to the slope and cross the upslope-downslope profiles. All the upslope-downslope profiles show a difference in resistivities between the upper and the lower part of the slope, where a complex and discontinuous resistive body with values higher than 50 kΩm is present. In the uppermost part of the profiles, the resistivities are lower than 10-15 kΩm.

The borehole data allowed the stratigraphy obtained from the ERT inverted profiles to be validated, concerning the distribution of frozen sediments as well as the depth of the detected structures. The results confirm that, in the Lapires site, permafrost is present in the lower parts of the talus slopes, whereas it is absent in the upper parts, as pointed out by other in situ investigations carried out in two other talus slopes of the area (Scapozza et al. 2010).

REFERENCES

- Delaloye, R. & Lambiel, C. 2005: Evidence of winter ascending air circulation throughout talus slopes and rock glaciers situated in the lower belt of alpine discontinuous permafrost (Swiss Alps). *Norsk Geografisk Tidsskrift*, 59, 194-203. DOI: 10.1080/00291950510020673.
- Hilbich, C., Hauck, C., Delaloye, R. & Hoelzle, M. 2008: A geoelectric monitoring network and resistivity-temperature relationships of different mountain permafrost sites in the Swiss Alps. *Proceedings of the Ninth International Conference on Permafrost*, Fairbanks, Alaska, 1, 699-704.
- Scapozza, C., Lambiel, C., Baron, L., Marescot, L. & Reynard, E. 2010: Internal structure and permafrost distribution in two alpine periglacial talus slopes, Valais, Swiss Alps. *Geomorphology*, submitted.

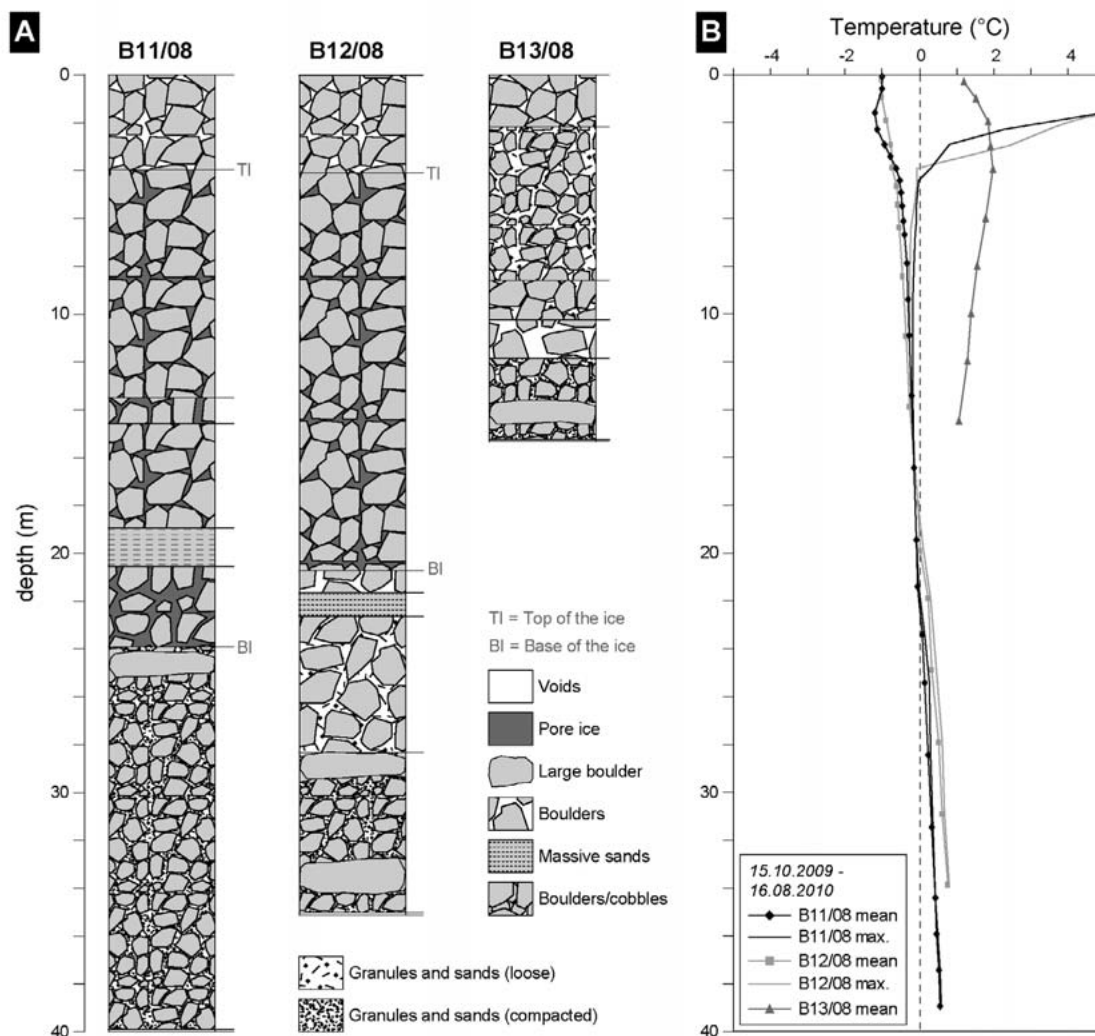


Figure 1. Stratigraphy (A) and thermal profiles (B) of the three boreholes on the Lapires talus slope.

7.17

Variability of topsoil organic carbon in semi-arid areas at different spatial scales

Wolfgang Schwanghart¹ & Thomas Jarmer²

¹ *Geologisch Geography and Environmental Change, Department of Environmental Sciences, University of Basel, Klingelbergstr. 27, CH-4056 Basel (w.schwanghart@unibas.ch)*

² *Institute for Geoinformatics and Remote Sensing, University of Osnabrueck, Barbarastrasse 22b, D-49076 Osnabrueck*

A key uncertainty in our understanding of the global carbon cycle is the lateral redistribution of carbon through the terrestrial system driven by erosion and deposition of soil derived particles (Kuhn et al., 2009). These processes create spatial patterns of soil organic carbon (SOC) depletion and accumulation in soils. Since soils are the major storage of carbon in the terrestrial biosphere, reliable estimates of spatial patterns of SOC are required for greenhouse gas inventories and carbon mitigation projects.

In order to generate SOC inventories various techniques of data gathering, analysis and modelling are required to obtain reliable results on SOC distribution. Here we present a combination of techniques comprising remote sensing, terrain analysis (Schwanghart & Kuhn, 2010) and geostatistics. Their application is exemplified with studies carried out in southern Spain and Israel.

The aim of the study carried out in Spain is to characterize spatial patterns of SOC in a Mediterranean, semi-arid area at different spatial scales and to assess the relationship between these patterns and terrain. We adopt a remote sensing based approach for the estimation of SOC in the topsoil. This approach utilizes the statistical relation between visible and near-infrared spectra of soils and SOC retrieved by Partial Least Squares (PLS) regression. Spatially distributed estimates (resolution 6 m) of SOC are obtained from the transfer of the statistical model to airborne hyperspectral data (HyMAP). Geostatistical techniques and digital elevation model analysis are used to characterize spatial patterns of SOC.

A similar approach was adopted in the Negev, Israel to derive spatial information on SOC distribution. Here, our focus was small scale variability of SOC and their relation to vegetation patterns and terrain.

The results indicate that the semi-arid hydrological and geomorphological process domain in both study areas exerts strong control on the lateral distribution of SOC generating high, small scale variability but also spatially contiguous patterns at larger scales. We conclude that hyperspectral remote sensing can be successfully applied to quantify the spatial distribution of SOC and provide a methodological framework for the analysis of the data.

REFERENCES

- Kuhn, N. J., Hoffmann, T., Schwanghart, W., Dotterweich, M. (2009): Agricultural Soil Erosion and Global Carbon Cycle: Controversy over?. *Earth Surface Processes and Landforms*, 34, 1033-1038.
- Schwanghart, W., Kuhn, N. J. (2010): TopoToolbox: a set of Matlab functions for topographic analysis. *Environmental Modelling & Software*, 25, 770-781.

7.18

Hypsometric analysis of glacial landscapes and its application to the European Alps

Pietro Sternai¹, Frédéric Herman¹, Matthew Fox¹ & Sébastien Castelltort¹

¹Eidgenössische Technische Hochschule - ETH Zurich (pietro.sternai@erdw.ethz.ch)

We investigate to what extent the hypsometric analysis of digital elevation models may be used to distinguish between glacial and fluvial landscapes.

Using theoretical topographies and a landscape evolution model, our results, similarly to other studies (Strahler, 1952; Brocklehurst & Whipple, 2004; Egholm et al., 2009), suggest that hypsometric curves can record how a fluvial-dominated landscape evolves to a glacial one (and vice-versa).

However, it appears difficult to use the hypsometric integral to assess the amount of glacial imprint on mountains. We derive here a new morphometric parameter that we term the hypsokyrto, which describes how the slope of the hypsometric curve evolves when landscapes switch between fluvial to glacial-dominated conditions.

We test the effectiveness of the hypsometric integral and hypsokyrto with a morphometric analysis of the Ben Ohau Range, New Zealand. With a numerical model we further test the geomorphic parameters in describing the morphologies of regions undergoing diverse climatic and tectonic conditions. The hypsokyrto has the advantage that it depends on the amount of glacial imprint and enables the production of maps that highlight regions where glacial erosion was maximized.

We use SRTM data and focus on two alternative geomorphic settings: the European Alps and the Apennines. The former has been affected by both fluvial and glacial erosion while the latter mainly exhibits a fluvially-dominated morphology.

The results demonstrate the efficiency of the hypsokyrto in differentiating domains affected by glacial and fluvial erosion. These observations, combined with present-day and last glacial maximum (LGM) equilibrium line altitudes (ELAs), suggest the prevalence of a "glacial buzzsaw" in the Alpine range, indicating that climate may put a limit on its topography.

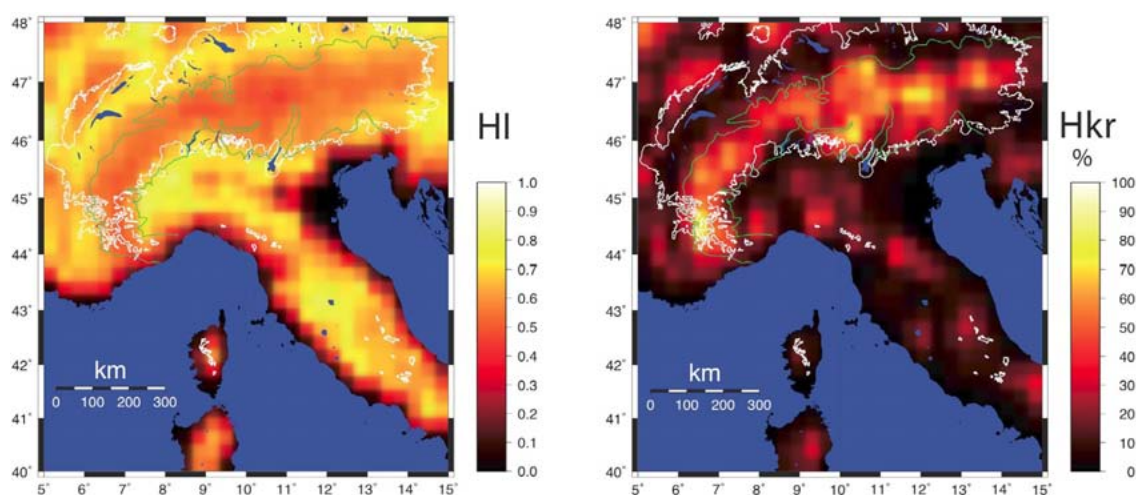


Figure 1. Maps of the hypsometric integrals (left) and hypsokyrto (right). The white line represents the Last Glacial Maximum (LGM) ice extent and the green lines delimit the region where the glaciated bedrock is exposed.

REFERENCES

- Brocklehurst, S., and Whipple K. X. 2004: Hypsometry of glaciated landscapes, *Earth Surface Processes and Landforms*, 29(7), 907-926.
- Egholm, D. L., Nielsen, S. B., Pedersen, V. K. & Lesemann J.-E. 2009: Glacial effects limiting mountain height, *Nature*, 460, 884-887.
- Strahler, A. 1952: Hypsometry (area-altitude) analysis of erosional topography. *Bull. Geol. Soc. Am.*, 63, 1117-1142

7.19

Vegetation border lines and border line ecotones influenced by geomorph dynamic processes.

An example of the timber line development since 1920 in the area of Grindelwald (Bernese Oberland).

Sarah Christine Strähl¹, Prof. Dr. N. J. Kuhn²

¹*Institut of Geography, Klingelbergstr. 27, CH-4056 Basel (sarah.straehl@unibas.ch)*

²*Institut of Geography, Klingelbergstr. 27, CH-4056 Basel*

Climate, soil, water and anthropogenic factors determine spatial patterns of vegetation, which appear as boundary ecotones ('treeline') in the landscape. The shift of boundary ecotones is considered to be an important indicator for the direction and the extent of the impact of global climate and environmental change on vegetation. The structure of expanding boundary ecotones is controlled by succession processes. The duration of succession can be several 100 years, but observed values in mountains vary widely depending on factors such as soil development and vegetation dispersion. Grindelwald is well suited to examine vegetation succession processes, due to well documented data of the glacial development during the past 100 years.

The aim of this study is to identify the role of succession for the spatial extent of border line ecotones in Grindelwald. In spite of global climate warming (1.5 °C) over the past 150 years timber lines show in several areas a decreasing trend, explaining the importance geomorph dynamic processes in the mountains for the structure and biodiversity of borderline ecotones.

Vegetation border lines and border line ecotones influenced by geomorph dynamic processes. An example of the timber line development since 1920 in the area of Grindelwald (Bernese Oberland).

REFERENCES

- Ellenberg, H. 1996. Vegetation Mitteleuropas mit den Alpen in ökologischer, dynamischer und historischer Sicht. Ulmer. Stuttgart.
- Holtmeier, F.-K. 2000. Die Höhengrenze der Gebirgswälder. Münster. Institut für Landschaftsökologie.
- Rössler, O. & Löffler, J. 2007. Uncertainties of tree line alterations due to climatic change during the past century in the central norwegian scandes. GEOÖKO. Volume / Band XXVIII. P. 104-112.
- Körner, C. 2003. Alpine Plant Life. A functional plant ecology of high mountain ecosystems. Springer. Berlin.
- IPCC-Report. 2007. Climate change 2007. Synthesis Report.

7.20

Flood hazard mapping in two Moroccan watersheds

Gabriela Werren¹, Mohamed Lasri², Emmanuel Reynard¹, Khalid Obda²

¹ Université de Lausanne, Institut de géographie, Anthropole, Quartier Dorigny, CH-1015 Lausanne (GeorgetaGabriela.Werren@unil.ch)

² Université de Fès-Saïs, Laboratoire d'Analyses Géo-Environnementales et d'Aménagement (LAGEA), Maroc.

Impacts of floods and fluvial hazards have increased during the last decades in Morocco, due to environmental changes and to rapid urban growth. In this context, the Swiss Agency for Development and Cooperation (SDC) has developed a program aimed at improving prevention and preparedness of local authorities to natural hazards. One part of this project is carried out by the universities of Fès and Lausanne and aims at preparing an indicative flood hazard map for two urbanized watersheds: Fès and Beni Mellal.

This poster presents the results of the first part of the project that is the map of water-related phenomena in the two watersheds (see also Werren et al., 2010; Lasri et al., 2010). The first step was to choose a mapping legend, based on the Swiss phenomena mapping method (Kienholz & Krummenacher, 1995) and on the French hydrogeomorphological mapping approach (Masson et al., 1996), with specific changes based on works carried out in arid and semi-arid areas. The main methodological challenge is related to the fact that the semi-arid catchments studied are prone to very irregular processes and that rain and discharge measurements are nearly absent. Field based mapping of water-related processes and landforms is, therefore, crucial to estimate hazards.

Phenomena are divided in three main morphogenetic domains: valleys, piedmonts, and alluvial plains. Another category of symbols concerns all the anthropic elements that influence the natural dynamics (presence of bridges, dikes, irrigation channels, dams, etc.). The cartographic approach faced several problems: 1) the quality of pre-existing data (e.g. plan de restitution (urban plan)) was poor and heterogeneous; 2) it was difficult to find a uniform and precise base map; 3) precise DTM are missing; 4) there was no list of former events; 5) the two watersheds have heterogeneous characteristics; it was, therefore, difficult to unify the legend; 6) important works are constantly carried out in the watersheds; there was, therefore, necessary to place a temporal limit for mapping.

The next steps will be to estimate discharge during intense events and to study – through interviews with local administrators and population – the vulnerability and its perception by local actors. Finally, an estimative map of the flood hazard will be produced.

REFERENCES

- Kienholz, H. & Krummenacher, B. 1995: Dangers naturels. Recommandations. Légende modulable pour la cartographie des phénomènes. Berne: OFEE/OFEFP.
- Lasri, M., Obda, K., Amyay, M., Taous, A. & Reynard, E. 2010: L'agglomération de Fès et sa périphérie face au risque d'inondation. Résultats préliminaires. In: Actes du colloque "Aménagement périurbain: processus, enjeux, risques et perspectives", 17-18 février 2010, sous presse.
- Masson, M., Garry, G. & Ballais, J.-L. 1996: Cartographie des zones inondables: approche hydrogéomorphologique. Ministère de l'Équipement, Ministère de l'Environnement, Les Editions Villes et Territoires, Paris: La Défense.
- Werren, G., Obda, K., Reynard, E & El Khalki, Y., E. 2010: Cartographie des phénomènes en vue de la réalisation de la carte indicative des dangers hydrologiques dans la ville de Beni Mellal, Maroc. In: Actes du colloque "La montagne marocaine: géomorphologie, environnement et développement", 5-6 mai 2010, sous presse.

7.21

Morphometric parameters and denudation rates in the Eastern Cordillera, Bolivia, affected by crustal bending?

G. Zeilinger¹, F. Kober², K. Hippe³

¹ Institute of Geosciences, University of Potsdam, Karl-Liebknecht-Str. 24/25, D-14476 Golm/Potsdam (zeilinger@geo.uni-potsdam.de)

² Institute of Geology, ETH Zurich, CH-8092 Zurich, Switzerland (kober@erdw.ethz.ch)

³ Institute of Isotope Geology and Mineral Resources, ETH Zurich, CH-8092 Zurich, Switzerland

Morphological parameters of catchments (Rio La Paz basin, Bolivia) incising the high Altiplano and draining into the Subandean zone by cutting transversely the Eastern Cordillera have been analyzed in order to understand feedback mechanism between active tectonics, focused orogenic precipitation and basin wide erosion. Specifically, a flexural rebound due to focused erosion has been postulated by Zeilinger & Schlunegger (2007). Subbasins with high erosion rates derived from cosmogenic nuclide analysis of catchment wide integrating samples in the Rio La Paz system are located close to the Cordillera, which is offset from major drainage divide, whereas subbasins with lower erosion rates are located in immediate vicinity of the Altiplano. This is in line with the proposed feedback mechanism. However, we do not recognize a correlation of mean slopes and mean relief in the subbasins and their respective erosion rates, as would be expected at first glance.

To investigate the feedback mechanism between erosion rates and surface morphology in more detail we conducted a study on the subbasins. The higher erosion rates correlate unexpectedly with a lower hypsometric integral, widely used to infer the stage of maturity of a basin. Analysis concentrates on of channel network parameters, particularly parameters like steepness index (k_s) and specific stream power (SSP) reveal the focus of erosion within the studied catchments. These spots of enhanced erosion coincide in general where bedrock incision is observed, and where the channel length profile show knickpoints. A spatial analysis of the geological properties detects those knickpoints induced by structures (faults and folds) and changes in lithology.

The cosmogenic nuclide erosion rates from the interior parts of the Rio La Paz catchments correlate only to certain extent with the surface morphology within the catchment. However, including the erosion rates and morphometric parameters from catchments sampled on the Altiplano, the correlation spanning data from both landscapes is more evident due to the extent in rates and parameters. This implies that the effects of feedback mechanisms between erosion and lithospheric deformation are substantial at the large scale. However, individual structures where the morphometry of catchments and channel morphologies are perturbed cannot be ignored. Which erosion processes (e.g. headwater expansion by landsliding and / or fluvial incision) is dominant might be influenced by tectonics and in some other parts controlled by climate-dominated processes. Consequently this may explain the spatially variable erosion rates and different surface morphologies and therefore the partly inconclusive correlations. The possible rebound effect due to enhanced erosion, located in the centre of the Rio La Pa catchment is hence only partially constrained at the moment, while more ongoing investigations further try to isolate this region.

REFERENCES

Zeilinger, G. & Schlunegger, F. (2007), Possible flexural accommodation on the eastern edge of the Altiplano in relation to focussed erosion in the Rio La Paz drainage system, *Terra Nova*, 19, 373-380,

8. Quaternary Research

Naki Akçar

Swiss Society for Quaternary Research (CH-Quat)

- 8.1 Akçar N., Deline P., Ivy-Ochs S., Christl M., Kubik P.W., Schlüchter C.: Surface exposure dating of 1717 AD rock avalanche deposits in the upper Ferret Valley (Italy) with cosmogenic ^{10}Be
- 8.2 Alpou S., Godefroid F. & Kindler P.: Origin of Bahamian laminar crusts: new geochronological and petrographic data
- 8.3 Chairi R.: Organic and mineral sedimentary deposits in the evaporators' environments of the Sahel of Tunisia (Mahdia): the Baghdadi swamp and the conjugated sebkha of Gotaia and Eliane
- 8.4 Colombaroli D., Henne P., Kaltenrieder P., Gobet E., Tinner W.: How did fire, human impact and climate change affect Holocene treeline dynamics in the Alps? A case of study from Gouille Rion (Valais, Switzerland)
- 8.5 Dehnert A., Kemna H. A., Anselmetti F. S., Drescher-Schneider R., Graf H. R., Lowick S., Preusser F., Züger A., Furrer H.: Erosion and filling of a glacially overdeepened trough in the northern Alpine Foreland as recorded in deep drill core NW09 from Niederweningen, Switzerland
- 8.6 Deplazes G., Haug G. H., Lückge A., Peterson L. C.: High-resolution sediment colour and geochemical analysis of Dansgaard-Oeschger events (Cariaco Basin, Northern Arabian Sea)
- 8.7 Girardclos S., Rachoud-Schneider A.-M., Brutsch N.: Rhone glacier deglaciation in western Lake Geneva : new sismo- and biochronostratigraphy results
- 8.8 Göktürk O.M., Fleitmann D., Badertscher S., Cheng H., Edwards L., Fankhauser A., Tüysüz O., Kramers J.: Climate in the southern Black Sea coast during the Holocene: Implications from the Sofular Cave record
- 8.9 Haghipour N., Kober F., Burg J.-P., Zeilinger G., Ivy-Ochs S., Kubik P., Faridi M.: Incision and deformation recorded by Quaternary fluvial terraces in Makran accretionary wedge, SE-Iran
- 8.10 Haudenschild E., Akçar N., Yavuz V., Ivy-Ochs S., Alfimov V., Kubik P.W., Schlüchter C.: The Kestanol Granite (Western Turkey) and its importance as a building stone: Application of cosmogenic ^{10}Be to an archaeological problem
- 8.11 Heiri O., Birks J., Brooks S., Kirilova E., Magyari E., Millet L., Mortensen M.F., Samartin S., Tinner W., Toth M., Veski S. & Lotter A.F.: European climate change at the end of the last glaciation: chironomid-based temperature reconstruction on a continental scale
- 8.12 Hippe K., Ivy-Ochs S., Kober F., Wieler R., Schlüchter C.: Reconstructing the deglaciation history of the Gotthard Pass area, Central Swiss Alps, using cosmogenic ^{10}Be and in-situ ^{14}C
- 8.13 Kind J., Hirt A., van Raden U.: Do magnetic properties reflect climate history in Swiss lakes?
- 8.14 Kremer K., Girardclos S.: Giant sub-lacustrine mass movement in Lake Geneva sediment record
- 8.15 Laigre L., Reynard E., Arnaud-Fassetta G., Baron L., Lambiel C.: Contribution of geoelectrical measurements and shallow drillings for detection of Holocene palaeochannels in the Saillon region (Valais)
- 8.16 Larocque-Tobler I., Quinlan R., Müller Stewart M., Grosjean M.: Chironomids as indicators of the past 1000 years of mean July air temperatures: the Sivaplana and Seeburgsee records
- 8.17 Lombardo U., Canal-Beeby E., Fehr S., Veit H.: Pre-Columbian human adaptation to seasonal inundations in the Llanos de Moxos, Bolivian Amazonia.

- 8.18 Malatesta L., Castelltort S., Picotti V., Mantellini S., Hajdas I., Simpson G., Willett S.: Holocene Climatic Variability In Central Asia; A Geo-Archaeological Case Study In Samarkand, Uzbekistan
- 8.19 Ott A., Ivy-Ochs S., Bauder A., Akçar N., Schlüchter C.: Holocene glacier oscillations at Damma
- 8.20 Plotzki A., Veit H.: Holocene landscape evolution of the Llanos de Moxos, NE Bolivia
- 8.21 Preusser F., Graf H.R., Keller O., Krayss E., Schlüchter C.: Quaternary glaciation history of northern Switzerland
- 8.22 Reber R., Tikhomirov D.A., Akçar N., Yavuz V., Schlüchter C.: Quaternary glacial chronology in Anatolia
- 8.23 Samartin S., Heiri O., Tinner W.: Late Glacial and early Holocene climatic changes in the Southern Swiss Alps, reconstructed using subfossil chironomid assemblages.
- 8.24 Schlüchter C., Burkhalter R.: Switzerland at the Last Glacial Maximum (LGM) A new map (2009) by swisstopo 1 : 500 000
- 8.25 Schmitt J., Seth B., Fischer H.: How to derive weathering rates from ice core measurements of atmospheric tetrafluoromethane?
- 8.26 Steinemann S., Hamann Y., Gilli A.: Detection of volcanic ash layers by high-resolution XRF core scanning
- 8.27 Stumm D., Fischer U.H., Schnellmann M., Haeberli W.: A review on tunnel valleys in northern Europe
- 8.28 Tikhomirov D., Alfimov V., Akçar N., Ivy-Ochs S., Schlüchter C.: Calibration of ^{36}Cl Production Rate on ^{39}K in Saturated Antarctica Samples
- 8.29 van Raden U., Gilli A., Kind J.: How does the elemental composition of Swiss lake sediments reflect past climate conditions?
- 8.30 Zech J., Zech R., Kubik P.W., Veit H.: Past glaciation in the Central Andes record alteration in the tropical circulation and the Southern Westerlies

8.1

Surface exposure dating of 1717 AD rock avalanche deposits in the upper Ferret Valley (Italy) with cosmogenic ^{10}Be

Akçar Naki¹, Deline Philip², Ivy-Ochs Susan³, Christl Marcus³, Kubik Peter W.³ & Schlüchter Christian¹

¹Institut für Geologie, Baltzerstrasse 1+3, CH-3012 Bern (akcar@geo.unibe.ch)

²EDYTEM Lab, Université de Savoie, CNRS, 73376 Le Bourget-du-Lac, France

³Laboratory of Ion Beam Physics, ETH Zurich, 8093 Zürich

One of the largest rock avalanches of the Alps occurred on September 12th 1717 AD in Mont Blanc Massif. In the upper Ferret Valley (Italy), a rock volume larger than 10 million m³ and a huge volume of ice from the Triolet glacier were mobilized and moved more than 7.5 km downvalley and reached the lower part of the valley (Deline and Kirkbride, 2009). This mass composed of ice and sediment destroyed two small settlements with 7 casualties and loss of their cattle.

Accumulations of granitic boulders and irregular ridges over a distance of 2 km in the upper Ferret terminate downvalley with a 5 m-high arcuate front (Deline and Kirkbride, 2009). This extensive deposit was first attributed to glacial deposits (Deline, 2009). In their detailed study, Porter and Orombelli (1980) interpreted this deposit as the rock avalanche of 1717 AD. Aeschlimann (1983) debated this interpretation and claimed that the main part of this deposit is a Lateglacial moraine (Deline, 2009). Recently, Deline and Kirkbride (2009) concluded that this deposit is a complex of glacial, an earlier rock avalanche and 1717 AD rock avalanche deposits. Can cosmogenic ^{10}Be tell us more on this dilemma?

With the aim of answering this question, 9 granitic boulders within the upper valley deposit and 3 from the boulders outside were sampled for surface exposure dating with ^{10}Be and prepared for AMS analysis. ^{10}Be exposure ages vary between 300 and 500 years within the limits of error. These exposure ages indicate that the extensive granitic boulder deposition with irregular ridges belongs to the 1717 AD rock avalanche. This relation confirms the main part of the Porter and Orombelli (1980) interpretations.

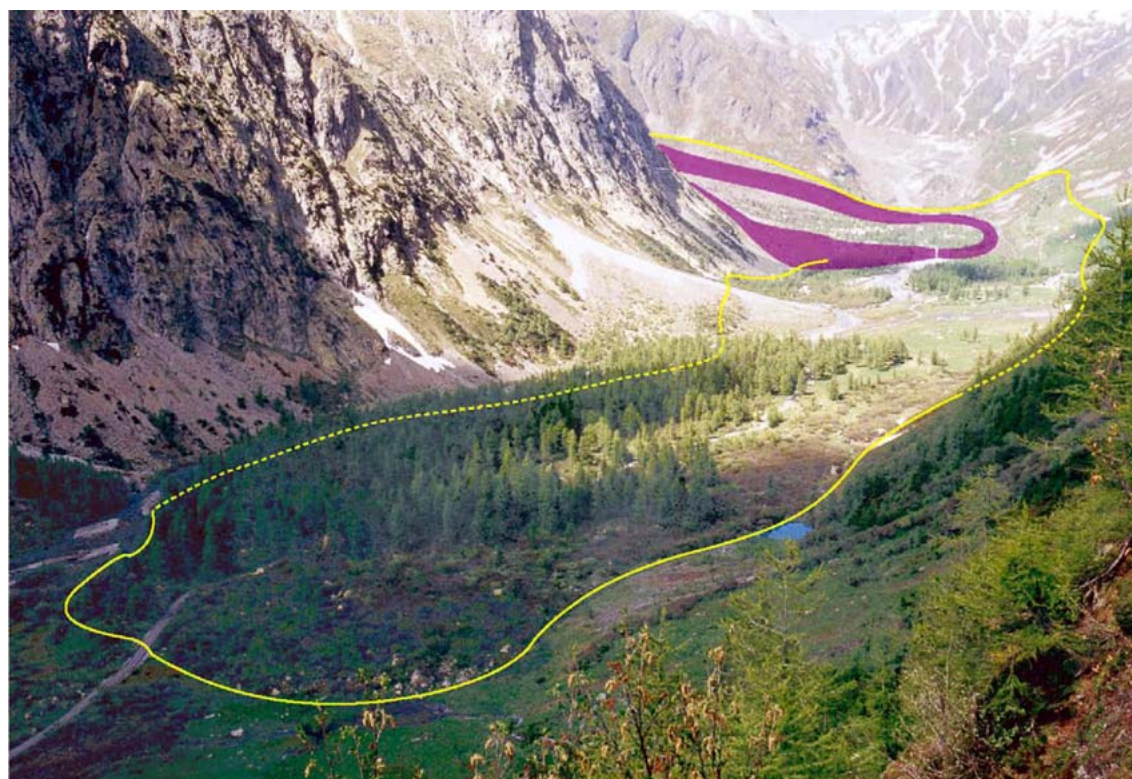


Figure 1. Deposits of upper Ferret Valley. Yellow line: extent of granitic boulder accumulations. Purple ribbon: limit of the recent morainic complex of Glacier de Triolet (Deline, 2009).

REFERENCES

- Aeschlimann, H., 1983: Zur Gletschergeschichte des italienischen Mont Blanc Gebietes: Val Veni - Val Ferret - Rutor. Ph.D. thesis, Universität Zürich, Switzerland.
- Deline, P. 2009: Interactions between rock avalanches and glaciers in the Mont Blanc massif during the late Holocene. *Quaternary Science Reviews*, 28, 1070-1083.
- Deline, P. & Kirkbride, M.P., 2009: Rock avalanches on a glacier and morainic complex in Haut Val Ferret (Mont Blanc Massif, Italy). *Geomorphology*, 103, 80–92.
- Porter, S.C. & Orombelli, G., 1980: Catastrophic rockfall of September 12, 1717 on the Italian flank of the Mont Blanc massif. *Zeitschrift für Geomorphologie*, 24, 200–218.

8.2

Origin of Bahamian laminar crusts: new geochronological and petrographic data

Alpou Sylvia¹, Godefroid Fabienne¹ & Kindler Pascal¹

¹ Section of Earth and Environmental Sciences, rue des Maraîchers 13, CH-1205 Genève (alpou5@etu.unige.ch)

Petrographic examination and radiometric dating of surficial laminar crusts collected from various Bahamian islands show that, contrary to previous thinking, these crusts mostly result from biologically controlled precipitation at the rock/atmosphere interface during the past 10 ka.

Laminar crusts are widely exposed on the Bahamas islands and have been interpreted as resulting mainly from physico-chemical precipitation during pedogenesis. Further, they have been identified as the lower horizon of a Wisconsinian paleosol, when occurring in association with clay-rich conglomerates between Pleistocene and Holocene carbonate units. To verify these hypotheses, we have examined microscopically and carbon dated several crusts collected from Mayaguana and San Salvador.

All studied profiles consist of one single, orange to brown, cm-thick crust, showing a smooth upper surface that rises and falls with the present topography. In all cases it rests on indurated Pleistocene limestone. At Green Cay (near San Salvador) and Betsy Bay (Mayaguana), the crust directly occurs at the rock/atmosphere interface, whereas at NW Point (Mayaguana) and Singer Bar Point (San Salvador) it is capped by a Holocene calcarenite, with intervening pockets of clay-rich breccia at the latter locality. The crust laminations correspond to mm-thin alternating zones of:

- (a) dense, orange, homogeneous or clotted micrite containing sparse calcitic spherulites
- (b) darker porous micrite containing rounded features with a cellular texture, and also peloids that have preserved their primary aragonitic mineralogy.

The boundary with the slightly altered underlying Pleistocene limestone is sharp, even at thin-section scale. Raw radio-carbon ages obtained from these crusts range from 9,210 to 3,270 years BP.

Our petrographic data show that biological factors, such as cyanobacterial, fungal, and pioneer-plant activity played a greater role than physico-chemical processes in the formation of these crusts. Their young age suggest that this biological activity could be related to the Holocene transgression, and that the overlying pockets of clay-rich breccia must be interpreted as a reworked soil sediment of Holocene age, rather than a Wisconsinian paleosol.

8.3

Organic and mineral sedimentary deposits in the evaporators' environments of the Sahel of Tunisia (Mahdia): the Baghdadi swamp and the conjugated sebkha of Gotaia and Eliane.

Raja CHAIRI

Laboratoire de Géoressources. Centre de technologie des eaux (CERTE), Technopole Borj cedria BP 273. 8020 SOLIMAN. TUNISIE
(Chairi_ra@yahoo.fr)

The mineral and organic sedimentary studies are realized on sedimentary columns of 1m of depth in evaporators systems in the sahel of Tunisia (Mahdia). These systems are the result of Tyrrhenian tectonic accidents.

The analysis of the organic matter by pyrolysis Rock-Eval 6 reveled the presence of a heterogeneous organic matter stock dominated by the ligneous fraction. The originated organic fraction is limited in bacteria activity. The hypersaline environments or evaporatores systems are known for the low biological variety. It is identified well by the presence of some biomarkers: alkylbenzenes (C18, C19 and C20), hopanes (norlupane ans oleane,) and steranes (stigmastane, cholestane).

silty fraction is the essential mineral fraction in the system of the Sahel from Tunisia. The quartz represents the main part of the mineral procession (90 %). Three clay minerals are presents: kaolinite, illite and smectite. Only the smectite is partially synthesized in these environments. The abundance of the kaolinite in peripheral sediments supports the significant terrigene contributions. The identified evaporates are halite, gypsum and calcite. In the center, the hailte constitutes the surface sediments.

Size distributions are influenced by the previous history of the sediment and climate condition. Clay particles are transported and deposit in the center of the system in low energy conditions. Sand located at the periphery is deposit by high energy. The presence of bimodal shape indicates the period of mudding in this evaporator system which is characterized by squat dynamic environment. However the levels of sand in the center specify the interruption by the cycle of important activity.

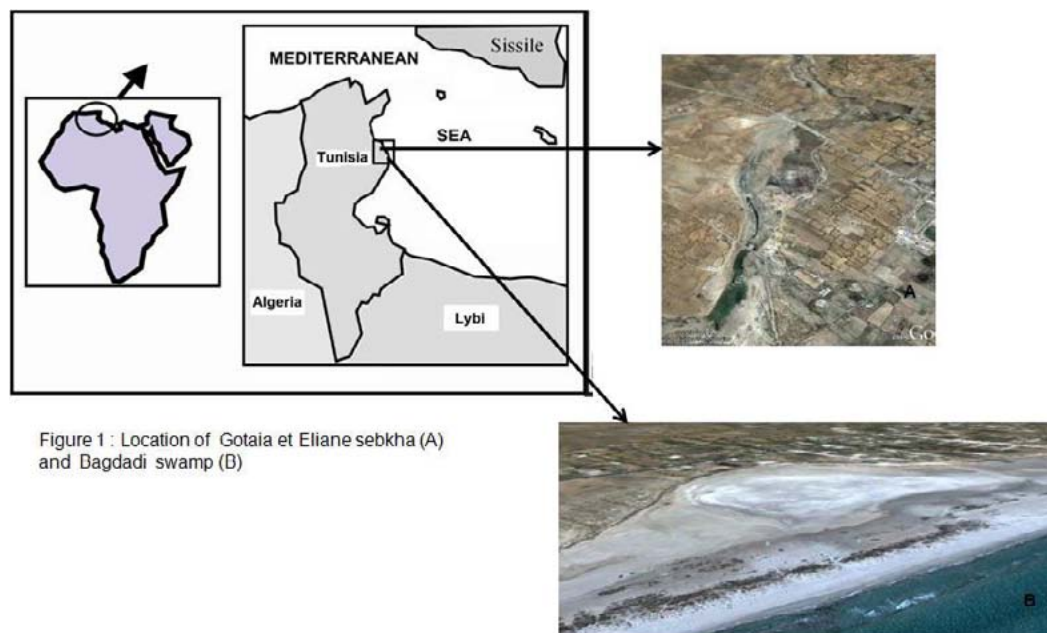


Figure 1 : Location of Gotaia et Eliane sebkha (A) and Baghdadi swamp (B)

REFERENCES

- Chairi R., Derenne S., Abdeljaoued S. & Largeau C. (2010): Sediment cores representative of contrasting environments in salt flats of the Moknine continental sabkha (Eastern Tunisia): Sedimentology, bulk features of organic matter, alkane sources and alteration.
- Chairi, R., 2005 : Etude du remplissage sédimentaire d'un système hypersalin de la Tunisie orientale au cours du quaternaire récent: la sabkha de Moknine. Quaternaire 16, 107–117.
- Disnard J.R., Jacob J. & Lavrieux M. 2008 : Marqueurs organiques et impact des activités humaines sur la sédimentation lacustre récente du Lac d'Aydat (Puy-de-Dôme). Comptes-rendus du 7ème Congrès International de Limnologie-Océanographie, Rouan, France.

8.4

How did fire, human impact and climate change affect Holocene treeline dynamics in the Alps?

A case of study from Gouillé Rion (Valais, Switzerland)

Colombaroli Daniele¹, Henne Paul¹, Kaltenrieder Petra¹, Gobet Erika¹ & Tinner Willy¹

¹ Institute of Plant Sciences and Oeschger Centre for Climate Change Research, University of Bern, CH-3013 Bern, Switzerland.

Corresponding author: daniele.colombaroli@ips.unibe.ch.

In the Alpine region, the treeline ecotone is highly sensitive to climatic and land-use changes. Rising temperatures induce upslope migration of individual species, allowing treeline expansion into unforested landscapes (Harsch *et al.* 2009). Additionally, ongoing agricultural abandonment favours afforestation in former high-elevation pastures (Rutherford *et al.* 2008). In contrast, forest fires affect the treeline ecotone, by reducing fuel loads and promoting dominance of fire-prone species. So far, few long-term paleoecological studies with high temporal-resolution investigated how fire variability affected treeline dynamics especially in the Alpine region, where people have altered fire regimes at least since the Neolithic (Gobet *et al.* 2003).

In this paper, we use a high-resolution record of macroscopic charcoal and plant macrofossil records from a lake in the Swiss Alps (Gouillé Rion, 2343 m a.s.l.) to: 1) investigate changes of biomass burning over the last 12,000 years; 2) to derive responses of tree-line vegetation to fire occurrence; 3) to disentangle the role of human vs. climatic factors for the observed variability in fire frequency. For our purposes, we used sediment charcoal to reconstruct the frequency of fire episodes around the lake (e.g. Gavin *et al.* 2007). Secondly, we used regression analyses between contiguous series of plant macrofossils, macroscopic charcoal and an available reconstruction of past summer temperature (Heiri *et al.* 2003), to derive species response to fire variability and to summer temperature. Finally, we used a dynamic landscape vegetation model (LANDCLIM), to explore potential forcing mechanisms of fire-regime change, specifically to disentangle the role of climate vs. humans on fire occurrence.

Our results show that fire was a natural disturbance agent at the treeline ecotone but since the Bronze Age (c. 4000 cal. years BP) human disturbance overrode the effect of climate in controlling fire variability. Also, anthropogenic fire and climate affected differently the composition of plant species at the treeline. For instance, when mean July temperatures were lower than modern mean July values, *Juniperus nana* and *Larix decidua* were at an advantage over *P. cembra*. With increasing anthropogenic fire, open lands with *J. nana* replaced *L. decidua* and *P. cembra* forest stands. *Pinus cembra* instead could expand during periods with temperature above the modern mean July temperature if fire disturbance was not too severe.

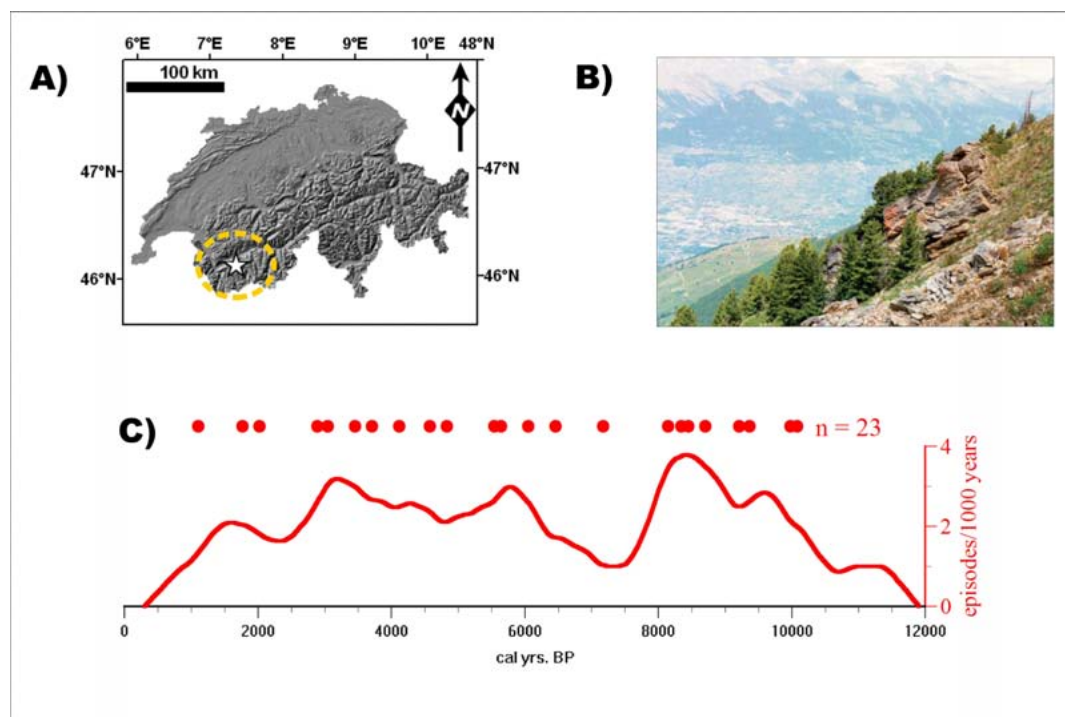


Figure 1.A) Location of the investigated site in the Valais. B) Occurrence of *Pinus cembra* near the site at the treeline (photo from Tinner 1996). C) Reconstructed local fire history over the last 12,000 years (modified from Colombaroli *et al.* in press).

Our study might be relevant for future development of Alpine ecosystems under global change scenarios, such as the response of the treeline ecotone to warming temperature and increasing anthropogenic fire (Tinner & Kaltenrieder 2005). Although climate change will alter vegetation composition, future dynamics of mountain forests will be co-determined by anthropogenic fire. For instance, high fire variability may delay or impede upslope establishment of forests in response to climatic warming as expected for this century, with serious implications for forest diversity.

REFERENCES:

- Colombaroli, D., Henne, P.D., Gobet, E., Kaltenreider, P. & Tinner, W.: Species responses to fire, climate, and human impact at tree-line in the Alps as evidenced by paleo-environmental records and dynamic simulation approaches. *Journal of Ecology* (in press).
- Gavin, D.G., Hallett, D.J., Hu, F.S., Lertzman, K.P., Prichard, S.J., Brown, K.J., Lynch, J.A., Bartlein, P. & Peterson, D.L. 2007: Forest fire and climate change in western North America: insights from sediment charcoal records. *Frontiers in Ecology and the Environment*, 5: 499-506.
- Gobet, E., Tinner, W., Hochuli, P.A., van Leeuwen, J.F.N. & Ammann, B. 2003: Middle to Late Holocene vegetation history of the Upper Engadine (Swiss Alps): the role of man and fire. *Vegetation History and Archaeobotany*, 12, 143-163.
- Harsch, M.A., Hulme, P.E., McGlone, M.S. 2009: Are treelines advancing? A global meta-analysis of treeline response to climate warming. *Ecology Letters*, 12, 10, 1040-1049.
- Heiri, O., Lotter, A.F., Hausmann, S. & Kienast, F. 2003: A chironomid-based Holocene summer air temperature reconstruction from the Swiss Alps. *The Holocene*, 13, 477-484.
- Rutherford, G.N., Bebi, P., Edwards, P.J. & Zimmermann, N.E. 2008: Assessing land-use statistics to model land cover change in a mountainous landscape in the European Alps. *Ecological Modelling*, 212, 460-471.
- Tinner 2006: Treeline studies In: Elias S.A. (ed.) *Encyclopedia of Quaternary Science* Elsevier, Amsterdam 2374-2383.
- Tinner, W. & Kaltenrieder, P. 2005: Rapid responses of high-mountain vegetation to early Holocene environmental changes in the Swiss Alps. *Journal of Ecology*, 93, 936-947.

8.5

Erosion and filling of a glacially overdeepened trough in the northern Alpine Foreland as recorded in deep drill core NW09 from Niederweningen, Switzerland

Andreas Dehnert¹, Hans Axel Kemna¹, Flavio S. Anselmetti², Ruth Drescher-Schneider³, Hans Rudolf Graf⁴, Sally Lowick⁵, Frank Preusser⁵, Andreas Züger⁶ & Heinz Furrer¹

¹ Palaeontological Institute and Museum, Karl Schmid-Strasse 4, CH-8006 Zurich (andreas.dehnert@pim.uzh.ch)

² Eawag, Swiss Federal Institute of Aquatic Science and Technology, CH-8600 Dübendorf

³ Schillingsdorferstrasse 27, A-8010 Kainbach bei Graz

⁴ Matousek, Baumann & Niggli AG, Mäderstrasse 8, CH-5401 Baden

⁵ Institute of Geological Sciences, Baltzerstrasse 1+3, CH-3012 Bern

⁶ Oeschger Centre for Climate Change Research, Zähringerstrasse 25 CH-3012 Bern

As the major weather divide in Europe, the Alps represent one of the most interesting areas for understanding past climate change and its impact on continental environments. However, our knowledge of the Quaternary environmental history of the region is still rather limited, especially for the time preceding the last glaciation of the Alps.

Geological and geophysical studies in the Wehntal, 20 km northwest of Zurich, in 2007 and 2008 have revealed the existence of a glacially overdeepened trough cut into Miocene molasse bedrock, which is today filled with ~90 to 180 m of Quaternary sediments.

In March 2009, a 93.6 m long sediment core NW09/1 has been drilled down to bedrock east of a famous mammoth-site in Niederweningen. This drill core represents one of the very few records in the northern Alpine Foreland that provides crucial insights into timing of erosion and infilling history of pre-Eemian glacially overdeepened structures and also helps to understand the climate and environmental history of multiple glacial-interglacial cycles.

On the basis of multi-proxy data and extended luminescence chronology, the recovered sediment succession is interpreted from bottom to top as: 4.1 m of in-situ molasse bedrock, overlain by 3.4 m of diamictic till. The glacial sediment was deposited by a lobe of the combined Walensee branch of Rhine Glacier and the Linth Glacier during Marine Isotope Stage (MIS) 8. It is suggested that this extensive ice advance, which once covered the entire Wehntal valley, caused the final erosion of the bedrock. The till merges seamlessly into a 29.5 m thick sequence of laminated, carbonate-rich, fine-grained siliciclastic sediments that are interpreted as proglacial lake sediments, which accumulated also during MIS 8. This unit was likely deposited in a proximal setting to a calving glacier-front confirmed by the presence of numerous dropstones.

The damming of this Wehntal palaeolake was most likely caused by a terminal moraine located ~3 km to the northwest of the drill site. The overlying 37.9 m of fine-grained lake sediments are comparable to the former unit, but absence of dropstones indicates a more distal proglacial lake facies and thus, a retreat of the feeding glacier lobe.

Low organic carbon contents point to almost no biological activity within the lake and suggest cold environmental conditions. Feldspar luminescence dating showed that the formation of this unit occurred over the whole MIS 7. This unit is unconformably overlain by 9.5 m of fine-grained material. The hiatus covers almost the complete MIS 6, which is believed to represent a major glaciation of the northern Alpine Foreland.

Although, a striking drop in carbonate content (from ~45 to 20 wt%) and shear strength, as well as an increase in grain-size (from clayey silt to fine sand) can be noticed, no obvious erosional features can be seen in the sediment fabric. The change in carbonate content is interpreted as a decoupling of the Wehntal catchment from the Rhein/Linth Glacier systems that originate in a carbonate-rich hinterland.

The top of the unit documents a gradual infilling of the palaeolake and onset of biological productivity due to climate warming during early MIS 5. This is also documented by occurrence of post-sedimentary pyrite and siderite concretions.

The prominent environmental change culminates in the abrupt accumulation of peat (1.8 m) during late interglacial MIS 5e (Eemian). Afterwards, the Wehntal was reoccupied by a younger palaeolake flooding the peat. The resulting 4.9 m of bluish-gray silty sediments have carbonate contents of ~25 wt% and relative high organic carbon contents (~1 wt%). Luminescence dates put this sediment unit into early MIS 3.

The source of sediment is interpreted as derived from the molassic Zurich Highlands and the Jurassic limestone of the Lägern mountain chain, which borders the Wehntal valley to the south. The actual cause of rise in water level subsequent to deposition of the Eemian peat, however, has not yet been identified.

Thereafter, the younger palaeolake was filled, resulting in the accumulation of 0.7 m of fossil-rich Middle Würmian peat, the so called 'Mammoth peat', which was finally covered with 2.0 m of post-Würmian-to-recent alluvial silts and sands.

8.6

High-resolution sediment colour and geochemical analysis of Dansgaard-Oeschger events (Cariaco Basin, Northern Arabian Sea)

G. Deplazes¹, G. H. Haug¹, A. Lückge², Larry C. Peterson³

¹ Geological Institute, ETH Zürich, Sonneggstr. 5, CH-8092 Zürich, Switzerland (gaudenz.deplazes@erdw.ethz.ch)

² Federal Institute for Geosciences and Natural Resources, Stilleweg 2, D-30655 Hannover, Germany

³ Rosenstiel School of Marine & Atmospheric Science, University of Miami, 4600 Rickenbacker Causeway, FL 33149, USA

The anoxic Cariaco Basin on the northern shelf of Venezuela preserves detailed records of past tropical climate variability. The sediment formation in this basin is controlled by the migration of the Atlantic Intertropical Convergence Zone (ITCZ) and the corresponding rain belt and trade winds. In the oxygen minimum zone off Pakistan in the northern Arabian Sea sediment archives of low-latitude monsoonal climate are preserved.

In this study sediments from the two settings that cover the last 80'000 to 110'000 years are compared with Greenland ice core records. Sediment colour analysis resulted in reflectance records with down to annual resolution. The reflectance records of the Cariaco Basin and the northern Arabian Sea faithfully mimic the Greenland ice core $\delta^{18}\text{O}$ record. An age model was set up by correlation of these records to the $\delta^{18}\text{O}$ record of NGRIP. The major element chemistry of the sediments was analysed with X-ray fluorescence scanning.

Colour variations in these marine sediments reflect changes in redox state and relative contributions of terrigenous and biogenic components. Changes in anoxia and productivity can be further explored using element proxies as molybdenum, manganese and bromine. Variability in the terrigenous input can be traced by elemental proxies as titanium.

The new high resolution proxy records indicate an unbroken association between warm climate conditions over Greenland, a northerly position of the Atlantic Intertropical Convergence Zone, and a strong Indian summer monsoon since the last glacial. The tight coupling is explained by a dominant role of the North Atlantic that is communicated largely through the atmosphere. New insights of dynamical mechanisms arise from comparison of individual Dansgaard-Oeschger events that suggests a threshold response of the tropics to North Atlantic cooling.

8.7

Rhone glacier deglaciation in western Lake Geneva : new sismo- and bio-chronostratigraphy results

Girardclos Stéphanie¹ Rachoud-Schneider Anne-Marie² & Brutsch Nicolas¹

¹ Dept Geology and Palaeontology, University of Geneva, Rue des Maraîchers 13, CH-1205 Geneva (stephanie.girardclos@unige.ch)

² Route de St-Cergue 116b, CH-1260 Nyon

Seismic reflection and geotechnical drilling were performed in spring 2009 in the western part of Lake Geneva within a public project to build a large bridge over the lake. Scientific analyse of this seismic and sediment record reveals new insights in the history of the Rhone glacier deglaciation and Lake Geneva formation.

Seismic data, acquired with a 1 in³ airgun and a pinger source, images the bedrock lake basin as well as eight sismostratigraphic units of glacial, glacio-lacustrine and lacustrine facies. In the eastern part of studied area, gas reduces seismic data quality but nevertheless, the lateral asymmetry of the basin geometry and of the sediment infill appears. In the western part, the bedrock (i.e. Molasse) forms a 3° ramp bending toward east which is topped by only maximum 30 m of sediment. In the centre and eastern part of the lake basin, the bedrock lies deeper and is covered by 70 to 110 m of glacial to lacustrine units.

The deepest unit (U1), which was detected on seismic lines but not drilled, is interpreted as glacial sediments left during an older glacial cycle (Fiore 2007). It is topped by the thick U6b and U7 units, interpreted as melt-out till of the Rhone glacier. Four 35 to 75 m-deep drillings confirm this interpretation and show that unit U6b was certainly compacted by a

re-advance of the Rhone glacier. This data reveals a new glacial stage, older than stages of Coppet and Nyon, with a glacial front near 'Le Reposoir'. The asymmetry of unit U7 also shows that the glacier melted first in the central and eastern part of the lake basin while it was still lying on the Molasse 'ramp' in the West.

The next sequence, represented by units U8-U12, is interpreted as glacio-lacustrine deposits. They have variable sedimentary facies ranging from massive silt to laminated clayed silt with rare sand layers. Gravels of alpine origin and 'galets mous' in the silty matrix, interpreted as dropstones', point to the recurrent presence of icebergs in the lake.

The seismic infill ends with lacustrine units U13-U14. These units consist of lacustrine marls with shells and organic debris. In unit U14, a thickness asymmetry between east and west side of the lake, as well as onlapping geometry toward west, point to sediment erosion and transport by currents down to 35-m-depth.

This result agrees with previous work on deep currents action in western Lake Geneva (Girardclos et al. 2003). Ongoing palynological analyses and C^{14} dating will give an age to glaciolacustrine and lacustrine units. Preliminary palynological results reveal that non-reworked pollen is surprisingly present in glacier melt-out till (U7).

This project is partly financed by the Fondation Ernest Boninchi, the Fondation Ernest et Lucie Schmidheiny and the Swiss Civilian Service. Thanks to De Cerenville Geotechnique and the State of Geneva for access to drillings and geotechnical data.

REFERENCES

- Fiore J. 2007: Quaternary subglacial processes in Switzerland: Geomorphology of the Plateau and seismic stratigraphy of Western Lake Geneva. *Terre et Environnement* 69. University of Geneva, 169 pp.
- Girardclos, S., Baster, I., Wildi, W. & Pugin A. 2003: Bottom-current and wind-pattern changes as indicated by Late-Glacial and Holocene sediments from western Lake Geneva (Switzerland). *Eclogae geologicae Helvetiae* 96 Suppl. 1, 39-48.

8.8

Climate in the southern Black Sea coast during the Holocene: Implications from the Sofular Cave record

Göktürk Ozan Mert^{1,2}, Fleitmann Dominik^{1,2}, Badertscher Seraina^{1,2}, Cheng Hai³, Edwards Lawrence³, Fankhauser Adelheid¹, Tüysüz Okan⁴, Kramers Jan¹

1: University of Bern, Institute of Geological Sciences, CH-3012 Bern, Switzerland (¹ gokturk@geo.unibe.ch)

2: Oeschger Center for Climate Change Research, CH-3012 Bern, Switzerland

3: University of Minnesota, Department of Geology and Geophysics, MN-55455 Minneapolis, USA

4: Istanbul Technical University, Eurasia Institute of Earth Sciences, TR-34469 Istanbul, Turkey

We present the updated Holocene section of the Sofular cave stalagmite stable isotope record from the southern Black Sea coast (northern Turkey). $\delta^{13}C$ time series of this record and the growth rates prove to be more useful than $\delta^{13}C$ in deciphering Holocene climate variations, as they apparently reflect the hydrological conditions above the cave.

Although the growth rates imply that precipitation amount was apparently higher in this region in the early to mid-Holocene and the rainfall patterns could well have been different than the present, there is no distinct difference in the effective moisture level; a finding which contrasts with the evidence from various Eastern Mediterranean sites. Moreover, some well-defined climatic anomalies such as the 4.2 and 8.2 kyr events are not clearly expressed in the Sofular cave record; at least they look unexceptional considering similar 'anomalous' periods.

We conclude that the peculiarities in our results reflect the influence of the Black Sea and the Anatolian topography in modifying the climate of this region, which should be important for the more subtle climatic changes during the Holocene. Nevertheless, the Sofular cave record does provide hints and pose new questions about the connection between regional and large scale climates, highlighting the need for a more extensive network of high quality paleoclimate records to better understand the Holocene climate.

8.9

Incision and deformation recorded by Quaternary fluvial terraces in Makran accretionary wedge, SE-Iran

Haghipour Negar ^{1,2}, Kober Florian¹, Burg Jean-Pierre¹, Zeilinger Gerold³, Ivy-Ochs Susan⁴, Kubik Peter⁵, Faridi Mohammad²

¹ Geological Institute, ETH Zurich, Sonneggstrasse 5, CH-8092 Zurich (negar.haghipour@erdw.ethz.ch)

² Geological Survey of Iran, Meraj Avenue, Azadi Square, P.O. Box 13185-1494, Tehran, Iran

³ Institute für Geowissenschaften, Universität Potsdam, D-14476 Golm, Deutschland

⁴ Institute of Ion Beam Physics, Particle Physics, ETH Zürich, CH-8093 Zürich, Switzerland and Department of Geography, University of Zürich, CH-8057 Zürich, Switzerland

⁵ PSI/ c/o Ion Beam Physics, Particle Physics, ETH Zürich, CH-8093 Zürich, Switzerland

The well-preserved sequences of marine and fluvial terraces found along coastal and inner Makran are the geomorphic expression of surface uplift. The Makran accretionary wedge is an excellent example where the poorly described quaternary sequences and driving forces for their genesis can be studied for a better understanding of the contribution and feedback of surface processes to the growth of the wedge. We focused on fluvial terraces to extract possible tectonic and climatic driving forces. For this purpose, we aim to correlate river terraces between catchments and between different segments of the same river to document the distribution of deformation-uplift on the wedge in recent times. We investigated four main catchments in the Iranian Makran where the rivers preserve several terraces. Four terrace levels can be traced from field survey and detailed mapping in all the catchments. Out of these four levels, two are regionally preeminent. Deformed terraces are localized and associated with active faults and folds. Due to the lack of organic material and sandy deposits in inner Makran, our dating method was restricted to Terrestrial Cosmogenic Nuclides. The preliminary ages for the abandonment of two preeminent terraces are around 90ka (T1) and 21ka (T2). The fluvial incision rates based on the ¹⁰Be exposures ages of these two levels are 0.5 mm/yr in the late Pleistocene and 1mm/yr in latest Pleistocene, which suggests enhancement of surface uplift rate in the latest Pleistocene and Quaternary. These preliminary results differ from previous work on marine terraces, which documented 0 to 0.2 mm/yr uplift rate in Pleistocene times. To avoid any false interpretation, especially on regional scale, more terrace dating is in progress.

8.10

The Kestanbol Granite (Western Turkey) and its importance as a building stone: Application of cosmogenic ¹⁰Be to an archaeological problem

Haudenschild Esther¹, Akçar Naki¹, Yavuz Vural², Ivy-Ochs Susan^{3,4}, Alifimov Vasily³, Kubik Peter W.³, & Schlüchter Christian¹

¹ Institut für Geologie, Baltzerstrasse 1+3, CH-3012 Bern (e.haudenschild@students.unibe.ch)

² Istanbul Technical University, Faculty of Mines, TR-80626 Maslak, Istanbul

³ Institute of Particle Physics, ETH Höggerberg, CH-8093 Zurich

⁴ Department of Geography, University of Zurich, CH-8057 Zurich

Kestanbol Granite, outcropping in the Ezine village of Çanakkale (Fig. 1), have been operated for the production and export of building stones since ancient times. It is known that the Romans were trading the Kestanbol Granite (Marmor Troadense) all over the Mediterranean region (Lazzarini, 1987). Today, leftovers of building stones can still be found in relict quarries. The types of building stones vary from pavement stones to 11 meters long columns (Fig. 2). There is a lack of inscriptions and of absolute dating of these quarries (Ponti, 1995), so that the archaeologists can roughly estimate the time of the quarrying of the Kestanbol Granite from 500 BC to 500 AD (Feuser, 2009). Such vague limitation gives neither any possibility for understanding the development in time of the exploitation area of the quarries nor about the historical and political context of the quarrying (Ponti, 1995).

Keeping these in mind, the aim of our study is to determine the distribution and operation periods of antique quarries near the Ezine village of Çanakkale. In order to achieve this, the detailed archaeo-geological map of the extent of ancient

human impact has been produced and surface exposure dating with in-situ produced cosmogenic ^{10}Be applied. For exposure dating, 27 samples from the quarries, building stones and natural (without any human impact) bedrock were collected. According to our first results from the bedrock samples, the landscape in the study area is older than 120 ka. The samples from building stones and quarries are still in progress. During our mapping, fundaments of several building of unknown purposes (not yet described in the literature) were determined. Furthermore, ore and slag pieces in the study area were found.

Our results give both insights to the importance of the quarries in the social structure in ancient cities in the region such as Neandreaia and Alexandria Troas and the chronological development of the areal quarry exploitation. In brief, the results of our study can contribute in short-term to the declaration of these quarries as a geoarchaeological heritage site, and in long-term to their rehabilitation as an open-air museum.

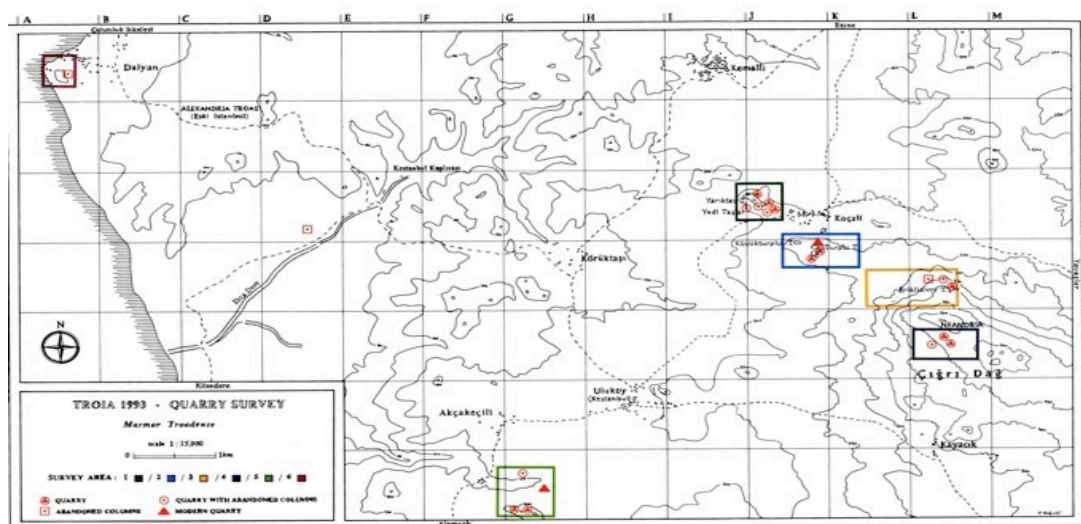


Figure 1. Map of the approximate areal distribution of the quarries in the Kestanol Granite (Ponti, 1995).



Figure 2. Ancient roman quarry “Yedi Taşlar” near Koçali.

REFERENCES

- Feuser, S., 2009: Der Hafen von Alexandria Troas. *Asia Minor Studien* 63, 16-17.
 Lazzarini, L., 1987: I graniti dei Monumenti Italiani e i loro problemi di deterioramento in: Bureca, A., Tabasso, M. L. & Palandri G.: *Materiali Lapidari II*, *Bollettino d'Arte Suppl.* 41, 157-172.
 Ponti, G., 1995: Marmor Troadense – Granite Quarries in the Troad. *Studia Troica* 5, 1995, 291-320.

8.11

European climate change at the end of the last glaciation: chironomid-based temperature reconstruction on a continental scale

Heiri Oliver^{1,2}, Birks John³, Brooks Steve⁴, Kirilova Emily², Magyari Enikő⁵, Millet Laurent⁶, Mortensen Morten Fischer⁷, Samartin Stéphanie¹, Tinner Willy¹, Toth Monika⁸, Veski Siim⁹ & Lotter André F.¹

¹ Institute of Plant Sciences and Oeschger Centre of Climate Change Research, University of Bern, Altenbergrain 21, CH-3013 Bern, Switzerland (oliver.heiri@ips.unibe.ch)

² Palaeoecology, Utrecht University, Budapestlaan 4, CD 3584 Utrecht, Netherlands

³ Department of Biology, University of Bergen, Allegaten 41, N-5007 Bergen, Norway

⁴ Natural History Museum, Cromwell Road, London SW7 5BD, UK

⁵ Hungarian Natural History Museum, P.O. Box 222, H-1476 Budapest, Hungary

⁶ Laboratoire de Chrono-Ecologie, 16 route de Gray, 25 030 Besançon, France

⁷ The National Museum of Denmark, Aarhus, Denmark

⁸ Balaton Limnological Research Institute, Klebelsberg Kuno 3, HU-8237 Tihany, Hungary

⁹ Institute of Geology at Tallinn University of Technology, Ehitajate tee 5, 19086 Tallinn, Estonia

In Europe the warming trend at the end of the last ice age was characterized by a number of abrupt temperatures shifts, including the rapid transitions to warmer climate at the beginning of the Lateglacial Interstadial and the Holocene, and the cooling at the start of the Younger Dryas cold period. The amplitude and spatial pattern of Lateglacial changes in temperature can provide information about the forcing factors causing these climate shifts and about processes affecting the European climate system during a transition to a warmer climate state. However, spatially resolved datasets describing temperature change across the European continent during the Lateglacial period at centennial or higher time resolution and based on the same standardized approach are presently not available. We aim to develop such a standardized dataset based on records of past summer temperature reconstructed from fossil chironomid assemblages preserved in lake sediments. A combination of regional calibration datasets provided the basis for a chironomid-based inference model for July air temperature which covers the range of expected temperatures and chironomid assemblage states expected for Europe during the Lateglacial period. This model, which is based on modern chironomid assemblages from 274 lakes in Norway and Switzerland and associated observed values of mean July air temperature, was then used to produce first chironomid-based temperature records from Estonia, Denmark, the Netherlands, southeastern France, southern Switzerland, and southern Romania. The preliminary results indicate distinct variations in the amplitude of reconstructed temperature changes across Europe with stronger shifts in inferred July air temperatures recorded in northern parts than at localities more to the south of the continent. Future work will expand this dataset to include additional sites on the British Isles, the Iberian Peninsula, Italy, Bulgaria and Scandinavia in order to confirm the observed spatial pattern of Lateglacial temperature changes.

8.12

Reconstructing the deglaciation history of the Gotthard Pass area, Central Swiss Alps, using cosmogenic ¹⁰Be and in-situ ¹⁴C

Hippe Kristina¹, Ivy-Ochs Susan², Kober Florian³, Wieler Rainer¹ & Schlüchter Christian⁴

¹ Institute of Geochemistry and Petrology, ETH Zürich, CH-8092 Zürich (hippe@erdw.ethz.ch)

² Institute for Particle Physics, ETH Zürich, CH-8093 Zürich

³ Institute of Geology, ETH Zürich, CH-8092 Zürich

⁴ Institute of Geological Sciences, University of Bern, CH-3012 Bern

During the Last Glacial Maximum (LGM) up to 500 m of ice covered the Gotthard Pass area (2106 m a.s.l.) at peak conditions (Florineth & Schlüchter 1998). This ice originated from the Rhone ice dome, one of the two big ice domes that existed in the Central Swiss Alps during the LGM. Ice from the Rhone glacier flowed over the Furka Pass down towards the Urseren area, where massive ice accumulated and flowed further south using the Gotthard Pass as a central pathway for mass transport. Ice flow over the Gotthard Pass ceased with the collapse of the LGM ice domes and the decrease of ice elevation in the Urseren area.

To determine the timing of ice retreat we have sampled glacially polished bedrock along an altitude transect at the western Gotthard Pass area. Surface exposure dating by cosmogenic ^{10}Be yield preliminary ages of ~9.5-12.8 ky (corrected for snow and erosion). The oldest age was obtained from the lowest elevation right in the pass area, while higher sampling points give younger exposure ages. This supports the concept that the pass area records the ice extent of the LGM whereas slightly higher elevations were affected by local ice, probably during the Lateglacial.

Our data are in agreement with ^{10}Be exposure ages from the nearby Grimsel Pass, giving a minimum age of ~14.0 ky for the final breakdown of ice domes in the Central Alps (Kelly et al. 2006). Within the errors, our ages also agree with radiocarbon data from the Gotthard region indicating a final retreat of small local glaciers at the beginning of the Holocene (Renner 1982).

Compared to radiocarbon ages from the Rhone valley (Welten 1982) and Simplon Pass (Müller 1984), which show completely ice-free main valleys, the Gotthard ages are slightly younger. Thus, to detect possible periods of post-LGM local ice coverage, especially in areas apparently only affected by LGM ice, cosmogenic in-situ ^{14}C is currently analyzed. The short-lived ^{14}C ($t_{1/2}$ 5730 y) decays during periods of burial and can provide information on complex exposure histories and the duration of burial episodes. Results will be presented at the meeting.

REFERENCES

- Florineth, D. & Schlüchter, C. 1998: Reconstructing the Last Glacial Maximum (LGM) ice surface geometry and flowlines in the Central Swiss Alps. *Eclogae geol. Helv.* 91, 391-407.
- Kelly, M. A., Ivy-Ochs, S., Kubik, P. W., von Blanckenburg, F. & Schlüchter, C. 2006: Chronology of deglaciation based on ^{10}Be dates of glacial erosional features in the Grimsel Pass region, central Swiss Alps. *Boreas* 35, 634-643.
- Müller, H.-N. 1984: Spätglaziale Gletscherschwankungen in den Westlichen Schweizer Alpen und im Nordisländischen Tröllaskagi-Gebirge. 205 pp. Buchdruckerei Küng, Näfels.
- Renner, F., 1982: Beiträge zur Gletschergeschichte des Gotthardgebietes und dendroklimatologische Analysen an fossilen Hölzern. *Physische Geographie* 8, 1-180.
- Welten, M., 1982: Vegetationsgeschichtliche Untersuchungen in den westlichen Schweizer Alpen: Bern-Wallis. *Denkschriften der Schweizerischen Naturforschenden Gesellschaft* 95, 1-105.

8.13

Do magnetic properties reflect climate history in Swiss lakes?

Jessica Kind¹, Ann Hirt¹, Ulrike van Raden²

¹ Institute of Geophysics ETH, CH 8096 Zurich, Switzerland (jessica.kind@erdw.ethz.ch)

² Institute of Climate Geology ETH, CH 8096 Zurich, Switzerland

The question of this study is whether magnetic parameters of lacustrine sediments from Swiss lakes can be used as high-resolution proxy for environmental change. We examine variations in the magnetic mineralogy from two lakes, Soppensee and Baldeggersee, covering the late Pleistocene and Holocene to investigate how the sediments are affected by changes in vegetation, erosional input, sedimentation, redox changes, and geochemistry. Magnetic mineralogy is determined by a combination of low-temperature measurements, coercivity distributions and extraction. The multi proxy climate records are currently being established. Magnetic properties are used to indicate the type and concentration of ferromagnetic minerals in the lake. We utilize a combination of: 1) concentration dependent parameters (magnetic susceptibility χ , anhysteretic remanent magnetization IRM), 2) composition indicative parameters (saturation isothermal remanent magnetization IRM/SIRM), and 3) grain size dependent parameters (ARM/IRM, hysteresis parameters).

Significant changes are seen in the sedimentology, geochemistry and magnetic mineralogy in the Soppensee that are related to the Wurm deglaciation, Bøling/Allerød (B/A), Younger Dryas (YD), and to the Holocene with the climatic optimum (Lotter, 2001, Lotter et al., 1997a, Lotter et al., 1997). The Wurm deglaciation is characterized by higher detrital input with a mixture of pseudo-single domain/multi domain (PSD/MD) magnetite and low concentration of superparamagnetic/single domain (SP/SD) hematite. Climatic transition from the colder Wurm period to the warmer B/A is characterized by an increase of low coercive magnetite/maghemite, as a consequence of decreasing detrital input. The beginning YD reflects more oxidizing conditions at the sediment-water interface, and is interpreted to be trigger for the appearance of magnetotactic bacteria (MTB), resulting in SD magnetite of uniform grain size, as shown in Figure 1.

The formation of siderite varves is initiated in the colder and anoxic YD with a subsequent transition to calcitic varves between 10 to 6 cal kyr PB (Lotter et al.,1997, Hajdas et al., 1993). Rising temperature during the climate optimum in Lake Soppen around 6 cal kyr BP increased primary production, leading to increased organic content. Varves disappear around 5.5 cal kyr BP as a consequence of geochemical changes at the sediment-water interface. The higher primary production at the surface leads to an uptake of oxygen at the bottom of the lake due to decomposition of organic matter. Hence this stage is marked by rapid increase of ferromagnetic minerals as displayed in Figure 1 a) and b). In conclusion, we can approve the initial question. The good agreement between the changes in magnetic properties and the climatic evolution demonstrate that the magnetic properties are a useful and fast tool to provide additional information for high resolution climate studies.

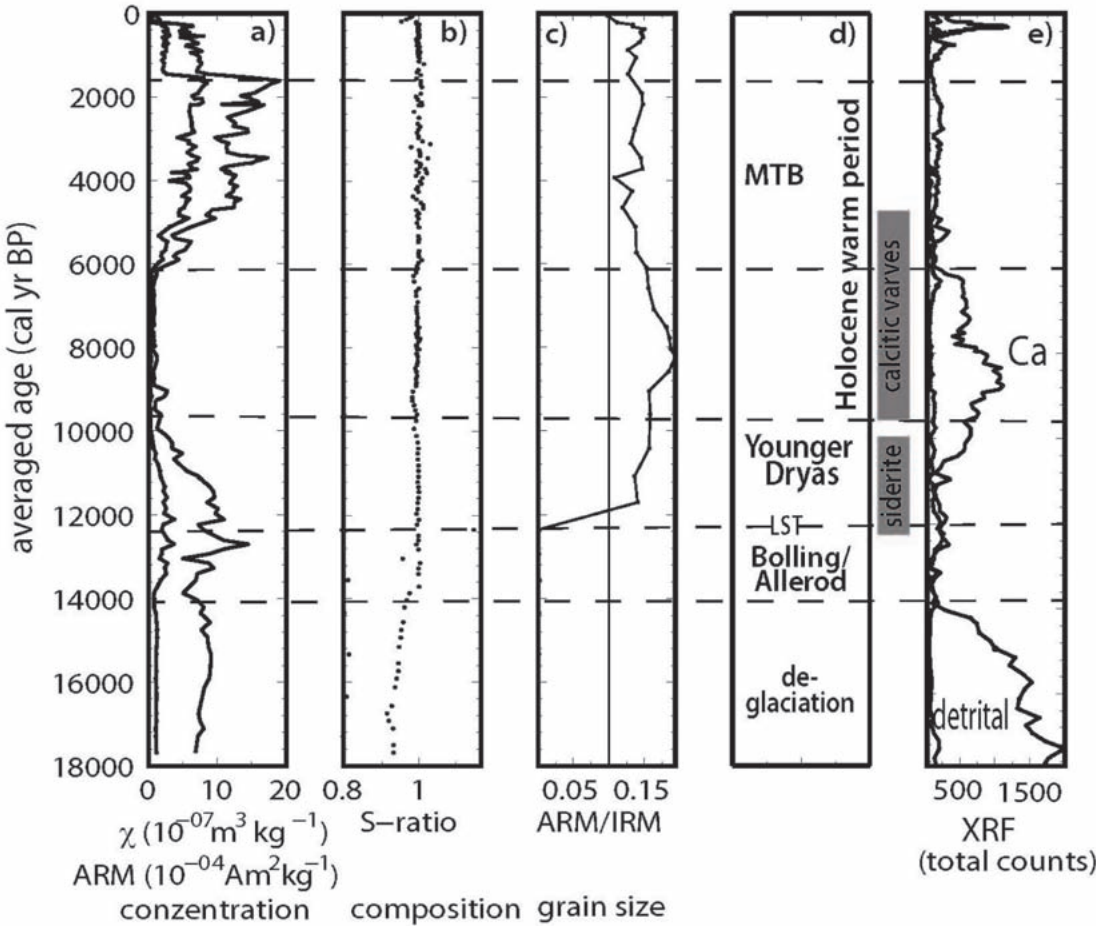


Figure 1: Magnetic properties from Lake Soppen a) low-field magnetic susceptibility, ARM intensity (120 mT AF with a bias field of 100 μT), b) S-ratio (IRM with a back field of 300 mT normalized by IRM at 1200 mT), c) ARM/IRM, e) Ca content, and sum parameter reflecting detrital input (Al,K,Ti;Rb;Zr) measured with XRF core scanning.

REFERENCES:

Hajdas I., Bonani G., Zolitschka B. (2000). Radiocarbon dating of varve chronologies: Soppensee and Holzmaar lakes after ten years. *Radiocarbon* 42, 349-353.

Lotter A. (2001). The paleolimnology of Soppensee (Central Switzerland), as evidence by diatoms, pollen, and fossil-pigment analyses. *Journal of Paleolimnology* 25, 65-79.

Lotter A., Merkt J., and Sturm M. (1997a). Differential sedimentation versus coring artefacts: a comparison of two widely used piston coring methods. *Journal of Paleolimnology* 18, 75-85.

Lotter A., Sturm M., Teranes J., and Wehrli B. (1997). Varve formation since 1885 and high resolution varve analyses in hypertrophic Baldeggersee (Switzerland). *Aquatic Science* 59, 304-325.

8.14

Giant sub-lacustrine mass movement in Lake Geneva sediment record

Kremer Katrina & Girardclos Stéphanie

Department of Geology and Palaeontology, University of Geneva, Switzerland (katrina.kremer@unige.ch)

Lake Geneva with an area of 582 km² and a maximal depth of 310 m, was formed during the Pleistocene by glacial erosion and is the first large sink for sediment transported by the Rhone river.

As part of a Swiss National Fund project on clastic sediment in lacustrine records (nr. 200021-121666/1), more than 100 km of high-resolution seismic reflexion profiles were acquired with a 3.5 kHz pinger source in the deepest part of lake Geneva.

Preliminary results show that the upper 5 m of this sequence consist of alternating seismic facies, interpreted as turbiditic and hemipelagic layers. These facies occur again from a 10-m depth downwards. Between these two sequences a 5-m-thick unit with chaotic/transparent facies, interpreted as a mass movement deposit, covers an area of 50 km². This unit, with an estimated minimum volume of 0.3 km³, represents the largest sub-lacustrine mass-movement deposit in Switzerland. The thickness map of this unit shows an increase towards east, thus attributing its origin to the Rhone delta area. Possible trigger of this mass movement is earthquake, rockfall, slope slide or a combination of these causes.

Ongoing 10-m-deep sediment coring will characterize the deposit as well as the age of the mass movement in order to link it to known historical and prehistorical events.

8.15

Contribution of geoelectrical measurements and shallow drillings for detection of Holocene palaeochannels in the Saillon region (Valais)

Laigre Laetitia¹, Reynard Emmanuel¹, Arnaud-Fassetta Gilles², Baron Ludovic³ & Lambiel Christophe¹

¹ Institut de Géographie, Université de Lausanne, Dorigny – Anthropole,
CH-1015 Lausanne (laetitia.laigre@unil.ch)

² Université de Paris Est-Créteil-Val-de-Marne – UMR 8591 CNRS – Laboratoire de Géographie Physique, Meudon.

³ Institut de Géophysique, Université de Lausanne, Dorigny – Amphipôle,
CH-1015 Lausanne

Upstream of Lake Geneva, the Rhône River underwent several morphological changes during the Holocene. Several geoelectrical measurements have been carried out between Sion and Martigny (Valais), particularly in the Saillon region, in order to identify former buried channels. Comparisons of several historical maps show that the Rhône River underwent fluvial metamorphoses during the 19th century (Reynard et al., 2009 ; Laigre et al., in press). The association of historical maps and DEM-LIDAR analyses helped us to identify some palaeochannels anterior to those indicated by maps.

Because of the different electrical responses given by gravels, sand, clay and silts, geoelectrical measurements can give precious information about the geometry of sediments. Furthermore, it helped us to localise former channels and to retrace fluvial dynamics (channel migration, change of fluvial pattern). Two sets of measurements were applied on a 500-m wide site: (i) a 5 m-depth profile, with a fine resolution, in order to observe recent architecture of sediments; (ii) a 40 m-depth profile, with a lower resolution that provided a deeper view of the sediment stratigraphy. In parallel, some hand hauger drillings (up to 3 m-depth) were done regularly along the geoelectrical profiles in order to compare the nature of the extracted sediments with returned electrical signals. These two resolution records show the existence of braided channels now buried at a depth of almost 20 m that disappear at a depth of 6 m. Some channel migrations are also visible in the first 5 meters, and bring fundamental information that helps us to reconstruct the fluvial dynamics of the Rhône River, that is little documented upstream of Lake Geneva.

REFERENCES

- Laigre, L., Arnaud-Fassetta, G., Reynard, E. Cartographie sectorielle du paléoenvironnement de la plaine alluviale du Rhône suisse depuis la fin du Petit Age Glaciaire: la métamorphose fluviale de Viège à Rarogne et de Sierre à Sion. Bulletin de la Murithienne (in press).
- Reynard, E., Arnaud-Fassetta, G., Laigre, L. & Schoeneich P. 2009: Le Rhône alpin sous l'angle de la géomorphologie : état des lieux. In: Le Rhône: dynamique, histoire et société (Ed. By Reynard, M., Evéquozy-Dayen, M. & Dubuis, P.) Sion: Cahier de Vallesia 21, 75-102.

8.16

Chironomids as indicators of the past 1000 years of mean July air temperatures: the Sivaplana and Seeburgsee records

Larocque-Tobler Isabelle¹, Quinlan Roberto², Müller Stewart Monique¹, & Grosjean Martin¹

¹ Oeschger Center and Institute of Geography, University of Bern, Erlachstrasse 9A, 3012 Bern (isabelle.larocque@giub.unibe.ch)

² Department of Biology, York University, 4700 Keele Street, Toronto, Ontario, Canada, M3J 1P3

Chironomid (non-biting midges) larvae preserved in lake sediments can be used to quantitatively and successfully reconstruct mean July air temperature, as shown by a comparison between chironomid-inferred temperatures and instrumental data (Larocque et al., 2009). Although they are one of the most promising biological proxy to reconstruct climate, they were, up-to-date, rarely used to reconstruct high-resolution climatic changes of the past 1000 years. The first near-annual temperature reconstruction was recently published (Fig. 1; Larocque-Tobler et al., 2010) and showed $\pm 1^\circ\text{C}$ temperature variations (compared to the climate normal (1961-1990) during the end of the "Medieval Climate Anomaly", the "Little Ice Age" and during the "Anthropocene" in Lake Silvaplana, Engadine. Lake Silvaplana ($46^\circ 26' 56''\text{N}$, $9^\circ 47' 33''\text{E}$) is at an altitude of 1791m a.s.l., it has a maximum depth of 77 m and a volume of $127 \times 10^6 \text{ m}^3$. Attempting a temperature reconstruction in such a deep, varved lake was, for chironomids, unprecedented at near-annual resolution.

Based on this success, a second attempt at reconstructing mean July temperature for the past 1000 years at high temporal resolution using chironomids preserved in the sediment of the meromictic Seeburgsee was made. Seeburgsee ($46^\circ 37'\text{N}$, $7^\circ 28'\text{E}$) is located at 1830 m a.s.l. in the northern Swiss Alps. The surface area of the lake is 0.06 km^2 , its volume is 0.38 km^3 and it has two basins with maximum depths of 15.5 and 9 m. Anoxia is one of the influential factors, other than climate, affecting chironomid assemblages and anoxic lakes are usually dismissed for climate reconstruction. However, biogenic varves are often created when anoxia is present. If anoxic lakes are disregarded for temperature reconstruction using chironomids, it hampers the possibility of high-resolution records. Here, we reconstructed climate using chironomids in the sediment of Seeburgsee to determine if a) chironomids in anoxic lake can be used to quantitatively and successfully reconstruct mean July air temperature and b) if the pattern of temperature changes for the past 1000 years in both cantons (Engadine and Bern) is similar.

Today, the analysis in Seeburgsee has been made for the Anthropocene period (Fig. 1). The pattern of temperature changes for the past 100 years is similar to the instrumental data (Larocque-Tobler et al. submitted) and similar to the Silvaplana record. 68 more samples are being currently analyzed and will be presented during the meeting, to complete the past 1000-year reconstruction of mean July temperature at Seeburgsee and compare with the Silvaplana record.

REFERENCES

- Larocque, I., Grosjean, M., Heiri, O., Bigler, C. & Blass, A. 2009: Comparison between chironomid-inferred July temperatures and meteorological data AD 1850–2001 from varved Lake Silvaplana, Switzerland. *J Paleolimnol* 41: 329–342
- Larocque-Tobler, I., Grosjean, M., Heiri, O., Trachsel, M. & Kamenik, C. 2010: Thousand years of climate change reconstructed from chironomid subfossils preserved in varved-lake Silvaplana, Engadine, Switzerland. *Quat Sci Rev* 29: 1940-1949

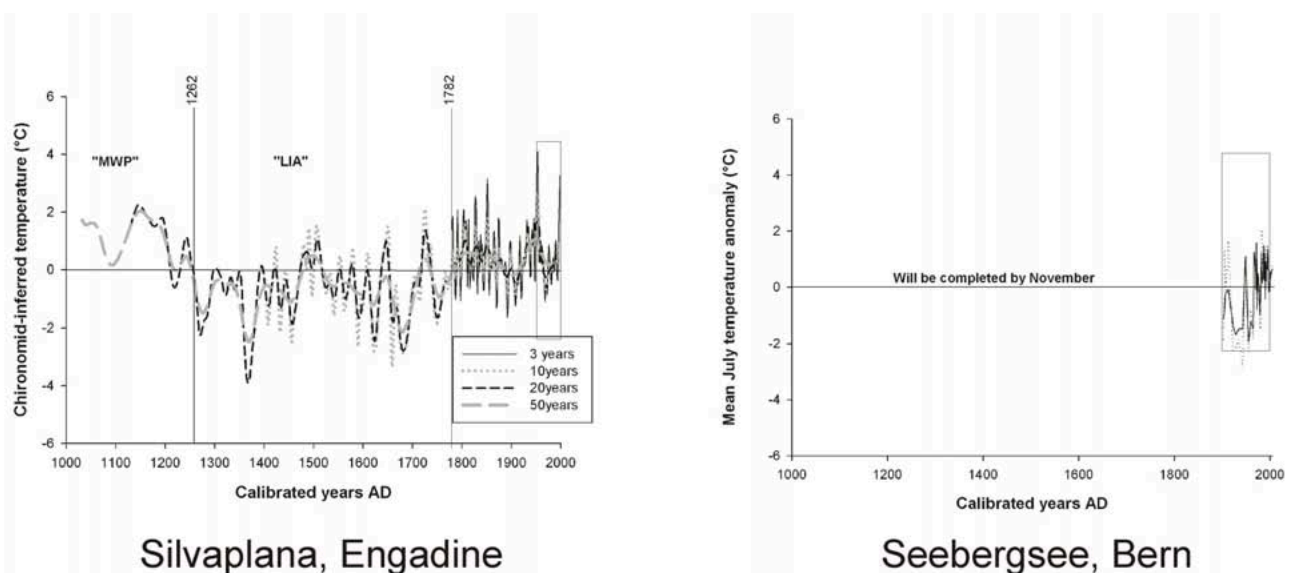


Figure 1. Temperature reconstructions using chironomids preserved in the sediment of Silvaplana (left graph; from Larocque-Tobler et al. 2010) and Seebergsee (right graph).

8.17

Pre-Columbian human adaptation to seasonal inundations in the Llanos de Moxos, Bolivian Amazonia.

Lombardo Umberto ¹, Canal-Beeby Elisa², Fehr Seraina ¹, Veit Heinz ¹

¹ Institute of Geography, University of Bern, Hallerstrasse CH-3012, Bern (lombardo@unibe.ch)

² School of International Development, University of East Anglia, UK

The Llanos de Moxos (LM), in Bolivia, is one of the largest seasonally flooded savannah in the world and covers most of the southeastern Amazon basin. In the last decade, the LM, has captured the interest of geographers and archaeologists because of the impressive amount of pre-Columbian earthworks it holds.

Different kinds of earthworks are found in different areas of the LM, but it is still unclear whether this is due to the different cultures that inhabited the LM or to differences in the geographical settings between the eastern and western sides of the region. The western Llanos holds an impressive amount of pre-Columbian agricultural fields (raised fields), (Lombardo et al. submitted) while the eastern Llanos is characterized by a dense distribution of monumental earth mounds, canals and causeways (figure 1) (Lombardo & Prümers, 2010). Earth mounds are huge buildings that can cover up to 20 hectares and can be up to 20 meters high. Archaeological excavations have shown that they are man made and date back to pre-Columbian times.

Current models suggest that raised field agriculture provided high yields without the need of fallow periods, representing a kind of pre-Columbian green revolution. However, evidence suggests that the highest level of social complexity was reached in the eastern Llanos, where raised fields are not present. Our research has focused on trying to explain this apparent contradiction.

An important difference between the eastern Llanos and the western Llanos which has often been overlooked is their hydrology. Flooding in the western Llanos is more severe than in the eastern Llanos because it is the result of local precipitations and river overflows, while further east it only responds to local precipitations. Therefore, in the western Llanos, in order to produce food, more far-reaching drainage infrastructures were needed than in the east, where conditions were more favorable for cultivation and canals were sufficient to drain the soil.

We believe that raised field agriculture was not a prehistoric green revolution, as suggested by some, but rather a flood risk mitigation strategy. Raised fields allowed pre-Columbian peoples in the western LM lessen the risk of more intense and frequent flooding than was experienced in the eastern LM. It would appear that pre-Columbian peoples adapted to

the harsh environmental conditions of the LM following different strategies in different areas: In the eastern LM a better natural drainage seems to have favored the flourishing of pre-Columbian societies with high levels of social complexity, while further west severe flooding obliged pre-Columbian peoples to build raised fields and constrained their growth and development.

This study highlights the importance of environmental constraints in conditioning population growth and cultural development in the Tropics.

REFERENCES

- Lombardo, U. & Prümers, H., 2010. Pre-Columbian human occupation patterns in the eastern plains of the Llanos de Moxos, Bolivian Amazonia. *Journal of Archaeological Sciences*, 37, 1875-1885
- Lombardo, U., Canal-Beeby, E., Fehr, S., Veit, H., 2010. Raised fields in the Bolivian Amazonia: a prehistoric green revolution or a flood risk mitigation strategy?. Submitted to *Journal of Archaeological Sciences*

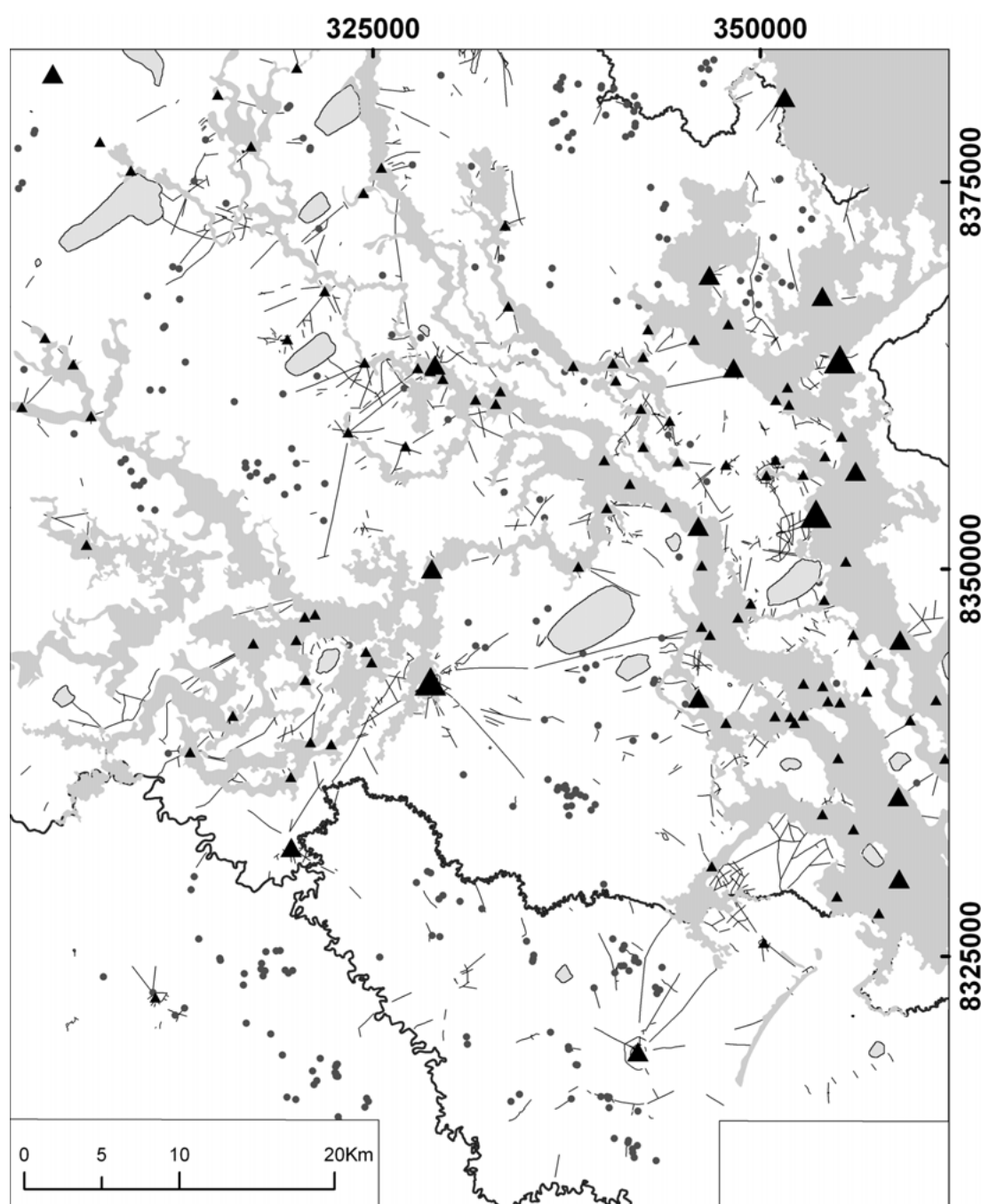


Figure 1. Map of the earth works in the eastern Llanos. The small triangles represent mounds of less than 8 hectares, the medium triangles represent mounds between 8 and 16 hectares and the large triangles represent mounds larger than 16 hectares. The dots represent forest islands and the black lines causeways and canals. The forest area is shaded in light grey and the lakes are a darker grey (Lombardo & Prümers, 2010).

8.18

Holocene Climatic Variability In Central Asia; A Geo-Archaeological Case Study In Samarkand, Uzbekistan

Malatesta L.¹, Castelltort S.¹, Picotti V.², Mantellini S.³, Hajdas I.⁴, Simpson G.⁵, Willett S.¹

¹ Institute of Geology, ETH Zurich, 8092 Zurich, Switzerland

² Dipartimento di Scienze della Terra e Geologico-Ambientali, Università di Bologna, 40127 Bologna, Italy

³ Facoltà di Conservazione dei Beni Culturali, Università di Bologna, 48100 Ravenna, Italy

⁴ Institute of Particle Physics, ETH Zurich, 8092 Zurich, Switzerland

⁵ Department of Geology and Palaeontology, University of Geneva, 1211, Geneva, Switzerland

The late Holocene (around 0-500 a. AD) climatic regime of Central Asia is characterised by cold winters, relatively cool summers and arid conditions (Oberhänsli et al., 2007). To the West, the Aral Sea experienced an important regression of over 20 m during the 4th c. AD (Boomer et al., 2000). The precipitation pattern in the Aral basin is linked by the Westerlies to the atmospheric changes in the Eastern Mediterranean, which is the main moisture source for the region (Sorrel et al., 2007). Paleoclimatic data for this region have been mostly gained by the study of sediment cores from the Aral Sea (Boomer et al., 2000). Furthermore Historical paleoclimatic data for the last two millennia in Eastern Asia indicate a cooling trend in the order of ca. 1.2°C between 250 and 350 a AD (Zheng et al., 2001).

The dense human History of the central Asian Mesopotamia – the land between the two tributaries of the Aral Sea, the Syr Darya and the Amu Darya – provides a potential supplementary record of paleoclimate evolution. Settlements, which were influenced by local climate variability, strongly modified in return the hydrologic regime of the catchment draining to the Aral Sea through extensive irrigation works (Kes, 1995; Oberhänsli et al., 2007).

This is particularly true in the Zeravshan Valley, an important tributary of the Amu Darya. From the 4th c. BC onwards, it was one of the Silk Road main paths. Large irrigation works were engineered to sustain the agriculture around the historical city of Afrosiab, now Samarkand (Mantellini, 2001; Stride et al., 2009).

The irrigation system upstream from the historical city of Afrosiab consists of two main canals, the Dargom and the Jangi Aryk (Stride et al., 2009). A particularly well studied dwelling next to the Dargom documents destructive floods. By applying sedimentological and surface processes methods to this archaeological site we bring original constraints to the framework and nature of precipitations at this time.

We dated the main flooding event at 160±80 a. AD. X-Ray Diffraction analysis of the flood-related sediments suggests a source for the sands further upstream in the valley, i.e. transported in the canal and not coming from the natural surrounding hillslopes. We estimate that an intense precipitation event of at least 65 mm/h for at least 2 hours allows for a 0.5 m deep flooding of the archaeological site based on a numerical model surface overland flow (Simpson and Castelltort, 2006). The usual construction type in the valley at this time, elevated dwellings, and the recurrence of flood horizons in the stratigraphy attest a repetition of floods of similar magnitude during the first centuries AD in western Central Asia.

REFERENCES:

Boomer, I., Aladin, H., Plotnikov, I., and Whatley, R., 2000, *Quaternary Sci Rev*, v. 19, p. 1259-1278.

Kes, A., 1995, *GeoJournal*.

Mantellini, S., 2001, *Cooperation in Archaeology and Islamic Studies*

Oberhänsli, H., Boroffka, N., and Sorrel, P., 2007, *Irrigation and Drainage Systems*

Simpson, G., and Castelltort, S., 2006, *Comput Geosci-Uk*, v. 32, p. 1600-1614.

Sorrel, P., Oberhänsli, H., Boroffka, N., Nourgaliev, D., Dulski, P., and Roehl, U., 2007, *Quaternary Res*, v. 67, p. 371-382.

Stride, S., Rondelli, B., and Mantellini, S., 2009, *World Archaeology*.

Zheng, J., Zhang, P., Ge, Q., and Man, Z., 2001, *Prog Nat Sci*, v. 11, p. 280-287.

8.19

Holocene glacier oscillations at Damma

Ott Andrea¹, Ivy-Ochs Susan², Bauder Andreas³, Akçar Naki¹ & Schlüchter Christian¹

¹Institut für Geologie, Baltzerstrasse 1+3, CH-3012 Bern (andrea.ott@students.unibe.ch)

²Laboratory of Ion Beam Physics, HPK, Schafmattstrasse 20, CH-8093 Zürich

³Versuchsanstalt für Wasserbau, Hydrologie und Glaziologie (VAW), Gloriastrasse 37-39, CH-8092 Zürich

In the recently free forefield of the Damma glacier in the Göschenalp, canton Uri, scientists of the BIGLINK project of the ETH Zurich are studying mineral weathering, soil formation and initial ecosystem development. In order to constrain in detail when the BIGLINK sampling sites became ice-free, a geomorphologic map was drawn, together with a short history of the glacier retreats and advances since 1956. For more information about the age of the moraines and associated landforms, some rock samples will be taken and measured.

For the mapping of the Damma glacier forefield, the focus was set on geomorphologic features. Characteristic for the area are the two big Holocene lateral moraines reaching about 100 m over the valley bottom. In between, a few much smaller distinct moraines are clearly visible.

The front position of the Dammafirn has been measured every year since 1921. Detailed documentation including reference points and sketch maps exists back to 1956. The measurements show a retreat phase before 1972 when the glacier re-advanced until 1991, followed by retreat still lasting until today. Observed front variations do not exactly match with existing moraines in the forefield. The data base allows us to geo-locate former observations and combine with maps and resolve inconsistency.

8.20

Holocene landscape evolution of the Llanos de Moxos, NE Bolivia

Plotzki Anna¹, Veit Heinz¹

¹Geographisches Institut, Universität Bern, Hallerstrasse 12, CH-3012 Bern (plotzki@giub.unibe.ch)

The Llanos de Moxos, which are located in the lowlands of north eastern Bolivia (Beni), are one of the largest seasonally inundated savannahs in the world. The region is characterized by a complex fluvial drainage pattern belonging to the Amazon system. In 2009, the University of Bern started to investigate the Holocene hydrogeomorphology and pre-Columbian water management in the Llanos de Moxos (funded by the Swiss National Science Foundation). As so far little data exist about human-environmental interactions in the Beni region, palaeoenvironmental and geoarchaeological studies are being conducted. First results with respect to landscape evolution are being presented here.

We examined sedimentary sequences along river banks across a 300-km-long N-S transect and found largely a systematic pedostratigraphic pattern. Sandy silts at the bottom are superimposed by yellow-ochre to red clayey silts. Above these sediments a palaeosol was found in all sections. Its maximum thickness is about 1.5 m and it is superimposed by silty-clayey deposits again. In some profiles we identified a second buried soil in these silty-clayey layers.

AMS ¹⁴C dates indicate that soil formation occurred between 9.3 to 3.4 cal ka BP and around 2.9 to 2.0 cal ka BP.

Based on the evaluation of the sedimentary sequences we developed a preliminary chronology of landscape evolution. The deposition of silty clays prior to 9.3 cal ka BP is interpreted as a low energetic sedimentary environment. It is assumed that relatively humid conditions prevailed, with seasonal inundation of the savannah. Between approximately 9.3 and 2.0 cal ka BP soil formation was the dominant process, suggesting a dryer early to mid-Holocene. Inundations during that period were absent or less severe. This long soil formation period was probably interrupted by several short more humid phases. The subsequent deposition of silty clays indicate a shift to modern wet conditions around 2 cal ka BP.

This interpretation is in accordance with pollen records from Noel Kempff Mercado National Park (Burbridge et al., 2004), lake level fluctuations of Lake Titicaca (Baker et al., 2001) and geomorphological and sedimentary analysis in the Bolivian Chaco (May et al., 2008 a,b). A dry early to mid Holocene could be the consequence of minimum summer insolation at 15-20°S during that time and a corresponding weakening of the South American Summer Monsoon (SASM).

REFERENCES

- Baker, P. A., Seltzer, G. O., Fritz, S. C., Dunbar, R. B., Grove, M. J., Tapia, P. M., Cross, S. L., Rowe, H. D. & Broda, J. P. 2001: The history of South American tropical precipitation for the past 25,000 years. *Science*, 291, 640-643.
- Burbridge, R. E., Mayle, F. E. & Killeen, T. J. 2004: Fifty-thousand-year vegetation and climate history of Noel Kempff Mercado National Park, Bolivian Amazon. *Quaternary Research*, 61, 215-230.
- May, J.-H., Argollo, J. & Veit, H. 2008a: Holocene landscape evolution along the Andean piedmont, Bolivian Chaco. *Palaeogeography, Palaeoclimatology, Palaeoecology*, 260, 505-520.
- May, J.-H., Zech, R. & Veit, H. 2008b: Late Quaternary paleosol-sediment-sequences and landscape evolution along the Andean piedmont, Bolivian Chaco. *Geomorphology*, 98, 34-54.

8.21

Quaternary glaciation history of northern Switzerland

Preusser Frank ¹, Graf Hans Rudolf ², Keller O.³, Krayss Edgar⁴, Schlüchter Christian ¹

¹ Institut für Geologie, Universität Bern, Baltzerstrasse 1+3, CH-3012 Bern
(preusser@geo.unibe.ch)

² Dorfstrasse 40, 8014 Gächlingen

³ Brühlstrasse 90, 9320 Arbon

⁴ Myrtenstrasse 9, 9010 St. Gallen

A revised glaciation history of the northern foreland of the Swiss Alps is presented by summarising field evidence and chronological data for different key sites and regions. The oldest Quaternary sediments of Switzerland are multiphase gravels intercalated by till and overbank deposits ('Deckenschotter'). Mammal remains place the oldest of these deposits into Mammalia Neogene Zone 17 (2.5-1.8 Ma). The presence of till within the sedimentary sequences implies glaciations of the Swiss alpine foreland during the Early Pleistocene. Important differences in the base level of the gravel deposits allow distinguishing two sub-units ('Höhere Deckenschotter', 'Tiefere Deckenschotter'), separated by a period of substantial incision. Each of the sub-units contains evidence for at least two but probably even four individual glaciations. The Early Pleistocene is separated from Middle Pleistocene deposition by a time of important erosion, probably related to tectonic movements and/or re-direction of the Alpine Rhine. The Middle-Late Pleistocene comprises four or five glaciations, named Möhlin, Habsburg, Hagenholz (uncertain, inadequately documented), Beringen, and Birrfeld after their key regions. Möhlin represents the most extensive glaciation of the Swiss alpine foreland and Beringen was only of just smaller extent. The last glacial cycle (Birrfeld glaciation) probably comprises two or even three independent glacial advances dated to about 105 ka, 65 ka, and 25 ka. For the last glacial advance, a detailed radiocarbon chronology for ice build-up and meltdown is presented.

8.22

Quaternary glacial chronology in Anatolia

Regina Reber¹, Dmitry Andreevich Tikhomirov¹, Naki Akçar¹, Vural Yavuz², Christian Schlüchter¹

¹*Institute of Geological Sciences, Baltzerstrasse 1+3, CH-3012 Bern,
(rreber@geo.unibe.ch)*

²*Istanbul Technical University, Faculty of Mines, TR-80626 Maslak, Istanbul,*

Surface exposure dating is a method used to place glacier fluctuations and moraine sequences into a chronological frame. Anatolia is one of the most sensitive places to the changes in atmospheric circulation patterns that influence the climate of the Eastern Mediterranean Region. Consequently it is important to construct the Quaternary glacial chronology to understand the climate changes in the past.

From cosmogenic ¹⁰Be, ²⁶Al and ³⁶Cl surface exposure ages it is known that the last local maximum glaciation occurred no later than around 20 ka in Uludağ (Zahno et al., 2010), 21 ka in Mount Erciyes (Sarıkaya et al., 2009), 20 ka Mount Sandıras (Sarıkaya et al., 2008); and between around 24 and 18 ka in the Dedegöl Mts. (Zahno et al., 2009), 22 – 18 ka in the Eastern Black Sea Mountains (Akçar et al., 2008 and references therein). This appear to be synchronous with the last maximum glaciation occurred in the European Alps, Central Apennines (Italy) and the Greek Mountains during the global Last Glacial Maximum (21± 2 ka) within Marine Isotope Stage-2.

At the Lateglacial subsequent glacier oscillations were dated: at around 16 ka in Mount Sandıras (Sarıkaya et al., 2008), 15 ka in Mount Erciyes (Sarıkaya et al., 2009); between around 16 and 15 ka in Uludağ (Zahno et al., 2010). Probably the Late Glacial advance in the Eastern Black Sea Mts. was restricted to the tributary valleys, but the timing of this advance is still unknown, however this advance continued until around 16 ka (Akçar et al., 2008 and references therein). So an oscillating glacier recession in Anatolia during Termination-1 is suggested by this evidence. In good agreement with this Anatolia data are published surface exposure ages related to the Lateglacial Gschnitz and Egesen moraines in the European Alps. This implies the parallel occurrence of major climatic shifts on millennial time-scale in the European Alps and Anatolia during MIS-2.

Already ice-free were the glacial valleys in SW Anatolia (Mt. Sandıras, Dedegöl Mountains) and in central Anatolia (Mt. Erciyes) during Younger Dryas (Sarıkaya et al., 2008, 2009; Zahno et al., 2009), whereas in the southern Black Sea coast, Younger Dryas occurred between around 13 ka and 11 ka (Akçar et al., 2008 and references therein; Zahno et al., 2010). During the Holocene after the deglaciation of the valleys in the Eastern Black Sea Mountains, rock glaciers and snow-avalanche ridges have been active processes. Then ¹⁰Be exposure ages from these ridges show that these events occurred during the Holocene and are therefore not linked to glacier fluctuations (Akçar et al., 2008 and references therein). In Anatolia Little Ice Age (LIA) moraines appear to be absent. Terrestrial geological records in Anatolia with regard to the Younger Dryas and the LIA cooling still remain to be studied in detail. Huge and active rock glaciers in the cirque areas may be related to the LIA cooling; absolute dates, however, are still absent. Dry and cold climatic conditions during the LIA could explain the absence of glacier advance, as the conditions were not conducive for the build-up of ice.

REFERENCES

- Akçar N., Yavuz V., Ivy-Ochs, S., Kubik P.W., Vardar M., Schlüchter C., 2008: A Case for a down wasting Mountain Glacier during the Termination-I, Verçenik Valley, NE Turkey. *Journal of Quaternary Science*, 23 (3), 273–285.
- Sarıkaya, M. A., Zreda, M., Çiner, A. and Zweck, C. 2008: Cold and wet Last Glacial Maximum on Mount Sandıras, SW Turkey, inferred from cosmogenic dating and glacier modeling. *Quaternary Science Reviews*, 27, 769-780.
- Sarıkaya, M. A., Zreda, M. and Çiner, A. 2009: Glaciations and paleoclimate of Mount Erciyes, central Turkey, since the Last Glacial Maximum, inferred from Cl-36 cosmogenic dating and glacier modeling. *Quaternary Science Reviews*, 28, 2326-2341.
- Zahno C., Akçar N., Yavuz V., Kubik P.W., Schlüchter C., 2009: Surface exposure dating of Late Pleistocene glaciations at the Dedegöl Mountains (Lake Beyşehir, SW Turkey). *Journal of Quaternary Science*, 24 (8), 1016–1028.
- Zahno C., Akçar N., Yavuz V., Kubik P.W., Schlüchter C., 2010: Chronology of Late Pleistocene glacier variations at the Uludağ Mountain, NW Turkey. *Quaternary Science Reviews*, 29, 1173–1187.

8.23

Late Glacial and early Holocene climatic changes in the Southern Swiss Alps, reconstructed using subfossil chironomid assemblages.

Stéphanie Samartin¹, Oliver Heiri¹ and Willy Tinner¹

¹ Institute of Plant Sciences and Oeschger Centre for Climate Change Research, University of Bern, CH-3013 Bern, Switzerland.

Lakes are archives of past environmental conditions. Biological, chemical, and physical components accumulate in the sediments, from within and without the lake (Douglas 2006). Larvae of the Chironomidae are found in most freshwater situations from the tropics to the arctic; some species are terrestrial or semi-terrestrial; some are even marine (Brooks et al. 2007). Due to their short generation times and the dispersal capacity of the winged adults, the Chironomidae rapidly respond to environmental changes. The strongly sclerotized head capsules of the Chironomidae larvae preserve well in lake sediments for thousands of years. Different taxa have specific ecological preferences and tolerances with respect to environmental variables, including temperature, pH, water depth, substrate morphology etc. (Brooks et al. 2007), making them useful as proxy indicators. Knowledge of chironomid ecology, together with the development of transfer functions, has allowed for the reconstruction of palaeotemperatures (Walker et al. 1991; Lotter et al. 1997). With these transfer functions summer air temperatures with a prediction error of 1-1.5°C can be reconstructed. Today, midges are widely used, especially as indicators of climatic change, and have been considered to be “the most promising biological method for reconstructing past temperature” (Battarbee 2000).

Available climatic reconstructions of Late Glacial and Holocene climate from the Northern, Western, and Central Alps and the Jura mountains are mainly based on pollen and chironomid assemblages (Lotter et al. 2000; Hofmann 2001; Heiri et al. 2003a, b, 2005; Ilyashuk et al. 2009). In the Southern Alps only few quantitative palaeoclimatic reconstructions are available so far (Frisia et al. 2005; Heiri et al. 2007, Larocque and Finsinger 2008). The absence of quantitative temperature reconstructions limits our comprehension of climatic patterns and of the biotic response of vegetation to temperature changes on both sides of the Alps. In this study we present a Late Glacial and early Holocene chironomid-based summer temperature reconstruction from Foppe (1470m a.s.l.) in the Southern Swiss Alps. Chironomid assemblages were studied in 58 samples along a 6.4m long sediment core covering the past 17200 years. Two training set (Swiss, Norwegian/Swiss) were used to infer summer temperatures (Heiri 2003a, Heiri unpublished).

On the basis of a preliminary chronology, our analyses suggest that midge assemblages have responded to major and minor climatic fluctuations during the last 17200 years, such as the Younger Dryas event in the Late Glacial and the Preboreal Oscillation at the beginning of the Holocene. The models reconstructed similar July air temperatures of around 9.2°C during the Oldest Dryas, an abrupt rise in temperature of about 3.6°C between 17000 and 15500 cal. BP (Pre-Bølling warming) up to 12.8°C. At this time afforestation in the Southern Alps started ca. 2000 years earlier than North of the Alps (i.e. before the Bølling onset at ca. 14700 cal. BP (Vescovi et al. 2007). This warming is in good agreement with high-resolution faunal, isotopic, and sedimentologic data from the European North Atlantic. These records indicate a strong temperature increase from 17500-17300 cal. BP (Lagerklint & Wright 1999). A climatic warming prior to the large-scale climate change at 15900 cal. BP was also recorded in the GRIP ice-core at ca. 17500-17000 cal. BP (Björck et al. 1998). A distinct cooling of about 1°C at around 14300 cal. BP (11.8°C, may be synchronous with the Older Dryas) is apparent. Temperatures increase gradually from 14500 cal. BP until 12800 cal. BP. Temperatures of about 12.8°C are reached at the end of the Allerød before temperatures decline again at the Allerød/Younger Dryas transition. Low temperatures of around 10.4°C are inferred during the Younger Dryas with several minor fluctuations. The Holocene starts with an abrupt warming of around 4.4°C and reaches values of about 14.8°C. At 11600 cal. BP the Foppe core shows a cooling of about 1.4°C which can probably be referred to as the Preboreal Oscillation. At Foppe the following amplitudes of change at climate transitions were recorded: Oldest Dryas/Bølling: 3.6°C, Allerød/Younger Dryas: 2.4°C, and Younger Dryas/Preboreal: 4.4°C. In a second step temperature reconstructions from the Southern, Northern and Central Alps will be compared with other records from the North Atlantic realm to infer spatial variability of summer temperature changes.

REFERENCES:

- Battarbee R.W., 2000. Palaeolimnological approaches to climate change, with special regard to the biological record. *Quat. Sci. Rev.* 19: 107-124.
- Björck S., Walker M.J.C., Cwynar L.C., Johnson S., Knudsen K.L., Lowe J.J. and Wohlfarth B., INTIMATE members, 1998. An event stratigraphy for the Last Termination in the North Atlantic region based on the Greenland ice-core record: a proposal by the INTIMATE group. *J. Quat. Sci.* 13: 283-292
- Brooks S.J., Langdon P.G. & Heiri O., 2007. The identification and use of Palaeartic chironomids in palaeoecology. *Quaternary Research Association Technical Guide Quat. Res. Assoc. Technical Guide*, 10: 1-276.
- Douglas M.S.V., 2006. Paleolimnology. In *Encyclopedia of Quaternary Sciences* (S.A. Elias Ed.), p. 2021. Elsevier, Amsterdam.

- Frisia S., Borsato A., Spötl C., Villa I.M. & Cucchi F., 2005. Climate variability in the SE Alps of Italy over the past 17000 years reconstructed from a stalagmite record. *Boreas* 34: 445-455.
- Heiri O., Lotter A.F., Hausmann S. & Kienast F., 2003a. A chironomid-based Holocene summer air temperature reconstruction from the Swiss Alps. *Holocene* 13: 477-484.
- Heiri O., Wick L., van Leeuwen J.F.N., van der Knaap W. & Lotter A.F., 2003b. Holocene tree immigration and the chironomid fauna of a small Swiss subalpine lake (Hinterburgsee, 1515m asl). *Palaeogeogr. Palaeoclimatol. Palaeoecol.* 189: 35-53.
- Heiri O. & Millet L., 2005. Reconstruction of Late Glacial summer temperatures from chironomid assemblages in Lac Lautrey (Jura, France). *J. Quat. Sci.* 20: 33-44.
- Heiri O., Filippi M.L. & Lotter A.F., 2007. Lateglacial summer temperatures in the Trentino area (Northern Italy) as reconstructed by fossil chironomid assemblages in Lago di Lavarone (1100m a.s.l.). *Studi Trentini di Scienze Naturali, Acta Geologica* 82 (2005): 299-308.
- Hofmann W., 2001. Late-Glacial/Holocene succession of the chironomid and cladoceran fauna of the Soppensee (Central Switzerland). *J. Paleolim.* 25: 411-420.
- Ilyashuk B., Gobet E., Heiri O., Lotter A.F., van Leeuwen J.F.N., van der Knaap W., Ilyashuk E., Oberli F. & Ammann B., 2009. Lateglacial environmental and climatic changes at the Maloja Pass, Central Swiss Alps, as recorded by chironomids and pollen. *Quat. Sci. Rev.* 28: 1340-1353.
- Lagerklint, M.I. and Wright J.D., 1999. Lateglacial warming prior to Heinrich event 1: The influence of ice rafting and large ice sheets on the timing of initial warming. *Geology* 27: 1099-1102.
- Larocque I. & Finsinger W., 2008. Late-glacial chironomid-based temperature reconstructions for Lago Piccolo di Avigliana in the southwestern Alps (Italy). *Palaeogeogr. Palaeoclimatol. Palaeoecol.* 257: 207-223.
- Lotter A.F., Birks H.J.B., Hofmann W. & Marchetto A., 1997. Modern diatom, cladocera, chironomid, and chrysophyte cyst assemblages as quantitative indicators for the reconstruction of past environmental conditions in the Alps. I. Climate. *J. Paleolim.* 18: 395-420.
- Lotter A.F., Birks H.J.B., Eicher U., Hofmann W., Schwander J. & Wick L., 2000. Younger Dryas and Allerød summer temperatures at Gerzensee (Switzerland) inferred from fossil pollen and cladoceran assemblages. *Palaeogeogr. Palaeoclimatol. Palaeoecol.* 159: 349-361.
- Vescovi E., Ravazzi C., Arpenti E., Finsinger W., Pini R., Valsecchi V., Wick L., Ammann B. & Tinner W., 2007. Interactions between climate and vegetation during the Lateglacial period as recorded by lake and mire sediment archives in Northern Italy and Southern Switzerland. *Quat. Sci. Rev.* 26: 1650-1669.
- Walker I.R., Smol J.P., Engstrom D.R. & Birks H.J.B., 1991. An assessment of Chironomidae as quantitative indicators of past climatic change. *Can. J. Fish. Aquat. Sci.* 48: 975-987.

8.24

Switzerland at the Last Glacial Maximum (LGM): A new map (2009) by swisstopo 1 : 500 000

Schlüchter Christian¹ & Reto Burkhalter²

¹ Institut für Geologie, Baltzerstrasse 1+3, CH-3012 Bern (christian.schluechter@geo.unibe.ch)

² Geologische Landesaufnahme, Swisstopo, CH – 3074 Wabern

Map-sheet No. 9 of the Atlas of Switzerland (1970) showing the area of the country at the Last Glacial Maximum by Eduard Imhof und Heinrich Jäckli has been sold out for many years. This simple fact and new data on the geometry of the inner-alpine LGM glaciers, mainly by Florineth (2000) and Kelly (2004), initiated the idea to produce a new map of the LGM in Switzerland. This idea was the beginning of a hard job which has kept us busy for almost 10 years. The new map 1 : 500 000 is available now through book- and map-stores and can be downloaded at www.swisstopo.ch.

What information is new on this map? This are the following reconstructions:

(1) The ice cover on the highest and central parts of the Jura Mountains is more extensive and more important than previously thought. The main data in support of this reconstruction is excellent mapping evidence to the northwest of the High Jura in France;

(2) The Highlands of the Napf in the central Swiss Midlands with a max. elevation of 1408 m has been covered with small, however well defined valley glaciers. This has not been recognised on the previous map. The local LGM valley glaciation of the Napf is supported by the existence of nivation areas and small glaciers in the adjoining hills;

(3) Detailed mapping of trimlines in the High Alps between the Engadine Valley to the east and the Mont Blanc area to the west shows the existence during LGM time of well defined ice dome areas in the Upper Engadine, in the Surselva and in the Upper Rhone Valley (including the ice plateau in the Zermatt area). All four such ice accumulations are situated to the south of the main orographic divide of the Alps with interesting implications on atmospheric paleocirculation patterns. As a result of this configuration ice flow was from south to north along certain transfluences accross the the High Alps. – The huge outlet glacier from the Matternal (draining the ice plateau in the upper valley of Zermatt) to the main valley of the Wallis was so important that the ice from the upper Rhone valley was blocked-off at Brig-Visp and diverted directly to the south accross Simplon pass (causing a complex divergent transfluent ice flow regime in the Brig-Visp area). With such a reconstruction of the paleo iceflow in the Rhone valley it is possible now fort he first time to explain the distribution of erratic indicator lithologies in the western Swiss Midlands;

(4) The glaciers in southern Switzerland display a narrow valley glacier morphology, quite different from earlier reconstructions. This morphology may reflect glaciers with very high mass turnover (compared to the glaciers in South Westland of New Zealand's South Island) as a result of the main track of precipitation to the Alps from the south. The positions of the LGM ice domes coincide with the centers of foehn controlled precipitation today.

REFERENCES

- Florineth, D. & Schlüchter, C., 2000: Alpine evidence for atmospheric circulation patterns in Europe during the last glacial maximum. *Quaternary Research*, 54, 295-308.
- Jäckli, H., 1970: Die Schweiz zur letzten Eiszeit, Karte 1:550 000. Atlas der Schweiz, Blatt 6, Bundesamt für Landestopographie, Wabern–Bern, Switzerland.
- Kelly, M., Buonchristiani, J.F., & Schlüchter, C., 2004: A reconstruction of the last glacial maximum (LGM) ice-surface geometry in the western Swiss Alps and contiguous Alpine regions in Italy and France. *Eclogae Geologicae Helvetiae*, 97, 57–75.

8.25

How to derive weathering rates from ice core measurements of atmospheric tetrafluoromethane?

Jochen Schmitt*, Barbara Seth* & Hubertus Fischer*

* *Climate and Environmental Physics, Physics Institute and Oeschger Centre for Climate Change Research, University of Bern, Switzerland (Schmitt@climate.unibe.ch)*

Fluorite, which is an accessory mineral found in rocks like granite and gneiss, contains trace amounts of tetrafluoromethane (Harnisch et al., 1996). Recent sources are dominated by anthropogenic emissions from aluminum smelters and the production for the semiconductor industry, whereas weathering of fluorite bearing rocks is the only natural source of this atmospheric trace gas.

As tetrafluoromethane (CF_4) is inert to destruction processes in the troposphere and stratosphere the only sink lies in the high mesosphere due to destruction by short wave UV radiation. As a consequence, CF_4 has a very long life time in the order of 50-100 ka or even longer.

As CF_4 is mainly released from weathering of granitic rocks we assume that its atmospheric concentration might show fluctuations on longer time scales as weathering intensity should change on glacial-interglacial timescales or longer. Also glacial erosion of the large continental ice sheets in Canada and Scandinavia could be important as these areas have widespread granitic or gneiss basement rocks and glacial erosion is more intense than ordinary fluvial erosion.

From firn air measurements we know that its preindustrial concentration was about 35 pptv (Worton et al., 2007). The only information from older times comes from a few measurements around the LGM and the last deglaciation on outcropping ice from Greenland, with almost constant values around 35 pptv (Muhle et al., 2010). So, there exists no indication of variations on time scales of 10000 years.

Our first low resolution measurements covering the last 750 ka show relatively constant CF_4 concentrations, ranging between 31 and 37 pptv. Additionally, we don't see marked concentration changes during glacial-interglacial transitions. However, a lot of questions have to be answered before past atmospheric CF_4 concentrations can be used to estimate weathering rates, e.g. only few rock samples per continent have been analysed on their CF_4 content (Harnisch et al., 1998, Harnisch et al., 2000). As the CF_4 concentration of these granite samples showed a large variability (one order of magnitude), it is clear that weathering in one region emits more CF_4 than other regions thus biasing any global estimate. With a better data basis on CF_4 rock concentration one could possibly identify key regions, which dominate the global CF_4 budget.

REFERENCES

- Harnisch J, Borchers R, Fabian P, Gaggeler HW, Schotterer U. Effect of natural tetrafluoromethane. *Nature* 1996; 384: 32.
- Worton DR, Sturges WT, Gohar LK, Shine KP, Martinerie P, Oram DE, Humphrey SP, Begley P, Gunn L, Barnola J-M, Schwander J, Mulvaney R. Atmospheric trends and radiative forcings of CF_4 and C_2F_6 inferred from firn air. *Environmental Science & Technology* 2007; 41: 2184.
- Muhle JM, Ganesan AL, Miller BR, Salameh PK, Harth CM, Gwinn BR, Rigby M, Porter LW, Steele LP, Trudinger CM, Krummel PB, O'Doherty S, Fraser PJ, Simmonds PG, Prinn RG, Weiss RF. Perfluorocarbons in the global atmosphere: tetrafluoromethane, hexafluoroethane, and octafluoropropane. *Atmospheric Chemistry and Physics* 2010; 10: 5145.
- Harnisch J, Eisenhauer A. Natural CF_4 and SF_6 on Earth. *Geophysical Research Letters* 1998; 25: 2401.
- Harnisch J, Frische M, Borchers R, Eisenhauer A, Jordan A. Natural fluorinated organics in fluorite and rocks. *Geophysical Research Letters* 2000; 27: 1883.

8.26

Detection of volcanic ash layers by high-resolution XRF core scanning

Steinemann Stefanie¹, Hamann Yvonne¹, Gilli Adrian¹

¹ Geological Institute, ETH Zurich, Sonneggstrasse 5, 8092 Zürich, Switzerland (ssteinem@student.ethz.ch)

Volcanic ash layers (tephras) in lake sediments are very important marker beds for establishing robust age models and to synchronize records from different archive. So far, detecting tephras in the sedimentary records of lacustrine lakes has been laborious as they are often very thin. X-ray fluorescence (XRF) core scanning, a rapid, non-destructive method to scan split sediment cores for their relative chemical composition, was now successfully used for the detection of tephras in the sedimentary records of four Swiss lakes (Soppensee, Gerzensee, Baldeggersee and Burgäschisee).

Having tested four different analytical settings for XRF core scanning on the Laacher See Tephra (12'880 varve years BP; Brauer et al., 1999) in the sediment core of Soppensee (So08-02 C2), it can be concluded that it is most likely to detect volcanic ashes with a maximum tube voltage of 2000µA, a high count time of 50s and a down core resolution of 0.2mm. The element peaks in the LST are higher in using setting 4 than in the other tested settings.

The Laacher See Tephra (LST), very prominent in the observed lakes and therefore easily detectable with this method, could be characterized by high element peaks of mainly K, Ca, Rb, Zr and Nb. The chemical composition of the surrounding sediment and the thickness of the ash influence the XRF expressions of the LST. Two invisible volcanic ash layers (cryptotephra) could be located by XRF core scanning. The Vasset Kilian Tephra (VKT) from the Massif Central (9407 ± 44 cal years BP; Hajdas et al., 1993) was found in Soppensee and the Icelandic Vedde Ash, erupted 12'225 –11'832 cal years BP (Blockley et al., 2007) could successfully be located in Baldeggersee and Burgäschisee, where it has not been found before. Both of these ashes have positive element peaks of K, Rb and Zr in XRF core scanning data. The XRF data of the VKT in the Soppensee core is shown in detail in Figure 1.

The evidence for having indeed detected a volcanic ash layer by XRF core scanning was given for all the named tephras by smear slides analysis, where the presence of volcanic glass shards could be confirmed (Fig. 2).

Detecting the Vedde Ash and the Vasset Kilian Tephra by XRF core scanning is a promising result, which shows the high potential of this application for nicely laminated and well-preserved sediment cores with homogeneous grain sizes. The possibility to apply this non-destructive, fast and easy technique to detect cryptotephra in sediment cores is a step to a more efficient use of tephrochronology in lake sediment studies.

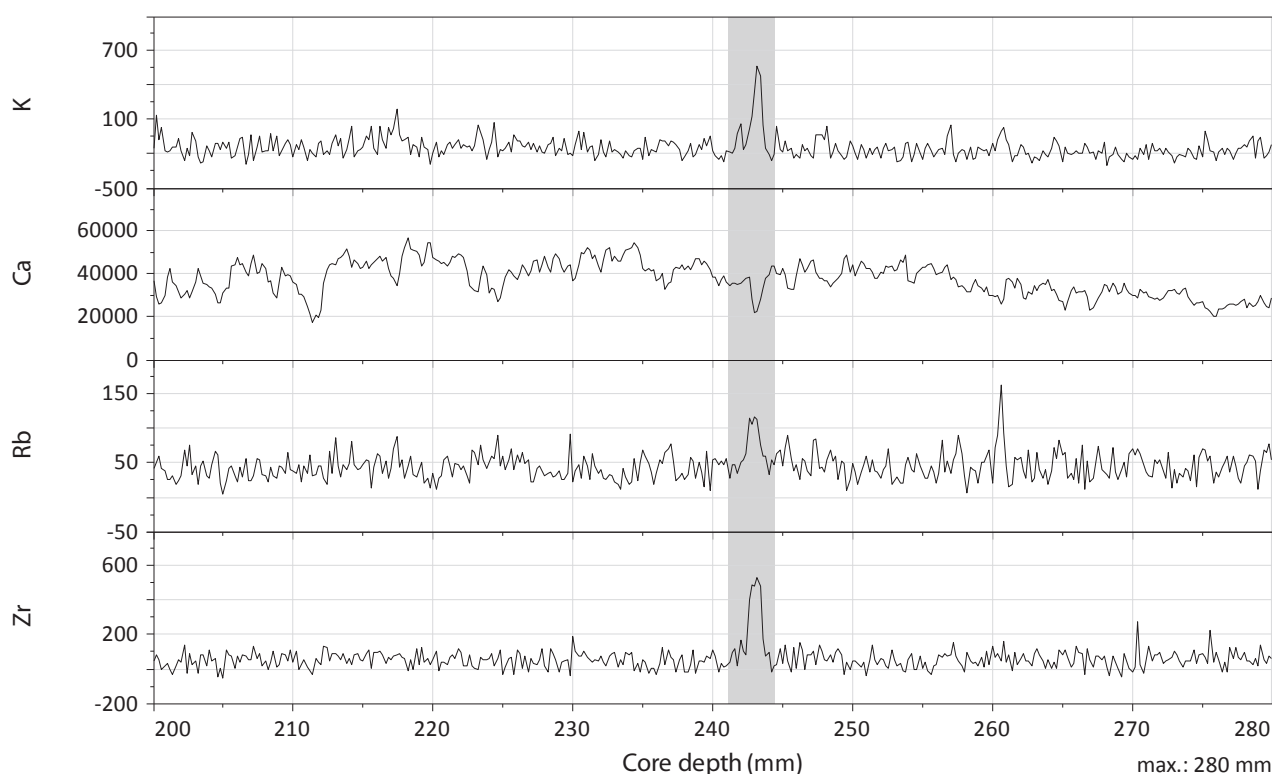


Fig. 1: XRF core scanning data (in total counts of peak surface) around the VKT (shaded area) in the Soppensee core (So08-01 B3)

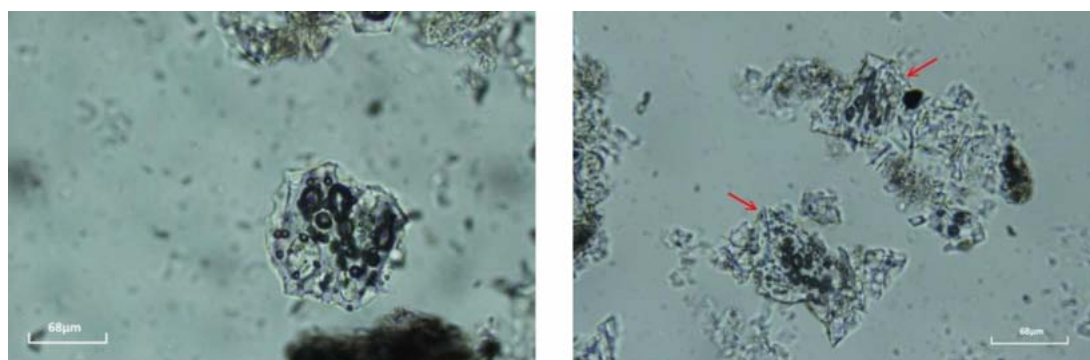


Fig. 2: Microscope picture of volcanic glass shards (smear slide) from the Laacher See Tephra layer in the Gerzensee core (left) and the Burgäschisee core (right)

REFERENCES

- Blockley S.P.E., Lane C.S., Lotter A.F., Pollard A.M., 2007. Evidence for the presence of the Vedde Ash in Central Europe. *Quaternary Science Reviews*, 26, 3030-3036.
- Brauer A., Endres C., Günter C., Litt T., Stebich M., Negendank J.F.W., 1999. High resolution sediment and vegetation responses to Younger Dryas climate change in varved lake sediments from Meerfelder Maar, Germany. *Quaternary Science Reviews*, 18, 321-329.
- Hajdas I., Ivy S.D., Beer J., Bonani G., Imboden D., Lotter A.F., Sturm M., Suter M., 1993. AMS radiocarbon dating and varve chronology of Lake Soppensee: 6000 to 12000 ^{14}C years BP. *Climate Dynamics*, 9, 107-116.

8.27

A review on tunnel valleys in northern Europe

Dorothea Stumm¹, Urs H. Fischer¹, Michael Schnellmann¹ & Wilfried Haeberli²

¹Nagra, Hardstrasse 73, CH-5430 Wettingen (Stummd@gmail.com)

²Department of Geography, University of Zurich-Irchel, Winterthurerstrasse 190, CH-8057 Zürich

The existence of buried Quaternary valleys indicates that glacial erosion is an important process in shaping the landscape of the Swiss alpine foreland. Considering the time of concern of 1 Ma for high-level nuclear waste repositories glacial erosion needs to be addressed for assessing their long-term safety. As one approach to better understand the formation processes of Quaternary valleys, a literature review with focus 'tunnel valleys' outside the alpine realm was carried out.

Deep glacial valleys have been documented in Europe, North America, Africa, Australia and Antarctica. However, the focus of the literature review is on tunnel valleys in northern Europe (North Sea, Denmark, northern Germany, the Netherlands and northern Poland) which have been investigated in detail. Here we give an overview of observed valley morphologies, their geographical distributions, bedrock morphologies and formation process theories.

Tunnel valleys are defined as large, elongated, overdeepened depressions cut into sediments or bedrock (Ó Cofaigh 1996). They occur as individual segments or as an anastomosing network, are often several kilometres long, maximum a few hundred metres deep and hundreds of metres up to a couple of kilometres wide (Jørgensen & Sandersen 2006). Usually they are steep-sided with flat undulating bottoms, begin and terminate abruptly and are open or filled with sediments (Kristensen et al. 2007; Fig. 1). Occasionally, eskers and lakes occupy the valleys. Tunnel valleys are formed below past ice sheet margins, and are generally oriented parallel to the subglacial hydraulic potential gradient. In some cases, the tunnel valleys terminate at major moraines where they may grade into large outwash fans.

The most important formation processes of tunnel valleys discussed in the literature include meltwater drainage, catastrophic outbursts (jökulhlaups) and sediment deformation, and are occasionally combined with direct glacial erosion (e.g. Boulton & Hindmarsh 1987; Jørgensen & Sandersen 2006). However, there is still controversy about the origin of tunnel valleys (Ó Cofaigh 1996).

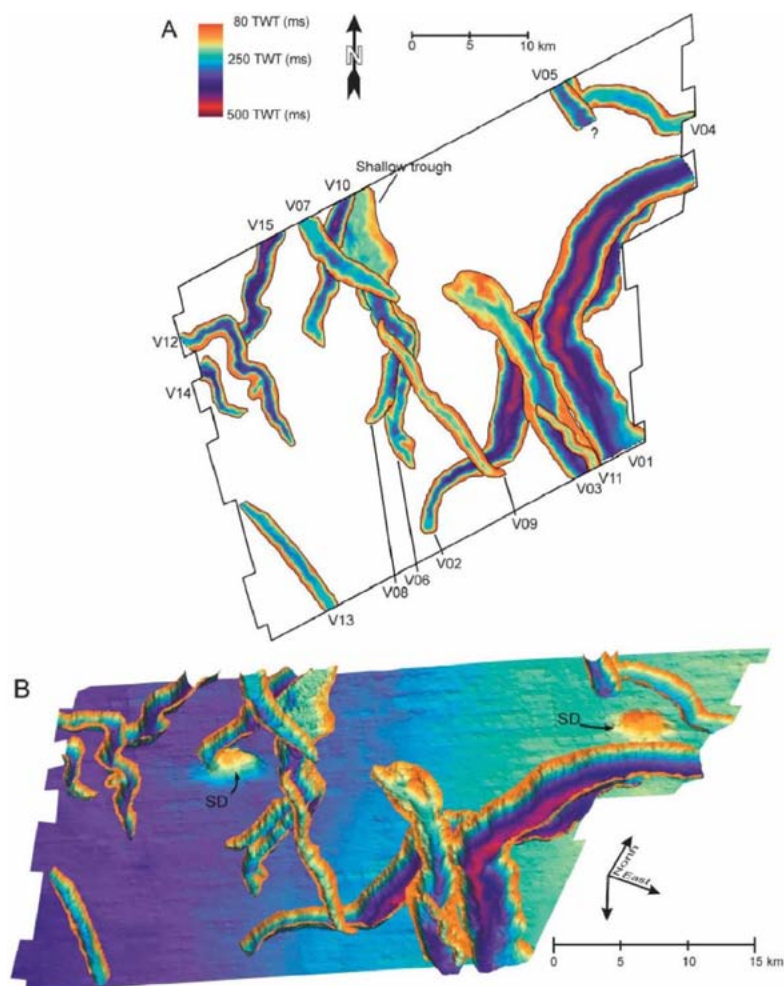


Figure 1. Example of buried tunnel valleys in the eastern North Sea in (A) plan and (B) perspective view (TWT: two-way-travel time). The seafloor is about 60 m b.s.l. (80 ms TWT) and the upper limit of the tunnel valleys, and the coloured plane is the Near Base Quaternary (NBQ) horizon. The tunnel valleys seem to deflect around two salt diapirs (SD) that possibly controlled the local subglacial drainage system (Kristensen et al. 2007).

REFERENCES

- Boulton, G.S. & Hindmarsh, R.C.A. 1987: Deformation of subglacial sediments: rheology and geological consequences. *Journal of Geophysical Research*, 92, 9059–9082.
- Kristensen, T.B., Huuse, M., Piotrowski, J.A. & Clausen, O.R. 2007: A morphometric analysis of tunnel valleys in the eastern North Sea based on 3D seismic data. *Journal of Quaternary Science*, 22, 801–815. ISSN 0267-8179.
- Jørgensen, F. & Sandersen, P.B.E. 2006: Buried and open tunnel valleys in Denmark – erosion beneath multiple ice sheets. *Quaternary Science Reviews*, 25, 1339–1363.
- Nagra 2008: Vorschlag geologischer Standortgebiete für das SMA- und das HAA-Lager. Geologische Grundlagen. Nagra Technischer Bericht NTB 08-04. Wettingen, Switzerland.
- Ó Cofaigh, C. 1996: Tunnel valley genesis. *Progress in Physical Geography*, 20, 1–19.

8.28

Calibration of ^{36}Cl Production Rate on ^{39}K in Saturated Antarctica Samples

Tikhomirov Dmitry¹, Alifimov Vasily², Akçar Naki¹, Ivy-Ochs Susa^{2,3}, Schlüchter Christan¹

¹ Institut fuer Geologie, Uni Bern, Baltzerstrasse 1+3, CH-3012 Bern (tikhomirov@geo.unibe.ch)

² Labor f. Ionenstrahlphysik, ETH Zürich

³ Geographisches Institut, Uni Zürich

The surface exposure dating of K-rich minerals like K-feldspar and biotite with the cosmogenic ^{36}Cl is presently limited by poorly known rate of ^{36}Cl production from ^{39}K . ^{36}Cl produced in situ on ^{39}K by secondary particles of cosmic rays in following nuclear reactions: high energy spallation, negative muon capture and thermal neutron capture. At the surface major contribution to ^{36}Cl production is made by spallation reactions, while the negative muon capture dominates below 2 meters of rock. Previously published ^{36}Cl production rates on ^{39}K by spallation reactions lies in wide band of numbers between 106 ± 8 and 228 ± 18 $\text{at}\cdot\text{g}(\text{K})^{-1}\cdot\text{yr}^{-1}$ (Evans 1997, Phillips 1996, Swanson 2001, Zreda 1991). More accurate evaluation of ^{36}Cl production rate from ^{39}K from is essential because the inaccuracy of the production rate translates into significant errors in derived ages.

Proper production rate calibration requires many conditions on samples to be met. K-rich minerals in the samples for calibration should contain low level of ^{40}Ca and ^{35}Cl to reduce the other ^{36}Cl production pathways. Exposure history (shielding, erosion) of the samples since their exposure should be clear. Exposure time must be well-determined by other independent methods or the steady state assumption must be justified.

In an ideal case, the obtained production rate can be uniquely scaled to any other latitude and altitude, and applied in any possible time span. However, due to present day knowledge of scaling procedures and past magnetic field variations, the scaling and application of production rates can have a certain bias due to scaling scheme and estimations of the magnetic field during time span of the calibrated site. These uncertainties can influence the application of the production rate at the level of up to 10%, therefore our estimated local production rates will be given together with all relevant local parameters.

Long term exposed samples of granites from Table Mountain, Antarctica were chosen (Ivy-Ochs 1995). Steady state of ^{36}Cl build up and independent dating by ^{10}Be make these samples perfect for calibration. However previous calibration based on similar samples gave a value, which is higher than all other available estimates. Verification and explanation of this outlier will be important for ^{36}Cl dating of long term exposed K-feldspars.

REFERENCES

- Evans, J.M., Stone, J.O.H., Fifield, L.K., Cresswell, R.G. 1997. Cosmogenic chlorine-36 production in K-feldspar. Nucl. Instr. Meth. Phys. Res., B123, 334-340.
- Phillips, F.M., Zreda, M.G., Flinsch, M.R. 1996. A reevaluation of cosmogenic ^{36}Cl production rates in terrestrial rocks. Geoph. Res. Lett., 23, 949-952.
- Swanson, T.W. & Caffee, M.L. 2001. Determination of ^{36}Cl production rates derived from the well-dated deglaciation surfaces of Whidbey and Fidalgo Islands, Washington. Quart. Res., 56, 366-382.
- Zreda, M.G., Phillips, F.M., Elmore, D., Kubik, P.W., Sharma, P., Dorn, R.I. 1991. Cosmogenic chlorine-36 production rates in terrestrial rocks. Earth Planet. Sci. Lett., 105, 94-109.
- Ivy-Ochs, S., Schlüchter, C., Kubik, P.W., Dittrich-Hannen, B., Beer, J. 1995. Minimum ^{10}Be exposure ages of early Pliocene for the Table Mountain plateau and the Sirius Group at Mount Fleming, Dry Valleys, Antarctica. Geology, 23, 1007-1010.

8.29

How does the elemental composition of Swiss lake sediments reflect past climate conditions?

Ulrike van Raden¹, Adrian Gilli¹, Jessica Kind²

¹ Geological Institute, ETH Zurich, CH-8096 Zurich, Switzerland (vanRaden@erdw.ethz.ch)

² Institute of Geophysics, ETH Zurich, CH-8096 Zurich, Switzerland

As part of an interdisciplinary multi-proxy study, we conducted a high-resolution XRF-core scan analysis on lacustrine sediments from Soppensee (Central Switzerland) covering the late Pleistocene and Holocene to answer the question of how the elemental composition of lake sediments reflects past climate conditions.

Climate has a strong influence on sedimentation rates, redox conditions, primary production, and the amount of erosive input of a lake, and this in turn affects the composition of the lake sediment. Since specific elements and element ratios often characterize specific lithological properties, XRF analysis helps to define the sediment's source and gives hints to reconstruct the paleo-environment and -climate.

At Soppensee, the sediment deposited at the end of the Würm glaciation mainly consist of detrital material, detected in high rates of K, Al, Rb, Ti, and Zr. We observe a strong decrease in these elements just at the onset of the Bölling/Alleröd (B/A) warm period. With the beginning of the B/A the Ca values start to increase indicating first authigenic calcite precipitation due to higher temperatures and developing primary production. Siderite is detected by XRD analyses (Fischer 1996) in sediments deposited during the B/A and Younger Dryas (YD). The presence of Siderite can also be seen in high Fe and at the same time low K, Al, Rb, Ti and Zr values in the XRF core scan results. This depositions coincide with a period of summer anoxia most probably caused by additional organic matter input from the catchment, as well as longer phases of stratification due to reduced wind exposure caused by the increased vegetation cover (Lotter 2001). At the same time first magnetotactic bacteria appear, resulting in single domain magnetite of uniform grain size.

At the end of the YD, first formation of calcitic varves starts. These annually laminated sediments, mainly reflected in high Ca values, indicate rising primary production at the lake surface due to warmer temperatures in the upper water column, and anoxic conditions at the sediment surface due to decomposition of organic material and poor mixing of the hypolimnion. Varves become darker, discontinuous and eventually faint at around 5500 cal y BP. For the same time period, previous studies report increasing air temperatures and a change in tree cover in the environment from mainly mixed oak forest to shadow-tolerant fir-beech forest (Lotter 2001). These changes in the environment lead to more organic matter produced within the epilimnion and also transported into the lake, which then decays at the lake bottom. This rotting process uses up oxygen and produces carbonic acid and hence leads to pH changes in the hypolimnion, which supposedly circumvents the build-up of calcite varves. In addition, these more acidic and reducing conditions result in an rapid increase of ferromagnetic minerals as well as increased mobility of metal ions, resulting in higher values of mainly Fe, but also Mn, Zn and Pb.

First human activity in the catchment and first local settlements may be seen in the sediment recorded by decreasing Ca and increasing Fe and Mn values at about 5500 and 3500 y cal BP due to anthropogenic changes of the environment. An abrupt increase in Fe and Mn during the Middle Ages (about 1500-500 y cal BP) coincides with massive deforestation in the catchment and around the lake. The lack of forest presumably enabled mixing of the lake water due to winds and increased soil erosion supplied additional nutrients to the lake. The topmost part of the lake sediment is strongly influenced by anthropogenic eutrophication of the lake due to intense agriculture in the catchment.

Our results not only confirm previously published climate reconstructions of Switzerland and Europe, but together with the interpretation of paleomagnetic properties of the exact same sediment core material, we are able to add new insights about the development and effects of past environmental and climate change.

REFERENCES

- Lotter, A. 2001: The palaeolimnology of Soppensee (Central Switzerland), as evidenced by diatom, pollen, and fossil-pigment analyses, *Journal of Paleolimnology*, 25, 65-79.
- Fischer A. 1996: Isotopengeochemische Untersuchungen ($\delta^{18}\text{O}$ und $\delta^{13}\text{C}$) im Wasser und in den Sedimenten des Soppensees (Kt. Luzern, Schweiz), Diss. ETH Nr. 11'924

8.30

Past glaciation in the Central Andes record alteration in the tropical circulation and the Southern Westerlies

Zech Jana¹, Zech Roland², Kubik Peter W.³ and Veit Heinz¹

¹Institute of Geography, University of Bern, Hallerstr. 12, 3012 Bern, Switzerland (jana.zech@giub.unibe.ch)

²Department of Geological Sciences, Brown University, Box 1846, Providence RI 02912, USA

³Laboratory of Ion Beam Physics, ETH Zurich, Schafmattstrasse 20, 8093 Zurich, Switzerland

The mass balance of glaciers is most sensitive to changes in precipitation and temperature. Thus the reconstruction of past glacial advances can provide important information about past climate changes. In the arid Central Andes, where glaciers are particularly sensitive to precipitation changes (Kull et al. 2008), the timing of glaciation documents how and when the three main atmospheric circulation systems - the South American Summer Monsoon (SASM), the El Niño Southern Oscillation and the Southern Westerlies - changed their intensity and position over time.

We dated several well preserved glacial stages in the Sierra de Quilmes (~26°S) applying ¹⁰Be surface exposure dating. Our results show that glaciers advanced in phase with the global last glacial maximum (LGM) at 25.8 ± 0.8 ka and during the Lateglacial at 13.5 ± 0.5 ka and 12.8 ± 0.5 ka. The Lateglacial advances coincide with the Tauca (16-14 ka) and Coipasa (13-11 ka) lake transgression phases on the Altiplano and reflect the precipitation sensitivity of glaciers in the arid Central Andes. A glacier climate modeling study corroborates that the Lateglacial advances occurred as a result of moderate to massive precipitation increases; reconstructed temperature depressions are -1.4 to -5.4°C (Schmidhauser 2007). Sufficient moisture for the Lateglacial glacial advance can be explained by enhanced upper tropospheric easterlies as response to an intensified tropical circulation and sustained la Niña-like conditions in the eastern Pacific. These results agree closely with previously reported Lateglacial advances farther north in NW Argentina (~22°S) (Zech et al. 2009) and Bolivia (~17°S) (Zech et al. 2010).

Our new glacial chronology from the Sierra de Quilmes, however, is unique, insofar as the oldest dated moraine documents an earlier glacial advance at ~34.6 ± 1.1 ka. This is roughly contemporaneous with the local LGM further south, dated to ~38 ka in northern Chile (~30°S) and Central Argentina (~39°S) (Zech et al. 2008). These pre-LGM advances document increased precipitation related to a northward shift and intensification of the Southern Westerlies, which affected the hydrological conditions in regions further north (north of 30°S) than previously assumed.

The new results from the Sierra de Quilmes thus raise questions regarding the southernmost migration of the tropical circulation system and the role of the Southern Westerlies for glacial advances even north of 30°S.

REFERENCES

- Kull, C., Imhof, S., Grosjean, M., Zech, R. & Veit, H., 2008: Late Pleistocene glaciation in the Central Andes: Temperature versus humidity control - A case study from the eastern Bolivian Andes (17°S) and regional synthesis. *Global and Planetary Change* 60, 148-164.
- Schmidhauser, A. 2007: Modelling glacier-climate interaction in the Central Andean Sierra del Quilmes, NW-Argentina, Diploma Thesis, University of Bern, 127.
- Zech, J., Zech, R., Kubik, P. W. & Veit, H., 2009: Glacier and climate reconstruction at Tres Lagunas, NW Argentina, based on ¹⁰Be surface exposure dating and lake sediment analyses. *Palaeogeography, Palaeoclimatology, Palaeoecology* 284, 180-190.
- Zech, J., Zech, R., May, J.-H., Kubik, P. W. & Veit, H., 2010: Lateglacial and early Holocene glaciation in the tropical Andes caused by La Niña-like conditions. *Palaeogeography, Palaeoclimatology, Palaeoecology* 293, 248-254.
- Zech, R., May, J.-H., Kull, C., Ilgner, J., Kubik, P. W. & Veit, H., 2008: Timing of the late Quaternary glaciation in the Andes from ~15 to 40° S. *Journal of Quaternary Science* 23 6-7, 635-647.

9. Trusting on soils in a changing world?

Samuel Abiven, Pascal Boivin, Elena Havlicek, Roxane Kohler Milleret, Claire Le Bayon

Swiss Soil Science Society

- 9.1 Bandowe BAM., Wilcke W.: Oxygenated Polycyclic Aromatic Hydrocarbons in Soil
- 9.2 Bigalke, M., Kersten, M., Kobza, J., Weyer, S., Wilcke, W.: Cu and Zn stable isotopes as tracers for sources, transport and biogeochemical transformations of Cu and Zn in polluted soils and sediments
- 9.3 Blanc N., Hassouna M., Pfeifer H.-R.: Environmental contamination of alpine soils in the Mont-Blanc massif by arsenic
- 9.4 Burri S., Sturm P., Knohl A., Buchmann N.: Impacts of Summer Drought on Short-Term Reactions of Plant and Soil Gas Exchange of a Managed Lowland Grassland in Switzerland
- 9.5 Hasinger O., Millièrè L., Verrecchia E. P., Cailleau G., Spangenberg J. E.: Carbon cycle in a scree slope soil: from organic matter to secondary carbonate (Villiers, Jura Mountains, CH)
- 9.6 Hoffmann, U., Kuhn, N.: Soil organic carbon in the rocky desert of northern Negev (Israel)
- 9.7 Johannes A., Kohler-Milleret R., Boivin P.: Evaluation of the effect of root exudates on the structure of two different soils
- 9.8 Maestrini B., Singh N., Abiven S., Schmidt M.W.I.: BC loss processes in a temperate forest topsoil: a long-term field manipulation experiment
- 9.9 Martignier L., Verrecchia E.: Pleistocene vs Holocene impact on soils: An example from the Jura Mountains
- 9.10 Melis S., Boivin P., Guiné V., Abiven S., Krebs R.: Cobaltihexamine and Metson CEC measures on different organic surfaces (biochars and hydrothermal chars)
- 9.11 Pfund S., Guenat C., Le Bayon C., Verrecchia E., Bullinger-Weber G.: Emme River (BE) restoration project: how to evaluate its success using soil parameters ?
- 9.12 Sadri S. & Wilcke W.: Initial analysis of a 10-year pH time series of litter leachate in an Ecuadorian catchment
- 9.13 Salomé C., Guenat C., Bullinger-Weber G., Gobat J.-M., Le Bayon R.C.: Structure formation in carbonate-rich alluvial soils along an altitudinal gradient: roles of lithogenic characteristics and biological agents.
- 9.14 Schmdit M. W.I., Torn M. S., Abiven S., Dittmar T., Guggenberger G., Janssens I. A., Kleber M., Kögel-Knabner I., Lehmann J., Manning D. A.C., Nannipieri P., Rasse D. P., Weiner S., Trumbore S. E.: Shifting paradigms - Soil organic matter turnover in a changing world
- 9.15 Schwarz M.T., Bischoff S., Krüger L., Michalzik B., Siemens J., Wilcke W.: Land-use intensity and biodiversity as controls of element cycling
- 9.16 Villacres D., Guiné V., Freyre N., Boivin P.: Contribution of earthworms in the maintenance of biobeds
- 9.17 Wilcke W., Ruppenthal M., Schwarz M.T., Oelmann Y.: Stable H and N isotope approaches to assess soil organic matter turnover and N transformations in ecosystems

9.1

Oxygenated Polycyclic Aromatic Hydrocarbons in Soil

Benjamin A. Musa Bandowe & Wolfgang Wilcke

Geographisches Institut, Universität Bern, Hallerstrasse 12, 3012 Bern (bandowe@giub.unibe.ch)

Extensive work has been published about polycyclic aromatic hydrocarbons (PAHs) in soil (Wilcke, 2000). However very little is known about their oxygenated derivatives (OPAHs, Fig. 1) in soil. The OPAHs are considered to be more toxic than their parent-PAHs because they are direct-acting mutagens compared to their parent compounds which require enzyme activation to exhibit their toxicity. They are also more water soluble and hence have higher ability to spread in the environment (Lundstedt et al., 2007). OPAHs are emitted together with parent-PAHs from anthropogenic sources or are products of microbial/physicochemical transformation of parent-PAHs. However the exact contribution of each of these sources in soil is unknown, but essential. In this paper, we present the results of the analysis of OPAHs and their parent-PAHs in soils from Angren industrial region (Uzbekistan) and Bratislava (Slovakia) with the aim of assessing the concentration, composition pattern, sources and vertical transport of OPAHs.

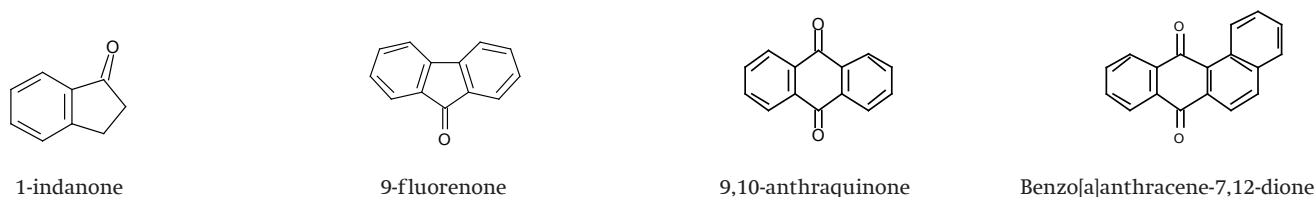


Figure 1. Structures of commonly found OPAHs in soil

At the Angren industrial region, we sampled mineral soils at two depths (0-10 and 10-20 cm) from 11 sampling points along a 20-km transect. In Bratislava, whole soil profiles (up to 5 horizons) at 9 locations and two additional topsoils were sampled. OPAHs and their parent-PAHs were extracted by pressurized liquid extraction, separated/purified using column chromatography and measured by GC-MS (Bandowe and Wilcke, 2010).

OPAHs were in all soils dominated by 1-indanone, 9-fluorenone, 9,10-anthraquinone and benzo[a]anthracene-7,12-dione (Fig. 1). The concentrations of these OPAHs were frequently higher than their regulated and frequently measured parent-PAHs (e.g., 9-fluorenone/fluorene: 13-126 and 9,10-anthraquinone/anthracene: 13-44 in Angren topsoils). This calls for the inclusion of OPAHs in monitoring programs.

The sum of OPAHs concentration (Σ OPAHs) was strongly correlated with their Σ parent-PAHs (Fig. 2) suggesting that OPAHs are emitted together with their parent-PAHs by primary anthropogenic sources. In Angren, this was further confirmed by the correlation of Σ OPAHs with industrially emitted trace metals (Ba, Pb, Th, Zn; Bandowe et al., 2010, $0.70 \leq r \leq 0.82$, $0.01 \leq p \leq 0.05$).

Evidence of faster vertical transport of OPAHs than their corresponding parent-PAHs was indicated by higher OPAH/parent-PAH concentration ratios in subsoil compared to topsoil at several sampling sites. We further showed that concentration ratio of OPAHs (concentration in uppermost subsoil to that in surface horizon) were significantly negatively correlated with their log octanol-water partitioning coefficient (K_{ow}) at several sites in Bratislava and one site in Angren. Again, larger contribution of the more water-soluble OPAHs (1-indanone and 9-fluorenone) at the expense of the of the less water-soluble 9,10-anthraquinone and benzo[a]anthracene-7,12-dione to total OPAH concentrations in subsoils indicated that the transport mechanism was mainly leaching as truly dissolved solute. This shows that groundwater will be increasingly affected by OPAHs and is another reason for monitoring these compounds.

REFERENCES

- Bandowe, B.A.M. & Wilcke, W. 2010: Analysis of polycyclic aromatic hydrocarbons and their oxygen-containing derivatives in soils. *Journal of Environmental Quality* 39,1349-1358.
- Bandowe, B.A.M., Shukurov, N., Kersten, M., & Wilcke, W. 2010: Polycyclic aromatic hydrocarbons (PAHs) and their oxygen-containing derivatives in soils from the Angren industrial area, Uzbekistan. *Environmental Pollution* 158, 2888-2899.
- Wilcke, w. 2000: Polycyclic aromatic hydrocarbons (PAHs) in soil. *Journal of Plant Nutrition and Soil Science* 163, 229-248.
- Lundstedt, S., White, P. A., Lemieux, C.L., Lynes, K.D., Lambert, I.B., Öberg, L Haglund, P. & Tysklind, M. 1992: Sources, fate, and toxic hazards of oxygenated polycyclic aromatic hydrocarbons (PAHs) at contaminated sites. *Ambio* 36, 475-485.

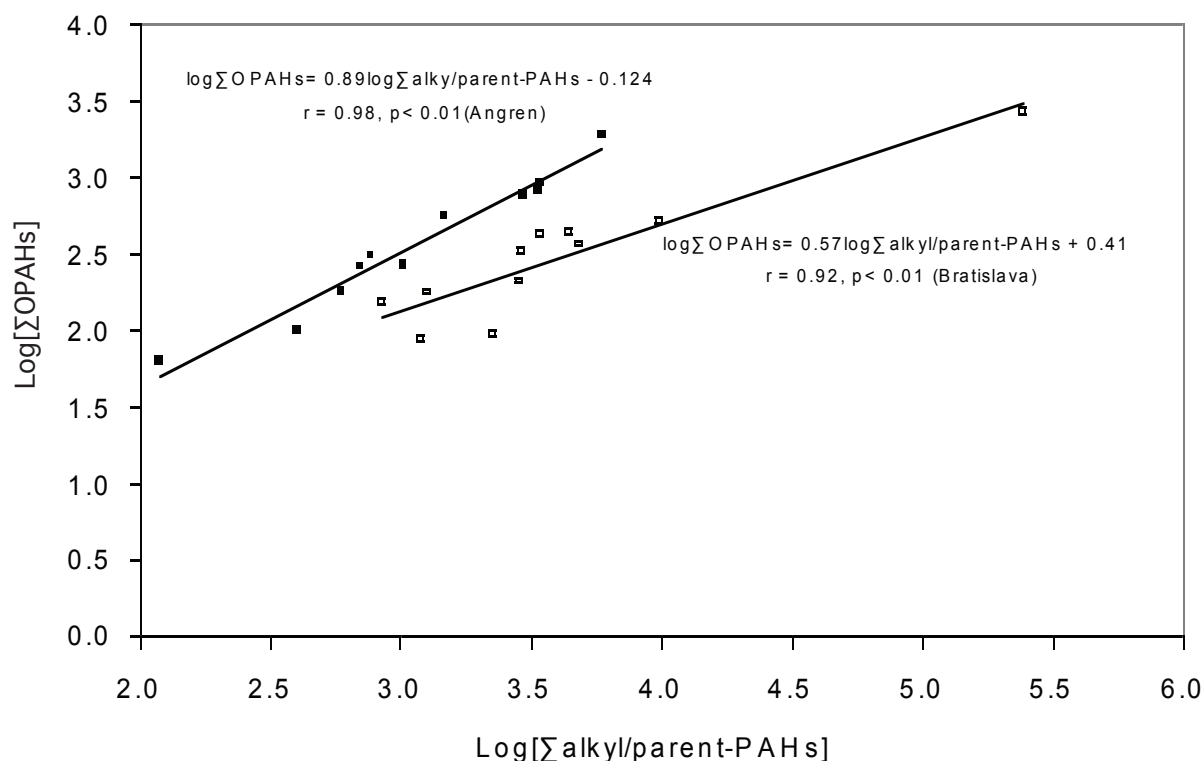


Figure 2. Relation between Σ OPACs and Σ parent-PAHs in Angren (closed boxes) and Bratislava (open boxes) mineral topsoils.

9.2

Cu and Zn stable isotopes as tracers for sources, transport and biogeochemical transformations of Cu and Zn in polluted soils and sediments.

Moritz Bigalke^{1,4}, Michael Kersten¹, Jozef Kobza², Stefan Weyer³, Wolfgang Wilcke⁴

¹ Earth System Science Research Center, Johannes Gutenberg University Mainz, Johann-Joachim-Becher-Weg 21, 55128 Mainz, Germany
(¹ correspondence: moritz.bigalke@giub.unibe.ch)

² University of Frankfurt, Institute of Geoscience, Altenhöferallee 1 60438 Frankfurt am Main, Germany

³ Soil Science and Conservation Research Institute, Mláde nícka 36, 974 04 Banská Bystrica, Slovakia

⁴ Geographic Institute, University of Berne, Hallerstrasse 12, 3012 Berne, Switzerland

The natural abundance of stable metal isotopes, which only recently became analytically accessible, may be used as new tool to discern sources and elucidate the fate of metals in soils. Zinc stable isotopes have already been used for Zn tracing from atmospheric sources (Mattielli et al., 2009) and identification of anthropogenic Zn in sediments (Sivry et al., 2008). In contrast, Cu isotopes have not yet successfully been used for source identification up to now. After metals reach soils or sediments they are prone to transport and different biogeochemical processes which might affect their isotope compositions.

We investigated three soil profiles at different distances from a Cu smelter in eastern Slovakia as well as sediments from a freshwater tideland near Hamburg (Germany).

Source identification:

The three soil samples were taken at 1.1, 3.8 and 5.3 km distance from a Cu smelter and showed very high metal concentrations with up to 8087 $\mu\text{g g}^{-1}$ Cu and 2084 $\mu\text{g g}^{-1}$ Zn. Additional to soil also samples from different waste material and bedrock were taken. The $\delta^{65}\text{Cu}$ values showed only little variation (-0.12 to 0.36‰) and overlapped in soils, bedrock, and most wastes. Therefore, no source identification with the help of $\delta^{65}\text{Cu}$ was possible. In contrast, the $\delta^{66}\text{Zn}_{\text{IRMM3702}}$ values had lighter isotope signals in ash (-0.41‰) and organic horizons (-0.85 to -0.32‰) compared to bedrock (-0.28‰) and slag (0.18‰), which is likely caused by fractionation of Zn isotopes during evaporation. This isotope fractionation caused different $\delta^{66}\text{Zn}$ values of smelter-derived Zn and native Zn and thus allowed for separation of different Zn sources.

A freshwater tideland was sampled to a depth of 35 cm in 2-cm intervals. The sediment showed elevated metal concentrations with up to 300 $\mu\text{g g}^{-1}$ Cu and 2100 $\mu\text{g g}^{-1}$ Zn. Variations of $\delta^{65}\text{Cu}$ and $\delta^{66}\text{Zn}$ in the profiles were small and for Zn within the analytical error, which might show that Zn sources were constant during time of sedimentation. The $\delta^{65}\text{Cu}$ values showed small but significant variation with depth. The $\delta^{65}\text{Cu}$ values became heavier down to a depth of 10 cm (Fig. 1). Below this depth $\delta^{65}\text{Cu}$ values fluctuated vertically, which might point at changing Cu sources in short time intervals (summer to winter) or biogeochemical fractionations.

Biogeochemical processes:

In the soil profiles at the Slovakian Cu smelter depth gradients of $\delta^{65}\text{Cu}$ and $\delta^{66}\text{Zn}$ showed contrasting behavior (fig. 1). The $\delta^{65}\text{Cu}$ values became lighter down to a depth of 0.4 m, probably because of equilibrium reactions between Cu species in soil solution and reactive surfaces during transport of smelter-derived Cu. Relating the leaching depth to the operating time of the smelter we calculated a mean leaching rate of ca. 0.0067 m yr^{-1} in the last 60 yr. In contrast, Zn isotope ratios shifted to heavier $\delta^{66}\text{Zn}_{\text{IRMM3702}}$ values with depth. Main variations of $\delta^{66}\text{Zn}_{\text{IRMM3702}}$ values occurred in the organic horizons and are probably caused by biogeochemical cycling in the plant-soil system. In the mineral soil, variations in $\delta^{66}\text{Zn}$ values were only minor and probably caused by mixing of smelter-derived Zn with native Zn in the soil.

In the tideland, $\delta^{65}\text{Cu}$ values became heavier with increasing depth, down to ca. 10 cm. This is the depth which is still subject to changing redox conditions, while at greater depth redox potentials (Eh) change to negative values and below a depth of ca. 18 cm nearly all Cu occurred in oxidizable fractions (e.g., sulphides). The trend of $\delta^{65}\text{Cu}$ values to become heavier in the area of changing redox conditions is similar to that observed in water influenced soils (Bigalke et al., 2010) and might be caused by changes in redox state and mobility of Cu. The fluctuating $\delta^{65}\text{Cu}$ values in the reduced sections of the sediment, might also be attributable to Cu isotope fractionation during formation of various reduced Cu species but can also be related to a priori different Cu isotope ratios in the source materials.

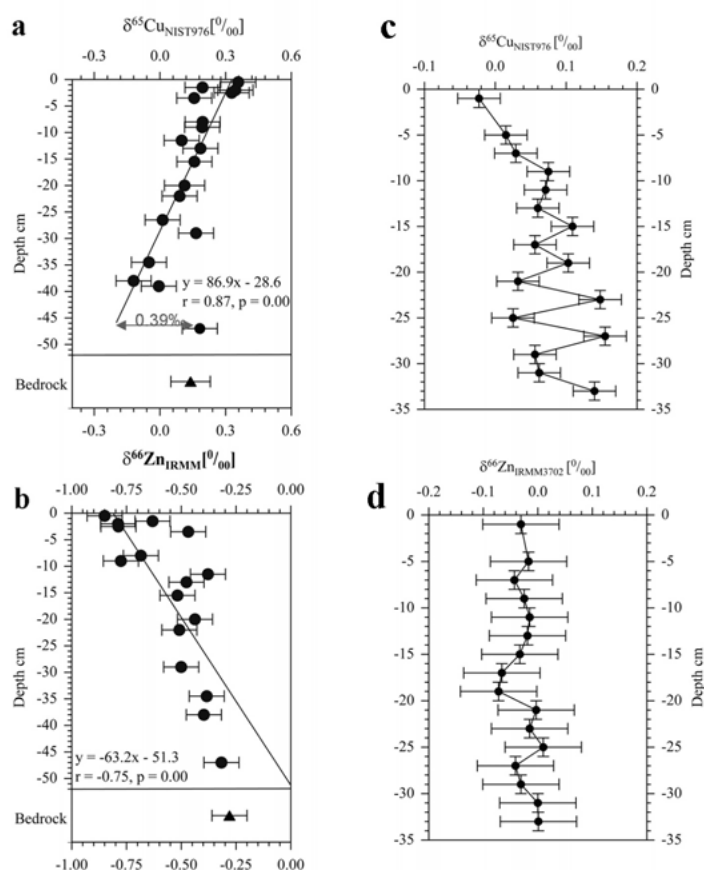


Figure 1. Vertical distribution of $\delta^{65}\text{Cu}$ (a, c) and $\delta^{66}\text{Zn}$ values (b, d) in polluted soils from Slovakia (a, b) and freshwater tideland sediments from Germany (c, d).

REFERENCES

- Bigalke, M., Weyer, S., and Wilcke, W., 2010. Stable copper isotopes: a novel tool to trace copper behavior in hydromorphic soils. *Soil Sci. Soc. Am. J.* 74, 60-73.
- Mattielli, N., Petit, J. C. J., Deboudt, K., Flament, P., Perdrix, E., Taillez, A., Rimetz-Planchon, J., and Weis, D., 2009. Zn isotope study of atmospheric emissions and dry depositions within a 5 km radius of a Pb-Zn refinery. *Atmosph. Environ.* 43, 1265-1272.
- Sivry, Y., Riotte, J., Sonke, J. E., Audry, S., Schafer, J., Viers, J., Blanc, G., Freydier, R., and Dupre, B., 2008. Zn isotopes as tracers of anthropogenic pollution from Zn-ore smelters The Riou Mort-Lot River system. *Chem. Geol.* 255, 295-304.

9.3

Environmental contamination of alpine soils in the Mont-Blanc massif by arsenic

Blanc Nicolas¹, Hassouna Mohammad¹ & Pfeifer Hans-Rudolf¹

¹ IMG-Centre d'Analyse Minérale, Bâtiment Anthropole, CH-1015 Lausanne

(nicolas.blanc.3@unil.ch, mohammad.hassouna@unil.ch, hans-rudolf.pfeifer@unil.ch)

Arsenic is widely recognized as a violent poison throughout the human ages. Many stories were written about it, but it became of interest for people only two decades ago, because it is responsible for some major public health problems around the world, like in the Bengal delta. Switzerland is also concerned by this phenomena, and even if it occurs on a smaller scale, a few communities can simply not deliver water complying with WHO's prescribed values for arsenic to their inhabitants.

Some alpine areas near the crystalline massifs show As-enriched zones with values well above geochemical background. The Petoudes area, in Val de Trient, Valais, is one of these. Located in the geological zone of the Mont-Blanc massif, this small mountain pasture shows a significant local contamination by As. All of the environmental compartments are concerned, but especially the values in the soils are important. This is because of the great affinity of arsenic with iron and aluminium oxyhydroxydes among others.

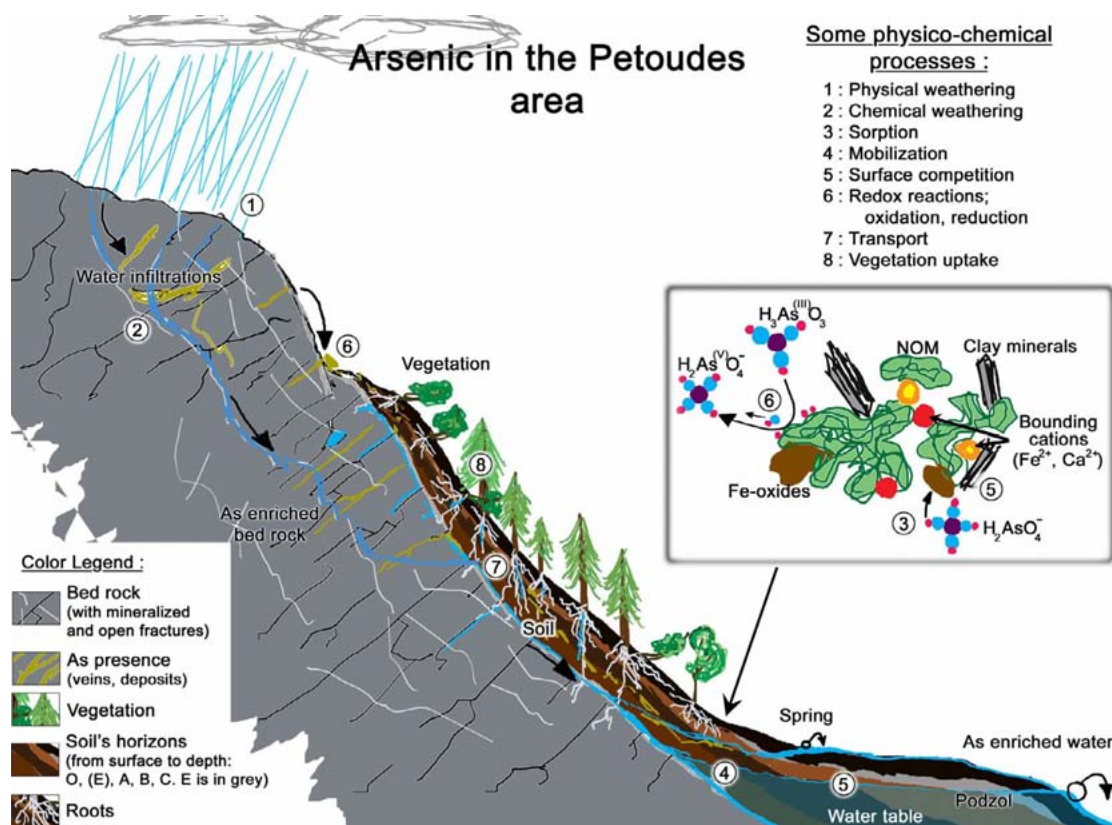


Figure 1. Arsenic fate in the Petoudes area (val de Trient, VS).

The proximity to As sources and the young age of the soils of this region make it an interesting study area. Two sample profiles were made along the slope, from the cliffs to the bottom of the mountain pasture. The top of one of these profiles is located right on a important As anomaly. The young and not well developed soil at this place is highly contaminated ($> \sim 1,000$ ppm) because of the fresh contribution from the As-rich mother rock. In the lower part, as soon as the soil profile gets layered and exhibits several horizons and also where the vegetation is more abundant, the As concentrations increases with depth. The same tendency is shown by iron and aluminium, but carbon and sulphur tend to behave oppositely to As.

Water extracts of the same soils show the inverse tendency: namely that surface horizons release much more As than deep ones. As contents here are in the order of hundred $\mu g \cdot kg^{-1}$ at maximum and this behaviour is quite the same for all analyzed metals, as the dissolved organic carbon. Unexpectedly, it cannot play an important role in the retention of As within the soil, compared with Fe and Al oxyhydroxydes or clay minerals.

Moreover, no significant relationship was revealed by UV-visible spectroscopic analysis of the organic matter. Nevertheless, it could play an indirect role by facilitating its solubilization from the surface horizons, where humic acids are predominant, and being a vector for its mobilization towards the deeper horizons.

It may be available for plants more or less in all horizons but it seems that they are one of the main path to bring As back to the surface in organic molecules as suggested by figure 1.

REFERENCES

- Hassouna, M., Massiani, C., Dudal, Y., Pech, N. & Theraulaz, F. 2010: Changes in water extractable organic matter (WEOM) in a calcareous soil under field conditions with time and soil depth, *Geoderma* 155, pp. 75–85.
- Kalbitz, L. & Wennrich, R. 1998: Mobilization of heavy metals and arsenic in polluted wetland soils and its dependence on dissolved organic matter, *The Science of The Total Environment*, vol. 209, Issue 1, pp. 27–39.
- Lenoble, V. 2003 : Elimination de l'Arsenic pour la production d'eau potable : oxydation chimique et adsorption sur des substrats solides innovants, Thèse de doctorat, Université de Limoges.
- Pfeifer, H.-R., Häussermann, A., Lavanchy, J.-C. & Halter, W. 2007: Distribution and behavior of arsenic in soils and waters in the vicinity of the former gold-arsenic mine of Salanfe, Western Switzerland, *Journal of Geochemical Exploration*, vol. 93, Issue 3, pp. 121–134.
- Von Raumer, J. F. & Bussy, F. 2004: Mont Blanc and Aiguilles Rouges ; Geology of their polymetamorphic basement (External massifs, Western Alps, France- Switzerland), *Mém. Géol. Lausanne*.

9.4

Impacts of Summer Drought on Short-Term Reactions of Plant and Soil Gas Exchange of a Managed Lowland Grassland in Switzerland

Burri Susanne¹, Sturm Patrick¹, Knohl Alexander¹, Buchmann Nina¹

¹ Institute of Plant, Animal and Agroecosystem Sciences, ETH Zurich, Universitätsstrasse 2, CH-8092 Zürich
(Susanne.Burri@ipw.agr.ethz.ch)

Global climate models not only project a gradual global climatic change in response to rising CO₂ concentrations for the future, but also a change in precipitation patterns and in occurrence of extreme weather events (Trenberth 2007). According to these projections, the terrestrial biosphere will not only be exposed to a gradual change in temperature, but also to a changed occurrence of heavy rainfall events, heat waves or droughts. There is, however, still a gap of knowledge in terms of how such climate variability and extreme weather events influence the terrestrial carbon cycle. CARBO-Extreme is a 4-year research project funded by the European Commission with the goal to improve the knowledge of the European terrestrial carbon cycle in response to climate variability and extreme weather events.

An ecosystem manipulation experiment was performed simulating summer drought on a managed lowland grassland in Switzerland in July 2010. The aim was to investigate the impact of summer drought on the short-term carbon cycle with a focus on plant ecophysiology and soil respiration.

Summer drought was simulated by rainout shelters excluding precipitation during the summer months. Soil respiration and its isotopic composition was continuously analyzed during approximately 4 weeks by a quantum cascade laser spectrometer (QCLAS-ISO, Aerodyne Research Inc., MA, USA) coupled to self-designed soil respiration chambers. A pulse labeling approach by adding 99.9 atom% ¹³C-CO₂ to canopy sections allowed tracing newly fixed carbon through the plant-soil system and back to the atmosphere by soil or root respiration. Thus, the short-term CO₂ exchange could be traced and diurnal fluctuations monitored.

Preliminary results allow a better insight into the impacts of summer drought on the carbon cycle of a lowland grassland, especially into the short-term reactions of plant and soil gas exchange and the transfer of assimilated carbon from aboveground to belowground processes.

REFERENCES

- Trenberth, K.E., Jones P.D., Ambenje P., Bojariu R., Easterling D., Klein Tank A., Parker D., Rahimzadeh F., Renwick J.A., Rusticucci M., Soden B. Zhai P. 2007: Observations: Surface and Atmospheric Climate Change. In: Solomon, S., Qin D., Manning M., Chen Z., Marquis M., Averyt K.B., Tignor M., Miller H.L. (eds.) 2007: *Climate Change 2007: The Physical Science Basis. Contribution of Working Group I to the Fourth Assessment Report of the Intergovernmental Panel on Climate Change*. Cambridge University Press, Cambridge, United Kingdom and New York, NY, USA. 996 pp.

9.5

Carbon cycle in a scree slope soil: from organic matter to secondary carbonate (Villiers, Jura Mountains, CH)

Hasinger Olivier¹, Millièvre Laure¹, Verrecchia Eric P.¹, Cailleau Guillaume¹, Spangenberg Jorge E.²

¹ Institute of Geology and Paleontology, University of Lausanne, Anthropole, CH-1015 Lausanne, Switzerland

² Institute of Mineralogy and Geochemistry, University of Lausanne, Anthropole, CH-1015 Lausanne, Switzerland

The role of soils in the global carbon cycle and their potential as carbon sinks in terrestrial ecosystems are attracting more and more research related to global warming (Janssens et al., 2003; Lal et al., 2009). Carbon transfers in aboveground ecosystems and biological systems are better understood compared to belowground processes (Ehleringer et al., 2002). The relationships between the organic matter cycle and soil secondary carbonates have been neglected for a long time, particularly in carbonate environments. Except at the global scale, carbon fluxes and their associated processes are still misunderstood (Prentice et al., 2001; Lal et al., 2009; Bond-Lamberty and Thomson, 2010).

Soil carbon dynamics in a scree slope deposit (where secondary carbonate precipitates abundantly as Needle Fiber Calcite or NFC) have been investigated by identifying and measuring the main carbon compounds (atmospheric CO₂, organic matter, soil CO₂, dissolved inorganic carbon, and secondary carbonates, see Fig. 1). The objective of the study is not a quantitative modelling of the carbon cycle, but rather a qualitative examination of the main contributing processes and pathways (Fig. 1). The main aim is to define the carbon origin contained in pedogenic carbonates (in this particular case, NFC, see Fig. 1). Most studies are related to the organic matter pool, but there is an obvious link between this compartment and secondary carbonates. The results of this study bring new insights to the belowground processes, in terms of carbon transfers in a carbonate scree slope soil.

The main result shows that the carbon contained in secondary carbonates (NFC) is mainly originating from atmospheric CO₂ (through photosynthesis fixation, organic matter mineralization and root respiration, dissolution of CO₂ in soil solution, and finally DIC precipitation), although lithogenic carbonates are present in large quantities in these scree slope deposits. The carbon isotopic signature of the soil solution reveals that carbon cycling is dominated by the heterotrophic respiration signal,

even if the soils are developing in a carbonate-rich substrate. This means that the weathering of lithogenic carbonates, in term of DIC carbon composition, can be neglected compared to the heterotrophic respiration. In addition, the influence of the physicochemical conditions of the medium is important. This is why various soil physicochemical parameters are measured to validate the interpretations about dominant carbon pathways.

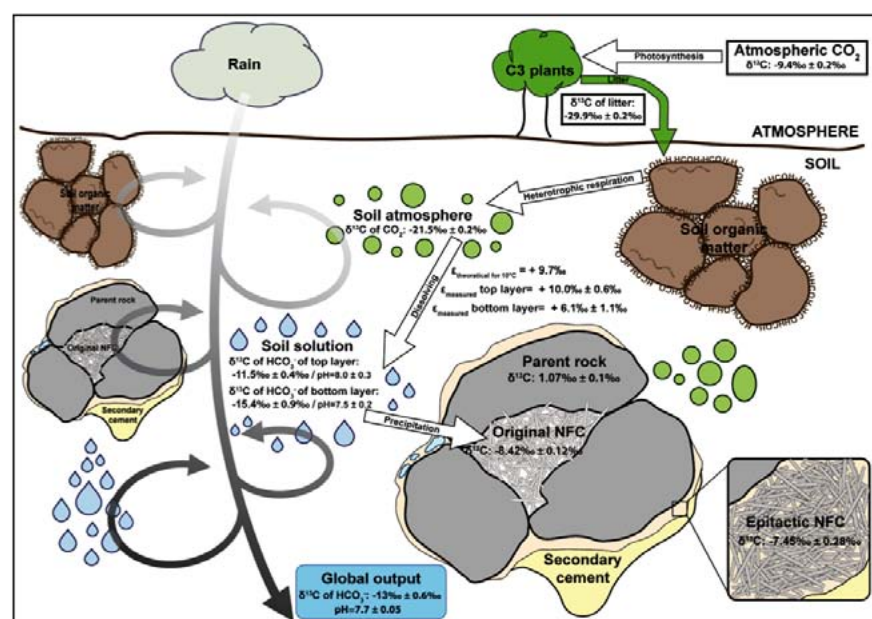


Figure 1. A model sketch of the carbon transfers between the various compartments in a scree slope soil, Villiers (CH). The compartments are characterized by their mean isotopic signatures (over one year of measurements). The white arrows represent the processes involved in the carbon transfers.

REFERENCES

- Bond-Lamberty B. & Thomson A. 2010 : Temperature-associated increases in the global soil respiration record, *Nature* 464, 579-582
- Ehleringer, J. R., Bowling, D., Fessenden, J., Flanagan, L.B., Helliker, B.R., Martinelli, L.A., and Ometto, J.P. 2002: Stable isotopes and carbon cycle processes in forests and grasslands. *Plant Biology* 4, 181-189.
- Lal, R. 2009: Sequestering carbon in soils of arid ecosystems. *Land Degradation & Development* 20, 441-454.
- Janssens I.A., A. Freibauer, P. Ciais, P. Smith, G.-J. Nabuurs, G. Folberth, B. Schlamadinger, R.W.A. Hutjes, R. Ceulemans, E.-D. Schulze, R. Valentini & A.J. Dolman, 2003: Europe's terrestrial biosphere absorbs 7 to 12% of European anthropogenic CO₂ emissions. *Science* 300, 1538-1542.
- Prentice, I.C., Farquhar G.D., Fasham M.J.R., Goulden M.L., Heimann M., Jaramillo V.J., Khashgi H.S., Le Quéré C., Scholes R.J., Wallace D.W.R. 1. 2001: The Carbon Cycle and Atmospheric Carbon Dioxide. In: *Climate Change 2001: The Scientific Basis. Contribution of Working Group I to the Third Assessment Report of the Intergovernmental Panel on Climate Change*. Cambridge University Press, United Kingdom and New York, USA, 881pp.

9.6

Soil organic carbon in the rocky desert of northern Negev (Israel)

U. Hoffmann, N. Kuhn

*Department of Physical Geography, University of Basel, Switzerland
(ulrike.hoffmann@unibas.ch / Fax: +41-61-2670740 / Phone: +41-61-2670736)*

The mineral soil represents a major pool in the global carbon cycle. However the behavior of mineral soil as a carbon stock is not fully understood and as a result there is a serious lack of comparable data on mineral soil organic carbon (SOC) at a regional scale. To improve our understanding of soil carbon stocks it is necessary to acquire regional estimates of SOC pools. So far the SOC literature is dominated by studies in the humid tropics with high deforestation rates and high biodiversity levels and Arctic ecosystems with high rates of warming and huge stocks of vulnerable carbon. Little attention has been given to dryland ecosystems, but they are often considered to be highly sensitive to environmental change, with large and rapid responses to even the smallest changes in climate conditions. Due to this fact, arid regions as an ecosystem with extensive surface area across the globe (6.15 billion ha) have been suggested as a potential component for major carbon storage. It is suggested that regional spatial patterns of SOC density (kg/m^2) in drylands are mostly affected by vegetation, soil texture, landscape position, soil truncation, wind erosion/deposition and the effect of water supply. However, there is minor research about the interaction between soil volume, geomorphic processes and SOC density. The goal of this study is to reveal that approaches to establish a SOC inventory used in humid areas with continuous runoff and fully developed soil profiles and Catenas are unlikely to work in arid areas with discontinuous runoff and patchy soil coverage. The focus of this paper is the assessment of a sampling approach based on the mapping of topographic-dependent hydrological response units (HRUs) and the establishment of a SOC inventory on a rocky desert slope in the northern Negev (Israel). The two objectives combine qualitative fieldwork in this area, statistical analysis and mapping of hydrological response units (HRUs).

Soil samples were taken in small transects at different representative slope positions across a range of elevations, soil texture, vegetation types, and terrain positions in a small catchment (600 ha) in the rocky desert (Negev). SOC concentrations of the soil samples were determined by a CHN-analyzer. Carbon densities (in kg/m^2) were estimated for the mineral soil layer in each soil sample. The results indicate a large spatial variability of the carbon contents ($0.12\text{--}6.07 \text{ kg/m}^2$), the soil depths (0.1 - 0.9 m) and the vegetation coverage (10 – 29 %) across the landscape. In general, topography exerts a strong control on the carbon contents and the soil depths in the study site. Lowest carbon contents are apparent at the hillslope tops with increasing contents downslope. Because of the significantly larger carbon content of the northern exposed slope, we suggest that aspect affects solar radiation and hence the plant productivity, as well as the decomposition rate which has major controls SOC. This regional SOC inventory makes a significant contribution in regional SOC-inventory-studies in arid environments, as these areas are generally mapped as stony-rocky deserts (WRB, FAO 1994), which are assumed to have negligible SOC stocks and are thus not considered in global inventories. The results show that SOC should not be ignored in arid areas due to the total amount of carbon storage in the study area (50791 kg C). Our results should provide an indication that carbon contents in dynamic environments are more affected and controlled by surface properties than by climate. In conclusion, climate is less important than the interaction of ecogeomorphological surface processes in arid ecosystems.

9.7

Evaluation of the effect of root exudates on the structure of two different soils

Alice Johannes¹, Roxane Kohler-Milleret² and Pascal Boivin¹

¹ Haute Ecole Paysage Architecture et Ingénierie (hepia) – Filière Agronomie – Laboratoire Sols et Substrats – Route de Presinge 150 – CH-1254 Jussy (alice.johannes@hesge.ch)

² Université de Neuchâtel – Institut de Biologie – Sol et Végétation – Rue Emile Argand 11 – CH-2009 Neuchâtel

An experiment to evaluate the effect of root exudates application on the structure of different soils (a silt loam Luvisol and a loamy Anthrosol) was conducted on repacked soil cores in the laboratory. A series of experiments were conducted by irrigating the two soils with exudates and fresh water.

The changes in the soil properties were analyzed using aggregate stability indexes and shrinkage analyses, and were compared to the previously reported literature.

The observed changes in aggregate stability, i.e. increase in aggregate stability with exudates application in the presence of bacteria, were in good agreement with the literature. Shrinkage analysis which allowed the characterization of the pore systems of the soil was never applied to exudates application so far. It mostly showed a change in the structural pore volume, with an increase of the largest pore volume on the Luvisol and a decrease of their hydro-structural stability on both soils with exudates application.

These results do not accord with previous findings of experiments conducted on mesocosms with plants and consequently natural leek root exudates, on which the large changes observed in the structural porosity were attributed to bacterial activity as stimulated by root exudates rather than to direct root penetration effect. Hence, further research is needed to better understand the combined effects of roots and bacteria on soil structure.

9.8

BC loss processes in a temperate forest topsoil: a long-term field manipulation experiment

Maestrini Bernardo¹, Singh Nimisha¹, Abiven Samuel¹, Schmidt Michael W. I¹.

¹ Department of geography, University of Zurich, Winterthurerstrasse, 190 8057 Zürich (Bernardo.maestrini@geo.uzh.ch)

Pyrogenic carbon (PyC) is playing an important role in the global carbon cycle as a C-sink. Since many years PyC has been considered a very recalcitrant matter (Goldberg, 1980) however the studies of the last decade have rejected the hypothesis of the negligibility of PyC decomposition (Schmidt and Noak, 2000). At least two field experiments (Hammes et al. 2008, Nguyen et al. 2008) and many incubation studies (Hamer, 2004, Baldock and Smernick, 2002 Zimmerman, 2010) are confirming the decomposition of PyC.

According to IPCC, 2007 N deposition will increase in thirty years by between 50 to 100% relative to year 2000. While the effect of N addition of SOM decomposition have been investigated (Hagedorn et al. 2003, Bowden, 2004) no specific studies have been carried out on the effect of N addition on PyC decomposition.

The experimental design is a field manipulation experiment: the equivalent of 2 gC kg⁻¹ of ¹³C (842‰), ¹⁵N (4,2 atom%) labelled powdered PyC has been added to 6 mesocosms installed in the soil in a clearance of a mixed temperate mountain forest. Additionally, 6 mesocosm has been added with 1gC kg⁻¹ of ¹³C (842‰), ¹⁵N (4,2 atom%) labelled wood powder.

The flux and $\delta^{13}\text{C}$ of the CO₂ evolving from the mesocosm and the ¹³C signal in the DOC is being measured to quantify the decomposition rate and the losses in water soil of labelled PyC over one year. According to the state of the art described above we investigated the decomposition rate and the relative mobilization processes of PyC over one year according to two scenarios: 1) actual N_{min} deposition 2) increasing N_{min} deposition (+60 KgN ha⁻¹ year⁻¹).

Results after the first ten months show a significant decomposition of PyC: a first raw estimation indicates that PyC decomposition is lower than 1%. After the first two months of application mesocosms added with N showed a lower decomposition. More detailed results will be shown in the talk. We can conclude that our first estimate of PyC decomposition in the field over the first ten months appears to be lower than the ones measured in incubation experiments, which can be explained of course by differences in T and moisture conditions.

REFERENCES

- Baldok J.A., Smernik R.J., 2002, Chemical composition and availability of thermally altered *Pinus resinosa* (Red pine) wood, *Organic geochemistry*, 33, 1093-1109.
- Bowden R. D., Davidson E., Savage K., Arabia C., Steudler P., 2004, Chronic nitrogen additions reduce total soil respiration and microbial respiration in temperate forest soils at the Harvard Forest, *Forest ecology and management* 196, 43-56.
- Goldberg, E. D. 1985. Black carbon in the environment. Environmental Science and Technology Series, Wiley and Sons, ISBN 978-0471819790.
- Hagedorn F., Spinnler D., Siegwolf R., 2003, Increased N deposition retards mineralization of old soil organic matter, *Soil biology and biochemistry*, 35, 1683-1692.
- Hamer U., Marschner B., Brodowski S., Amelung W. 2004, Interactive priming of black carbon and glucose mineralization, *Organic geochemistry* 35 823-830.
- Hammes, K., Torn, M.S., Lapenas, A.G. and Schmidt, M.W.I. 2008. Centennial black carbon turnover observed in a Russian steppe soil. *Biogeosciences* 5:1339-1350.
- IPCC (Intergovernmental Panel on Climate Change). 2007. Climate Change 2007: Synthesis Report. http://www.ipcc.ch/pdf/assessment-report/ar4/syr/ar4_syr.pdf
- Nguyen B. T., Lehmann J., Kinyangi J., Smernik R. J., Riha S.J., Engelhard M. H. 2008. Long-term black carbon dynamics in cultivated soil. *Biogeochemistry* 89(3):295-308.
- Schmidt M. W. I. and Noack A. G., 2000, Black carbon in soils and sediments: analysis, distribution, implications, and current challenges. *Global biogeochemical cycles*, 14, 777-793
- Zimmerman A.R, 2010, Abiotic and microbial oxidation of laboratory produced black carbon, *Environmental science and technology*, 44, 1295-1301.

9.9

Pleistocene vs Holocene impact on soils: An example from the Jura Mountains

Martignier Loraine¹ & Verrecchia Eric¹

¹ University of Lausanne, Institute of Geology and Paleontology, Quartier UNIL-Dorigny, 1015 Lausanne (loraine.martignier@unil.ch)

Soil develops at the interface between mineral, hydrological, and living worlds. As an emerging property, each of the soil's constituents tells a story of the past or presently occurring pedogenetic dynamics. The coarse and fine fractions are witnesses of these different processes through time. Consequently, what is the origin of the coarse fraction of soils? What about their fine fraction? Do climatic processes such as frost leave a durable imprint?

To answer these questions, a toposequence is studied in the Jura Mountains where the coarse fraction, fine fraction, and soil processes have interacted since the LGM. In the Jura Mountains (Amburnex Valley, 1360-1420 m a.s.l.), a toposequence of soils is developing on a succession of Cretaceous marls, marly limestones, and limestones. At its highest point, the topography is characterized by a small bench. The soil is mainly composed of a mixture of local moraine deposits. The bench slopes off steeply into forest, where the bedrock outcrops. The soil is thin and mainly organic. The lowest part of the slope is characterized by a colluvium of stones and rocks within a finer fraction of runoff particles. The slope gently decreases towards the wooded pasture. Soils are deeper and much finer grained. Finally, the last part of the slope leads to the lowest point of this toposequence in a small swampy plain, filled by peat bog.

Three main environments are responsible of the coarse fraction of soils. The first type of coarse material is directly inherited from moraine deposited during the LGM. The second type is related to periglacial processes and is mainly composed of scree slope deposits. Finally, part of these materials is removed and mixed with in situ weathered parent material and displaced along the slope forming a colluvium.

The fine material is constituted by two main phases: an allocthonous one mainly composed by loess deposits (Pochon, 1978) and an autocthonous one related to weathered products of bedrock. The in situ loess deposits have been characterized using grain size analysis on surficial horizons compared with deeper horizons. The grain size distribution of these horizons is clearly leptokurtic with a median around 10 μm . The mineralogical composition of these horizons confirms the presence of alpine minerals emphasizing the distal origin of this aeolian material. Nevertheless, another fraction characterizes the fine material, i.e. the weathered products of the parent material. A phyllosilicates vs quartz plot allows the

two different origins of these fractions to be discriminated. A linear relationship can be drawn between the parent material and its autochthonous or subautochthonous weathered products, whereas the linear relationship linking the loess samples is totally independent, emphasizing their allochthonous origin.

Soil thin sections are a powerful tool to observe pedogenetic features. In the Amburnex Valley, thin sections show reticular cracks left by ice lensing, frost shattering of soil features, and frost-disrupted clayey to loamy matrix. All these characteristics demonstrate the important role of frost in pedogenesis. Nevertheless, it is likely that part of these frost imprints is related to past processes as well as to present conditions, at least in the upper part of the soils. In addition, thin sections show the present day weathering of silicates. These processes also include clay leaching and ion lixiviation and redistribution (Fig.1).

The gathering of all these processes builds the history of the landscape since the LGM. At this time, a local glacier was probably situated in the Amburnex Valley and formed the moraine deposit observed at the top of the toposequence. Marly levels were eroded and weathering products were redistributed up and down along the valley flank, forming subautochthonous surficial deposits. At the end of the glaciation, loess originating from the Swiss Plateau was brought up by the wind. These loessic deposits lay directly on top of the carbonate moraine. They underwent runoff along the slope, sometimes mixed with colluvium, and accumulated on benches, overlaying the weathered products of bedrocks. Vegetation, and consequently pedogenesis, started to develop when the climate was warming. Weathering of minerals was enhanced by organic acids, and soil structured with the action of fauna and vegetation. Therefore, soils are the products of a long story recorded by their various features, at various scales.

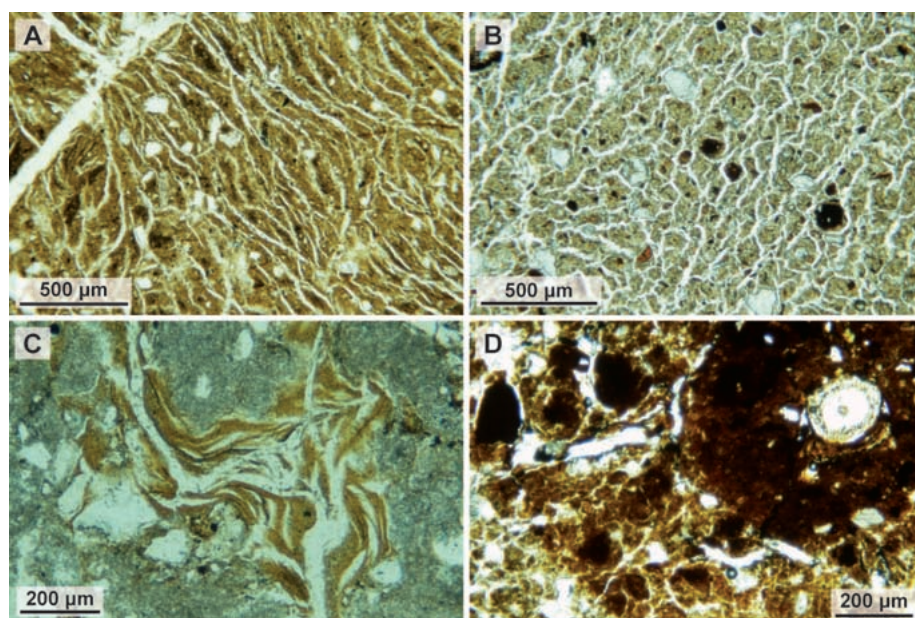


Figure 1. Soil thin sections illustrating A) frost-disrupted clayey matrix, B) reticular cracks left by ice lenses, C) clay coatings due to leaching processes, D) iron redistribution related to root activity. (Photographs by L. Martignier)

REFERENCES

- Pochon, M. 1978: Origine et évolution des sols du Haut Jura Suisse. Mémoires de la Société Helvétique des Sciences Naturelles. Band/Vol. XC, 190 p.

9.10

Cobaltihexamine and Metson CEC measures on different organic surfaces (biochars and hydrothermal chars)

Sylvain Melis¹, Pascal Boivin¹, Véronique Guiné¹, Samuel Abiven² and Rolf Krebs³

¹ Haute Ecole Paysage Architecture et Ingénierie (hepia) – Filière Agronomie – Laboratoire Sols et Substrats – Route de Presinge 150 – CH-1254 Jussy (sylvain.melis@etu.hesge.ch)

² University of Zurich - Physical Geography - Soil Science and Biogeography - Winterthurerstrasse 190 - CH-8057 Zurich

³ Zurich University of Applied Sciences (ZHAW) - Institut für Umwelt und Natürliche Ressourcen - Schloss – CH-8820 Wädenswil

Pyrogenic matter (organic matter heated under oxygen-depleted atmosphere) is known to be relatively efficient for immobilization and degradation of organic contaminants by surface adsorption. Recent, pyrogenic matter has been proposed to be used in agriculture, under the name of biochar. However there is little information on the effectiveness of different chars (hydrothermal char and slow-pyrolysis char) on the immobilization of heavy metals.

In the present study we have evaluated the cationic exchange capacity (CEC) of different type of chars (3 different biochars prepared by slow pyrolysis and 3 different hydrothermal chars) exposed to different types of surface treatment (HCl, acetone, H₂O vapor) with two different methods (cobaltihexamine and Metson). The CEC of compost and peat were also measured using the same protocols.

The first results show that (1) hydrophobic surfaces (biochars without surface treatment) may reduce the CEC of a factor 10; (2) CEC is controlled by pH and CEC performed at pH 7±0.5 (Metson) may be 10 times higher than CEC performed at pH 4±0.5; (3) the CEC measured on the organic surfaces follow the order: compost > coco fiber > peat >> biochars >> hydrothermal chars.

These surfaces reactivity results will be confirmed by acid-base titrations and Cu sorption isotherms.

9.11

Emme River (BE) restoration project: how to evaluate its success using soil parameters ?

Simona Pfund^{1,2}, Claire Guenat³, Claire Le Bayon², Eric Verrecchia¹ & Géraldine Bullinger-Weber¹

¹Laboratory Biogeosciences, Institute of Geology and Palaeontology, University of Lausanne, Anthropole, 1015 Lausanne, Switzerland

²Laboratory Soil & Vegetation, Institute of Biology, University of Neuchâtel, Emile Argand 11, CP 158, 2009 Neuchâtel, Switzerland

³Laboratory ECOS & WSL, Station 2, EPFL, 1015 Lausanne, Switzerland

During the XIX century, several Swiss rivers have been canalized, in order to respond to different human needs (flood protection and water exploitation). In more recent times, river management strategies focus on restoring fluvial dynamics (widening of the river bed) to provide better protection against floods, as well as to increase biodiversity. Different evaluation methods of river restoration are used (hydrology, biodiversity, landscape, etc.) but until now, soils have generally not been considered in floodplain restoration assessment, despite their crucial function in ecosystems.

In this study, we propose to assess the Emme River restoration project using soil parameters (soil morphology and humus characteristics). The restoration aims to increase three evaluation criteria: soil diversity, soil dynamism and soil typicality. Each criterion is related to several quantitative indicators, such as Shannon index, number of horizons and presence hydromorphic features. This methodology has been previously applied to the Thur River (TG), which has been recently restored. Thus, the aim of the present study is also to test if this methodology may be used in other restored rivers.

The Emme River site is one of the first restoration projects in Switzerland. This river had been embanked until 1991/92 when a 500 m stretch was widened. The evaluation is made on comparisons between restored and embanked floodplains. The two zones are located near Aefligen and Burgdorf (canton of Bern) at a mean altitude of 500 m and with an estimated discharge of 19 m³/s. Alluvial deposits are mainly composed of calcareous pebbles and sands. Soil descriptions based on morphological parameters along 13 geomorphological transects (260 auger boring profiles) allow classifying soil profiles into different morphological groups (using clustering analysis). In addition, these soil profile groups have been named according to the “Référentiel Pédologique” classification (AFES, 2008).

In a second analysis, we focus on topsoil layer (humus or new recent deposits) of representative soil profile groups. Several physicochemical analyses have been made, i.e. organic carbon and nitrogen contents, structural stability, particle size distribution, total calcareous material, and porosity.

Seven soil profile groups have been identified in the restored and embanked floodplains. Restoration modifies the presence and the relative importance of each soil group. The soil diversity increases in the restored floodplain, where seven groups are present, while only four are found in the embanked zone. The soil typicality also increases in the restored floodplain, where typical alluvial soils have been created (i.e. FLUVIOSOL BRUTS reflecting a high fluvial dynamics with erosion processes). Analyses on topsoil layers show less distinct differentiation between groups.

Based on our analysis, we conclude that the Emme River restoration was a partial success. The three criteria show that restoration improved floodplain health, but only very locally. Despite the time elapsed and the occurrence of several flood events, restoration was only efficient around the initial widening. We hypothesize that no change may be expected in the future due to the widening characteristics (short length, abrupt transition between river and floodplain). Concerning the methodology, our results show that the proposed methodology is applicable to another braided river, but a comparison with a natural reference seems necessary.

10.12

Initial analysis of a 10-year pH time series of litter leachate in an Ecuadorian catchment

Sara Sadri and Wolfgang Wilcke

Geographic Institute, University of Bern, Hallerstrasse 12, CH-3012 Bern

Corresponding author: sara.sadri@giub.unibe.ch

Over the past decades, there has been increasing concern about tropical rainforest ecosystems of the Amazon. These rainforest systems are being rapidly converted into agricultural areas and pastures via burning, resulting in pollutant deposition both in the soil and in the atmosphere. Boy et al. (2008) studied the resulting increase in acidity of soil of montane rainforests of the Ecuadorian south Andes. Increase of soil acidification results in plant micronutrient losses of Ca, Mg, K as well as associated anions such as sulfate and nitrate. Furthermore, an increasing use of mineral fertilizers is expected to increase the soil nitrogen loads in the form of ammonium, which eventually oxidizes to nitrate and results in more increase of soil acidity (Galloway et al., 2004). In tropical rainforests, the thick organic layer contains almost all of the plant roots. In such a scenario, the loss of nutrient from litter leachate (i.e., the flux from the organic layer into the underlying mineral soil) can be seen as the loss from soil-plant nutrient cycle resulting in further impoverishment of already-nutrient-poor ecosystem. Therefore, in this study, the focus is on the litter leachate soil pH; we aim to understand the impact of manmade changes. The same catchment as in Boy et al. (2008), located in the rim of the Amazon basin was selected for this study. Litter leachate was collected with lysimeters introduced directly below the organic layer without disturbing it on a weekly basis from October 1998 to October 2008. The pH was measured in unfiltered aliquots of the samples immediately after sampling. All analyses of pH data then translated into hydrogen proton activity in water which is the negative logarithm of the molar concentration (i.e., H^+). There were 85 weeks of missing data out of 521 weeks of sampling, which were interpolated linearly.

The upper graph in Figure 1 shows the time series of H^+ from October 1998 to October 2008. The nonparametric Mann-Kendall (MK) test was performed on the time series. The results show that a positive trend in the series exists with 99.99% probability. The residual autocorrelation graph (the lower graph of Figure 1) shows the absence of any discernible seasonal trend (Brockwell and Davis, 2002). The time series graph shows that there was not much change in the leachate data until 2002. Beyond 2002, the data starts moving up and down with multiple quick spikes. For future development of a model capable of forecasting these data, it is important to find the principal regulators of pH values in litter leachate. This will be further studied and analyzed.

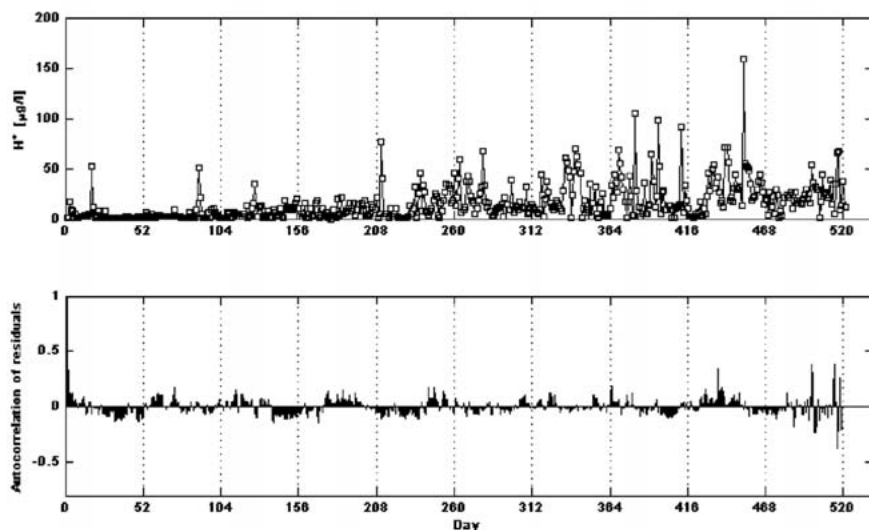


Figure 1. Time series of pH in litter leachate in a 10 year period. Data are taken weekly (on horizontal axis 0 stands for October 9, 1998 and 521 stands for October 11, 2008) [top]. Autocorrelation of residual data reveals no detectable seasonal trend [bottom].

REFERENCES

- Boy, J., C. Valarezo, & W. Wilcke (2008a), Water flow paths in soil control element exports in an Andean tropical montane forest, *European Journal of Soil Science*, 59, 1209-1227.
- Brockwell, P. J., & R. A. Davis (2002), *Introduction to Time Series and Forecasting*, 2nd ed., Springer.
- Galloway, J., F. Dentener, D. Capone, E. Boyer, and R. Howarth (2004), Nitrogen cycles: past, present, and future, *Journal of Biogeochemistry*, 70, 153-226.

9.13

Structure formation in carbonate-rich alluvial soils along an altitudinal gradient: roles of lithogenic characteristics and biological agents.

Salomé C.¹, Guenat C.², Bullinger-Weber G.³, Gobat J.-M.¹ and Le Bayon R.C.¹

¹ Laboratory Soil and Vegetation, University of Neuchâtel, Emile Argand 11, CP 158. 2009 Neuchâtel Switzerland
(clemence.salome@unine.ch)

² ECOS laboratory, Station 2, EPFL, EPFL -1015 Lausanne Switzerland

³ Biogeosciences Laboratory, Institute of Geology and Paleontology, University of Lausanne, Anthropole, 1015 Lausanne, Switzerland.

Floodplains are known to be areas of extraordinary biodiversity with a mosaic of shifting habitats with high interdependency. Nowadays, these ecosystems are subject to conservation and protection. Regarding pedology, floodplains contain a wide range of all steps of soil evolution, i.e. from newly deposited sediment to several hundred year old stable soils. However, less attention has been paid in this context to pedogenesis, especially the very first steps of soil structuring in the youngest and the least developed soils (FLUVIOSOLS).

In this context, our aim is to understand and to compare the structuring processes along a soil stabilization gradient as well as along an altitudinal gradient, testing out the relative importance of mineral inherited deposits due to fluvial dynamics, and the in situ pedogenesis due to biological agents. Our main hypothesis is that at the subalpine level, pedogenesis processes are assumed to be slower than at the hill level. As a consequence, the thickness of soil structured layers as well as the stability of soil aggregates should be higher at the hill level compared to the subalpine one.

To assess these assumptions, we study physicochemical parameters and biological variables (earthworms as ecosystem engineers) in carbonate-rich and calcium saturated environments along:

1. an altitudinal gradient (subalpine, mountain and hill levels).
2. a gradient perpendicular to the river, stratified by vegetation: pioneer willow stage, intermediate alder forest and finally ash mature forest.

All the ecosystems chosen are still influenced by the fluvial dynamic, undergoing regular flooding. In order to evaluate the heterogeneity within each site, three replicates are made in each vegetation unit resulting in a total of 45 samples.

Soil descriptions and laboratory measurements of structural stability (mean weight diameter and percentage of water stable macroaggregates, according to Kemper and Rosenau, 1986) were done. To test the factors that influence soil aggregation, Multiple Linear Regressions (MLR) with earthworms and physicochemical data were performed for each structure variable (MWD and %MAS) .

Our results showed that at the aggregate scale, soil aggregation depends on i) the initial characteristics of deposited sediments and ii) earthworms acting as ecosystem engineers. Biomass of both endogeic and anecic earthworms explained structure in the whole soil profile. At the profile scale, the thickness of structured soil does not significantly vary with altitude despite strong tendencies. This result is due to the dynamic of alluvial system that permits new depositions on soil surface, resulting in soil rejuvenation.

9.14

Shifting paradigms – Soil organic matter turnover in a changing world

Michael W.I. Schmidt¹, Margaret S. Torn², Samuel Abiven¹, Thorsten Dittmar³, Georg Guggenberger⁴, Ivan A. Janssens⁵, Markus Kleber⁶, Ingrid Kögel-Knabner⁷, Johannes Lehmann⁸, David A.C. Manning⁹, Paolo Nannipieri¹⁰, Daniel P. Rasse¹¹,¹², & Susan E. Trumbore¹³

¹ University of Zurich, Department of Geography, Switzerland, (michael.schmidt@geo.uzh.ch)

² Earth Sciences Division, Berkeley Lab, CA, USA

³ Max Planck Institute for Marine Geochemistry, Carl von Ossietzky University, Germany

⁴ Institute of Soil Science, Leibniz Universität Hannover, Germany

⁵ Department of Biology, University of Antwerp, Belgium

⁶ Department of Crop and Soil Science, Oregon State University, USA

⁷ Lehrstuhl für Bodenkunde, Technische Universität München, Germany

⁸ Department of Crop and Soil Sciences, Cornell University, NY USA

⁹ School of Civil Engineering and Geosciences, Newcastle University, UK

¹⁰ Department of Plant, Soil and Environmental Sciences, University of Firenze, Italy

¹¹ Norwegian Institute For Agricultural and Environmental Research, Norway

¹² Structural Biology, Weizmann Institute, Israel

¹³ Max-Planck Institute for Biogeochemistry, Germany

Global changes in climate and atmospheric chemistry will influence soil carbon cycling in myriad ways. This presentation will consider these myriad pathways of influence, how they are represented in current ecosystem models, and considerations for a research agenda to improve predictions of soil response to global change factors.

Our understanding of how soil organic matter is stabilized informs how we think about and model its vulnerability to environmental change. In many disciplines, conceptions of soil organic matter cycling and its expression in mathematical models rest heavily on the concept of recalcitrance – that some organic structures are intrinsically inert. However, a wide array of research, using isotopic, spectroscopic, and molecular marker tools finds little evidence that selective preservation of plant derived material or of resynthesis products determines the long residence time of organic carbon in soil. Even the decomposition rates of fire-derived organic material depend on the soil environment, and it can degrade more quickly than other pools of organic matter in some soils. Thus, intrinsic chemical recalcitrance can no longer be considered a dominant control for long-term organic matter preservation.

Much more likely is that rates of carbon cycling are determined by the interaction of the organic matter and the soil environment including microorganisms, mineralogy, climate, and so on. This does not mean compound chemistry is not important, rather it means it is not important for creating a universal recalcitrance but is very important for determining the potential for stabilization (e.g., tendency to form stable bonds with mineral interfaces) and of the requirements for decomposition (e.g., oxygen requirements to degrade lignin). This understanding is well expressed in recent papers on, for example, physical stabilization, organic carbon-mineral interactions, and the role of microbial by-products in stabilization.

The next step, then, is to consider how these pathways of stabilization affect vulnerability to global change. Changes in plant productivity and root depth alter the input of high energy substrates to the subsoil, which has been shown to be important for priming decomposition of subsoil organic matter. Molecular tools show that nitrogen deposition alters microbial communities, the enzymes expressed, and the byproducts produced. Perhaps least well understood is how predicted changes in soil temperature and moisture will interact with physical and mineralogical modes of stabilization, and thus the vulnerability of very old or deep soil organic matter.

Without the foundational principle that chemical composition defines the rate of decomposition, many tenets of old models are not supported, for example regarding decomposition response to change in temperature or plant species composition. At the same time, the demands on models have expanded to include interest in long time spans and the whole soil profile. Given these new demands and new results, current models may not be adequate. There is a need to develop numerical models that include the pathways and mechanisms that are (1) important for stabilization and destabilization and (2) likely to be affected by global change. These models need to be able to be run globally and yet be testable in point mode against observations.

Much progress could be made in the near term to improve soil carbon models by, for example, improving representations of oxygen diffusion and limitation, root carbon inputs, isotopic tracers, and making depth- or transport-related processes explicit. In other areas, new research is needed to translate recent findings into new parameters, for example, to replace texture with parameters for reactive mineral surface area to represent organo-mineral interaction.

Likewise, solubility and other properties of molecular moieties should be investigated to create parameterizations that may better predict response to future change. Furthermore, much is not known at a structural level, for example, about the interaction of warming with altered moisture regimes, the importance of priming by new plant inputs, or the resolution at which microbial genomics and gene expression must be represented. For these and other knowledge gaps, a new generation of soil experiments are needed to generate understanding of long-term, whole-profile processes that will govern SOC dynamics in a dynamic world.

9.15

Land-use intensity and biodiversity as controls of element cycling

Martin T. Schwarz¹, Sebastian Bischoff², Lisa Krüger³, Beate Michalzik², Jan Siemens³ & Wolfgang Wilcke¹

¹ Geographisches Institut, Universität Bern, Hallerstrasse 12, CH-3012 Bern (martin.schwarz@giub.unibe.ch)

² Institut für Geographie, Friedrich-Schiller Universität Jena, Löbdergraben 32, D-07743 Jena

³ Institut für Nutzpflanzenwissenschaften und Ressourcenschutz, Rheinische-Friedrich-Wilhelms-Universität Bonn, Nussallee 13, D-53115 Bonn

Intensification of land use has modified the cycling of C, N, and possibly P in terrestrial ecosystems globally and threatens biodiversity due to the application of fertilizers on regional scales (Vitousek et al., 1997). Biodiversity and land-use intensity are thought to be related (Paillet et al., 2010) therefore their respective effects on ecosystem services such as nutrient cycling can hardly be separated. Within the German Biodiversity-Exploratories project we try to solve this issue by establishing element budgets along gradients of land-use intensity and associated biodiversity. We hypothesize that element cycling is related to land-use intensity and associated biodiversity.

The Biodiversity Exploratories are a large-scale and long-term interdisciplinary research platform to study the functional role of biodiversity for ecosystem processes and services, and the consequences of land-use change for biodiversity. It comprises three research areas (Hainich Dün, Schorfheide-Chorin, and the Schwäbische Alb) each consisting of 50 forest and 50 grassland plots arranged in a standardized hierarchical design. Currently 40 subprojects contribute to the Biodiversity-Exploratories (Fischer et al., in press). Our subproject BECycles studies waterbound fluxes of C, N, P, Ca, K, Mg, Na, and Si in rainfall, throughfall, and soil solution, and throughfall, stemflow, litter leachate, and soil solution in 29 grassland and 27 forest plots, respectively.

Preliminary results demonstrate that PO_4^{3-} fluxes in forest throughfall at the Schwäbische Alb are not related to forest type (i.e. spruce age-class forest, beech age-class forest, extensively managed beech stands; $p=0.33$; main effects-ANOVA). However, they were closely correlated to NaOH-extractable inorganic P concentrations in topsoil ($r=0.90$; $p<0.01$), which is thought to reflect the moderately labile P fraction determined by the accompanying project DYNPHOS (Negassa and Leinweber, 2009). Therefore, we conclude that higher P availability increases P recycling via canopy leaching. However, throughfall PO_4^{3-} fluxes were not correlated to the directly available inorganic P fraction (NaHCO_3 -extractable; $r=0.38$, $p=0.31$). The DYNPHOS group showed that besides soil pH, land-use intensity is a driver of P distribution among different pools and predominantly effects the NaOH-extractable P fraction. Furthermore, mean o-PO_4^{3-} fluxes in throughfall correlate with the metric “planning land-use and disturbance intensity” index established by the forest inventory subproject of the Biodiversity Exploratories ($r=0.76$; $p>0.05$) and seems therefore to be influenced by management practices. It may be hypothesized that higher land-use intensity increases internal P cycling in forest ecosystems by driving plants to gain access to less available P sources.

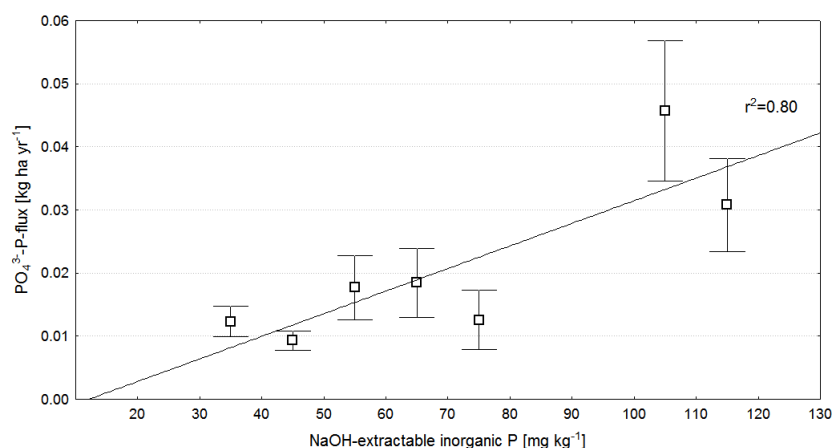


Figure 1. Relationship between moderately labile P fraction in topsoils and mean PO_4^{3-} flux with throughfall (mean±standard error) in forests at the Schwäbische Alb.

Besides element budgeting, our further aims in the project are to explore biodiversity as a control on element cycling in forests and grasslands. Our special focus will be the cycling of N. In a first step, we will determine $\delta^{15}\text{N}$ and $\delta^{18}\text{O}$ of NO_3^- in the collected sample types to detect the presence of various N transformation processes in the canopy and in the soil. Additionally, we will determine gross N transformation rates with the help of complex Monte-Carlo-Markov-Chain sampling technique in a ^{15}N tracer study (Rütting and Müller, 2007). We further address the importance of land-use intensity and biodiversity for soil acidification and carbon leaching. Overall aims will be to adjust models for element cycling and simulate scenarios like land-use change and to establish transfer functions for nutrient turnover in soil to extrapolate our findings from plot to landscape scales.

REFERENCES

- Fischer, M., Bossdorf, O., Gockel, S., Hänsel, F., Hemp, A., Hessenmöller, D., Korte, G., Nieschulze, J., Pfeiffer, S., Prati, D., Renner, S., Schöning, I., Schumacher, U., Wells, K., Buscot, F., Kalko, E.K.V., Linsenmair, K.E., Schulze, E.-D. & Weisser, W.W. 2010. Implementing large-scale and long-term functional biodiversity research: The Biodiversity Exploratories. *Basic and Applied Ecology*, in press.
- Negassa, W. & Leinweber, P. 2009. How does the Hedley sequential phosphorus fractionation reflect impacts of land use and management on soil phosphorus: A review. *Journal of Plant Nutrition and Soil Science*, 172, 305–325.
- Paillet, Y., Berges, L., Hjalten, J., Odor, P., Avon, C., Bernhardt-Roemermann, M., Bijlsma, R.-J., De Bruyn, L., Fuhr, M., Grandin, U., Kanka, R., Lundin, L., Luque, S., Magura, T., Matesanz, S., Meszaros, I., Sebastia, M.T., Schmidt, W., Standovar, T., Tothmeresz, B., Uotila, A., Valladares, F., Vellak, K. & Virtanen, R. 2010. Biodiversity differences between managed and unmanaged forests: Meta-analysis of species richness in Europe. *Conservation Biology*, 24, 101–112.
- Rütting, T. & Müller, C. 2007. ¹⁵N tracing models with a Monte Carlo optimization procedure provide new insights on gross N transformations in soils. *Soil Biology and Biochemistry*, 39, 2351–2361.
- Vitousek, P.M., Aber, J.D., Howarth, R.W., Likens, G.E., Matson, P.A., Schindler, D.W., Schlesinger, W.H. & Tilman, D.G. 1997. Human alteration of the global nitrogen cycle: Sources and consequences. *Ecological Applications* 7, 737–750.

9.16

Contribution of earthworms in the maintenance of biobeds

Daniela Villacres, Véronique Guiné, Nicolas Freyre and Pascal Boivin

Haute Ecole Paysage Architecture et Ingénierie (hepia) – Filière Agronomie – Laboratoire Sols et Substrats – Route de Presinge 150 – CH-1254 Jussy (veronique.guine@hesge.ch)

Biobeds, made of a mixture of straw and soil, are dedicated to the depuration of pesticide effluents in agriculture. One of their limitations is the need to mix them with new added straw every year. To overcome this limitation, we tested the ability of different worm species (i) to survive in contact with organic pesticides effluents and (ii) to efficiently incorporate fresh organic matter to the substrate of a Biobed.

In a first step, classical ecotoxicology assessment were performed in laboratory experiments, on *Eisenia Fetida* sp. using different substrate and cypermethrin. Although the DL50 concentration was smaller than previously reported results, all worms survived in solutions with treatment and effluent concentrations, respectively.

In a second step, different worm species were settled on mesocosms (columns of 1 m length) of biomix substrates (evolved and recent mixture of straw and soil) and irrigated with (i) fresh water, (ii) an artificial effluent made of a mix of 8 commonly used pesticides molecules and (iii) cypermethrin at effluent and treatment concentrations. The soil surface was covered with labeled fresh organic matter, and layers of substrate were separated by colored silts.

These experiments showed a good survival of the different worm species and a strong mixing of the layers, with the generation of large pores and incorporation of the topsoil organic matter to the whole substrate profile. Although different questions remain opened prior to the practical use of worms for substrate renewal in Biobeds, our study conclude that worm present a good potential for that but long term effects of pesticides and climatic constraints on worm activity must be studied.

9.17

Stable H and N isotope approaches to assess soil organic matter turnover and N transformations in ecosystems

Wolfgang Wilcke^{1,1}, Marc Ruppenthal², Martin T. Schwarz¹, Yvonne Oelmann²

¹ Geographic Institute, University of Berne, Hallerstr. 12, 3012 Berne, Switzerland (wolfgang.wilcke@giub.unibe.ch)

² Institute of Integrated Natural Sciences, Geography, University of Koblenz-Landau, Universitätsstr. 1, 56070 Koblenz, Germany

Turnover processes of organic matter and N in soils must usually be determined in laborious laboratory incubations or isotope tracer experiments. Alternatively, stable isotope signals in the environment might be used to infer type and sometimes even rate of turnover processes. Such approaches have already been followed using stable C and N isotope ratios of bulk soils. However, C stable isotopes usually show little fractionation during mineralization of organic matter and N isotope fractionation in bulk soils can be attributed to many different processes. We tested (i) whether H stable isotope ratios can be used to assess organic matter turnover expecting that H isotope fractionation is much larger than that of C because of the more pronounced mass difference of the two H isotopes (Ruppenthal et al., 2010) and (ii) whether the N isotope ratio in a well defined N species, nitrate, offers better insight into N transformation processes (Schwarz et al., 2010).

H isotope ratios.

Prior to be able to use H isotope ratios ($\delta^2\text{H}$ values) as proxies for organic matter turnover, the relationship between the varying H isotope signals of precipitation and soil organic matter needs to be known (and eliminated). We hypothesize that the $\delta^2\text{H}$ value of isotopically nonexchangeable H in bulk soil (composed of C-bonded H in soil organic matter (SOM) and the nonexchangeable fraction of O-bonded H in pedogenic clay minerals) is correlated with the mean $\delta^2\text{H}$ value of local precipitation water at the place and time of biomass production and clay mineral neoformation, respectively. We equilibrated soil samples with water of known isotopic composition prior to $\delta^2\text{H}$ analysis with an Elemental Analyzer-Isotope Ratio Mass Spectrometer (EA-IRMS) to determine the $\delta^2\text{H}$ value of isotopically nonexchangeable H in soil. We analyzed 12 topsoil samples from different climate zones (temperate zone, subarctic zone and tropics). The $\delta^2\text{H}$ values of nonexchangeable H in soil ranged from -75‰ to -167‰ . The $\delta^2\text{H}$ values of nonexchangeable H in soil were highly correlated with predicted average annual $\delta^2\text{H}$ values of local precipitation at the sampling sites ($r = 0.89$, $p < 0.001$, Fig. 1). The $\delta^2\text{H}$ values of nonexchangeable H in soils from Siberia were up to 80‰ depleted in ^2H compared to soils from Central Europe, which directly corresponds to the difference in average annual $\delta^2\text{H}$ values of precipitation from Central Europe and Siberia. We will use this information to test whether the deviation of the expected $\delta^2\text{H}$ value from precipitation in soil correlates with organic matter turnover determined in laboratory incubations.

N isotope ratios in nitrate.

Knowledge of the fate of deposited N in the possibly N-limited, highly biodiverse north Andean forests is important because of the possible effects of N inputs on plant performance and species composition. We analyzed concentrations and fluxes of NO_3^- -N, NH_4^+ -N and dissolved organic N (DON) in rainfall, throughfall, litter leachate, mineral soil solutions (0.15 and 0.30 m depths) and stream water in a montane forest in Ecuador and used the natural ^{15}N abundance in NO_3^- during the passage of rain water through the ecosystem and bulk $\delta^{15}\text{N}$ in soil to detect N transformations. Depletion of ^{15}N in NO_3^- and increased NO_3^- -N fluxes during the passage through the canopy and the organic layer indicated nitrification in these compartments (Fig. 2) but seasonal variations occurred. During leaching from the organic layer to mineral soil and stream, NO_3^- concentrations progressively decreased and NO_3^- was enriched in ^{15}N but did not reach the $\delta^{15}\text{N}$ of solid phase organic matter ($\delta^{15}\text{N}=5.6\text{--}6.7\text{‰}$). The ^{15}N enrichment during leaching could be described as a Rayleigh fractionation. Hence, we attribute the observed $\delta^{15}\text{N}$ values to a combination of nitrification and denitrification in mineral soil. The stable N isotope composition of NO_3^- gave valuable indications of N transformations during the passage of water through the forest ecosystem from rainfall to the stream.

REFERENCES

- Ruppenthal, M., Y. Oelmann & W. Wilcke (2010): Isotope ratios of nonexchangeable hydrogen in soils from different climate zones. *Geoderma* 155, 231-241.
- Schwarz, M.T., Y. Oelmann & W. Wilcke (2010): Stable N isotope composition of nitrate reflects N transformations during the passage of water through a montane rain forest in Ecuador, *Biogeochemistry*, published online on 11/04/2010, doi: 10.1007/s10533-010-9434-5.

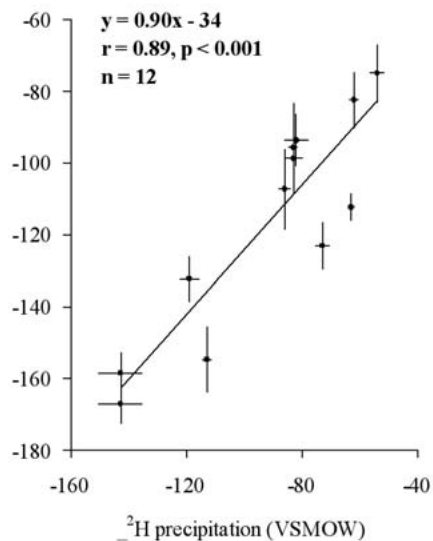


Figure 1: Regression of $\delta^2\text{H}_n$ values of soil samples on predicted mean annual $\delta^2\text{H}$ values of local precipitation at the sampling site. Y axis error bars depict the overall uncertainty ($\pm\text{SD}$).

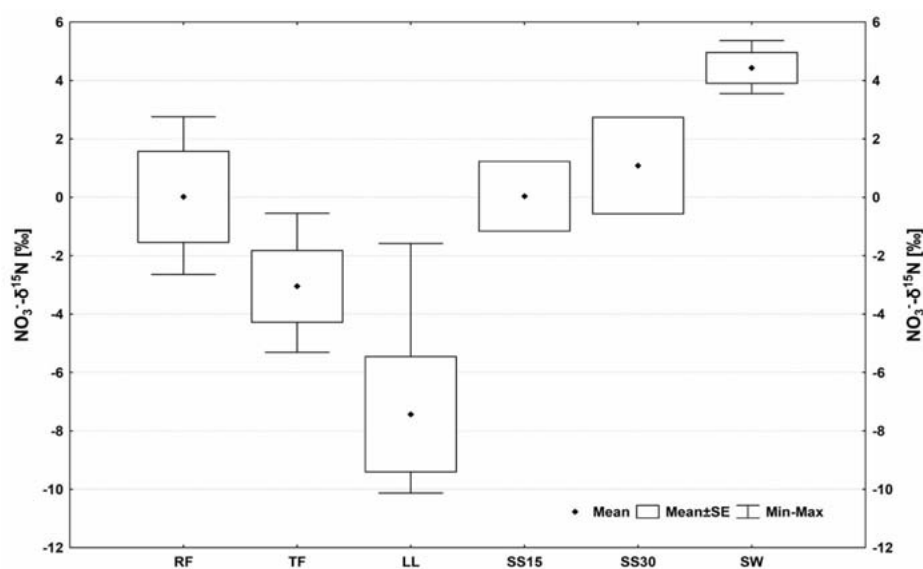


Figure 2. Box plots of the $\delta^{15}\text{N}$ values in nitrate during its passage through an Ecuadorian montane forest (RF=rainfall, TF=throughfall, LL=litter leachate, SS15=soil solution at 15 cm depth, SS30=soil solution at 30 cm depth, SW=stream water).

10. Open Cryosphere Session

A. Bauder, M. Hoelzle, B. Krummenacher, J. Nötzli, C. Lambiel, M. Lüthi, J. Schweizer, M. Schwikowski

Swiss Snow, Ice and Permafrost Society

- 10.1 Boeckli L., Brenning A., Noetzli J., Gruber S.: An empirically-based permafrost distribution model for the entire Alps
- 10.2 Etzelmüller B., Farbrót H., Guomundsson Á.: Seven years of permafrost monitoring in Iceland - updated results and geomorphological implications
- 10.3 Eugster M.: Snow, ice and permafrost study in Swiss schools: From local student observations to global understanding
- 10.4 Gabbi J., Farinotti D., Bauder, A.: Past and future changes and impacts on runoff conditions in the Mauvoisin region
- 10.5 Huss M.: Present and future contribution of glacier storage change to runoff from macroscale drainage basins in Europe
- 10.6 Huss M., Machguth H., Jörg P., Zemp M., Salzmann N., Linsbauer A., Hoelzle M.: Re-analysis of mass balance measurements on Findelengletscher 2005-2009
- 10.7 Huss M., Stokvis M., Salzmann N., Hoelzle M.: Towards short-term monitoring of glacier mass balance and snow accumulation distribution
- 10.8 Keller A., Funk M.: Ice deformation measurement in boreholes on Rhonegletscher
- 10.9 Lambiel C., Baron L.: Mapping ground ice distribution in an ice-cored moraine with electrical resistivity tomography, Col des Gentianes, Swiss Alps
- 10.10 Linsbauer A., Paul F., Künzler M., Frey H., Haeberli W.: Formation of new lakes in deglaciating regions of the Swiss Alps
- 10.11 Lüthi M.P., Bauder A., Funk M.: Volume change reconstruction of Swiss glaciers from length change data
- 10.12 Matzl M., Steiner S., Schneebeli M., Steinfeld D., Köchle B., Singer J.: 3-D-reconstruction and visualization of microscale snow stratigraphy and weak layers
- 10.13 Morard S., Bochud M., Delaloye R.: Rapid changes of the ice mass configuration in the dynamic Diablotins ice cave– Fribourg Prealps, Switzerland
- 10.14 Nath S.K., Huss M.: Glaciological investigations on three glaciers at Les Diablerets, Alpes Vaudoises
- 10.15 Salzmann N., Machguth H.: The Swiss Alpine Glacier's Response to the "2°C Target"
- 10.16 Scapozza C., Baron L., Lambiel C.: Borehole logging in alpine periglacial talus slopes, Valais Alps, Switzerland
- 10.17 Scherler M., Hauck C.: Modelling of permafrost evolution under climate change scenarios
- 10.18 Schneider S., Hoelzle M.: Investigation of the high variability of mountain permafrost
- 10.19 Walthard P., Gulley J., Benn D., Martin J.: Using speleological methods to test dye tracing interpretations in glaciology
- 10.20 Zech R., Huang Y., Zech M., Tarozo R., Zech W.: Permafrost carbon dynamics controlled atmospheric CO₂ and Pleistocene climate
- 10.21 Zenklusen Mutter E., Phillips M.: Active Layer development in Alpine permafrost

10.1

An empirically-based permafrost distribution model for the entire Alps

Lorenz Boeckli¹, Alexander Brenning², Jeannete Noetzli¹ & Stephan Gruber¹

¹ Department of Geography, University of Zurich, Switzerland
(lorenz.boeckli@geo.uzh.ch)

² Department of Geography, University of Waterloo, Ontario, Canada

Permafrost distribution modelling in highly populated mountain regions is an important task and several differing modelling approaches exist. Most permafrost models in the Alps are calibrated for a local region and only applicable for a specific area. For analyzing the permafrost distribution and evolution on an alpine-wide scale, one consistent model for the whole domain is needed, instead of differing and incomparable models. We present a statistical permafrost model for the entire Alps based on permafrost evidences. The evidences were collected in the framework of the PermaNET project and contain different data (e.g. rock glacier inventories, borehole temperatures, ground surface temperatures).

Two models were developed, one for the debris covered area (debris model) and one for steep rock faces (rock model). In both cases the predictor variables are mean annual air temperature (MAAT) and potential direct solar radiation. For the debris model we use a logistic regression to predict the probability of active against inactive rock glacier. For the rock model a linear regression was used to model rock temperatures based on temperature loggers located in steep rock walls. To distinguish between those two surface characteristics a third model (surface type model) is used, which is based on slope only. The final output product combines these three models and provides alpine-wide permafrost probabilities.

10.2

Seven years of permafrost monitoring in Iceland - updated results and geomorphological implications

Bernd Etzelmüller¹, Herman Farbrót¹, Águst Guðmundsson²

¹ Department of Geosciences, University of Oslo Department of Geosciences, University of Oslo (bernde@geo.uio.no)

² Jarðfræðistofan Geological Services, Iceland

The distribution of mountain permafrost has been mapped and monitored mainly in locations with relatively continental climates characterized by a stable snow cover and low winter temperatures. In contrast, there is a paucity of systematic ground temperature investigations from maritime mountain areas such as Iceland and transitional areas between the Scandinavian mountain permafrost zone and the continuous permafrost in Svalbard. Knowledge of the present distribution and thermal characteristics is crucial for assessing the response of permafrost to climate change and its geomorphological and geotechnical impact.

Intensive field-based studies on the distribution of permafrost and the dynamics of selected periglacial landforms were carried out in northern (Tröllaskagi peninsula) and eastern Iceland since 2003. Since then ground thermal monitoring has continued at four sites. This presentation reviews and synthesises the main results of the 7 years of monitoring, and draws lines to former and future geomorphic process dynamics and landscape development.

The presentation demonstrates that permafrost is widespread at elevations above c. 900 m a.s.l. in Iceland, mainly depending on the snow cover regime. At this elevation, permafrost temperatures are close to 0°C, and thus highly vulnerable for climate variability. Modelling exercises show quite rapid responses of ground temperatures from changes in snow conditions and air temperatures. Climate variability has been large during the period of instrumental measurement of meteorological variables (start late 18. Century). This is due to the large influence of sea ice, occasionally occurring close to northern Iceland, resulting in lower winter temperatures. During the LIA and parts of the last century (e.g. the 1970ies) permafrost must have been much more widespread than today, mainly because of the lower winter temperatures. Furthermore, the modelling indicates that under future climate scenarios the permafrost will degrade at these sites on the order of decades depending on climate scenarios chosen and subsurface ice content.

10.3

Snow, ice and permafrost study in Swiss schools: From local student observations to global understanding

Eugster Markus

Sekundarschule, Schöntalstrasse 2, 9244 Niederuzwil

Introduction:

I will present to you a way to implement polar science in Swiss classrooms. With local measurements, fundamental experiments and worldwide exchange within the GLOBE network students come to a better understanding of the Earth as a system and especially of the changing cryosphere. Method: Learning by doing.

GLOBE

Switzerland is a member (<http://www.globe-swiss.ch/de/>) of GLOBE (= Global Learning and Observations to Benefit the Environment; <http://globe.gov>), and our school joined GLOBE in 2003.

Seasons and biomes

GLOBE started several Earth System Science Projects (ESSP) in 2007, among them “Seasons and Biomes” was part of the IPY. I was invited to attend two workshops in Fairbanks, Alaska, with teachers from all over the world.

Spaceship Earth

In collaboration with Nicolas Gessner, the director of 52 short films about our planet, I designed 52 worksheets to help my students understand the outside influences that determine the Earth’s systems.

Ice seasonality

My students observe the covering of snow and the ice on our school pond, fill in protocols and take pictures to document freeze-up and break-up. This helps them to become aware of seasonal cycles.



Figure 1: School pond Sek Uzwil



Figure 2: Ice protocol

Frost tubes

We manufacture and test different types of frost tubes. In addition we measure soil temperatures with buried sensors. Taking measurements helps my students understand the different behaviour of air and soil. This leads to questions about permafrost and the active layer and the consequences of thawing permafrost in Polar Regions as well as in our Alps.

Learning Activities

I’m developing low cost experiments to equip my students with basic knowledge about snow, ice, fresh and sea water ice, ocean currents and glaciers.

Workshops

I was invited to the Oslo IPY conference (<http://ipy-osc.no/>) in June 2010. I attended the PolarTeacher’s conference with all its workshops and presentations and establish new contacts with teachers and scientists from around the world.

In August 2010 I gave my first Swiss teacher’s course (“Ewiger Schnee”) in the Pizol region. I would be glad to find a glaciologist for next year’s course.



Figure 3: Students controlling frost tubes

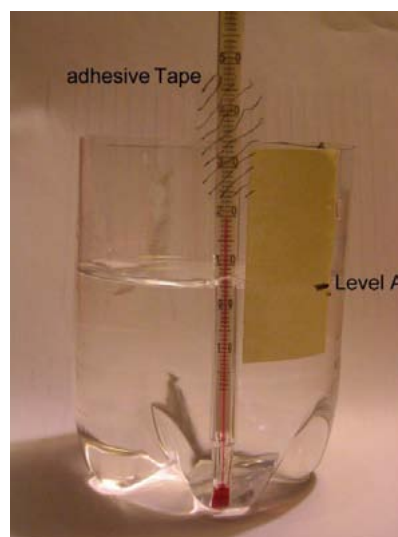


Figure 4: Experiment Melting ice



Figure 5: Pizol glacier (all pictures by M. Eugster)

10.4

Past and future changes and impacts on runoff conditions in the Mauvoisin region

Gabbi Jeannette¹, Farinotti Daniel¹ & Bauder Andreas¹,

¹Versuchsanstalt für Wasserbau, Hydrologie und Glaziologie (VAW), ETH Zürich, CH-8092 Zürich (gabbij@vaw.baug.ethz.ch)

The progressive ice mass loss in Alpine regions is a response to the ongoing global climate change. In the near future an even pronounced glacier retreat is expected due to a further temperature rise confirmed by several climate studies (e.g. Frei, 2007; van der Linden and Mitchell, 2009). Hence, the runoff conditions in high mountain valleys will significantly change.

The runoff conditions and the evolution of the glaciers in the Mauvoisin area are determined until the end of the 21st century using the Glacier Evolution and Runoff Model (GERM, Huss et al., 2008). The GERM is based on a distributed temperature-index melt model combined with an accumulation model. Further, a runoff routing, an evaporation and a glacier evolution model is implemented. The glacier surface is updated in annual time steps. In order to compute the future glacier extension the knowledge about the initial ice thickness distribution is fundamental. The current ice volume is derived using the ice thickness estimation approach by Farinotti et al. (2009) which is based on principles of the ice-flow mechanics. If radar-echo soundings are available the radar profiles are included in the ice thickness analysis. The incorporated climate scenarios are adopted from a study of Frei (2007) which provides temperature and precipitation projections for the North and the South of Switzerland in seasonal resolution for the years 2030, 2050 and 2070 and the corresponding 95% confidence interval. Three different climate regimes are deduced: a best-case (cold and wet), a median and a worst-case (warm and dry) scenario. The parameters of the model are calibrated on the basis of past ice thickness changes derived from topographic maps and areal photographs, discharge data and direct mass balance measurements.

As a consequence of the enhanced melting the runoff of the Mauvoisin area increases in the near future. The duration of the period with pronounced discharge depends mainly on the climate scenario. In the cold and wet climate regime the maximal annual runoff is even suspected to arise after the end of the 21st century. In case of the median and worst-case scenario the maximal runoff is achieved in 2060. After reaching the peak runoff the discharge diminishes significantly due to the strong reduction of the glacierized area. The amount of reduction depends on the characteristics of the catchment and the chosen climate scenario. Due to the glacier loss the runoff regime is mainly influenced by snow-melt instead of ice-melt. The peak runoff is shifted to earlier times in the season whereas the summer runoff is strongly reduced. All glaciers in the Mauvoisin area show a considerable ice volume loss until the end of the 21st century (Fig. 1). But the proceeding of the glacier retreat is different for the individual glaciers depending on the current ice volume and its distribution in relation to the altitude.

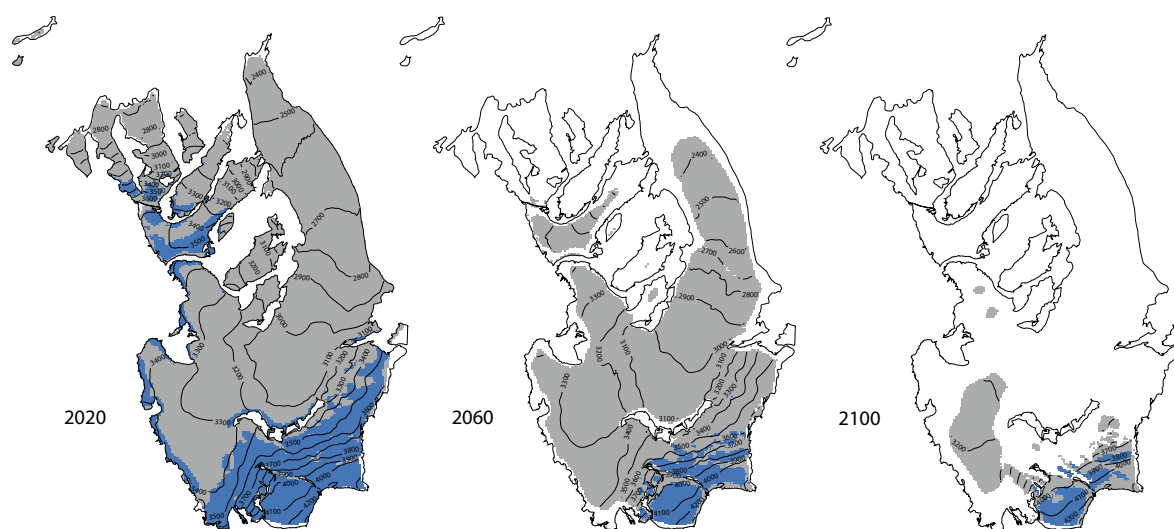


Figure 1. The glacier geometry of the Glacier de Corbassière and the Glacier du Petit Combin for the years 2020, 2060 and 2100 in the median climate scenario. The blue area indicates positive mass balances and the grey area negative mass balances.

REFERENCES

- Farinotti, D., Huss, M., Bauder, A., Funk, M. & Truffer, M. 2009: A method to estimate the ice volume and ice-thickness distribution of alpine glaciers, *Journal of Glaciology*, 55(191), 422–430.
- Frei, C. 2007: Die Klimazukunft der Schweiz. In: *Klimaänderung und die Schweiz 2050 – Erwartete Auswirkungen auf Umwelt, Gesellschaft und Wirtschaft*. Beratendes Organ für Fragen der Klimaänderung (OcCC): 12-16, <http://www.occc.ch>.
- Huss, M., Farinotti, D., Bauder, A. & Funk, M. 2008: Modelling runoff from highly glacierized alpine drainage basins in a changing climate, *Hydrological Processes*, 22, 3888–3902.
- van der Linden, P. & Mitchell, J. (2009): ENSEMBLES: Climate change and its impacts: Summary and results from the ENSEMBLES project, Met Office Hadley Centre, Exeter EX1 3PB, UK, 160pp.

10.5

Present and future contribution of glacier storage change to runoff from macroscale drainage basins in Europe

Huss Matthias¹

¹ Department of Geosciences, University of Fribourg, Fribourg, Switzerland

Glaciers are important seasonal storage components in the hydrological cycle. In this study, the importance of glacier storage change in the summer months for runoff from large-scale drainage basins in Europe is analyzed. Along the major streams draining the Alps – Rhine, Rhone, Po and Danube – the contribution of snow- and icemelt from glacierized catchments to discharge is evaluated for three to seven measurement stations. The analyzed drainage basins vary in size from 200 to 800'000 km², and have a glacierization of between 60% and 0.06%.

Detailed information on glacier storage change is available from monthly mass balance data for 50 glaciers in the Swiss Alps. Mass balance time series were derived based on a comprehensive set of field data covering the entire 20th century combined with distributed modelling (Huss et al., 2010a,b). Using climate scenarios the transient future glacier retreat and consequent changes in monthly runoff contribution were calculated for each glacier individually until 2100. Based on glacier inventory data, storage changes are extrapolated to all glaciers in the European Alps.

By comparison of the monthly runoff yields from glacierized surfaces in the summer months and the measured discharge from large-scale catchments the relative portion of glacier melt water is calculated.

For a typical macroscale catchment with a size of 96'000 km², and a glacierization of 1% (Rhone at Beaucaire, France), glacier storage change potentially contributed to August runoff by 19% over the last century (Fig. 1). Even on the lower Danube with an ice-covered fraction of only 0.06% glaciers make a contribution of 2.2% to observed runoff volume in August. In the extreme year of 2003 glacier contribution was higher by a factor of 2 to 3. It is shown that the relative importance of glacier contribution to runoff does not scale linearly with the percentage of glacierization. As the runoff regime changes from nivo-glacial to pluvial (with a minimum in summer) moving away from the Alps, the relative importance of glacier melt water increases downstream.

Over the 21st century most Alpine glaciers will shrink to less than 10% of their current size according to the model results. Thus, glacier storage change will be strongly reduced due to a lack of both snow- and icemelt. In consequence, a decrease in runoff contribution from previously glacierized catchments to summer discharge by about two thirds is expected until 2100. This will intensify issues with water shortage in the summer months, not only mountainous drainage basins, but as well in poorly glacierized macroscale catchments.

REFERENCES

- Huss, M., Hock, R., Bauder, A. & Funk, M. (2010a). 100-year glacier mass changes in the Swiss Alps linked to the Atlantic Multidecadal Oscillation. *Geophysical Research Letters*, 37, L10501.
- Huss, M., Usselman, S., Farinotti, D. & R., Bauder, A. (2010b). Glacier mass balance in the south-eastern Swiss Alps since 1900 and perspectives for the future. *Erdkunde*, 64(2), 119-140 .

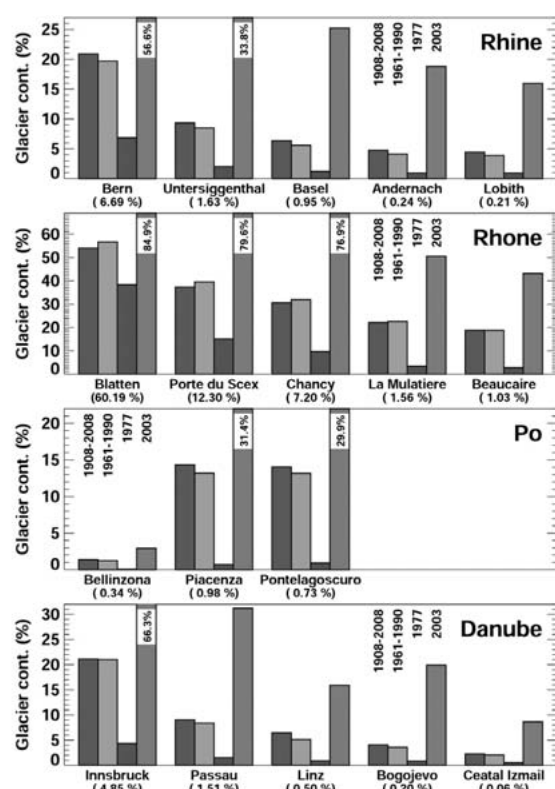


Figure 1. Relative contribution of glacier storage change in August to runoff from several drainage basins along the four streams leaving the Alps. The name of the gauging station and catchment glacierization is given. Data are evaluated for the period 1908-2008, 1961-1990, and the extreme years of 1977 and 2003. Note that the bar for 2003 is cut off in some cases, and the contribution is stated using numbers.

10.6

Re-analysis of mass balance measurements on Findelengletscher 2005-2009

Huss Matthias¹, Machguth Horst², Jörg Philip Claudio², Zemp Michael², Salzmann Nadine^{1,2}, Linsbauer Andreas² & Hoelzle Martin¹

¹Department of Geosciences, University of Fribourg, Fribourg, Switzerland

²Department of Geography, University of Zurich, Zurich, Switzerland

In the Swiss Alps, long-term glacier mass balance series are currently only maintained on three glaciers using the direct glaciological method. Moreover, these glaciers are rather small and may disappear within the coming decades. The representativeness of mass balance series in Switzerland thus needs to be enhanced by including larger glaciers in the monitoring network.

Since 2004 direct mass balance measurements have been performed on Findelengletscher, Valais, but no glacier-wide mass balances have been calculated so far. Since 2009, the mass balance measurements are jointly performed by the Universities of Zurich and Fribourg, and the program was extended. Recently, high-accuracy Digital Elevation Models (DEMs) for the years 2005 and 2009 (LiDAR), and 2007 (photogrammetry) became available. These DEMs allow the calculation of ice volume changes for Findelen- and Adlergletscher.

The aim of this study is the re-analysis of the mass balance measurements performed between 2005 and 2009 resulting in homogenized glacier-wide seasonal mass balances for both glaciers. We focus on the comparison of the results to the independently determined geodetic mass changes (DEM comparison) allowing the quantification of systematic uncertainties in both data sources.

Annual point measurements of mass balance are evaluated using a distributed daily accumulation and melt model that is calibrated to the field data in each year individually (Huss et al., 2009). In this method, winter accumulation data availab-

le for 2005, 2009 and 2010 are crucial for determining the spatial mass balance variability. In addition, first results of the helicopter-borne Ground Penetrating Radar (GPR) survey of April 2010 are included in the analysis. Electromagnetic waves are reflected at the snow-ice interface providing continuous records of snow layers (Machguth et al., 2006). In the firn area up to four annual firn layers are detectable in the radar soundings. Thus, accumulation rates over the last years at high elevation may be reconstructed (Fig. 1). Although the interpretation and temporal allocation of the firn layers obtained from GPR is not trivial, this data source is valuable in regions above 3300 m a.s.l. – representing half of the glacier surface – as there are no direct field data available.

The re-analysis of the mass balance data yields a cumulative thickness change of -1.40 m water equivalent (w.e.) for Findelengletscher, and -0.87 m w.e. for Adlergletscher between October 2005 and 2009. Whereas mass losses were above average in 2005/2006, the mass budget of Findelengletscher was nearly balanced in 2008/2009 due to high winter accumulation. Comparison with the geodetic ice volume change between 2005 and 2009 based on LiDAR DEMs (Jörg et al., 2010), however, indicates that mass losses were higher by about 50%.

The significant disagreement between the glaciological and geodetic method needs to be reduced, and the uncertainties in both methods have to be understood before the Findelengletscher mass balance series can be used for climatic interpretation. Several reasons could potentially contribute to this misfit: (1) Accumulation might be overestimated in the re-analysis due to very sparse direct observations at high altitude. However, high-resolution snow probings up to 3800 m a.s.l., and the firn layer thickness inferred from GPR (Fig. 1) indicate that accumulation rates are well reproduced by the model. (2) Converting ice volume change obtained by DEM comparison into mass change is difficult as the density of the volume change is unknown leading to a considerable uncertainty in the geodetic mass change over short periods. (3) Several additional uncertainties have yet to be explored, and might be important.

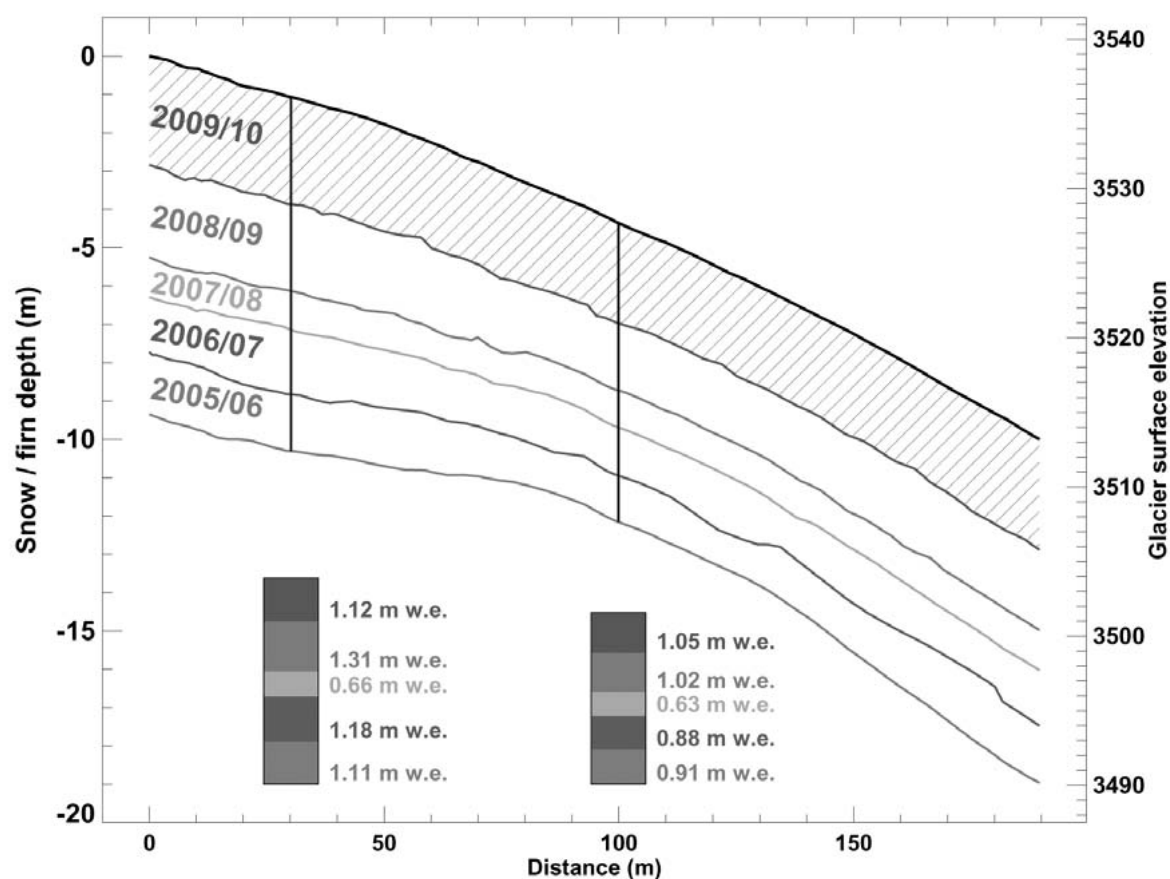


Figure 1. Thickness of firn layers between the mass balance years 2005/2006 and 2008/2009 inferred with helicopter-borne GPR. The uppermost layer represents the winter snow 2009/2010. The surface topography (right axis) is vertically exaggerated. Two profiles through the accumulation layers are shown. Thickness is converted into water equivalent using estimated firn densities.

REFERENCES

- Huss, M., Bauder, A. and Funk, M. (2009). Homogenization of long-term mass balance time series, *Annals of Glaciology*, 50(50), 198–206.
- Jörg, P.C., Morsdorf, F. and Zemp, M. (2010). Operational use of airborne laserscanning for glacier monitoring in Switzerland. *Geophysical Research Abstracts*, EGU2010-750.
- Machguth, H., Eisen, O., Paul, F. & Hoelzle, M. (2006). Strong spatial variability of snow accumulation observed with helicopter-borne GPR on two adjacent Alpine glaciers. *Geophysical Research Letters*, 33, L13503.

10.7

Towards short-term monitoring of glacier mass balance and snow accumulation distribution

Huss Matthias¹, Stokvis Mazzal¹, Salzmann Nadine¹ & Hoelzle Martin¹

¹Department of Geosciences, University of Fribourg, Fribourg, Switzerland

Glacier mass balance is an important indicator of climate change. Mass balance monitoring programs mostly report annual values because field measurements are laborious. For climatic interpretation, the separation of the components of mass balance – accumulation and melt – is important. This can be achieved by performing seasonal mass balance surveys. However, the monthly or even daily glacier mass change over one year, which is crucial for analyzing e.g. the importance of glacier melt contribution to the hydrological cycle, was only modelled so far, and not observed directly in the field. A second gap in current mass balance monitoring programs is the spatial distribution of snow accumulation showing a high variability in space that is difficult to capture with direct measurements.

Here, we outline a new method that allows a temporally continuous monitoring of glacier mass balance, as well as the spatial snow accumulation variability over glacierized surfaces. The method is based on two data sources that can be acquired remotely, i.e. without direct field site contact. Thus, also inaccessible regions of the glacier surface can be included. We use repeated digital photography of the glacier, and snow distribution measurements at the end of winter using helicopter-borne Ground Penetrating Radar (GPR).

In April 2010, an automatic digital camera was installed on Unterrothorn overlooking the entire catchment of Findelengletscher, Valais, Switzerland. Photos are taken at hourly intervals and directly transmitted to a server. The snow-line in selected pictures is delineated, and the photos are deskewed, orthorectified and georeferenced (Corripio, 2004). It has been shown that snow accumulation distribution in the lower reaches of a glacier can be derived using repeated photography combined with simple modelling (Farinotti et al., 2010).

First results of the helicopter-borne Ground Penetrating Radar (GPR) survey of April 2010 are used in this study. Electromagnetic waves are reflected at the snow-ice interface providing continuous records of snow layers (Machguth et al., 2006). In total, about 13 km of snow profiles on Findelengletscher are available for April 2010.

The method to continuously determine total mass balance relies on the Accumulation Area Ratio (AAR) that can be determined for each day from the repeated glacier photography. Here, the AAR is defined as the percentage of the glacier surface covered with winter snow. The relation between glacier-wide mass balance and the AAR mainly depends on (1) the quantity and the spatial distribution of snow (given by the GPR surveys), and (2) the characteristics of glacier geometry, e.g. hypsometry, exposure (obtained from a digital elevation model).

We present the snow accumulation distribution on Findelengletscher in April 2010 and the depletion pattern of winter snow throughout the melting season of the year 2010 as depicted by repeated georeferenced photography. Rating curves for AAR versus glacier-wide mass balance are derived based on a simple model. The method to continuously determine glacier mass balance using remotely sensed data is illustrated with first results for the year 2010.

REFERENCES

- Corripio, J. G. (2004). Snow surface albedo estimation using terrestrial photography. *International Journal of Remote Sensing*, 25(24), 5705–5729.
- Farinotti, D., Magnusson, J., Huss, M. & Bauder, A. (2010). Snow accumulation distribution inferred from time-lapse photography and simple modelling. *Hydrological Processes*, 24, 2087–2097.
- Machguth, H., Eisen, O., Paul, F. & Hoelzle, M. (2006). Strong spatial variability of snow accumulation observed with helicopter-borne GPR on two adjacent Alpine glaciers. *Geophysical Research Letters*, 33, L13503.



Figure 1. Findelengletscher as seen by the Automatic Camera installed on Unterrothorn. The picture is taken on July 6, 2010. The current snowline is indicated.

10.8

Ice deformation measurement in boreholes on Rhonegletscher

Keller Arne, Funk Martin

Versuchsanstalt für Wasserbau, Hydrologie und Glaziologie, Gloriast. 37-39, CH-8092 Zürich

In order to provide boundary conditions for numerical flow modeling, information on the basal motion of temperate glaciers are necessary. Whereas basal processes are usually not directly accessible and cannot easily be inferred from surface measurements, borehole deformation measurements allow via determination of velocity profiles to investigate the contributions of both sliding and internal ice deformation to surface motion.

In summer 2009 borehole deformation measurements covering both vertical and shear strain have been carried out on the tongue of Rhonegletscher (Valais, Switzerland). Unlike earlier studies using uniquely gravitation sensors for inclinometry, our experimental setup includes both gravimeters and magnetometers. This allows to determine the borehole deformation with respect to a fixed coordinate system given by gravitational and geomagnetical fields.

The inclination angle of the boreholes shows characteristic diurnal variations. Those are correlated with the variations of englacial water pressure measured in a nearby borehole. The mechanism governing this effect is not entirely clear yet.

10.9

Mapping ground ice distribution in an ice-cored moraine with electrical resistivity tomography, Col des Gentianes, Swiss Alps

Lambiel Christophe¹, Baron Ludovic²

¹ Institut de Géographie, Université de Lausanne (christophe.lambiel@unil.ch)

² Institut de Géophysique, Université de Lausanne

The mapping of ground ice in sedimentary deposits other than rock glaciers necessitates in most cases the use of geophysical methods. That is particularly the case for glacier forefields. For this, several ERT profiles were carried out in the Col des Gentianes moraine, on the orographic left side of the Tortin glacier (Verbier area). The site is located at 2900 m a.s.l., that is within the alpine permafrost belt. Ground temperatures recorded in a 20 m deep borehole since 2002 attest the presence of permafrost conditions in the moraine (Lambiel 2006). A cable car station was built on the northern part of the moraine at the end of the 1970's (Figure 1). Massive ground ice was encountered at this occasion. In October 2006, excavations for ski-run landscaping purposes revealed outcrops of congelation and sedimentary ice at depths of 50 cm to 2 m (Lambiel & Schuetz 2008). Sedimentary ice is also regularly observed in the internal flank of the moraine, just below the building, after the slide of surface debris on buried ice due to the glacier retreat at the foot of the slope.

The main results show that a band up to 40 meters wide with ground resistivities (at around 10 m depth) between 100 kWm and more than 2000 kWm occupies the inner part of the moraine on the edge of the glacier (Figure 1). This corresponds to sedimentary ice buried under superficial debris. At the place of the excavations of 2006, values up to 200 kWm have been measured. Between those 2 sectors, resistivities around 10-20 kWm are present. This probably indicates a low ice content (only congelation ice ?). Finally, at the base of the building the resistivities are lower than 4 kWm, showing that ice observed during the construction has completely melted. This has been resulting in the subsidence of the moraine.

The large range of resistivities measured, interpreted as different types of ice that do not systematically coincide with topogeomorphological evidences, probably results from a complex history of glacier-permafrost interactions during the Little Ice Age. Today, the evolution of this ice-cored moraine is both controlled by glacier retreat and permafrost creep.

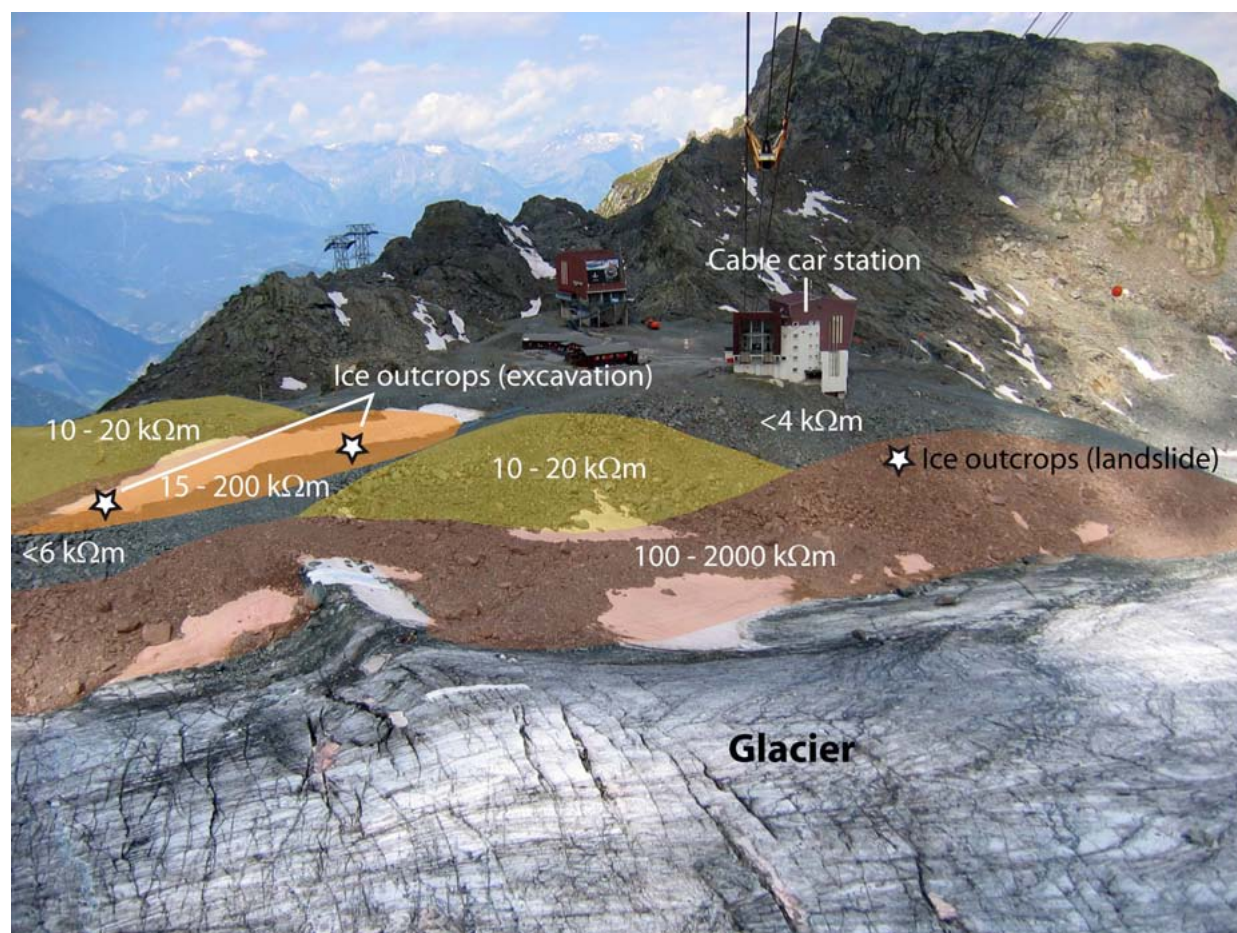


Figure 1. Distribution of the resistivities at around 10 m depth in the Col des Gentianes moraine.

REFERENCES

- Lambiel, C. 2006: Le pergélisol dans les terrains sédimentaires à forte déclivité: distribution, régime thermique et instabilités. Thèse, Université de Lausanne, Institut de Géographie, coll. "Travaux et Recherches" n° 33, 260 p.
- Lambiel, C., & Schuetz, P. 2008: Ground characteristics and deformation of a frozen moraine affected by tourist infrastructures (Col des Gentianes, Valais). *Klima-veränderungen auf der Spur. Studien des Europäischen Tourismus Instituts an der Academia Engiadina, Samedan*, 5, 110-122.

10.10

Formation of new lakes in deglaciating regions of the Swiss Alps

Linsbauer Andreas¹, Paul Frank¹, Künzler Matthias¹, Frey Holger¹ & Haeberli Wilfried¹

¹ Glaciology, Geomorphodynamics and Geochronology Group, Department of Geography, University of Zurich, Switzerland (andreas.linsbauer@geo.uzh.ch)

The alpine environment is strongly affected by climate change and the ongoing increase in mean temperature has a severe impact on glaciers in the Alps. With the ongoing rapid glacier shrinking or even vanishing, characteristics of the surface topography over wide regions will now and in the future undergo strong changes with considerable impacts on the environment at all scales.

For future assessments and modeling of glacier retreat scenarios and their impacts, it is crucial to have a better knowledge on both glacier bed topography and ice volumes for a large number of glaciers (e.g. Linsbauer et al. 2009, Farinotti et al. 2009). Thereby, glacier bed topography is calculated by subtracting modeled ice thickness distributions from a surface DEM. These beds can then be used among others for the modeling of future glacier evolution, glacier flow, detection of overdeepenings with potential future lake formation and hazard assessment.

In this study we have modeled bed topographies and ice thickness distributions of all Swiss glaciers >0.1 km² with a simple but robust GIS-tool (Paul & Linsbauer subm.). Subsequently, we analyzed the geomorphometric characteristics of the glacier beds and the detected overdeepenings, which can be seen as potential sites for future lake formation (Frey et al. 2010). Such new lakes can be attractive for tourism and hydropower production, but also constitute serious hazard potentials as they come into existence in an increasingly destabilized environment (e.g. steep rock walls, warming permafrost, de-buttressing of over-steepened slopes from glacier vanishing).

The analysis of the hypsographic distribution of the ice thickness with reference to the glacier beds reveals that huge ice masses are based on bedrock with low altitude (below 2400 m a.s.l.). This has wide implications for future glacier development as it supports the self-acceleration of mass loss, i.e. glacier tongues cannot retreat to higher elevations. Some larger valley glaciers with a prominent tongue reaching down to elevations below 2500 m a.s.l. are selected to map elevation profiles of the glacier surface and bed along their central flowline. These profiles reveal the moderate slope of the low glacier beds and the large number of overdeepenings. Summing up the total area of all detected overdeepenings, expose a potential of 50 - 60 km² of new lake area under currently still existing glaciers. By applying the GIS-based modeling of the glacial sediment balance (Zemp et al. 2005), a statement on the sedimentary/rocky nature of the glacier bed can be made and helps to indicate whether a depressions may fill with water or with sediment after the glacier has disappeared. By using a simplified model of future glacier retreat (Paul et al. 2007), the potential lake formation sites are further roughly classified for their date of appearance (next decade, first half of the century or later).

REFERENCES

- Frey, H., Haeberli, W., Linsbauer, A., Huggel, C. & Paul, F. 2010: A multi-level strategy for anticipating future glacier lake formation and associated hazard potentials. *Natural Hazards and Earth System Sciences*, 10, 339–352.
- Farinotti, D., Huss, M., Bauder, A. & Funk, M. 2009: An estimate of the glacier ice volume in the Swiss Alps. *Global and Planetary Change*, 68, 225–231.
- Linsbauer, A., Paul, F., Hoelzle, M., Frey, H., & Haeberli, W. 2009: The Swiss Alps without glaciers – a GIS-based modelling approach for reconstruction of glacier beds. *Proceedings of Geomorphometry 2009, Zurich, Switzerland*, 243–247.
- Paul, F., Maisch, M., Rothenbuehler, C., Hoelzle, M. & Haeberli, W. 2007: Calculation and visualisation of future glacier extent in the Swiss Alps by means of hypsographic modelling. *Global and Planetary Change* 55(4), 343–357.
- Paul, F. & Linsbauer, A. subm: Modeling of glacier bed topography from glacier outlines, central branch lines and a DEM. *International Journal of Geographical Information Science*.
- Zemp, M., Kääb, A., Hoelzle, M. & Haeberli, W. 2005: GIS-based modelling of glacial sediment balance. *Zeitschrift für Geomorphologie*, 138, 113–129.

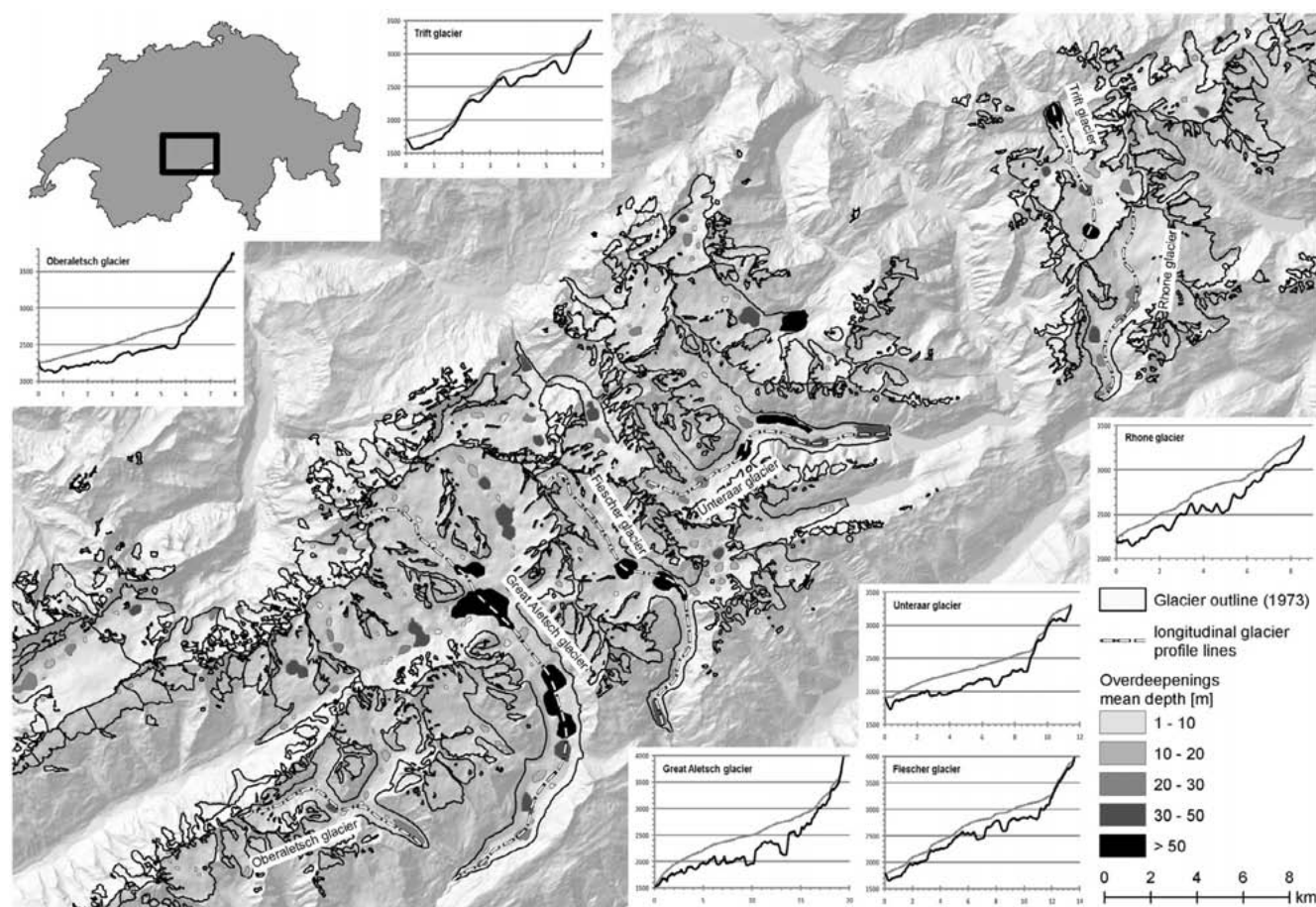


Figure 1. Glacier subset around Great Aletsch glacier in the Bernese Oberland and Valais: The detected overdeepenings in the modeled glacier bed topographies are classified by their mean depth. The plots show the longitudinal profile lines (distance in km) of glacier surface and bed (elevation in m a.s.l.) of some major glaciers of the region.

10.11

Volume change reconstruction of Swiss glaciers from length change data

Martin P. Lüthi, Andreas Bauder and Martin Funk

Versuchsanstalt für Wasserbau, Hydrologie und Glaziologie, ETH Zürich, CH-8092 Zürich (luethi@vaw.baug.ethz.ch)

A novel method to reconstruct glacier volume changes from a measured length record is presented, and tested for 13 glaciers in the Swiss Alps. The response of a glacier to changes in climate is modeled with a two-parameter dynamical system in the variables “length” and “volume”. Driven by a history of equilibrium line altitude (ELA), the model yields variations of glacier length and volume. A dynamically equivalent simple model (DESM) is determined for each glacier by matching modeled and measured length changes. The volume changes predicted with the DESM agree well with measurements for twelve glaciers, whereas agreement is poor for one glacier with topographic breaks in the terminus area. For all glaciers, which are located in different climate regions, the length and volume changes are reproduced with the same ELA history. This agreement shows that the macroscopic glacier response to the climate history is well correlated over a whole mountain range. Modeling the future evolution of the glaciers under a constant present-day climate reveals that fast-reacting glaciers are close to equilibrium, whereas length and volume of the large valley glaciers would be reduced during the next century by an amount similar to the volume lost during the last 150 years.

REFERENCES

- Lüthi, M.P., Bauder, A. & Funk, M., 2010. Volume change reconstruction of Swiss glaciers from length change data. *Journal of Geophysical Research; Earth Surface Processes*, (in press).
- Lüthi, M.P. & Bauder, A., 2010. Analysis of Alpine glacier length change records with a macroscopic glacier model. *Geographica Helvetica*, (in press).
- Lüthi, M.P., 2009. Transient response of idealized glaciers to climate variations. *Journal of Glaciology*, 55(193):918–930.

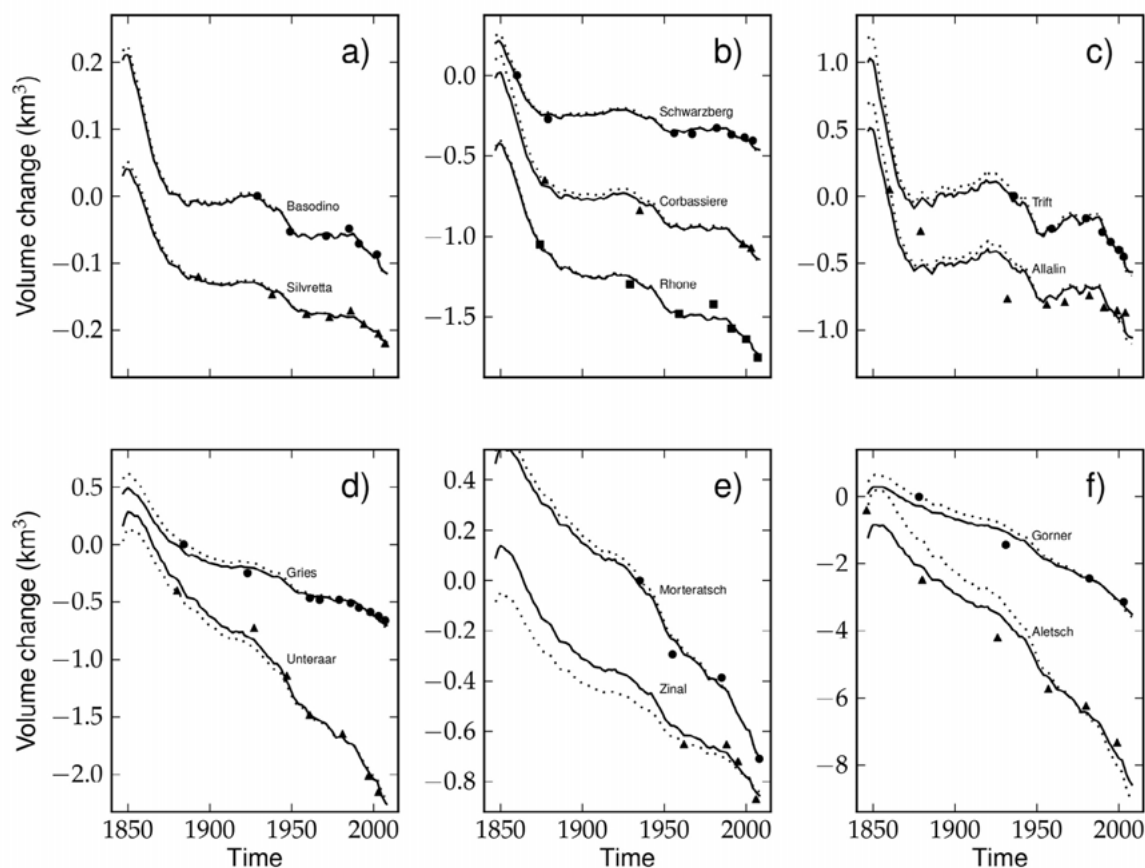


Figure 1. Modelled glacier volume changes for 13 glaciers are shown with lines. Measured volume changes for glaciers are indicated with symbols for comparison. The glacier names are given next to curves.

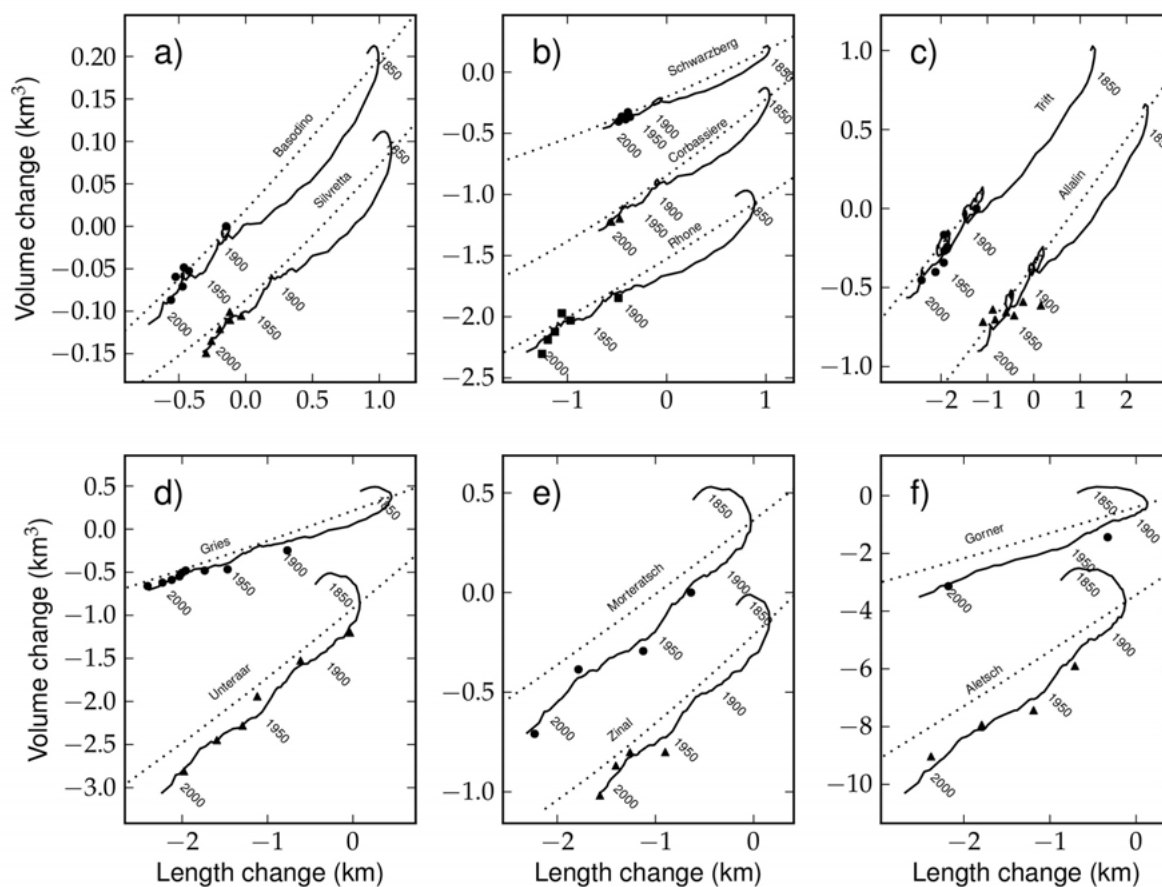


Figure 2. Phase space diagrams of modeled length and volume changes for 13 glaciers in the Swiss Alps (solid lines). Measured volume and length changes are shown with symbols. Dotted lines indicate the locus of the steady states. Clearly, small and steep glaciers are close to a steady state at present, whereas large and flat glaciers (Aletsch, Morteratsch, Unteraar) are far out of equilibrium.

10.12

3-D-reconstruction and visualization of microscale snow stratigraphy and weak layers

Matzl Margret¹, Steiner Stephen¹, Schneebeli Martin¹, Steinfeld Daniel¹, Köchle Bernadette¹ & Singer Julia¹

¹ WSL Institute for Snow and Avalanche Research SLF, Flüelastr. 11, CH-7260 Davos Dorf (matzl@slf.ch)

During the last 10 years X-ray microtomography (micro-CT) has proved to be the first successful method to measure the true three-dimensional (3-D) structure of snow on the ground. However, due to its constriction to small samples (with a typically evaluated size of 5 x 5 x 5 mm³) only more or less homogeneous samples have been analyzed. A new replica method introduced by Heggli et al. (2009) for 3-D micro-CT samples now allows the visualization of snow samples up to 70 mm height, and about 10 mm diameter, with a resolution of 10 µm. Based on this method, we casted highly fragile snow samples, like new snow, buried surface hoar and other weak layers during winter 2009-2010. The samples show a fascinating new image of how complex snow layers are. Many samples show strong density gradients within a structurally similar layer. From some 3D-reconstructions we created anaglyph images allowing to see the intricate structures in 3D. In addition, several snow packs were characterized by stability tests, Near Infrared Photography and SnowMicroPen. We think that this technique will improve our understanding of snow metamorphism and snow properties and that such visualizations of the snow microstructure could be a useful tool both for practitioners and researchers to improve the understanding of fracture processes during avalanche formation.

REFERENCES

Heggli, M.; Frei, E.; Schneebeli, M., 2009: Instruments and Methods. Snow Replica method for three-dimensional X-ray microtomographic imaging. *J. Glaciol.* 55, 192: 631-639.

10.13

Rapid changes of the ice mass configuration in the dynamic Diablotins ice cave– Fribourg Prealps, Switzerland

Morard Sébastien¹, Bochud Martin^{2,3} & Delaloye Reynald¹

¹ Geography Unit, Department of Geosciences, Chemin du Musée 4, CH-1700 Fribourg (sebastien.morard@unifr.ch)

² Geology Unit, Department of Geosciences, Chemin du Musée 6, CH-1700 Fribourg

³ Spéléo-Club des Préalpes Fribourgeoises (SCPF), Rue François Guillimann 7, CH-1700 Fribourg

Located at 2'000 m.a.s.l. in the entrance zones of the Gouffre des Diablotins (-652m), the Diablotins ice cave is the most important massive ice volume known in the Fribourg Prealps (Switzerland). Most part of the ice is encountered 10m inside the lower entrance of the cave and extends discontinuously in a lower horizontal gallery for about 40 meters until the intersection with a vertical shaft leading to the upper entrance 100m above.

The particularity of this ice cave is founded in the rapid changes of the ice mass configuration observed during the last two decades and relayed in the archive of the SCPF. In 1983, the lower gallery was plugged by ice. However in summers 1991 and 1992, the ice content was very low, allowing intense explorations of the karstic network during these years. Since 1994 the ice mass has sharply increased making difficult the speleological explorations, and plugging completely the lower gallery in 1995. Since then it has been impossible to reach again the intersection with the vertical shaft from the lower entrance. In fall 2009 it was still possible to penetrate the ice cave beyond about 20m to an intermediate room with a particular flat ice ceiling.

In order to better understand the processes occurring in this ice cave, the lower entrance was equipped in 2009 with several devices to measure airflow characteristics (temperature, humidity, velocity and direction), rock temperature and external air temperature. First results have shown that a chimney-effect ventilation system occurred currently in the ice cave: airflow direction reverses in the lower entrance when the external air temperature crosses a threshold of about +2°C.

The continuous cave climate measurements have also showed the predominant role of winter atmospheric air conditions to drive both the efficiency of chimney-effect circulation and the seasonal modifications of the ice mass. Important cooling and drying phases were thus recorded in winter 2009-2010 and main part of the ice loss is currently due to sublimation in wintertime. In contrast, formation of new ice was observed in spring during snowmelt period.

Winter meteorological conditions were also reconstructed between 1980 and 2009 to estimate the causes of the rapid changes observed in the 1990s. The results showed that winters 1989, 1990, 1992 and 1993 were mild, less snow-covered and with dry air conditions. These years correspond with the low ice content period of the ice cave. In contrast opposite meteorological conditions were encountered during winters 1994 and 1995, when the strong increase of the ice mass was observed.

10.14

Glaciological investigations on three glaciers at Les Diablerets, Alpes Vaudoises

Nath Sovik Kumar¹, Huss Matthias¹

¹ Department of Geosciences, University of Fribourg, Chemin du Musée 4, 1700, Fribourg, Switzerland (sovikkumar.nath@unifr.ch)

Glaciers in the Swiss Alps responded to climate change over the last century with strongly differing rates of mass loss. In order to correctly extrapolate glacier mass balance observed at individual glaciers to unmeasured ice masses the differences in glacier response driven by the same climatic changes need to be understood.

For this reason we focus on three glaciers around Les Diablerets, Alpes Vaudoises, with strongly different characteristics descending from the same mountain. Area changes over the 20th century appear to be strongly different according to glacier inventory data (Müller et al., 1976): Glacier de Tsanfleuron, an east-exposed and relatively flat glacier, has lost almost half of its area between the maximum of the Little Ice Age (around 1850) and 1973. In contrast, Glacier de Prapio, a small and steep cirque glacier, has only decreased in area by 12% over the same period. Glacier du Sex Rouge is a small north-exposed glacier with a flat accumulation area and a steep ablation zone (formerly called Glacier du Dar) that has recently separated from the main ice body and is about to disappear (Fig. 1). Glacier du Sex Rouge showed an area change of -26% between 1850 and 1973. Whereas Glacier de Tsanfleuron still has a size of more than 3 km², the two other glaciers are around 0.3 km². Due to the important differences in area that are observed in the past, we expect that the rate of mass loss – which is more directly related to climate change – shows a similar behavior.

The University of Fribourg plans to set up an integrative cryospheric monitoring site at Les Diablerets. Here, first results of glaciological investigations on the three glaciers around Les Diablerets are presented. Since winter 2009/2010 several types of field observations have been performed. Stakes were placed on the glacier surface to measure snow accumulation and ice ablation (Fig. 1). Manual probings of the snow depth including snow density surveys have been carried out in April 2010 to determine the winter balance of Glacier de Tsanfleuron. We present a first evaluation of the seasonal glacier mass balance of Tsanfleuron for the year 2009/2010. In addition, Ground Penetrating Radar (GPR) was used to measure the ice thickness (Fig. 1). On Glacier de Tsanfleuron ice thicknesses of up to 180 m were measured. On Glacier du Sex Rouge ice thickness is still higher than 60 m over considerable parts, which is surprising for its limited size.

The long-term evolution of the glaciers is investigated based on old topographic maps that are available for all glaciers for the years 1880, 1950, 1961, 1986, 1992 and 2006. By digitizing contour lines, Digital Elevation Models (DEMs) of the glaciers were established allowing the calculation of ice volume changes in decadal periods (Bauder et al., 2007). The uncertainty in the DEMs was assessed by comparing surface elevation in glacierized areas yielding an error of about 2 m. Between 1950 and 2006 we find mean changes in glacier surface elevation of -31 m for Glacier de Tsanfleuron, -21 m for Glacier du Sex Rouge, and of -14 m for Glacier de Prapio. Ice volume changes were further evaluated using a distributed accumulation and temperature-index melt model (Huss et al., 2009). Based on this method mass balance series covering the 20th century were derived for all glaciers.

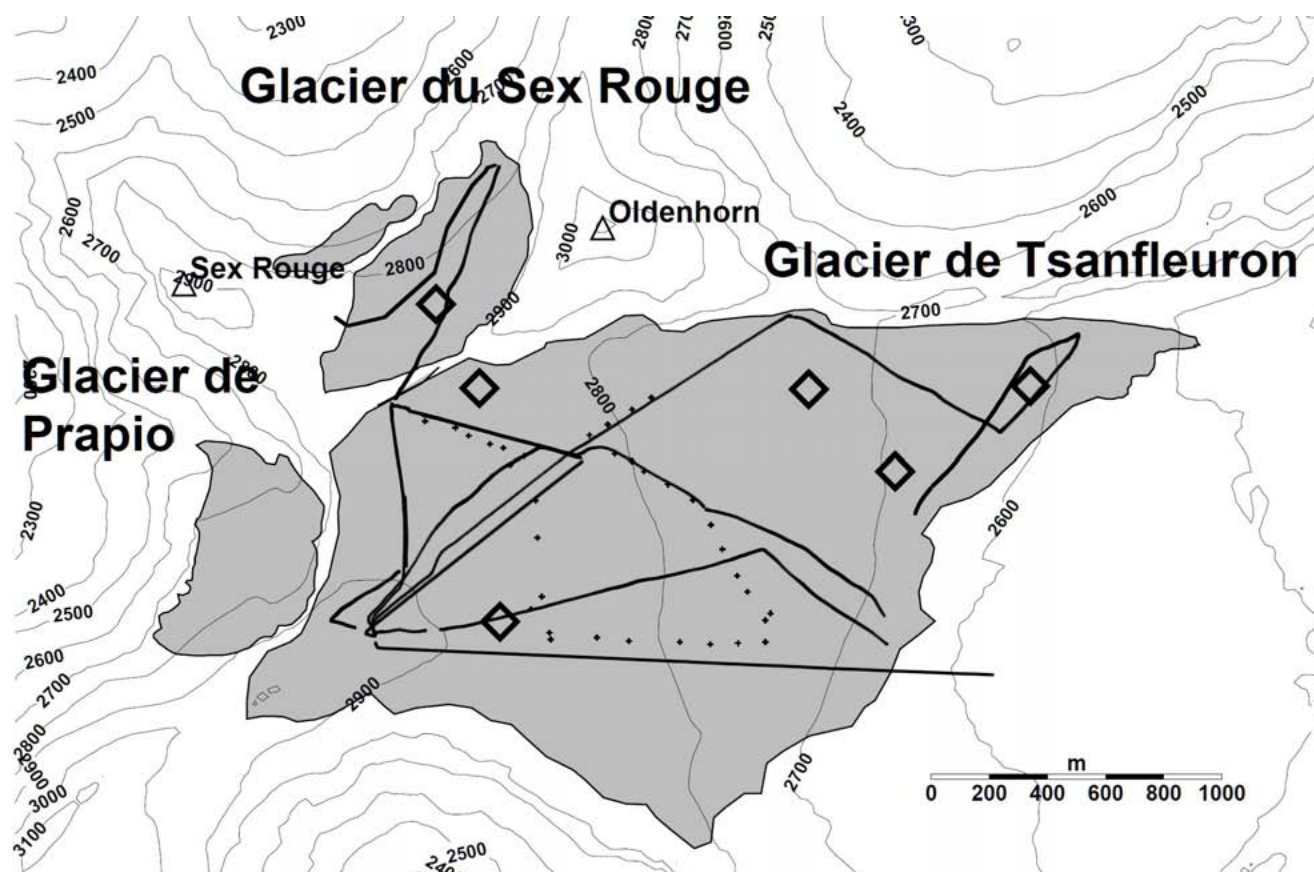


Figure 1: Overview map the three glaciers around Les Diablerets. The contour line interval is 100 m. Diamonds indicate the position of stakes to measure annual mass balance. Lines show the GPR profiles realized in April 2010, and small crosses measurements of the winter snow depth.

REFERENCES

- Bauder, A., Funk, M. & Huss, M. (2007): Ice-volume changes of selected glaciers in the Swiss Alps since the end of the 19th century. *Annals of Glaciology*, 46, 145–149.
- Huss, M., Bauder, A. & Funk, M. (2009). Homogenization of long-term mass balance time series. *Annals of Glaciology*, 50(50), 198–206.
- Müller, F., Caflisch, T. & Müller, G. (1976). *Firn und Eis der Schweizer Alpen: Gletscherinventar*, No. 57, Geographisches Institut der ETH Zürich, Zürich.

10.15

The Swiss Alpine Glacier's Response to the "2°C Target"

Nadine Salzmann^{1,2} Horst Machguth^{2,3}

¹ (1) *Alpine Cryosphere and Geomorphology, Department of Geosciences, University of Fribourg, Switzerland*
(nadine.salzmann@unifr.ch)

² *Glaciology and Geomorphodynamics Group, Department of Geography, University of Zurich, Switzerland*

³ *Marine Geology and Glaciology, Geological Survey of Denmark and Greenland - GEUS, Copenhagen, Denmark*

The "2°C target" for global warming (relative to pre-industrial level) became a main focus in the climate change debate since the UN Climate Change Conference in Copenhagen (COP15) in December 2009 at the latest. While this target implies to be a 'clear' goal for politicians and decision makers, the effective impacts that a global mean air temperature increase of 2°C has on natural and human systems on regional to local scales remain complex. Her, we present an approach to assess the potential impact of a 2°C warming on the Swiss Alpine glaciers.

In glacierized mountain regions, where glaciers represent an important source for fresh water and control a great part of the hydrological cycle, the retreat or disappearance of glaciers as a consequence of climatic changes will have major socio-economical consequences on the people living there and the adjacent lowland. A trend to negative glacier mass balances is observed and well documented for many mountain ranges all over the world (WGMS, 2009).

Global climate change, however, is not equally distributed around the globe. Observations show that the last century's air temperature trends significantly differ between regions, and this is true even within Switzerland. The 12 homogenized air temperature series available for Switzerland for example, show a range of trends between 0.82°C/100y for Lugano, to 1.63°C/100y for Chateau-d'Oex. (Meteoschweiz, 2009).

Our study is (i) based on the 12 homogenized air temperature series to define the warming that has already taken place in the past, and (ii) on results from a selection of Regional Climate Model (RCM) simulations that have been completed in the frame of the recently finished EU-funded ENSEMBLES program, for the transient simulation and to define the 'remaining' temperature increase up to the level of 2°C. The RCM results are bias-corrected and then taken as input for a distributed mass balance model (Machguth et al. 2009) in order to assess time and mass balance trends for the Swiss Alpine glaciers with regard to a 2°C increase. The different runs of the glacier mass balance model show a range of future scenarios, mainly as a result of the different driving RCMs. All scenarios have in common that numerous glaciers will lose their accumulation area before or when the 2°C target is reached. Because a global 2°C temperature rise is likely to impact with a warming of more than 2°C on the Swiss Alps, our scenarios represent a lower limit for the changes to be expected. Therefore, we additionally considered a 4°C increase in our study.

REFERENCES

WGMS 2009: Glacier Mass Balance Bulletin, No. 10, 96 pp

Meteoschweiz 2009: Originale und homogene Reihen im Vergleich. Dezember 2009.

Machguth, H., Paul, F., Kotlarski, S., Hoelzle, M. 2009: Calculating distributed glacier mass balance for the Swiss Alps from regional climate model output: A methodical description and interpretation of the results. *Journal of Geophysical Research*, 114, D19106, doi:10.1029/2009JD011775

10.16

Borehole logging in alpine periglacial talus slopes, Valais Alps, Switzerland

Scapozza Cristian¹, Baron Ludovic², Lambiel Christophe¹

¹ Institut de Géographie, Université de Lausanne, Anthropole-Dorigny, CH-1015 Lausanne
(cristian.scapozza@unil.ch ; christophe.lambiel@unil.ch)

² Institut de Géophysique, Université de Lausanne, Amphipôle-Sorge, CH-1015 Lausanne (ludovic.baron@unil.ch)

Recent drilling projects in three periglacial talus slopes of the Valais Alps, Switzerland (see Scapozza et al. 2010a, b), opened up the possibility of carrying out borehole geophysical measurement to study the stratigraphy and the permafrost structure of the prospected talus. Borehole logging is an important tool for investigating the vertical distribution of some physical parameters, such as density (gamma-gamma), natural radioactivity (gamma-ray) and hydrogen content (neutron-neutron) (Vonder Mühll & Holub 1992).

In Les Attelas site, three boreholes were drilled destructively along an upslope-downslope transect. Frozen sediments are present only in the two lowest boreholes, whereas the upper borehole does not present ground ice. The internal structure of some of the boreholes could be observed with a hand-made borehole camera. Other information about the borehole structure comes from the field experience of the drilling team and from observations of the characteristics of the expelled materials. As the boreholes were drilled destructively and not cored, it was not possible to quantify the volumetric ice content of the ground. Only a qualitative estimation (low or high content of ice) was established on the basis of the nature of the expelled materials. Logging had to be done in dry holes, what has limited the choice of the logging methods.

Borehole geophysics at the studied talus slope confirms the borehole stratigraphy. In Les Attelas site, for example, an important shift in the logs separate the surface layer of unfrozen sediments (high activity in the gamma-gamma and

neutron-neutron logs) and the layer characterised by ice-rock mixture (low activity in the gamma-gamma and neutron-neutron logs). The ice content in the frozen layer is not homogeneous, as pointed out by the important variations in the three logs. Where layers relatively rich in ice are present (ice content estimated between 10 and 50 %), a decreasing activity in the gamma-gamma log and an increasing activity in the neutron-neutron log can be observed. This behaviour is particularly evident for the borehole B01/08 (fig. 1).

As drilling in mountain permafrost (and in particular in talus slope) is often expensive and complicated, it is necessary to derive as much information from a borehole as possible. For this reason, borehole logging is a very powerful method for studying the stratigraphy of a borehole when it is not cored. In this framework, the borehole geophysics performed in the studied talus slope allows: (1) to confirm the permafrost stratigraphy derived from direct observations and thermal measurements and; (2) to perform the calibrations of the width and the nature of the structures detected by surface geophysical prospecting.

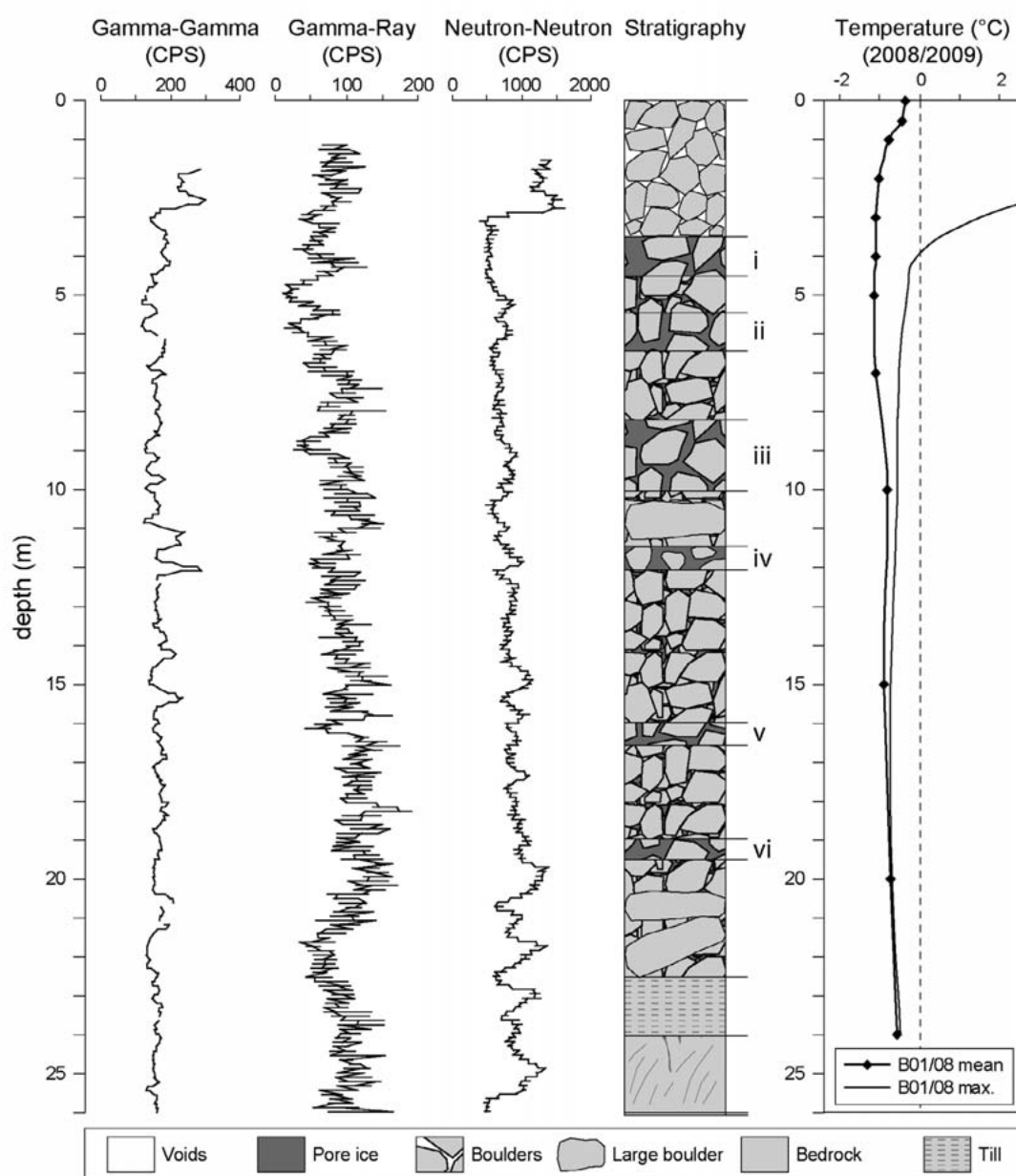


Figure 1. Results of borehole geophysics in borehole B01/08 (lower part of the slope) in Les Attelas talus slope. i-vi: layers relatively rich in ice.

REFERENCES

- Vonder Mühl, D. & Holub, P. 1992: Borehole logging in alpine permafrost, Upper Engadin, Swiss Alps. *Permafrost and Periglacial Processes*, 3, 125-132. DOI: 10.1002/ppp.3430030209.
- Scapozza, C., Lambiel, C., Baron, L., Marescot, L. & Reynard, E. 2010a: Internal structure and permafrost distribution in two alpine periglacial talus slopes, Valais, Swiss Alps. *Geomorphology*, submitted.
- Scapozza, C., Lambiel, C., Abbet, D., Delaloye, R. & Hilbich, C. 2010b: Internal structure and permafrost characteristics of the Lapires talus slopes (Nendaz, Valais). 8th Swiss Geoscience Meeting, Fribourg, this volume.

10.17

Modelling of permafrost evolution under climate change scenarios

Scherler Martin¹, Hauck Christian²

¹ Alpine Cryosphere and Geomorphology (ACAG), Department of Geosciences, University of Fribourg, Fribourg, Switzerland (martin.scherler@unifr.ch)

² Alpine Cryosphere and Geomorphology (ACAG), Department of Geosciences, University of Fribourg, Fribourg, Switzerland (christian.hauck@unifr.ch)

The model used in this study is a one-dimensional coupled soil water and heat transfer model of the soil-snow-atmosphere boundary layer (Jansson & Karlberg 2001). It accounts for the accumulation and melt of a seasonal snow cover, as well as for the freezing and thawing of the soil. The model is driven by the following meteorological parameters: air temperature, relative humidity, global radiation, incoming long-wave radiation, wind speed, and precipitation. A complete energy balance is calculated for the snow or soil surface, yielding a surface temperature representing the upper thermal boundary condition of the soil profile. A constant geothermal heat flux determines the lower thermal boundary.

The model has been applied to simulate ground temperatures together with water and ice content evolution of two high-altitude alpine permafrost sites in Switzerland. The sites are Schilthorn in the Bernese Oberland and Murtèl in the Engadin. The sites were chosen because of their different morphologies and substrates, i.e. a rock slope with a substantial fine-grained surficial cover at Schilthorn and a bouldery surface with large blocks at rock glacier Murtèl. The aim of the simulations was the long term modelling (9 years for Schilthorn and 6 years for Murtèl) and the calibration of the model for the two study sites. The model is validated with borehole temperature data.

In a next step the model was driven by daily mean values of meteorological parameters which were taken from regional climate model (RCM) output (ENSEMBLES Project) for the time period of 1991 to 2101. The bias in relation to the measured climate data has been determined on the basis of an observation period from 1999 to 2008 for Schilthorn and from 1997 to 2008 for Murtèl. These deviations have been corrected in the model input by addition or subtraction of the so determined bias. One of the given scenarios shows that the active layer at the Schilthorn site varies between 5m and 10m for the next 30 years. After that period, the thaw layer does not freeze up anymore and a talik develops. In the subsequent years the permafrost degrades as the permafrost table gradually declines.

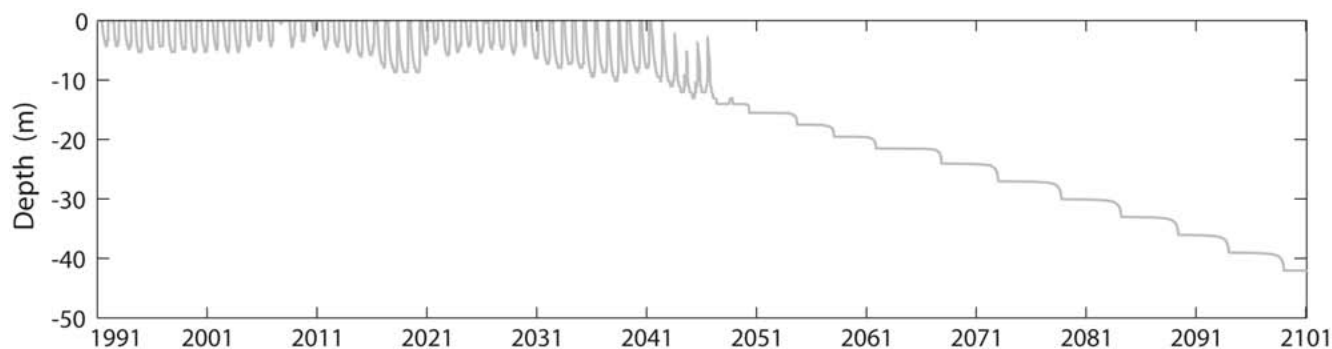


Figure 1. Thaw layer depth projection for Schilthorn based on a model run driven with regional climate model (RCM) data

REFERENCES

ENSEMBLES Project. <http://ensemblesrt3.dmi.dk/>

Jansson P-E. & Karlberg L. 2001: Coupled heat and mass transfer model for soil-plant-atmosphere systems. Royal Institute of Technology, Dept of Civil and Environmental Engineering, Stockholm.

10.18

Investigation of the high variability of mountain permafrost

S. Schneider & M. Hoelzle

Alpine Cryosphere and Geomorphology (ACAG), Department of Geosciences, University of Fribourg, Switzerland

Compared to polar regions permafrost in high mountain areas occurs in a great variation of surface and subsurface material and texture within short distances. Therefore, the thermal regime of the active layer strongly depends on site-specific factors like the grain size, the pore volume and type of material beside climatic factors such as air temperature, incoming radiation, precipitation and infiltration.

The background of this work is the analysis of the seasonal and long-term temperature changes in a permafrost region with different materials, whereas the microclimatic factors (like air temperature, wind speed and direction, relative humidity and incoming solar radiation) as well as the topographic situation (exposition, inclination) are the same. Therefore, observed changes in subsurface temperatures are due to the different subsurface materials and their corresponding, material depending processes. The aim of this work is to understand these different processes and to calculate the different sensitivities of the ground thermal regime to changes in the microclimate.

Borehole temperature data from 2002 – 2009 down to 6 m depth will be presented for five different sites. All sites are located at the Murtèl- Corvatsch area (Hanson and Hoelzle 2004) and some of them are not more than 25m away from each other. The material in which the boreholes were drilled varies from bedrock to coarse blocky and fine-grained substrate with corresponding changes in ice content. Some of them have only seasonal frost whereas others are drilled within a rock glacier with approximately 10m of ice.

Figure1 shows the mean annual temperature for three of these boreholes. The thermal regime of the bedrock site (a) is mainly driven by heat conduction within the rock. During summer the temperature decreases almost linear with depth (respectively increases in winter). At the talus slope (b) the permafrost table is recognizable at 3.5 m depth where the temperature is around 0°C throughout the whole year. Hence, this depth is the lower boundary where the colder air can circulate. This process is called balch- effect, i.e. warm air of the subsurface will be replaced by subsiding cold air. The temperature at the rock glacier site (c) at 2.5 – 6m depth is strongly influenced by the ice content of the rock glacier. Due to the high air temperature and the cooling by the ice, a high temperature gradient is present during summer.

To estimate the sensitivity of permafrost to climatic changes the thermal diffusivity and the soil heat flux was calculated for all sites (for the period 2003 – 2009). The thermal diffusivity describes the degree of how fast a material may change its temperature. Whereas high values of apparent diffusivity indicate the occurrence of non-conductive processes, while low diffusivity values indicate the dominance of conductive heat transfer. At all sites the diffusivity is quite low at the surface ($10^{-5} - 10^{-6} \text{ m}^2 \text{ s}^{-1}$). That means that the thermal regime near the surface is mainly conductive. As expected the diffusivity values within the subsurface vary strongly, depending on the subsurface material. The bedrock sites show low values down to 6m depth, due to conductive processes. The values at the rock glacier site increase at the permafrost table at 2.5m as a consequence of a temperature close to 0 °C and therefore the melting of the ice.

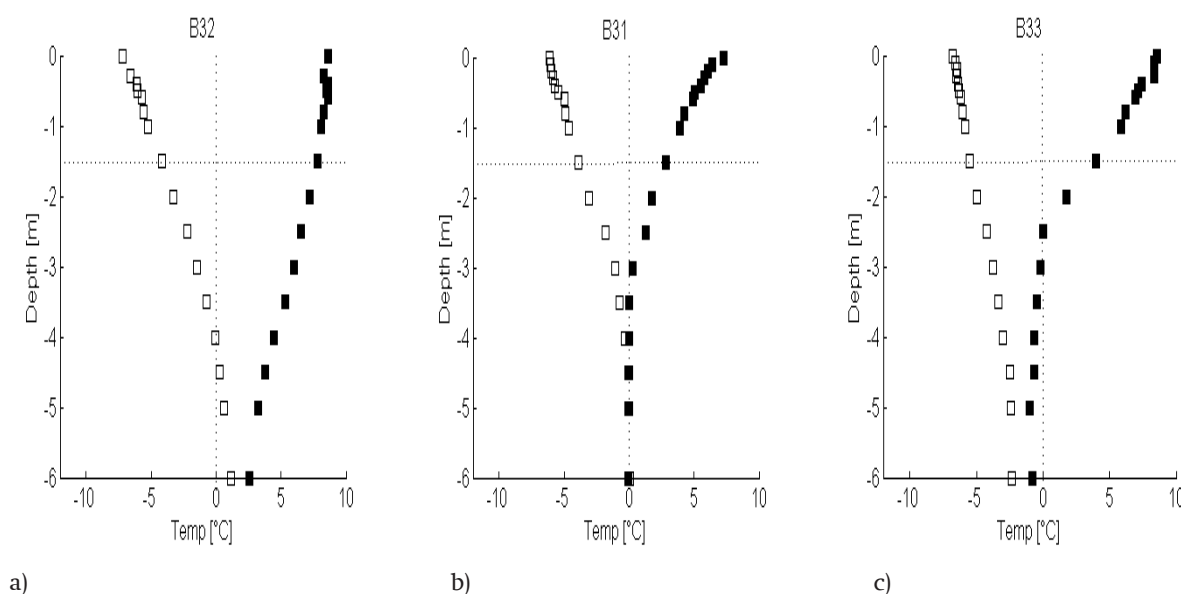


Figure1: mean summer (black) and winter (white) temperature data from 2003-2008 for a) bedrock, b) talus slope and c) rock glacier

The analysis of this temperature data and their development over the last years show strong differences depending on the material. Understanding the different processes and calculating the time which is needed for the energy transport in the subsurface is the first step to estimate the sensitivity of mountain permafrost to climatic changes. In addition, the calculated thermal diffusivities and the soil heat flux for different materials might be important input parameters for modeling the development of mountain permafrost.

REFERENCES

Hanson, S. and Hoelzle, M., 2004. The thermal regime of the active layer at the Murtèl rock glacier - based on data from 2002. *Permafrost and Periglacial Processes*, 15(3): 273-282.

10.19

Using speleological methods to test interpretations of dye tracing results in glaciology

Walther Peter^{1,2}, Gulley Jason³, Benn Douglas¹, Martin Jon³

¹ University Centre in Svalbard, Pb 156, NO-9171 Longyearbyen

² Geographisches Institut, Klingelbergstrasse 27, CH-4056 Basel

³ Department of Geological Sciences, 241 Williamson Hall, US-32611 Gainesville, FL

Hydrological properties of glacial drainage systems are an important control on glacier dynamics and are thought to influence short term variations in sliding speed. Since most drainage systems remain inaccessible to direct exploration, the development of drainage systems during melt season is usually investigated by quantitative dye tracing.

Previous studies showed that the dye breakthrough curve (BTC) usually shows low transit velocities (TV) and peak concentrations (PC) at the beginning of the melt season and high TV, PC later in the season, and that this transition takes place once the snow line is retreating beyond the injection moulin.

This behaviour is interpreted as a change in the configuration of the subglacial drainage system: Dispersed BTC with low TV, PC are seen as an indicator of a distributed drainage system, where water flows through linked cavities and water films at the glacier bed, whereas high TV, PC are seen as an indicator of an efficient drainage system through a subglacial conduit. The transition between the two BTC patterns is then explained as a collapse of a distributed system and its replacement by an efficient channelized system.

Due to the physical inaccessibility of most subglacial drainage systems, this hypothesis has not yet been tested by direct exploration.

In 2009/10, both speleological mapping and dye tracing investigations have been conducted in a subglacial conduit in Rieperbreen, a cold-based glacier in central Spitzbergen, Svalbard, Norway. The conduit, which had been mapped before in 2007 was remapped after the melt season 2009 and explored again before and after the melt season 2010. During melt season 2010, numerous dye trace investigations were conducted by injection of Rhodamine W/T via a supraglacial stream that discharges into the explored subglacial conduit. Dye return was measured in the proglacial river near the glacier snout. BTC-Patterns could then be compared to the observed changes in the morphology of the subglacial channel.

Speleological exploration shows that the subglacial conduit is located at the bed of the glacier where it is partly incised in frozen till. The ice thickness above the conduit is less than 30 m. The conduit has the morphological traits of a classic cut and closure conduit that developed by incision of a supraglacial channel and must have developed after 1996, when the drainage of Rieperbreen was mainly supraglacial.

Repeated mapping and exploring using speleological methods indicates that the geometry of the conduit shows no significant changes between the investigated seasons, and, according to the mapping of 2007, also doesn't change significantly between years.

Dye tracing results showed the pattern mentioned above, with low TV, PC in the early, and high TV, PC in the peak melt season.

The conduit is not subject to changes in morphology, so this factor can be eliminated as a cause of the observed hydrological changes. Instead, we infer that the BTC characteristics reflect changes in recharge, and the varying effects of channel roughness at different discharge rates. These results imply that recharge rates must be taken into account when interpreting the results of tracer studies in glacial drainage systems.

10.20

Permafrost carbon dynamics controlled atmospheric CO₂ and Pleistocene climateZech Roland¹, Huang Yongsong¹, Zech Michael², Taroza Rafael¹ & Zech Wolfgang²¹Geological Sciences, Brown University, Providence, USA (godotz@gmx.de)²Institute of Soil Science, University of Bayreuth, Germany

The prevailing ‘ocean hypothesis’ explains lower levels of atmospheric CO₂ during glacials (~180 ppm) compared to interglacials (~280 ppm, pre-industrial) with reduced deep ocean ventilation and resultant trapping of CO₂. The blind spot of this hypothesis, however, is that the assumed large pool of old radiocarbon in the deep ocean has not been found so far (Broecker and Barker 2007), and that current climate and carbon models can not adequately simulate the CO₂ trapping (Tagliabue et al. 2009). One should therefore be open-minded to alternative hypothesis, namely that carbon sequestration and storage in terrestrial ecosystems increased during glacials.

Revised carbon storage estimates highlight that the soil organic carbon pools in northern permafrost regions have been extremely underestimated so far (>1670 Pg C, Tarnocai et al. 2009). Good preservation of soil organic matter more than compensates for low biomass productivity. Although reports of increasing permafrost degradation and related CO₂ and methane emissions have fueled concerns about a strong positive climate feedback to anthropogenic warming, the potential role of permafrost carbon dynamics on longer, glacial-interglacial timescales has largely escaped scientific interests.

We investigated a 15 high, 240 ka old permafrost loess profile in NE-Siberia using standard geochemical techniques, as well as compound-specific deuterium measurements (δD) on plant-derived long-chain n-alkanes. Our results show that organic-rich horizons accumulated during cold (glacial) periods as indicated by more negative δD values, whereas soil organic material degraded and mineralized more intensively during warm (interglacial) periods (more positive δD values, Fig. 1). These findings reflect and illustrate the long-term carbon dynamics of permafrost soils, and spatial extrapolation of these dynamics to the vast, non-glaciated Siberian plains indicates that more than 1000 Pg soil organic carbon might have accumulated slowly during each glacial (Zimov et al. 2009). Similar amounts of carbon would have been released rapidly during terminations, an equivalent to ~500 ppm CO₂ in the atmosphere. This implies that the oceans would have acted as sinks during terminations rather than sources, as suggested by the ‘ocean hypothesis’.

On long, glacial-interglacial timescales, permafrost carbon dynamics are controlled by mean annual temperatures, which are externally forced by integrated annual insolation. The ~40 ka periodicity of ice ages during the early Pleistocene can thus readily be linked to the orbital parameter obliquity, which controls high-latitude integrated annual insolation (Huybers 2006). Our proposed ‘permafrost glacial hypothesis’ can also readily explain the Mid-Pleistocene Transition after ~1 Ma, when the periodicity of ice ages changed to ~100 ka: The overall Pleistocene cooling trend caused permafrost to reach mid-latitudes (~45°N), where integrated annual insolation is no longer controlled by obliquity, but eccentricity. As a consequence, obliquity cycles (glacial terminations) were skipped, unless they coincided with increasing eccentricity, resulting in 80 or 120 ka glacial cycles.

REFERENCES

- Broecker, W. & Barker, S. 2007: A 190‰ drop in atmosphere's Δ14C during the “Mystery Interval” (17.5 to 14.5 kyr). *Earth Planet. Sci. Lett.* 256: 90-99.
- Huybers, P. 2006: Early Pleistocene Glacial Cycles and the Integrated Summer Insolation Forcing. *Science* 313: 508-511.
- Tagliabue, A., Bopp, L. & Roche, D. M. et al. 2009: Quantifying the roles of ocean circulation and biogeochemistry in governing ocean carbon-13 and atmospheric carbon dioxide at the last glacial maximum. *Clim. Past* 5: 695–706.
- Tarnocai, C., Canadell, J. G. & Schuur, E. A. G. et al. 2009: Soil organic carbon pools in the northern circumpolar permafrost region. *Global Biogeochem. Cycles* 23: GB2023.
- Zimov, N. S., Zimov, S. A. & Zimova, A. E. et al. 2009: Carbon storage in permafrost and soils of the mammoth tundra-steppe biome: Role in the global carbon budget. *Geophys. Res. Lett.* 36: L02502.

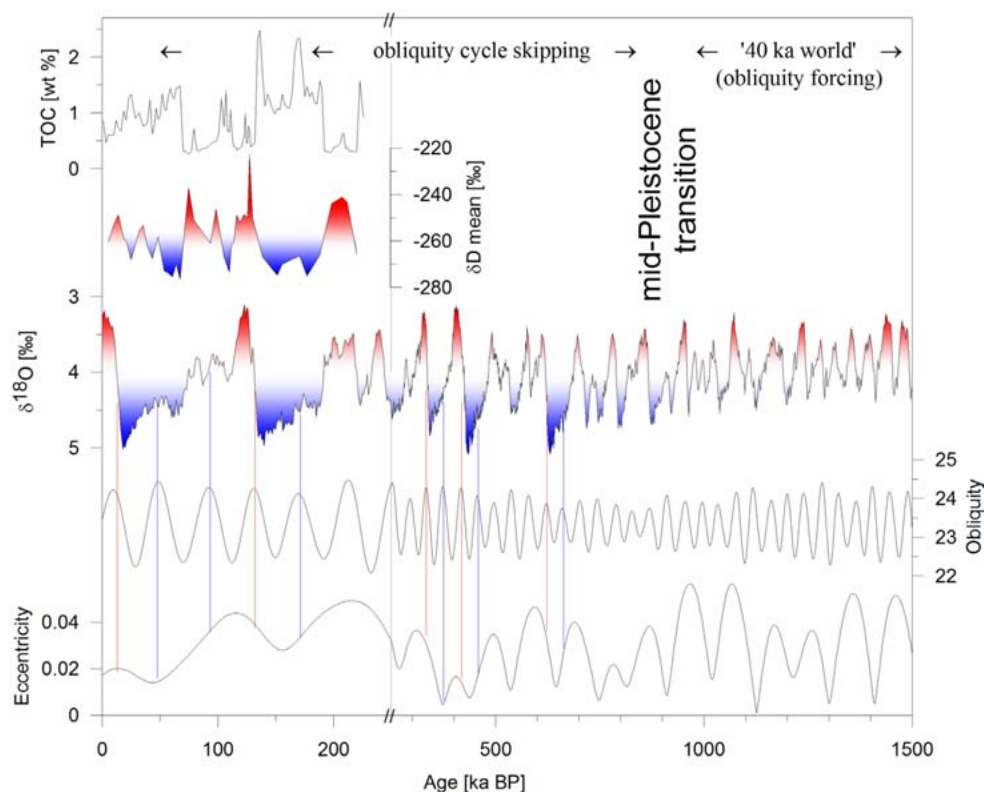


Figure 1. Sketch of the permafrost glacial hypothesis. More total organic carbon (TOC) is sequestered in our Siberian loess profile during cold periods as indicated by more negative δD , and increased global ice volume as indicated by more positive $\delta^{18}O$ (marine stack). Terminations coincide with obliquity maxima, and after the MPT also with increasing eccentricity (note break in time scale).

10.21

Active Layer development in Alpine permafrost

Zenkhusen Mutter Evelyn¹ & Phillips Marcia¹

¹ WSL Institute for Snow and Avalanche Research SLF, CH-7260 Davos Dorf, Switzerland

The active layer is the ground layer above permafrost that thaws in summer and refreezes in winter. Its thickness is defined thermally as the maximum seasonal depth of penetration of the 0°C isotherm into the ground (Burn 1998). Mainly controlled by air temperature, ground surface characteristics, moisture content and snow cover, the active layer thickness can vary both spatially and temporally. Warming air temperatures may lead to increasing active layer thickness and induce slope or infrastructure instability in mountain permafrost.

In this study active layer properties in ten permafrost boreholes in the Swiss Alps have been studied and compared using borehole temperatures. All ten sites show different active layer depths ranging from 0.5m to 5m depth. A characteristic depth at which ground temperature inside the active layer is analysed had to be determined to allow reasonable comparisons between the sites. We used the ground temperature series measured (if available) or interpolated in the middle of the active layer for each location (see legend of Figures 1 and 2 in brackets). To keep things simple the interpolation of these thermal data was effected linearly, yet taking into consideration the phase shift with increasing depth.

The active layer depths and the different stages in the seasonal course of the characteristic active layer temperature series (autumn and spring zero curtains, winter cooling and warming rates and active layer duration) have been analysed. Furthermore the relation between thawing degree days and active layer thickness (Harlan & Nixon 1978, Smith et al. 2009) has been compared with the results found in studies on circumpolar permafrost locations.

The results show that maximum active layer depths are relatively stable at the different sites (Fig. 1). The impact of the exceptionally hot summer 2003 is, however, clearly visible at two sites, but there was almost complete recovery from this striking active layer deepening in the course of the following two years. In contrast to the thickness, the duration of the active layer shows an increasing tendency for all sites (Fig. 2).

Autumn and spring zero curtain durations are highly variable ranging from 0 to 90 days. Rates of cooling and thawing during the frozen stage of the year are similar for the different sites and range from -0.006 to $-0.001^{\circ}\text{C}/\text{day}$ for cooling and from 0.001 to $0.01^{\circ}\text{C}/\text{day}$ for warming. The relation between thawing degree days and active layer depth only shows significant positive correlations for the early active layer season (May to July). At many sites with coarse grained surface material in the Alps the active layer is underlain by a relatively ice-rich permafrost table which prevents a further active layer deepening later in the summer (Phillips et al. 2009).

REFERENCES

- Burn, C.R. 1998: The active layer: two contrasting definitions. *Permafrost and Periglacial Processes*, 9, 411-416.
- Harlan, R.L. & J.F. Nixon 1978: *Ground thermal regime*. MacGraw-Hill, New York.
- Phillips, M., E. Zenklusen Mutter, M. Kern-Luetsch & M. Lehning 2009: Rapid Degradation of Ground Ice in a Ventilated Talus Slope: Flüela Pass, Swiss Alps. *Permafrost and Periglacial Processes*, 20, 1-14.
- Smith, S.L., S.A. Wolfe D.W. Riseborough & F.M. Nixon 2009: Active Layer Characteristics and Summer Climatic Indices, Mackenzie Valley, Northwest Territories, Canada. *Permafrost and Periglacial Processes*, 20, 201-220.

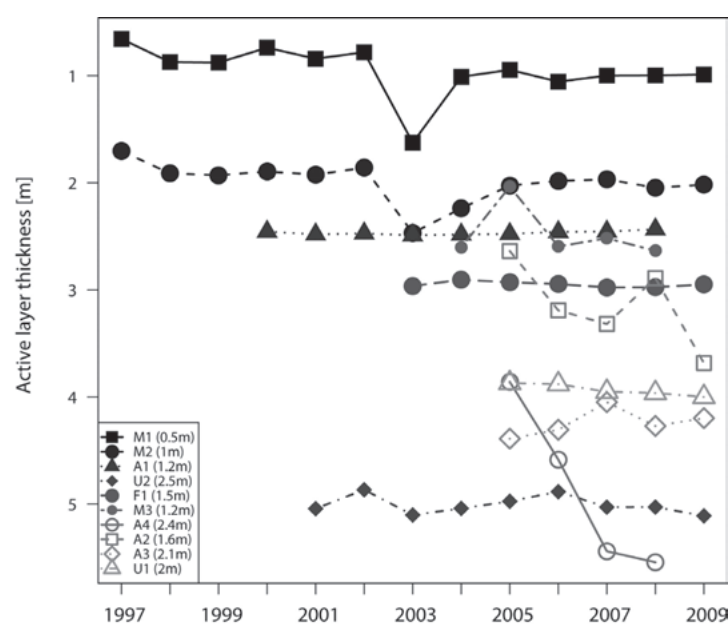


Fig. 1: Active layer thickness at the ten borehole sites. In brackets: characteristic depth in the middle of the active layer for the corresponding site.

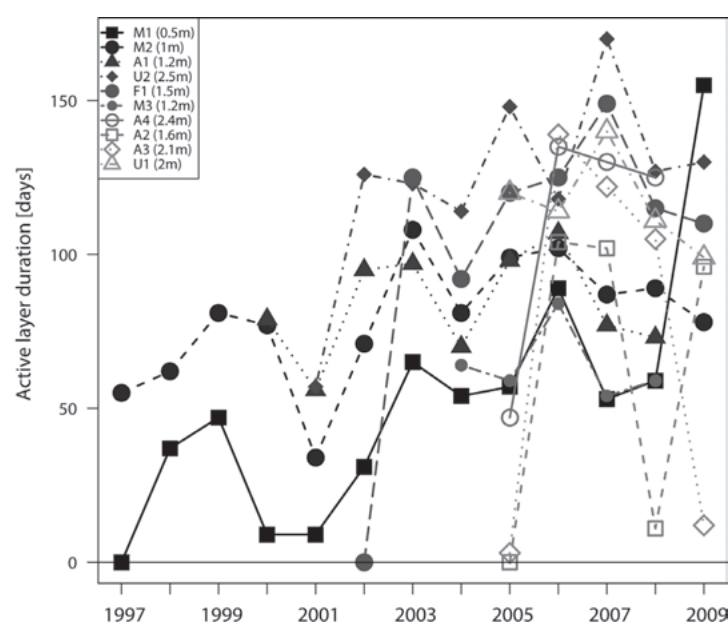


Fig. 2: Active layer duration at the ten borehole sites. In brackets: characteristic depth in the middle of the active layer for the corresponding site.

11. Meteorology and Climatology

Rolf Philipona, Markus Furger

Swiss Meteorological Society

- 11.1 Brönnimann S.: Weather extremes in the past 140 years in a historical reanalysis data set
- 11.2 Bukowiecki N., Zieger P., Hüglin C., Weingartner E., Baltensperger U.: Detection of Eyjafjöll volcano ash at Jungfrauoch, Switzerland
- 11.3 Calanca P., Philipona R., Trebejo I., Alarcón Velazco C.: Simple approaches to the evaluation of net radiation and reference evapotranspiration
- 11.4 Ediang O.A., Ediang A.A.: Dynamics of abrupt climatic change over the climate regions in Nigeria.
- 11.5 Hächler P.: Schneefrühwarnungen in den Schweizer Alpen
- 11.6 Henne S., Brunner D.: Simulating the dispersion of the Eyjafjalla volcanic ash plume over Europe
- 11.7 Hiller R., Stieger J., Neininger B., Buchmann N., Eugster W.: Aircraft and ground based CH₄ measurement of a high moor in Switzerland
- 11.8 Hurter F., Perler D., Geiger A.: Monitoring atmospheric water vapor in the Zermatt region with GNSS
- 11.9 Kuhlemann J., Raible C.C., Luterbacher J., Schuster C., Krumrei I., Reinecker J., Kubik P., Westphal H.: Climate of the Little Ice Age: A Mediterranean-scale anomaly pattern with LGM similarities
- 11.10 Neininger B., Schneider B., Oldani D.: Airborne observation of the Eyjafjallajökull volcanic ash plume over Switzerland
- 11.11 Perler D., Geiger G., Rothacher M.: Water vapor retrieval with parameterized GPS tomography: Longterm study in Switzerland
- 11.12 Sesartic A., Dalla Fior T., Storelvmo T., Lohmann U.: Modelling global emissions of bacteria and fungal spores acting as ice nuclei
- 11.13 Strauss F., Formayer H., Asamer V., Schmid E.: High resolution climate change data for Austria until 2040
- 11.14 Weibel B., Röser I., Liniger M., Appenzeller C.: NCCR Climate related research at MeteoSwiss - The Swiss climate of today and tomorrow
- 11.15 Willi M., Frei C.: Gridding of daily sunshine duration by combination of station and satellite data

11.1

Weather extremes in the past 140 years in a historical reanalysis data set

Brönnimann Stefan

Institute of Geography and Oeschger Centre for Climate Change Research, University of Bern, Hallerstr. 12, 3012 Bern (stefan.broennimann@env.ethz.ch)

Information on weather extremes is important for stakeholders. Because extremes are rare by definition, conventional meteorological data sets often contain only few events and hence there is a need for extending these data sets back in time. Recently, a global reanalysis has been performed that provides six-hourly 3-dimensional data back to 1870 based on the assimilation of only surface pressure data (Compo et al. 2010, see: http://www.esrl.noaa.gov/psd/data/gridded/data.20thC_ReanV2.html).

The suitability of the new data sets for studying extremes (and eventually changes thereof) needs to be assessed. In my presentation I will show some selected extreme events from this data set and compare the results with available in-situ observations, focusing on storms, cold air outbreaks, and heat-waves. In general, a good agreement between historical information and the reanalysis is found at northern midlatitudes. The agreement is worse in other parts of the globe, and there are systematic biases that need to be accounted for. Nevertheless, the data set provides a unique source of information that will find a wide range of applications from atmospheric sciences to impact modelling.

REFERENCES

Compo, G.P., J.S. Whitaker, P.D. Sardeshmukh, N. Matsui, R.J. Allan, X. Yin, B.E. Gleason, R.S. Vose, G. Rutledge, P. Bessemoulin, S. Brönnimann, M. Brunet, R.I. Crouthamel, A.N. Grant, P.Y. Groisman, P.D. Jones, M. Kruk, A.C. Kruger, G.J. Marshall, M. Maugeri, H.Y. Mok, Ø. Nordli, T.F. Ross, R.M. Trigo, X. Wang, S.D. Woodruff, S.J. Worley (2010) The Twentieth Century Reanalysis Project. *Q. J. R. Meteorol. Soc.* (submitted)

11.2

Detection of Eyjafjöll volcano ash at Jungfraujoch, Switzerland

Bukowiecki Nicolas¹, Zieger Paul¹, Hüglin Christoph², Weingartner Ernest¹, Baltensperger Urs¹

¹ *Laboratory of Atmospheric Chemistry, Paul Scherrer Institut, CH-5232 Villigen PSI, Switzerland (nicolas.bukowiecki@psi.ch)*

² *Empa, Swiss Federal Laboratories for Materials Science and Technology*

The Eyjafjöll volcano ash plume was detected at the Jungfraujoch during three episodes in April and March 2010. The large variety of aerosol properties being measured continuously at the Jungfraujoch (including mass and number concentration, cloud condensation nuclei, size distribution, as well as light absorption and scattering coefficients) will help for an in-depth physical and chemical characterization of the airborne volcanic ash.

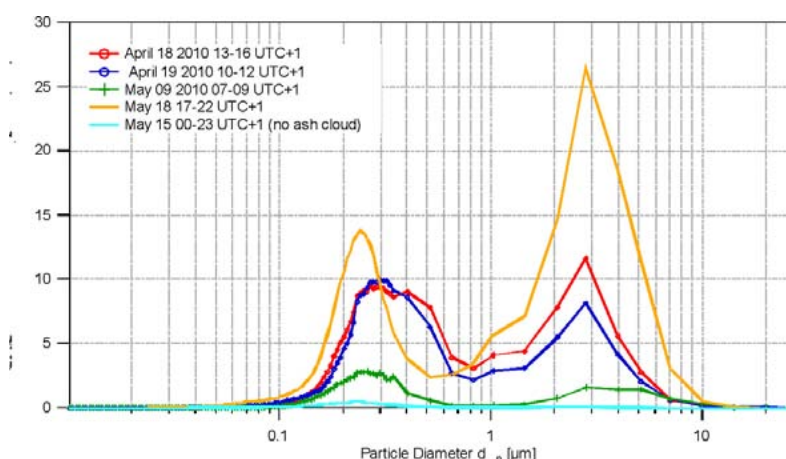


Figure 1. The size distribution of volcanic ash at the Jungfraujoch. The indicated diameter axis represents the mobility diameter for $d_p < 0.3 \mu\text{m}$ and the corrected OPC diameter¹ for $d_p > 0.3 \mu\text{m}$.

11.3

Simple approaches to the evaluation of net radiation and reference evapotranspiration

Calanca Pierluigi¹, Philipona Rolf², Trebejo Irene³, Alarcón Velazco Constantino

¹ Agroscope Reckenholz-Tänikon ART, Environmental Resources and Agriculture, Reckenholzstrasse 191, CH-8046 Zurich (pierluigi.calanca@art.admin.ch)

² Federal Office of Meteorology and Climatology MeteoSwiss, Aerological Station, CH-1530 Payerne

³ Servicio Nacional de Meteorología e Hidrología, SENAMHI, Casilla 11 1308, Lima 11, Perú

Net radiation (NR) and the so-called reference evapotranspiration (ET₀) are key variables in agrometeorology, providing the basis for the assessment of crop water requirements and irrigation needs. Standard methods are available for inferring NR and computing ET₀ from routinely observed meteorological data. Many of them have been developed and tested with respect to environmental conditions as found at low altitudes. In the context of climate change and its impacts on agriculture there is, however, an increasing necessity for applying such methods to mountain areas. These have been identified as among the most vulnerable environments and have for this reason become the focus of several research programmes such as e.g. the Climate Change Adaptation Programme in Peru (PACC), initiated by the Swiss Agency for Development and Cooperation (SDC) in 2008, and the EU funded project ACQWA.

In this contribution we review simple approaches to the evaluation of NR and ET₀ on a daily time scale with a potential for application in mountain areas and impact studies. Examples are drawn from our investigations in the Swiss Alps and Peruvian Andes. Concerning NR we consider both methodologies that address the shortwave and longwave radiative fluxes individually, as well as the possibility to simply express NR as a linear function of global radiation. Several studies from the 1960s but also radiation data from various sources, including a 10-year field experiment conducted on the Swiss Plateau and the Alpine Surface Radiation Budget (ASRB) network, indicate that the latter approximation is quite robust and applicable in many circumstances. However, little has been done in the past to consider cloudless and cloudy conditions separately.

Regarding ET₀, we focus our attention on the Penman-Monteith equation and its adiabatic term, i.e. the contribution arising from the vapour pressure deficit (VPD) of the air. While the computation of the VPD from routine weather observations is unproblematic, the way in which the VPD could be affected by climate change is only rarely considered in impact studies, given that projections for either the changes in vapour pressure or relative humidity are normally overlooked. In this case, simplified expression essentially relying only on temperature can at least provide means for conducting sensitivity studies.

11.4

Dynamics of abrupt climatic change over the climate regions in Nigeria.

Ediang Okuku Archibong, Ediang Aniekan Archibong

Research Division, Nigeria Meteorological Agency, pmb 1215, Oshodi Lagos, Nigeria. (ediang2000@yahoo.com)

The paleoclimate record of past environmental change clearly shows that the instrumental record contains only a subset of possible climate system behavior. This is highlighted, for example, by paleoclimatic evidence that the climate system repeatedly switches, in a matter of years to decades especially between significantly different climatic modes.

Climate change is overviewed over the climate regions in Nigeria using a 48years (1961 – 2009) climatological data of air temperature (0600utc – 1400 utc) minimum and maximum temperature and relative humidity (0900utc) for forty five stations.

The climatic regions are sahel savannah, sudan savannah, Guinea savannah, tropical rainforest and mangrove swamp. The result generally showed increased in temperature over the decades and decrease in relative humidity.

In conclusion, although the significance of past abrupt climatic changes is heightened by the fact that they cannot be studied using instrumental data, and because their origins are poorly understood. Careful work is needed to map out the spatial – temporal patterns of change associated with past abrupt events that occur in the climatic regions in Nigeria, how to determine their causes, and also how to determine if they are predictable.

11.5

Schneefrühwarnungen in den Schweizer Alpen

Hächler P.

MeteoSchweiz, Kräbühlstr. 58, 8044 Zürich

Seit über 10 Jahren erlässt MeteoSchweiz, der nationale Wetterdienst, Warnungen vor Starkschneefällen. Sie dienen dazu, die Lawinensituation rechtzeitig einzuschätzen, insbesondere im Falle von Ereignissen, die auch Dörfer und Verbindungsrouten gefährden können. Das SLF, Fachleute für Verkehrswege sowie Krisenverantwortliche stützen ihre Entscheidungen darauf ab.

Prognosen von seltenen Ereignissen sind aber naturgemäss mit sehr vielen Schwierigkeiten beladen. Der Vortrag zeigt verschiedene Aspekte dazu auf: die Rolle spezieller Wetterlagen, klimatologische Überlegungen, Prognosemethoden und Erfolgszahlen.

11.6

Simulating the dispersion of the Eyjafjalla volcanic ash plume over Europe

Henne Stephan¹, Brunner Dominik¹

¹ Empa, , Swiss Federal Laboratories for Materials Science and Technology (stephan.henne@empa.ch)

Air traffic over Europe came to a stand still following the eruption of the Eyjafjalla volcano on Iceland. In this situation, aviation had to rely upon the model simulations and advice given by the Volcanic Ash Advisory Center responsible for the north Atlantic flight corridor that is hosted by the UK MetOffice in London (VAAC London). As an independent source of information Empa provided model forecasts of volcanic ash concentrations over Europe to the Swiss Federal Office of Civil Aviation using the Lagrangian Particle dispersion model FLEXPART (Stohl, et al., 2005) driven by NCEP/GFS forecasts. In this paper we analyze the challenges encountered when simulating the dispersion of a volcanic ash plume in the atmosphere. We compare the VAAC advisory charts with our model predictions and satellite products. Furthermore, results taken from an optimized simulation are shown that relies on information not available during the event (ECMWF analysis wind fields, quality controlled plume heights, and absolute ash mass emissions). This simulation is driven by volcanic

ash emissions as derived from observed initial plume heights and a one-dimensional volcanic plume model (Mastin, 2007). Results are quantitatively compared with in-situ observations of particle mass from the high-altitude observatories Jungfrauoch, Switzerland, and Zugspitze, Germany. In addition, the qualitative correspondence of our simulations with satellite data and ground-based in-situ measurements is demonstrated. Concluding remarks will draw attention to future developments in forecasting volcanic ash concentrations and in particular the need for more accurate and detailed information on the initial plume characteristics.

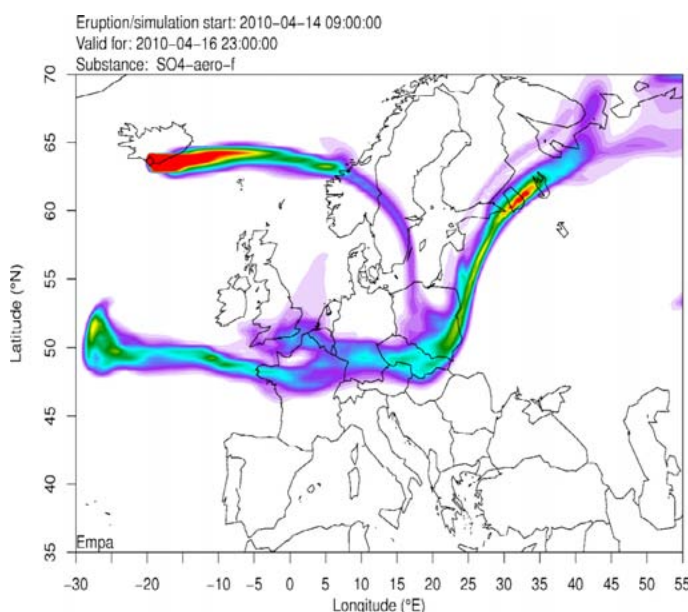


Figure 1. Total column of simulated volcanic ash aerosol at 2010-04-16 23:00.

REFERENCES

- Mastin, L. G., 2007. A user-friendly one-dimensional model for wet volcanic plumes, *Geochemistry Geophysics Geosystems* 8, Q03014, doi:10.1029/2006GC001455.
- Stohl, A., Forster, C., Frank, A., Seibert, P. and Wotawa, G., 2005. Technical note: The Lagrangian particle dispersion model FLEXPART version 6.2, *Atmospheric Chemistry and Physics* 5, 2461-2474.

11.7

Aircraft and ground based CH₄ measurement of a high moor in Switzerland

Rebecca V. Hiller¹, Jacqueline Stieger¹, Bruno Neininger², Nina Buchmann¹, Werner Eugster¹

¹Institute of Plant, Animal and Agroecosystem Sciences, ETH Zürich, Universitätsstrasse 2, CH-8092, Zürich (hillerr@ethz.ch)

²MetAir, AG, CH- 8915 Hausen am Albis

Wetlands are the largest natural methane source at the global scale, contributing 20-60% to the total CH₄ emissions (Zhuang and Reeburgh, 2008). Aircraft based measurements bare the advantage to observe a larger area than a single flux tower, allowing conclusions on a regional scale (Oechel et al. 1998). Thus, to assess the source strength of a typical mid latitude high moor, we conducted several flights over the high moor near Rothenthurm (SZ), covering flight levels of 50 m up to 400 m a.g.l. During the flights, we continuously measured the CH₄ concentration by a Fast Methane Analyzer (Los Gatos Research Inc, Mountain View (CA), USA) plus many other environmental variables, such as wind, temperature, humidity, CO₂. Complementary, ground based concentrations of CH₄, CO₂ and H₂O were measured by a Fast Greenhouse Gas Analyzer (Los Gatos Research Inc., Mountain View (CA), USA) at 1 Hz mounted on a bicycle trailer. The cycling route was recorded by a GPS unit. Additionally, we quantified the soil moisture at various locations. Ground based CH₄ measurements ranged between 1.75 and 9.46 ppm (q_{25} =1.82 ppm, q_{50} =1.85 ppm, q_{75} =1.87 ppm) where highest concentrations were observed next to a manure heap. On August 19th, the wind pattern was dominated by the local wind system and we observed a slight concentration gradient along the valley axis with increasing methane concentration the longer the air travelled over the moor. More preliminary results from the three flight days during the second part of August 2010 will be presented.

REFERENCES

- Zhuang, Q. & Reeburgh, W. S. 2008: Introduction to special section on Synthesis of Recent Terrestrial Methane Emission Studies, *J. Geophys. Res.*, doi: 10.1029/2008JG000749
- Oechel, W. C.; Vourlitis, G. L.; Brooks, S.; Crawford, T. L. & Dumas, E. 1998: Intercomparison among chamber, tower, and aircraft net CO₂ and energy fluxes measured during the Arc System Science Land-Atmosphere-Ice Interactions (ARCSSLAI) Flux Study, *J. Geophys. Res.*, doi: 10.1029/1998JD200015

11.8

Monitoring atmospheric water vapor in the Zermatt region with GNSS

Hurter Fabian¹, Perler Donat¹, Geiger Alain¹

¹Institut f. Geodäsie u. Photogrammetrie, Schafmattstr. 34, 8093 Zürich (fabian.hurter@geod.baug.ethz.ch)

To take appropriate short time measures to mitigate flood risks from mountain rivers, the location, time and intensity of extreme rain events must be known. One of the limiting factors for nowcasting such events with numerical weather prediction models are insufficient initial conditions with respect to water vapor distribution. A method that delivers information on the atmospheric water vapor makes use of GNSS and is a research focus at the Geodesy and Geodynamics Lab, ETH Zürich. A recently started project in this field will be presented in this talk.

Water vapor in the atmosphere causes path delays in measurements of GNSS receivers. Deploying a receiver network allows the 3D retrieval of the atmospheric water vapor from these path delays with a tomographic algorithm. The inversion problem of the water vapor tomography is mixed-determined and hence, needs to be constrained with additional information. In order to introduce as weak constraints as possible, a very dense network of GNSS receivers is required. Such a network has been set up in a field campaign in the Zermatt region from the 15th July to the 12th August, 2010 to investigate the atmosphere above Zermatt.

33 geodetic receivers were placed such as to optimize resolution of the water vapor field. Suitable station locations were selected on the basis of an a priori error analysis of the tomographic solution. For validation of the water vapor retrieval by GNSS, 25 radiosondes were launched. In collaboration with the hydrology group of Prof. Burlando we also have access

to rain gauge measurements along a terrestrial profile in the Zermatt region. The rain gauge measurements together with the water vapor determined from the GNSS receivers will serve as a basis to investigate the devolution of rain events in an alpine region and how to make better use of GNSS for nowcasting of extreme rain events.

The focus of this talk will be on the setup of the field campaign and how the station locations were selected. Advantages and drawbacks of the used algorithm will be discussed and the eventual setup evaluated.

11.9

Climate of the Little Ice Age: A Mediterranean-scale anomaly pattern with LGM similarities

Kuhlemann Joachim^{1,2}, Raible Christoph C.³, Luterbacher Jürg^{3,4}, Schuster Christina^{2,5}, Krumrei Ingrid², Reinecker John², Kubik Peter⁶, Westphal Hildegard⁷

¹ Eidgenössisches Nuklearsicherheitsinspektorat ENSI, Industriestrasse 19, CH-5200 Brugg, KUJ@ensi.ch

² Univ. Tübingen, Inst. für Geowissenschaften, Sigwartstr. 10, D-72076 Tübingen, vorname.name@uni.tuebingen.de

³ Univ. Bern, Climate and Environmental Physics & Oeschger Center for Climate Change Research, Sidlerstrasse 5 CH-3012 Bern, raible@climate.unibe.ch

⁴ Univ. Giessen, Inst. für Geographie, Senckenbergstrasse 1, D-35390 Giessen, Juerg.Luterbacher@geogr.uni-giessen.de

⁵ TU München, Fachgebiet für Ökoklimatologie, Hans-Carl-von-Carlowitz-Platz 2, D-85354 Freising-Weihenstephan, christina.schuster@wzw.tum.de

⁶ ETH Zurich, Institute of Particle Physics, HPK H30, CH-8093 Zurich, kubik@phys.ethz.ch

⁷ Univ. Bremen, MARUM, Leobener Straße, 28359 Bremen, hildegard.westphal@uni-bremen.de

Mediterranean paleoclimate reconstructions for the late Maunder Minimum (1675-1715), the most likely coldest period within the Little Ice Age (LIA), point to 0.5 to 1°C colder and slightly wetter conditions compared to today (Frank et al. 2010).

Here, we present evidence of a Mediterranean key region which experienced anomalously cold and wet conditions during the LIA and other cold spells of the Holocene. The results shed new light on atmospheric circulation during the LIA and expose some similarities with the preferential wintery meridional atmospheric circulation during cold spells, including the Last Glacial Maximum (LGM).

The special role of the Mediterranean climatic key region of Corsica and presumably the Gulfs for Genoa and Lion is evident from the enormous fluctuation of the climatic snowline, reconstructed from niche glacier advances and their equilibrium line altitude (ELA). During the coldest phase of the LIA, the ELA was situated as low as 2200 m a.s.l. in the center of the island Corsica. In comparison, the recent ELA (1961-1990) is situated at about 2800 m in the coldest and wettest spot of Corsica (Kuhlemann et al. 2008), which demonstrates ELA fluctuation in the range of 600 m. The regional ELA distribution pattern in Corsica at present and during several cold spells of the LIA are very similar.

At Mediterranean scale, the ELA depression in Corsica merges into a branch which extends across southern Italy towards Montenegro. We assume a more frequent generation of Genoa cyclones and probably also more frequent invasion of polar air in the mid troposphere (500 hPa level appr. 5500 m above sea level) to explain this ELA depression.

Global climate modelling (GCM) yields the highest late Holocene potential for glacier advances in the 17th century in the western Mediterranean. In the eastern and western parts of the Mediterranean, cold spells are partly out of phase, due to internal variability of the climate. An increase of cyclone activity during the Maunder Minimum is also found in climate model simulations.

In the western Mediterranean the difference between the 1000-hPa and 500-hPa geopotential height shows negative anomalies north of Spain in winter and Genoa in spring and positive anomalies over Iceland and the Caspian Sea. The jet stream (zonal wind in the 300 hPa level) is shifted southwards over the western Mediterranean, suggesting that it more frequently meandered to the south during periods favourable for glacier growth.

REFERENCES

- Frank, D.C., J. Esper, C.C. Raible, U. Buentgen, V. Trouet, B. Stocker nad, F. Joos 2010: Ensemble reconstruction constraints on the global carbon cycle sensitivity to climate, *Nature*, 463, 527-530.
- Kuhlemann, J., Krumrei, I., Rohling E., Kubik, P., Ivy-Ochs S., Kucera, M. 2008: Regional synthesis of Mediterranean atmospheric circulation during the Last Glacial Maximum. *Science* 321, 1338-1340.

11.10

Airborne observation of the Eyjafjallajökull volcanic ash plume over Switzerland

Bruno Neininger 1) 2) Boris Schneider 1) and David Oldani 1)

1) METAIR AG, Hausen am Albis

2) ZHAW – Zurich University of Applied Sciences

When it became clear on April 16 that the ash plume (actually over northern Europe) might reach Switzerland on an eastern trajectory (e.g. NOAA HYSPLIT), the staff of METAIR decided to try a measurement with the existing configuration of our small research aircraft (Neininger et al., 2004 and 2001), which included a MetOne optical particle counter for particles of the optical diameter >0.3 and >0.5 μm . These flights up to 6 km altitude allowed collecting the only in-situ data from the ash layer over the continent for the beginning of the episode in April. Surprisingly for us – the initial motivation was pure curiosity - the data was then also used for decision making, which expedited the opening of the Swiss air space on April 20, and prevented another closing on May 9. After the first phase in April, the data quality was improved for the second phase in co-operation with PSI (additional Grimm OPC with an optimised intake). Based on these additional flights, the data was also improved for the first phase, with an estimate on the mass concentration. Other parameters like CO , CO_2 , O_3 (and the sulphurous smell in the cloud on April 17) helped to characterise the plume.

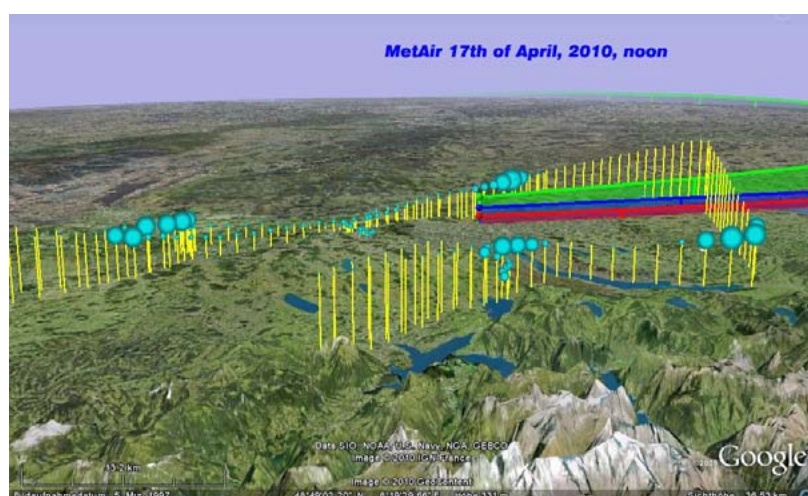


Figure 1. Flights from April-17, crossing the plume (blue balloons) when flying up and down over Eastern Switzerland (backward trajectories red/blue/green)

REFERENCES

- Neininger, B. (2004): AN UPDATE ON METAIR'S MULTI-PARAMETER RESEARCH AIRCRAFT EMS Annual Meeting Abstract EMS04A-00261, Vol. 1, 00261, 2004, European Meteorological Society.
- Neininger, B., W. Fuchs, M. Bäumle, A. Volz-Thomas, A.S.H. Prévôt, and J. Dommen (2001): A small aircraft for more than just ozone: MetAir's 'Dimona' after ten years of evolving development. Proceedings of the 11th Symposium on Meteorological Observations and Instrumentation. Albuquerque, NM, USA, 14-19 January 2001, pp 123-128.

11.11

Water vapor retrieval with parameterized GPS tomography: Longterm study in Switzerland

D. Perler, A. Geiger, M. Rothacher

Institute of Geodesy and Photogrammetry, ETH Zurich, Schafmattstrasse 34, HPV G56, 8093 Zürich

Can nonconstant parameterization of the grid voxels decrease systematic errors in tomographic reconstruction of the water vapor field in the troposphere? Investigations of different grid resolutions have show that best results are achieved with a vertically highly resolved grid (43 layers). A challange in working with such highly resolved grids is to cope with the increasing illposedness of the system. Usually the system is stabilized with pseudoobservations.

However increasing the grid resolution decreases the relative information content comming from actual observations. To

avoid this we use nonconstant parameterized voxels, which provides a smooth transition between voxels and achieves results with a similar quality as with constant parameterized voxels, but with a coarser resolved grid.

Investigations with 1 year of data have shown that the use of nonconstant parameterization can decrease the rms and the standard deviation by 13.5% and 17.8%, respectively. Improvements are especially observed at low altitudes (below 3000 m) where a decrease of the rms of 30% is observed. At altitudes above 3000 m, the constant parameterized method achieves slightly better results than the nonconstant parameterized ones.

11.12

Modelling global emissions of bacteria and fungal spores acting as ice nuclei

Sesartic Ana¹, Dallafior Tanja¹, Storelvmo Trude², Lohmann Ulrike¹

¹ Institute for Atmospheric and Climate Science, ETH Zurich, Universitätstrasse 16, CH-8092 Zurich (ana.sesartic@env.ethz.ch)

² Department of Geology and Geophysics, Yale University, 210 Whitney Ave., USA-06520-8109 New Haven (CT)

Primary biological aerosols, like bacteria and fungal spores, have been shown in laboratory studies to be efficient ice nuclei (IN) and an important component of the biological aerosol population in the atmosphere (Diehl et al., 2006; Kieft, 1988; Jaenicke et al., 2007). It is necessary to know their global emissions in order to investigate their potential impact on clouds and precipitation.

Bacteria in general and those with ice nucleating abilities in particular are commonly found on plant leaves (Lindemann et al., 1982), which aids in determining global bacteria concentrations depending on different plant functional types. Plant functional types and their seasonally changing leaf area index from the JSBACH dynamic vegetation model (Raddatz et al., 2007) were combined with observed near surface bacteria concentrations (Burrows et al., 2009a), which served as an input for ECHAM5-HAM general circulation model (GCM) (Lohmann et al., 2007) for an online calculation of bacteria emissions. A fraction of the bacteria (10%) is considered to initiate ice formation by serving as ice nuclei.

A review of available fungal spore concentration data has been undertaken by Dallafior (2010). Those data from literature have been assigned to an ecosystem and converted to surface fluxes. The fluxes have been calculated offline based on ecosystem areas from JSBACH and fungal spore properties (e.g. mass, density).

The average global fungal spore number concentrations were found to be two orders of magnitudes lower than the modelled average number concentrations of bacteria (10^6 m^{-3}) and mineral dust (10^8 m^{-3}).

Results from the ECHAM5-HAM with bacteria serving as IN will be shown in this talk. Here the influence of bacteria on mixed-phase clouds will be highlighted. Also the fungal spore emissions will be compared with emissions from bacteria and mineral dust.

REFERENCES

- Burrows, S. M. et al. 2009a: Bacteria in the global atmosphere – Part 1: Review and synthesis of literature data for different ecosystems, *Atmos. Chem. Phys.*, 9, 9263–9280.
- Dallafior, T. 2010: Global Fungal Spore Emissions. Review and Synthesis of Literature Data. Bachelor Thesis at IAC ETH Zürich.
- Diehl, K. et al. 2006: Numerical sensitivity studies on the impact of aerosol properties and drop freezing modes on the glaciation, microphysics, and dynamics of clouds, *J. Geophys. Res.*, 111, D07202.
- Kieft, T. L. 1988: Ice nucleation activity in lichens, *Applied & Env. Microbiol.*, 54, (7), 1678–1681.
- Jaenicke, R. et al. 2007: Omnipresence of biological material in the atmosphere, *Environ. Chem.*, 4, 217–220.
- Jacobson, M. Z. & Streets, D. G. 2009: Influence of future anthropogenic emissions on climate, natural emissions and air quality, *J. Geophys. Res.*, 114, D08118.
- Lindemann, J. et al. 1982: Plants as sources of airborne bacteria, including ice nucleation-active bacteria, *Applied & Env. Microbiol.*, 44, (5), 1059–1063.
- Lohmann, U. et al. 2007: Cloud microphysics and aerosol indirect effects in the global climate model ECHAM5-HAM, *Atmos. Chem. Phys.*, 7, 3425–3446.
- Raddatz, T. J. et al. 2007: Will the tropical land biosphere dominate the climate-carbon cycle feedback during the twenty-first century?, *Clim. Dyn.*, 29 (6), 565–574.

11.13

High resolution climate change data for Austria until 2040

Strauss Franziska¹, Formayer Herbert², Asamer Veronika¹ & Schmid Erwin¹

¹Institut für Nachhaltige Wirtschaftsentwicklung, Universität für Bodenkultur Wien, Feistmantelstraße 4, A-1180 Wien
(franziska.strauss@boku.ac.at)

²Institut für Meteorologie, Universität für Bodenkultur Wien, Peter-Jordan-Straße 82, A-1190 Wien

The relatively poor spatial resolution of General Circulation Models (GCMs) restricts the usefulness of results to global and continental scales. To model weather developments on regional scales, various methods have been developed which are commonly dubbed as “Downscaling-Methods”. In this case, downscaling means to transfer the information of the GCM to finer spatial and temporal scales. Scenarios of GCMs as well as of Regional Climate Models (RCMs) imply many uncertainties arising from:

- I) different initializations and parameterizations (many climate components or interactions in the atmosphere can only be assessed by simplified calculations)
- II) assumptions on economic and population growths as well as on possible impacts of new technologies, and
- III) greenhouse gas emissions resulting from assumptions made in ii).

As an alternative to RCMs, we have developed a daily climate change dataset for Austria and the period from 2008 to 2040 with temporal and spatial resolution of one day and one km² using linear regression and bootstrapping methods. The representation of spatial frames and temporal variations are important in climate modeling, because regions often show a wide range of different climate patterns (Böhm, 2006). We think that local variations and the development of regional climates in the next three decades can be better captured in statistical climate change models using historical meteorological data than by downscaling.

The aim of this article is to present a statistical climate change model to develop a spectrum of high resolution climate change data for Austria until 2040. Hence, daily meteorological data from 34 weather stations and the period 1975-2007 have been used to construct 60 spatial climate clusters with homogeneous climates with respect to mean annual precipitation sums and temperatures in the period 1961-1990 (Auer et al. 2000). We have performed regression model analyses to compute a set of daily climate change data for each climate cluster (Figure 1). The integral parts of our regression model are i) the extrapolation of the observed linear temperature trend from 1975 to 2007 using an average national trend of ~0.05 °C per year, derived from a homogenized dataset (Auer et al. 2007), and ii) the repeated bootstrapping of temperature residuals and of observations for solar radiation, precipitation, relative humidity, and wind speed to ensure consistent spatial and temporal correlations (Strauss et al. 2010). This bootstrapping procedure has been performed for all weather parameters based on the observed climate variations in the period 1975-2007. To account for a wider range of precipitation patterns, we have also developed precipitation scenarios including higher or lower annual precipitation sums, as well as unchanged annual precipitation sums with seasonal redistribution. These precipitation scenarios, together with the bootstrapped scenarios of temperature, solar radiation, relative humidity and wind speed constitute our climate change spectrum for Austria until the year 2040.

REFERENCES

- Auer, I., Böhm, R., Mohnl, H., Potzmann, R. & Schöner, W. 2000: ÖKLIM: A digital Climatology of Austria 1961-1990. Proceedings of the 3rd European Conference on Applied Climatology, 16 to 20 October 2000, Pisa. CD Rom, Institute of Agrometeorology and Environmental Analysis, Florence.
- Auer, I., Böhm, R., Jurkovic, A., Lipa, W., Orlik, A., Potzmann, R., Schöner, W., Ungersböck, M., Matulla, C., Briffa, K., Jones, P.D., Efthymiadis, D., Brunetti, M., Nanni, T., Maugeri, M., Mercalli, L., Mestre, O., Moisselin, J.-M., Begert, M., Müller-Westermeier, G., Kveton, V., Bochnicek, O., Stastny, P., Lapin, M., Szalai, S., Szentimrey, T., Cegnar, T., Dolinar, M., Gajic-Capka, M., Zaninovic, K., Majstorovic, Z. & Nieplova, E. 2007: HISTALP – Historical instrumental climatological surface time series of the greater Alpine region 1760-2003. *International Journal of Climatology* 27, 17-46.
- Böhm, R. 2006: ALP-IMP. Multi-centennial climate variability in the Alps based on Instrumental data, Model simulations and Proxy data. Final report for RTD Projekt, Wien.
- Strauss, F., Formayer, H., Asamer, V. & Schmid, E. 2010: Climate change data for Austria and the period 2008-2040 with one day and km² resolution. Diskussionspapier DP-48-2010, Institut für nachhaltige Wirtschaftsentwicklung, Universität für Bodenkultur Wien.

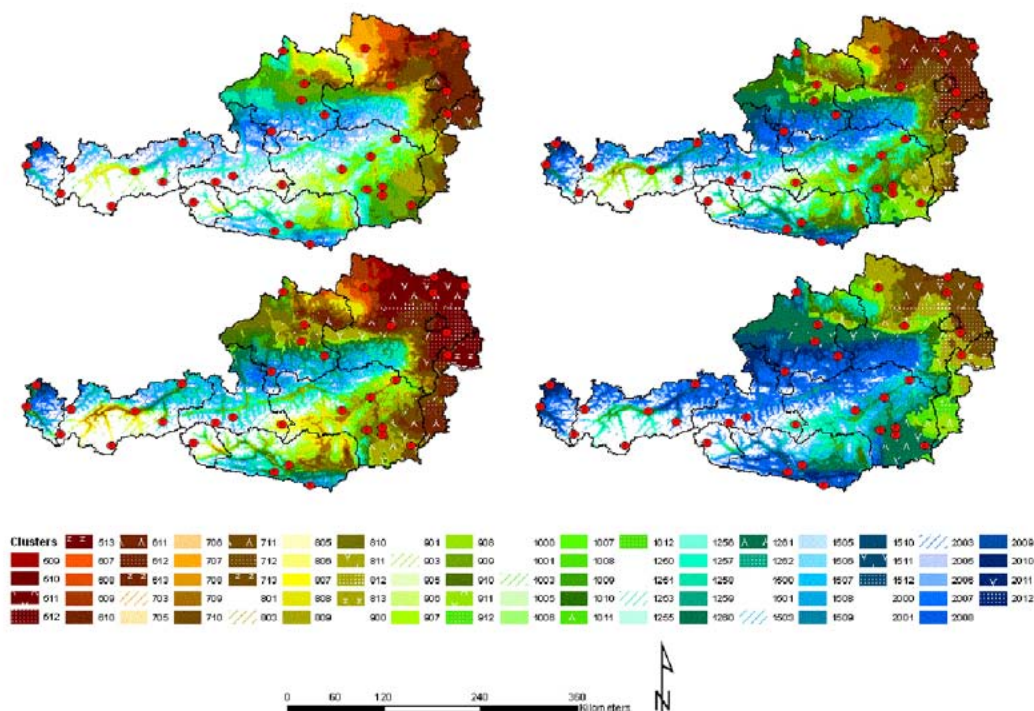


Figure 1. Climate clusters in Austria between 1975 and 2007 (upper left), and between 2008 and 2040 (upper right), as well as with 20% lower annual precipitation sums (lower left), and with 20% higher annual precipitation sums (lower right). For example, the climate cluster 509 (500+9) represents annual precipitation sums between 400 mm and 500 mm and mean annual temperatures between 8.5 °C and 9.5 °C. Red dots indicate the locations of the respective weather stations.

10.14

NCCR Climate related research at MeteoSwiss - The Swiss climate of today and tomorrow

Weibel Bettina, Röser Ines, Liniger Mark, Appenzeller Christof

Federal Office of Meteorology and Climatology MeteoSwiss, Krähbühlstrasse 58, CH-8044 Zurich, Switzerland (bettina.weibel@meteoswiss.ch)

Climate change affects Europe and Switzerland in particular. There is a demand and a social responsibility to present information about specific changes and possible adaptations. As a governmental office one of our roles is to provide high quality climate information on the past, current and future conditions to the public, research and decision makers in federal offices, policy and private sector. MeteoSwiss is developing the scientific basis to create such an information framework bundling resources from different external fundings and a substantial internal contribution. MeteoSwiss is an active member of the C2SM (Center for Climate Systems Modeling) and participant of various research projects, in particular of the SNF NCCR Climate (Swiss National Center of Competence In Research – Climate), COST-Actions and projects funded by the European Union.

The project will provide climate background information to answer questions about the effect of climate change in Switzerland in the future: Will there be palm trees in Lucerne in 30 years? Will there be more floods causing damages? Will agriculture profit from the new conditions? And what about today's climate: What precipitation field could cause a major flood event? Is a Swiss harvest at danger in the upcoming weeks?

The research project at MeteoSwiss runs from 2009 until 2012 and is divided into four subprojects: Preclim, BiotoP, CombiPrecip and Euro4M. Preclim will provide climate scenarios for Switzerland for the current century based on regional climate models. BiotoP will link climate change scenario data to the pest models, in order to investigate the potential threat of plant diseases under conditions of a changing climate. The idea behind CombiPrecip is to combine information

from the two classical rainfall measurements – radar and rain gauges – with statistical methods for climatological and near-real time applications such as hydrology. EURO4M will provide a new high-resolution daily gridded Alpine wide precipitation data set over the last 40 years based on rain gauge observations.

According to the key areas defined by the Stern Review (Stern et al., 2006), it is our goal to provide high resolution climate data (Euro4M, CombiPrecip) and to refine climate scenarios for user needs (Biotop, PreClim) in order to link the scientific community with real world applications.

REFERENCES

Stern, N., Peters, S., Bakhshi, V., Bowen, A., Cameron, C., Catovsky, S., Crane, D., Cruickshank, S., Dietz, S., Edmonson, N., Garbett, S.-L., Hamid, L., Hoffman, G., Ingram, D., Jones, B., Patmore, N., Radcliffe, H., Sathiyarajah, R., Stock, M., Taylor, C., Vernon, T., Wanjie, H., and Zenghelis, D. 2006: Stern Review - The Economics of Climate Change, HM Treasury, London.

10.15

Gridding of daily sunshine duration by combination of station and satellite data

Willi Marco¹, Frei Christoph¹

¹ Swiss Federal Office of Meteorology and Climatology, Kräbühlstrasse 58, CH-8044 Zürich

Parameters of solar irradiance are of great importance in many fields of application which demand data of high temporal and spatial resolution. For example, such data are required in agricultural- and hydrological models to calculate the daily available solar energy and its variability, and to assess trends in climatic conditions.

The distribution of sunshine duration in Switzerland is spatially highly structured and markedly influenced by weather phenomena related to the topography (e.g. low-level stratus in winter, topographically triggered clouds in summer). Operational surface station networks are hardly able to resolve the fine-scale patterns associated with such phenomena.

The aim of the present study is to develop and test a new method for the spatial analysis (gridding) of daily relative sunshine duration, which combines surface station measurements with satellite data. Input for the method are in-situ measurements from 77 SwissMetNet stations and a 5-year data set of a Heliosat Clear-Sky Index (CSI, resolution 2 km) derived from Meteosat Second Generation albedo measurements.

The combination of measurements from the two observation platforms is accomplished by extracting dominant patterns of sunshine variability via Principal Component Analysis (PCA) of suitably transformed CSI satellite data. These patterns are determined individually for each season and reveal physically plausible sunshine patterns associated with recurring weather situations in Switzerland including their pertinent km-scale structures. Subsequently, the PCA patterns are used as explanatory variables in a kriging model with external drift (KED). The spatial covariance structure of KED was modeled by climatological variograms for each calendar month. The design of the method is such that satellite information enters in a statistical sense only and hence the method can be applied for pre-satellite periods without restriction. The final settings of the method were carefully chosen from detailed considerations of test cases, and systematic evaluations.

Specific and systematic evaluation showed the method's ability to interpolate station measurements for days with various cloudiness distributions reasonably. Leave-one-out cross-validation yields a median mean absolute error of about 10 % relative sunshine duration during winter and about 7.5 % during summer. Explained spatial variance varies considerably from day to day, typically between 50-80 % in winter and between 40-70 % in summer. Comparisons with a reference kriging setup, which uses no satellite data, highlight the added value of the combination. While the average skill differs only slightly, the combination is especially more skillful than the reference on days when the reference method has a poor skill. The benefit from satellite information is particularly evident in cases when the relative sunshine distribution is influenced by small-scale topographic features, not resolved by the station network, such as situations with low-level stratus.

The analysis method is applied to conduct experiments with different station networks. Results suggest that network size and configuration (location of stations) play a crucial role for the quality of the daily spatial analysis. Interpolation quality improves with increasing station density. Moreover, a scheme is proposed to find “optimal” network configurations from the satellite data (via rotation of principal components), which would yield more accurate spatial analyses compared to the actual station network for this specific parameter and temporal resolution.

The new analysis method will become part of the operational gridding suite at MeteoSwiss.

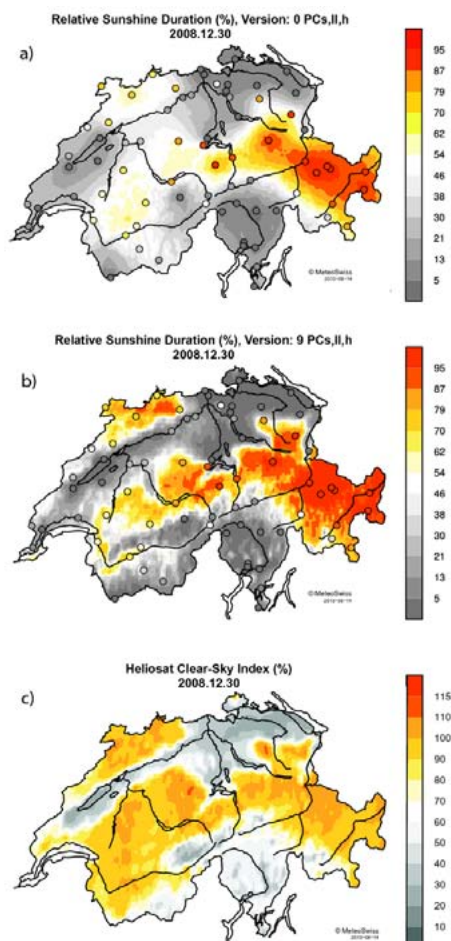


Figure 1: Sample day (30 December 2008), when a low-level stratus was extending over the Swiss Plateau. Comparisons between gridded fields from a reference method (a), the newly derived combination method (b) and the satellite CSI field (c). Circles denote stations used for the interpolation, colors indicate measured/estimated relative sunshine duration (%) for panels a and b.

12. Phenology and Seasonality

This Rutishauser, Martine Rebetez, Thomas Herren

MeteoSwiss, University of Bern, Oeschger Centre for Climate Change Research

- 12.1 Basler D. and Körner Ch.: Spring flush of native forest trees at rising spring temperatures is controlled by photoperiodism and temperature
- 12.2 Bloesch B., Spring J.-L., Viret O., Dubuis P.-H.: Climate change and grapevine's vegetative growth development in Western Switzerland
- 12.3 Clot B., Gehrig R.: Airborne pollen: phenological aspects and observed trends
- 12.4 Dobbertin M.: Forest phenology and extreme climatic events
- 12.5 Dobbertin M., Baltensweiler W., Giuggiola A., Li M.-H., Cherubini P.: 50 years of needle length measurements on Larch in the Engadin Valley closely reflect spring temperature changes
- 12.6 Egli S., Ayer F., Franc A.: Trends in fruiting phenology of wild forest mushrooms from 1975-2006 in the fungus reserve La Chanéaz (FR)
- 12.7 Eugster M.: Phenological and seasonal observations in Swiss schools
- 12.8 Hansmann J., Loew S., Evans K.F.: REROD – A mathematical model for reversible rockslope deformations, caused by seasonal variations in the groundwater table, observed in the central Swiss Alps
- 12.9 Herren T., Meier N., Rotach M.W., Liniger M.A., Appenzeller C.: The Swiss Spring Index as a novel integral metric for spring phenology
- 12.10 Kottmann D.: A comparison of ground-based phenological observations and NOAA AVHRR NDVI data
- 12.11 Morin X., Chuine I., Bugmann H.: Predicting the impact of warming on tree phenology: experimental and modelling results
- 12.12 Rixen C.: Changes in alpine plant phenology under future climate conditions
- 12.13 Rutishauser T., Brügger R., Jeanneret F.: Altitude, slope and aspect: Are there local-scale effects in temporal trends in a spatially high-resolved plant phenological network in the Swiss Alps 1971–2000?
- 12.14 Rutishauser T., Mitinitiantinnen und -initianten: KPS – eine Kommission für Phänologie und Saisonalität bei der «Plattform Geosciences»
- 12.15 Vitasse Y., François C., Delpierre N., Dufrêne E., Kremer A., Chuine I., Delzon S.: Assessing the effects of climate change on the phenology of European temperate trees
- 12.16 Wolf S., Eugster W., Buchmann N.: Ecosystem carbon budgets of tropical pasture versus afforestation

12.1

Spring flush of native forest trees at rising spring temperatures is controlled by photoperiodism and temperature

David Basler and Christian Körner

Botanisches Institut, Schönbeinstr. 6, 4056 Basel (david.basler@unibas.ch)

Warmer spring temperatures, as caused by climate warming, led to an earlier spring bud burst and an extended growing season in many temperate and boreal species. To which extent will the phenology of these species keep tracking rising temperatures in future? Phenology is controlled by three important factors: the degree of winter chilling, photoperiod and temperature. Contrary to the high inter-annual variation of spring temperatures, the length of photoperiod is an astronomical and thus weather independent signal for the progression of the season. Photoperiodic control of spring development protects trees from flushing too early under mild winter and early spring temperatures, before the period of potentially fatal freezing damage is over. Photoperiod sensitive species may therefore stop tracking climate the closer temperature modulated bud break is shifted toward the genetically fixed photoperiod threshold. We assessed the photoperiod sensitivity of spring bud break in several common temperate tree species using phytotron experiments with variable photoperiod x temperature interaction. While early successional species showed photoperiod-insensitive and thus mostly temperature controlled bud break, the timing of bud break in late successional species was strongly photoperiodic. Climate warming will thus not lead to much longer growing seasons in such species, as is often assumed.

12.2

Climate change and grapevine's vegetative growth development in Western Switzerland

Bloesch Bernard, Spring Jean-Laurent, Viret Olivier and Dubuis Pierre-Henri.

Agroscope Changins-Wädenswil, Rte de Duillier, 1260 Nyon, contact: pierre-henri.dubuis@acw.admin.ch

The main development stages of grapevine have been recorded for the cultivar Chasselas since 1925 in Pully (VD) and 1958 in Changins (VD). The increasing temperatures observed during the last two decades did influence the development of grapevine. The early stages, from bud break (BBCH 09) to initiation of flowering (BBCH 51) do not show any tendency to precocity related to temperature increase, while flowering (BBCH 65), fruit maturation and grape harvest (BBCH 89), were in average ten days earlier during the last years, reducing thus considerably the vegetation period. When considering a longer period of time as in the observation made in Pully, such conditions have already been observed during the decade 1940 – 1950. Before the forties and after the fifties, slower development periods have been registered. The earliness of the last two decades, marked by significant warming especially during the summer months, must be put into perspective by the climate variability of our regions and the cyclic character of warmer or cooler episodes succession overlapping the global trend of climate evolution.

REFERENCES

- Bloesch, B., Viret, O., Fabre, A.-L. & Spring J.-L. 2009: Evolution climatique et phénologie de la vigne de 1958 à nos jours. *Revue Suisse Vitic. Arboric. Hortic.* 41(3), 146-149
- Spring, J.-L., Viret, O. & Bloesch, B. 2009 : Phénologie de la vigne : 84 ans d'observation du Chasselas dans le bassin lémanique. *Revue Suisse Vitic. Arboric. Hortic.* 41(3), 151-155

12.3

Airborne pollen: phenological aspects and observed trends.

Clot Bernard & Gehrig Regula

Federal Office of Meteorology and Climatology MeteoSwiss, Station aérologique, CH - 1530 Payerne (bernard.clot@meteoswiss.ch)

In Switzerland, airborne pollen monitoring with volumetric method started in Basel in 1969, in Neuchâtel in 1979 and in Zürich in 1981. Since 1993, MeteoSwiss is responsible for the National pollen network, comprising 14 stations. The main goal of this service is to deliver information and forecasts for prevention and treatment of allergic diseases. As airborne pollen reflects in large part the flowering of local anemophilous plants, it also represents an interesting source of phenological data.

In spring and early summer, the pollen season has shifted remarkably towards earlier occurrence dates, as it has also been observed in many European countries. The pattern of trend is not linear, but a shift towards earlier dates seems to have occurred in the late Eighties. Trends in the abundance of pollen are not uniform: some taxa show a positive trend in SPI (seasonal pollen index), other a negative trend; both increases and decreases can occur for the same species in different regions. The local vegetation and land use management have probably had up to now a stronger influence on pollen abundance than the effect of climate change.

12.4

Forest phenology and extreme climatic events

Dobbertin, M.¹

¹WSL Swiss Federal Research Institute for Forest, Snow and Landscape Research (matthias.dobbertin@wsl.ch)

Phenological observations on trees in forests have been made at various stations in Switzerland and on different forest tree species since 2000. In contrast to the classical phenological observations on selected shrubs and tree species in open-grown conditions in the tree phenological network several trees in forest stands are assessed. For the study of climate and climate change effects on forest growth and condition, the actual assessment of forest tree phenology is important. Extreme climatic events that may become visible in forest phenology includes late frost, warm spring months and drought.

In this preliminary evaluation the first 8 – 9 years of available data were used to study the phenological phases of leaf unfolding, flowering, leaf discoloration and leaf fall for common beech (*Fagus sylvatica*), oaks (*Quercus petraea* and *Qu. robur*), common ash (*Fraxinus excelsor*), European larch (*Larix decidua*) and Norway spruce (*Picea abies*).

First, differences between species, social crown position, and locations were compared. Second, the two extreme warm years 2003 and 2007 were compared against the other years. Although within site and species variation can be high, differences between species could be detected as was expected. These differences varied between years showing different reactions of species to warming versus radiation. The years 2003 for spring and summer pheno phases and in particular 2007 for spring pheno phases were significant. Possible differences in assessment were also discussed.

Long-term time series of phenological observations of forest trees species growing in forests give additional information to the existing network of phenological observation sites. Thus a continuation of these sites is highly recommended.

REFERENCES

- Brügger, R. & Vasella, A., 2003: Pflanzen im Wandel der Jahreszeiten – Anleitung für phänologische Beobachtungen. Geographica Bernensia. p.19, 23, 50-53, 116-121.
- Jolly, W.M., Dobbertin, M., Zimmermann, N.E. & Reichstein, M. 2005: Divergent growth responses of Alpine forests to 2003 heat wave. Geophys. Res. Lett. 32 (18): Art. No. L18409, DOI:10.1029/2005GL023252.
- Menzel A. & Fabian, P. 1999: Growing season extended in Europe. Nature 397: 659.
- Reist, M. 2006: Auswirkungen von Frühling und Sommer 2003 auf die Phänologie der Buche und Esche. Wintersemesterarbeit 2006. Universität Bern, 36 p.
- Rutishauser, T., Luterbacher, J., Defila, C., Frank, D. & Wanner, H. 2008: Swiss spring plant phenology 2007: Extremes, a multi-century perspective, and changes in temperature sensitivity. Geophys. Res. Lett. 35: L05703.

12.5

50 years of needle length measurements on Larch in the Engadin Valley closely reflect spring temperature changes

Dobbertin, M.¹, Baltensweiler, W.³, Giuggiola A.², Li M.-H.², Cherubini, P.²

¹WSL Swiss Federal Research Institute for Forest, Snow and Landscape Research (matthias.dobbertin@wsl.ch)

²WSL Swiss Federal Research Institute for Forest, Snow and Landscape Research

³ passed away 2008.

Phenological observations have been used to determine and to quantify the effect of warming on vegetation development. While long-term observations of plant phenological phases are numerous, almost no studies exist that have actually measured the seasonal growth of foliage. Here, we present results from almost 50 years of needle length measurements of deciduous European larch (*Larix deciduas* Mill.) at two high altitude sites (1630 m a.s.l. and 1830 m a.s.l.) in the Engadine valley and relate it to spring temperature and outbreaks of the larch bud moth (*Zeiraphera diniana* Gn). Measurements had been initiated to monitor the interaction between defoliation by the larch bud moth and needle growth.

Needles of larch are formed annual in clusters on short shoots or in spirals on long shoots. Needles on short shoots grow simultaneously allowing periodic measurements of its mean needle length. Needle length was measured on 3 short shoots proximal and 3 distal to the base of the 2-year old shoots of branches of the same trees. Needle elongation in early June in percent of the final needle length was computed for each tree and site and correlated with mean April and May temperature obtained from the adjacent MeteoSwiss climate station. Measurements at the site Sils started in 1963 and at the site Brail in 1965. Before 1971 the individual tree and short shoot measurements have been lost, but mean plot-wise means for each observation dates are available.

Data were grouped into five decades (i.e. 1963-1970, 1971-1980, ..., 2001-2010) and into the period until 1987 and following 1987 when a strong temperature increase was observed in spring. Symmetric sigmoidal logistic growth curves were separately fit for the needle length in mm and for the relative needle length in percent of the final length against the day of year. The day of year when 50% of the final needle length is reached was determined as the parameter estimate of the function. For each year the percentage of final needle length reached by the end of May were also determined and compared. Larch bud moth outbreaks have been determined from larvae counts and visual needle discolorations.

Larch bud moth outbreaks, that occurred every 7 to 10 years and usually last 2 years, reduced needle length in the year following an outbreak, but had no influence on phenology. Needle length increased during the observation period for both sites. However, this was mainly due to the lack of severe larch bud moth outbreaks in recent decades. 50% needle length at the lower site was on average reached 8-10 days before the high altitude site. The relative needle length to final needle length at the beginning of June correlated highly with April-May temperatures. Needle elongation during 1988-2006 occurred 8 to 11 days earlier than during 1972-1987. Needle growth at the higher site is identical or earlier than growth at the lower site before 1987 suggesting a more than 200 m shift in altitude. This is in agreement with the observed warming of 1.6 °C in April and May. In 2007, with the warmest April ever recorded in Switzerland, needle development was even 15 days earlier than during the period up to 1987 and 23 days earlier than during the period since 1987. The presented results stress the importance of long-term ecological observations to assess the impacts of environmental change.

REFERENCES

- Baltensweiler, W., Weber, U.M. & Cherubini, P. 2008: Tracing the influence of larch-bud-moth insect outbreaks and weather conditions on larch tree-ring growth in Engadine (Switzerland). *Oikos* 117: 161-172.
- Baltensweiler, W. 1993: Why the larch bud-moth cycle collapsed in the subalpine larch-cembra pine forests in the year 1990 for the first time since 1850. *Oecologia* 94: 62-66.
- Bjornstad, O.N., Peltonen, M., Liebhold, A.M. & Baltensweiler, W. 2002: Waves of larch budmoth outbreaks in the European Alps. *Science* 298: 1020-1023

12.6

Trends in fruiting phenology of wild forest mushrooms from 1975-2006 in the fungus reserve La Chanéaz (FR)

Egli Simon¹, Ayer François², Franc Alain³

¹Eidg. Forschungsanstalt für Wald, Schnee und Landschaft WSL, Zürcherstrasse 111, CH-8903 Birmensdorf (simon.egli@wsl.ch)

²Routes des roches 8, CH-1553 Châtonnaye

³UMR Biodiversité Gènes et Communautés INRA, 69 route d'Arcachon, F-33612 Cestas Cedex

Increasing spring temperature and delayed arrival of biological winter have lengthened the green-cover season and influenced phenological events in many plants and animals (Penuelas et al., 2009; Root et al., 2003; Menzel et al. 2006).

The study of temporal trends in the fruiting phenology of mushrooms by Kauserud et al. (2008) showed that the mean time of fruiting of 83 examined fungal species has changed considerably over the period 1940-2006 in Norway. Across the whole period there has been a delay of 13.3 day in mean time of fruiting. These findings do not exactly correspond to those of Gange et al. (2007). They noticed an expansion of the mushroom fruiting season in both directions in the United Kingdom.

The studies of Gange et al. (2007) and Kauserud et al. (2008) are based on herbarium collections, which may contain biases in the data (e.g. possible temporal shifts in the collecting effort).

Our study was carried out in the fungus reserve "La Chanéaz" established in 1975 in Southwestern Switzerland, located in a representative forest type of the Swiss Central Plateau at 575 m a.s.l., a mixed old-growth forest with deciduous and coniferous tree species of different age beech (*Fagus sylvatica* L.), oak (*Quercus robur* L.), spruce (*Picea abies* (L.) Karst.), fir (*Abies alba* Mill.), pine (*Pinus sylvestris* L.), and larch (*Larix decidua* Mill.). Fruit bodies of the epigeous mycorrhizal and saprotrophic macromycetes were identified and counted at weekly intervals from May to December (weeks 21-52). When first recorded, the fruit bodies were marked with methylene blue on the cap to avoid double counting in the subsequent week. The survey was started in 1975 and continued until 2006.

A general trend for later starting and later ending of the mushroom season can be detected. However, the changes differ strongly between species and groups of species. Total duration of mushroom season was more or less stable.

In the weighted time of fruiting a clear shift can be observed, with an average delay of about 2 weeks since 1975 (Fig. 1), for the mycorrhizal as well as for the saprobic species.

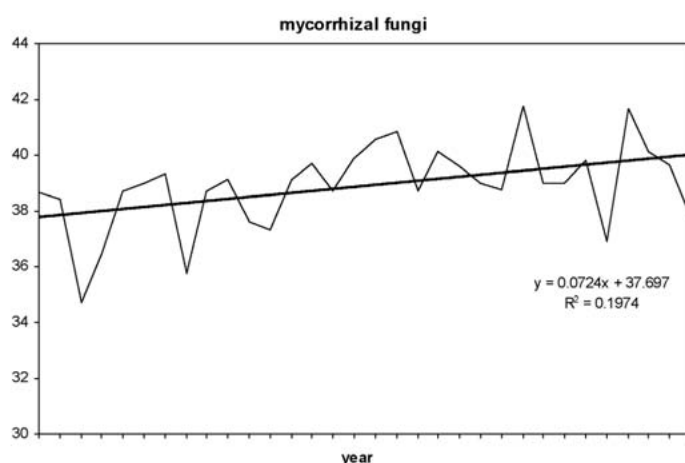


Figure 1. Weighted fruit body appearance (week number) of all 275 mycorrhizal species in the fungus reserve La Chanéaz 1975-2006.

REFERENCES

- Gange, A.C., Gange, E.G., Sparks, T.H., Boddy, L. (2007). Rapid and recent changes in fungal fruiting patterns. *Science* 316: 71.
- Kauserud, H., Stige, L.C., Vik, J.O., Okland, R.H., Hoiland, K., Stenseth, N.C. (2008). Mushroom fruiting and climate change. *PNAS* 105/10: 3811-3814.
- Menzel, A., Sparks, T., Estrella, N., Koch, E., Aasa, A. et al. (2006) European phenological response to climate change matches the warming pattern. *Global Change Biology* 12: 1969-1976.
- Penuelas, J., Rutishauser, T., Foliella, I. (2009). Phenology feedbacks on climate change. *Science* 324: 887-888.
- Root, T.L., Price, J.T., Hall, K.R., Schneider, S.H., Rosenzweig, C., Pounds, A. (2003). Fingerprints of global warming on wild animals and plants. *Nature* 421: 57-60.

12.7

Phenological and seasonal observations in Swiss schools

Eugster Markus

Sekundarschule, Schöntalstrasse 2, 9244 Niederuzwil

Introduction:

I will show you how I integrated phenological and seasonal observations into our curriculum. Students observe plants in their region and around the school, enter data in a database and compare it with meteorological data and observations of other schools. They take pictures to document seasonal changes.

GLOBE

Switzerland is a member (<http://www.globe-swiss.ch/de/>) of GLOBE (= Global Learning and Observations to Benefit the Environment; <http://globe.gov>), and our school joined GLOBE in 2003.

Seasons and biomes

GLOBE started several Earth System Science Projects (ESSP) in 2007, among them “Seasons and Biomes”. The Seasons and Biomes project is an inquiry- and project-based initiative that monitors seasons, specifically their interannual variability in order to increase students’ understanding of the Earth system. This project connects GLOBE students, teachers, and communities with educators and scientists. By monitoring the seasons in their biome, students will learn how interactions within the Earth system affect their local environment and how it in turn affects regional and global environments.

Spaceship Earth

In collaboration with Nicolas Gessner, the director of 52 short films about our planet, I designed 52 worksheets to help my students understand the outside influences that determine the Earth’s systems and with that the conditions for life on Earth and the forming of different biomes.

Phenological calendar

During the growing season we discuss the development of the vegetation and fill in an adapted protocol referring to the official list for the phenological observations of Meteo Schweiz.

Budburst and green-up

In spring my students determine the date of budburst for several trees and shrubs around our school. Henceforth they measure the length of the leaves that came out of the observed buds until they are fully grown in summer.

Green-down

In autumn the students protocol the color of tagged leaves until the leaves fall. Together with the green-up observations we define the length of the growing season.

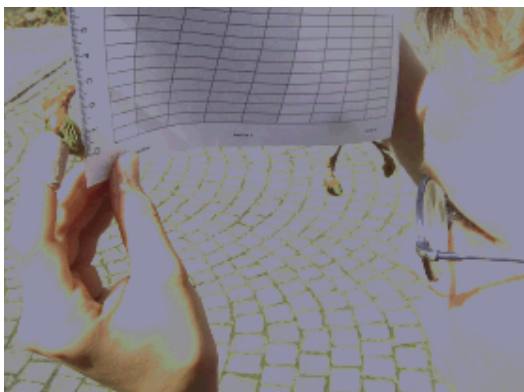


Figure 1: Green-up: Length of leaf



Figure 2: Green-down: Color table

GLOBE Phenological Garden (GPG)

According to the GLOBE instructions we made a phenological garden. The plants are the same in every GPG (clones). The students observe different phenological stages, fill in protocols and submit data to the international data base.

Data handling

I will explain how we collect and enter data and how it can be used by other people.

Student Research Campaign

GLOBE schools are organized by biomes into Global Learning Communities and students monitor their seasons through local research campaigns. Students interact with other students in schools from the Taiga, Tundra, Deciduous Forest, Desert, Grassland and other biomes in Global Learning Communities.

Seasons in my biome (SIMB) <http://www.seasonsandbiomes.net>

I started this project in 2009: Students, teachers and other persons choose a typical biome in their region and take a picture every month (exactly the same view). We document the seasonal changes and by comparing pictures get a new understanding of the diversity of biomes, the range of seasonal changes within a biome and how the Earth's systems interact.



Figure 3: My homepage SIMB
(All pictures by M. Eugster)

Photo phenology

We collect series of pictures to show seasonal changes and try to detect phenological stages. We have applied for a project of the Swiss Federal Institute of Technology Zurich that works with automated digital cameras to get phenological data.

12.8

REROD – A mathematical model for reversible rockslope deformations, caused by seasonal variations in the groundwater table, observed in the central Swiss Alps

Juergen Hansmann, Simon Loew¹ & Keith F. Evans¹

¹ Geologisches Institut, Ingenieurgeologie, ETH Zürich, Sonneggstrasse 5, CH-8092 Zürich (Juergen.Hansmann@erdw.ethz.ch)

In the framework of the construction of a deep tunnel in crystalline rock in central Switzerland, a high-precision automatic geodetic monitoring network has been installed above the tunnel trajectory in order to detect possible ground surface deformations during the construction phase. This monitoring network includes a cluster of several total stations and reflectors that are located along profile lines in three alpine valleys. Measurements have been initiated several years before the tunneling process started. During this period only natural processes influenced ground surface motions and deformations.

The recorded deformation signal normal to the valley axis, observed before the tunnel excavation was initiated, undergoes a seasonal, periodic change, reaching maximum extension in early summer and maximum compression in late winter time. The deformation appears to be elastic, as the amplitude remains quite constant. A strong correlation between measured deformations and the timing and amount of spring snow melt and summer rainstorm precipitation can be clearly shown. While in winter time the ground water reservoir depletes, deformation measurements indicate extensive movements of the valley slopes. Within only some days after intensive rainfall events or with the onset of snow melt, the groundwater reservoir is recharged and the measurements indicate that the valley slopes move towards each other.

The amplitude of the measured deformation signal differs with the elevation of the measured points. Reflector pairs in higher elevation show larger amounts of relative horizontal displacement (or strain) than reflector pairs close to the valley bottom. Furthermore a difference in the amount of deformation could be observed in different valleys. This paper identifies possible reasons for these differences in horizontal reversible deformations. Possible causes that are explored include (1) the geometry of the valley slopes, especially steepness and exposition of the terrain, (2) differences in hydromechanical rock mass properties, especially hydraulic conductivity and stiffness, (3) differences in soil cover, (4) differences in climatic

conditions, especially altitude dependent precipitation and snow melt, and (5) variations in size of mountain chains separating the valleys.

Based upon precipitation and snow height data, a mathematical model has been formulated, that predicts the expected natural deformation components for each valley profile. This model takes into account three key processes influencing the natural deformations: (1) infiltration of snow melt water, (2) infiltration of rainstorm precipitation during snow-free periods, and (3) depletion of the groundwater reservoir during times when there is no recharge. The correlation between the measured and modeled natural deformations is very good and the model allows to predict the temporal evolution of such deformations.

12.9

The Swiss Spring Index as a novel integral metric for spring phenology

Herren Thomas, Meier Nicole, Rotach Mathias W, Liniger Mark A., Appenzeller Christof

Federal Office of Meteorology and Climatology MeteoSwiss, Krähbühlstrasse 58, CH-8044 Zürich

Numerous studies have shown the tendency to earlier onset of spring in response to climate change. Most of these studies were confined to one single phenological phase, observations from one location or combinations of such results. To achieve more generalised information, a multispecies estimate for spring phenology was worked out using principal components analysis (PCA) on a combination of 10 spring phases from the Swiss phenological network.

Universally applicable information on the beginning of spring is often difficult to devise, because the appearance date of a single phenological phase may vary strongly between regions depending on the actual temperatures and individually observed plants. Using PCA analysis of the data from a combination of different species it can be shown that the dominant spatial pattern of spring phenology is essentially uniform in Switzerland and highly correlated to temperature. Thus a Spring Phenological index is constructed from the first principle component which yields spatially averaged information on spring appearance rather than an information for a specific location or a specific phenological phase. A further advantage of the method, is the fact that it is not mandatory to have every observation at all stations to give a suitable result.

However, the main benefit of the spring index lies in its simplicity. Comparable to an annual mean temperature the spring index provides one single value for a whole region, that can be monitored over longer periods of time thus establishing the pattern of spring phenological phases and their relation to climate signals.

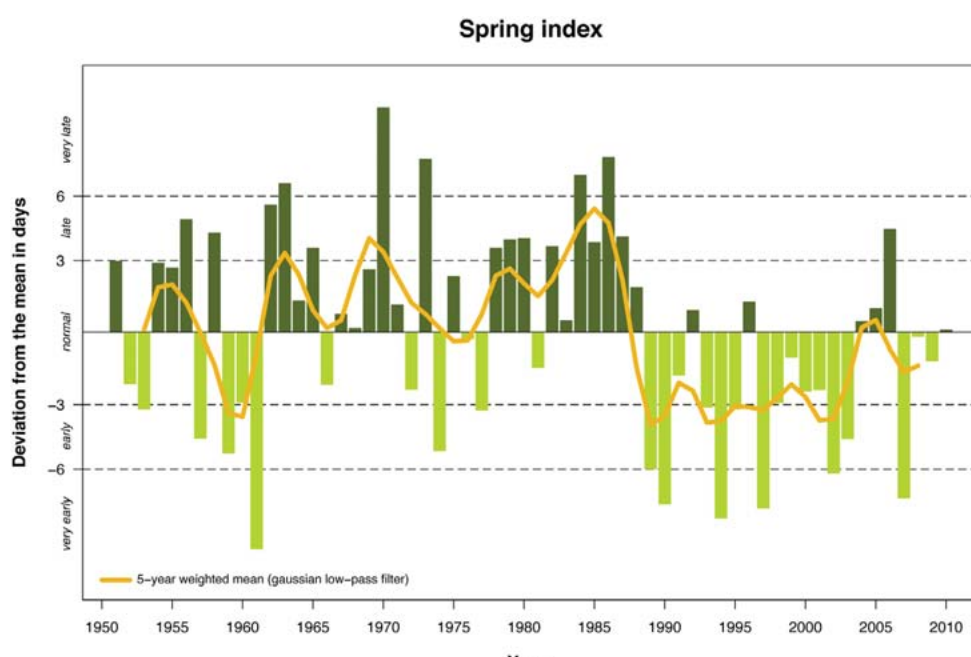


Figure 1: The spring index as a graph. From 1978 to 1988 the development of the vegetation was almost exclusively late, whereas between 1989 and 2003 greening in spring was mainly early. Similar to 2008 the timing of the actual year was at an average.

12.10

A comparison of ground-based phenological observations and NOAA AVHRR NDVI data

Dominic Kottmann

Geographic Institute of the University of Berne, Hallerstrasse 12, CH-3012 Bern

Seasonal variations of the Normalized Difference Vegetation Index (NDVI) are closely related to vegetation phenology, such as green-up, peak and offset of growing cycle. Methods have been developed in order to estimate the timing of single phenological dates and characteristics, such as the start of the growing season (Beck et al., 2006). This thesis aims to compare 11 years (1998 - 2008) of NDVI time series data derived from the North Oceanic and Atmospheric Administration (NOAA) Advanced Very High Resolution Radiometer (AVHRR) with ground-based phenological observations provided by MeteoSchweiz in order to reveal the potential of modelling specific phenological phases on a local or regional scale.

To reduce noise in the NDVI time series, a 10-day Maximum Value Composite (MVC) has been applied on the daily data (Holben, 1986). Also, two smoothing functions – an asymmetric Gaussian function-fitting (Jönsson & Eklundh, 2002) approach and a double logistic function-fitting (Beck et al., 2006) approach – have been separately applied on the NDVI time series. Another method concerning noise reduction lied within enlarging the area of interest to approximately 10 km x 10 km surrounding each phenological station and summing up land cover information derived for the years between 1992 and 1997, information derived from a digital elevation model (DEM), information on scan geometry, a cloud mask and a distance-based gradient to weighting procedures which all in all aimed to lead to a realistic representation of the vegetation dynamics observed at the stations (Doktor et al., 2009). In order to extract phenological information from the smoothed NDVI time series, a threshold-based method regarding the annual maximum NDVI and its amplitude has been used.

It has been shown, that applying these weighting procedures, especially concerning land cover statistics and altitude, lead to a slight improvement in the linear correlation of the two datasets. Even though the phenological dataset provided by MeteoSchweiz was rather small, high correlations ($r > 0.5$) for specific regions and onsets of phenological phases have been found. Still, the overall correlations are not yet high enough to establish a model on a regional nor temporal scale. But the results indicate that better and more accurate results can be achieved by using bigger phenological datasets and by analysing longer time series. In near future, other, more advanced remote sensing technologies such as the Moderate Resolution Imaging Spectroradiometer (MODIS) will provide a longer time span of records with a more accurate spatial resolution which will be leading to an improved possibility of comparison with the available ground-based phenological observations. Concerning noise reduction, especially at high altitudes, it could also be considered to take datasets into account which give information about water stress or snow cover.

REFERENCES

- Beck, P. S. A., Atzberger, C., Høgda, K. A., Johansen, B., Skidmore, A. K. 2006: Improved monitoring of vegetation dynamics at very high latitudes: A new method using MODIS NDVI. *Remote Sensing of Environment*, 100, 321-334.
- Doktor, D., Bondeau, A., Koslowski, D., Badeck, F. 2009: Influence of heterogeneous landscapes on computed green-up dates based on daily AVHRR NDVI observations. *Remote Sensing of Environment*, 113, 2618-2632.
- Holben, B. N. 1986: Characteristics of maximum-value composite images from temporal AVHRR data. *International Journal of Remote Sensing*, 7(11), 1417-1434.
- Jönsson, P., & Eklundh, L. 2002: Seasonality Extraction by Function Fitting to Time-Series of Satellite Sensor Data. *IEEE Transactions On Geoscience And Remote Sensing*, 40(8), 1824-1832.

12.11

Predicting the impact of warming on tree phenology: experimental and modelling results

Morin Xavier¹, Chuine Isabelle² & Bugmann Harald¹

¹Forest Ecology, ETH Zürich, Universitätstr. 22, CH-8092 Zürich (xavier.morin@env.ethz.ch)

²CEFE, CNRS, 1919 route de Mende, FR-34293 cedex 5, France

Because phenological events are strongly responsive to environmental factors such as temperature, they have been among the first documented fingerprints of climate change. Phenological changes in temperate forests have been observed in the last decades (Menzel et al. 2006). These changes have important implications, not only for forest products and biodiversity, but also for the global climate itself. Although other drivers such as photoperiod will also constrain the future response of trees (Körner and Basler 2010), accurate predictions of the response of tree phenology to climate change are urgently required to better forecast the future of forest ecosystems (Chuine et al. 2010). Here we present modelling and experimental results on the effect of warming on budburst phenology of European and North American tree species.

First we aimed to experimentally determine whether projected levels of warming for the upcoming decades will lead to linear changes in the phenology of trees or to more complex responses. We report the results of a 3-year common garden experiment designed to study the phenological response to artificial climate change – obtained through experimental warming and reduced precipitation – of several populations of three European oaks: two deciduous species (*Quercus robur*, *Quercus pubescens*), and one evergreen species (*Quercus ilex*), in a Mediterranean site (Morin et al. 2010).

Experimental warming advanced the seedlings vegetative phenology, causing a longer growing season, and caused higher mortality. However, the rate of advancement of leaf unfolding date was decreased with increasing temperature (Fig. 1). On the contrary, soil water content did not affect the phenology of the seedlings nor their survival.

Second, we showed predictions of change in budburst date made at the species distribution level with phenological models. Indeed, to advance our understanding of phenological responses to climate change, more reliable predictions made with process-based models are required.

We calibrated and validated models of leaf unfolding for 22 North American tree species. Using daily meteorological data predicted by two scenarios (A2: +3.2°C and B2: +1°C) from the HadCM3 GCM, we predicted and compared range-wide shifts of leaf unfolding in the 20th and 21st centuries for each species. Model predictions suggest that climate change will affect leaf phenology in almost all species studied, with an average advancement during the 21st century of 5.0 days in the A2 scenario and 9.2 days in the B2 scenario (Morin et al. 2009).

Our model also suggests that lack of sufficient chilling temperatures to break bud dormancy will decrease the rate of advancement in leaf unfolding date during the 21st century for many species. Some temperate species may even have years with abnormal budburst due to insufficient chilling. At the interspecific level, we predicted that early-leafing species tended to show a greater advance in leaf unfolding date than late-leafing species; and that species with larger ranges tend to show stronger phenological changes.

Thus our results show that the phenological response of temperate and boreal trees to climate change may be non-linear, and suggest that predictions of phenological changes in the future should not be built on extrapolations of current observed trends.

REFERENCES

- Chuine, I., X. Morin, and H. Bugmann. 2010. Warming, photoperiods, and tree phenology. *Science* 329:277-278.
- Körner, C. and D. Basler. 2010. Phenology under global warming. *Science* 327:1461.
- Menzel, A., T. H. Sparks, N. Estrella, E. Koch, A. Aasa, R. Aha, K. Alm-Kubler, P. Bissolli, O. Braslavskaya, A. Briede, F. M. Chmielewski, Z. Crepinsek, Y. Curnel, A. Dahl, C. Defila, A. Donnelly, Y. Filella, K. Jatczka, F. Mage, A. Mestre, O. Nordli, J. Penuelas, P. Pirinen, V. Remisova, H. Scheffinger, M. Striz, A. Susnik, A. J. H. Van Vliet, F. E. Wielgolaski, S. Zach, and A. Züst. 2006. European phenological response to climate change matches the warming pattern. *Global Change Biology* 12:1969-1976.
- Morin, X., M. J. Lechowicz, C. Augspurger, J. O'Keefe, D. Viner, and I. Chuine. 2009. Leaf phenology changes in 22 North American tree species during the 21st century. *Global Change Biology* 15:961-975.
- Morin, X., J. Roy, L. Sonié, and I. Chuine. 2010. Climate change impact on the phenology of three European oak species: results from a field experiment. *New Phytologist* 186: 900–910.

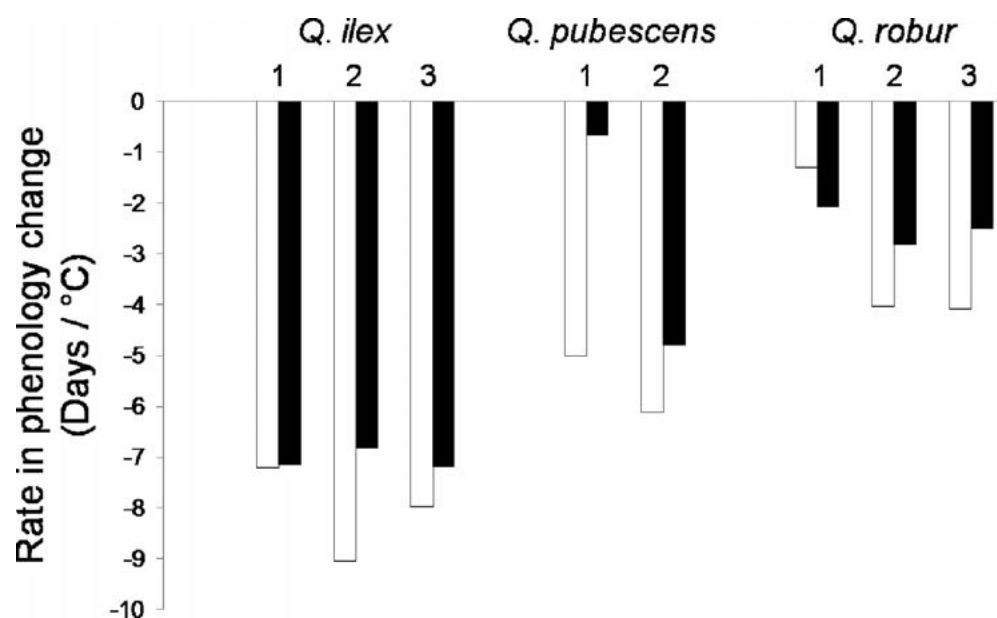


Figure 1.: Mean advancement rates between the warming treatments (T+: open bars, and T++: black bars) and the control treatment in days/°C (Rate+: advancement rate in days/°C for the T+ treatment, Rate++: advancement rate in days/°C for the T++ treatment) for each sampled population. The number corresponds to different populations.

Note: T+: level of warming about +1.5°C, and T++: level of warming about +3°C.

12.12

Changes in alpine plant phenology under future climate conditions

Rixen Christian¹

¹Alpine Ecosystems Group, WSL Institute for Forest, Snow and Landscape Research (rixen@slf.ch)

Alpine shrub- and grasslands are shaped by extreme climatic conditions such as a long-lasting snow cover and a short vegetation period. Such ecosystems are expected to be highly sensitive to global environmental change. Prolonged growing seasons and shifts in temperature and precipitation are likely to affect plant phenology and growth.

In a unique experiment, climatology and plant growth was monitored for almost a decade at 17 snow meteorological stations in different alpine regions along the Swiss Alps. Regression analyses revealed highly significant correlations between mean air temperature in May/June and snow melt out, onset of plant growth, and plant height.

These correlations were used to project plant growth phenology for future climate conditions based on the gridded output of a set of regional climate models runs. Melt out and onset of growth were projected to occur on average 17 days earlier by the end of the century than in the control period from 1971–2000 under the future climate conditions of the low resolution climate model ensemble.

Plant height and biomass production were expected to increase by 77% and 45%, respectively. The earlier melt out and onset of growth will probably cause a considerable shift towards higher growing plants and thus increased biomass.

Our results represent the first quantitative and spatially explicit estimates of climate change impacts on future growing season length and the respective productivity of alpine plant communities in the Swiss Alps.

12.13

Altitude, slope and aspect: Are there local-scale effects in temporal trends in a spatially high-resolved plant phenological network in the Swiss Alps 1971–2000?

Rutishauser This¹, Brügger Robert¹ & Jeanneret François¹

¹Geographisches Institut, Hallerstrasse 12, CH-3012 Bern (rutis@giub.unibe.ch)

Shifts in phenology of plants and animals have been widely observed as consequence of climate change impacts and temperature increase. Species-specific data are often assigned to limited and generalized site information on the precise location of the observation. However, as much meta-information as possible on the individual plant under observations is necessary to assess the impacts of changing weather patterns at the local scale that are related to changes in radiation, fog, frost and dominating circulation.

Here we used plant phenological data of the BERNCLIM network that collects data in the Canton of Bern (Switzerland) and adjacent areas covering a total area of 7,000 km² since 1970 (Messerli 1978, Jeanneret and Rutishauser 2010). The number of observation sites reached up to 600 observation sites with detailed meta-information of several locations within each site. The precision of coordinates for each location is generally less than one hectare. This information allows differentiating several terrain-types, based on altitude, slope and aspect. We used original observations including the blooming of hazel (*Corylus avellana* L.) for early spring, dandelion (*Taraxacum officinale* aggr.) for mid spring, and apple trees (*Malus domestica* Borkh.) for late spring.

For this contribution we analysed the impact of local terrain differences on phenological trends of three plant species. Specifically, we addressed the question whether differences in altitude, slope and aspect lead to systematic differences in temporal trends for the 1971–2000 period. Whereas altitude shows generally high correlations with phenology, we aimed at quantifying additional impacts on phenological trends such as microclimate and local adaptation of individual plants. Strongest variations between locations are expected for *Corylus* and *Malus* whereas *Taraxacum* is most strongly influenced by temperature along altitudinal gradients. This information derived from a regional observations network with long-term observations and high precision meta-information can be useful for detailed analyses of large data sets that stored in a number of European databases.

REFERENCES

- Messerli, B. 1978: Klima und Planung. Ziele, Probleme und Ergebnisse eines klimatologischen Forschungsprogrammes im Kanton Bern, Jahrbuch der geographischen Gesellschaft von Bern, 52, 11-22.
- Jeanneret, F. & Rutishauser, T., 2009: Phenology for topoclimatological surveys and large-scale mapping, in: Keatley, M. & Hudson, I. (eds.): Phenological Research: methods for environmental and climate change analysis, pp. 153-169, Springer.

12.14

KPS – eine Kommission für Phänologie und Saisonalität bei der «Plattform Geosciences»

Rutishauser This¹ und Mitinitiantinnen und -initianten

¹Geographisches Institut, Hallerstrasse 12, CH-3012 Bern (rutis@giub.unibe.ch)

Der Wissenschaftszweig der Phänologie dokumentiert und erforscht Ablauf und Entwicklung der Jahreszeiten im System Erde («Timing»). Insbesondere untersucht sie die biotischen und abiotischen Faktoren, die auf das zeitliche Eintreten der untersuchten Erscheinungen (z. B. Blattentfaltung des Laubes und Blattfall, Beginn der Schneedecke) einwirken. Unter dem übergeordneten Begriff der Saisonalität werden die verschiedenen im Jahresverlauf wiederkehrenden Erscheinungen sowohl in der belebten Natur (Biosphäre: Pflanzen und Tiere) als auch in der unbelebten Natur (Hydrosphäre bzw. Kryosphäre: Schnee und Eis; Atmosphäre: Nebel, Pollen) zusammengefasst. Abfolge, Interaktionen und langfristige Veränderungen im Eintreten der Jahreszeiten beeinflussen Stoff- und Energieflüsse zwischen Boden, Vegetation und Atmosphäre im Erdsystem als auch Interaktionen in der belebten Natur («Matching»), machen saisonale Veränderungen des Klimas und der Umwelt sichtbar und haben wichtige Einflüsse auf Menschen und Wirtschaft in der Schweiz.

Die Kommission für Phänologie und Saisonalität (KPS) hat zum Ziel, die phänologische Forschung national und international zu stärken, weiter zu entwickeln und breiter abzustützen. An Schweizer Universitäten und Eidgenössischen Forschungsanstalten ist eine Vielzahl von phänologischen Forschungsprojekten angesiedelt. Die Fragestellungen und Zielsetzungen sind so verschieden wie die Institutionen, Interessen und Anwendungen der Forschenden. Die Auswertungen von weltweit einzigartigen Archivaufzeichnungen (Pfister 1999, Rutishauser et al 2007), die Analyse von Satellitenbilddaufnahmen (Stöckli und Vidale, 2003), die Entwicklung und Anwendung von neuartigen Sensortechniken, Bildaufnahme und -auswertungsverfahren (Ahrends et al. 2008, Fontana et al. 2008) sowie experimentelle Studien (Asshoff et al 2006) im Gebirgsland Schweiz tragen zur facettenreichen Forschungslandschaft bei. Die herausragende Qualität der Forschung findet international grosse Beachtung: So etwa darin, dass in den vergangenen eineinhalb Jahren drei Artikel in «Science» erschienen sind, die von Schweizer Autoren oder Co-Autoren verfasst worden sind (Peñuelas et al. 2009, Körner und Basler 2010, Chuine et al. 2010). Substantielle Beiträge konnte die Schweizer phänologische Forschung auch zum Bericht der Working Group II des IPCC (2007) beitragen.

Die KPS will die Phänologie als Instrument der integrativen Umweltbeobachtung fördern, den Nutzen der Phänologie zur Erfassung und besserem Verständnis komplexer Umweltveränderungen bekannter machen und Anwendungen der phänologischen Forschung vorantreiben. Dabei baut sie auf intensiven Austausch mit Beobachtenden verschiedener Netzwerke und fördert die geowissenschaftliche Bildung zusammen mit dem Bildungsprogramm GLOBE, mit pädagogischen Hochschulen und Schulen aller Stufen.

Die KPS vertritt mit ihren Zielen konkret die Mission der SCNAT. Insbesondere mit konkreten Aktivitäten fördert die KPS (1) die Bedeutung der Naturwissenschaften für unser tägliches Leben, (2) den direkten Dialog mit der Gesellschaft vor Ort, (3) inter- und transdisziplinäre Forschungsansätze, und legt (4) mit Initiativen zur Nachwuchsförderung die Basis für die nächste Generation von Naturwissenschaftlerinnen und Naturwissenschaftlern. Die KPS initiiert die Herausgabe eines Newsletters mit wissenschaftlichen und populärwissenschaftlichen Beiträgen. Sie wird 2011 erstmals aktiv sein und viele Aufgaben vom «Phänologiekreis Schweiz» übernehmen (www.phaenologiekreis.ch.vu, www.cerclephenologique-suisse.ch.vu, www.circolofenologicosvizzera.ch.vu, www.swissphenologicalcircle.ch.vu)

REFERENCES

- Ahrends, H. E., Brügger, R., Stöckli, R., Schenk, J., Michna, P., Jeanneret, F., Wanner, H. & Eugster, W. 2008: Quantitative phenological observations of a mixed beech forest in northern Switzerland with digital photography, *Journal of Geophysical Research – Biogeosciences*, 113, G04004, doi:10.1029/2007JG000650.
- Asshoff, R., Zotz, G. & Körner, Ch. 2006: Growth and phenology of mature temperate forest trees in elevated CO₂. *Global Change Biology*, 12, 1-14.
- Chuine, I., Morin, X. & Bugmann, H. 2010: Warming, Photoperiods, and Tree Phenology, *Science*, 329, 277-e, doi: 10.1126/science.329.5989.277-e
- Fontana, F., Rixen, C., Jonas, T., Aberegg, G. & Wunderle, S. 2008: Alpine Grassland Phenology as seen in AVHRR, VEGETATION, and MODIS NDVI Time Series - a Comparison with in Situ Measurements. *Sensors* 8: 2833-2853.
- Körner, Ch. & Basler, D. 2010: Phenology Under Global Warming, *Science*, 327, 1461-1462.
- Peñuelas, J., Rutishauser T. & Filella I. 2009: Phenology Feedbacks on Climate Change, *Science*, 324, 887–888.
- Pfister, C. 1999: *Wetternachhersage. 500 Jahre Klimavariationen und Naturkatastrophen*, Paul Haupt, Bern.
- Rutishauser, T., Luterbacher, J., Defila, C., Frank, D. & Wanner, H. 2008: Swiss Spring Plant Phenology 2007: Extremes, a multi-century perspective and changes in temperature sensitivity. *Geophysical Research Letters*, 35, L05703. doi: 10.1029/2007GL032545.
- Stöckli R. & Vidale P.L. 2004: European plant phenology and climate as seen in a 20 year AVHRR land-surface parameter dataset, *International Journal of Remote Sensing*, 25, 3303-3330.

12.15

Assessing the effects of climate change on the phenology of European temperate trees

Vitasse Yann¹, François Christophe^{2,3}, Delpierre Nicolas², Dufrêne Eric³, Kremer Antoine⁴, Chuine Isabelle⁵ & Delzon Sylvain¹

¹ Université Bordeaux, UMR BIOGECO-1202, Av. des Facultés, F-33405 Talence, France,

² Université Paris-Sud, UMR ESE-8079, F-91405 Orsay, France

³ CNRS, F-91405 Orsay, France

⁴ INRA, UMR BIOGECO-1202, 69 route d'Arcachon, F-33612 Cestas, France

⁵ Centre d'Ecologie Fonctionnelle et Evolutive, UMR 5175, Equipe BIOFLUX, CNRS, 1919 route de Mende, 34293 Montpellier cedex

Modelling phenology is crucial to assess the impact of climate change on the length of the canopy duration and the productivity of terrestrial ecosystems. Focusing on six dominant European tree species, the aims of this study were (i) to examine the accuracy of different leaf phenology models to simulate the onset and ending of the leafy season, with particular emphasis on the putative role of chilling to release winter bud dormancy, (ii) to predict seasonal shifts for the 21st century in response to climate warming.

Models testing and validation were done for each species considering two or three years of phenological observations acquired over a large altitudinal gradient (1500 m range, 57 populations). Flushing models were either based solely on forcing temperatures (1-phase models) or both on chilling and forcing temperatures (2-phases models). Leaf senescence models were based on both autumn temperature and photoperiod.

We show that most flushing models are able to predict accurately the observed flushing dates. The 1-phase models (based on forcing temperatures) are as efficient as 2-phases models (based both on forcing and chilling temperatures) for most species suggesting that chilling temperatures are currently sufficient to fully release bud dormancy. However, our predictions for the 21st century highlight that chilling temperature could be insufficient for some species at low altitude. Overall, flushing is expected to advance in the next decades but this trend substantially differed between species (from 0 to 2.4 days per decade).

The prediction of leaf senescence appears more challenging, as the proposed models work properly for only two out of four deciduous species, for which senescence is expected to be delayed in the future (from 1.4 to 2.3 days per decade). These trends to earlier spring leafing and later autumn senescence are likely to affect the competitive balance between species. For instance, simulations over the 21st century predict a stronger lengthening of the canopy duration for *Quercus petraea* than for *Fagus sylvatica*, suggesting that shifts in the altitudinal distributions of these species might occur.

12.16

Ecosystem carbon budgets of tropical pasture versus afforestation

Wolf Sebastian, Eugster Werner & Buchmann Nina

ETH Zurich, Institute of Plant, Animal and Agroecosystem Sciences, Universitaetsstrasse 2, LFW A54.1, CH-8092 Zurich

Tropical ecosystems play an important role for the global carbon cycle and account for about 60% of the global terrestrial gross primary production (Beer et al., 2010). They contain 40% of the carbon in the terrestrial biosphere and are considered to sequester large amounts of anthropogenic released carbon from the atmosphere (Grace et al., 2001). However, with ongoing deforestation and land-use changes, the tropical carbon sink is increasingly influenced by agroecosystems and pastures (Fearnside, 2005). It is not yet fully understood how carbon cycling in the tropics responds to climate and land-use change. In addition, the carbon sequestration potential of tropical afforestation and the carbon balance of tropical pasture are largely unknown. Land-use change from tropical forest to pasture was found to increase intra-annual variations in CO₂ fluxes, the sensitivity to seasonal drought and to modify ecosystem carbon budgets (Saleska et al., 2009). Despite the general importance of tropical ecosystems for global climate and carbon cycling, continuous flux measurements in the tropics are still scarce and thus, globally underrepresented.

Therefore, we performed comparative eddy covariance flux tower measurements of CO₂ in a tropical pasture and adjacent native tree species afforestation in Sardinilla, Panama from 2007 to 2009. We observed pronounced seasonal variations in gross primary productivity (GPP), total ecosystem respiration (TER) and net ecosystem exchange (NEE) that were closely related to irradiance, soil moisture and C₃ versus C₄ plant physiology. Shallow rooting depth of grasses compared to trees resulted in a higher sensitivity of the pasture ecosystem to water limitations in the dry season. During 2008, we observed an annual GPP of 2345 g C m⁻² at the pasture and 2082 g C m⁻² at the afforestation site: significant amounts of carbon were sequestered at the afforestation (-442 g C m⁻², negative value denotes ecosystem carbon storage) and we found close agreement with biometric observations in 2008. Soil carbon isotope data of δ¹³C elucidate the C₄ to C₃ vegetation change and indicate the rapid carbon turnover in this tropical ecosystem. The pasture ecosystem was a strong carbon source in 2008 (261 g C m⁻²) and 2009 (260 g C m⁻²) and our results provide evidence that these carbon losses were induced by high stocking densities and periodical overgrazing.

Our results indicate that tropical afforestation can sequester large amounts of carbon, reduce the intra-annual variability of gross primary production and enhance the ecosystem resilience to seasonal drought. In contrast, we present the first multi-year eddy covariance measured carbon budgets for a tropical C₄ pasture, with persistent carbon losses observed over 2.5 years. These results have large implications on land management and suggest reduced livestock stocking densities and the benefit of increased afforestation efforts in the tropics. Moreover, the conversion from pasture to afforestation may become more relevant for Panama and other Latin American countries in the future, within the carbon accounting of the Clean Development Mechanism (CDM) as part of the Kyoto protocol.

REFERENCES

- Beer, C., Reichstein, M., Tomelleri, E., Ciais, P., Jung, M., Carvalhais, N., Rodenbeck, C., Arain, M.A., Baldocchi, D., Bonan, G.B., Bondeau, A., Cescatti, A., Lasslop, G., Lindroth, A., Lomas, M., Luysaert, S., Margolis, H., Oleson, K.W., Rouspard, O., Veenendaal, E., Viovy, N., Williams, C., Woodward, F.I. & Papale, D. 2010: Terrestrial Gross Carbon Dioxide Uptake: Global Distribution and Covariation with Climate. *Science*, 329(5993): 834-838.
- Fearnside, P.M. 2005: Deforestation in Brazilian Amazonia: History, rates, and consequences. *Conservation Biology*, 19(3): 680-688.
- Grace, J., Mahli, Y., Higuchi, N. & Meir, P. 2001: Productivity of tropical forests. In: J. Roy, B. Saugier and H. Mooney (Editors), *Terrestrial Global Productivity*. Academic Press, San Diego, CA, USA.
- Saleska, S., da Rocha, H., Kruijt, B. and Nobre, A.D. 2009: Ecosystem carbon fluxes and Amazonian forest metabolism. In: M. Keller, M. Bustamante, J. Gash and P.S. Dias (Editors), *Amazonia and Global Change*. American Geophysical Union, Washington, DC, pp. 389-408.

14. Geoscience and Geoinformation - From data acquisition to modelling and visualisation

Nils Oesterling, Adrian Wiget, Massimiliano Cannata

Swiss Geological Survey; Swiss Geodetic Commission; Swiss Geotechnical Commission; Swiss Geophysical Commission; Swiss Hydrogeological Society

- 14.1 Almqvist B.S.G., Zappone A., Bruijn R.H.C., Diamond L.W., Ramseyer K., Burg J.-P.: Physical and mechanical characterization of potential reservoir and cap rocks for geological storage of carbon dioxide in Switzerland
- 14.2 Ambrosi C.: The landslide inventory of Canotn Ticino: statistical analysis and updating issues
- 14.3 Ambrosi C., Bernoulli D., Soma L.: Quaternary Geologic Map of Mendrisiotto (Ticino)
- 14.4 Ambrosi C., Cannata M.: MIARIA - Adaptive Idrogeological Monitoring supprtuing the Area Integrated Risk Plan
- 14.5 Antonovic M., Cannata M.: Authentication and authorization management to ogc services with Geoshield: introducing Web Feature Service protection
- 14.6 Baruffini M., Ambrosi C.: A GIS-tool for risk assessment due to natural hazards in mountain regions. An exploratory study on an hypothetical event: the Val Canaria flood.
- 14.7 Baumberger R., Bossart P.: The Mont Terri Borehole Information System – development towards a 3D planning tool
- 14.8 Bilgot S., Parriaux A.: GIS-based 3D modelling for landslide hazard assessment: increasing the objectivity of hazard maps.
- 14.9 Burri T., Kündig R., Sinnreich M.: The Hydrogeological Map of Switzerland 1:100'000: From a pure print product of the 1970's to an interactive GIS-tool
- 14.10 Jolimet T., Tacher L., Parriaux A., Weidmann M., Giorgis D.: Première étape de la modélisation géologique 3D du canton de Vaud : la feuille de Nyon
- 14.11 Jordan P.: 3D geological mapping and visualisation as a tool for the analysis of overdeepened valleys
- 14.12 Molinari M., Cannata M., Troung X.L.: WPS application for shallow landslide hazard assessment
- 14.13 North R.P., Livingstone D.M.: Comparison of Cubic Splines and Linear Interpolation Methods for Lake Time Series Analysis
- 14.14 Oesterling N., Kühni A.: Geology Portal - Enhancing the availability of geological information
- 14.15 Wannaz C., Fantke P., Rainer F., Jolliet O.: Multi-scale, multimedia modeling to compare local and global life cycle impacts on human health
- 14.16 Wu J., Gilliéron P., Merminod B.: An integrated methodology for change detection via terrestrial laserscanning: case study of the landslide in Flamatt

14.1

Physical and mechanical characterization of potential reservoir and cap rocks for geological storage of carbon dioxide in Switzerland

Almqvist Bjarne S. G.¹, Zappone Alba², Bruijn Rolf H. C.¹, Diamond Larry W.³, Ramseyer Karl³, Burg Jean-Pierre¹

¹ *Geologisches Institut, ETH Zürich.*

² *Schweizerischer Erdbebendienst, ETH Zürich.*

³ *Institut für Geologie, Universität Bern.*

In July 2010 the Mauna Loa Observatory on Hawaii reported that the concentration of CO₂ in the atmosphere was ~390 ppm, a value that is about 40% higher than the atmospheric CO₂ concentration before industrialization began. This rapid increase and elevated level are mainly due to burning of fossil fuels. The atmospheric CO₂ is believed to affect the Earth climate system in a way that can have an adverse impact on current ecosystems and human society, which has led to the initiation of a worldwide effort in reducing anthropogenic emissions using carbon dioxide capture and storage (CCS) systems. Carbon management in power generation (CARMA) represents a joint initiative of several academic and industrial institutions in Switzerland, for the purpose of CCS. One aspect of the project focuses on the potential for storage in Swiss bedrock. A preliminary evaluation indicates that the Swiss Molasse Basin (SMB) is the most suitable region for storage in Switzerland (Chevalier et al., in press). However, characterization of the potential reservoir and cap rocks is needed in terms of their geomechanical and physical properties (e.g., porosity, permeability, density, elasticity), in ambient settings and in laboratory settings that simulate storage conditions in the crust. A certain amount of information exists already in academic and non-academic literature, although access remains restricted or difficult to obtain in the latter case. The task is to compile the information into a single database, and to carry out field sampling and use existing drill core for laboratory measurements to fill the missing information. The Swiss Atlas of Physical Properties of Rocks (SAPHYR), a multiyear project developed by the Swiss Geophysical Commission (www.sgpk.ch) goes in this direction, and data collected throughout Switzerland are presented in a geographical frame (GIS). The development of a database containing detailed information on mechanical and physical properties for potential reservoir and cap rocks is of value not only for CO₂ sequestration, but also for other initiatives such as nuclear waste storage and geothermal energy.

REFERENCES

Chevalier, G., Diamond, L. W. & Leu, W., 2010: Potential for deep geological sequestration of CO₂ in Switzerland: a first appraisal. *Swiss Journal of Geosciences* 103 (3), In press (December issue).

14.2

The landslide inventory of Canton Ticino: statistical analysis and updating issues

Christian Ambrosi

SUPSI, Institute of Earth Sciences C.P. 72 CH-6952 Canobbio (Ticino, Switzerland)

The landslide Inventory of the alpine areas of Cantone Ticino (about 1000 km², southern Switzerland) is a large database with more than 2000 phenomena. The inventory is aimed to provide a support tool for landslide hazard assessment.

Inventory was done by means of aerial photo-interpretation. The interpretation of optical images is commonly applied in support of landslide inventories. Based on aerial photography interpretation complemented by field surveys and historical records, landslide inventory maps were produced. The aerial photographs (swisstopo) are available at 1:20'000 scale and were taken in the last 50 years. Using stereoscopic images landslides were distinguished by typology, depth and activity. The high resolution of aerial photographs has also permitted to recognize the geomorphological features associated by mass movements, such as scarps, counterscarps, trenches, debris flows, debris fans and rockfalls. The state of activity was performed by means of available monitoring data, SAR measurements and morphological features.

A statistical analysis was performed on the landslide dataset and it enhances the relationships between landsliding and several geological and environmental factors. Lithology exerts a strong control on landslide distribution. Such control is both direct (mechanical properties and weathering), and indirect (slope form and gradient). Finally, by using GIS techniques, the susceptibility of the region to landsliding was analysed.

REFERENCES

- Strozzi T. and Ambrosi C. 2007: Sar Interferometric Point Target analysis and interpretation of aerial photographs for landslides investigations in Ticino Southern Switzerland. Envisat Symposium, Montreux Switzerland, 13-27 April
- Ambrosi C. and Crosta G.B. 2006: Large sackung along major tectonic features in the Central Italian Alps. *Engineering Geology*, 83 183-200.
- Ambrosi C. and Crosta G.B. 2006: Effects of slope geometry and in situ stress on large slope instabilities. General Assembly of the European Geophysical Union, Vienna, Austria, 2-7 April.

14.3

Quaternary Geologic Map of Mendrisiotto (Ticino)

Ambrosi Christian¹, Bernoulli Daniel², Soma Linda¹

¹SUPSI Istituto Scienze della Terra, CP72 CH-6952 Canobbio (linda.soma@supsi.ch)

²Institute of Geology and Palaeontology, Basel University, Basel, Switzerland

Within the making of the 1:25.000 scale geological map (1373-Mendrisio sheet), in 2010, the part concerning the quaternary deposits has been completed. The territory that has been inquired is located in the Southern part of Switzerland, it's the area enclosed between Lugano's lake to the North and Como's lake to the East.

The map, made using ArcGis 9.3 software, contains information collected and processed during the geological survey integrated with previous GESPOS (IST-SUPSI database) drilling data.

Innovative techniques have been used during the data acquisition phase, such as landslide photointerpretation and 2 meter DEM analysis to recognize and characterize shapes present on the Mendrisiotto's area.

The approach to distinguish deposits is litostratigraphic; glacial and fluvioglacial deposits are characterized using, as temporal limit, the LGM (Late Glacial Maximum). To distinguish deposits older than LGM or referable to LGM, these criterias have been used: alteration of granitoid clasts, depth of decarbonation profile and pedogenic development.

This approach has turned out very useful, most of all because it allows to create an easily readable digitalized map that represents an important item for practical applications.

14.4

MIARIA - Adaptive Idrogeological Monitoring supporting the Area Integrated Risk Plan

Christian Ambrosi¹ & Massimiliano Cannata¹

¹ SUPSI, Institute of Earth Sciences C.P. 72 CH-6952 Canobbio (Ticino, Switzerland)

MIARIA is a project funded as part of the Italy/Switzerland Operational Programme for Trans-frontier Cooperation 2007-2013 (INTERREG Italy/Switzerland).

The project aims to build innovative systems and technologies for the distributed acquisition of regional data and the communication of that data to second-generation operating control rooms, the aggregation of the information on a phenomenological basis, and the generation of dynamic integrated risk scenarios in trans-frontier Alpine environments, with particular regard to domino effects (Area Integrated Risk Plan-denominated scenarios).

More specifically, the specific distributed monitoring action - which is based on Wireless Sensor Networks technology (which complements pre-existing sensor stations) - will provide data that will go to make up a dynamic map of the risk associated with a specific area. This will be integrated with a static map of technological risk and network present in the region, in order to provide an Integrated Risk Plan for the Alpine Area. At the same time, the monitoring system will allow the dynamic forecasting of risk around emergency situations, using real-time information coming from the field.

Within this frame the Institute of Earth Sciences of the Applied University of the Southern Switzerland (IST-SUPSI) is responsible for the application of the project in the case study of the Canaria valley and is leader of the modelling work package.

This poster present the currently performed activities and the relative results.

14.5

Authentication and authorization management to ogc services with Geoshield: introducing Web Feature Service protection

Antonovic Milan¹, Cannata Massimiliano¹

¹ SUPSI Istituto Scienze della Terra, CP72 CH-6952 Canobbio

The usage of OGC standards in public administration has to deal with security of sensible data. Today a few possibilities are available and most of them are extremely complicated and not specific for geospatial services. The definition of users authentications and privileges are essential in developing specific applications like emergency response management systems.

For this reason we studied how the OGC services could be secured and how a filtered access for different groups and users could be realized. The result of this studies is the design and realization of Geoshield, a project born to offer a centralized way to define security access-control to OGC services. Basically it acts like a proxy, intercepting all the communications between clients and OGC compliant services (WMS, WFS).

Geoshield is able to manage users and groups, it handles authentication and privileges settings among groups and registered services. It is capable to analyse requests applying the filters setted to the user and manipulating the response.

For example handling WMS or WFS security, with GeoShield we can:

- define access privilege for each layer provided by the service,
- specify if a layer can be viewed or not,
- define geometrical extent of view permission
- define permissions based on data attributes

Actually all WMS and WFS privileges on single layers are based on Common Query Language (CQL) filters, that allow interesting combination of permissions definition that operate in a hidden way to end-user.

Currently the Geoshield service is applied in production environments for the securing of two application for the Public Administration in Switzerland, the presentation will provide some consideration about actual security issues in OGC standards and detailed informations about technical implementation, performance report, and future enhancement of the GeoShield software.

REFERENCES

- GeoShield project - <http://istgeo.ist.supsi.ch/site/projects/geoshield>
 OGC Standards (Open Geospatial Consortium) - www.opengeospatial.org
 Geotools Java GIS Toolkit - <http://geotools.codehaus.org/>

14.6

A GIS-tool for risk assessment due to natural hazards in mountain regions. An exploratory study on an hypothetical event: the Val Canaria flood.

Baruffini Mirko¹ & Christian Ambrosi¹

¹Istituto Scienze della Terra IST-SUPSI, C.P. 72, CH-6952 Canobbio (ist@supsi.ch)

Numerous large landslides are located in the Alps of Ticino, Southern Switzerland. In particular, The Val Canaria landslides are located near Airolo in the upper Leventina valley. The Val Canaria landslides consist of failed rock masses on both sides of the valley with a total volume of about 80 million m³

The area is historically known for its instability. The first reports date back to 1846 where failures were reported from the southern slope of the valley. Despite of the average long-term displacements that are of the order of a few centimetres per year, the snow melt in the spring of 1992 caused total slope displacements of 2 to 7 m. The landslide masses blocked the torrent creating a natural dam, which disappeared after a few days, without causing flooding or debris flows (Seno and Thüring, 2006).

In fact, the channel of the torrent Canaria at the slope's toe is filled with unvegetated landslide debris. A natural dam could form again after a landslide event with a possible subsequent disastrous failure and destructive consequences on the important traffic lines passing in the main valley.

This scenario, although characterized by a very low probability of occurrence, is nevertheless possible and could have effects that would certainly be devastating for a big part of the Swiss economic system. A damaged infrastructure would cause serious material damage that would require extraordinary repairs or restorations. The inactivity of services, as a result of a malfunction, would generate important financial losses and problems in essential services supply in the region (Maggi R. et al, 2009). These are elements that justify a risk analysis of this region.

The risk is a matter not directly measurable but with a Geographical Information System adapted to run with a tool developed to manage risk analysis it is possible to survey the data in time and space, obtaining an important system for managing natural risks (Frigerio and van Westen, 2010). The aim is to join and to organize the various data currently available to carry out a qualitative and semi-quantitative analysis giving an overview of the risk (BUWAL, 1999). The tool is developed in ESRI ArcObjects and runs in ArcGIS. The outcomes can provide an answer to the questions: "what can happen?" and "how achieve maximum safety with a minimum of effort?" or, depending on the desired depth, they can represent also input to start an increasing order of analytical analysis (i.e a cost-benefit analysis or so on). In this way the study could develop a methodology that makes possible a risk analysis aiming to optimize the infrastructure vulnerability and therefore allows to obtain a model designed to optimize the functionality of the network infrastructure.

REFERENCES

- BUWAL 1999: Risikoanalyse bei gravitativen Naturgefahren - Methode, Fallbeispiele und Daten (Risk analyses for gravitational natural hazards). Bundesamt für Umwelt, Wald und Landschaft (BUWAL). Umwelt-Materialien Nr. 107, 1-244.
 Frigerio, S., van Westen, C. J., 2010: RiskCity and WebRiskCity: Data Collection, Display, and Dissemination in a Multi-Risk Training Package. Cartography and Geographic Information Science, Volume 37, Number 2, April 2010, 119-135(17).
 Maggi R. et al, 2009: Evaluation of the optimal resilience for vulnerable infrastructure networks. An interdisciplinary pilot study on the transalpine transportation corridors, NRP 54 "Sustainable Development of the Built Environment", Projekt Nr. 405 440, Final Scientific Report, Lugano
 Seno, S., Thüring, M., 2006: Large landslides in Ticino, Southern Switzerland: Geometry and kinematics. Engineering Geology, 83 (2006) 109-119.

14.7

The Mont Terri Borehole Information System – development towards a 3D planning tool

Roland Baumberger ¹, Paul Bossart ¹

¹ *swisstopo, Swiss Geological Survey, CH-3084 Wabern, Switzerland (roland.baumberger@swisstopo.ch)*

The Mont Terri Rock Laboratory is located in the Swiss Jura Mountains (Folded Jura, Mont Terri Anticline). It can be accessed via the security gallery of the Mont Terri Highway tunnel. Inside the rock laboratory, mechanical, hydrogeological and geochemical properties of the Opalinus Clay Formation, a potential host rock for deep geological disposal in Switzerland, are being investigated. Since 1996 thirteen partners from Europe, the United States and Japan carry out various kinds of experiments in this facility (developing test methodology, performing demonstrations and understanding processes).

Data specification

Most of the experiments are performed in drill holes of various lengths. Their stability and the proper quality of the corresponding drill cores denote important preliminaries to the success of the experiments. Drilling techniques used (simple, double, triple core barrel) are based on various drilling fluids (gas or oil-based), but not on water.

Since the beginning of the Mont Terri project, each drill hole has been exactly surveyed. Their relative positions in the laboratory as well as geology, orientation (length, dip, azimuth) and technical information (diameter, technique, fluid) have been mapped. Additional information as borehole history, photos, core mapping and core sampling are stored as well.

The Borehole Information System

The complete set of data (~900 cores) is accessible through the Mont Terri Borehole Information System (BIS). It is a Perl, VRML and HTML based graphical tool that can be used using Internet Explorer browser in offline mode. As a highlight, the BIS allows to navigate through the rock laboratory in 3D (see Figure 1). Corresponding drill holes can be accessed either by graphical search or an option-based approach using drop-down menus in the browser. swisstopo is in charge of managing and updating the BIS as well as for its distribution to the partners.

Data acquisition

Up to now, data acquisition follows a purely manual procedure at swisstopo and reaches from (1) data mapping, (2) quality control, (3) update the BIS to (4) the generation of the 3D view. Since there are no automated testing methods yet during data input (e.g. naming of geological facies, general grammar, coordinates etc.), it is necessary to manually check each entry and to eventually adjust any errors according to previously specified standards. Following the above-mentioned workflow, data acquisition is a time consuming, defective and cost-intensive procedure. Updates of the BIS are sent to the partners on CD-ROM annually.

Starting in late 2010, the workflow described above is adapted to meet long lasting requirements of the operators and to adopt the BIS to modern functionality as well. As a main improvement, quality control, updating the existing BIS and generation of the 3D view is automated. As a consequence, the complete dataset has a higher accuracy and is up to date on a daily basis.

Outlook

Having improved the BIS to a semi-automated data handling and management, the basis for future development is built. It is planned to migrate the complete BIS in 2011 to a web based framework that manages the data in a database and can then either be run online or offline. Search queries will be possible and data updates will be provided as database dump by FTP.

In a final development step in 2012, the BIS will be pushed to a 3D planning tool, where the partners will be able to plan the boreholes needed in their experiments directly in the system. For the success of these experiments, it is crucial that they do not interfere. Since the available rock volume is finite, it is increasingly difficult to guarantee the needed spatial independence. In this context, the envisioned BIS will be an essential planning instrument.

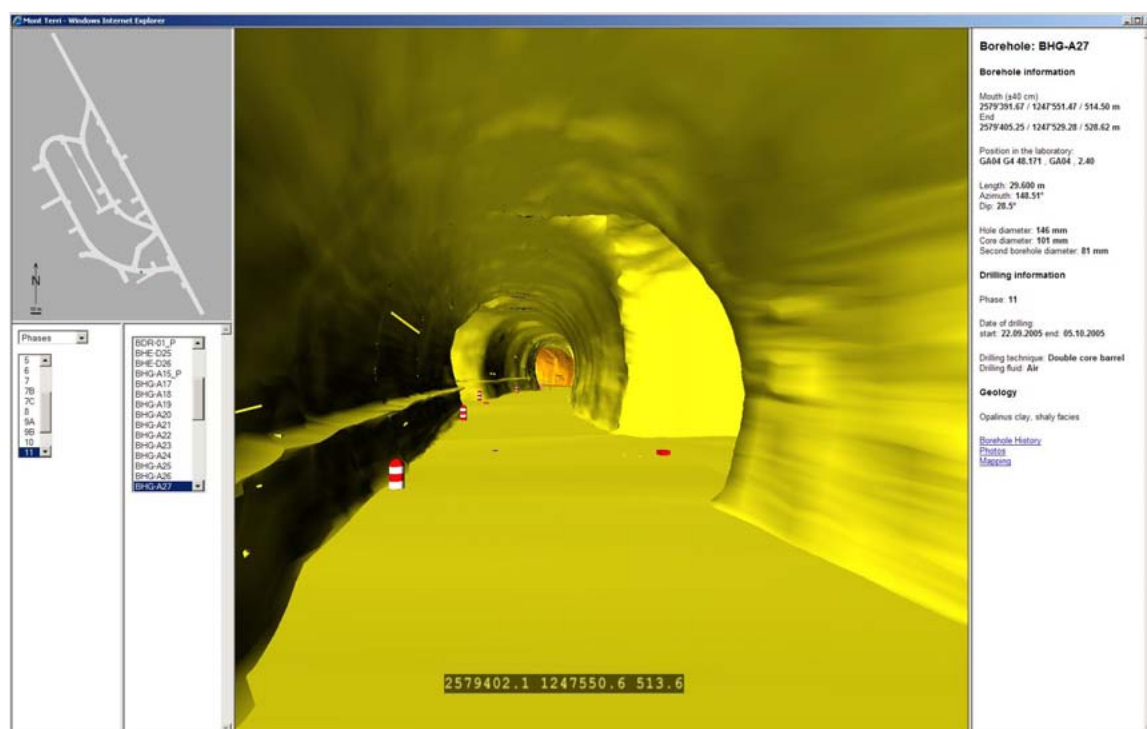


Figure 1. Screen shot of the Mont Terri BIS. The 3D view in the center of the screen serves as main approach for drill hole query. Navigation is either possible through (1) the 3D window, (2) the interactive floor plan in the upper left corner or (3) the option-based choice using drop-down menus in the lower left corner. Detailed information of the corresponding drill hole is provided in the area on the right hand side of the screen. The plugin “blaxxun Contact” (<http://www.blaxxun.com>) is necessarily needed to run the tool. Therefore, the BIS is technically bound to MS Internet Explorer.

14.8

GIS-based 3D modelling for landslide hazard assessment: increasing the objectivity of hazard maps.

Bilgot Séverine¹, Parriaux Aurèle¹

¹ EPFL ENAC IIC GEOLEP, Station 18, CH-1015 Lausanne (severine.bilgot@epfl.ch)

Recent decades have been marked by many disasters caused by natural hazards. Gravitational phenomena in particular have resulted in several deaths and extensive damage to infrastructure.

Nearly 10% of Swiss territory is considered unstable. It therefore requires an effective methodology for the mapping of areas likely to be affected by this type of hazard.

The aim of this project is to establish the bedrock of a new methodology for the implementation of hazard maps related to landslides based on the evaluation of slope instability predisposition.

The first step of this methodology is a systematic field survey on a given study area. The information is organized by type (faults, dip, formations, boreholes, springs, streams, etc..) and then imported into a GIS.

Once these data interpolated and converted into a grid of points, we obtain on the one hand a three-dimensional geological model (supplemented by geotechnical and hydrodynamic parameters measured in situ and extrapolated to the entire study area) and on the other hand an approximation of the gradient of hydraulic potential in the area. It is then possible to calculate a safety factor at each point of the model and thus to assess the susceptibility of the slope to instabilities. After crossing with a map of moderating factors (altitude, aspect, vegetation) in order to take into account the context of the slopes, it is validated by comparison with the map of phenomena to obtain the final hazard map. Achieving it is thus entirely transparent.

14.9

The Hydrogeological Map of Switzerland 1:100'000: From a pure print product of the 1970's to an interactive GIS-tool

Burri Thomas¹, Kündig Rainer¹, Sinreich Michael²

¹ Swiss Geotechnical Commission, ETH Zentrum, NO F35, 8092 Zürich (thomas.burri@erdw.ethz.ch, rainer.kuendig@erdw.ethz.ch)

² Federal Office for the Environment FOEN (Bundesamt für Umwelt BAFU), Hydrogeology section, CH-3003 Bern (michael.sinreich@bafu.admin.ch)

The Hydrogeological Map of Switzerland (HYGA100) displays on a set of sheets lithological and hydrogeological information on solid and unconsolidated rock at a scale of 1:100'000. This contains, among others, spatial surface distribution of the rocks and aquifers, their permeability, groundwater flow direction as well as locations of springs, abstraction wells or major boreholes. The extent of the individual sheets is generally consistent with those of the topographic map of Switzerland. Currently, 12 out of 23 sheets are published in collaboration of the Swiss Geotechnical Commission SGTK and the Federal Office for the Environment FOEN. Although the map provides a lot of detailed information, the scale is rather adequate as a planning and information instrument for regional to interregional or even international purposes, than for local studies. Nonetheless, the map may also be used for applied geological investigations in order to get a quick overview of a specific area, e.g. in the framework of a larger project.

Work on HYGA100 has started under the guidance of prof Heinrich Jäckli in the late 1960's, at that time a pioneer work in Europe. In the beginning, the map was intended as a purely print-based product. As an important drawback, once printed, the map loses its actuality with time, due to increasing information on regional aquifer characteristics and modifications in point data with time (aquifer modelling, spring and borehole inventories). The focus in map production during the last 40 years has clearly been set on the Swiss Plateau, the region with the most productive aquifers supplying the majority of Swiss population with drinking water. Other important aquifers in the Alpine area, such as Ticino or Valais, are not yet mapped to date.

With the upcoming of Geographic Information Systems GIS, the focus of publication has moved from a pure print product to an interactive GIS-based map, even though actual map sheets will remain available in print format. A first sheet in the digital version, which covers parts of Swiss Jura Mountains and the eastern edge of the Plateau was published in 2006 (Fig. 1). At the same time, the procedure of map compilation changed from an AUTHOR-Redaction-system to an Author-REDACTION-system. The reason is simple, as much data is now available online and no longer needs to be collected and sorted by the authors themselves. Furthermore, many geological maps have been published in the last decades. Collection and integration of this data is now also part of the work of the editorial board of the SGTK.



Fig. 1: Extract of the Hydrogeological Map of Switzerland 1:100'000, sheet Vallorbe – Léman nord.

These fundamental changes created new requirements and, respectively, resulted in several important innovations: Firstly, an extendable data model had to be established for the whole project. A preliminary, non-reviewed version is now available. This data model has to be integrated in the current draft of the GIS project. For the purpose of compatibility, it incorporates as much as possible and meaningful of the geologic data model of the Swiss Geological Survey. Secondly, the GIS-based map is a sheetline-free project of whole Switzerland, which requires consistent (unambiguous) description criteria for the whole area. Relevant sections of neighbouring countries, e.g. in the area of Basel, are also included making the map an international project. Thirdly, this new information can be combined and intersected with other GIS-based data and related subjects can relatively easily be inferred from it, e.g. lithological maps, vulnerability maps or permeability maps. Not least, information inside the map must and will be updated in appropriate intervals.

In the near future, several important and challenging steps must be simultaneously accomplished in the framework of the project:

- Establishment of a revised data model and setup of the sheetline-free GIS project for the whole country.
- Production of the remaining sheets as a concurrent GIS-based and print product.
- Digitalisation and updating of the published maps, as well as integration into the larger GIS project.
- Production of the explanatory notes and digitalisation of the so far published notes.
- Enabling of higher interactivity within the GIS project with data query possibilities providing base information and links to the data host (Federal or cantonal internet sites, on-line surveys etc.).

14.10

Première étape de la modélisation géologique 3D du canton de Vaud : la feuille de Nyon

Thomas Jolimet ¹, Laurent Tacher ¹, Aurèle Parriaux ¹, Marc Weidmann ², David Giorgis ³

¹ EPFL/ENAC/IIC/GEOLEP, Station 18, CH-1015 LAUSANNE

² Sentier du Molard 3, CH-1805 JONGNY

³ Etat de Vaud-OIT, Av. de l'Université 5, CH-1014 Lausanne

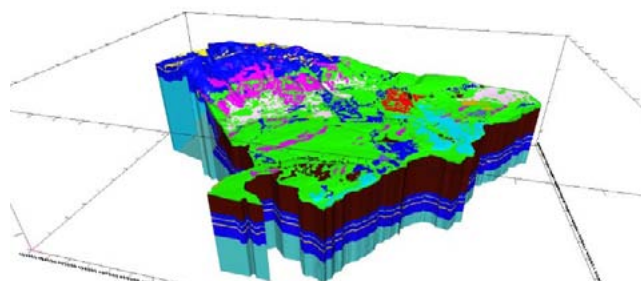
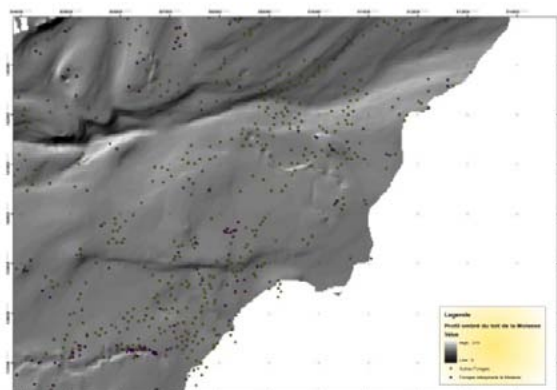
Dans une démarche de développement durable, un accent particulier doit être mis dans la connaissance du territoire, et notamment de son sous-sol, afin de pouvoir en valoriser tous les potentiels. Même si, en Suisse, une première priorité a été placée sur les milieux urbains, il n'en reste pas moins important de pouvoir développer cette connaissance sur l'ensemble d'un canton. Dans cette optique, nous proposons de montrer l'exemple mis en place dans le canton de Vaud avec la modélisation géologique 3D d'une feuille entière: la feuille 1261-Nyon [1].

La connaissance géologique des territoires nécessite d'utiliser des moyens informatiques performants afin de stocker, élaborer et visualiser des données brutes ou complexes après modélisation. Beaucoup de ces données géologiques sont centralisées par l'administration cantonale (Office de l'Information du Territoire) et disponibles sur le guichet cartographique [2]. De plus, l'information géologique nécessite l'intégration de données dans les trois dimensions ainsi que la maîtrise de l'enchaînement des différentes couches/types de roches. Les systèmes d'information géographique (SIG) proposent rarement la maîtrise de la troisième dimension, mais se limitent le plus souvent à une représentation 2D ou 2 ½ D. L'élaboration d'une information géologique compréhensible par le plus grand nombre, et plus seulement limitée aux spécialistes, se fera donc par l'intermédiaire d'une modélisation utilisant un logiciel spécialisé comme Geolep 3D développé par le GEOLEP, Laboratoire de Géologie de l'ingénieur de l'EPFL.

Le choix de la feuille Nyon a été dicté par la variété des terrains géologiques de ce territoire qui présente un Quaternaire complexe sur le plateau molassique, tandis que le NW de la feuille relève du Jura avec une structure plissée tout aussi complexe. Dans un souci d'harmonisation de l'information géologique, nous avons choisi d'établir ce modèle sur la base des géotypes [3]. Pour pouvoir mieux appréhender les différentes structures des terrains meubles glaciolacustres (GL) et fluvioglaciaires (FG) et leurs relations avec les moraines de fond (MF), il est nécessaire de bien connaître la morphologie du substratum molassique marno-gréseux sur lequel elles reposent. Une carte en isohypses de la surface molassique a ainsi été établie à l'aide de toutes les données disponibles (sondages mécaniques [2], mesures gravimétriques et sondages électriques [4]). Cette carte précise la profondeur et l'extension du très important sillon d'érosion, probablement sous-glaciaire, reconnu jusqu'ici de Gingins à Bursinel, dont le remplissage témoigne d'au moins quatre occupations glaciaires. La carte suggère aussi que les importants décrochements EW qui hâchent la Molasse et le Jura ont parfois, mais pas systématiquement, guidé les érosions glaciaires ou sous-glaciaires.

Par ailleurs, le défi de la modélisation 3D est de produire une image continue fiable de la géologie à partir d'informations ponctuelles. Tout l'enjeu pour le géologue est donc de densifier l'information. Dans notre étude, à partir des documents de références, cette densification est passée par :

- l'établissement de différentes coupes géologiques pour identifier les structures du Quaternaire,
- la création de cartes structurales simplifiées pour les plis du Jura,
- l'utilisation de méthodes d'extrapolation de type « cosines » pour les failles principales.



Figures 1 et 2 : Carte ombrée du toit de la Molasse et modèle géologique

L'image de la feuille de Nyon ainsi construite est perfectible : elle montre bien où se situent actuellement les limites technologiques de la représentation graphique, ainsi que les incertitudes de l'interprétation géologique. Elle est notamment susceptible d'être partiellement remise en cause à chaque nouveau sondage disponible. Elle représente néanmoins pour l'Etat de Vaud la ligne de départ menant à de nombreuses applications à caractère géologique ou géotechnique, telles que l'établissement de cadastre de potentiels géothermique ou de risque sismique.

REFERENCES

1. Arn R., Conrad M.-A., Weidmann M. (2004): Feuille 1261 Nyon, avec notice explicative.- Atlas géol. Suisse 1:25'000, carte 117, O.F.E.G., Ittigen/Berne.
2. Vaud, Guichet cartographique: <http://www.geoplanet.vd.ch/index.php>.
3. Parriaux A. & Turberg P. (2007): Les géotypes, pour une représentation géologique du territoire.- Tracés, 15/16, 11-17.
4. Données transmises par R. Olivier, Inst. Géophysique Univ. Lausanne;
5. Baumgartner F. (1996): Développement d'une nouvelle méthode de prospection géophysique lacustre appliquée à l'étude du bassin lémanique.- Thèse Fac. Sci. Univ. Lausanne, Inst. de Géophysique.

14.11

3D geological mapping and visualisation as a tool for the analysis of overdeepened valleys

Peter Jordan¹

¹Böhringer AG, 4104 Oberwil (peter.jordan@boe-ag.ch)

Based on surface and borehole information, together with pre-existing regional and local interpretations, a 7,150 square kilometre Raster Digital Elevation Model (DEM) of the bedrock surface of northern Switzerland was constructed using a 25 m cell size. This model represents a further important step in the understanding of Quaternary sediment distribution and is open to a broad field of application and analysis, including the analysis of the overdeepened valleys.

In most cases, overdeepening is restricted to the areas covered by the Last Glaciation Maximum (LGM). However, at various locations relatively narrow overdeepened valleys outreach the tongue basins and the LGM ice shield limits. Therefore, an earlier and further-reaching glacial event has probably contributed significantly to the overdeepening of these valleys. However, overdeepening ends far inside the Most Extensive Glaciations (MEG) limits.

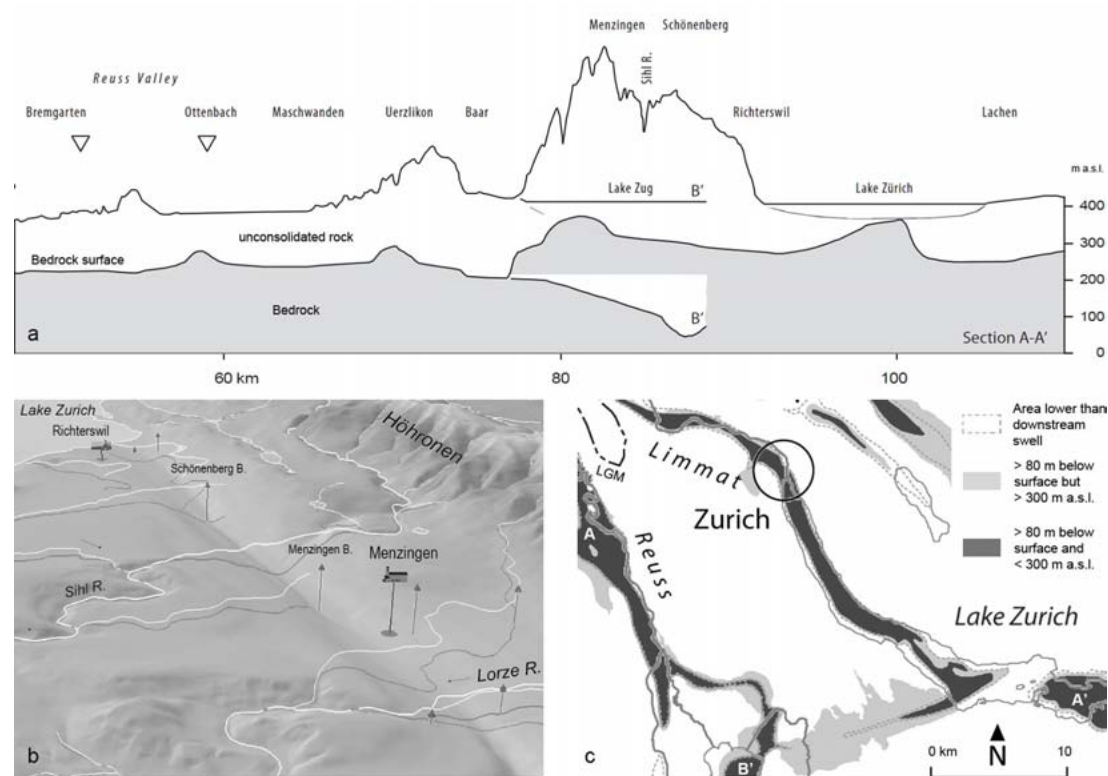


Figure 1. Analysis and visualization of abandoned Richterswil - Menzingen valley and surrounding overdeepened basins using DEM of land and bedrock surface: a) Section along thalweg; b) bird's eye view with boreholes; c) map showing depth of bedrock, unconsolidated rock thickness and drainless basins.

The paper addresses different methods and techniques of creating and combining various 3D and 2D digital raster models to localize, visualize and analyze the extent of overdeepening as a function of pre-existing drainage systems, bedrock geology and glacial advances and retreats. The products give a better understanding glacial and fluvial erosion processes, actual unconsolidated rock thickness and distribution, and past and future landscape development.

REFERENCES

- Jordan, P. 2007: Digitales Höhenmodell Basis Quartär (DHM B_QU, "Felsmodell") - Grundlagen, Erarbeitung, Ergebnisse, Stand Juni 2007. Nagra Arbeitsbericht NAB 07-12.
- Jordan, P. 2010: Analysis of overdeepened valleys using the Digital Elevation Model of the bedrock surface of Northern Switzerland. Swiss Journal of Geosciences (in press).

14.12

WPS application for shallow landslide hazard assessment

Molinari Monia Elisa¹, Cannata Massimiliano¹, Troung Xuan Luan²

¹ *Institute of Earth Sciences – SUPSI, Trevano, C.P 72, CH-6952 Canobbio*

² *Hanoi University of Mining and Geology – Dong Ngac, Tu Liem, Hanoi, Vietnam*

This research aims to illustrate the development of a web-based framework for shallow landslide hazard assessment. These phenomena, generally triggered by intense rainfall, are often extremely dangerous and they can cause severe damage to infrastructure and population; mathematical models can be an important resource to reduce this risk allowing the assessment of where shallow landslide may occur and what area is involved.

The application we propose couples two models widely used for landslide hazard assessment, TRIGRS (Baum et al., 2008) and DFWALK (Cannata & Molinari, 2008), respectively capable to estimate instabilities areas and runout extents.

The procedure has been performed using the standard OGC WPS (Web Processing Service) which allows to produce geoprocessing services and provides them to different client platforms. WPS (OGC, 2005) defines a standard communication through Internet between client and server: it establishes how a client has to submit a processing task to a server and how the outputs of the process are delivered. It offers three types of requests: DescribeProcess to have information about the available processes, GetCapabilities to know the input parameters and the generated outputs of a process and Execute to invoke the execution of the process.

Through the procedure implemented the client provides rainfall data and obtains in real time the landslide hazard maps created by the simulation models; a user-friendly interface has been realized to insert the data and visualize the maps.

REFERENCES

- Baum R.L., Godt J.W., Savage W.Z., 2008: TRIGRS – A fortran program for transient rainfall infiltration and grid-based regional slope-stability analysis, Version 2.0. U.S. Geological Survey Open-File Report 08-1159.
- Cannata M., Molinari M.E., 2008: Natural Hazard and Risk Assessment: the FOSS4G, Proceeding of the 2008 Free and Open Source Software for Geospatial Conference, Cape Town, South Africa.
- OGC, 2005: OpenGIS Web Processing Service, document available on www.opengeospatial.org/standards

14.13

Comparison of Cubic Splines and Linear Interpolation Methods for Lake Time Series Analysis

North Ryan P., Livingstone David M.

*Swiss Federal Institute of Environmental Science and Technology (EAWAG), Überlandstrasse 133, CH-8600 Dübendorf
(ryan.north@eawag.ch)*

Understanding the impact of climate change on aquatic systems is only possible through detailed study over long periods of time. Analysis of spatial and temporal time series observations has the potential to allow the interpretation of changes to aquatic systems. However, long and complete time series are rare. Field measurements often include gaps of missing data and irregular measurement intervals. In order to properly analyze time series, regularly spaced, complete time series are needed. Using available data, interpolation fills gaps and creates regularly spaced intervals. The challenge is to select the ideal interpolation method from the wide range of available techniques.

Cubic spline and linear interpolation methods are compared for temporal and spatial (profile) interpolation of lake data. The comparison methodology creates artificial gaps in a long time series and uses interpolation to replace them. This is repeated over the whole data set for varying gap lengths and for four variables (temperature, oxygen, phosphorus and chloride). The accuracy is determined using the normalized root mean square error (RMSE) of the interpolated value in relation to the measured value.

Results indicate that the choice of method is dependent on the type of interpolation (temporal or spatial) as well as the variable. The latter is related to the change in time series and profile shape with a variable. In general, the simpler linear method proves more or equally as accurate as the cubic spline method.

14.14

Geology Portal - Enhancing the availability of geological information

Oesterling Nils & Kühni Andreas

Swiss Geological Survey, Federal Office of Topography swisstopo, Seftigenstrasse 264, CH-3084 Wabern (nils.oesterling@swisstopo.ch)

Main tasks of the Swiss Geological Survey (SGS) are to collect geological, geotechnical and geophysical data, to transform this data into information and to make both available to related fields of expertise and to the public (Kühni & Oesterling 2009). Responding to the fast growing demand on digital geological information the SGS sped up its internal processes by integrating GIS methods into the map production cycle (Kühni et.al. 2006) and designed a Geological Information System aiming to facilitate the access to digital data for the customers of the SGS (Oesterling et al. 2009, Oesterling 2009).

- The major objectives of the Geological Information System are:
- Improve accessibility to all data/information relevant to geology
- Give an overview of tasks, responsibilities etc. of the Swiss Geology Community
- Increase the awareness of the importance of geological data/information in the public

Public access via the internet ensures the accessibility to the above mentioned data/information and is crucial for the success and the acceptance of the information system. In order to guarantee this web accessibility the Geology (Web-) Portal is being built up.

The conceptual basis for the web portal including the definition of goals, target groups, architecture etc. was finished end 2009 (Oesterling 2009). Furthermore the system boundaries between the Geological Information System (technical backbone), the Geology Portal (central gateway to the Geological Information System) and the embracing organisation (defining rules, content and processes) have been defined.

As the Swiss Geology Community is rather heterogeneous and a vast number of potential content for the information system already exists, coordination between the players of the Geology Community is the key factor. The fact that when putting up a web portal which aims to integrate content from all the different players in Switzerland all of these have to be involved into the conceptual phase of the project goes without saying.

In order to incorporate the different needs concerning content, structure, functionality, design etc., a working group has been established. It comprises members of the following organisations:

- Platform Geosciences of the Swiss Academy of Science (SCNAT): Representing the academic sectors needs
- Swiss Association of Geologists (CHGEOL): Representing the private sectors needs
- Swiss Geotechnical Commission (SGTK): Representing the academic and private sectors needs
- Swiss Geophysical Commission (SGPK): Representing the academic sectors needs
- SGS: Representing the administrative sectors needs

Since the demand for digital geological data/information is continuously growing, it is important to develop and to provide the Geology Portal as soon as possible. Therefore a two-step approach is followed:

- Develop an initial version of the Geology Portal. Use existing IT infrastructure. Accept imperfectness. Goal: Go Live as soon as possible (planned spring 2011)
- Redefine technical needs and develop necessary applications and services. Implement the second version of the Geology Portal into the technical infrastructure of the National Spatial Data Infrastructure (NSDI) which is in the process of being established. Goal: Detect user needs during the operative phase of the initial version of the Geology Portal. Improve the portal and Go Live in 2012-13

The Geology Portal is intended to be the central gateway to geological information. Geological data/information (maps, datasets etc.) as well as information on the Swiss Geology Community will be easily accessible for all users from professional geologists to layman.

REFERENCES

- Kühni A., Oesterling N., Sartori M., and Jaboyedoff M. (2006): Integration of GIS into the geological map production cycle of the Swiss Geological Survey, 5th European Congress on Regional Geoscientific Cartography and Information Systems (ECONGEO-06) proceedings, volume 2, 177-179
- Oesterling, N., Kühni, A. and Kündig, R. 2009: The Geological Information System Switzerland, 6th EUREGEO Proceedings, Volume 1, 235-237.
- Kühni, A. & Oesterling, N. 2009: Towards a Swiss Geological Information System, 7th Swiss Geoscience Meeting, Neuchâtel Proceedings, 245-246
- Oesterling, N. 2009: Geological Information System Switzerland – Supplying geoscientific geoinformation to the NSDI, Master Thesis, UNIGIS MSc programme, Salzburg University

14.15

Multi-scale, multimedia modeling to compare local and global life cycle impacts on human health

Wannaz Cedric¹, Fantke Peter², Friedrich Rainer², Jolliet Olivier¹

¹ The University of Michigan, School of Public Health, 1415 Washington Heights, 48109-2029 Ann Arbor, USA
(wannaz@umich.edu, ojolliet@umich.edu)

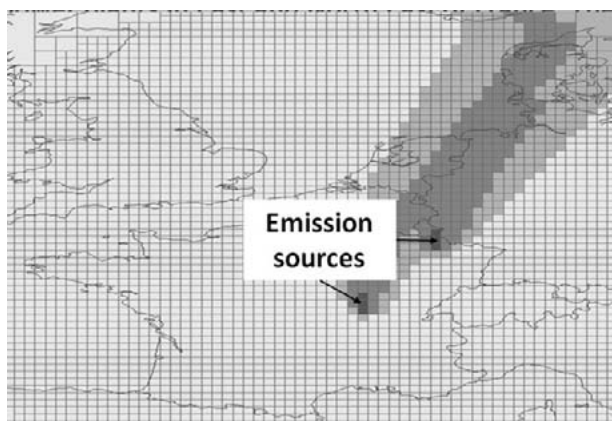
² University of Stuttgart, Institute of Energy Economics and the Rational Use of Energy, Germany
(peter.fantke@ier.uni-stuttgart.de, Rainer.Friedrich@ier.uni-stuttgart.de)

How can we quantify and consistently compare local and global impacts of pollutants that undergo multimedia fate and lead to multi-pathway exposure?

To address this question, there is a clear need to utilize a multimedia approach. However, none of the currently published and operational multimedia models is able to properly reflect local to global impacts.

This study therefore develops and implements a flexible multi-scale modeling framework named Pangea, which allows us to model chemical fate and population exposure, obtaining steady-state and dynamic solutions at local to global scales. It was presented at SETAC 2010 (Jolliet et al., 2010). This model allows us to study the local and global spatial impacts of various pollutants, as illustrated for the fate and exposure of 1,2-Dichlorobenzene (figures 1, 2). A crucial feature is its ability to dynamically generate problem-specific multi-scale grids in air, water, and terrestrial media, which significantly reduces calculation time to only include high resolution where needed (illustrated in (fig. 3) for the air). We obtain this flexibility by extending the Pangea core engine with the ArcGIS Geoprocessor. This allows parameterization of the model using GIS datasets (windspeed, river network, population, etc) specific to each study. These datasets can be used as potentials for refinement (e.g. population density and proximity to source) that drive the grid refinement, and they are dynamically projected on the grids.

As an illustration, we compare the local impact (in the emission cell) to the global impact of a pollutant emitted from two coal power plants. For pollutants with long residence time in air like 1,2-Dichlorobenzene, figure 2 shows that the long distance population intake from a 1,2-Dichlorobenzene point source can be much higher (98.5%) than the local intake within the emission cell. Specifically, the emissions from two coal power plants in the East and North-East of France have most of their impacts occurring in western Germany due to the high population density of that region and the prevalent wind direction.



The ability of this engine to have high resolution in places of interest with a coarser grid elsewhere (made feasible by its interaction with GIS) allows increased accuracy while keeping the computational requirements reasonably low.

Figure 1. Resulting air concentrations [in kg/m³] for a 1 kg/day 1,2-Dichloro-benzene emission from two coal power plants in East and North East of France. This chemical has a half-life in air of 21.1 days.

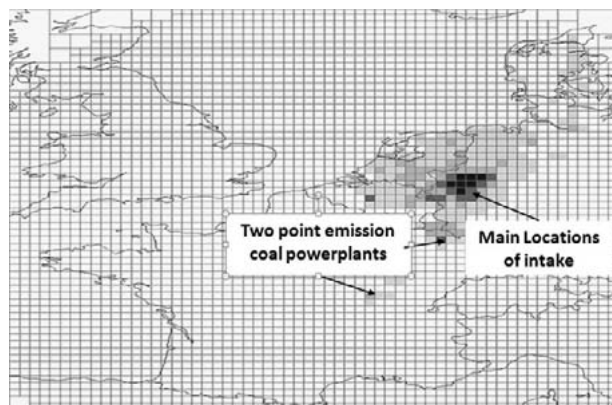


Figure 2. Intake map of 1,2-Dichloro-benzene due to emissions at two coal powerplants in France. The highest impacts occur for regions that have both high air concentrations and high populations. Only 1.5% of the total intake is inhaled at the emission location, compared with 98.5% in the rest of Europe, mostly in western Germany.

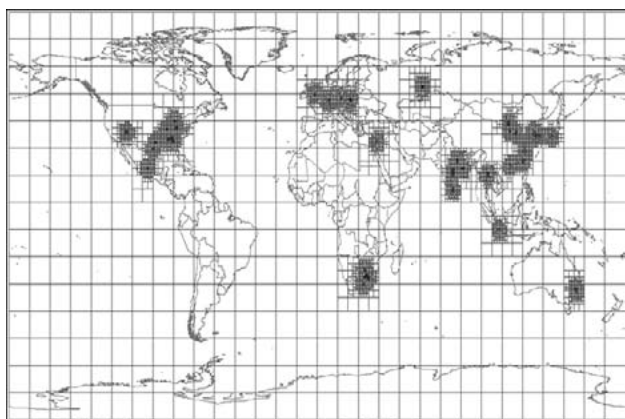


Figure 3. Global multi-scale grid. This new engine allows us to have a high resolution in places of interest, while keeping the numerical dimension and data requirements low elsewhere.

REFERENCES

- Jolliet, O., Wannaz, C., Fantke, P., 2010. Multiscale, Multimedia modelling to compare local and global life cycle impacts on human health. Conference Proceedings, SETAC Europe 20th Annual Meeting “Science and Technology for Environmental Protection”, Seville, Spain.

14.16

An integrated methodology for change detection via terrestrial laser-scanning: case study of the landslide in Flamatt

Jing Wu, Pierre-Yves Gilliéron, Bertrand Merminod

Laboratoire de Topométrie, Ecole Polytechnique Fédérale de Lausanne (EPFL) Bâtiment GC, Station 18, CH-1015 Lausanne

Email: jing.wu@epfl.ch, pierre-yves.gillieron@epfl.ch, bertrand.merminod@epfl.ch

Landslides are natural phenomena, which mainly affect mountainous regions. During the last 36 years (1972-2007), an average annual financial damage about 20 millions CHF and an average of 1 death per year are directly caused by landslides in Switzerland (Hilker et al., 2009). The impact of this dynamic process depends primarily on its size, speed and location, especially when crossing infrastructure or constructions. Due to the complexity of the phenomena, the monitoring of landslide is still a challenge and can also be expensive according to its location.

For decades landslides have been studied with classical surveying techniques like theodolites, photogrammetry, levels and more recently GPS (Global Positioning System) (Noverraz et al, 1998). These techniques mostly focus on the monitoring of specific points (landmarks, geodetic control network, etc.) with time series of coordinates. Another approach is now possible with the laser scanning which is an excellent candidate for the fast and dense data acquisition of the ground surface. The acquisition of a large number of points (called point clouds) is used for the identification of geomorphological features. Point clouds allow a surface-based analysis, especially when a multi-epoch comparison is required in change detection.

Usually the instability is induced by natural process such as heavy rainfall or by man-made activities including road or building construction, land use changes, etc. The size of the area can vary from some square metres to several square kilometres.

The estimation of the ground surfaces movements, called change detection, is mainly based on terrain models which provide a uniform spatial and/or temporal interpolation such as algebraic polynomials and spline functions for the whole region (Dermanis et. Al., 2006). These models are focusing on the monitoring of some pre-selected partial regions with a priori knowledge. In contrast, our approach is to generate a more informative description automatically – so called “deformation map” (i.e. providing analysis of 3D displacements including horizontal movement, vertical movement, rotations, etc. for different partial regions), without any prior information. This “deformation map” can be computed by a so called “split/merge” approach. At this stage of the development, we present this preliminary algorithm for the estimation of the subsidence along the Z direction.

Firstly, space of the whole terrain region is split into many continuous and adjacent 3D uniform cells. By using R-tree spatial access method (Manolopoulos et al., 2005), the point clouds inside a given cell of two epochs can be acquired efficiently. The cell size has a high impact on the ability to detect changes. Secondly, the detection of movements between epochs is mainly based on the following statistical parameters: the minimum value of the elevation (Z value), its mean, its median, its maximum or its value in the center of the cell, as obtained by a surface regression on the points contained in the cell. All these parameters are applied to each cell. The change of each cell is described by a subsidence value. Then we can compare the effects of using different parameters by the subsidence distribution. Thirdly, the computed subsidences for all the cells are merged and presented in a map of subsidence. In this procedure, the adjacent cells with similar values for the changes are combined together and small discrepancies between neighbouring cells are considered as noise and are removed.

Our approach has been applied for a landslide near Flamatt, Switzerland, which has affected a major railway line. The map of the subsidence (Fig. 1) illustrates:

- most subsidence values of this region are centred around 0 m;
- part in the middle has decreased: - 0.2 m;
- lower edge has slightly increased: + 0.2 m;
- two spots of this area have increased: more than + 0.5 m.

While a., b., and c. have a predominantly natural cause, d. is due to earthworks realized to allow construction vehicles to access the site. Fig 2 shows the subsidence distribution of this region by using different detection parameters (min, max, median, mean and center). Fig. 2 (a), (b), (c) and (d) shows the results with similar distribution. However, some residual noises still remain in the result of centre method which needs to be improved (Fig 2 e.).

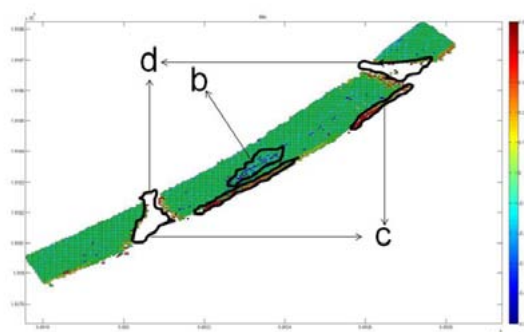


Figure 1: The map of subsidence for the railway embankment (Flamatt)

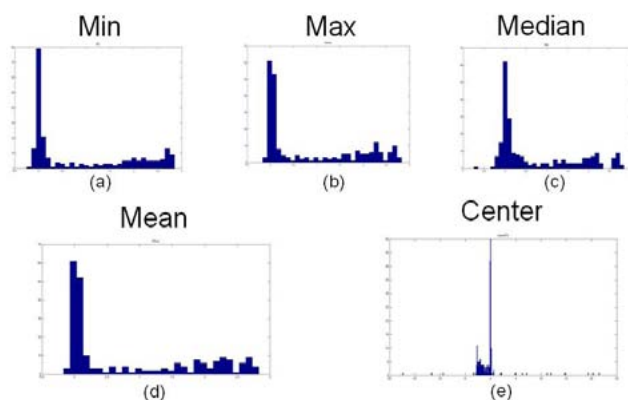


Figure 2: Distribution of the subsidence of different parameters

ACKNOWLEDGMENTS

Many thanks to the CFF (Swiss federal railway company) and the BBHN SA (surveying company) for the provision of laser-scanning data from the Flamatt region.

REFERENCES

- Dermanis, A. & Kotsakis, C. 2006: Estimating Crustal Deformation Parameters from Geodetic Data: Review of Existing Methodologies, Open Problems and New Challenges, *Geodetic Deformation Monitoring: From Geophysical to Engineering Roles*, Springer Berlin Heidelberg, 131, 7-18.
- Hilker, N., Badoux, A., & Hegg, C. 2009: The Swiss flood and landslide damage database 1972-2007, *Natural Hazards and Earth System Science*, 9, 913-925.
- Manolopoulos Y., Nanopoulos A., Papadopoulos A.N. & Theodoridis Y. 2005 : *Rtrees: Theory and Applications*. Series in Advanced Information and Knowledge Processing, ISBN: 1-85233-977-2, Springer.
- Noverraz, F., Bonnard, C., Dupraz, H. & Huguenin, L. 1998: *Grands glissements de versants et climat. Rapport final PNR 31*. Zürich, vdf – Hochschulverlag AG, ETH Zürich, 1998, 314 p.

15. Decision oriented modelling of the geosphere

M. Stauffacher, O. Smrekar, C. Ritz, H.-R. Egli

*Swiss Academic Society for Environmental Research and Ecology (SAGUF),
Swiss Geography Association,
Proclim*

- 15.1 Bugmann H.: Global Change, Goods and Services from Mountain Ecosystems, and Stakeholders
- 15.2 Hauck C., Hölzle M., Salzmann N.: Communication of uncertain cryospheric model results in the view of the public environmental awareness
- 15.3 Scheringer M.: How free are we in our choices of methods for scientific work in transdisciplinary projects?
- 15.4 Schneider F.: Bridging science and society through transdisciplinary research
- 15.5 Zinsstag J.: Cross-species transmission modelling and economics of zoonotic diseases

15.1

Global Change, Goods and Services from Mountain Ecosystems, and Stakeholders

Harald Bugmann*

* Forest Ecology, Institute of Terrestrial Ecosystems, Department of Environmental Sciences, ETH Zürich, 8092 Zurich
(harald.bugmann@env.ethz.ch)

Mountain regions and their ecosystems fulfill a multitude of functions, from freshwater provision and carbon storage to aesthetic beauty. The fate of the vegetation cover of mountain regions under a changing climate, changing land use and changing atmospheric composition is important for the capability of ecosystems to provide many of the goods and services that humanity depends on. In mountain ecosystems, several factors are of crucial importance that may be nearly negligible elsewhere, such as slope stabilization by root systems. These factors are often interlinked, making the integrity of mountain systems dependent on the integrity of their weakest element.

In the context of the EU project ATEAM, we have addressed these issues by taking into account stakeholder views as an integral component of the research. What may appear frightening at first sight, including the need to discuss the research questions with non-scientists, turned out to be highly fruitful, shaping the project in ways that we would not have anticipated.

In this presentation, I will outline the setup of the project, introduce the stakeholder dialogue, and discuss selected scientific results from the project, thereby pointing out the pivotal role that stakeholders played in the project.

15.2

Communication of uncertain cryospheric model results in the view of the public environmental awareness

Christian Hauck, Martin Hoelzle and Nadine Salzmann *

** Department of Geosciences, University of Fribourg
(martin.hoelzle@unifr.ch)*

The currently undergoing strong changes in the cryosphere are caused by changes in the atmosphere, leading to related impacts through natural hazards such as rock falls and debris flows. Authorities and the public are aware of these processes and demand a better prediction of such events from the scientific community. However, the process knowledge and the corresponding knowledge about the uncertainties within this field are still severely limited. Today, sophisticated model approaches to couple whole process chains (e.g. climate – cryosphere – subsurface – instability – natural hazard – impact) are increasingly applied by using regional climate model output as direct input for local scale cryosphere models. However, such processes oriented modelling approaches across different temporal and spatial scales are challenging and include the treatment of the large uncertainties involved. The question arises then for the scientists how to communicate the existing uncertainties of all these model results to the public and/or the authorities. Despite the considerable uncertainties, we believe that the current climate – cryosphere models are the only tools to provide plausible scenarios for the future, and with appropriate usage they furnish sound support for decision makers.

15.3

How free are we in our choices of methods for scientific work in transdisciplinary projects?

Martin Scheringer *

** Institute for Chemical and Bioengineering, ETH Zürich
(scheringer@chem.ethz.ch)*

An important driver for scientific progress is the goal that scientists aim to use methods that are as advanced as technically and conceptually possible, and to continuously improve these methods. This motivation is characteristic of the academic and often disciplinary context, but it is also limited to this context; it cannot be easily reconciled with the need for robust, transparent and not overly expensive methods suitable for practical applications. In other words, there is a tension between method-focused progress within individual disciplines and the need for broadly applicable methods in transdisciplinary research.

In what way can it be justified to use in transdisciplinary research methods that are less sophisticated and advanced than current state-of-the-art methods? This question will be discussed in the context of environmental chemistry and chemical risk assessment. Chemical risk assessment encompasses both poles, scientific research aiming to improve methods, concepts and data bases as well as practical implementation by government authorities, international organizations, and industry.

REFERENCE

Jaeger J., Scheringer M. 1998. Transdisziplinarität. Problemorientierung ohne Methodenzwang. GAIA 7(1): 10-25

15.4

Bridging science and society through transdisciplinary research - insights from theory and practice on stakeholder involvement in sustainability research in Switzerland and Developing Countries

Flurina Schneider

*Centre for Development and Environment (CDE), University of Bern, Hallerstrasse 12, 3012 Bern
(flurina.schneider@cde.unibe.ch)*

Based on a summary of the state of the art of theory on sustainability science we show that the most appropriate way for bridging science and society is through transdisciplinary approaches of knowledge co-production between scientists and non-academic stakeholders related to a certain societal defined research question. How are the theoretical concepts implemented into practice, and which are key challenges, potentials and limitations of stakeholder involvement in the solution of real world problems? Such questions will be discussed on the basis of concrete cases representing experiences of CDE in Switzerland (MontanAqua, NFP61) and the Swiss National Centre of Competence in Research (NCCR North-South).

15.5

Cross-species transmission modelling and economics of zoonotic diseases

Jakob Zinsstag *

** Swiss Tropical and Public Health Institute, PO Box, 4002 Basel
(jakob.zinsstag@unibas.ch)*

Zoonotic diseases are transmissible between animals and humans. Bovine Spongiform Encephalitis (BSE), Rabies, Bovine Tuberculosis and Brucellosis have been eliminated in many industrialized countries with massive state intervention and good veterinary and public health management. However most of the developing countries have insufficient means and technical capacity to eliminate such diseases. Prior to engaging in such efforts, developing countries need more information on the profitability and cost-effectiveness of such interventions. We have estimated the profitability and cost-effectiveness of brucellosis control in Mongolia and Rabies control in N'Djaména, Chad, using highly reductionist deterministic models between animals and humans. These models were as much as possible adapted to the decision criteria of the local authorities. The tradeoff between reductionism and urgent need for evidence will be discussed in the framework of transdisciplinary engagement between science and policy.

16. Hydrological and Limnological Perspectives in Times of Global Changes

Petra Schmocker-Fackel, Beat Oertli, Bruno Schädler

*Swiss Society for Hydrology and Limnology (SGHL / SSSL),
Swiss Hydrological Commission (CHy)*

- 16.1 Balin D., Schulla J., Lambiel C., Scapozza C., Metzger R., Horton P., Reynard E.: Hydrological modelling under present and future scenarios in two alpine catchments
- 16.2 Davin E. L., Seneviratne S. I.: The role of diffuse/direct radiation partitioning in land-atmosphere interactions and terrestrial water cycling
- 16.3 De Jong R., Kamenik C., Larocque-Tobler I., Grosjean M.: Aquatic organisms as indicators of past climate variability
- 16.4 Doering M., Blaurock M., Robinson C.T.: Landscape transformation of an Alpine floodplain influenced by humans: Historical analysis from aerial images
- 16.5 Giuliani G., Ray N., Lehmann A.: Modelling global changes impacts on the Black Sea catchment
- 16.6 Halder J., Decrouy L., Vennemann T.: Hydrodynamics of Lake Geneva inferred from Stable H- and O-Isotope Compositions
- 16.7 Hines J., Gessner M.: Life-history plasticity in a detritivore determines ecosystem response to climate warming
- 16.8 Kauzlaric M., Rey E.: Approaching water stress in the Alps- Water management options in the Crans-Montana-Sierre region, Valais (MontanAqua): estimation of available natural water resources
- 16.9 Köplin N., Viviroli D., Schädler B., Weingartner R.: Hydrological change in Switzerland: Which catchments are most sensitive? - A comprehensive assessment of climate change impact
- 16.10 Leuzinger S., Körner C.: Rainfall distribution is the main driver of runoff under future CO₂-concentration in a temperate deciduous forest
- 16.11 Magnusson J., Jonas T., Kobierska F., Farinotti D., Zappa M., Bavay M., Bosshard T.: Climate change effects on snow melt and discharge of a partly glacierized watershed in central Switzerland
- 16.12 Meyer R., Schädler B., Viviroli D., Weingartner R.: Low water in a changing climate
- 16.13 Niemann H., Anselmetti F. S., Sinninghe Damsté J. S., Gilli A., Lehmann M. F., Peduzzi R., Peduzzi S., Ravasi D., Sax N., Schubert C. J., Stadnitskaia A., Stötter T., Tonalla M., Wirth S. B.: The Holocene sediment record of Lake Cadagno: Over-view and initial results from a comprehensive paleoenvironmental study
- 16.14 Rey E., Kauzlaric M.: Approaching water stress in the Alps – Water management options in the Crans-Montana-Sierre region, Valais, (MontanAqua): Measuring network and influence of land use and land use changes on water balance.
- 16.15 Rosset V., Oertli B.: Freshwater biodiversity under climate warming pressure: identifying the winners and losers in temperate small waterbodies
- 16.16 Schilder J., Heiri O., Van Hardenbroek M., Lotter A.: Stable nitrogen isotopes in chitinous remains: Exploration of a new palaeoenvironmental proxy for past freshwater environments
- 16.17 Staudinger M., Seibert J., Stahl K., Lehner I.: Towards uncertainty reduction of low flow modeling using $\delta^{18}\text{O}$ as additional information

16.1

Hydrological modelling under present and future scenarios in two alpine catchments

Balin Daniela¹, Schulla Jörg², Lambiel Christophe¹, Scapozza Cristian¹, Metzger Richard³, Horton Pascal³ & Reynard Emmanuel¹

¹ Institut of Geography, University of Lausanne (daniela.balin@unil.ch)

² Hydrology Software Consulting, Zürich

³ Institute of Geomatics and Risks, University of Lausanne

This study intends to presents the main results of a two-year research that was done within the frame of a SNF Marie Heim-Vögtlin program that aimed to model the coupled hydro-geomorphologic system and to evaluate its hazard potential in two contrasting catchments, in south-western Switzerland under uncertainty and from the climate change perspective.

The study catchments are represented by the Avançon catchment (80 km²), that include as head catchment the Vallon de Nant catchment - a natural reserve and the experimental basin of the Environmental and Geosciences Faculty from University of Lausanne, and the Tinte catchment (10km²), a small catchment in the Verbier basin with a strong human impact.

One of the latest versions of the WASIM-ETH model (Schulla, 1997), that includes among others a glacier, snow, permafrost and slope instability modules, was used to simulate the water balance and slope instability in the two catchments at daily and hourly time steps. The uncertainty in the hydrological modelling was quantified by means of a Bayesian Monte Carlo Markov Chains approach (Balin et al, 2010, Balin et al, 2010). This approach enables computation of uncertainty due to the model parameters and the predictive uncertainty which includes in a lumped way other sources of uncertainty (i.e. input and model structure). The scenarios used in the present study are issued from the dynamic REMO-UBA regional model (Jacob, 2008) and will enable identifying the trend and the most important impacts of the changing climate on the hydro-geomorphologic hazards in two study catchments. The year 2050 has been chosen as projected horizon of the climate scenarios as (1) the climatic scenarios are more likely to happen and (2) this is more likely to interest the decision making and to influence the present challenges of the society in high alpine regions.

REFERENCES

- Balin Talamba, D., E. Parent, and A. Musy 2010: Bayesian multiresponse calibration of TOPMODEL: Application to the Haute-Mentue catchment, Switzerland, *Water Resour. Res.*, 46, W08524, doi:10.1029/2007WR006449.
- Balin, D., H. Lee, and M. Rode 2010: Is point uncertain rainfall likely to greatly impact on distributed complex hydrological modelling?, *Water Resour. Res.*, doi:10.1029/2009WR007848, *in press*.
- Jacob D, Göttel H, Kotlarski S, Lorenz P, Sieck K. 2008: Klimaauswirkungen und Anpassung in Deutschland – Phase 1: Erstellung regionaler Klimaszenarien für Deutschland. Abschlussbericht zum UFOPLAN-Vorhaben 20441138, Max-Planck-Institut für Meteorologie (MPI-M), Hamburg.
- Schulla, J. 1997. Hydrologische Modellierung von Flussgebieten zur Abschätzung der Folgen von Klimaänderungen. *Zürcher Geographische Schriften*, Heft 69. ETH-Zurich, Geographisches Institut (in German), p. 161.

16.2

The role of diffuse/direct radiation partitioning in land-atmosphere interactions and terrestrial water cycling

Davin Edouard¹ & Seneviratne Sonia¹

¹Institute for Atmospheric and Climate Science, Universitätstrasse 16, CH-8092 Zürich (edouard.davin@env.ethz.ch)

The nature of light (diffuse or direct) and not only its quantity is important for ecosystem functioning. In particular plant photosynthesis is sensitive to the partitioning between diffuse and direct light. This has implications not only for the carbon cycle but also for water cycling, since photosynthesis is tightly coupled to plant transpiration.

In order to quantify the effect of diffuse/direct radiation partitioning on surface fluxes and climate, we use the newly developed COSMO-CLM² model. COSMO-CLM² is a coupled biosphere-atmosphere Regional Climate Model (RCM) combining the COSMO-CLM atmospheric model and the NCAR Community Land Model. An evaluation of the model against observations will first be presented.

A set of diffuse/direct radiation partitioning experiments over Europe will then be analyzed. Two situations are compared: a first situation where the proportion of diffuse versus direct light (constituting surface incoming shortwave radiation) is set constant temporally and spatially; a second situation where the land model explicitly receives diffuse and direct short-wave components as calculated by the atmospheric radiation scheme. Comparison with observations reveals that the atmospheric radiation scheme provides a rather realistic description of diffuse/direct radiation partitioning at the surface (more direct light in summer compared to winter, more diffuse light with increasing latitude, etc). This in turn has a strong influence on photosynthesis and transpiration. However, the effect on total evapotranspiration is limited, due to the existence of a compensating mechanism involving ground evaporation. For this reason the overall impact on the European climate remains relatively small. We note however that the effect of diffuse/direct radiation partitioning might be stronger for more productive ecosystems such as tropical forests. To shed some light on this question, similar experiments over Africa are currently under way.

16.3

Aquatic organisms as indicators of past climate variability

De Jong Rixt, Christian Kamenik, Isabelle Larocque-Tobler & Martin Grosjean

Oeschger Centre for Climate Change Research and Institute of Geography, Bern University, Erlachstrasse 9a, CH-3004 Bern (dejong@giub.unibe.ch)

Aquatic organisms such as chironomids (non-biting midges), diatoms and chrysophytes (golden-brown algae) are known to be sensitive to changes in e.g. lake water chemistry, nutrient levels and the availability of light. However, they may also be highly sensitive to air temperature, which makes the sedimentary remains of these organisms very promising proxies for climatic reconstructions. The head-capsules of chironomid larvae are generally well-preserved in lake sediments. Since the temperature optimum and tolerance range of these are known for the Swiss Alpine region, these can be used to reconstruct past July temperatures (Larocque-Tobler et al., 2010). Chrysophyte algae produce siliceous cysts that are also preserved in lake sediments. Previous work in the Austrian (Kamenik and Schmidt, 2005) and Swiss (De Jong and Kamenik, *in press*) Alps and the Pyrenees (Pla and Catalan, 2005) has demonstrated their sensitivity to cold-season temperatures. The total biogenic silica (bSi) content of sediment samples was also shown to be a potential proxy for June-July-August temperatures (Trachsel et al., *in press*).

In these studies (Larocque-Tobler et al, 2010; De Jong and Kamenik, *in press*; Trachsel et al., *in press*) detailed analyses of bSi, chrysophyte cysts and chironomid head capsules were conducted on the varved sediments of Lake Silvaplana (Engadine, 1800 m asl). Here we present a reconstruction of winter and summer temperatures covering the past 1000 years at near-annual resolution. Comparison to independent records (meteorological timeseries, other proxy records) shows that these methods yield excellent results for the Alpine region (Fig. 1). This study clearly highlights the potential of aquatic organisms as proxies for past temperature variability.

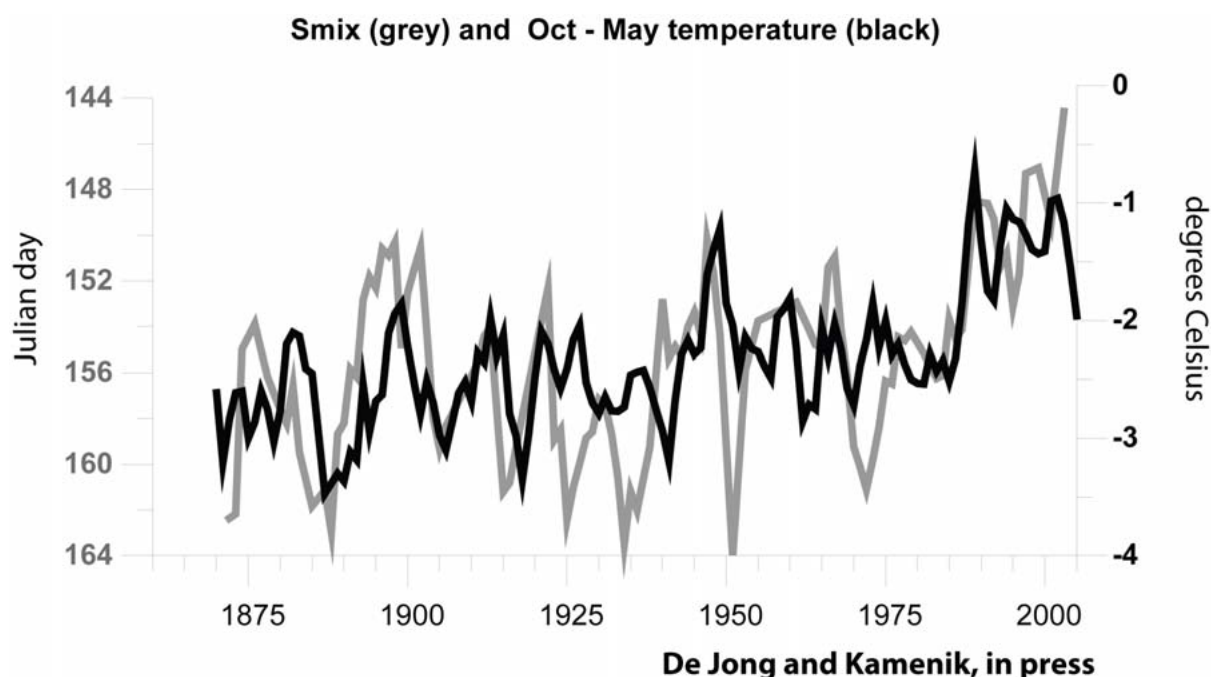


Figure 1: Comparison of reconstructed climate parameter Smix (date of spring mixing, based on chrysophyte stomatocysts, grey line) with measured Oct- May temperatures from Sils Maria (black line) (from De Jong & Kamenik, *in press*)

REFERENCES

- De Jong R & Kamenik C: Validation of a chrysophyte stomatocyst-based cold-season climate reconstruction from high-Alpine Lake Silvaplana. *Journal of Quaternary Science*, *in press*
- De Jong R, Kamenik C & Grosjean M, in prep: Alpine cold-season temperature during the past millennium
- Kamenik C & Schmidt R, 2005: Chrysophyte resting stages: a tool for reconstructing winter/spring climate from Alpine lake sediments. *Boreas* 34: 477-489.
- Larocque-Tobler I et al, 2010: Thousand years of climate change reconstructed from chironomid subfossils preserved in varved lake Silvaplana, Engadine, Switzerland. *Quaternary Science Reviews*, *in press*
- Pla S & Catalan J, 2005: Chrysophyte cysts from lake sediments reveal the submillennial winter/spring climate variability in the northwestern Mediterranean region throughout the Holocene. *Climate Dynamics* 24: 263-278.
- Trachsel M et al. *in press*: Quantitative summer temperature reconstruction derived from a combined biogenic Si and chironomid record from varved sediments of Lake Silvaplana (south-eastern Swiss Alps) back to AD 1177. *Quaternary Science Reviews*.

16.4

Landscape transformation of an Alpine floodplain influenced by humans: Historical analysis from aerial images

M. Doering, M. Blaurock and C.T. Robinson

Natural floodplains are among the most productive and biologically diverse ecosystems worldwide, but they are also among the most endangered due to climate change and human impacts such as water storage, flood control and hydro-power production (Tockner & Stanford, 2002). Floodplains are composed predominantly of different aquatic (e.g. channel and pools) and terrestrial (e.g. riparian forests, islands, gravel bars) habitats affected by major hydrological forces that shape habitat heterogeneity and distribution, and channel migration and turnover (Whited. et al., 2007). Despite their highly dynamic nature, the relative abundance of different habitat elements in natural floodplains seems to remain more or less constant over ecological time periods. This phenomenon is also described as the “shifting mosaic steady state” by Ward et al. (2002). Therefore, spatial changes in habitat heterogeneity and abundance can be used to quantify the effects of human interference such as from flow regulation and water abstraction that have profoundly changed most braided alpine floodplains (Kollmann et al., 1999). We investigated the spatio-temporal transformation of floodplain habitats and channel complexity for a 3.4-km long and up to 600-m wide alpine floodplain (Sandey, Innertkirchen, Canton Bern, 850 m a.s.l.) from its near natural state in 1940 to 2007 by analyzing a series of historical aerial images. Indices such as the

braiding index (Thalweg length main channel/ thalweg length main and side channel) and shoreline length ratio (shoreline length/river length) were derived from the analysis. Within this time period, the floodplain was subject to several hydrological and morphological modifications that included water abstraction (ca. 30 % of average annual discharge) in the upper catchment (from 1950) and the construction of several levees within the active floodplain. Results showed that habitat heterogeneity and channel complexity changed substantially between 1940 and 2007. We could distinguish two main time periods of change. First, a period from 1940 to 1986 with strong decreasing habitat heterogeneity, e.g. more than 90% of island area lost and parafluvial areas (gravel areas without established vegetation that are frequently flooded) decreased by about 34%. Channel complexity was also reduced as indicated by the braiding index and shoreline length ratio changing from 1.8 to 1.3 and 3.1 to 2.4, respectively. Second, a period from 1986 to 2007 when habitat heterogeneity and channel complexity partly recovered. Islands were reestablished in the system (area increase of 50%) and the parafluvial area increased by about 64%. The braiding index and shoreline length ratio increased to 1.6 and 2.9, respectively. This increase in habitat heterogeneity and channel complexity parallels an increasing yearly frequency of high precipitation events ($> 60 \text{ mm } 24 \text{ h}^{-1}$) in the region. However, habitat and channel conditions are still below the status before floodplain impairment by humans. The study clearly demonstrates the negative effect of water abstraction and flood protection on habitat heterogeneity and channel complexity of the floodplain but also raises the question whether elevated frequencies of high flow events induced by climate change can contribute to floodplain restoration.

REFERENCES

- Kollmann, J., Vieli, M.; Edwards, P.J., Tockner, K. & Ward, J.V. (1999) Interactions between vegetation development and island formation in the Alpine river Tagliamento. *Applied Vegetation Science*, 2, pp. 25-36
- Tockner, K., Stanford, J.A. (2002) Riverine flood plains: present state and future trends. *Environmental Conservation*, 29, pp. 308-330
- Ward, J.V., Tockner, K., Arscott, D. B., et al. (2002) Riverine landscape diversity. *Freshwater Biology*, 47, pp. 517-539
- Whited, D. C., Lorang, M. S., Harner, M. J., et al. (2007) Climate, hydrologic disturbance, and succession: Drivers of floodplain pattern. *Ecology*, 88, pp. 940-953

16.5

Modelling Global Changes Impacts on the Black Sea Catchment

Giuliani Gregory^{1,2}, Ray Nicolas^{1,2}, Lehmann Anthony^{1,2}

¹ Université de Genève, Institut des Sciences de l'Environnement, Route de Drize 7, CH-1227 Carouge

² UNEP/DEWA/GRID-Europe, Maison Internationale de l'Environnement, Chemin des Anémones 11, CH-1219 Châtelineau

The Black Sea Catchment is recognized for its great historical and cultural value, but also for its ecologically unsustainable development and inadequate resource management leading to severe environmental, social and economical problems. The EU FP7 EnviroGRIDS @ Black Sea Catchment project (www.envirogrids.net) is addressing these issues by bringing several new emerging information technologies that are totally revolutionizing the way we will be looking at our planet in the future. The aim of the project is to build capacities in the Black Sea region to use new international standards to gather, store, distribute, analyze, visualize and disseminate crucial information on past, present and future states of this region, in order to assess its sustainability and vulnerability. To achieve its objectives, EnviroGRIDS will build a Grid-enabled Spatial Data Infrastructure (gSDI) serving data, information and services in the Global Earth Observation System of Systems (GEOSS), and being compatible with the European directive on Infrastructure for Spatial Information in the European Union (INSPIRE), as well as the United Nations Spatial Data Infrastructure (UNSDI). EnviroGRIDS will particularly target the needs of the Black Sea Commission (BSC) and the International Commission for the Protection of the Danube River (ICPDR) in order to help bridging the gap between science and policy.

The scientific aim of the EnviroGRIDS project is to start building an Observation System that will address and assess several GEOSS Societal Benefit Areas under global changes. This system will incorporate a shared information system that operates on the boundary of scientific/technical partners, stakeholders and the public. It will contain an early warning system able to inform in advance decision-makers and the public about risks to human health, biodiversity and ecosystems integrity, agriculture production or energy supply caused by climatic, demographic and land cover changes on a 50-year time horizon.

To achieve and support the vision and objectives of enviroGRIDS, the gSDI (currently under development) will provide interoperable and standardized data storing, discovery, accessibility and retrieval as well as processing capabilities based on the Grid infrastructure of the Enabling Grids for E- Science (EGEE) project. In consequence, one of the key challenges

of the enviroGRIDS project is to bridge the technological gap between SDIs and Grid infrastructures and to make these infrastructures interoperable. In its four-year timeframe (started in April 2009), enviroGRIDS aims to benefit from the EGEE infrastructure to run a high resolution (spatially and temporally) water balance model on the entire Black Sea catchment (2.1 mio. square km.) using the Soil and Water Assessment Tool (SWAT). The project will also implement methods to access and process near real-time data from sensors and satellite images allowing to develop early warning systems and decision support tools. In term of analysis capacities, this will offer the possibility to shift from a traditional single desktop computer to sizable computing resources, allowing environmental scientists to leverage the full potential of high-resolution spatio-temporal data sets. The EnviroGRIDS gSDI will probably be one of the first implementation of such a grid-enabled infrastructure in a trans-national framework.

REFERENCES

- Abbaspour, K., Vejdani, M. & Haghighat, S. 2007: SWAT-CUP Calibration and Uncertainty Programs for SWAT, MODSIM 2007 International Congress on Modelling and Simulation, Modelling and Simulation Society of Australia and New Zealand.
- Arnold, J., Srinivasan R., Muttiah R. , & Williams, J. 1998: Large area hydrologic modeling and assessment - Part 1: Model development, Water resources bulletin, 34(1), 73-89.
- European Commission 2007: Directive 2007/2/EC of the European Parliament and the Council of 14 March 2007 establishing an Infrastructure for Spatial Information in the European Community (INSPIRE). Brussels, 14p.
- GEO secretariat 2005: Global Earth Observation System of Systems 10-Year Implementation Plan Reference Document, Geneva, 210p.
- Giuliani, G., Ray, N., Charvat, K. & Lehmann, A. 2009: EnviroGRIDS interoperability guideline. EnviroGRIDS Deliverable 2.1, 92p.
- Giuliani, G., Ray, N., Schwarzer, S., De Bono, A., Peduzzi, P., Dao, H., Van Woerden, J., Witt, R., Beniston, M. & Lehmann A. 2011: Sharing environmental data through GEOSS. International Journal of Applied Geospatial Research.
- Gorgan, D., Bacu, V., Ray, N. & Maier, A. 2009: EnviroGRIDS data storage guideline. EnviroGRIDS Deliverable 2.2, 67p.
- Henricksen B. 2007: UNSDI Compendium: A UNSDI Vision, Implementation Strategy, and Reference Architecture, New York, 174p.
- Srinivasan, R., Ramanarayanan, T., Arnold, J. & Bednarz, S. 1998: Large area hydrologic modeling and assessment - Part II: Model application, Water resources bulletin, 34(1), 91-101

16.6

Hydrodynamics of Lake Geneva inferred from Stable H- and O-Isotope Compositions

Janine Halder¹, Laurent Decrouy¹, and Torsten Vennemann¹

¹ *Faculté des géosciences et de l'environnement, Institut de minéralogie et géochimie, L' Anthropole, CH-1015 Lausanne (Janine.Halder@unil.ch)*

The expected increase of average annual temperatures and changes in precipitation patterns linked to the changes in climate, but also the human influence in terms of surface runoff and waste water inputs, may alter the physical, chemical, and biological dynamics of a lake and could thus affect future water quality in ways that are still unknown. Because the stable H- and O- isotope compositions of water are clearly linked to temperatures of precipitation from the ambient air mass and the origin of the air mass, variations in the H and O isotopic compositions as a function of time and place within a big lake such as Lake Geneva may help to interpret changes in its hydrology and dynamics of the water budget. The main research goal of this study is to evaluate the variability of the H- and O-isotope composition of Lake Geneva in order to apply it to a qualitative and quantitative assessment of the water budget.

Lake Geneva, Europe's largest freshwater reservoir located in a temperate climate zone, is mainly recharged by the Rhone river (~ 75%). Given the large volume (89 km³, maximum depth 310 m) and long residence time of water (~11.4yrs), its dynamic system, that is the interaction with surface and underground in/out-flows, precipitation, and evaporation fluxes may well be complex. Results from water samples and CTD profiles taken from morphometrically different basins of the lake in August 2009 (Fig.1) indicate a stratified water body. The epilimnion (uppermost 2-12 m) is relatively enriched in ¹⁸O with $\delta^{18}\text{O}$ values between -11.8 and -12.1‰ at the water surface. All profiles show a progressive depletion in ¹⁸O with depth, reaching minimum values in the middle of the metalimnion (20 m) of between -12.4 and -12.8‰ .

In the lower part of the metalimnion (20-40 m) the water becomes increasingly enriched in ^{18}O with depth again (-12.1 and -12.3‰), reaching more or less constant values in the hypolimnion. However, winter profiles taken in March 2010 are homogenous in all sampling points and layers (-12.3‰).

The difference in the isotope composition is related to the thermal stratification of the lake and mixing of glacial-sourced Rhone water, which has an average isotope composition of -13.9‰. Plotting all available isotope data from the watershed also indicates that water samples from the metalimnion are located between the Rhone and lake water on the LMWL. Rhone water can thus be traced to move through the lake over 50km as a stream in the thermocline/chemocline region. This phenomenon, previously described already as „La bataillère“, represents a cold silt-laden density current of glacial Rhone meltwater, which has a low content of dissolved solids and is therefore producing water of an intermediate density (Gorceix & Kreitmann 1930).

To better understand the extension of this stream, four cross sections of water profiles were taken in the lake in a second sampling campaign in August 2010. The results show the same curved progression of isotopic variation with depth as in the year before and demonstrate that the stream is also extending to relatively shallow bay regions. In comparison to August 2009, where the samples most depleted in ^{18}O and D were found at about -20m, those most depleted in these isotopes in August 2010 were found at -10m at the same sampling points. This difference can be explained as 2010 was influenced by more windy and cooler weather conditions than the year before, which results in a shallower thermocline region than the year before.

In contrast to the isotopic compositions, the results from the major ion analyses indicate that the lake water and its different sources are well-mixed as the variations are smaller than the analytical errors associated with the analyses via liquid chromatography. This underlines the sensitivity and strength of the application of stable isotopes in order to evaluate mixing of different waters and in contrast to other methods, like turbidity measurements, this method allows for a direct, natural tracing of the water sources and hydrodynamics of Lake Geneva. In order to apply the results to a qualitative and quantitative assessment of the water budget one further sampling campaign will be conducted in fall 2010 to trace the seasonal mixing of the water layers. In addition, water samples were also analysed for micropollutant concentrations and it is planned to evaluate correlations between these and the isotope compositions in order to trace micropollutant fate in the lake.

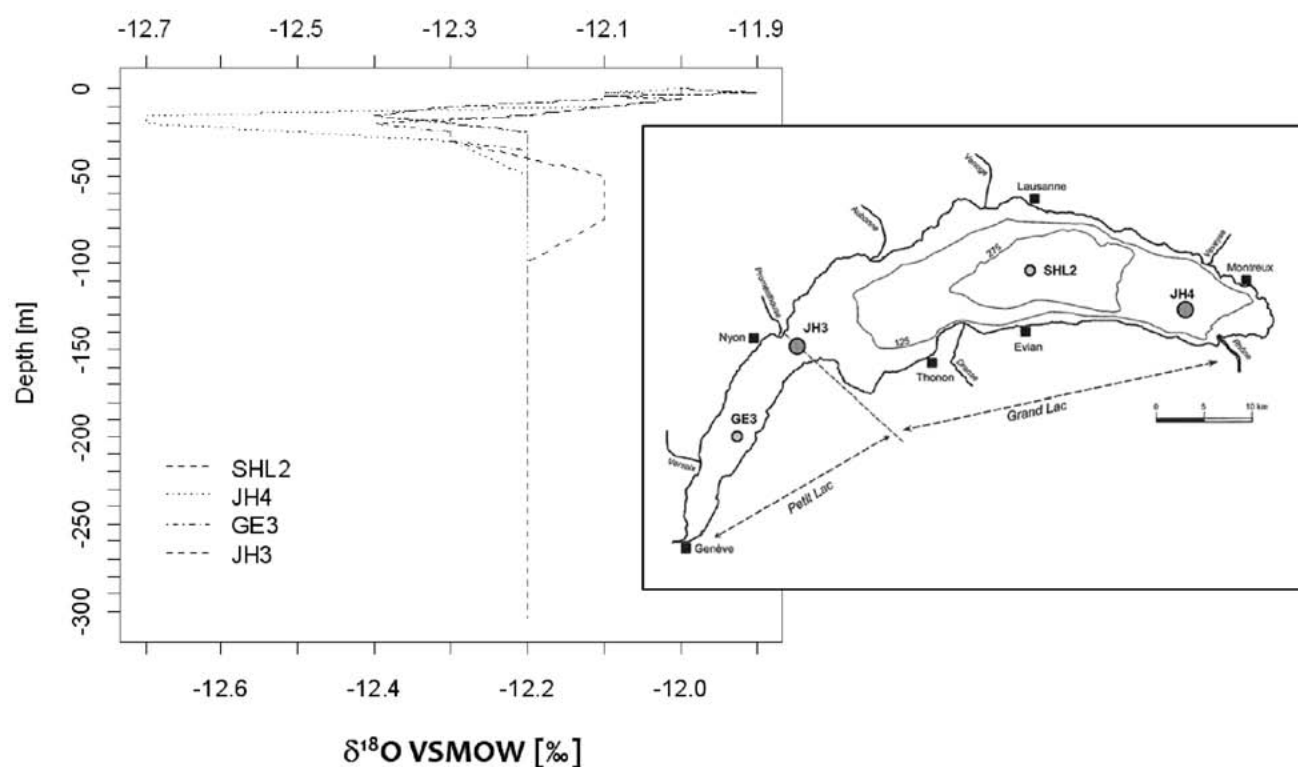


Figure 1.: $\delta^{18}\text{O}$ values in relation to depth of four sampling points in Lake Geneva (August 2009).

REFERENCES

- CIPEL 2009: Rapp. Comm. Int. prot. eaux Léman contre pollut., Campagne 2008. Fiche Signalétique du Léman et de son bassin Versant, 7-9.
- Gorceix, C & Kreitmann, L. 1930 : Etude thermique de « La Bataillère » sur le Léman. Revue géographie alpine. Tome 18. 3, 537-551

16.7

Life-history plasticity in a detritivore determines ecosystem response to climate warming

Hines Jes, Gessner Mark

Eawag: Swiss Federal Institute of Aquatic Science and Technology, Ueberlandstrasse 133, 8600 Dübendorf, CH

Many ectotherms grow faster in warmer environments. However, life history tradeoffs in growth rate, body size, and fecundity can constrain the influence of warming on an individual's resource consumption. Additionally, although warmer temperatures can cause phenological shifts in some species, changes in the timing of resource demand may vary across taxa, functional groups, and trophic levels. Using a randomized complete block 2x2 factorial field enclosure experiment, we examined the consequences of increased temperature (+4°C, ambient), and resource availability (nitrogen subsidized, ambient) on littoral zone communities feeding on *Phragmites australis* leaf litter. We find that life history plasticity of a key benthic consumer (*Limnephilus* spp., Trichoptera) in response to climate warming can strongly affect rates of leaf litter decomposition. However, community dynamics can buffer species specific responses. Our results demonstrate that experimental field studies that capture species responses in complex communities will be necessary to accurately predict the effects of climate change on ecosystem functioning.

16.8

Approaching water stress in the Alps- Water management options in the Crans-Montana-Sierre region, Valais (MontanAqua): estimation of available natural water resources

Kauzlaric Martina¹, Rey Emmanuel¹

¹ Geographisches Institut, Hallerstrasse 12, CH-3012 Bern (martina.kauzlaric@giub.unibe.ch)

The main objective of the current transdisciplinary project is to develop strategies moving towards a more sustainable water resources management in the Crans-Montana-Sierre region (Valais), together with actors involved. The study region is situated in the driest part of Switzerland and has been subject to dynamic economic, tourism and urban development during the last decades. The proposed research on more sustainable water management options will evaluate co-ordination and adaptation of water demand to water availability under changing biophysical and socioeconomic conditions.

For the detailed assessment of the available water resources in the study area, today and in the future, two distinct sources of water must be considered: (1) the in-situ water resources resulting from the natural water balance; (2) water which is transferred from different sources (e.g. glaciers, reservoirs) through the system by natural flows (rivers, subsurface flows) and by artificial channels within the irrigation scheme.

The study area is highly differentiated across the altitudinal range, and does not cover a classical hydrological basin as the water flows frequently across natural hydrographic boundaries, what is a big challenge from a hydrological point of view. Assessment of present hydrological conditions by observation will be the basis for establishing a detailed hydrological model for the entire study region (sub-module MODEL). In-depth assessment of the present and future availability of water will allow identifying areas with water surplus and deficits respectively. Results will be strongly related to the issue of evaluating the impact of different land use practices.

In the higher parts of the area, snow is a major hydrological element, which is highly sensible and is expected to be significantly affected by climate change. The Plaine Morte, a typical plateau glacier situated on the main divide between the cantons of Berne and Valais, seems to be an important water resource for the region, will also be sensitive to climate change. Despite the geological investigation of Wildberger [Wildeberger, 1981] and a few glaciological investigations, its role as well as the influence of its karstic environment in the water balance is still not fully understood and remains uncertain.

Therefore the role of snow (sub-module MODEL) and ice (sub-modules GLACIER and KARST with external collaboration), both valuable water sources for the region, will be thoroughly investigated.

The finite volume method conserves mass and as such is more appropriate for hydrological applications and for the estimation of available water resources.

Besides the choice of approach, a fundamental problem of modelling water balance is that often many of the equations we use to represent processes require calibration, thus their parameters cannot be directly measured.

This is true even of “physically based” equations because they are invariably applied at a scale different to that at which they were derived [Grayson et al., 2000].

It should be stressed the limited possibilities to calibrate-validate a model in the region based on historical data, due to the lack of extensive discharge and soil moisture measurements. What in turn reduces margins of conceptualization of the processes occurring in the region, as well as penalizes any need for parameter estimation.

Therefore the Penn State Integrated Hydrologic Model (PIHM) has been selected for the estimation of water resources in the study area,

It is a semi-discrete, physically-based model which includes: channel routing, overland flow, subsurface saturated unsaturated flow, rainfall interception, snow melting and evapotranspiration (refer to Fig.1).

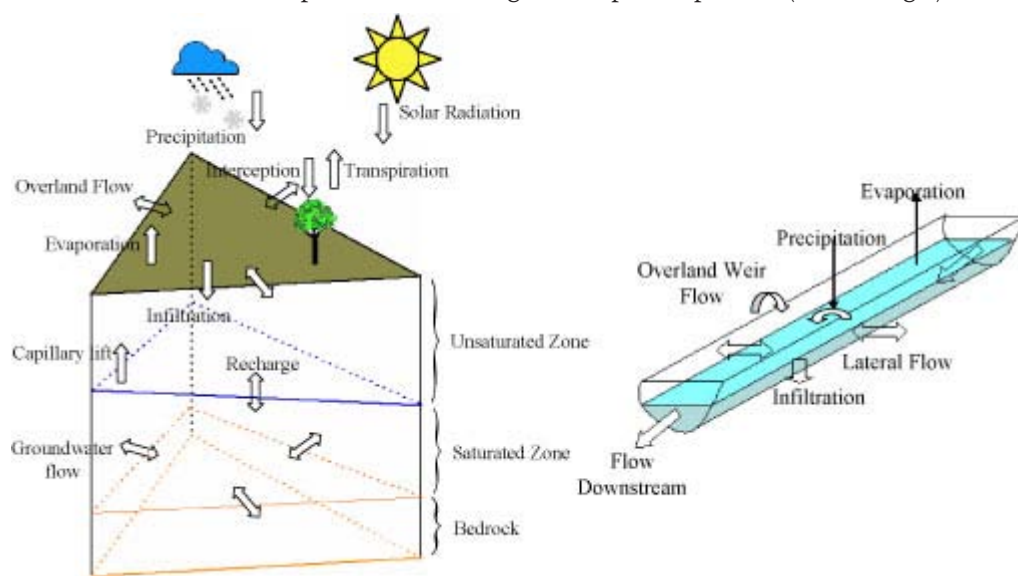


Fig.1: All the interacting hydrologic processes in PIHM are defined on prismatic watershed elements or linear river elements. ODEs corresponding to each process from all across the model domain are solved together to predict state variables at next time step. (source http://www.pihm.psu.edu/pihm_home.html)

In principle the domain is decomposed using the catchment boundary and stream network as constraints, however the choice of including other thematic maps for the catchment decomposition is left to the user.

The 2-D TIN is vertically projected creating prismatic volumes. The prismatic volume is divided into layers and a local system known as the kernel is created in which all the relevant hydrological processes occur within the prismatic volume. Hydrological processes are governed by both ordinary differential equations (ODEs) and partial differential equations (PDEs). PDEs are reduced to ODEs using the semi-discrete method, also known as the finite volume method. Coupling between elements is controlled by the fluxes across the boundary element [Minogue, 2008].

Some of the parameters are fixed with values obtained from the literature and extensive calibration is performed only for a limited number of parameters to which the model is the most sensitive. This allows a ‘constrained’ calibration [Ivanov et al., 2004], which will be based on case studies, where historical data are available, as well as on the dense measuring network built within the framework of the project.

The progressing of the understanding of catchment processes and system behaviour for the assessment of currently available water resources will allow landuse change scenarios and related consequences to be coupled in a comprehensive potential climate-change impact assessment, addressing sensitivity and uncertainty of the proposed scenarios as well as corresponding results.

REFERENCES

- [Grayson et al., 2000] Spatial patterns in catchment hydrology : observations and modelling; R.Grayson, G. Blöschl, Cambridge University Press, ISBN 0-521-63316-8 (2000)
- [Ivanov et al., 2004] Preserving high-resolution surface and rainfall data in operational-scale basin hydrology: a fully-distributed physically-based approach; V. Y. Ivanov, E. R. Vivoni, R. L. Bras, D. Entekhabi, Journal of Hydrology 298 80–111 (2004)
- [Minogue, 2008] Preliminary Hydrological Modelling of River Thur Revitalisation Scheme Using the Physically Based Distributed Model PIHM; A. T. Minogue (2008)
- [Wildeberger, 1981] Zur Hydrogeologie des Karstes im Rawil-Gebiet.; Wildberger Andreas ,Beiträge zur Geologie der Schweiz – Hydrologie, Nr. 27. Geographischer Verlag Kümmerly & Frey, Bern (1981)

16.9

Hydrological change in Switzerland: Which catchments are most sensitive? - A comprehensive assessment of climate change impact

Köplin Nina^{*,**}, Viviroli Daniel^{*,**}, Schädler Bruno^{*,**}, Weingartner Rolf^{*,**}

¹ Institute of Geography, University of Bern, Hallerstrasse 12, CH-3012 Bern (nina.koeplin@giub.unibe.ch)

² Oeschger Centre for Climate Change Research, University of Bern, Zähringerstrasse 25, CH-3012 Bern

We assess future impacts of climate change on hydrological systems in Switzerland through hydrological modelling with the semi-distributed and conceptual yet process-oriented PREVAH model (Viviroli et al. 2009), that we force with scenario data as climate input.

The anticipated climate change in Switzerland will result in changing precipitation patterns and increasing temperatures, and these changes will have an impact on the hydrological systems. The objective of our study is to determine those catchments that exhibit sensitivity towards a change in climate, and to identify specific catchment characteristics causing this sensitivity. Both issues will be addressed in the framework of the joint research project “Climate Change in Switzerland – Hydrology” (CCHydro, Volken 2010).

We apply climate scenarios of expected changes (deltas) in the annual cycle of temperature and precipitation. For each day of the year and observational station site, the delta between the control (1980–2009) and the scenario periods (2021–2050, 2070–2099) is provided (Bosshard et al. in preparation). For every site, a total of 10 model chains from the ENSEMBLES-project (Hewitt & Griggs 2004), each consisting of one general circulation model (GCM) driving one regional climate model (RCM), were analyzed. All model chains assume the SRES A1B emission scenario. Differences between the 10 different model chains represent modelling uncertainty.

The annual cycle of expected changes is superimposed on the observed time series to generate a set of climate scenarios with which the models for the catchments considered are forced. The hydrological modelling system PREVAH is run with hourly meteorological input and on basis of a spatial resolution of 500 x 500 m². Thus, we examine approximately 200 mesoscale catchments with an average area of 150 km² and a range of 30 to 2000 km² to specify process-based relationships between climate sensitivity and specific catchment characteristics. An application of climate scenarios to such an extensive set of catchment models that are processed at this spatial and temporal resolution is new so far. This approach is, however, necessary to meet the high degree of heterogeneity of mountainous environments as well.

In addition, changes in land use, i.e. an alteration of glaciated and forested area, will be included in the framework to study the respective impacts on the hydrological systems.

REFERENCES

- Bosshard, T., Kotlarski, S., Ewen, T. & Schär, C.: Spectral representation of the annual cycle in the climate change signal, in preparation.
- Hewitt, C. D. & Griggs, D. J. 2004: Ensembles-Based Predictions of Climate Changes and Their Impacts, *Eos Transactions AGU*, 85(52), doi: 10.1029/2004EO520005.
- Viviroli, D., Zappa, M., Gurtz, J. & Weingartner, R. 2009: An introduction to the hydrological modelling system PREVAH and its pre- and post-processing tools. *Environmental Modelling & Software*, 24(10), 1209–1222.
- Volken, D. 2010: CCHydro – Auswirkungen der Klimaänderung auf die Wasserressourcen und die Gewässer in der Schweiz, *Hydrologie und Wasserbewirtschaftung*, 54, 143–146.

16.10

Rainfall distribution is the main driver of runoff under future CO₂-concentration in a temperate deciduous forest

Sebastian Leuzinger¹, Christian Körner²

¹Forest Ecology, ETHZ, CH-8092 Zurich (Leuzings@ethz.ch)

²Botanisches Institut der Universität Basel, CH-4056 Basel

Reduced stomatal conductance under elevated CO₂ results in increased soil moisture, provided all other factors remain constant. Whether this results in increased runoff critically depends on the interaction of rainfall patterns, soil water storage capacity and plant responses. To test the sensitivity of runoff to these parameters under elevated CO₂, we combine transpiration and soilmoisture data from the Swiss Canopy Crane FACE experiment (SCC, 14 30–35m tall deciduous broad-leaved trees under elevated CO₂) with 104 years of daily precipitation data from an adjacent weather station to drive a three-layer bucket model (mean yearly precipitation 794mm). The model adequately predicts the water budget of a temperate deciduous forest and runoff from a nearby gauging station. A simulation run over all 104 years based on measured sap flow responses resulted in only 5.5mm (2.9%) increased ecosystem runoff under elevated CO₂. Out of the 37 986 days (1 January 1901–31 December 2004), only 576 days produce higher runoff in the elevated CO₂ scenario. Only 1 out of 17 years produces a CO₂-signal >40mm, which mostly depends on a few single days when runoff under elevated CO₂ exceeds runoff under ambient conditions. The maximum signal for a double preindustrial CO₂-concentration under the past century daily rainfall regime is an additional runoff of 46mm. More than half of all years produce a signal of <5mm, because trees consume the 'extra' moisture during prolonged dry weather. Increased runoff under elevated CO₂ is nine times more sensitive to variations in rain pattern than to the applied reduction in transpiration under elevated CO₂. Thus the key driver of increased runoff under future CO₂-concentration is the day by day rainfall pattern. We argue that increased runoff due to a first-order plant physiological CO₂-effect will be very small (<3%) in a landscape dominated by temperate deciduous forests, and will hardly increase flooding risk in forest catchments. Monthly rainfall sums are unsuitable to realistically model such CO₂ effects. These findings may apply to other ecosystems with comparable soil water storage capacity.

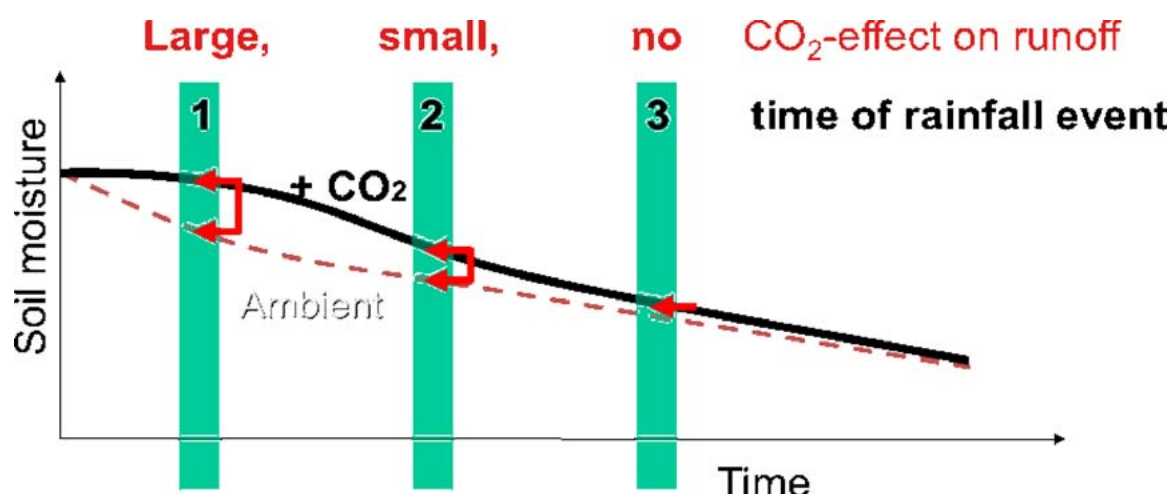


Figure 1. The graphic illustrates the importance of the timing of the rainfall event for the CO₂-effect on runoff.

16.11

Climate change effects on snow melt and discharge of a partly glacierized watershed in central Switzerland

Jan Magnusson¹, Tobias Jonas¹, Florian Kobierska¹, Daniel Farinotti², Massimiliano Zappa³, Mathias Bavay¹ & Thomas Bosshard⁴

¹ WSL Institute for Snow and Avalanche Research SLF, Davos, Switzerland (magnusson@slf.ch)

² Laboratory of Hydraulics, Hydrology and Glaciology (VAW), ETH Zurich, Switzerland

³ Swiss Federal Institute for Forest, Snow and Landscape Research WSL, Birmensdorf, Switzerland

⁴ Institute for Atmospheric and Climate Science (IACETH), ETH Zurich, Switzerland

In the Alps, streamflow regimes and water resource availability critically depend on snow and glacier melt. While the capabilities of numerical models have made significant progress in recent years, it remains challenging to accurately quantify the hydrological response of mountain watersheds to climate warming. Apart from uncertainties that relate to atmospheric forcing data for predictive model runs, dealing with snow and glacier melt, steep terrain, complex micro climatic effects, and unknown groundwater processes poses substantial difficulties to numerically reproduce the hydrological behavior of alpine watersheds.

Here we present results of a comprehensive hydrological study in the drainage area of a hydropower reservoir in central Switzerland. The total basin is partly glacierized (20 %) and spans over 92 km² of alpine topography covering elevations between 1800 and 3600 m asl. As is often the case, long-term hydrometeorological data is largely unavailable for the area, apart from reservoir water level measurements. Among other measuring infrastructure, three automatic meteorological stations, continuous discharge measurements at three sites, and two remote camera systems for snow-covered area were installed at the beginning of this study in 2007.

Discharge measurements in feeding streams display strong diurnal fluctuations due to snowmelt in spring and glacier melt later in summer. Three different modeling approaches have been tested to reproduce the measured discharge dynamics: 1) a detailed energy-balance model primarily designed for snow simulations; 2) a temperature-index model developed for glacier mass balance studies; 3) a conceptual runoff model system suitable for mountain hydrology applications. A considerable effort has been put in distributing available meteorological station data to the model grids as forcing data. In particular, the energy-balance model was sensitive to different precipitation distribution methods. With this model, an algorithm accounting for terrain curvature and slope turned out to provide a promising approach.

The recent EU regional climate modeling initiative ENSEMBLES provided up-to-date climate predictions for two periods in mid and late 21st century. These were used to estimate changes in the water supply of the hydropower reservoir in response to expected climate shifts. Our simulations suggest a drastic shortening of the snow covered season by about two months at all elevations by the end of this century. Even at the highest elevations, in many areas the snow cover will no longer persist throughout the summer with evident consequences for the glacier accumulation zones. Thus, peak streamflow in spring from snowmelt will take place earlier, while late-summer streamflow will decrease considerably.

16.12

Low water in a changing climate

Meyer Raphael^{1,2}, Schädler Bruno^{1,2}, Viviroli Daniel^{1,2} & Weingartner Rolf^{1,2}

¹Institute of Geography, University of Bern, Hallerstrasse 12, CH-3012 Bern (raphael.meyer@giub.unibe.ch)

²Oeschger Centre for Climate Change Research, University of Bern

Water resources management requires knowledge about the possible magnitude of runoff in the near and the far future, in order to take consequent measures for adaptation. Providing this knowledge is difficult enough for a more or less stationary system. Facing the ongoing and anticipated changes in climate and land use as well as future socio-economic change renders the task even more challenging.

The interdisciplinary research project CCHydro (Volken 2010) analyses changes in water balance as well as in flood and low water behavior in Switzerland caused by climate change. In the present sub-project we focus on low water. The aim is a projection of low water runoff in the Swiss Midlands for the periods 2021 to 2050 and 2070 to 2099 with an appropriate model. The European heat wave of 2003 showed that low water might be a problem even in Switzerland. Especially in the Swiss Midlands conflicts between water users and ecosystem requirements (like perennial runoff in rivers) are likely during summer months. Therefore low water is investigated here exclusively for catchments in the Swiss Midlands and only for a time window from May to October.

Runoff projections into 2050 or 2099 are a difficult task in general and often based upon weak assumptions. In low water projection, as in all projections, the choice of the model is most important. There are two questions to answer: 1) Which model represents best the entity under research – i.e. low water – in the investigated area and 2) which model is able to represent this entity under climate change. It is crucial to have a process based model in order not to model the errors of the model structure in 2050 or 2099 but the impact of climate change on the water cycle. In addition, low water research in Switzerland suffers from the fact that the occurrence of this runoff extreme is very rare. Model choice, model calibration and model validation are thus difficult. In addition, in the rare periods of low water, the measuring accuracy of water flow is most sensitive for determining low water.

In order to cope with all these problems we decided to find a well-founded modelling approach, based on the analysis of base flow. Starting with the importance of accurate runoff measurements, runoff gauges were selected based on the NQ-stat database (BAFU 2005) quality declaration. 59 catchments all over Switzerland matched these quality requirements (Fig. 1).

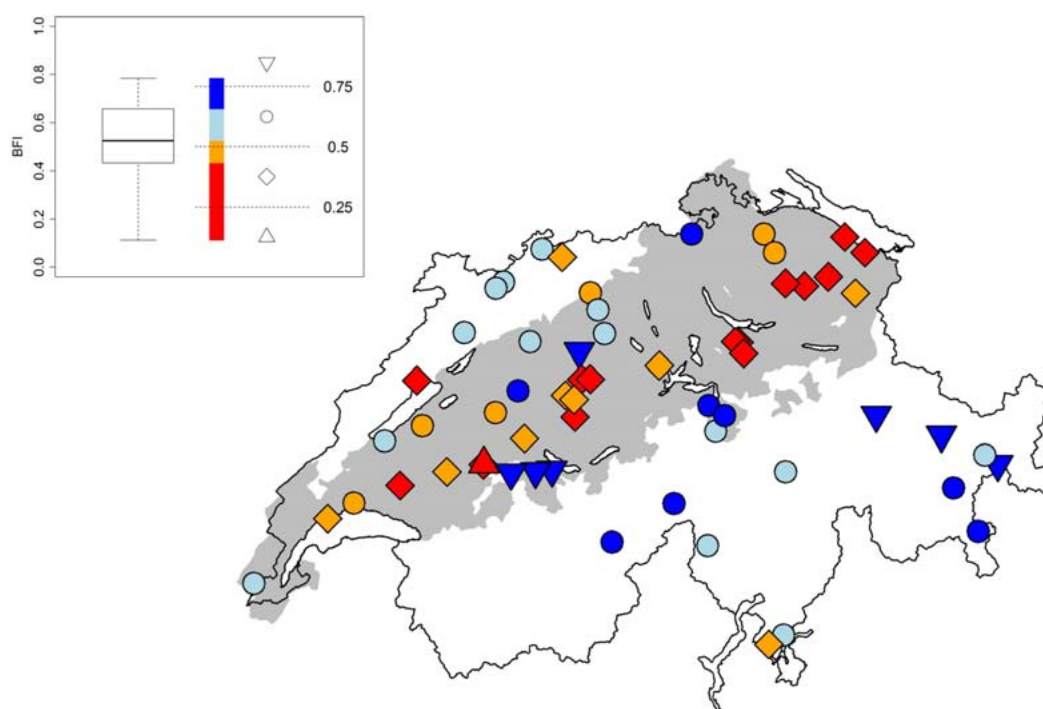


Figure 1. Spatial distribution of the 59 catchments under investigation. Each symbol represents one associated gauge. The shape of the symbol shows an absolute classification of the BFIs, whereas the color shows a relative classification, relative to the totality of obtained BFIs (see inset on top left). The extension of the Swiss Midlands is shaded in grey.

For all of these 59 catchments base flow was determined. Base flow allows an investigation of the complete time series of interest, without any regard to the occurrence of a low water period. The separation of base flow is possible even during high water periods. Base flow is that part of total runoff which originates from delayed sources. It is only this part of runoff which supplies the river with water during periods without rain, and consequently this part of runoff is of interest for our investigation. The base flow index (BFI) is a useful index to describe the low water character of a catchment at a glance. BFI is the ratio between base flow and total discharge over a given time. A BFI of 0.9 thus describes a catchment which generates a stable water supply to the river, whereas a BFI of 0.1 means very little storage of water, quick runoff after a rainfall event and almost no runoff during prolonged periods without rain. Figure 1 shows that low BFIs are almost uniquely located in the Swiss Midlands whereas high BFIs can be found all over Switzerland. By using this BFI we want to empower our model to cope with climate change.

Most models do have their weak points in the groundwater module. So does PREVAH, which we decided to use in an adapted manner for our low water projection. PREVAH is already an established model for average water and high water in Switzerland (Viviroli 2007). With the calibration of its groundwater module against the gained BFI, we prove PREVAH to cope correctly with climate change from the low water point of view.

REFERENCES

- BAFU (Bundesamt für Umwelt) 2005: Die Niedrigwasser-Datenbank NQStat. Bedienungsanleitung. Bern.
- Viviroli, D. 2007: Ein prozessorientiertes Modellsystem zur Ermittlung seltener Hochwasserabflüsse für ungemessene Einzugsgebiete der Schweiz. Weiterentwicklung und Anwendung des hydrologischen Modellsystems PREVAH. Geographica Bernensia, Bern.
- Volken, D. 2010: Projektbericht. CCHydro - Auswirkungen der Klimaänderung auf die Wasserressourcen und die Gewässer in der Schweiz. Hydrologie und Wasserbewirtschaftung 54 (2), 143–146.

16.13

The Holocene sediment record of Lake Cadagno: Overview and initial results from a comprehensive paleoenvironmental study

H. Niemann (1), F. S. Anselmetti (2), J. S. Sinninghe Damsté (3), A. Gilli (4), M. F. Lehmann (1), R. Peduzzi (5), S. Peduzzi (5), D. Ravasi (6), N. Sax (1), C. J. Schubert (7), A. Stadnitskaia (3), T. Stötter (1), M. Tonolla (6), S. B. Wirth (4)

- (1) Institute for Environmental Geosciences, University of Basel
- (2) Swiss Federal Institute of Aquatic Science and Technology (EAWAG), Dübendorf
- (3) Royal Netherland Institute for Sea Research (NIOZ), Texel
- (4) Swiss Federal Institute of Technology (ETH), Zürich
- (5) Fondazione Centro di Biologia Alpina, Piora
- (6) Microbiology unit, BioVeg Dept. UNIGE, c/o Istituto cantonale di microbiologia, Bellinzona
- (7) Swiss Federal Institute of Aquatic Science and Technology (EAWAG), Kastanienbaum

Lake Cadagno is a relatively small (840 m long, 420 m wide, 21 m deep) high-alpine lake situated in the Piora valley in the southern part of Switzerland (Ticino) at an altitude of 1921 m. The lake basin was created by glacial erosion. The bedrock of the valley contains dolomite and gypsum, and sulphate-rich water from underwater springs lead to high sulphate concentrations in the anoxic hypolimnion. Microbial sulphate reduction and the subsequent accumulation of sulphide in combination with a strong density gradient result in meromictic conditions of the lake's water body, with a permanent oxicleine at about 9 m water depth. High abundances of purple and green sulphur bacteria (*Chromatiaceae* and *Chlorobiaceae*, respectively) at the redox interface in the modern lake, as well as their organic geochemical remnants and signatures in surface sediments at the bottom of the lake were the subject of several research campaigns. Paleoenvironmental studies at lake Cadagno, on the other hand, were restricted to short sediment cores covering the last centuries.

Within the frame work of the SNF funded project "FloodALP" we conducted a seismic survey and recovered a 10.5 m-long composite core from the deepest part of the lake, covering, according to preliminary ¹⁴C dating, the last 12000 years. After recovery, the core was sub sampled in high resolution (about every 10 cm) for sedimentological, organic geochemical (lipid biomarker) and molecular (16S rDNA) as well biogeochemical analyses (pore water constituents, methane, element composition and speciation). In this presentation, we provide a progress report on various collaborative research projects that all aim at reconstructing the paleoenvironmental conditions at Lake Cadagno during the Holocene.

The sediments of Lake Cadagno can be divided into three different types: regular background sediment, flood deposits and intervals of reworked material. The different types of deposits were identified and separated by visual observations (layer thickness, grain size/grading, macro-fossil content, thin sections) or by C and N analysis (%C, %N, C/N ratios, $\delta^{13}\text{C}$, $\delta^{15}\text{N}$). The detailed analysis of the flood layers indicates that the flood events during the Holocene were most intense between 3500 and 4500 years BP. This evidence towards wetter climatic conditions during the Bronze Age is in agreement with previous work. The sediments sequences of the Little Ice Age cold period (ca. 16th - 19th century) also indicate an elevated reoccurrence of episodic flood events.

We also reconstructed paleo temperatures in the lake Cadagno catchment area using a novel, lipid-based proxy, the MBT/CBT paleothermometer. The MBT/CBT approach is based on the ratio of specific organic compounds derived from fossilised remains (GDGTs) of presumably soil bacteria that are preserved in the lakes sedimentary sequence. Our preliminary results are in very good agreement with estimated values of atmospheric air temperature at Lake Cadagno ($\sim 0^\circ\text{C}$, Swiss Meteo), and are consistent with climatological evidence from the sedimentological investigations. Furthermore, temperature variations recorded by the MBT/CBT paleothermometer match published temperature reconstructions for the last two millennia at nearby locations in timing and magnitude and reflect the extension of the Great Aletsch Glacier during the last 3500 years. Major climate anomalies recorded by the independent proxies and by the MBT/CBT paleothermometer are, for instance, the Medieval Warm Period (ca. 1000 years BP) and a cold spell ~ 1500 years BP. We could also detect a cold period at about 2500 years ago that correlates in timing with the disappearance of the last lake dwellings in the European Alps. Additional cold periods were observed during the Bronze Age (~ 3500 and ~ 4500 years BP) and we found evidence for elevated temperature during the so-called Holocene Climate Optimum (8000 - 5000 years BP).

Ongoing and future work addresses the possible links between climate and environmental/biogeochemical changes within the lake. First bulk C and N isotope results indicate that both the C and N cycles of Lake Lugano have been dynamic during the Holocene. Diagenetic effects on the bulk signals cannot be ruled out completely and will be constrained through compound-specific isotope analyses of shielded organic compounds. An ongoing lipid biomarker/pigment study aims at reconstructing the population dynamics of anoxygenic, phototrophic bacteria and the reconstruction of past redox conditions in the lake. Biomarker data will be integrated with sedimentary data on fossil DNA. Preliminary results indicate that the recent microbial community is not a unique phenomenon of the modern lake and its recent past, as we were able to detect both purple and green sulphur bacteria in several sediment horizons, indicating extended intervals of water column anoxia at Lake Cadagno during the Holocene.

These studies were supported by the Swiss National Science Foundation (SNF grants 200021-121909 & IZK0Z2-131407)

16.14

Approaching water stress in the Alps – Water management options in the Crans-Montana-Sierre region, Valais, (MontanAqua): Measuring network and influence of land use and land use changes on water balance.

Rey Emmanuel¹, Kauzlaric Martina¹

¹Geographisches Institut, Hallerstrasse 12, CH-3012 Bern (emmanuel.rey@giub.unibe.ch)

The main objective of the current transdisciplinary project is to develop strategies moving towards a more sustainable water resources management in the Crans-Montana-Sierre region (Valais), together with actors involved. The study region is situated in the driest part of Switzerland and has been subject to dynamic economic, tourism and urban development during the last decades. The proposed research on more sustainable water management options will evaluate co-ordination and adaptation of water demand to water availability under changing biophysical and socioeconomic conditions.

For the detailed assessment of the available water resources in the study area, today and in the future, two distinct sources of water must be considered: (1) the in-situ water resources resulting from the natural water balance; (2) water which is transferred from different sources (e.g. glaciers, reservoirs) through the system by natural flows (rivers, subsurface flows) and by artificial channels within the irrigation scheme.

The study area is highly differentiated across the altitudinal range, and does not cover a classical hydrological basin as the water flows frequently across natural hydrographic boundaries, what is a big challenge from a hydrological point of view. Assessment of present hydrological conditions by observation will be the basis for establishing a detailed hydrological model for the entire study region. In-depth assessment of the present and future availability of water will allow identifying

areas with water surplus and deficits respectively. Results will be strongly related to the issue of evaluating the impact of different land use practices.

The observations are made through a dense measuring network (Fig. 1), which was installed in spring and summer 2010. The network will stay on place for the duration of the MontanAqua project. Weather stations, rain gauges and totalisators were installed at different altitudinal ranges to assess the input of water in the system. The output is measured by discharge stations which are installed on the main rivers of the area. We also use several weather stations and discharge stations installed and used by other organization or by private offices. To complete the measuring network a hillside lysimeter is built in the study area in an extensive meadow on the lower area. This will precisely measure the evapotranspiration of an unirrigated typical vegetation type of the area. Soil humidity, with tensiometer will also be investigated in the main land use types.

The diversity in land use and land cover is another main characteristic of the study area: the lowest slopes are dominated by vineyards, above which an area with intensive as well as extensive farming (intensive meadow and extensive pasture) and expanding dry forests is situated. In the medium altitudes, tourist resorts and tourist activities are predominant. The highest part of the area is a typical alpine landscape with alpine meadows used for cattle grazing at summer time. The land use practices in the different altitudinal zones of the study area have different water requirements and water use efficiency that will be assessed by the tensiometers and the hillside lysimeter (Fig. 2, next page). Identification of optimal agricultural land management practices (vineyard, meadow, pasture, forest and alpine meadow) will be conducted, especially in the context of irrigation, and their influence on the water budget today and under climate change. A model such as SWAP used in Netherland or in India could be used (Singh et al. 2006a,b, Van Dam et al. 2008) Additionally, we will assess new land use options, which are better adapted to climate variability and extremes. Such investigations have been made in various parts of the world and have been partly capitalized on by the global WOCAT program (<http://www.wocat.net/en.html>). For the Swiss mountain region, such studies are missing in large measure.

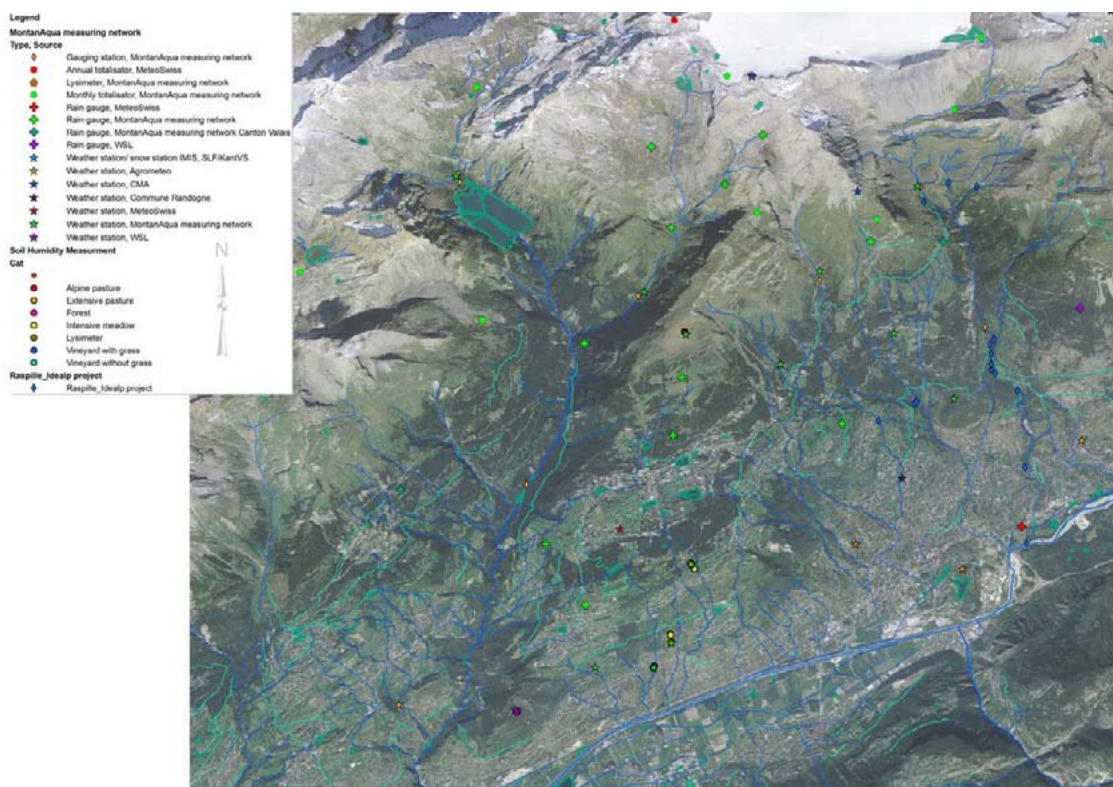


Figure 1. Measuring network of the MontanAqua project.

REFERENCES

- Singh R., Kroes J.G., van Dam J.C. & Feddes R.A. 2006a: Distributed ecohydrological modelling to evaluate the irrigation system performance in Sirsa district. I. Current water management and its productivity, *J. Hydrol.* 329, 692-713
- Singh R., Jhorar R.K., van Dam J.C. & Feddes R.A. 2006b: Distributed ecohydrological modelling to evaluate the irrigation system performance in Sirsa district. II. Impact of alternative water management scenarios, *J. Hydrol.* 329, 714-723
- Van Dam J.C., Groenendijk P, Hendriks R.F.A., Kroes J.G. 2008: Advances of modelling water flow in variably saturated soil with SWAP, *Vadose Zone J.* 7:640-653.



Figure 2. Hillside Lysimeter with exte tensiometer and weather station, Lens-Chermignon, August 2010.

16.15

Freshwater biodiversity under climate warming pressure: identifying the winners and losers in temperate small waterbodies

Rosset Véronique^{1,2} & Oertli Beat¹

¹ University of Applied Sciences Western Switzerland, 1254 Jussy-Geneva, Switzerland (veronique.rosset@hesge.ch)

² University of Geneva, 1227 Carouge, Switzerland

Climate warming is affecting the composition of communities all around the world, resulting in the expansion or contraction of the geographical range of species, and leading to colonisation (winners) and extinction (losers) events in ecosystems. It is crucial for the conservation of biodiversity to identify the potential winners and losers involved in such changes.

We focus here on small standing waterbodies in Switzerland and on five taxonomic groups: vascular plants, snails, beetles, dragonflies and amphibians. We first investigated the sensitivity of each species to climate warming through their thermal preferences, using altitudinal and latitudinal distribution as a surrogate for temperature. We then investigated the resilience of species to perturbations through five ecological and biogeographical criteria applicable to the perturbation “warming”: dispersal ability, degree of habitat specialisation, geographical extent in the study area, future trend in geographical extent, and future trend of habitat availability for species.

When considering only the thermal preferences of species, the proportion of potential losers ranged from 0% to 33% of the regional species pool according to the taxonomic groups. The set of potential winners was much larger; it comprised from 53% to 63% of the regional species pool for dragonflies and amphibians. The resilience criteria combined into a multimetric index added complementary information on the sensitivity of species to warming and enabled to classify all species along a gradient of extinction risk. This threat linked to warming appeared to be different from the threat identified by the present Red Lists and should therefore be used as a complementary label by the managers in charge of species conservation.

16.16

Stable nitrogen isotopes in chitinous remains: Exploration of a new palaeoenvironmental proxy for past freshwater environments

Schilder Jos^{1,2}, Heiri Oliver^{1,2}, Van Hardenbroek Maarten² & Lotter André²

¹ Institute of Plant Sciences and Oeschger Centre for Climate Change Research, University of Bern, CH-3013 Bern, Switzerland (j.c.schilder@gmail.com)

² Institute of Environmental Biology, Palaeoecology, Laboratory of Palaeobotany and Palynology, Utrecht University, 3584 CD Utrecht, The Netherlands

In ecological studies stable nitrogen isotope ratios ($\delta^{15}\text{N}$) are used to trace food web structure, based on the observation that $\delta^{15}\text{N}$ of organisms is on average $3.4 \pm 1.1\text{‰}$ higher than that of their food source. Additionally, $\delta^{15}\text{N}$ can be used to identify changes in the source of nitrogen in an ecosystem. However, $\delta^{15}\text{N}$ has rarely been measured in fossil remains preserved in lake sediments even though this would potentially allow the reconstruction of past food web structure and changes in the nitrogen source of lakes.

We show in an experimental setup with larvae of the chironomid midge *Chironomus riparius* that $\delta^{15}\text{N}$ of both soft tissue and fossilizing head capsules faithfully reflect the $\delta^{15}\text{N}$ of their food source and that there is a constant offset between the $\delta^{15}\text{N}$ of soft tissue and the $\delta^{15}\text{N}$ of fossilizing structures. This is in agreement with findings by Perga (2010), who found that $\delta^{15}\text{N}$ of cladoceran exoskeletons reflects the values measured in soft body tissue, albeit with a consistent offset.

A field study showed that there is considerable variability in $\delta^{15}\text{N}$ of cladocerans and chironomids in Lake De Waay (the Netherlands). This variability was apparent within taxa, between taxa and between seasons. Moreover, analysis of samples

of subfossil remains showed spatial (i.e. within lake) variability in $\delta^{15}\text{N}$. Repeated sampling of fossils from core-tops retrieved at the same location resulted in consistent results, however.

A downcore record of $\delta^{15}\text{N}$ in fossil cladoceran and chironomid remains was produced and compared to trends in bulk sediment organic matter $\delta^{15}\text{N}$ and trends in nitrogen deposition on the Netherlands. The results suggest that bulk sediment organic matter $\delta^{15}\text{N}$ increases and decreases as lake productivity rises and declines due to changes in anthropogenic nitrogen deposition on the Netherlands. More importantly, the $\delta^{15}\text{N}$ of fossil remains of cladocerans and chironomids show similar trends, yet with an amplitude two to three times larger than bulk sediment organic matter $\delta^{15}\text{N}$.

The results of this study show that $\delta^{15}\text{N}$ of chitinous remains of chironomids and cladocerans provides a good approximation of $\delta^{15}\text{N}$ of tissues of once living organisms. In Lake De Waay, and possibly in similar lakes, $\delta^{15}\text{N}$ measured on these remains can be used to reconstruct past changes in nitrogen source of the lake system. Our results suggest that $\delta^{15}\text{N}$ of chitinous remains of aquatic invertebrates is more sensitive to changes in nitrogen source $\delta^{15}\text{N}$ than $\delta^{15}\text{N}$ measured on bulk sediment organic matter. This study may lead to the development of $\delta^{15}\text{N}$ in chitinous remains as a new indicator for past trophic conditions in lakes.

REFERENCES

Perga, M-E. 2010: Potential of $\delta^{13}\text{C}$ and $\delta^{15}\text{N}$ of cladoceran subfossil exoskeletons for paleo-ecological studies, *Journal of Paleolimnology*, 44, 387-395.

16.17

Towards uncertainty reduction of low flow modeling using $\delta^{18}\text{O}$ as additional information

Staudinger Maria ¹, Seibert Jan ¹, Stahl Kerstin ² & Lehner Irene ³

¹Hydrology & Climate, Department of Geography, University of Zurich, Winterthurerstrasse 190, CH-8057 Zurich (maria.staudinger@geo.uzh.ch)

² Institute of Hydrology, University of Freiburg, Fahnbergplatz, D-79098 Freiburg

³ Institute for Atmospheric and Climate Science, ETH Zurich, Universitätsstrasse 16, CH-8092 Zurich

Droughts and low flow have severe consequences for both natural and social systems including impacts on ecosystems, agriculture, water supply and energy production. An early recognition of critical drought conditions is favorable to society and economy and thus essential for drought risk management. A common tool to estimate hydrological responses is the use of hydrological models. Often conceptual rainfall runoff models are applied, because they are able to capture the dominant catchment dynamics while remaining parsimonious and computationally efficient. However, modeling brings uncertainty along, which should be quantified. The identification of the sources of uncertainty is crucial for reducing uncertainty through changes in structure, parameterization and error models, which account for uncertainty in the forcing and output data. Little work has been done particularly regarding the sources of uncertainty in the modeling of low flow situations. We modeled low flow in a small-scale research catchment in Switzerland (Rietholzbach catchment, www.iac.ethz.ch/groups/seneviratne/research/rietholzbach) using multiple conceptual hydrological models. The various sources of uncertainty were estimated using the Bayesian total error analysis (BATEA) framework (Kavetski et al., 2006). Within this framework the modeler can transparently incorporate, test, and refine existing understanding of all sources of data uncertainty in a specific application, including both rainfall and stream flow measurement uncertainties. The hydrological models differed in the structures known to be important to capture low flow processes i.e. percolation as well as soil and groundwater storages in modeling. The models are extended to enable mass transport and thus allow modeling the isotopic signal for all model components. After optimizing also for the simulation of the isotopic signal ($\delta^{18}\text{O}$) the uncertainty is re-analyzed.

REFERENCES

Kavetski D., Kuczera G., Franks S. 2006: Bayesian analysis of input uncertainty in Hydrological modeling: 1. Theory, *Water Resources Research*, 1-9

17. Groundwater and Climate change

Marc Schürch, Eduard Hoehn, Pascal Turberg, Federico Matousek

Swiss Hydrogeological Society

- 17.1 Akinfiyev N.N., Diamond L.W.: Thermodynamic model of aqueous CO₂–H₂O–NaCl solutions from 22 to 100 °C and from 0.1 to 100 Mpa
- 17.2 Alt-Epping P., Diamond L.W.: Reactive-transport modelling applied to geological sequestration of CO₂ in Switzerland
- 17.3 Chevalier G., Diamond L.W., Leu W.: Potential for deep geological sequestration of CO₂ in Switzerland: a first appraisal
- 17.4 Diem S., Schirmer M.: RIBACLIM – Riverbank filtration under climate change scenarios
- 17.5 Figura S., Livingstone D.M., Hoehn E., Kipfer R.: Climate change and groundwater: analysis of historical records
- 17.6 Germann P.: Infiltration depths due to increased rain intensities and durations as a consequence of climate change
- 17.7 Hessenauer M., Flury F.: Evolution, sur plus de 20 ans, de quelques paramètres hydrochimiques des eaux souterraines suivies dans le cadre de l'étude d'impact de l'autoroute Transjurane (A16, Canton du Jura)
- 17.8 Huguenberger P., Butscher Ch.: Modeling the effects of climate change on the vulnerability of karst groundwater resources
- 17.9 Käser D., Perrochet P., Renard P., Schirmer M., Zwahlen F., Hunkeler D.*: Influence of groundwater/stream water interactions in sustaining environmental flow and water supply in a changing climate: the case of an Alpine alluvial aquifer, the Upper Emme
- 17.10 Moeck C., Baillieux A., Schirmer M., Hunkeler D.: Groundwater shortage due to climate change
- 17.11 Stoll S., Hendricks Franssen H.-J., Butts M. & Kinzelbach W.: Analysis of the impact of climate change on groundwater related hydrological fluxes
- 17.12 Tacher L., Turberg P., Breguet A., Parriaux A.: Modelling the sensibility of the alpine and perialpine hydrogeological systems in climate change
- 17.13 Vögeli Albisser C., Prasuhn V.: Irrigation and groundwater quality in times of climate change

17.1

Thermodynamic model of aqueous CO₂–H₂O–NaCl solutions from –22 to 100 °C and from 0.1 to 100 MPa

Akinfiev Nikolay¹, Diamond Larry W.²

¹ Institute of Geology of Ore Deposits, Petrography, Mineralogy and Geochemistry, Russian Academy of Sciences, Staromonetny per. 35, Moscow 119017, Russia

² Rock–Water Interaction Group, Institute of Geological Sciences, University of Bern, Baltzerstrasse 3, CH-3012 Bern, Switzerland (diamond@geo.unibe.ch)

Accurate knowledge of the thermodynamic properties of aqueous solutions containing CO₂ and NaCl has become essential to many branches of technology. Among these are industries dealing with the production of petroleum and gas, including enhanced oil recovery, desalination of seawater, supercritical fluid extraction and oxidation, fertilizers and treatment of waste water. In the geosciences the ternary CO₂–H₂O–NaCl system is recognized to be an important model of the chemically more complex fluids that are present in the subsurface of the earth. Geoscience fields that make use of such models include geothermal energy, permafrost, hydrothermal ore deposits, fluid inclusions in minerals, and geological sequestration of anthropogenic emissions of CO₂.

Experimental measurements of the solubility of CO₂ in aqueous NaCl solutions have been assembled from 21 literature studies and tested for consistency using analytical and thermodynamic criteria. Of the 508 data compiled, 170 data (33%) were discarded and 36 were reserved to test the high-pressure dependency of the model. Possible reasons for the observed discrepancies between datasets are discussed. The 302 measurements that satisfy the acceptance criteria have been used to fit Pitzer parameters. These have been incorporated into a semi-empirical, γ – ϕ type thermodynamic model that builds upon published equations of state for the unary and binary subsystems.

The accepted experimental solubilities are reproduced by the model with a precision of better than 1.6% (one standard deviation) over the entire P–T–x range considered. The new model provides a thermodynamically consistent description of numerous properties of the aqueous liquid in the ternary CO₂–H₂O–NaCl system, including: CO₂ solubility (Fig. 1, next page) the activity coefficients, activities and partial molar volumes of CO_{2(aq)} and Na⁺ Cl[–]_(aq); the activity coefficient and osmotic coefficient of the solvent H₂O; the Setchenow coefficient; saturation indices of all four solid phases in the system (CO₂–clathrate–hydrate, ice, hydrohalite and halite); and the molar volume, excess molar volume and density of the bulk liquid. These properties can be calculated for any CO₂ concentration up to saturation, and for any NaCl concentration (whether stable or metastable).

The model is available as a computer code at <www.geo.unibe.ch/diamond>.

REFERENCES

- Akinfiev, N. N. & Diamond, L. W., 2010: Thermodynamic model of aqueous CO₂–H₂O–NaCl solutions from –22 to 100 °C and from 0.1 to 100 MPa. *Fluid Phase Equilibria* 295, 104–124.
- Diamond, L. W. & Akinfiev, N. N., 2003: Solubility of CO₂ in water from –1.5 to 100 °C and from 0.1 to 100 MPa: Evaluation of literature data and thermodynamic modelling. *Fluid Phase Equilibria* 208, 263–288.

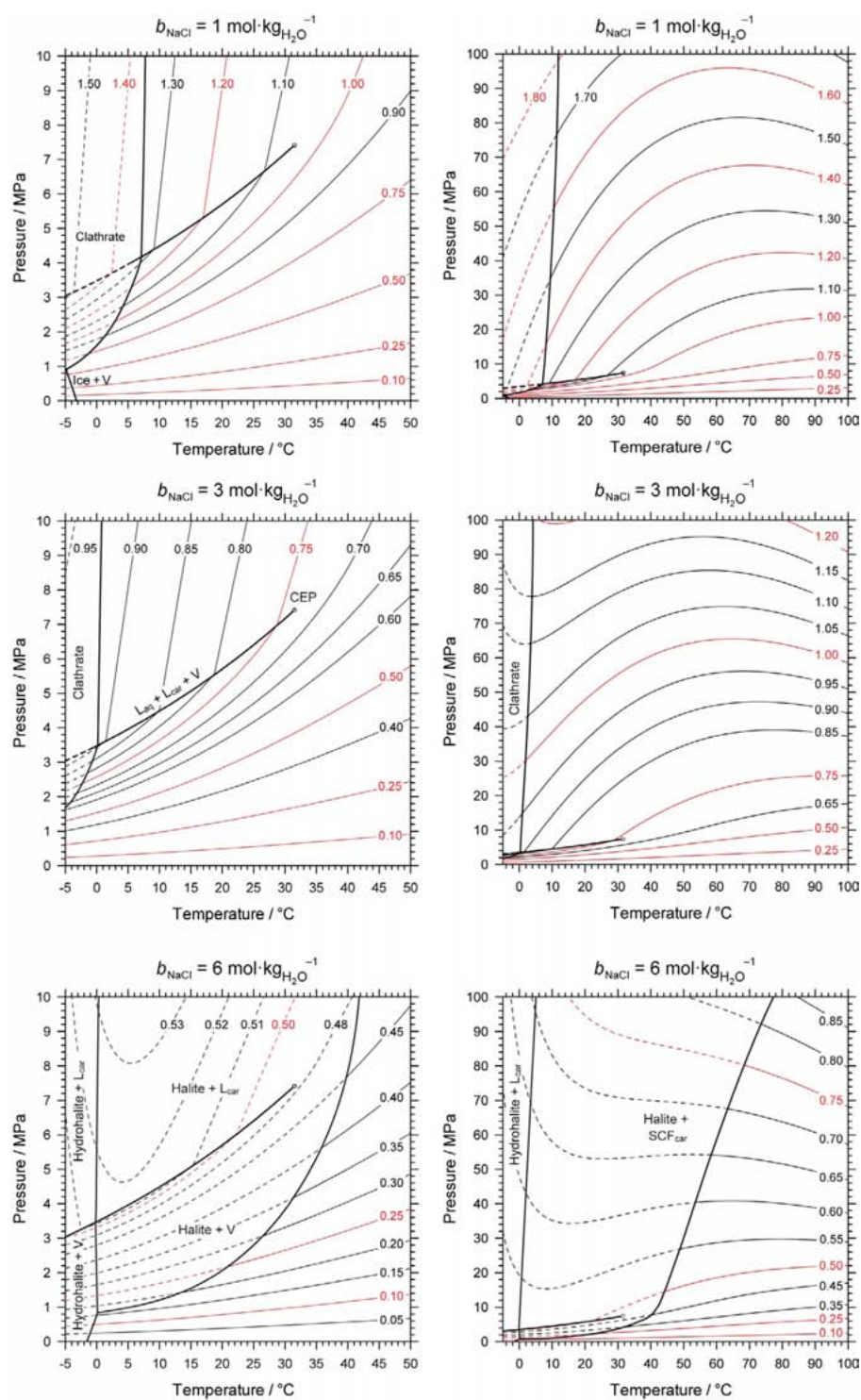


Figure 1. Contours of CO₂ solubility in aqueous solutions, calculated using our model. Each contour represents an isoplethic bubble curve of the system.

17.2

Reactive-transport modelling applied to geological sequestration of CO₂ in Switzerland

Alt-Epping, Peter¹, Diamond Larry W.¹

¹Rock–Water Interaction Group, Institute of Geological Sciences, University of Bern, Baltzerstrasse 3, CH-3012 Bern, Switzerland (alt-epping@geo.unibe.ch)

A recent study (Chevalier et al., 2010) has identified several deep saline aquifers in the Swiss Molasse Basin, which may potentially be useful as reservoirs to store waste CO₂. A further step in the evaluation of their potential is to consider issues of storage capacity, injectivity and fluid–rock reactivity, all of which are relevant to the safety and feasibility before, during and after the injection of CO₂. Only partial answers to these questions can be gained by in-situ testing and laboratory experiments. Therefore, predictive numerical models are required to assess the accompanying processes over spatial- and time-scales that are inaccessible to direct observation.

The numerical simulation of the physical and chemical processes during and after the injection of CO₂ is a challenging task because of the complexity and the coupled nature of the phenomena. The dominant physical/chemical processes and the trapping mechanisms during and after the injection of supercritical CO₂ into a geological formation vary significantly over time. During and shortly after injection, CO₂ displaces the brine in a drainage-like process, and vertical and lateral flow paths are created as CO₂ migrates laterally away from the injection wells and to the top of the injection aquifer due to buoyancy forces. Once injection stops, CO₂ continues to migrate upward and displace water at the leading edge of the plume, while at the trailing edge water displaces CO₂ in an imbibition-like process. A trail of residual, immobile CO₂ is left behind the plume as it migrates laterally and upward. The residual CO₂ and the CO₂ at the plume/brine interface slowly dissolves into the formation water, altering its chemical composition. Over longer time scales the fluid may then be involved in reactions with the rock and under favourable conditions dissolved CO₂ may precipitate and be permanently trapped as carbonate minerals.

A model that incorporates these processes and is constrained by the geological, physical and chemical characteristics of the injection site can be used for predicting the evolving system during and after CO₂ injection and for assessing the risks that may be posed by CO₂ geological storage. Some of the specific issues include the compositional perturbation of formation waters, the possible mobilisation of heavy metals and toxic hydrocarbons, the evolution of porosity and permeability as a function of mineral reaction progress in the reservoir and caprock lithologies, the chemical consequences of hypothetical leakage of CO₂ into overlying aquifers and into concrete-filled abandoned boreholes, the consequences of pressure build-up in the aquifer during injection, and other “what-if” scenarios.

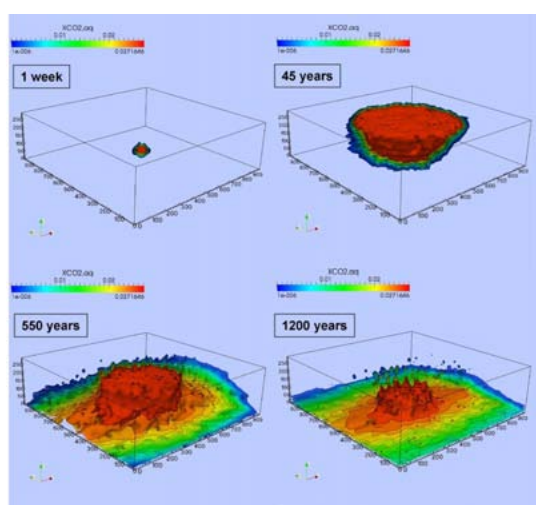


Figure 1: Model of an aquifer with heterogeneous permeability distribution.

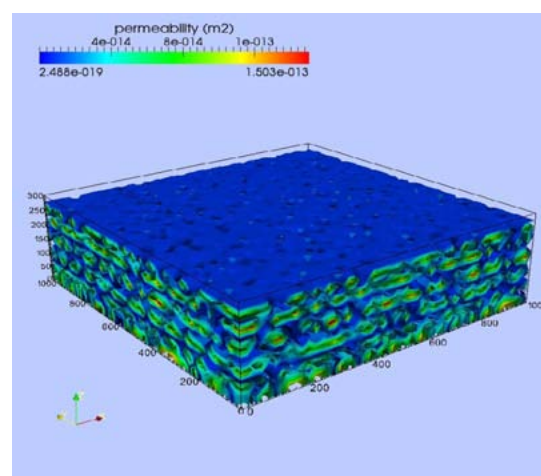


Figure 2: Mole fraction of dissolved CO₂ in the aquifer plotted at the indicated times. Injection rate: 2kg/s (63072 t/yr), total injection time: 30 years.

We are conducting numerical simulations with the code PFLOTTRAN (Mills et al., 2009) to address some of the above issues. The code is founded upon parallel data structure and solvers and specifically designed for high-performance computing. It permits fully coupled simulations involving multiphase fluid flow, solute transport, heat transport and chemical reactions (homogeneous and heterogeneous reactions, ion exchange, surface complexation and multirate kinetic sorption). Thus, insight is obtained into effects of spatial heterogeneities in the aquifer on multiphase flow, into effects on the integrity of caprocks in 3D and over distances in the order of km, and into kinetically-determined fluid-rock interaction over the envisaged periods of CO₂ confinement (hundreds to thousands of years). Here we present preliminary results of a numerical simulation of CO₂ injection into a stratified, heterogeneous aquifer (Figs. 1 and 2). This generic model scenario serves as an analogue of aquifers found in the Swiss Molasse Basin, and it illustrates the functionality of PFLOTTRAN and its suitability for the complex physical/chemical processes involved.

REFERENCES

- Chevalier, G., Diamond, L. W. & Leu, W., 2010: Potential for deep geological sequestration of CO₂ in Switzerland: a first appraisal. *Swiss Journal of Geosciences* 103 (3), In press (December issue).
- Mills, R.T., Hammond, G.E., Lichtner, P.C., Sripathi, V., Mahinthakumar, G., Smith, B.F., 2009, Modeling subsurface reactive flows using leadership-class computing. *Journal of Physics Conference Series*, in press.

17.3

Potential for deep geological sequestration of CO₂ in Switzerland: a first appraisal

Chevalier Gabriel¹, Diamond Larry W.¹, Leu Werner²

¹Rock–Water Interaction Group, Institute of Geological Sciences, University of Bern, Baltzerstrasse 3, CH-3012 Bern, Switzerland (diamond@geo.unibe.ch)

²Geoform Ltd., Via San Gottardo 56, CH-6648 Minusio, Switzerland

Possibilities to sequester anthropogenic CO₂ in deep geological formations are being investigated worldwide, but the potential within Switzerland has not yet been evaluated. This study presents a first-order appraisal based solely on geological criteria collated from the literature.

The Swiss Molasse Basin (SMB) and the adjacent Folded Jura are the only realms of the country where CO₂ could conceivably be stored in saline aquifers. Evaluation of geological criteria at the basin-wide scale shows that the SMB-Jura has moderate potential (score of 0.6 on a scale from 0 to 1) when compared to basins elsewhere. At the intrabasinal scale, inspection of the stratigraphy reveals four regional candidate aquifers that are sealed by suitable caprocks: top Basement plus basal Mesozoic sandstones, all sealed by the Anhydrite Group; Upper Muschelkalk sealed by the Gipskeuper; Hauptrogenstein sealed by the Effinger Member, and Upper Malm plus Lower Cretaceous sealed by the Lower Freshwater Molasse. Nine geological criteria are defined to evaluate the storage potential of these and other smaller-scale candidates. A numerical scoring and weighting scheme allows the criteria to be assessed simultaneously, permitting the storage potential to be depicted using the 0–1 scale in contoured maps (e.g. Fig. 1).

Approximately 5000 km² of the central SMB exhibits potentials between 0.6 and 0.96. The Fribourg–Olten–Luzern area is the most favoured owing to the presence of several sealed aquifers within the preferred 800–2500 m depth interval, and to its low seismicity, low geothermal gradient, low fault density, and long groundwater residence times. Smaller areas with good potential lie between Zürich and St. Gallen. In contrast, western Switzerland, the Jura and the southern SMB have markedly poorer potential. Considering only the portions of the aquifers with potential above 0.6, the theoretical, effective storage capacity of the basin is estimated to be 2680 million tonnes of CO₂.

REFERENCES

- Chevalier, G., Diamond, L. W. & Leu, W., 2010: Potential for deep geological sequestration of CO₂ in Switzerland: a first appraisal. *Swiss Journal of Geosciences* 103 (3), In press (December issue).

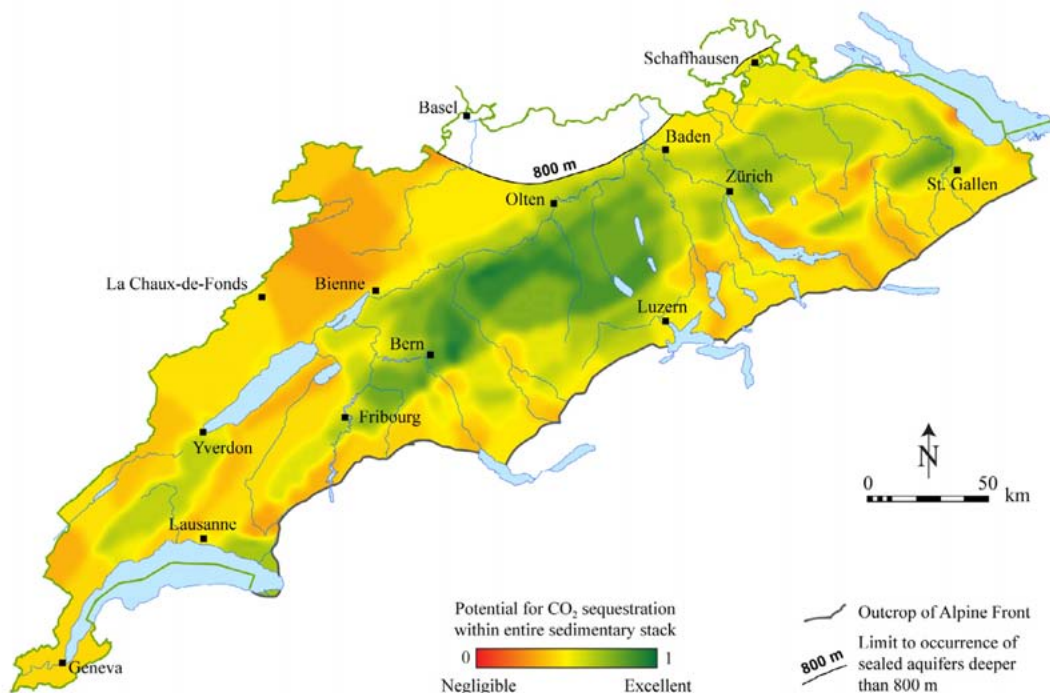


Figure 1. Potential of SMB and Jura for geological storage of CO₂. Colours show potential of entire sedimentary stack below each point in map.

17.4

RIBACLIM – Riverbank filtration under climate change scenarios

Diem Samuel¹ & Schirmer Mario¹

¹ Eawag, Swiss Federal Institute of Aquatic Science and Technology, Department of Water Resources & Drinking Water, Überlandstrasse 133, CH-8600 Dübendorf (samuel.diem@eawag.ch)

The National research programme NRP61 'Sustainable water management' aims at providing a scientific basis and methods for a sustainable management of water resources. In Switzerland about 80% of the drinking water is derived from groundwater of which 30% originates from riverbank filtrate. Riverbank filtration is a multipurpose treatment step that removes particles, natural and effluent organic matter and also micropollutants by filtration, adsorption and biodegradation. In the Swiss context, riverbank filtration is often the only barrier between river water and drinking water. This is possible because of the high wastewater treatment standards, the usually high dilution in receiving rivers and the fact that groundwaters are usually oxidic. However, a redox zonation has been observed in aquifers, which is induced by seasonal variations in river water temperature and increased loads of organic matter due to wastewater discharge (von Gunten et al. 1991). It has been shown that the degradation of organic micropollutants and dissolved organic matter (DOM) strongly depends on the redox milieu and the temperature. Therefore it's questionable, if safe drinking water supply can be guaranteed under scenarios of changing boundary conditions due to climate change.

RIBACLIM is one of 16 projects within NRP61 and intends to better understand how the fate of DOM, the coupled redox zonation and the degradation of micropollutants develop in riverbank filtration systems under different climate change scenarios. The project is subdivided in three blocks, each one being a PhD subject. The first block deals with photochemical transformation of DOM and micropollutants in the river. The second one investigates the redox zonation and degradation of DOM and selected micropollutants by means of column experiments. Laboratory data will be used to calibrate a 1D reactive transport model and the resulting kinetic parameters will be used to setup a 2D vertical reactive transport model on the field scale as part of block three.

We want to present the objectives of thesis three and show the different steps, which are planned to achieve them. Over the past two decades, numerical methods were developed to model transport, kinetic microbial degradation and geochemistry simultaneously and were applied to investigate different kinds of organic contaminant-impacted aquifers in 1D, 2D and 3D (Mayer et al. 2002; Molson et al. 2002). In parallel, several models were developed to simulate the behavior of or-

ganic contaminants within riverbank filtration (Horner et al. 2007; von Gunten & Furrer 2000). These models often consider just advective transport and all of them are related to an isothermal system and 1D geometry. Thus to date, a quantitative link between the 1D laboratory column scale and the 2D or 3D field scale has been lacking in modeling bank filtration.

In block three of the project RIBACLIM we will first perform 1D numerical simulations to determine transport parameters (porosity, longitudinal dispersivity) and to help design suitable experimental conditions for the column experiments (boundary conditions, flow rates, sampling locations and frequency). For the reactive transport modeling we use the state-of-the-art model BIONAPL, which simulates flow and coupled reactive transport for multiple aqueous contaminants in a porous system (Molson et al. 2002). Column experiments are carried out for baseline scenarios first, followed by several climate change scenarios consisting of temperature changes and/or changes of the fraction of wastewater effluent and with that also DOM concentrations. We will simulate column data to draw quantitative conclusions and assess the kinetic parameters for the degradation of DOM and the micropollutants under different temperature and redox conditions.

The test site Niederneunforn at the river Thur was chosen for the development of the 2D vertical numerical flow and transport model at field scale (www.ces.ethz.ch/projects/nature/Record/sites). Firstly, we will establish a 2D horizontal groundwater flow model using FEFLOW (DHI-WASY GmbH) to understand and reproduce the groundwater flow field in this highly dynamic river-groundwater system. For its calibration, we are monitoring groundwater and surface water levels, temperatures and electrical conductivities at about 30 points. Secondly, we will set up the cross-sectional 2D flow and transport model along an identified groundwater flow path using the conceptual model of the 1D modeling as an initial base case. Sampling of ground and river water for micropollutants and redox parameters should allow us to re-calibrate kinetic parameters and their temperature and redox dependencies, if necessary. We will then simulate a range of different climate scenarios with different flow conditions, different temperature regimes and DOM loads. This enables us to anticipate effects on the redox zonation, DOM degradation and the fate of micropollutants, all relevant for drinking water supplies. This will be the first quantitative modeling study of a 2D field scale and temperature-dependent reactive bank filtration system linked to detailed laboratory-derived reaction rates.

REFERENCES

- Horner, C., Holzbecher, E. & Nützmann, G., 2007: A coupled transport and reaction model for long column experiments simulating bank filtration. *Hydrological Processes* 21(8), 1015-1025.
- Mayer, K.U., Frind, E.O. & Blowes, D.W., 2002: Multicomponent reactive transport modeling in variably saturated porous media using a generalized formulation for kinetically controlled reactions. *Water Resources Research* 38(9), 131-1321.
- Molson, J.W., Barker, J.F., Frind, E.O. & Schirmer, M., 2002: Modeling the impact of ethanol on the persistence of benzene in gasoline-contaminated groundwater. *Water Resources Research* 38(1), 4/1-4/12.
- von Gunten, H.R. et al., 1991: Seasonal biogeochemical cycles in riverborne groundwater. *Geochimica Et Cosmochimica Acta* 55(12), 3597-3609.
- von Gunten, U. & Furrer, G., 2000: Steady-state modelling of biogeochemical processes in columns with aquifer material: 2. Dynamics of iron-sulfur interactions. *Chemical Geology* 167(3-4), 271-284.

17.5

Climate change and groundwater quality: analysis of historical records

Figura Simon¹, Livingstone David¹, Hoehn Eduard¹ & Kipfer Rolf^{1, 2}

¹ Eawag: Swiss Federal Institute of Aquatic Science and Technology, Ueberlandstrasse 113, 8600 Duebendorf (simon.figura@eawag.ch)

² Institute of Isotope Geology and Mineral Resources, Swiss Federal Institute of Technology Zurich (ETH)

Although climate change is expected to have a strong impact on the hydrological cycle, little is known about its effect on groundwater in general, and on groundwater quality in particular (Bates et al., 2008). In our study, we attempt to assess the effect of climatic forcing and climate change on the quality of Swiss groundwaters based on a statistical analysis of historical time-series of physical and chemical variables measured in groundwater wells.

We (Figura et al., in prep.) analysed historical temperature records from five granular, unconsolidated, river-fed aquifers located on the Swiss Plateau (Fig. 1). Two statistical tests were applied to identify abrupt changes in these and in other relevant time-series. Groundwater temperatures, river temperatures and air temperatures were all found to have under-

gone an abrupt increase in the late 1980s, when annual mean groundwater temperatures increased by 0.4°C to 1°C, and annual mean air and river water temperatures increased by 0.6°C to 1.4°C. Additionally, annual mean groundwater temperatures were found to be highly correlated with annual mean air and river temperatures ($r^2 > 70\%$; $p < 0.01$).

Our pilot analysis suggests that fluctuations in the temperature of groundwaters recharged by rivers are strongly dominated by fluctuations in regional air temperature. The abrupt temperature shift in the late 1980s, which is commonly observed in various other environmental and aquatic systems, including Swiss rivers (Hari et al., 2006), is now acknowledged to be a manifestation of a large-scale climate regime shift associated with changes in the behaviour of the North Atlantic Oscillation (e.g., Conversi et al., 2010). Hence, our work suggests that the late 1980s climate regime shift also had a strong effect on the temperature of river-fed groundwaters.

In a next step, we will statistically model future groundwater temperatures based on climate predictions for Switzerland, and will analyse the conditions under which increasing groundwater temperatures might affect other groundwater quality metrics. For example, do higher groundwater temperatures lead to reduced oxygen concentrations, thus changing the redox conditions in Swiss groundwaters?

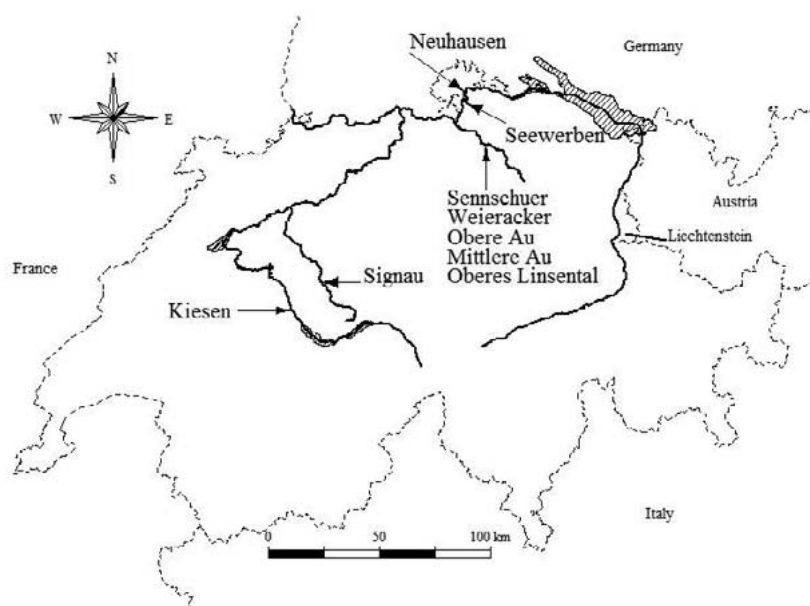


Figure 1: Locations of aquifers investigated by Figura et al. (in prep.).

REFERENCES

- Bates, B. C., Kundzewicz, Z. W., Wu, S. & Palutikof, J. P. 2008: Climate change and water. Technical paper of the Intergovernmental Panel on Climate Change. Technical report, IPCC Secretariat, Geneva.
- Conversi, A., Umani, S. F., Peluso, T., Molinero, J. C., Santojanni, A. & Edwards, M. 2010: The Mediterranean Sea regime shift at the end of the 1980s, and intriguing parallelisms with other European basins. *PLoS ONE* 5 (5): e10633. doi: 10.1371/journal.pone.0010633
- Figura, S., Livingstone, D. M., Hoehn, E. & Kipfer, R. 2010: manuscript in preparation.
- Hari, R. E., Livingstone, D. M., Siber, R., Burkhardt-Holm, P. & Guetinger, H. 2006: Consequences of climatic change for water temperature and brown trout populations in Alpine rivers and streams. *Global Change Biology*, 12 (1), 10-26.

17.6

Infiltration depths due to increased rain intensities and durations as a consequence of climate change

Peter Germann^{1, 2}

¹ SGH-Arbeitsgruppe "Grundwasser und Klima" (pf.grmann@bluewin.ch)

² Geographisches Institut der Universität Bern, Hallerstrasse 12, Bern

The climate change scenario for the Swiss Plateau predicts increased intensities and durations, and increased spatial and temporal heterogeneities of rainfall. Recently, some of the predictions already seem to have materialized.

While soils may dry up more pronounced than in the past decades, preferential flow of rains with increased intensity may carry infiltrating water fast to greater depths (Gerke et al., 2010). The plants may additionally suffer from water deprivation, thus enhancing the demand for crop irrigation. Moreover, water that has passed the biologically active and rooted soil horizons - mainly the A-horizons that are rich in organic matter - is much less exposed to bio-chemical filtering and may carry germs and chemicals to greater depths where it faster reaches wells and groundwater bodies.

Recent progress in the research of preferential infiltration applies Stokes theory to flow in soils and similar permeable media, like unconsolidated sediments and fissured rocks. The following considerations are relevant to our assessment. The wetting front velocity, v_w (m s⁻¹) is fairly conservative and may remain constant over depth ranges from 0.2 to at least 20 m (i.e., Rimón et al., 2007; Germann and al Hagrey, 2008; Ochoa et al., 2009). It scales to the intensity q_s (m s⁻¹) of infiltration according to

$$v_w = F^2 \cdot (g/3 \cdot \eta) \quad (1)$$

The wetting front depth, $z_w(t)$ (m) moves with the constant velocity v_w during a period that lasts 3/2 times the duration t_s (s) of the rain. After that the wetting front slows down and it progresses in proportion to the third power of time. Equation (1) is based on

$$v_w = F^2 \cdot (g/3 \cdot \eta) \quad (2) \quad \text{and} \quad q_s = F^3 \cdot L \cdot (g/3 \cdot \eta) \quad (3)$$

where F (m) is the thickness of the water film, L (m⁻¹) is the vertical contact area per unit volume of the permeable medium onto which momentum dissipates, g (=9.81 m s⁻²) and η (=10⁻⁶ m² s⁻¹) are acceleration due to gravity and kinematic viscosity of water. Hincapié and Germann (2009) reported approximate ranges of $5 \leq F \leq 100$ (μm) and $0.2 \leq L \leq 20$ (km⁻¹)

To illustrate the abstract, relative durations and intensities were doubled in five steps that yielded the relative increase of the wetting front depths in the maximum range of 1 : 3.18. The increases are in many cases strong enough to move a substantial amount of rain markedly beyond the root zone that would have stayed there under non-disturbed (i.e., pre-climate-change scenario) conditions.

REFERENCES:

- Gerke, H.H., P. Germann, and J. Nieber (2010) Preferential and unstable flow: From the pore to the catchment scale. *Vadose Zone J.* 9:207–212. doi:10.2136/vzj2010.0059
- Germann, P.F., and S.A. al Hagrey (2008) Gravity-driven and viscosity-dominated infiltration into a full-scale sand model. *Vadose Zone J.* 7:1160–1169; doi:10.2136/vzj2007.0172.
- Hincapié, I., and P.F. Germann (2009) Abstraction from infiltrating water content waves during weak viscous flows. *Vadose Zone J.* 8:996–1003.
- Ochoa, C.G., A.G. Fernald, S.J. Guldán, and M.K. Shukla (2009) Water movement through a shallow vadose zone: A field irrigation experiment. *Vadose Zone J.* 8:414–425.
- Rimón, Y., O. Dahan, R. Nativ, and S. Geyer (2007) Water percolation through the deep vadose zone and groundwater recharge: Preliminary results based on a new vadose zone monitoring system. *Water Resour. Res.*, 43, W05402, doi:10.1029/2006WR004855.

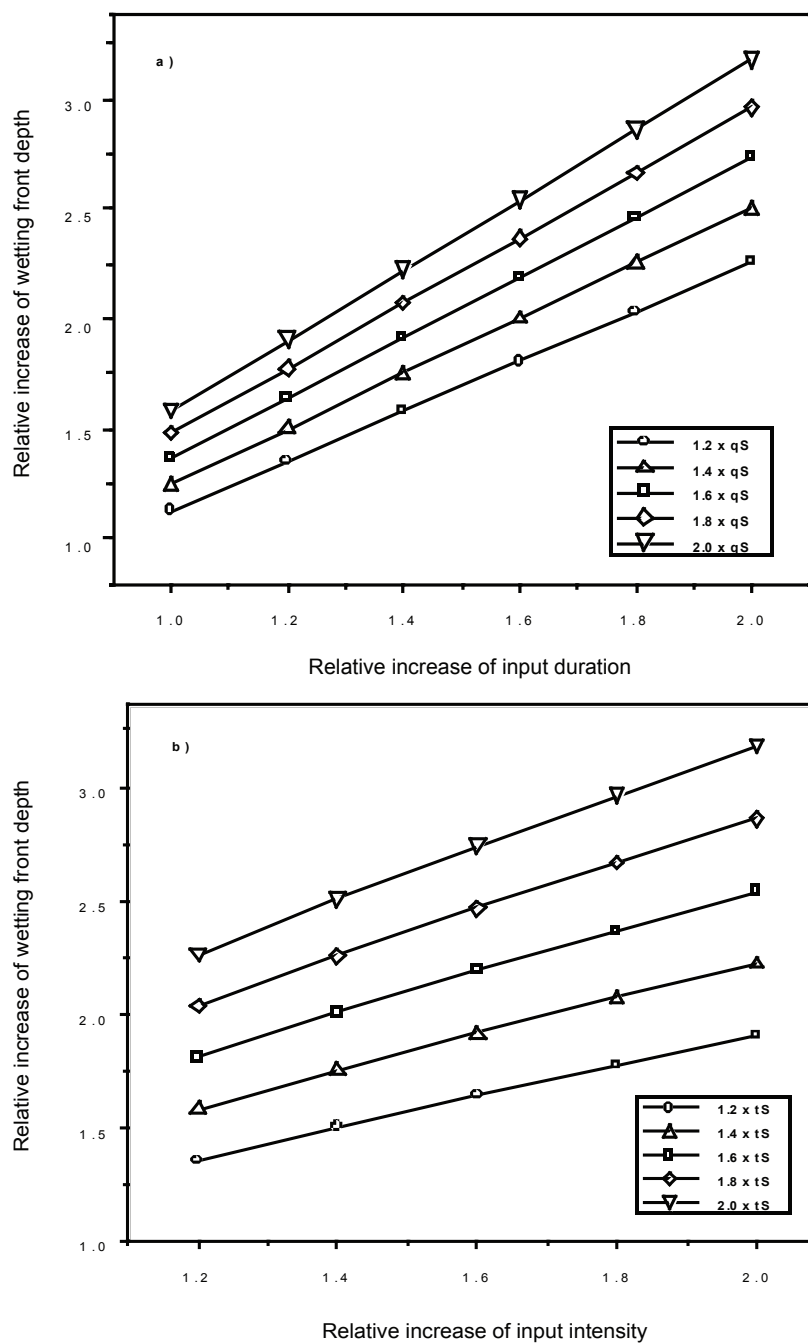


Figure 1: Relative increases of wetting front depths due to rainfall increase of a) duration, b) intensity, where qS and tS are relative rates and durations of rain fall events.

17.7

Evolution, sur plus de 20 ans, de quelques paramètres hydrochimiques des eaux souterraines suivies dans le cadre de l'étude d'impact de l'autoroute la Transjurane (A16, Canton du Jura)

Marc Hessenauer¹, François Flury¹

¹ MFR Géologie-Géotechnique SA, 9 rue de Chaux 2800, Delémont

Les sections 1 à 3 de l'autoroute A16 traversent le plateau karstique de l'Ajoie dans le Jura tabulaire (NW Canton JU), entre les communes de Porrentruy et Boncourt.

Dans le cadre de l'étude d'impact sur l'environnement (EIE) de ce projet, un réseau hydrologique de surveillance quantitative et qualitative a été mis en place dès 1989. Sur une superficie de l'ordre de 100 km², celui-ci se compose d'une cinquantaine de points d'eau regroupant des puits en nappe alluviale, des sources essentiellement karstiques pérennes exploitées ou non, des sources temporaires de crue, des rivières souterraines, des piézomètres et une rivière (Allaine).

Le suivi quantitatif consiste à mesurer automatiquement (pas de temps de 15 minutes), sur 17 stations, le débit et/ou le niveau d'eau ainsi que la conductivité électrique et la température. Ce réseau bénéficie donc actuellement d'une période de suivi de plus de 20 ans.

En ce qui concerne la débitmétrie, les chroniques présentent une bonne corrélation avec les données météorologiques (précipitations). Par contre, ces chroniques ne montrent pas de cycle, ni d'évolution statistique notoire. Il n'en est pas de même pour les chroniques de température et notamment pour les enregistrements dans la rivière souterraine la Milandraine. Les moyennes mensuelles calculées depuis 1990 rendent compte de l'évolution globale des températures à ce point d'eau de type karstique. On observe notamment des variations saisonnières, d'une amplitude variant de 0.1 à 0.5 °C, marquées par un pic de température en général vers octobre et un minimum de température vers mars-avril. Le décalage par rapport à la température de l'air à l'extérieur de la grotte est donc de l'ordre de 2 mois.

Une tentative de corrélation de ces valeurs mensuelles en fonction du temps (Figure 1) montre qu'il existe une évolution notoire qui semble suivre un cycle pluriannuel. La tendance globale indique une augmentation de la température de l'eau de 0.3 °C depuis 1990.

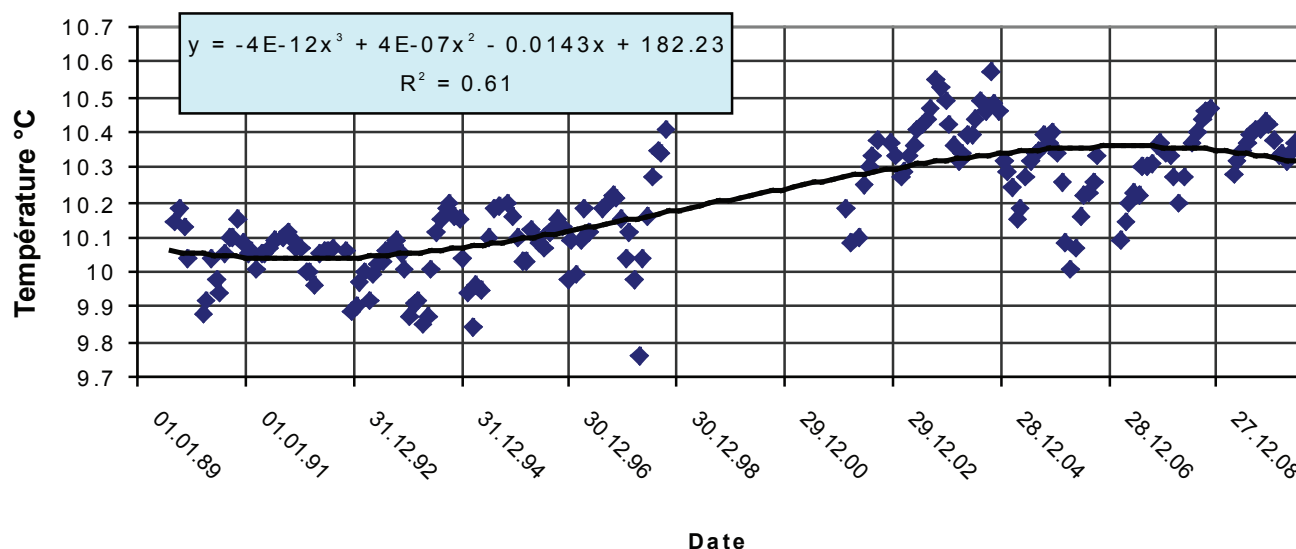


Figure 1 : Evolution des moyennes mensuelles de la température de l'eau dans la Milandraine

Le suivi qualitatif, quant à lui, a été systématisé à partir de 2003 : les prélèvements sur une quarantaine de points d'eau se font avec une fréquence trimestrielle pour les paramètres physico-chimiques et une fréquence semestrielle pour les micropolluants (hydrocarbures et métaux lourds). Grâce à ce projet autoroutier, l'évolution des paramètres hydrochimiques peut donc être appréciée sur une longue période de suivi (actuellement 20 ans), complétée, sporadiquement, par des données antérieures. Une démarche rigoureuse utilisant une distribution statistique de chaque paramètre physico-chimique sur chaque point d'eau a permis de mettre en évidence, sur certains d'entre eux, des évolutions à long terme. Il s'agit, en particulier, du bicarbonate (HCO_3^-), du pH, de l'oxydabilité, des sulfates (SO_4^{2-}) et des chlorures (Cl^-). L'évolution du bicarbonate montre, par exemple, une nette augmentation, quasi linéaire, de 60 mg/l au cours des 25 dernières années (Figure 2).

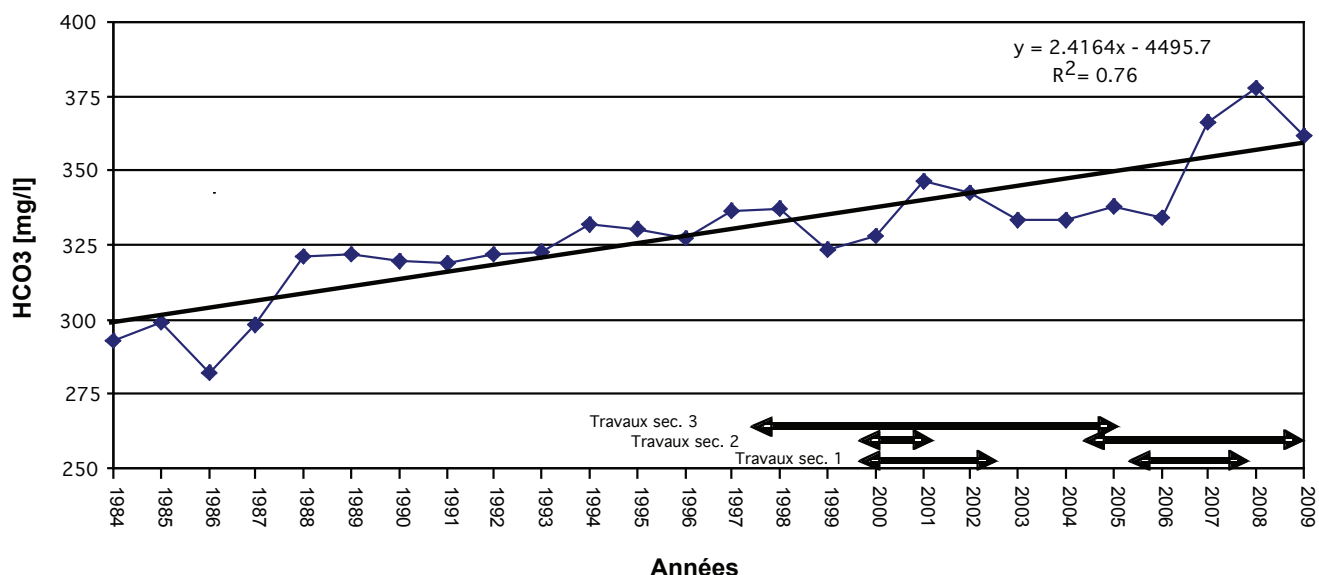


Figure 2 : Evolution de la teneur moyenne annuelle en bicarbonate sur 15 points d'eau

En ce qui concerne le paramètre température, seule une faible proportion des points d'eau surveillés (1/6^{ème}) montre une évolution notoire marquée, de la même manière qu'avec les mesures automatiques, par un cycle pluriannuel.

La mise en évidence de ces évolutions de grande amplitude temporelle fait appel à certaines réflexions et questions :

- à priori, ces évolutions ne semblent pas imputables à l'A16 ;
- s'agit-il de phénomènes liés à des cycles naturels ?
- serait-ce le résultat d'impacts anthropiques (pluies acides, réchauffement climatique, pratiques agricoles, réseau routier,...) ?
- y a-t-il un lien entre les différents paramètres ?
- existe-t-il une différenciation géologique dans l'observation de ces évolutions ?
- les autres paramètres présentent-ils aussi, au moins sporadiquement, de telles évolutions notaires ?
- d'autres cas similaires ont-ils été observés ailleurs ?

REFERENCES

- MFR Géologie-Géotechnique SA 2009 : A16 Sections 1 à 3. EIE eaux souterraines et superficielles. Annuaire des données Madd, années 2005 à 2006. Service des Ponts et Chaussées, Delémont (non publié)
- MFR Géologie-Géotechnique SA 2010 : A16 Sections 1 à 3. EIE eaux souterraines et superficielles. Suivi qualitatif des eaux par point de prélèvement. Service des Ponts et Chaussées, Delémont (non publié)

17.8

Modeling the effects of climate change on the vulnerability of karst groundwater resources

Peter Huggenberger & Christoph Butscher

University of Basel, Applied and Environmental Geology, Switzerland

Many river basins rely on karst groundwater as feeder of springs, brooks, rivers and streams. However, karst aquifers are very sensitive to changes in the hydrological conditions of the recharge areas. These conditions depend on the interaction of precipitation, evapotranspiration and retention capacity of the soil and epikarst. Global warming due to the greenhouse effect is predicted to cause changes in precipitation patterns and evapotranspiration. In the context of the ongoing debates on the impact of climate change to society, it is important to see how the vulnerability of karst systems is influenced by changing hydrological conditions.

A model is presented that allows making predictions of the behavior and vulnerability of karst systems under time-variant groundwater recharge conditions. It is used to assess the effects of predicted climate change on karst groundwater vulnerability based on two climate scenarios, one accounting for heat waves such as observed in central Europe 2003, the other accounting for severe precipitation events, which are predicted to become more and more frequent. The model simulations indicate that decreasing groundwater recharge during dry summers result in increasing vulnerability to persistent pollutants (e.g. pesticides) due to reduced dilution effects, but decreasing vulnerability to easily-degradable pollutants (e.g. fecal bacteria) due to reduced infiltration into the karst system. The increase in extreme rainfall events, in contrast, is expected to have the opposite effect. Which of the two countering processes becomes most relevant to the groundwater vulnerability of an individual karst basin will depend on the actual characteristics of both the recharge conditions and the karst system, as well as on the human activity in the catchment area. The proposed numerical model provides an effective tool for predicting karst groundwater vulnerability at the basin scale under varying climatic conditions.

17.9

Influence of groundwater/stream water interactions in sustaining environmental flow and water supply in a changing climate: the case of an Alpine alluvial aquifer, the Upper Emme

Käser Daniel¹, Perrochet Pierre¹, Renard Philippe¹, Schirmer Mario¹, Zwahlen François¹ & Hunkeler Daniel¹

¹ Centre de hydrogéologie et géothermie, Rue Emile-Argand 11, CH-2000 Neuchâtel (christian.moeck@unine.ch)

² Eawag, Überlandstrasse 133, CH- 8600 Dübendorf

In many regions of the world, including Switzerland, groundwater is a key resource during droughts. In low flow conditions, water stored in the wet season becomes available for both, ecosystems and society. With stock depletion, however, the competition between these two entities increases, thus raising a number of questions driven by management considerations: How long can the abstraction rate be maintained without damaging the ecosystem? What is the optimal abstraction rate that would promote water availability on the long term? What are the controls on groundwater/surface water exchanges? And more generally: how can one expect such systems to behave, in response to various climate change scenarios?

The present project addresses these issues through a study case: the alpine alluvial system of the Upper Emme, in the Canton of Bern. The alluvial aquifer, which drains a X km² basin, is approximately 15 km long and 30 m deep. A riverbank filtration scheme, located at the outlet of the watershed, is allowed to extract 0.4 m³/s, as long as the nearby stream flow is higher than 0.11 m³/s. The mixed snowmelt-rainfall regime means that dry periods occur, in average, twice a year: during the hotter summer and in winter, when precipitation is stored as snow.

The poster presents the methodological approach, the data requirements, the modeling strategy, and the expected outputs of this study. The alluvial plain will be represented by a 3D model that integrates surface and subsurface flow (HydroGeoSphere). Field work includes the installation of observation wells, weather stations, flow monitoring stations, as well as measurements of differential flow, hydraulic head, and snow volume. Spatial and temporal variations of oxygen and hydrogen isotopes are also monitored in the rain, the river and the groundwater, in order to characterize transit times at the catchment scale.

17.10

Groundwater shortage due to climate change

Möck Christian¹, Baillieux Antoine¹, Schirmer Mario², Hunkeler Daniel^{1,1}

¹ Centre de hydrogeologie et geothermie, Rue Emile-Argand 11, CH-2000 Neuchâtel (christian.moeck@unine.ch)

² Eawag, Überlandstrasse 133, CH- 8600 Dübendorf

In Switzerland, nearly 40 % of drinking water comes from springs and consists one of the main water supply for many regions. The 2003 heat wave and the consecutive drought have shown how vulnerable the system is. The response of the groundwater systems, especially springs to drought, however, is complex and not readily predictable. While some show a decrease of discharge and a lowering of the water table, others do not react, or only slightly, to such extreme weather conditions. In this context, the aim of this study is to understand what are the factors driving the hydrodynamic of groundwater emergences and to estimate their vulnerability under different climate scenarios, especially to droughts.

In this purpose, two different field sites are chosen. The first site is located at Wohlenschwil, in the Reuss valley (400 m a.s.l.) in a relatively flat moraine landscape with a porous aquifer. Because of the water abstraction scheme, no spring discharge can be observed but the dynamic of this system is typical of a spring behavior. The second site is near Langnau, in the Upper Emme valley (860 m.a.s.l.) and consists of several springs discharging from a mostly fractured molasse.

Tracer tests and isotopes measurements, as well as geophysical and hydraulic methods are applied for unsaturated and saturated zones to quantify dynamics, recharge processes and estimate the buffer capacity of the systems during dry phases. All field results are used to build up a fully coupled numerical model which aims to evaluate the dynamic of the system.

Preliminary results from tracer tests and numerical modeling show that, only with an integral approach that includes both the saturated and unsaturated zones, a global assessment of transit times and of the buffer capacity is possible. Furthermore, numerical modeling based partly on soil water measurements and water table observation of the "Wohlenschwil" catchment shows that recharge processes are only controlled by precipitation and that inflow from borders are of minor role. The dynamic of this area is strongly dependant on the local climate.

Therefore, the next step of this study will be a more detailed investigation of the soil moisture at different location in the catchment. This approach should help to obtain a better understanding of the direct recharge and the flow processes under various meteorological conditions.

17.11

Analysis of the impact of climate change on groundwater related hydrological fluxes

Stoll Sebastian¹, Hendricks Franssen Harrie-Jan², Butts Michael³ & Kinzelbach Wolfgang¹

¹ Institute of Environmental Engineering, ETH Zurich, CH-8093 Zurich (stoll@ifu.baug.ethz.ch)

² Agrosphere, ICG-4, Forschungszentrum Jülich GmbH, D-52425 Jülich

³ DHI Water and Environment, DK-2970 Hørsholm

Climate change related changes in the spatio-temporal distribution of precipitation and evapotranspiration will have an impact on groundwater resources. This study presents a modelling approach exploiting the advantages of integrated hydrological modelling and a broad climate model basis. We applied the integrated MIKE SHE model on a perialpine, small catchment in northern Switzerland near Zurich. To examine the impact of climate change we forced the hydrological model with data from eight regional climate models (RCM) showing systematic biases which are corrected by three different statistical downscaling methods, not only for precipitation but also for the variables that govern potential evapotranspiration. The downscaling methods are evaluated in a split sample test and the sensitivity of the downscaling procedure on the hydrological fluxes is analyzed. The RCMs resulted in very different projections of potential evapotranspiration and, especially, precipitation. All three downscaling methods reduced the differences between the predictions of the RCMs and all corrected predictions showed no future groundwater stress which can be related with more expected precipitation during winter. It turned out that especially the timing of the precipitation and thus recharge is very important for the future development of the groundwater levels. However, the simulation experiments revealed the weaknesses of the downscaling methods which directly influence the predicted hydrological fluxes, and thus also the predicted groundwater levels. The downscaling process is identified as an important source of uncertainty in hydrological impact studies, which has to be accounted for. Therefore it is strongly recommended to test different downscaling methods by using verification data before applying them on climate model data.

17.12

Modelling the sensibility of the alpine and perialpine hydrogeological systems in climate change

Tacher Laurent¹, Turberg Pascal¹, Breguet Alain¹, Parriaux Aurèle¹

¹ GEOLEP, EPFL ENAC IIC, GC B, station 18, 1015 Lausanne

(Laurent.tacher@epfl.ch, pascal.turberg@epfl.ch, alain.breguet@epfl.ch)

The effects of climate change on Swiss groundwater systems still remain little studied and are consequently poorly known. It thus seems important to know if this climate change could have a significant influence on this water resource and, if necessary, to determine what will be the types of aquifers the most sensitive to climate changes.

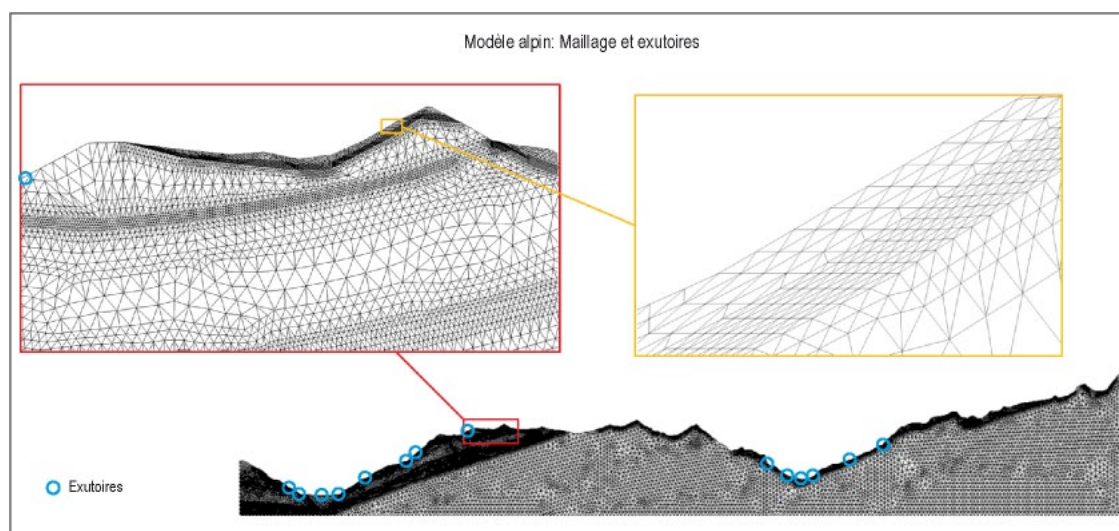
The climatic effects on groundwater systems of the alpine environment are studied on the basis of a 2D vertical transient numerical model. The geological, hydrogeological, topographic and altitude conditions defined for this model are fictive but inspired by those of the alpine environment.

The initial recharge conditions are extracted from typical meteorological chronicles (data from MeteoSwiss) and their evolution for the next 50 years due to climate changes are based on the OcCC report data (2007).

The main objectives of this modeling process are to characterize the foreseen variations in recharge conditions for different types of aquifers, to determine the quantitative effects of these variations on the groundwater systems and their re-surgences and finally to raise a comparative assessment of the sensibility of these different aquifers to climate change in alpine environment.

The structure of the alpine model, its hydrogeological parameters, the processing and the use of data in relation with the recharge of the aquifer systems are described and explained.

The first results of this model are presented. The behavior of these groundwater systems in response to the recharge evolution, in terms of hydraulic potential and discharge rate, and the possible impact of these variations on the groundwater supply of alpine populations are discussed.



REFERENCES

OcCC 2007: Les changements climatiques et la Suisse en 2050.

OcCC 2005 : Canicule de l'été 2003, Rapport de synthèse.

OcCC 2002 : Le climat change, en Suisse aussi.

EEA Report No 8/2009 : Regional climate change and adaptation.

Frei, C, Christensen, J. H., De´que, M., Jacob, D., Jones R. G. & Vidale, P. L. 2003 : Daily precipitation statistics in regional climate models:

Evaluation and intercomparison for the European Alps, Journal of geophysical research, VOL. 108, NO. D3.

17.13

Irrigation and groundwater quality in times of climate change

Christiane Vögeli Albisser¹ and Volker Prasuhn¹

¹ Agroscope Reckenholz-Tänikon Research Station ART, Reckenholzstrasse 191, CH-8046 Zürich

The hot summer of 2003 showed what weather conditions – according to climate forecasts – are increasingly to be expected in future. High temperatures combined with long dry spells during the main growing season will also make irrigation increasingly necessary in Switzerland. By examining the extent to which nitrates and plant-protection products leach into the groundwater supply, this study aims to determine whether irrigation or lack of irrigation during a dry spell can threaten groundwater quality.

Twelve roofed and weighable lysimeters with a surface area of 3.14 m² and two different soils are available for three cultivation periods (2010-2012) to answer this question. Each cultivation period is dedicated to an agricultural crop, beginning with maize, with three irrigation treatments (?) repeated twice and tested in parallel on both soils. As a reference treatment (Treatment 1), the 2003 drought, without additional watering, is simulated for four lysimeters. The other lysimeters are subjected to two different irrigation intensities. The first of these, Treatment 2, is meant to represent optimum watering, where we let the useful field capacity (uFC) drop to 50%, then irrigate until the soil has reached 80% uFC. With Treatment 3, however, the 80% uFC irrigation point deemed to be optimum is exceeded until the soil exhibits 120% uFC. This simulates a situation of over-irrigation.

The leachate from the lysimeters is sampled at regular intervals over the entire year and tested for contents of nitrate and the plant-protection product sprayed in the spring. The comparison of the treatments is intended to show the extent to which irrigation during dry spells affects groundwater quality. Results from the first experimental year are presented. In addition, in a next step, different ways of managing irrigation are assessed by means of simulation models with a view to making irrigation recommendations.

This study was initiated and financed by the Swiss Federal Office for the Environment.

18. Troubling water: modes of socialization of a natural resource

Olivier Ejderyan & Olivier Graefe

Swiss Geography Association (ASG)

- 17.1 Hemund C., Weingartner R., Jorde K.: Integrated Assessment of the Small Hydropower Potential in Switzerland
- 18.2 Homewood C.: MontanAqua: an assessment of the socio-economic and institutional setting
- 18.3 Meyer U.: Water and women in rural Amhara: A <naturalized> connection reflecting a restricting political agenda in Ethiopia
- 18.4 Schneider F., Rist S., Weingartner R., Herweg K., Liniger HP., Schädler B., Kauzlaric M., Rey E., Graefe O., Hoelzle M., Homewood C., Reynard E., Bonriposi M.: Water Scarcity in Inner-Alpine Regions Options for sustainable water use in the Crans-Montana-Sierre region (Valais)
- 18.5 Schweizer R.: Les bisses et leurs modes d'organisation au XXIe siècle, un modèle de gestion durable ?

18.1

Integrated Assessment of the Small Hydropower Potential in Switzerland

Hemund Carol ^{1,2}, Weingartner Rolf ^{1,2} & Jorde Klaus ³

¹ Institute of Geography, University of Bern, Hallerstrasse 12, CH-3012 Bern (hemund@giub.unibe.ch)

² Oeschger Centre for Climate Change Research, University of Bern, Zähringerstrasse 25, CH-3012 Bern

³ SFOE - Research program "Waterpower", Entec AG, St. Leonhardstrasse 59, CH-9000 St. Gallen

Consequences arising out of Climate Change and increasing energy demand urge nations to adapt their energy policies. Special emphasis is put on renewable energy production. Increased efforts are made not only in the European Union (EU 2000) but also in particular states such as Switzerland (Swiss Confederation 2007).

Until today Switzerland's largest part of energy production has been provided by hydropower. Thus, about 90% of all the rivers are already being used for electricity production. At first glance promoting the expansion of renewable energies such as hydropower seems to be inappropriate. However, recent studies reveal the possibility of an increase, taking into account the feasible Small Hydropower SHP potential and improvements in efficiency (SFOE 2000).

In order to accomplish the targets set in SFOE (2008), incentives have been introduced in 2009 to facilitate renewable energy projects (KEV). Subsequently, responsible authorities are being overcharged with numerous proposals including Small Hydropower plants. The conflicting demands of protection and utilisation flare up anew and interfere with approved solutions. Authorities clearly lack an adequate tool supporting that decision making process.

The aim of our study is to provide such a method allowing a holistic assessment of the SHP potential in a region. Accordingly, we suggest a method considering sustainability and water management from a large-scale perspective. Results will contribute to the joint research project "Investigation of the Small Hydropower Potential in Switzerland" on behalf of the Federal Office of Energy SFOE.

To cover the complexity of a river system and all the conflicting demands at its best, the authors suggest a multi-level approach. In the area of interest the streams and their adjacent area are assessed with the highest possible objectivity by means of criteria raster. That resulting value indicates the current state; it is then balanced against the hydro-electrical potential to reveal areas with priority protection. Finally, maps showing different distribution patterns for SHP implementation will be provided. These scenarios will be based on selectable intensities of use, depending on the scheduled extension of SHP production in the region considered.

In a first attempt the proposed methodology has been applied to the hydroelectrically interesting river basin Lütschine in the Bernese Alps. However, the preliminary results show that adjustments are required. Hence, additional applications to further test areas are performed. Furthermore, key factors need to be extracted to condensate and simplify the overall method. To provide a practicable and widely accepted tool, the complexity of the assessment tool has to be reduced.

Finally results are intended to be a basic display for site-related studies such as environmental impact assessments of SHP projects.

REFERENCES

- EU 2000: Richtlinie 2000/60/EG des europäischen Parlaments und des Rates zur Schaffung eines Ordnungsrahmens für Maßnahmen der Gemeinschaft im Bereich der Wasserpolitik. Amtsblatt der europäischen Gemeinschaften L327, L 327/1-72, 2000, European Parliament & Council of the European Union.
- SFOE 2008: Strategie Wasserkraftnutzung Schweiz. Herausgegeben von Bundesamt für Energie BFE. Swiss Federal Office of Energy, Bern.
- SFOE 2009: Das Potential der Kleinwasserkraft klären. In: energiea - Newsletter of Swiss Federal Office of Energy SFOE, H. 5, S. 12–13.
- Swiss Confederation 2007: Die Energieperspektiven 2035 - Band 1. Synthese. Ed. Federal Department of the Environment, Transport, Energy and Communication DETEC & Swiss Federal Office of Energy SFOE, Bern.

18.2

MontanAqua: an assessment of the socio-economic and institutional setting

Homewood Christine¹

¹Department of Geosciences, University of Fribourg, Chemin du Musée 4, CH-1700 Fribourg (christine.homewood@unifr.ch)

Part of the project “Approaching water stress in the Alps – Water management options in the Crans-Montana-Sierre region, Valais (MontanAqua)” from the Swiss National Research Programme «Sustainable Water Management» (NRP 61), my work aims at assessing the socio-economic and institutional setting in the region.

The main objective of this transdisciplinary project is to develop strategies moving towards a more sustainable water resources management in the Crans-Montana-Sierre region (Valais), together with actors involved. The spatial perimeter is not limited to the Crans-Montana tourist resort (communes of Icogne, Lens, Chermignon, Montana, Randogne and Mollens), but is extended to the whole valley side, including high mountain areas as well as urban (Sierre) and periurban municipalities (Miège, Venthône and Veyras) situated close to the Rhone River valley. The study region is situated in the driest part of Switzerland and has been subject to dynamic economic, tourism and urban development during the last decades. The proposed research on more sustainable water management options will evaluate co-ordination and adaptation of water demand to water availability under changing biophysical and socioeconomic conditions.

Based on the framework of Bourdieu's theory of practice, the research focus will be on the analysis of the relationships between socio-economic change and the waterscape of the Crans-Montana-Sierre region in order to understand to what extent and how water supply is negotiated. The hypothesis is that the shape of the water distribution system, in its orientations and fragmentations, is a result of supply-oriented management, which is in the process of being transformed towards demand-driven management.

REFERENCES

- Bourdieu, P. (1980) : Le sens pratique. Ed. de Minuit, Paris.
- Mollinga, P. (2008): Water, Politics and Development : Framing a Political Sociology of Water Resources Management. *Water Alternatives* 1(1) : 7-23.
- Reynard, E. (2000): Gestion patrimoniale et intégrée des ressources en eau dans les stations touristiques de montagne. Le cas de Crans-Montana-Aminona et Nendaz (Valais). Thèse de doctorat. Université de Lausanne, Lausanne, Institut de Géographie, Travaux et Recherches n° 17,2 vol.

18.3

Water and women in rural Amhara: A 'naturalized' connection reflecting a restricting political agenda in Ethiopia

Meyer Ursula

Institut de Géographie, Chemin du Musée 4, Université de Fribourg (ursula.meyer@unifr.ch, ursula.meyer@unil.ch)

The connection between water and women in the rural context of a country of the Global South commonly seems to be the concern of development project experts treating the subject mostly from a local actor's perspective. By doing so, political, historical and societal frame conditions are often not sufficiently considered in understanding why women are so 'naturally' connected to water and fail to improve their status in society beyond their usual function as domestic water managers. The presented MA thesis suggests an alternative approach to understanding women's social role in rural Ethiopian society as part of a broader power setting.

By applying Pierre Bourdieu's three concepts of *Habitus*, *Field* and *Symbolic Violence* to water supply in a rural district in Amhara, improved access to drinking water for the rural population can no longer be assessed purely positively. Rather this theoretical approach reveals hidden power mechanisms functioning in different societal relations that speak for a clearly repressive political regime. Such power relations are especially efficient because of their incorporation into social practices of both, the powerful and the powerless.

Deriving from the results of field research conducted in rural Amhara, the author of the MA thesis argues that by granting easier access to safe drinking water, women's daily work load might be reduced, hence, water access improvements appear as positive. But, as the 'naturalized' connection between water and women is not questioned in a broader political sense, improvements in water access hide the curtailing effect such technical interventions have on women's room for manoeuvre and self-determination in an overall repressive political situation. Rather, they serve an authoritarian government to distract the population's and the international community's attention from the fact that improved access to safe drinking water only provides basic need and welfare, but further, more profound personal and political rights and freedoms are deliberately withheld and denied.

REFERENCES

- Biseswar, I. 2008: A new discourse on 'gender' in Ethiopia, Research article, *African Identities*, 6/ 4, 405 - 429
- Dörfler, Th., Graefe, O. & Müller-Mahn, D. 2003: *Habitus und Feld, Anregungen für eine Neuorientierung der geographischen Entwicklungsforschung auf der Grundlage von Bourdieus „Theorie der Praxis“*, *Geographica Helvetica*, 58/ 1, 11- 23
- Lefort, R. 2007: Powers – mengist – and peasants in rural Ethiopia: the May 2005 elections, *Journal of Modern African Studies*, 45/ 2, 253 - 273
- O'Reilly, K. 2006: „Traditional“ women, „modern“ water: Linking gender and commodification in Rajasthan, India, *Geoforum*, 37, 958-972

18.4

Water Scarcity in Inner-Alpine Regions**Options for sustainable water use in the Crans-Montana-Sierre region (Valais)**

Schneider Flurina, Rist Stephan, Weingartner Rolf, Herweg Karl, Liniger Hanspeter, Schädler Bruno, Kauzlaric Martina, Rey Emmanuel¹, Graefe Olivier, Hoelzle Martin, Homewood Christine², Reynard Emmanuel, Bonriposi Mariano³

¹ Institute of Geography, University of Bern, Gruppe für Hydrologie and Centre for Development and Environment–CDE

² Geography Unit, University of Fribourg

³ Institute of Geography, University of Lausanne

Climate change as well as societal and economic development will in future significantly modify the supply and consumption of water, and consequently fuel existing or create new conflicts of interest. Dry valleys in the Alps will be particularly affected, as one has to assume that in these regions general water offer will become even scarcer and seasonal distribution might be changing significantly. At present, the use and distribution of water is generally organized at the communal level and follows historically evolving norms and regulations.

Water management is the expression of a historically evolving interaction between biophysical and social factors. The regulation of these socio-ecological dynamics is the core of water management, which determines where water is tapped and stored as a public good, and how it is distributed to the different water users according to socially negotiated rules. Until now, one could usually assume that water supply is more or less constant—taking into account natural annual and seasonal fluctuations. As a result, water management focused on distributing available water; it did this according to water demand. One therefore took it for granted that water yield was not a limiting factor. But as this might change—at least seasonally—due to climate change, water management needs to be fundamentally revisited: what changes in the availability of water resources should we expect and how can actors who decide on the distribution and use of water react constructively to these changes? These are the central questions addressed by “MontanAqua”, a research project briefly presented here.

The transdisciplinary research project “MontanAqua” investigates water related problems and issues of the study area, the Crans-Montana-Sierre region in the Valais, integrating biophysical and socioeconomic dimensions. It is divided into three work packages (doctoral theses) and one synthesis package (post-doc). Available water resources will be measured and modelled in and for the different altitudinal zones, from the Plaine-Morte glacier down to the Rhone valley (WP1). The study of water use will focus on drinking water, energy production, agri- and viticulture, as well as tourism (WP2). Decision-making related to water use will be studied through the socioeconomic structure, incorporating various levels from the municipality to the canton (WP3).

The synthesis package (SP) aims at investigating the links existing between the issues addressed by the three work packages, using the multifunctional landscape as an integrative bridging concept. This concept implies studying the different and simultaneous functions of specific parts of a landscape (e.g. vineyards and alpine pastureland), as well as analyzing the interactions between, and priorities of these functions. On the basis of such an analysis, it is possible to deduce existing, competing, and contradictory claims to the landscape made by the different parts of the population. By showing how the multifunctionality of landscapes is modified under different climate change scenarios and socio-economic development options, it will be possible to highlight future actor-specific claims to landscapes and make them accessible for discussion and planning.



The aim of these coordinated interdisciplinary studies is to develop options for optimal and at the same time balanced distribution and management of water resources. Local actors will be involved in a dialogue about what might constitute optimal and balanced management, while considering biophysical and socioeconomic factors likely to change. The project thus creates a space for transdisciplinary communication aiming at the co-production of knowledge between researchers and representatives of policy makers, administration and civil society.

PICTURE 1: The study area: Crans – Montana – Sierre
(Photo: Bruno Schädler)

18.5

Les bisses et leurs modes d'organisation au XXI^e siècle, un modèle de gestion durable ?

Schweizer Rémi¹

¹ Institut de Hautes Etudes en Administration Publique (IDHEAP), Quartier UNIL Mouline, CH-1015 Lausanne (remi.schweizer@idheap.unil.ch)

L'approvisionnement en eau d'irrigation des régions de montagne subissant un climat sec ou aride a, de tout temps, représenté un défi majeur pour les communautés s'installant dans ces zones. Sur le plan matériel, cette lutte pour l'eau s'est traduite par la construction de canaux d'irrigation plus ou moins spectaculaires – dont les bisses du Valais représentent un célèbre exemple –, tandis que sur le plan social, elle a mené à la mise en place de modes de gestion et d'organisation communautaires qui représentent de bons exemples de *CPR institutions* (Ostrom 1990) et qui sont caractérisés par des modalités de partage et de distribution de l'eau particulièrement strictes.

Ces modes d'organisation font l'objet d'une abondante littérature, notamment en ce qui concerne les bisses du Valais. Toutefois, ces travaux adoptent souvent une perspective historique, et une minorité seulement traite de l'exploitation telle qu'elle se pratique à l'heure actuelle. Paradoxalement, en dépit de cette méconnaissance des modes de gestion contemporains liés à l'exploitation des bisses, il a été affirmé à plusieurs reprises dans la littérature que ces derniers représentaient des « modèles de gestion durable ». Or, des conclusions en termes de durabilité ne sauraient être tirées de l'analyse des modalités historiques de gestion et requièrent au contraire de répondre à une série de questions complexes qui restent pour l'heure sans réponse : comment ces modalités de gestion ont-elles évolués en parallèle à la complexification des réseaux d'irrigation et à l'évolution socio-économique de son environnement ? quelle place reste-t-il pour les modalités historiques de gestion ? quels rôles jouent la souplesse et l'informalité dans la gestion de réseaux autrefois caractérisés par des modalités très strictes de distribution de l'eau ? C'est à ces questions, qui nous paraissent centrales dans le contexte actuel de regain d'intérêt – patrimonial, touristique, mais surtout plus récemment environnemental – dont les bisses font l'objet, que la présente communication entendra tout d'abord répondre, afin d'offrir quelques éclairages sur la manière dont les modes de gestion qui encadrent les usages des bisses se composent à l'heure actuelle.

Dans un deuxième temps, l'objectif sera, sinon d'apporter une réponse définitive quant au caractère durable ou non des systèmes d'irrigation liés à l'exploitation des bisses, en tous les cas de proposer une grille de lecture novatrice à même d'évaluer les modalités de gestion contemporaines sous l'angle de la durabilité. Pour ce faire, notre analyse s'appuiera sur le cadre théorique des *Régimes Institutionnels de Ressources* (RIR). Ce cadre théorique, qui est le fruit des réflexions d'une équipe de chercheuses et de chercheurs menée par Peter Knoepfel, Ingrid Kissling-Näf et Frédéric Varone (2001, 2003), considère que l'état physique des ressources naturelles est fonction de l'ingénierie sociale qui l'entoure, soit, plus spécifiquement, des règles qui en régulent les usages. L'objectif est de tenir compte de la complexité de la gestion des ressources et d'intégrer l'ensemble des dimensions régulatrices pertinentes afin d'en identifier, dans des situations concrètes, les lacunes et les incohérences. Le postulat central de ce modèle consiste à considérer que plus les usages d'une ressource seront régulés de manière étendue et cohérente, plus les conditions de son exploitation pourront être considérés comme durables. La mise en œuvre de ce cadre théorique nous permettra, à travers l'assimilation d'un réseau d'irrigation à un complexe multiresourciel composé des ressources *eau*, *bisse* (infrastructures du réseau) et *sol*, d'élaborer une grille de lecture dont l'application rigoureuse rendra possible l'évaluation, sur le terrain, de la durabilité des modes de gestion mis en place.

Ces deux objectifs – clarifier les modalités de gestion actuelle liés à l'exploitation des bisses et élaborer puis tester une grille de lecture pour évaluer leur durabilité – seront atteints à travers une étude empirique réalisée à Savièse. Cette commune, où la gestion est caractérisée par l'imbrication de modes de gestion appartenant aux sphères privée, publique, communautaire (consortages) et associative d'une part, et par l'importance de la souplesse et de l'informalité de l'autre, représente un terrain d'étude particulièrement riche en enseignements.

REFERENCES

- Ostrom E. 1990, *Governing the Commons: the Evolution of Institutions for Collective Action*, University Press, Cambridge, 280 pp.
- Knoepfel P., Kissling-Näf I., & Varone F. (Eds) 2001, *Institutionelle Regime für natürliche Ressourcen : Boden, Wasser und Wald im Vergleich*, Helbing & Lichtenhahn, Basel/Genf/München, 258 pp.
- Knoepfel P., Kissling-Näf I., & Varone F. (Eds) 2003, *Institutionelle Regime natürlicher Ressourcen in Aktion*, Helbing & Lichtenhahn, Basel/Genf/München, 376 pp.

19. The global / local in our research

Marina Richter & Patricia Felber

Swiss Geography Association (ASG), International Geographical Union (IGU)

- 19.1 Backhaus N.: The local and the global in spatial appropriation
- 19.2 Kayani S.: Psychosocial effects of natural (cosmic) phenomena: a case study
- 19.3 Richter M.: Jumping scale: dealing with the local and the global in a transnational research project

19.1

The local and the global in spatial appropriation

Norman Backhaus

Dept. of Geography, University of Zurich, Winterthurerstr. 190, CH-8057 Zurich
norman.backhaus@geo.uzh.ch

Research on spatial appropriation is at the core of human geographical studies. Regardless of the form of appropriation, this process is mostly regarded as a local activity and has, on the first glance, little to do with globalization. However, even in its strictest form of physical appropriation there is almost always a global aspect involved. In my presentation I want to in a first part address different forms of spatial appropriation, i.e. physical appropriation, mental appropriation, spatial alienation, and disappropriation and their relation to the local and the global (cf. Backhaus & Müller, 2006). In a second part I want to present a few vignettes of research projects to illustrate the close connection of the local and the global:

- The appropriation of the sea in Bali between local traditions and global markets (Backhaus, 1998).
- Domestic tourism in Malaysian national parks: global rules for local leisure time (Backhaus, 2005).
- The UNESCO World Heritage Site Jungfrau-Aletsch: a global label in conflict with local needs (Müller, 2007).
- Appropriation of public space by skaters in Zug: global sub-culture meets local opposition (Carminitana, 2009).

I want to conclude with a few remarks about methodological issues concerning research of spatial appropriation that ought to be open to both local and global processes although especially the global can be a very elusive aspect when being “in the field”.

REFERENCES

- Backhaus, N. (1998). Globalization and Marine Resource Use in Bali. In V. T. King (Ed.), *Environmental Challenges in South-East Asia* (pp. 169–192). Singapore: Curzon.
- Backhaus, N. (2005). *Tourism and Nature Conservation in Malaysian National Parks*. Münster: Lit.
- Backhaus, N., & Müller, U. (2006). Regionalisierung: eine konstruktivistische Perspektive. In N. Backhaus & U. Müller-Böker (Eds.), *Gesellschaft und Raum – Konzepte und Kategorien* (Vol. 22, pp. 13–29). Zürich.
- Carminitana, F. (2009). *Raumaneignung von Jugendlichen – Vergleich von zwei Jugendgruppen in der Stadt Zug*. Universität Zürich, Zürich.
- Müller, U. (2007). *Die Kraft der Bilder in der nachhaltigen Entwicklung – Die Fallbeispiele UNESCO Biosphäre Entlebuch und UNESCO Weltnaturerbe Jungfrau-Aletsch-Bietschhorn*. Zurich: vdf Hochschulverlag AG an der ETH Zurich.

19.2

Psychosocial effects of natural (cosmic) phenomena: a case study

Kayani Saheeb-Ahmed

National University of Sciences and Technology, H-12, Islamabad-44000, Pakistan (saheebk@ceme.nust.edu.pk)

Every now and then on a clear night, if you get a chance of spending a few hours out in the open, I hope you will be able to catch the faint trail of a shooting star or two. And I believe you would always like to make a wish (something we all are told while growing up) before the trailblazer vanishes into the darkness of the atmosphere. Historically these poor nocturnal adventurers (not really as they fall to earth all around the clock) have demonstrated a remarkable ability to impact people's lives in many ways. Myths surrounding meteorites have influenced collective psychology of societies far and wide to the extent that even belief systems evolved based on either reverence or fear of a fallen meteorite. With the kind of cosmological information we have today, our understanding and attitudes have changed so much that at times we seem to ignore that even today in distant cultures, people still take meteorites as evil omens and harbingers of death and destruction. For any one interested, a good starting point can be *Cosmic Debris: Meteorites in History* (Burke 1986) in which the author explores human society's often strange relationship with these natural (cosmic) phenomena.

Recently I was engaged in a small project related to identification of a meteorite debris near village Lehri (33°09'09"N; 73°33'35"E) in district Jhelum, Pakistan (Kayani 2009). This debris consists of apparently extremely weathered stones scattered on an area about 250 metres in length and 100 metres across. The site referred to as Pind or village in the local dialect Pothohari on which this debris has been discovered had been under cultivation and is filled with levelled fields (that are worked no more) and their raised boundaries. On these raised boundaries and also in the fields lie countless small pottery shards of different shapes and sizes. The largest concentration of these shards is found on the boundaries of fields, as the farmers while ploughing and clearing must have pushed them to the sides. Presence of this much quantity of broken earthenware points towards existence of a human settlement on this site that was abandoned in a rather hastily manner at some point in history. A few samples of these pottery shards were examined by late Dr. Ahmed Hassan Dani, one of Pakistan's leading archaeologists and he in his preliminary analysis identified them from muslim era in Indian subcontinent (roughly from 12th century onwards).

Local oral history contains no mention of a village on this site. Local written history does not exist at all. The usage of the term 'Pind' by residents of nearby villages for this site (that would have been used to point towards a settlement in normal circumstances) provides a clue as the name has entered the referral system used locally for identification of different places and is still in use today long after the disappearance of the village it referred to. One of the oldest and largest villages in this area is Lehri (half a kilometre south of this site). Historical records indicate that this village has been inhabited since 15th century. It is probable that this site (Pind) was also occupied at the same time and a small village existed on this location. But in the first land reforms carried out by the British in 1860, this site has been recorded as being used for agricultural purposes and not as a settlement. So here we can identify a general time period from 1400-1860, during which a village that existed on this site was abandoned due to some unknown reasons.

The presence and peculiar mixing of this meteorite debris with pottery shards may help us with a reason for the sudden abandoning of the village. It seems like for the residents of this presumed settlement tragedy came from the sky. Worse if it came during a winter's night when the dark and gloomy ravines surrounding the village site are filled with chilling north wind. Suddenly the sky would have illuminated with thousands of fireballs. The silence of the hitherto peaceful night would have been replaced with screams of horror and destruction as smouldering meteorite debris hit people's rooftops, causing panic and probably damage to life and property. The terrible spectacle may have evoked the primeval fear of mountain people that they have been attacked by demons and the village site is cursed. The villagers relocated abandoning the site for good, leaving broken clay ware and meteorite debris as reminder of the chaos and tragedy that befell this sad and forgotten site.

REFERENCES

- Burke, J. 1986: *Cosmic debris: meteorites in history*. Berkeley: University of California Press.
- Kayani, SA. 2009: Using combined XRD-XRF analysis to identify meteorite ablation debris. In: *Proceedings of Fifth IEEE International Conference on Emerging Technologies*, Islamabad, December 19-20, 2009, 219-220.

19.3

Jumping scales? dealing with the local and the global in a transnational research project

Richter Marina

*Soziologie, Sozialpolitik und Sozialarbeit, Universität Fribourg, Rte des Bonnesfontaines 11, 1700 Fribourg,
Marina.richter@unifr.ch*

The scales are a basic concept in geography and much geographical research would not exist without the local, the regional, the national, or the global. Many debates have centered on the usage of scales in geographical research. For instance, feminist geographers have claimed the body as a scale of social action in and about space that is nested in the local. Recently, Sally Marston, John Paul Jones and Keith Woodward claimed that scales are not only a social construction – as Sally Marston pointed out earlier – but they tried to imagine the world without looking through the scalar lens. They called this perception of the social world a “flat ontology”: a network of sites, where actions and interactions are just about to happen.

These debates seem very interesting on the theoretical level. But how can we make use of the flat ontology for our empirical work? The paper will address this question by looking first at the theoretical debates around scales and will then discuss especially the recent article by Jones, Woodward and Marston that aims to sketch an empirical usage of their flat ontology. Lastly, I will try to reflect on these thoughts from the literature by looking at my own research on second generation migrants from Spanish parents in Switzerland and their transnational social networks and their perception of transnational social spaces. Are we jumping scale as researchers when getting on an airplane in order to fly to another country, following the transnational connections of our research subjects? How can we grasp another scale than the local when meeting and interviewing people always in concrete sites?

20. Geotopes and Geoparks

Jean-Pierre Berger, Emmanuel Reynard, Pierre-Yves Jeannin, Markus Felber

Swiss Working Group on Geotopes (Platform Geosciences, SCNAT)

- 20.1 Berger J.-P. et al.: Geotopes of national significance: report 2010
- 20.2 Martin S. & Ghiraldi L.: Static and dynamic mapping of geosites
- 20.3 Morard S., Staub A., Oggier P.: Geomorphology and geology in the Regional Nature Park (RNP) Pfyn-Finges (Valais): identification, assessment, educational and touristic promotio
- 20.4 Perret A., Guyomard A., Coutterand S., Reynard E., Delannoy J.-J.: Glacial heritage of the Chablais area (FR-CH): understanding glacier flows and identifying geosites
- 20.5 Regolini-Bissig G., Martin S.: Quality assessment of natural heritage trails

20.1

Geotopes of national significance : report 2010

Groupe de travail "Geotopes d'importance nationale", coord. Berger Jean-Pierre¹

¹Dept. Geosciences-Earth Sciences, chemin du Musée 6, 1700 Fribourg (jean-pierre.beerger@unifr.ch)

Starting in 2006, the revision of the inventory of Geotopes of national significance (see Berger et al. 2008) comes to the last step. We present here the last report, which will be submitted to the BAFU at the end of this year.

Thank to the collaboration of several swiss earth scientists, this version will be considered as the first stable list on geotopes of national importance, including about 350 sites.

The present contribution will discuss the general list with some typical examples of problems occurring during the realization of the report.

We will also take the opportunity to discuss the present list as well as the different aspects concerning the future of this report : it is clear that this process need a regular update, concerning for example the following topics :

- procedure for adding new geotopes
- procedure for cancelling geotopes already listed (because of destruction, for example)
- database updating
- creation of a separate database concerning geotopes discussed but finally removed of the list during the years 2005-2010
- publication(s) of the results in local to international public
- future of the Working Group

We hope to see a lot of colleagues to participate to the discussion.

Special thanks to the BAFU and SCNAT for financial support and to all the colleagues who help us to compile and choice paleontological sites.

REFERENCES

Berger J.-P., Reynard E., Bissig G., Constandache M., Dumas J., Felber M., Häuselmann P., Jeannin P.Y., Schneider H. 2008 : Révision de la liste des géotopes d'importance nationale : rapport du groupe de travail 2006-2007. – Groupe de Travail pour les Géotopes en Suisse, 22 p.

20.2

Static and dynamic mapping of geosites

Martin Simon¹, Ghiraldi Luca²

¹ *Université de Lausanne, Institut de géographie, Anthropole, Quartier Dorigny, CH-1015 Lausanne (simon.martin@unil.ch)*

² *Museo regionale di Scienze Naturali, Sezione di Mineralogia, Petrografia e Geologia, Via Giolitti 36, I-10100 Torino (luca.ghiraldi@gmail.com)*

The use of maps in the field of geoheritage research and promotion is growing. Several attempts to formalize the mapping process – especially for geotourist maps – have been proposed these last years (Coratza & Regolini-Bissig, 2009; Martin & Reynard, 2009; Regolini-Bissig, 2010). Until now, they are limited to traditional, static maps. However, dynamic tools such as web-mapping and web-GIS have been used to publish and communicate information about geosites.

Three different maps are presented and compared: a static map showing the Swiss geosites of national significance, a web-mapping tool based on the same inventory, and a geotourist and interpretive map of Tanaro Valley. The specific advantages of both static and dynamic maps are exposed, according to Cartwright & Peterson (1999) and Meng (2003).

Following Regolini-Bissig (2010), geosite maps are classified in three categories according to their objectives: inventory maps, geotourist maps and interpretive maps (tab. 1).

Map type	Objectives
Inventory maps	to localize sites; compare attributes (values)
Geotourist maps	to inform the public about tourist facilities and services and communicate geo-scientific information
Interpretive maps	to visually transfer geoscientific knowledge between specialists and the public

Table 1. Typology of maps in the field of geoheritage research and promotion.

The first category is not well developed. Mostly static maps can be found, used as synthesis tools presenting the sites' localization and sometimes a few attributes of these. As a matter of fact, GIS are poorly used to manage geosite inventories and assessment, despite the fundamental spatial dimension of the objects.

We have carried out a web-mapping project based on the Swiss inventory of geosites of national significance. Compared with the static map, this project exemplifies the advantages of a dynamic and interactive map. While keeping the objectives of a basic inventory map, it also becomes a query tool, allowing spatial and thematic requests. Dynamically based on a database, the web-map is, thereby, not only a storage tool, but also an exploration and publication tool. The interface allows the user to choose which task he wants to perform. It is an attempt to design a tool intended for both specialists and amateurs.

The two last categories are designed for a non-specialist public. Geotourist maps aim to inform the reader whereas interpretive maps tend to communicate a message and explain a landscape's specificities.

The third example is a bird's-eye view map with two sides. In the front there is geotourist information on Tanaro Valley region (Italy), while the back is more interpretive, and explains the landscape's evolution using a series of drawings supported by synthetic text explanations. This example shows that a static map can also meet several objectives and illustrates the importance of focusing on one theme only.

As a conclusion, some perspectives are drawn for the use of dynamic tools to support geotourist and interpretive maps. Interactive maps allow the users to select the content according to their interests and competence, or the time they want to spend on it. Along with multimedia, interactivity gives the opportunity to dynamically show processes and the evolution of landscape. Finally, dynamic maps can be a good alternative to the frontal-teaching aspects of traditional maps, allowing the user to build his own knowledge of a theme.

REFERENCES

- Cartwright, W., & Peterson, M. P. 1999: Multimedia cartography. W. Cartwright, M. Peterson & G. Gartner: Multimedia cartography, 1-10. Berlin: Springer.
- Coratza, P., & Regolini-Bissig, G. 2009: Methods for mapping geomorphosites. E. Reynard (ed.): Book on geomorphosites, 89-103. München: Pfeil.
- Martin, S., & Reynard, E. 2009: How can a complex geotourist map be made more effective? Popularisation of the Tsanfleuron heritage (Valais, Switzerland). Bayerisches Landesamt für Umwelt (ed.): 6th European Congress on Regional Geoscientific Cartography and Information Systems: Earth and Man. Proceedings, 2, 261-264. München: Landesamt für Vermessung und Geoinformation.
- Meng, L. 2003: Missing theories and methods in digital cartography. 21st International Cartographic Conference, Durban: International Cartographic Association.
- Regolini-Bissig, G. 2010: Mapping geoheritage for interpretive purpose. Definition and interdisciplinary approach. G. Regolini-Bissig & E. Reynard (eds.): Mapping geoheritage. Geovisions, 35, 1-13. Lausanne: IGUL.

20.3

Geomorphology and geology in the Regional Nature Park (RNP) Pfyn-Finges (Valais): identification, assessment, educational and touristic promotion

Morard Sébastien¹, Staub Alexandra² & Oggier Peter²

¹ Geography Unit, Department of Geosciences, Chemin du Musée 4, CH-1700 Fribourg (sebastien.morard@unifr.ch)

² Pfyn-Finges Naturpark Wallis, CH-3970 Salgesch

The Regional Nature Park (RNP) Pfyn-Finges project is located in central Valais and covers a surface of about 250 km² from the Bishorn summit in the Turtmann valley to the Plaine Morte glacier north of the Rhone river. The RNP perimeter also crosses the three main geological domains of the Swiss Alps (Austroalpine, Penninic, Helvetic nappes and crystalline basement).

During the first phase of the RNP project in 2008, a general inventory of landforms was realized. Due to the wide range of altitudinal zones (500 to 4'000 m. a.s.l.) and the geological diversity, numerous various geomorphic landforms and processes were identified. A database of scientific publications and thematic maps about geomorphology and geology in the Pfyn-Finges region was also performed.

The multi-thematic method for landscape assessment developed by the Federal Office of Environment was then used to evaluate the value of the geomorphic and geological landforms. Several of them have obtained a high notation, like the Illgraben scarp, the wild Rhone, the Siders Bergsturz and the glacial valley of Turtmann. Others well developed and preserved features like the uphill-facing scarps morphology in the Fäsilalpü, the pyramids of the Raspille, the narrow gorge of Feschel incised in the Helvetikum limestone nappes, the numerous rockglaciers of Turtmanntal or the hydro-karstic systems of the Russubrunnu are of particular interest. Some of these landforms are also important in term of marketing: the Illgraben for instance is now considered as the main geomorphic hotspot and one of the main visual identities of the RNP Pfyn-Finges.

On the basis of this assessment, several projects of educational and touristic promotion were developed. The panel of offers to discover geomorphology and geology was improved since a few years. In addition to guided excursions and information's flyers, a geological garden with 36 different rocks from the RNP was realized in the Nature and Landscape Center in Salgesch during summer 2010. Objectives of this permanent exposition are to show the long geological history of the Alps and to be used as educational tool for schools. Another project initiated this summer concerns the development of an educational place in collaboration with the three gravel companies located in the wild Rhone area. It will host an Illgraben model (in order to create artificial debris flows) and others didactical activities (rocks identification, understanding of aquifers...) for school classes. In the next years, the diversification and the improvement of the geotouristic offers is one of the main objectives of the RNP Pfyn-Finges.

20.4

Glacial heritage of the Chablais area (FR-CH): understanding glacier flows and identifying geosites

Perret Amandine^{1,2}, Guyomard Anne³, Coutterand Sylvain², Reynard Emmanuel² & Delannoy Jean-Jacques¹

¹ Laboratoire EDYTEM, UMR 5204 du CNRS, Pôle Montagne, Campus scientifique, FR-73376 le Bourget-du-Lac (amandine.perret@univ-savoie.fr)

² Institut de Géographie, Université de Lausanne, Dorigny – Anthropole, CH-1015 Lausanne

³ Syndicat Intercommunal d'Aménagement du Chablais, Square Voltaire, Rue des Allobroges 2, FR-74201 Thonon-les-Bains

The Chablais area possesses a very interesting glacial heritage. It is considered as one of the cradles of glaciology, theory elaborated with difficulty but widely accepted since the middle of the XIXth century (De Charpentier 1841). Since then, several generations of researchers have focused on this region with various approaches like geology, hydrogeology, geomorphology, geophysics, etc. Today, the territory shows strong glacial characteristics, of which knowledge remains paradoxically incomplete, because most of the studies are very localized (Perret 2010) without a global overview of the system (Rhône and Dranse glaciers).

Within the framework of a territorial project including the creation of a regional geopark, an itinerant exhibition and an inventory of natural sites, we have a mandate to complete the knowledge on the regional Quaternary palaeogeography, and to present a coherent glacial history to the public, through a regional inventory of geosites.

To better understand the current indicators of the former glaciers, it is necessary to reconstruct the flows of ice, which followed each other in this area (Fig. 1). It will then be possible to explain the visible elements in the landscape and to identify key sites of the glacial history. This stage of reconstruction includes the study and mapping of the glacial and associated morphologies, through a geomorphological approach coupled with a more geological approach (study of natural and artificial cuttings). Although we are not looking to establish an absolute chronology of the events, it is also planned to date some landforms such as erratic blocks.

The objective of promoting geology through a territorial project (geopark) guided the choice of an approach by geosites as well as the constitution of an inventory. In this way, we select particularly representative or rare sites (Grandgirard, 1997), with a strong integrity, in order to present the most striking objects (Fig. 2) to the public but we try also to approach a wide panel of landforms capable of reporting all the glacial processes which operated in the region.

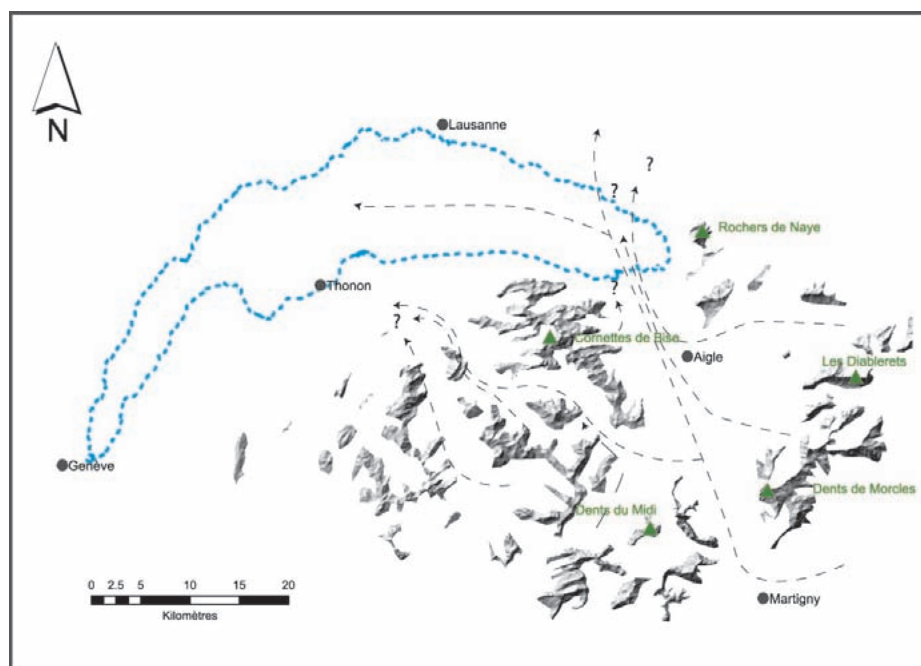


Figure 1. Map of the last width glacial extension in the Chablais area, after S. Coutterand, 2010.



Figure 2. The “Pierre à Martin” (Ballaison, FR), erratic block, potential geosite in the French Chablais.

REFERENCES

- Coutterand, S. 2010: Etude géomorphologique des flux glaciaires au Pléistocène récent dans les Alpes Nord-occidentales. Du maximum de la dernière glaciation aux étapes de la déglaciation. Thesis. University of Savoie, Laboratory EDYTEM.
- De Charpentier, J. 1841 : Essai sur les glaciers et sur les terrains erratiques du bassin lémanique. Lausanne: M. Ducloux, 363 p.
- Grandgirard, V. 1997 : Géomorphologie, protection de la nature et gestion du paysage. Thesis. University of Fribourg, Geography Institute. 210 p.
- Perret, A. 2010: Les glaciations quaternaires dans le Chablais, synthèse bibliographique. Lausanne, Chambéry. Unpublished report.

20.5

Quality assessment of natural heritage trails

Regolini-Bissig Géraldine¹, Martin Simon¹

¹ Université de Lausanne, Institut de géographie, Anthrope, Quartier Dorigny, CH 1015 Lausanne (geraldine.regolini@unil.ch) (simon.martin@unil.ch)

Natural heritage trails and educational panels are a widespread form of scientific communication. Commissioned by public entities as well as by private associations, they concern both local peculiarities and internationally known features. While some projects inventory the trails in a given region to more efficiently spread the information among the public (e.g. www.randonature.ch) other works analyse the scientific topics highlighted by trails (Cayla, 2009). Up to now, no method has been developed to assess their scientific and educational value. However, evaluation is important to guarantee products of quality and of high interest for the public (Martin et al., submitted).

In 2010, the natural sciences society of Valais (*La Murithienne*) launched a project to certify products about natural heritage in Valais, Switzerland. A label –Marque Valais – will be attributed to products of high scientific quality and a significant socio-economic impact within a sustainable development model. The assessment of the socio-economic impact will be carried out by the Institute of Economics & Tourism of HES-SO Valais and is not subject of this contribution.

Considering the directives of the awarding committee (Bernard & Kunz, 2009) – improvement of the product quality through a consulting service and labialisation – five evaluation categories (Fig. 1) were taken into account for the develop-

ment of the assessment method presented here. They regard the domains individuated as important for guiding the implementation process of a valorisation product (Martin et al., submitted). Each of these categories is composed of a set of criteria (Tab. 1) with explicitly formulated scores in order to reduce subjectivity as much as possible and, therefore, differences of appreciation among evaluators (Bruschi & Cendrero 2005). Six evaluators tested the method before applying it at a large scale (250 natural heritage trails, of which 80 have already been assessed as a priority). Their remarks helped us to reformulate some ambiguous criteria and to adapt the method to practical considerations of evaluation in the field.

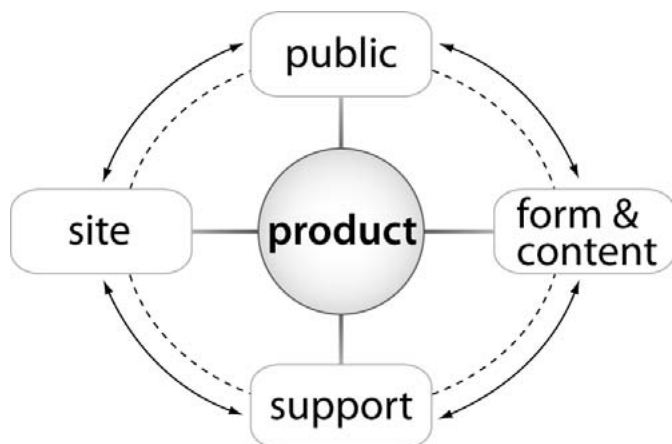


Figure 1. Evaluation categories for the assessment of the scientific and educational quality of natural heritage trails.

Domain	Criteria
1) site	a) rareness, b) integrity, c) cultural and historical value, d) educational interest
2) support	a) design (general appearance) for permanent supports (ex. panels): b) maintenance, c) location, d) integration for mobile supports (ex. brochure, mobile phone, etc.): b) quality, c) navigation (structure), d) size
3) form	a) layout, b) readability, c) information structure, d) diversity and quality of illustrations, e) relevance of illustration, f) available languages
4) content (theme and message)	a) preciseness of theme, b) coherence of the message, c) comprehension of natural complexity, d) general and social interest of the message
content (scientific content*)	a) accuracy and scientific rigour, b) honesty, c) scientific interest of the site or features, d) relevance of information, e) respect of intellectual property
content (educational content)	a) level of complexity, b) accessibility and complexity, c) attractiveness, d) adequacy between quantity of information and length of the trail
5) public	a) visitors' orientation, b) site protection, c) car park management, d) vulnerability awareness message e) information availability

*this section has to be assessed by an expert

Table 1. Evaluation categories and corresponding assessment criteria.

The analysis of the obtained results will provide an overview of the global value of products in Valais and help to develop the consulting service. Moreover, the presented assessment method could be modified to fit the evaluation of products other than trails.

REFERENCES

- Bernard, R. & Kunz P. 2009: Nature & Tourisme. Projet 2010-2011. Sion.
- Bruschi, V.M. & Cendrero A. 2005: Geosite evaluation; can we measure intangible values? *Il Quaternario*, 18/1, 291-304.
- Cayla, N. 2009: Le patrimoine géologique de l'arc alpin. De la médiation scientifique à la valorisation géotouristique. Thèse de doctorat, Le Bourget-du-Lac, Université de Savoie.
- Martin, S., Regolini-Bissig, G., Perret, A. & Kozlik, L. (submitted): Elaboration et évaluation de produits géotouristiques. Propositions méthodologiques. *Téoros*, Revue de recherche en tourisme.

<http://www.randonature.ch> (consulted 26.8.2010)

21. Mars: water, climate & geology

Pierre Brisson & François Zwahlen

Chyn and Mars Society Switzerland

- 21.1 Bibring J.-P.: Mars, Water, Habitability.
- 21.2 Brisson P.: Mars, a remote, now accessible, geologic object.
- 21.3 Frankel C.S.: Putative oceans and Hydrothermal activity on Mars.
- 21.4 Gautsch S.: Atomic Force Microscopy on Mars.
- 21.5 Gillmann C., Lognonné P.: Volatiles in the atmosphere of Mars: the effects of volcanism and escape.
- 21.6 Golabek G., Keller T., Gerya T., Zhu G., Tackley P., Connolly J.: Core and early crust formation on Mars
- 21.7 Hofmann B., Josset M., Josset J.-L.: The potential of Close-up imaging on the surface of Mars
- 21.8 Josset J.-L.: The ExoMars Rover Mission, Goals & Instruments.

21.1

Mars, Water, Habitability

Bibring J.-P.

Institut d'Astrophysique Spatiale, Université de Paris-Sud

With the data acquired by the ongoing space missions, Mars history is profoundly re-visited. It now exhibits an ancient era where sustained liquid water has likely been present, as recorded by specific hydrated minerals. Mars might have harboured habitable conditions, before the end of the heavy bombardment, while its dynamo was still operating. It happens that sites having preserved this record are still present at its very surface. If life emerged other than on the Earth, the upcoming Mars missions (NASA/MSL and ESA/ExoMars) should be able to find bio-relics, in a few areas well documented, and accessible to rovers. Moreover, their exploration will give unprecedented clues on the environment which characterized the early Earth, when life appeared. Astrobiology is truly entering its scientific era.

21.2

Mars, the most interesting, now accessible, remote geological object.

Pierre Brisson

President of the Mars Society Switzerland, Member of the board of Association Planète Mars (French branch of the Mars Society), Founding member of the Mars Society (USA). Neuchâtel, Switzerland.

Mars is far away, small and dry but it is, apart the Moon, the most accessible large celestial body. Its gravity is twice that of the Moon. It has days of 24h40 minutes, instead of 14 days. It has water ice at the poles, in the subsoil almost everywhere and in veils of clouds in its sky, much more than the traces detected on the Moon. During its early geological history, liquid water has run on its surface and altered the magmatic and lava rocks into hydrated rocks. It has an atmosphere even though very thin and unbreathable (CO_2). Almost all erosion stopped 3.5 billion years ago and since there has been no plate tectonic, the surface has almost not changed, providing an open book for what our Earth could have been at such an early stage, when life started to emerge.

We have been there with robots and we learnt a lot but men on the spot could be much more efficient and facilitate exploration. Sending them there, would be feasible within ten years if we decided to. Thanks to the “Mars Direct” theory, we could use nowadays technology and stay within a budget smaller than that of the International Space Station. If we use the Martian atmosphere to produce locally the fuel and combustive necessary to return to Earth, then the mass which we need to propel off the Earth gravity pit would be reduced to the level at which we can use the equivalent of the Saturn V rockets which carried men to the Moon forty years ago.



Image Association Planète Mars

REFERENCES:

- Robert Zubrin, *The Case for Mars*, Simon & Schuster, 1996.
- Richard Heidmann, *Planète Mars, Une attraction irresistible*, Editions Alvik 2005.
- Mars, *Planète Bleue*, Jean-Pierre Bibring, Odile Jacob, 2009.
- Adrian Brown et al., “Hydrothermal formation of Clay-Carbonate alteration assemblages in the Nili Fossae region of Mars”; *Earth & Planetary Science Letters* (2010), doi 10.1016/j.epsl.2010.06.018 (Elsevier).
- Dorothy Z. Oelher & Carlton C. Allen: “Evidence for pervasive mud volcanism in Acidalia Planitia, Mars”; *Icarus* 208 (2010) p. 636 to 657 (Elsevier).
- Paul B. Niles et al. « Stable Isotope Measurements of Martian Atmosphere CO_2 at the Phoenix Landing Site », *Science*, vol 329, Sept. 10th 2010, p.1334 to 1337.
- Strategies for Mars: A guide to Human Exploration, Edited by Carol R. Stoker & Carter Emmart, An American Astronautical Society Publication, Vol 86 Science & Technology series, Published by Univelt Inc. 1996.
- Donald Rapp, *Human Missions to Mars; Enabling technologies for Exploring the Red Planet*, Springer-Praxis 2008.

21.3

Putative oceans and hydrothermal activity on Mars

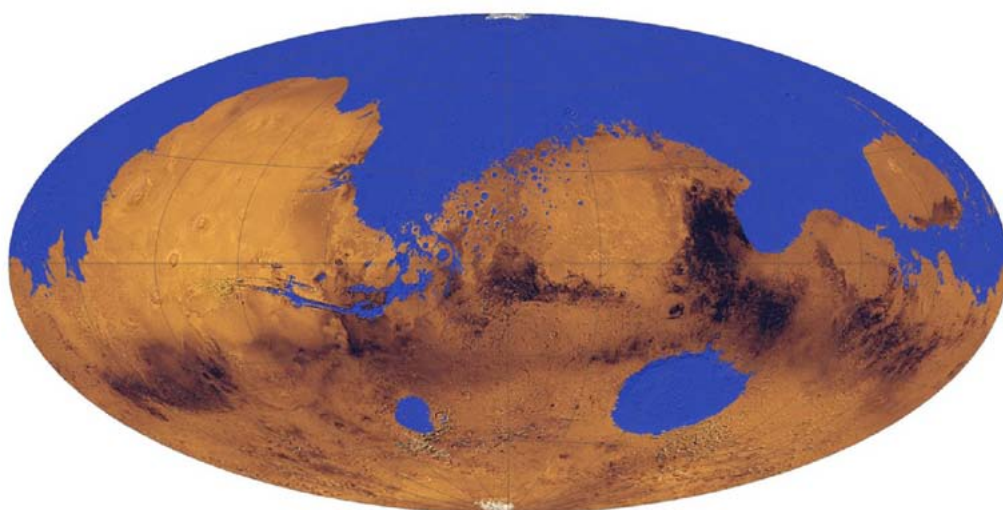
Charles Frankel*

* Association Planète Mars, Visiting Professor at Middlebury College (Vermont, USA)

Mars has a rich water history. The ancient Southern highlands show evidence of rainfall with runoff recorded by river systems that have shown up at higher resolutions to constitute denser, more integrated networks than previously believed [1]. This early Noachian period also coincides with clays identified from orbit (see presentation by J.P. Bibring).

Abundant water reemerges from the ground in later events throughout the history of Mars, most notably during the Hesperian period, approximately 3.8 billion years ago. Evidence includes catastrophic outflow channels out of the highlands towards the Southern hemisphere Hellas impact basin and most importantly towards the Northern lowlands. Recognition of the extreme smoothness of the Northern plains and of the common altitude at which channels flow into this boreal basin have led to the hypothesis of an ancient sea occupying the basin, nicknamed Oceanus Borealis [2]. We examine the status of this theory [3].

Since volcanism and vast amounts of underground ice and liquid water have interacted in the past, it is fair to assume that hydrothermalism has been prevalent throughout Martian history, probably up to this day. Indirect evidence has come in the form of mineral associations found on the ground, such as streaks of opaline silica discovered by the Mars Exploration Rover Spirit [4]. The search for hydrothermal mounds from orbit is also accelerating, as we shall examine [5,6]. The search for life on Mars is bound to focus in the future on these promising sites.



Putative oceans on Ancient Mars (University of Colorado)

REFERENCES

- [1] Hynek B. & Phillips R. 2003: New Data Reveal Mature, Integrated Drainage Systems on Mars Indicative of Past Precipitation, *Geology*, vol 31, N°9, 757-760.
- [2] Baker, V. et al., 1991: Ancient Oceans, Ice Sheets and the Hydrological Cycle on Mars, *Nature*, 352, 589-594.
- [3] Di Achille, G. & Hynek B. 2010: Ancient Ocean on Mars Supported by Global Distribution of Deltas and Valleys, *Nature Geoscience* 3, 459-463.
- [4] Squyres, S. et al. 2008: Detection of Silica-Rich Deposits on Mars, *Science*, vol. 320, N° 5879, 1063-1067.
- [5] Schulze-Makuch, D. et al. 2007: Exploration of Hydrothermal Targets on Mars, *Icarus*, 189, 308-324.
- [6] Allen, C., & Oehler D. 2008: A case for Ancient Springs in Arabia Terra, Mars, *Astrobiology*, Vol. 8, N°6, 1093-1112.

21.4

AFM MEASUREMENTS OF MARTIAN SOIL PARTICLES – RESULTS FROM THE PHOENIX MISSION

S. Gautsch¹, D. Parrat¹, N. F. de Rooij¹, U. Staufer², J.-M. Morookian³, M. Hecht³, S. Vijendran⁴, H. Sykulska⁵, T.W. Pike⁵

¹ SAMLAB, EPFL STI, Jaquet-Droz 1, 2002 Neuchatel, Switzerland

² MNE - Laboratory, TU Delft, Mekelweg 2, 2628 CD Delft, The Netherlands; u.staufer@tudelft.nl

³ Jet Propulsion Laboratory, California Institute of Technology, Pasadena, CA 91109, USA

⁴ ESTEC, Keplerlaan 1 Postbus 299, 2200 AG Noordwijk, The Netherlands

⁵ Dept. of Electrical and Electronic Eng., Imperial College, South Kensington Campus, London SW7 2AZ, UK

Light scattering experiments conducted on Mars [i] indicated that soil particles have dimensions around 1 μm . Particles in that range play an important role in the gas exchange between sub-surface water ice and the atmosphere. The Phoenix mission [ii] therefore decided to analyze soil and dust particles in the sub- range using an Scanning Force Microscope (SFM) for the first time on another planet.

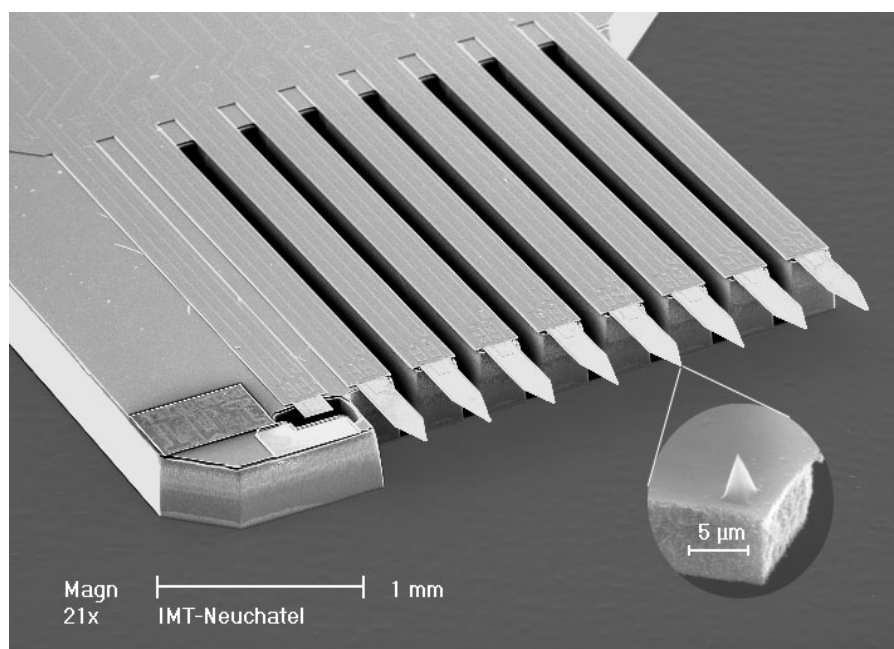


Figure 1: SEM image of the sensor chip with eight support beams and cantilevers. The inset shows the tip formed by KOH etching at the end of the cantilever.

A MEMS approach combined with mechatronic concepts for the scanner was selected for implementing the SFM. For redundancy, the sensor chip (Figure 1) featured eight, about 6 μm thick cantilevers each with an KOH-etched 7 to 8 μm high silicon tip. The cantilevers could be cleaved off if contaminated. The cantilever deflection was measured using implanted, p-type piezo-resistors. Thermal drifts were compensated by a reference piezo-resistor. The chip was glued on a triangular platform, which was suspended from the rigid body of the scanner by means of symmetrically arranged polyimide springs. The later also contained the electrical contacts to the chip. Three magnets were attached in the corners of the platform. An electrical coil mounted underneath each magnet allowed deflecting them. The whole scanner measured 12mm×18mm×24mm and weighted 15g.

The sample stage featured 10 sets of 6 substrates and 10 calibration samples. It could be moved out of the enclosure to receive a soil or air-fall sample. Once rotated in front of the microscope, the sample wheel moved first to the focus position of the optical microscope. An OM image was taken on which, the position for the SFM measurement was selected. The stage was then used to approach the sample to the SFM tip.

During NASA's Phoenix Mission, which operated on the red planet from May to October 2008, we could demonstrate successful SFM operations (see Figure 2). The instrument produced data of soil particles for scientific analysis. From an engineering point of view, operating the SFM within the constraints of a mission was the biggest challenge.

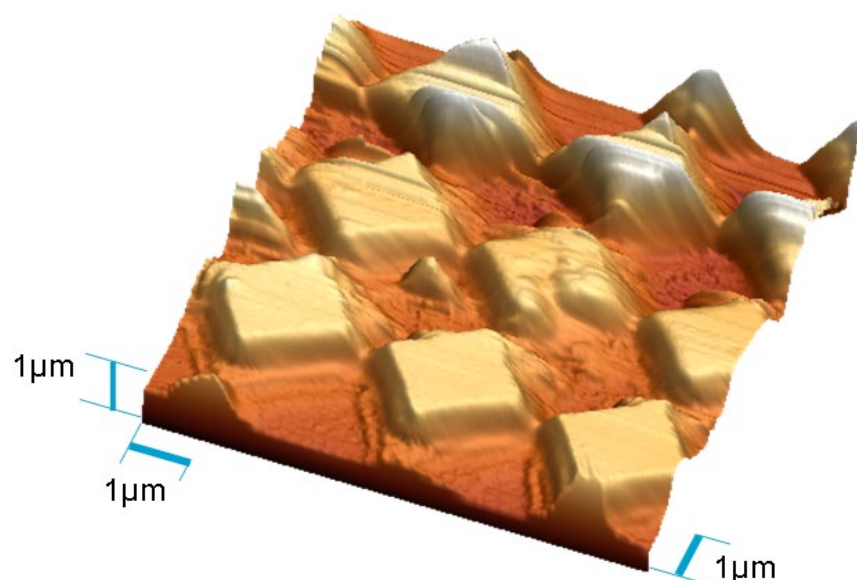


Figure 2: Dynamic mode SFM image of a 2D calibration sample recorded on sol 64 of the Phoenix Mission on Mars.

REFERENCES

- [i] W. J. Markiewicz, et al., "Optical properties of the Martian aerosols as derived from Imager for Mars Pathfinder midday sky brightness data", *J. Geophys. Res.*, 104 (E4), 9009–9017 (1999).
- [ii] PH. Smith, et al., "Introduction to special section on the Phoenix Mission: Landing Site Characterization Experiments", *Mission Overviews, and Expected Science J. of Geophys. Res. - Planets* 113, Article Number: E00A18 (2008).

21.5

Volatiles in the atmosphere of Mars: the effects of volcanism and escape.

Gillmann Cédric*, Lognonné Philippe**

*Institut für Geophysik, ETH Zürich, Switzerland (cedric.gillmann@erdw.ethz.ch)

**Géophysique spatiale et planétologie, IGP, Paris, France

Habitability of terrestrial planets and of Mars in particular, is governed by their atmospheric conditions; that is the surface pressure and temperature and the abundance of diverse volatiles, such as water and CO₂. Over time, Mars has known several main phases of evolution that were characterized by vastly different surface conditions and sometimes the presence of flowing liquid water. To better understand the history of the planet, we study the long term influence of volcanism and atmospheric escape on the evolution of the conditions on the surface of Mars during the last four billion years. We use the recent observation and modeling to constrain our model with the help of isotopic data from Carbon, Nitrogen and Argon. Water is also a focus of our study.

CO₂ is the main object of our study, as it represents the bulk of the present, and probably past, atmosphere. Volcanic degassing and atmospheric escape through non-thermal processes are the two most straightforward processes that can have an effect on the atmosphere of Mars, and, as such, it is important to quantify their respective influences.

Volcanic degassing is obtained from crust production models, observation of the surface, and realistic volatile contents of the lavas. ASPERA measurements and modeling of the escape rates produced by ionic escape, sputtering and dissociative recombination constitute the sink of volatiles. History of Argon (and the ⁴⁰Ar/³⁶Ar ratio) constrains the maximum escape flux of CO₂. This imposes limited escape flux, consistent with the recent lowering of the expected escape efficiency on Mars. With low escape rates, our model is able to reproduce present day ³⁶Ar abundance and ⁴⁰Ar/³⁶Ar ratio.

We also show that the present-day atmosphere of Mars is likely to be constituted by a large part of volcanic gases, as it only takes 150 ppm CO₂ in the lavas to obtain a “volcanic/early” ratio of 50% and 90% or more are obtained with a content of 450 ppm. We also find that it is unlikely that lavas on Mars could have contained more than several hundred ppm CO₂. Likewise, the mean age of the atmosphere is estimated to be no more than 1.9 to 2.3 billion years old and could be less in case recent volcanism was more intense than taken into account in the model. Atmospheric pressures and variations on Mars are predicted to be low, as the result of degassing and non-thermal escape. In our model, they do not exceed 50 mbar during the considered period. This seems in line with the assumption of a heavy loss of volatiles during the first 500 Myr.

Isotopic ratios lead us to propose that Nitrogen is probably old in the Martian atmosphere and has been subjected to the fractionation of atmospheric escape. The ¹²C/¹³C, on the other hand is more stable and indicates that Carbon is younger and that a part of it might come from cometary bodies. Water is moderately abundant on Mars during the whole 4 billion years evolution but is unlikely to reside in the atmosphere or in liquid form unless large scale perturbations occur (changes in obliquity, large input of greenhouse gases due to a short burst of volcanism).

21.6

Core and early crust formation on Mars

Golabek Gregor*, Keller Tobias**, Gerya Taras*, Zhu Guizhi*, Tackley Paul & Connolly James**

*Institut für Geophysik, Sonneggstrasse 5, CH-8092 Basel (gregor.golabek@erdw.ethz.ch)

**Institut für Mineralogie und Petrologie, Clausiusstrasse 25, CH-8092 Zürich

One of the most striking surface features on Mars is the crustal dichotomy. It is the oldest geological feature on Mars and was formed more than 4.1 Ga ago by either exogenic or endogenic processes (Nimmo et al., 2008; Keller & Tackley, 2009). In order to find an internal origin of the crustal dichotomy, located within a maximum of 400 Ma of planetary differentiation, the thermal state of the planet resulting from core formation needs to be considered. Additionally, it was suggested that a primordial crust with up to 45 km thickness can be formed already during the Martian core formation (Norman, 1999). We suggest that the sinking of iron diapirs delivered by predifferentiated impactors induced impact- and shear heating-related temperature anomalies in the mantle that fostered the formation of early Martian crust. Thus, the crustal thickness distribution would largely be a result of planetary core formation, late impact history and the onset of mantle convection.

In this study, we examine parameter sets that will likely cause hemispherical asymmetry in both core formation and onset of mantle convection. To test this hypothesis we use numerical models to simulate the formation of the Martian iron core and the resulting mantle convection pattern, while peridotite melting is enabled to track melting caused by shear and radioactive heating.

We perform 2D simulations using the spherical-Cartesian code I2ELVIS (Gerya & Yuen, 2007) for planetary accretion and the spherical code STAGYY (Hernlund & Tackley, 2008) for the consequent onset of mantle convection. We apply a temperature-, stress- and melt-fraction dependent viscoplastic rheology inside a Mars-sized planet. Radioactive and shear heating as well as consumption of latent heat by silicate melting are taken into account.

The depth of neutral buoyancy of silicate melt with respect to solid silicates is determined by the difference in compressibility of the liquid and solid phase. To self-consistently simulate the silicate phase changes expected inside a Mars-sized body, we use the thermodynamical database *Perple_X* (Connolly, 2005). As initial condition for core formation (I2ELVIS), we apply randomly distributed iron diapirs with 75 km radius inside the planet, representing the cores of stochastically distributed impactors. Additionally, we explore the effect of one giant impactor core on the planetary evolution.

Results indicate that the presence of a large impactor core induces hemispherically asymmetrical core formation. The amplitude of shear heating anomalies often exceeds the solidus of primitive mantle material and thus, the formation of a considerable amount of silicate melt is observed.

The resulting temperature field after core formation is then read into the mantle convection code STAGYY. The hemispherical magma ocean induced by one late giant impactor favours a dichotomous crust formation during and shortly after core formation. Afterwards, the extraction of excess heat produced by the sinking of the giant impactor through the mantle leads to a localized region of massive magmatism, comparable to Tharsis, which is sustained during later evolution by a single plume forming beneath the province. The rest of the mantle is dominated by a sluggish convection pattern with limited crust formation that preserves the early formed dichotomous crustal structure until recent time.

REFERENCES

- Connolly, J.A.D. 2005: Computation of phase equilibria by linear programming: A tool for geodynamic modeling and its application to subduction zone decarbonation. *Earth Planet. Sci. Lett.*, 236, 524-541.
- Gerya, T.V., & Yuen, D.J. 2007: Robust characteristics method for modelling multiphase visco-elasto-plastic thermo-mechanical problems. *Phys. Earth Planet. Int.*, 163, 83-105.
- Hernlund, J.W., & Tackley, P.J. 2008: Modeling mantle convection in the spherical annulus. *Phys. Earth Planet. Int.*, 171, 48-54.
- Keller, T., & Tackley, P.J. 2009: Towards self-consistent modeling of the martian dichotomy: The influence of one-ridge convection on crustal thickness distribution. *Icarus*, 202, 429-443.
- Nimmo, F., Hart, S.D., Korycansky, D.G., & Agnor, C.B. 2008: Implications of an impact origin for the martian hemispheric dichotomy. *Nature*, 453, 1220-1223.
- Norman, M.D. 1999: The composition and thickness of the crust of Mars estimated from rare earth elements and neodymium-isotopic compositions of Martian meteorites. *Meteorit. Planet. Sci.*, 34, 439-449.

21.7

The potential of Close-up imaging on the surface of Mars

Hofmann Beda A.*, Josset Marie**, Josset Jean-Luc**

*Naturhistorisches Museum Bern, Bernastrasse 15, CH-3005 Bern (beda.hofmann@geo.unibe.ch)

**Space Exploration Institute, Neuchâtel

Close-up imaging is here defined as imaging at resolutions of 10 to 100 microns per pixel, corresponding to macro-photography. Imaging of this type has been implemented in past Mars Missions (Beagle 2, 50micron/pixel b/w; Mars Exploration Rovers, 30 microns/pixel b/w; Phoenix, 23-120 micron/pixel colour) and similar instruments will be used during upcoming Mars surface missions (Nasa's Mars Science Laboratory, ESA's ExoMars). The resolution is intermediate between that of Panoramic cameras and of microscopes. In preparation for the ExoMars mission, where the Swiss Instrument CLUPI (Close UP Imager, 15 microns/pixel in colour, 2652x1768 pixel detector) will provide this type of information, we are performing tests to acquire knowledge concerning the types of information that can be gained from CLUPI-type images (Hofmann, 2008).

The main goal for ESA's ExoMars Rover Mission with the Pasteur instrument payload (launch planned for 2018) is to search for traces of past or present life using a sophisticated set of instruments for geological context characterization and life search. The operation strategy of the Pasteur Rover consists of a) search for an interesting site; b) site characterization; c) detailed investigation of selected sites including drilling to 2 m followed by drillcore analysis in a lab inside the rover. CLUPI will be used mainly in steps b) and c), possibly also a). During site characterization, CLUPI images will be crucial for the interpretation of the characteristics of soil and rock surfaces. During detailed investigations, CLUPI will yield images of drilling fines and of drillcores obtained (after this drillcores are destroyed for analyses). The preparation of image interpretation has two main goals:

First we aim to be able to characterize soils and rocks in the best possible way using CLUPI-type images, and to obtain information about the uncertainties involved by performing blind tests. A specific interest will be the recognition and characterization of evidence for the past presence of water.

Second, we prepare for the search for and interpretation of possible signatures of life at CLUPI resolution. Stromatolitic textures in past surface environments and filamentous fabrics in past subsurface environments (Hofmann et al., 2008) are prime candidates of interest in this context. The types of biosignatures present on Earth at this resolution needs to be investigated and criteria for their interpretation (biogenic versus nonbiogenic) need to be evaluated.



Figure 1. CLUPI-type close-up image obtained with a commercial camera using the identical detector as CLUPI. Image width is 5.7 cm (corresponding to 21.5 microns per pixel). Inset shows detail in full resolution. The "stalactitic" fabric are encrustations of microbial filaments in a cavity in Mesozoic basalts from the Black Head Quarry, Ballina, NSW, Australia. Such fabrics are an example of an easily identifiable potential signature of past life on Mars.

REFERENCES

- Hofmann, B.A., 2008, Morphological biosignatures from subsurface environments: Recognition on planetary missions: *Space Science Reviews*, v. 135, p. 245-254.
- Hofmann, B.A., Farmer, J.D., von Blanckenburg, F., and Fallick, A.E., 2008, Subsurface filamentous fabrics: An evaluation of possible modes of origins based on morphological and geochemical criteria, with implications for exoplaeontology: *Astrobiology*, v. 8, p. 87-117.

21.8

ExoMars Rover : Goals and instruments

Josset Jean-Luc*, Sandoz Alain*, Josset Marie*, Choueiri Ted*, Jordan Fabien*, Josset Laureline*

**Space-Exploration Institute (Space-X), Fbg de l'Hôpital 68, CH-2000 Neuchâtel
jean-luc.josset@space-x.ch*

ExoMars is an approved Mars exploration programme of the European Space Agency (ESA) involving a broad cooperation with NASA. The programme is composed of two missions:

A first launch will take place in 2016, with three goals: deploy an orbiter module that will analyse trace gases of the Martian atmosphere; demonstrate ESA's capability to deliver a payload to the surface with an Entry, Descent and Landing (EDL) module ; and provide with the orbiter a communication relay between Mars and the Earth, in particular for the ExoMars rover.

In a second step, the ESA ExoMars Rover will be launched together with the NASA Max-C Rover. Using a NASA « Skycrane » descent module, the rovers will be delivered to the surface at the same time in early 2019.

Along with technological demonstration goals (surface mobility with a rover, access to sub-surface samples, sample preparation and distribution for analysis by scientific instruments), the programme has the following scientific aims:

- to search for signs of past and/or present life on Mars;
- to investigate the water/geochemical environment as a function of depth in the shallow subsurface;
- to investigate Martian atmospheric trace gases and their sources.

Research in geology and exobiology will be conducted using the scientific payload of the ExoMars rover. The Pasteur payload consists of 9 instruments. A first set of four instruments will conduct preliminary observations:

PanCam, an instrument equipped with wide-angle multi-spectral stereoscopic high resolution panoramic imagers, will provide a 3D model of research sites and geological information thanks to its optical filters.


CLUPI (CLOse UP Imager) will provide high-resolution color images (2400 x 1700 x 3 bits per image with a 15µm/bit resolution at 20cm) of the immediate surroundings of drill spots and of retrieved samples. Space-X is the institute responsible for delivering CLUPI and the PanCam stereoscopic imagers to the ExoMars mission.

Together with these visible imaging systems, Ma_Miss (Mars Multispectral Imager for Sub-surface Science, a wide-range infrared spectrometer to conduct mineralogical investigations) and WISDOM (Water Ice & Subsurface Deposit Observations on Mars, a polarimetric ground-penetrating radar) will bring additional information to characterize the drilling sites.

At six drill sites during the 180-sol surface mission of the ExoMars rover, a core sample will be retrieved from two meters under the surface and delivered to the scientific instruments inside the rover. After having been imaged using CLUPI, the samples will be crushed and distributed to the following five instruments inside the rover:

MIRU (Micromega InfraRed Unit, Infrared Microscope for hyperspectral imaging), RAMAN IOH (Raman Spectrometer), MARS XRD (X-Ray Diffractometer), MOMA (Mars Organic Molecule Analyser, Gas Chromatographer / Mass Spectrometer) and LMC (Life Marcher Chip).

The combination of all the results produced by the ExoMars rover's Pasteur scientific payload will produce the first full set of data on sub-surface Martian samples.



The image shows a detailed rendering of the ExoMars rover on the surface of Mars. The rover is a six-wheeled vehicle with a solar panel and various scientific instruments. In the background, the ESA Mars Express orbiter is visible in the sky, with its large dish antenna and solar panels. The ESA logo is in the top right corner of the image.

exomars

→ LIFE ON MARS?

ExoMars to investigate one of the most exciting questions of our time.

Are we alone in the Universe or is there life beyond Earth? The European Space Agency (ESA), in cooperation with NASA, has launched the ExoMars programme to look for the answer on and below the surface of Mars.

Recent research stemming from ESA's Mars Express orbiter mission has confirmed the presence of methane in the martian atmosphere. On Earth, most of this gas is produced by living organisms. Liquid water and moderate temperatures on the Red Planet, in the past or present, could be capable of supporting complex organic molecules and possibly living organisms.

The two ExoMars missions will investigate the martian environment and demonstrate new technologies for the next big international scientific challenge: the return of samples from Mars in the 2020s.

<http://exploration.esa.int>

www.esa.int European Space Agency

Figure 1. ExoMars Rover.